Early Jurassic (Toarcian) dinoflagellate cysts from the Timor Sea, Australia

JAMES B. RIDING and ROBIN HELBY

RIDING, J.B. & HELBY, R., 2001:09:21. Early Jurassic (Toarcian) dinoflagellate cysts from the Timor Sea, Australia. *Memoir of the Association of Australasian Palaeontologists 24*, 1-32. ISSN 0810 8889.

An Early Jurassic (Toarcian) dinoflagellate cyst association is recorded as a rare component (normally <1%) of abundant and diverse palynofloras from the lower Plover Formation in the Jabiru and Skua Fields, Timor Sea, offshore north-western Australia. This represents the first detailed report of dinoflagellate cysts from the Toarcian in Australia. One genus, *Skuadinium*, and nine species of dinoflagellate cysts are described as new. The new species are: *Luehndea septata*, *Mendicodinium echinatum*, *Mendicodinium scabratum*, *Moorodinium tessellatum*, *Nannoceratopsis spinosus*, *Skuadinium asymmetricum*, *Skuadinium biturbinatum*, *Skuadinium reticulatum* and *Susadinium*? *australis*. The dinoflagellate cyst association is termed the *Luehndea* Assemblage. Within this association, it is possible to delineate a lower *Susadinium*? Suite and an overlying *Skuadinium* Suite. Correlations with Europe are indicative of an early Toarcian age for the *Luehndea* Assemblage, and the occurrence of this association may be associated with a global eustatic base level rise at this time. The *Luehndea* Assemblage is, however, markedly different to coeval marine palynofloras from the Northern Hemisphere and is interpreted as being marginal marine.

James B. Riding, Australian Geological Survey Organisation, GPO Box 378, Canberra, ACT 2601, Australia (present address: British Geological Survey, Keyworth, Nottingham NG12 5GG, UK [e-mail: jbri@bgs.ac.uk]); Robin Helby (corresponding author), 356A Burns Bay Road, Lane Cove, NSW 2066, Australia (e-mail: rhelby@ozemail.com.au). *10 November 2000.*

Keywords: dinoflagellate cysts, Early Jurassic, Australia, biostratigraphy, taxonomy

THE PALYNOLOGICAL zonation of the Australian Mesozoic published by Helby *et al.* (1987) was the first attempt to provide an integrated, pan-Australian microplankton and spore-pollen zonation. Only the basic zonal framework was given in anticipation that further contributions, particularly documentation of new taxa, would occur as the zonation scheme evolved. This paper is one of a series providing the taxonomic foundation necessary to formalise the widely used unpublished subdivisions of these zones. These subzones have widespread currency within the hydrocarbon industry due to the legislative requirement for the release of technical data under the Petroleum (Submerged Lands) Act 1967. The informal subdivisions of the Helby *et al.* (1987) zonation have been entered into the Australian Geological Survey Organisation (AGSO) STRATDAT database. A diagrammatic update of the Helby *et al.* (1987) zonal scheme is presented by Foster (this volume), and will be fully described by Helby & Partridge (in prep.). This taxonomic project is an initiative of the Petroleum and Marine Division of AGSO.

This paper provides taxonomic descriptions of previously undescribed taxa from Early Jurassic (Toarcian) dinoflagellate cyst assemblages recorded in samples from the Skua and Jabiru fields and other areas in the Timor Sea (Figure 1; Appendices 1, 2; Foster, this volume). The dinoflagellate cyst associations are normally extremely sparse, with more than three quarters of samples in which they occur yielding less than 0.5% dinoflagellates as a proportion of total palynomorphs (Appendix 1). The dinoflagellate cyst associations are grouped as the *Luehndea* Assemblage. Helby *et al.* (1987, figs. 9S-X) illustrated *Susadinium*? *australis* sp. nov, one of the species described here, as *Susadinium* sp. A, from Enderby-1 well in the Carnarvon Basin, Western Australia. It was suggested that *Susadinium* sp. A is confined to the uppermost part of the *Dapcodinium priscum* dinoflagellate cyst Oppel Zone and is associated with the basal part of the *Callialasporites turbatus* spore-pollen Oppel Zone and the uppermost part of the *Corollina torosa* spore-pollen Oppel Zone (Helby *et al.*, 1987, p. 17, figs 8, 12). However, there is no

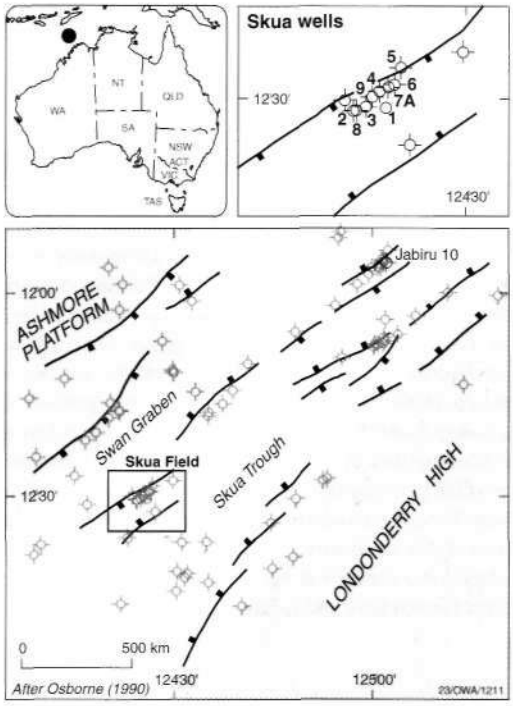

Fig. 1. Map illustrating the location of the Skua Field, Skua wells 1-9 and Jabiru 10 Well in the Timor Sea. The spot in the map at top left represents the area illustrated in the main map (bottom).

overlap of ranges between *Dapcodinium priscum* Evitt 1961 and *Susadinium* sp. A (*Susadinium? australis*) as illustrated in Helby *et al.* (1987, fig. 8). The specimens of *Susadinium* sp. A in the uppermost *Dapcodinium priscum* dinoflagellate cyst Oppel Zone are poorly preserved specimens of *D. priscum* which were misidentified. In Australia, there is a significant stratigraphical gap between the top of *D. priscum* in the late Pliensbachian and the base of *Susadinium* sp. A/ *Susadinium? australis* in the early Toarcian. This was discovered during the course of studies on the Toarcian of development drilling wells in the Skua and Jabiru fields and other areas on the Northwest Shelf. This hiatus in the Australian Early Jurassic dinoflagellate cyst record is reminiscent of the situation in Europe where dinoflagellate cysts are absent or extremely rare in the Hettangian-early Sinemurian and early Pliensbachian intervals (Woollam & Riding, 1983; Riding, 1984a; Riding & Thomas, 1992). *Susadinium? australis* was also recorded as ?*Susadinium* sp. A of Helby *et al.* 1987, from two seabed dredge samples from offshore Western Australia by Burger (1996), who placed them in the *Corollina torosa* spore-pollen Oppel Zone and assigned a Pliensbachian-Toarcian age.

The geology of the Skua Field was discussed by Osborne (1990). The reservoir sands in this field are located in the truncated Plover Formation, with the top of the unit becoming younger, from Toarcian in the south-west to Bathonian in the north-east (Fig. 2; see also Mory, 1988; Osborne, 1990, figs 8, 9). MacDaniel (1988a,b) outlined the geology of the Jabiru Field. The reservoir in this field includes the basal Oxfordian *Wanaea spectabilis* sand, overlying the truncated surface of the lower Plover Formation which was termed the *Corollina torosa* sand (MacDaniel, 1988a,b).

The figured specimens herein are from the lower Plover Formation in Jabiru-10, Skua-4, Skua-5, Skua-6 and Skua-7A wells (Figs 1, 2), although the assemblage has also been recorded in 23 other wells in the Timor Sea region (Appendices 1, 2; Foster, this volume). These data were collected by one of us (RH) between 1983-1998, and most recorded in open file well completion reports. The assemblage has also been recorded in wells in the Carnarvon Basin. Apart from Coojong-1 and Enderby-1 wells, these are not discussed.

SYSTEMATIC PALYNOLOGY

One genus and nine species of dinoflagellate cysts from the lower Plover Formation of the Timor Sea are described as new. The genera are in alphabetical order; the suprageneric classification of Fensome *et al.* (1993) is not used. Dimensions are in micrometres (µm). For descriptive purposes, the cyst sizes, small, intermediate and large, follow Stover & Evitt (1978, p. 5), with intermediate sized cysts having a maximum dimension of 50 to 100µm. Small and large forms are less than 50µm and over 100µm respectively. Most of the morphological terminology for dinoflagellate cysts is as used by Evitt (1985). Where appropriate, the cyst paraplate notation system used is Kofoidian, rather than the 'Taylor-Evitt' scheme of Evitt (1985). References to author citations of taxa discussed may be found in Williams *et al.* (1998, p. 747-817). All figured specimens are housed in the Commonwealth Palaeontological Collection (CPC) of the Australian Geological Survey Organisation (AGSO), Canberra (see Appendix 3).

This study has used, almost exclusively, single and multiple grain mounts and most figured specimens are from these single species slides. All the samples are from sidewall cores. The photomicrographs in Figs 3-11 were taken using an Olympus DP10 digital camera system coupled to a Zeiss Axioskop photomicroscope, housed at AGSO. Some extraneous palynodebris, not

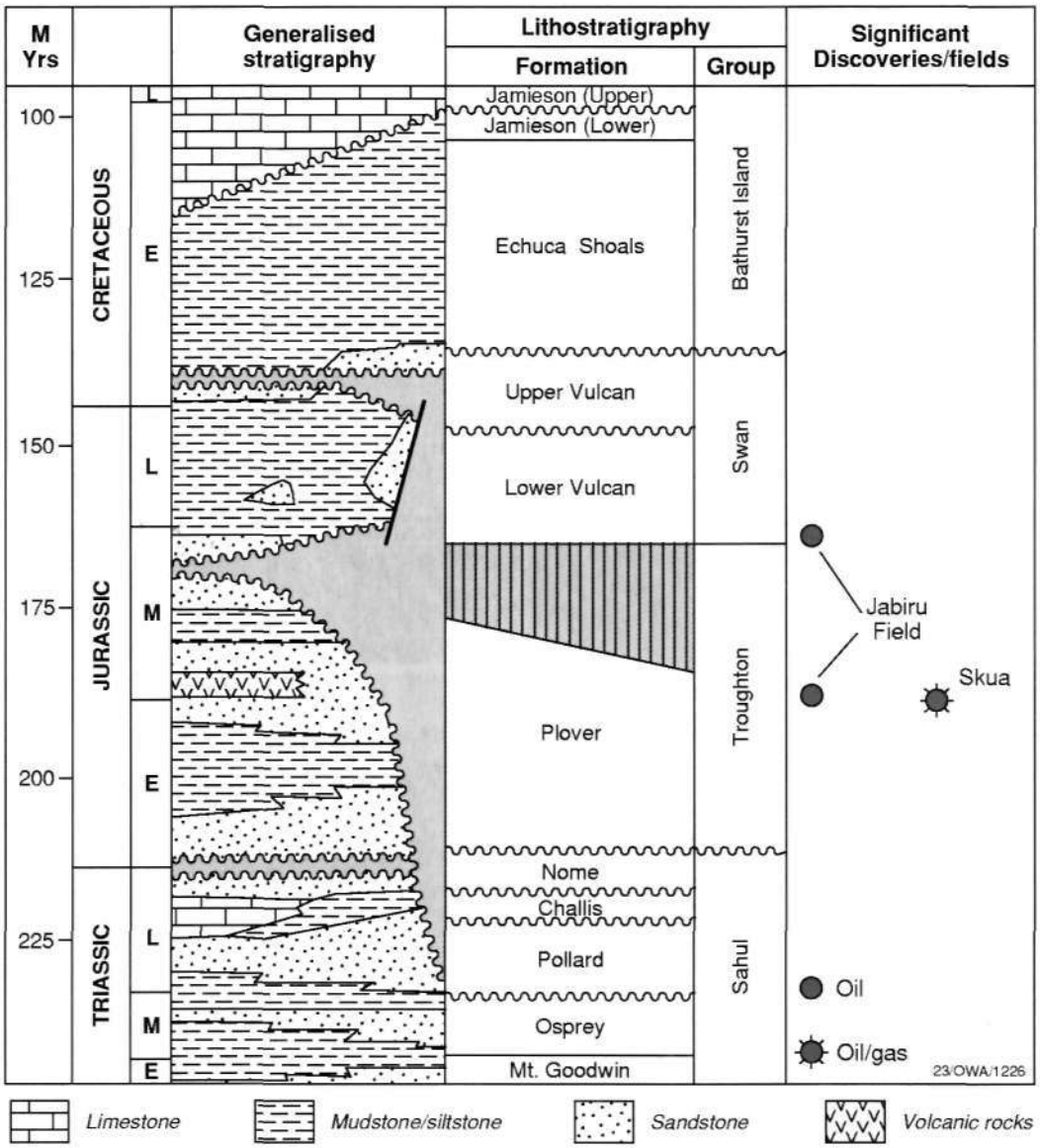

Fig. 2. The regional Mesozoic stratigraphy of the Timor Sea region including the positions of the Jabiru and Skua fields (adapted from Osborne, 1990).

adherent to the figured specimens has been digitally removed in selected images.

The images in Figs 3-11 are stored in a digital database. Many more digital images exist than have been figured. Sample details, morphological data and measurements of each imaged specimen are on open file spreadsheets. The image database is accessible on the AGSO website (http://www.agso.gov.au).

Many of these new taxa have been used in unpublished reports, which are now on open file. To maximise their utility, these informal names are listed separate from the formal synonymy under 'Previous Australian usage'. For continuity, where practical, these informal names have been retained.

Dinoflagellate cysts

Luehndea Morgenroth 1970 emend.

1970 *Luehndea* Morgenroth, p. 346, 347.
1997 *Luehndea* Morgenroth 1970 emend. Bucefalo Palliani *et al.*, p. 114, 115.

Type species. Luehndea spinosa Morgenroth 1970

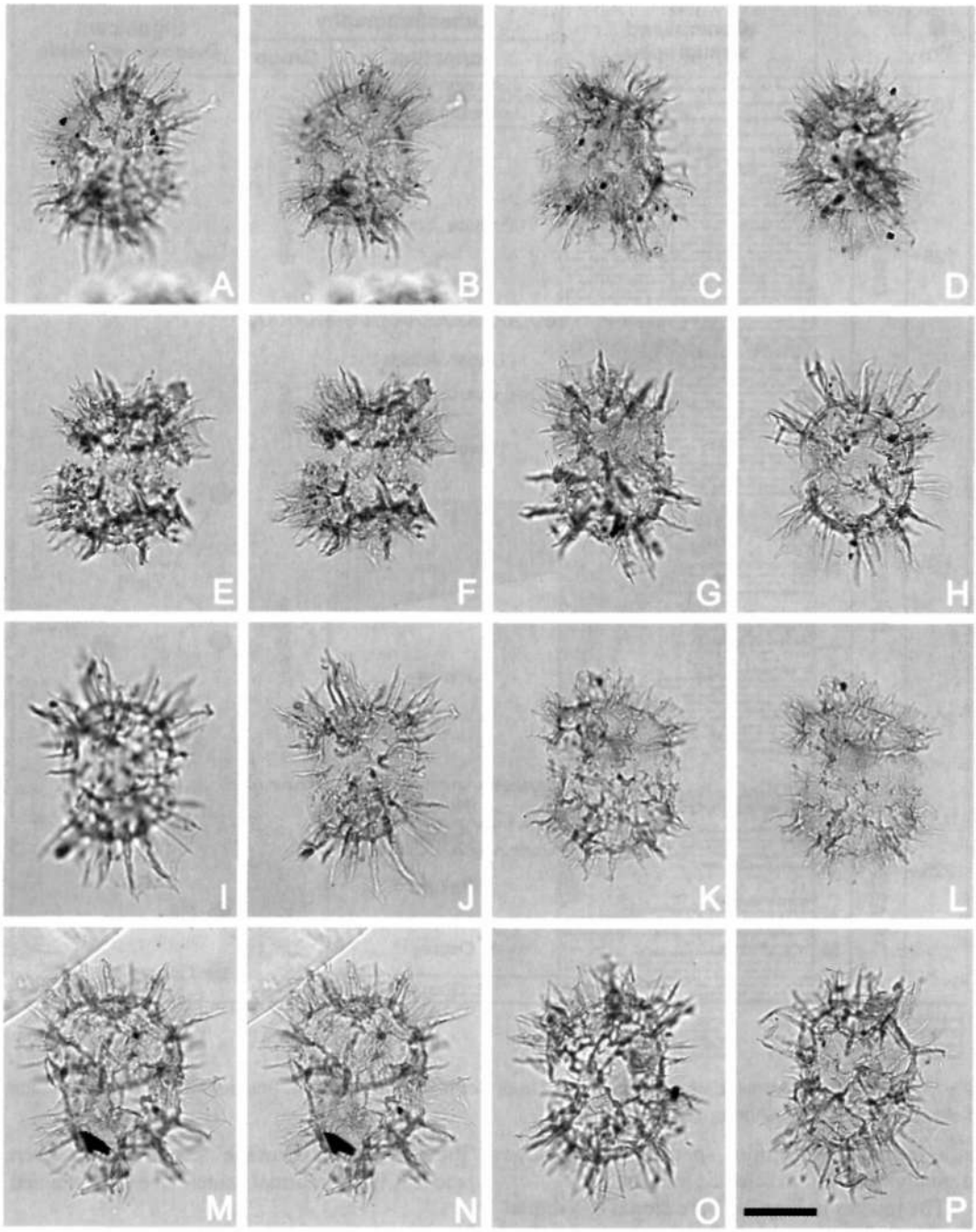

Fig. 3. Luehndea septata sp. nov. All specimens from sidewall cores in Skua-6 well at 2385.00m (Figs 3A-G, K-N) and Skua-7A well at 2440.00m (Figs 3H-J, O-P). All photomicrographs taken using plain transmitted light. The scale bar in Fig. 3P refers to all photomicrographs and is 25µm. Fig. 3O is the holotype, the remainder are paratypes. Note the septa connecting the processes, the prominent paracingular area and the epicystal archaeopyle. A, B - CPC 35107, paratype; ventral view, high and low focus respectively. C - CPC 35108, paratype; ventral view, median focus. D - CPC 35109, paratype; dorsal view, median focus. E, F - CPC 35110, paratype; ventral view, median and low focus respectively. Note the clear epicystal archaeopyle and the relatively low processes and septa. G - CPC 35111, paratype; ventral view, median focus. H - CPC 35112, paratype; dorsal view, low focus. I, J - CPC 35113, paratype; dorsal view, high and median focus respectively. K, L - CPC 35114, paratype; dorsal view, median and low focus respectively. Note the relatively low processes and septa. M, N - CPC 35115, paratype; ventral view, median and low focus respectively. O - CPC 35116, holotype; dorsal view, median focus. P - CPC 35117, paratype; ventral view, low focus.

Emended diagnosis. As emended here, the generic diagnosis incorporates the diagnosis of Bucefalo Palliani *et al.* (1997a, p.115), and is further extended to include species that have parasutural septa which connect the gonal and intergonal processes and cysts that are intermediate in size.

Comments. *Luehndea* is emended to accommodate forms intermediate in size and with parasutural septa. Previously, it was restricted to small forms with low, smooth parasutural ridges or crests (Bucefalo Palliani *et al.*, 1997a, fig. 3).

Luehndea septata sp. nov. (Figs 3A-P)

Previous Australian usage
'Epicystal species' – Helby.

Description. A species of *Luehndea* which is subquadrangular to ellipsoidal in outline, and intermediate in size. Apparently two-layered, the periphragm is extended into solid, slender, distally-pointed gonal and intergonal processes which are normally connected by thin septa. The paracingular paraplates, however, appear to lack vertical parasutural septa. The absence of spines and septa in the broad paracingular region imparts a characteristic indented outline or waist. The processes are straight or slightly curved. Gonal spines are present at all major paraplate boundaries and may be separated by up to two, slightly shorter, intergonal spines. No intratabular processes, or other positive ornamentation, have been observed. The septa are smooth and the distal extremities are commonly concave. The autophragm is smooth or microscabrate. The archaeopyle is epicystal with the operculum typically attached ventrally.

Dimensions (µm, n=31): Min. (Mean) Max.
Overall length (incl. processes): 62 (80) 94
Length of cyst body (excl. processes): 40 (54) 67
Overall width (incl. processes): 55 (67) 77
Width of cyst body (excl. processes): 36 (44) 50
Length of processes: 7 (15) 27

The measured specimens are from sidewall core samples in Skua-5 (2646.00m), Skua-6 (2385.00m) and Skua-7A (2440.00m) wells.

Comments. This distinctive species of *Luehndea* is distinguished by its relatively large size compared to the other species within the genus and the prominent thin parasutural septa. These septa connect the gonal and intergonal processes, except at the paracingulum (Fig. 3). Each septum is concave and smooth distally. There are no vertical paracingular septa, therefore the equatorial area is devoid of ornamentation. The septa define the paratabulation pattern, which is consistent with that determined for the genus (Below, 1990, fig. 10; Bucefalo Palliani *et al.*, 1997a). In a few samples the septa are suppressed; more commonly they may be reduced. The processes in *Luehndea septata* exhibit significant variety in length and those gonal spines associated with the two antapical paraplates are consistently the longest, often exceeding 20µm in length. These relatively long antapical processes can be frequently be used as an orientational criterion. The processes close to the equatorial region are normally the smallest and these may be as short as 10µm in length. Furthermore, the intergonal spines are normally shorter than the gonal spines.

Comparison. *Luehndea septata* is distinguished by the high parasutural septa between the processes (see Morgenroth, 1970, pl. 9; Below, 1990, pl. 8). *Luehndea cirilliae* Bucefalo Palliani *et al.* 1997, *L. spinosa* Morgenroth 1970 and *L. microreticulata* Bucefalo Palliani *et al.* 1997 all have low, smooth parasutural crests or ridges (Bucefalo Palliani *et al.*, 1997a, fig. 3). Furthermore, *Luehndea septata* is about twice the average size of the European species (see *Dimensions*, above). The latter have average lengths of 36-39µm and average widths of 28-34µm (Bucefalo Palliani *et al.*, 1997a, fig. 3).

Derivation of name. From the Latin *septum*, meaning wall or partition.

Holotype and type locality. Fig. 3O, CPC 35116, Skua-7A well, sidewall core at 2440.00m.

Stratigraphical distribution. See Appendix 1 and Fig. 12.

Mendicodinium Morgenroth 1970 emend. Bucefalo Palliani *et al.* 1997

Type species. *Mendicodinium reticulatum* Morgenroth 1970

Mendicodinium echinatum sp. nov. (Figs 4A-L)

Previous Australian usage
Mendicodinium spinosum – Helby.
Hemicystodinium sp. – Morgan.

Description. A proximochorate *Mendicodinium*

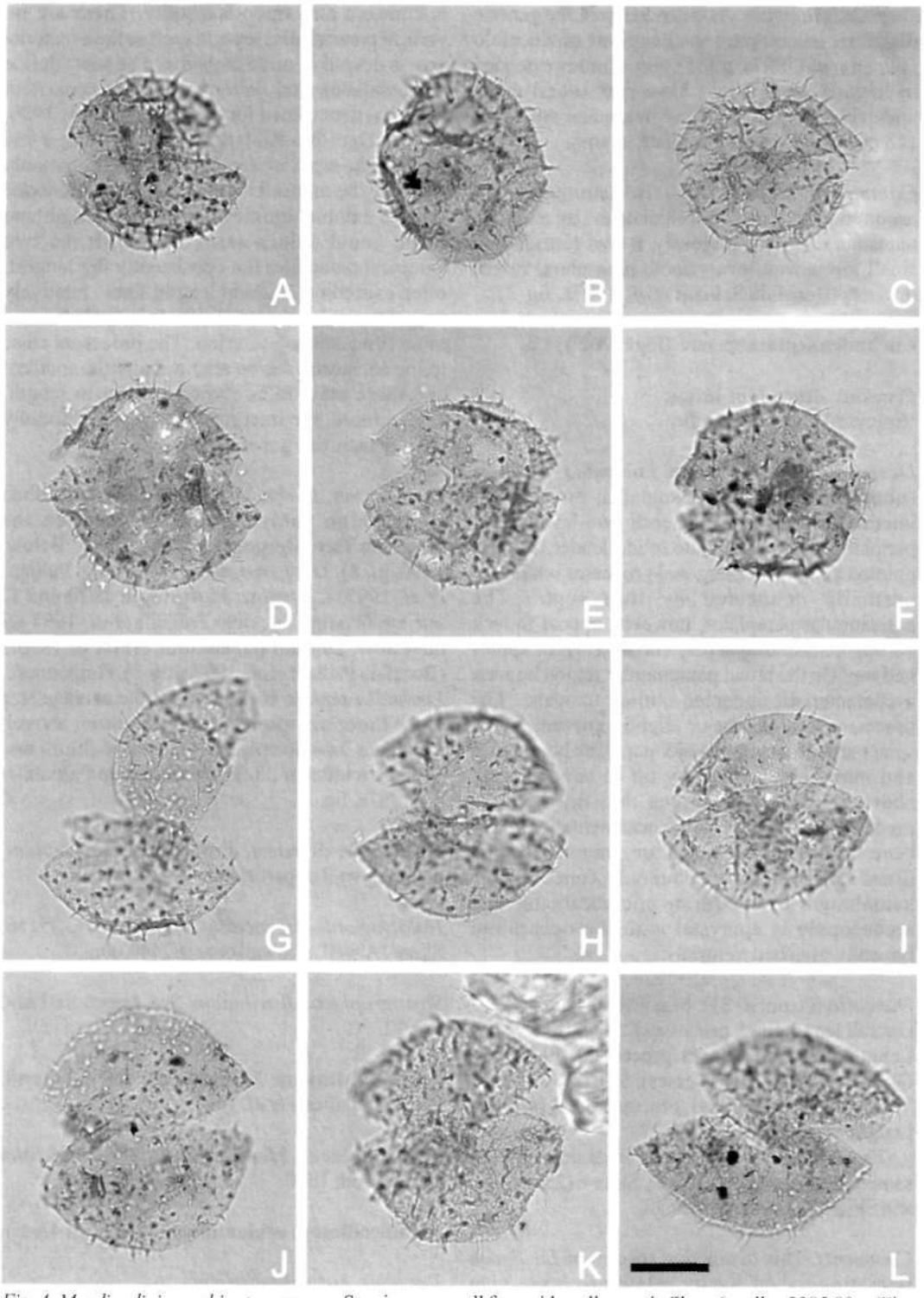

Fig. 4. Mendicodinium echinatum sp. nov. Specimens are all from sidewall cores in Skua-6 well at 2385.00m (Figs 3A-B, F, J, L) and 2391.50m (Figs 3C-E, G-I, K). All photomicrographs were taken using plain transmitted light. The scale bar in photomicrograph 4L refers to all the photomicrographs and represents 25µm. The holotype is Fig.4H; the remainder are paratypes. Note the relatively short processes, the variable density of the spines and the epicystal archaeopyle of this species. A - CPC 35118, paratype; ventral view, (continued opposite)

of intermediate size, subcircular to ellipsoidal in dorsoventral outline. Hypocyst equal in size to, or slightly larger than, the epicyst. The hypocyst is frequently subangular in the antapical area (paraplate 1''''), and is often somewhat flattened. The cyst is normally slightly wider than long. The autophragm is moderately thick, scabrate to rugulate, bearing up to 150 nontabular simple, short, slender, solid, straight to recurved, distally-pointed spines. In the rarer, rugulate forms, the low-relief ornamentation is often present as short, smooth, randomly oriented ridges and scattered grana.

Dimensions (µm, n=31): Min. (Mean) Max.
Length of cyst body (excl. spines): 47 (60) 75
Width of cyst body (excl. spines): 54 (65) 78
Length of spines: 3 (6) 12

The measured specimens are from sidewall core samples in Skua-5 (2646.00m) and Skua-6 (2385.00m and 2391.50m) wells.

Comments. The wide range in the measured cyst body length of this genus is due to the compactional style, which varies markedly. Where the epicyst and the hypocyst are attached in open-lid mode, the measured height of the cyst is exaggerated (Fig. 4G). In contrast, the epicyst may be compressed into the hypocyst, giving a relatively low cyst length.

Comparison. *Mendicodinium echinatum* is similar to the early Toarcian *Mendicodinium spinosum* Bucefalo Palliani *et al*. 1997 in being proximochorate, bearing solid, distally-pointed, nontabular spines. No other validly described species of *Mendicodinium* are spine-bearing. *Mendicodinium spinosum* ranges from 16µm to 27µm in cyst body length (Bucefalo Palliani *et al*., 1997b, fig. 2) and therefore is considerably smaller than *M. echinatum*. The length of the cyst body in *M. echinatum* varies from 47µm to 75µm, hence the size difference between the two species is mutually exclusive and there appears to be no possibility of an overlap. Furthermore, the autophragm of *M. echinatum* is of average thickness (c. 1µm) and is rugulate to scabrate. The wall of *M. spinosum* is markedly thicker and, in *M. spinosum* subsp. *spinosum* is psilate. The autophragm of *M. spinosum* subsp. *perforatum* is perforate. *Mendicodinium echinatum* also has a denser cover of spines than *M. spinosum*.

Derivation of name. From the Latin *echinatus*, meaning prickly.

Holotype and type locality. Fig. 4H, CPC 35125, Skua-6 well, sidewall core sample at 2391.50m.

Stratigraphical distribution. See Appendix 1 and Fig. 12.

Mendicodinium scabratum sp. nov. (Figs 5A-I)

1996 *Mendicodinium* cf. *M. groenlandicum auct. non* (Pocock & Sarjeant 1972) Davey 1979; Burger, fig. 5.

Previous Australian usage
Mendicodinium sp. – Helby.

Description. A proximate *Mendicodinium* of intermediate size and ellipsoidal dorsoventral outline. The hypocyst is frequently larger than the epicyst. Paraplate 1'''' is normally slightly concave or flattened. The cyst is normally slightly wider than long. The autophragm is of moderate thickness and scabrate, microscabrate or granulate. The paracingulum may be faintly indicated on the hypocyst by a low parasutural ridge or a lineation of ornamentation. There may also be a slight inset or concavity at the paracingulum.

Dimensions (µm, n=30): Min. (Mean) Max.
Length: 41 (52) 67
Width: 45 (54) 62

The measured specimens are from sidewall core samples in Skua-5 (2646.00m) and Skua-6 (2385.00m and 2391.50m) wells.

Comments. *Mendicodinium scabratum* typically has a scabrate autophragm (Figs 5A-F), but microscabrate (Figs 5G-I) or granulate individuals have been recorded. The type and density of ornamentation in this species is somewhat

median focus. B - CPC 35119, paratype; ?ventral view, median focus. Note that the archaeopyle has not fully formed. C - CPC 35120, paratype; ventral view, low focus. D - CPC 35121, paratype; ventral view, median focus. E - CPC 35122, paratype; ventral view, high/median focus. F - CPC 35123, paratype; ventral view, low focus. G - CPC 35124, paratype; dorsal view, median focus. Note the almost completely detached epicyst (operculum). H - CPC 35125, holotype; ventral view, high focus. I - CPC 35126, paratype; dorsal view, high focus. J - CPC 35127, paratype; ventral view, low focus. K - CPC 35128, paratype; ventral view, median focus. Note the flat antapical area. L - CPC 35129, paratype; ventral view, median focus.

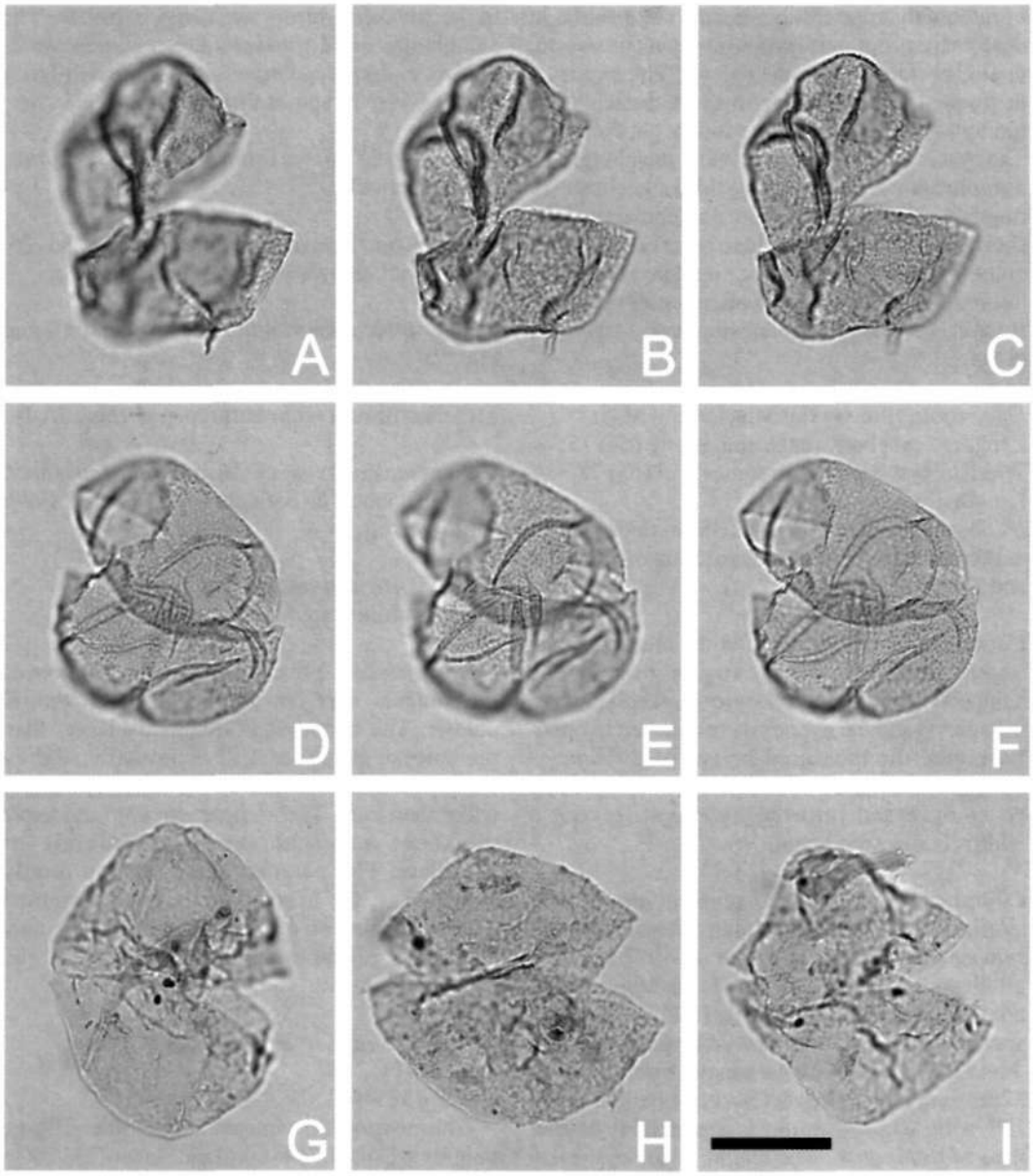

Fig. 5. Mendicodinium scabratum sp. nov. Specimens are all from sidewall cores in Skua-5 well at 2646.00m (Figs 5A-F) and Skua-6 well at 2391.50m (Figs 5G-I). All photomicrographs were taken using plain transmitted light. The scale bar in Fig. 5I refers to all the photomicrographs and represents 25µm. The holotype is Figs 5D-F; the remainder are paratypes. Note the variably scabrate/microscabrate nature of the autophragm and the epicystal archaeopyle. A-C - CPC 35130, paratype; dorsal view, high, median and low focus respectively. A densely scabrate specimen in 'open-lid' preservational mode; the paracingulum is faintly indicated on the hypocyst. Note the slight concavity in the antapical region. D-F - CPC 35131, holotype; oblique ventral view, high, median and low focus respectively. A scabrate individual. G - CPC 35132, paratype; dorsal view, median focus. An elongate, microscabrate form. H - CPC 35133, paratype; ventral view, median focus. Note the microscabrate autophragm. The epicyst is significantly more cone-shaped than the hypocyst, which has a somewhat flattened antapex. I - CPC 35134, paratype; dorsal view, median focus. A biconical specimen with microscabrate autophragm.

variable (Fig. 5). Occasionally, the paracingulum is faintly indicated on the hypocyst by a low parasutural ridge or lineation of ornament (Fig. 5B) and may also be marked by a slight indentation or concavity. The relatively high size range in the cyst body dimensions is due to the occurrence of 'open-lid' preservational style (Figs 5A-C).

Comparison. Mendicodinium scabratum is similar to several members of the plexus of small *Mendicodinium* described from the Toarcian of central Italy by Bucefalo Palliani *et al.* (1997b). These are *M. brunneum, M. microscabratum* and *M. umbriense,* none of which exceeds 38µm in width (Bucefalo Palliani *et al.*, 1997b, fig. 2); they are all significantly smaller than *M. scabratum. Mendicodinium brunneum* has a thick autophragm and is granulate. The cyst wall of *M. microscabratum* Bucefalo Palliani *et al.* 1997 varies from smooth to microscabrate, and the autophragm of *Mendicodinium umbriense* is characterised by relatively large granules. *Mendicodinium reticulatum* Morgenroth 1970, the genotype, is also small but it differs from *M. scabratum* in having a coarsely reticulate autophragm. The seven remaining validly described species of *Mendicodinium* listed by Williams *et al.* (1998, p. 397, 398) are all significantly larger in size and, incidentally, younger than *M. scabratum. Mendicodinium caperatum* Brideaux 1977 and *M. granulatum* Kumar 1986 are both scabrate/granulate. Two Mid to Late Jurassic species *Mendicodinium groenlandicum* (Pocock & Sarjeant 1970) Davey 1979 and *M. quadratum* Kumar 1987 have characteristically psilate autophragms. The autophragm of *M. kemperi* Heilmann-Clausen (in Heilmann-Clausen & Thomsen 1995) is ornamented by thin discontinuous ridges, rugulae and granules. *Mendicodinium microreticulatum* Kumar 1986 and *Mendicodinium morgenrothum* Butler 1995 have microreticulate and verrucate autophragms respectively.

Derivation of name. From the Latin *scabra,* meaning rough.

Holotype and type locality. Figs 5D-F, CPC 35131, Skua-5 well, sidewall core sample at 2646.00m.

Stratigraphical distribution. See Appendix 1 and Fig. 12. *Mendicodinium scabratum* also ranges into Aalenian/Bajocian strata which are referable to the upper *Callialasporites turbatus* Oppel Zone equivalent of Helby *et al.* (1987) (Oliver-1 well at 3057.00m, see Appendix 1).

Moorodinium Backhouse 1988

Type species. Moorodinium spinatum Backhouse 1988

Moorodinium tessellatum sp. nov. (Figs 6A-P)

Description. Proximate, acavate, longitudinally elongate dinoflagellate cysts belonging to the genus *Moorodinium* which are intermediate in size. The outline in dorsoventral view is highly variable around a broad subpentagonal theme. There are two basic varieties; firstly, forms with a broad, bulbous epicyst and a subconical hypocyst normally with a single antapical horn (Figs 6I-P). Secondly, individuals with rounded subtriangular epicysts with an apical horn or protuberance and three-sided hypocysts with a straight or concave antapex (Figs 6A-H). The latter variety may have up to four antapical horns or protuberances (Fig. 6G). Rarely, one or more lateral protuberances may also occur. The epicyst is normally longer than the hypocyst. A reticulum is formed by low smooth ridges which normally define hexagonal and quadrate fenestrae; the autophragm is otherwise smooth. Paratabulation presumably gonyaulacalean, indicated only by the paracingulum, archaeopyle and the presumed gonal position of the antapical horns or protuberances, where developed. The paracingular parasutures are marked by smooth ridges or low crests. Parasulcus indented. Archaeopyle probably epicystal.

Dimensions (µm, n=33): Min. (Mean) Max.
Length of autocyst: 63 (82) 102
Width of autocyst: 46 (59) 75
Length of epicyst: 26 (47) 62
Length of hypocyst: 25 (36) 52
Epicyst as % of overall length: 37 (56) 69
Length of apical horns: 3 (6) 10
Length of antapical horns: 3 (8) 18
Diameter of fenestrae: 4 (8) 12

The measured specimens are all from a sidewall core sample in Skua-6 well at 2385.00m.

Comments. Moorodinium tessellatum is a relatively large cyst (see *Dimensions*, above), however using the criteria of Stover & Evitt (1978, p. 5), it is mainly within the intermediate range. The species has an extremely variable outline around a broad, subpentangular theme (Fig. 6). The highly variable number of horns or

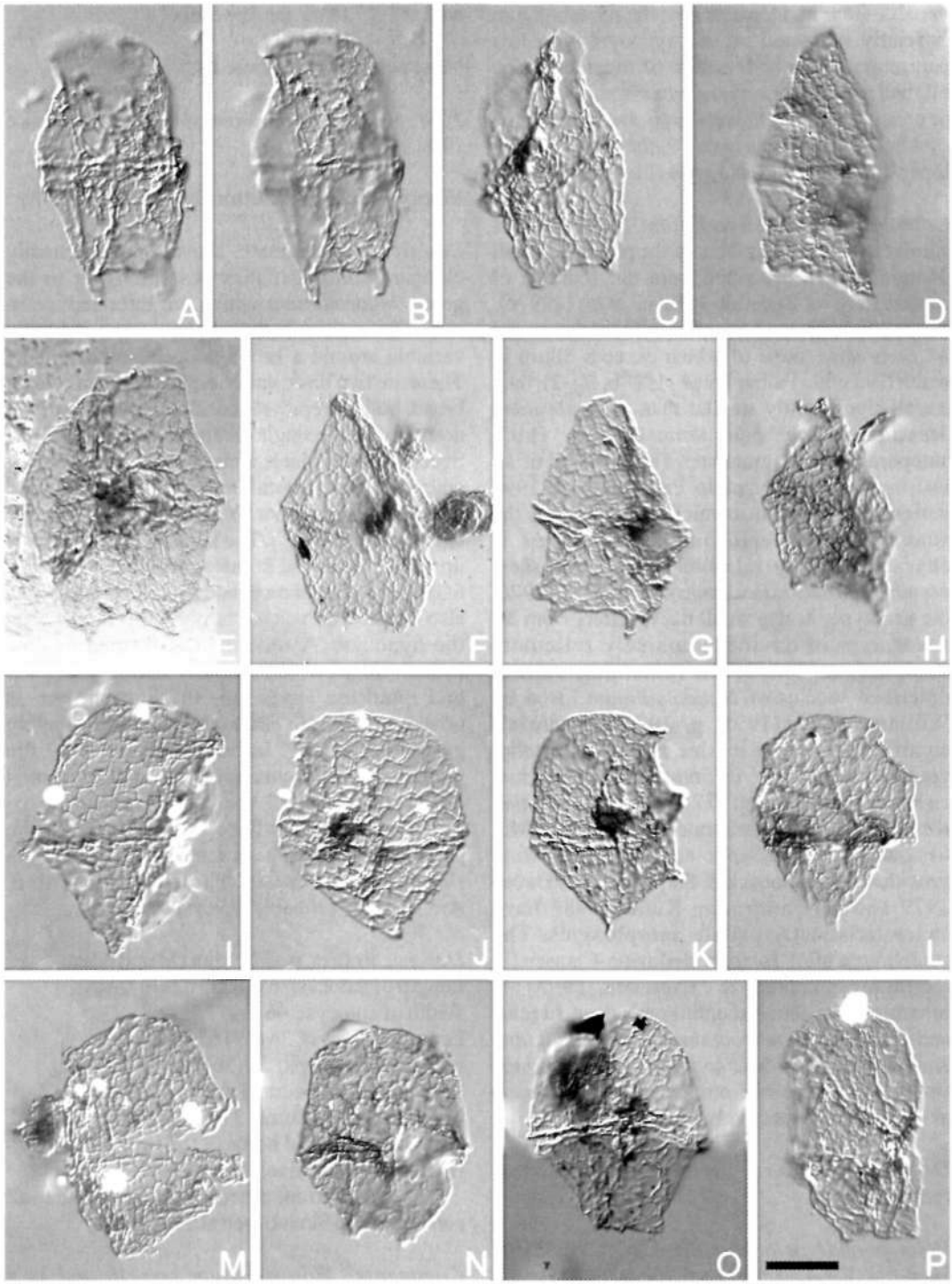

Fig. 6. Moorodinium tessellatum sp. nov. Specimens are all from a sidewall core at 2385.00m in Skua-6 well. All photomicrographs were taken using Nomarski Interference Contrast. The scale bar in Fig. 6P refers to all the photomicrographs and represents 25µm. Fig. 6J is the holotype and the remainder are paratypes; Figs 6K, L, 0 are composite photomicrographs. Figs 6A-H are 'deltoid' morphotypes and Figs 6I-P are 'bulbous' morphotypes. Note the highly variable cyst outline, the prominent paracingulum, the reticulate nature of the autophragm and the apparently epicystal archaeopyle in Fig. 6M. A, B - CPC 35135, paratype; ventral view, median and low focus respectively. C - CPC 35136, paratype; dorsal view, median focus. (continued opposite)

protuberances are of similarly variable sizes and shapes. They are normally subconical with distally rounded terminations but may have bluntly pointed extremities. The epicyst is commonly bulbous but may be subconical and these latter forms, which comprise the minority, are informally termed 'deltoid morphotypes' (Figs 6A-H). Most have a bulbous epicyst and typically have a single antapical horn which is assumed to be inserted at, or close to, the centre of the antapical (1'''') paraplate. These are informally referred to as 'bulbous morphotypes' (Figs 6I-P). Dinoflagellate cysts with a single horn present on the hypocyst are extremely rare, another Jurassic example being *Wanaea* Cookson & Eisenack 1958. Up to four antapical horns/protuberances may be present (Fig. 6G). When four are present, they are presumably inserted at the gonal points on the 1'''' paraplate. Rarely, lateral horns or protuberances may also be present (Figs 6K, L). The horns or protuberances may be broken off in poorly-preserved material. The autophragm is relatively thin and readily folded. A relatively large, brown, subcircular accumulation body is present close to the paracingulum in many specimens. Commonly, the only indication of paratabulation is the paracingulum, which is low in height and is weakly laevorotatory; it is indicated by prominent, distally smooth ridges or crests. The paracingulum is typically low in position on the cyst and normally appears to offset or cut the mosaic-like reticulate pattern which is developed over all the autophragm. Rarely, the paracingulum is either not developed or suppressed. In one specimen (Fig. 6M), the fields forming the reticulum are rectangular to square on either side of a split which may be the principal archaeopyle suture. These four-sided fields may be paracingular paraplates. The lack of a consistently developed epicystal archaeopyle is intriguing. However, some specimens have a split apparently immediately anterior to, or within, the paracingulum (Fig. 6M).

The reticular units of *Moorodinium tessellatum* are overwhelmingly six-sided. The effect of the superpositioning of the ventral and dorsal surfaces often tends to obscure this feature. The species is assumed to have a gonyaulacalean paratabulation. The characteristic regular reticulum is reminiscent of gymnodinioid and suessioid forms. If *Moorodinium tessellatum* was gymnodinioid, each polygonal field defined by the reticulum would represent an amphiesmal vesicle in the parent theca (Fensome *et al.*, 1993, fig. 41). The species is not considered likely to have a suessioid affinity because paraplates arranged in latitudinal series are generally lacking and the paracingulum in *Moorodinium tessellatum* is relatively narrow. This may indicate that the reticulum is a feature of ornamentation, perhaps to give strength to the cyst wall, and that the fields do not necessarily represent paraplates. However, in Fig 6M, there appears to be a paracingulum indicated by two equatorial rows of four-sided fields, which may represent paraplates. This broadly resembles *Suessia* Morbey 1975 (see Morbey 1975, figs 12-15), which has an equatorial paracingulum comprising many paraplates, most of which are four-sided. However, both Below (1987, figs 43, 53) and Stover & Helby (1987, figs 21A, B) illustrated suessioid paratabulation patterns in which the paracingular paraplates are only four-sided. Should these rectangular and square areas represent the paracingulum, it would mean that the surrounding hexagonal fields are also reflected thecal plates. As this phenomenon in *M. tessellatum* is only observed on a single specimen, its suessioid affinity must be deemed equivocal at present. When first described by Backhouse (1988), the genus was deemed to be an index for lacustrine or estuarine deposition.

Comparison. *Moorodinium tessellatum* is superficially similar to suessioid dinoflagellate cysts in having an autophragm which is subdivided into numerous fields. *Moorodinium*, however, is significantly longer than the five suessioid genera, apparently has an epicystal archaeopyle and the fields are more numerous and possibly do not reflect paratabulation (Bucefalo Palliani & Riding, 1997, fig. 7). *Moorodinium*

D - CPC 35137, paratype; ventral view, median focus. An elongate specimen. E - CPC 35138, paratype; ventral view. A large, 'deltoid' specimen. F - CPC 35139, paratype; ventral view, median focus. G - CPC 35140, paratype; ventral view, median focus. Note the small, regular antapical horns at gonal points around the antapical (1'''') paraplate. H - CPC 35141, paratype; dorsal view, low focus. I - CPC 35142, paratype; dorsal view, low focus. Note the hexagonal reticulum. J - CPC 35143, holotype; dorsal view, low focus. Note the regular, hexagonal reticulum. K- CPC 35144, paratype; dorsal view. Note the lateral horns or protuberances. L - CPC 35145, paratype; ventral view. Note the mid lateral horn/protuberance on the epicyst. M - CPC 35146, paratype; ?right lateral view, median focus. Note the distinctly quadrate fields along the possibly epicystal archaeopyle. N- CPC 35147, paratype; dorsal view, low focus. O - CPC 35148, paratype; ventral view. A bilaterally symmetrical specimen. P - CPC 35149, paratype; ventral view, low focus. Note the elongate, subrectangular outline.

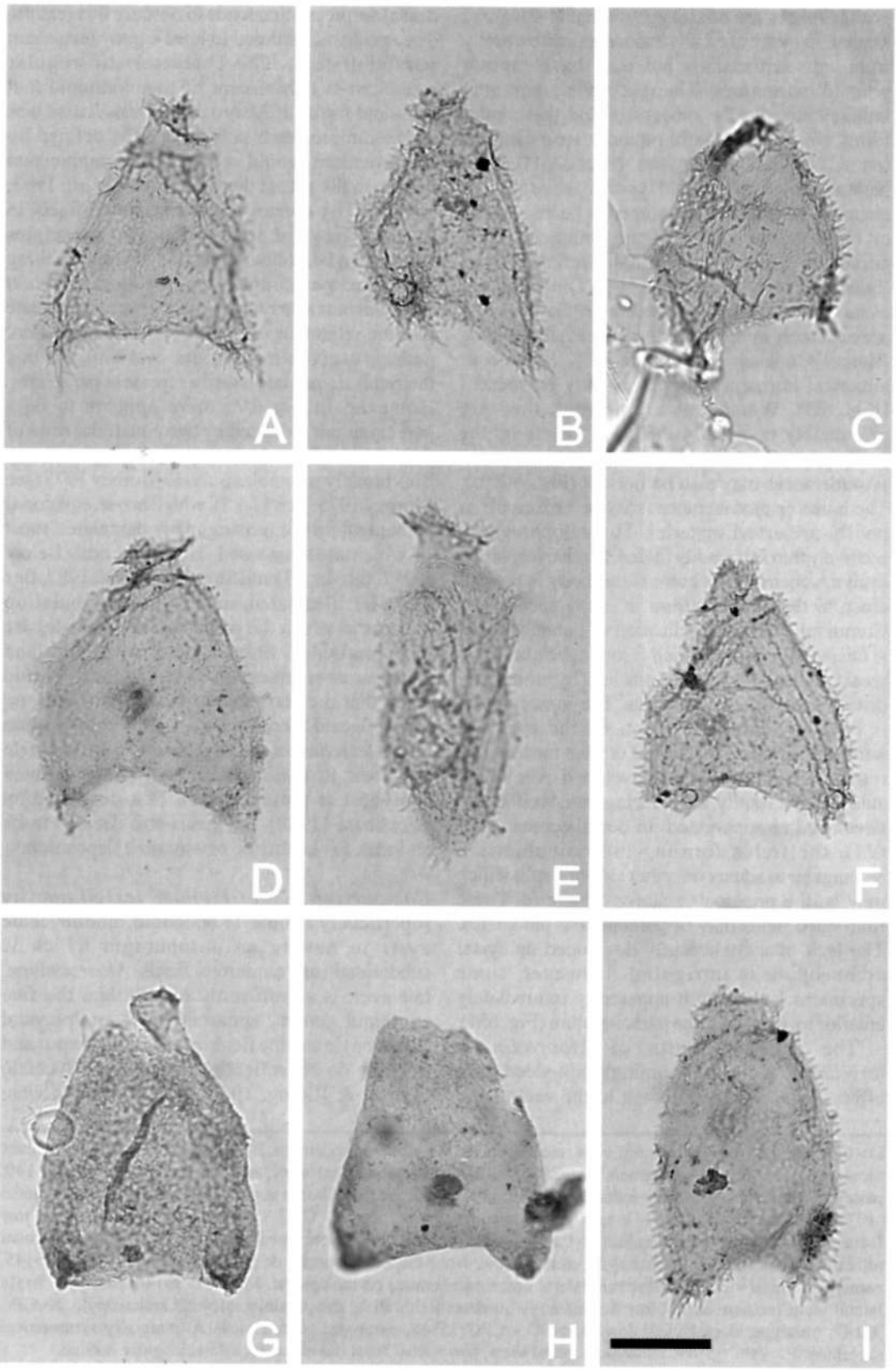
A
B
C
D
E
F
G
H
I

tessellatum has some similarities with representatives of *Cassiculosphaeridia* Davey 1969 and *Valensiella* Eisenack 1963, which may have fine and irregularly reticulate autophragms, are ovoidal and have apical archaeopyles. *Scriniocassis* Gocht 1964 emend. Preuss 1989 also has a reticulate autophragm, yet is ovoidal, has much thicker autophragm and has a combination apical/precingular archaeopyle.

Derivation of name. From the Latin *tessellatus*, meaning mosaic.

Holotype and type locality. Fig. 6J, CPC 35143, Skua-6 well, sidewall core sample at 2385.00m.

Stratigraphical distribution. See Appendix 1 and Fig. 12.

Nannoceratopsis Deflandre 1939 emend.

1939 *Nannoceratopsis* Deflandre, p. 183.
1961 *Nannoceratopsis* Deflandre 1939 emend. Evitt, p. 306.
1980 *Nannoceratopsis* Deflandre 1939 emend. Piel & Evitt, p. 102.
1992 *Nannoceratopsis* Deflandre 1939 emend. Poulsen, p. 44.

Type species. Nannoceratopsis pellucida Deflandre 1939.

Emended diagnosis. The emended generic diagnoses of Piel & Evitt (1980) and Poulsen (1992) are accepted but the genus is further emended here to include species which are proximochorate and/or have parasutural crests.

Comments. The genus *Nannoceratopsis* is emended here to accommodate proximochorate forms which have parasutural crests. This is due to the discovery of *Nannoceratopsis spinosus* sp. nov. (see below), which bears numerous short processes, most specimens being proximochorate and having parasutural crests. Previously, the genus was restricted to proximate forms (see Prauss, 1989, fig. 3; Bucefalo Palliani & Riding, 1998, fig. 9). The processes in *Nannoceratopsis spinosus* sp. nov. exhibit significant variation in length. Most are less than 10% of the minimum diameter of the cyst body. However the processes frequently exceed 10%, especially the antapical spines close to the paired dorsal and ventral horns, therefore the diagnosis of *Nannoceratopsis* needed to be formally emended to include proximochorate forms (Sarjeant, 1982, p. 392).

Nannoceratopsis spinosus sp. nov. (Figs 7A-F, I)

Previous Australian usage
Nannoceratopsis spinosus – Helby.

Description. An acavate, relatively elongate species of *Nannoceratopsis*, intermediate in size and having two prominent, distally tapering, antapical horns of essentially similar size. The horns are distally pointed or rounded. The antapex is consistently markedly concave due to the presence of the large, subequal antapical horns. Paracingulum is well developed and is devoid of ornamentation on the paraplate surfaces, although high crests, surmounted by spines, are developed on, or close to, the anterior and posterior parasutures. The autophragm varies in thickness. Numerous short, solid, distally-pointed, thorn-shaped processes arise from the parasutures bordering the sagittal band, surmounting parasutural crests in the dorsal, ventral and antapical areas of the hypocyst, on the paracingular parasutures and on the epicyst. The processes at and close to the distal parts of the antapical horns are frequently significantly longer than the spines elsewhere on the cyst. Spines may also be scattered in nontabular positions on

Fig. 7. Nannoceratopsis spp. All specimens are from a sidewall core at 1790.00m in Jabiru-10 well. The photomicrographs were all taken using plain transmitted light. The scale bar in Fig. 7I refers to all the photomicrographs and represents 25µm. 7A-F, I - *Nannoceratopsis spinosus* sp. nov. Fig. 7I is the holotype, the remainder are paratypes. Figs. 7A, E are composite photomicrographs. Note the prominent paracingulum and the spinose nature of the cyst. A - CPC 35150, paratype; left lateral view. A form with a particularly prominent paracingulum. B - CPC 35151, paratype; right lateral view, median focus. C - CPC 35152, paratype; right lateral view, low focus. A damaged specimen, lacking the relatively small epicyst. D - CPC 35153, paratype; right lateral view, low focus. A relatively broad specimen. E - CPC 35154, paratype; oblique ventral view. Note the corona of short apical spines. F - CPC 35155, paratype; right lateral view, median focus. Note the sagittal parasutural ridges. I - CPC 35156, holotype; right lateral view, median focus. Note the prominent, regular spines in the sagittal areas. G, H - *Nannoceratopsis* sp. A. Note the relatively small antapical horns and the weakly concave antapical margin. G - CPC 35157, left lateral view, high focus. H - CPC 35158, left lateral view, high focus. Note that the entire epicyst has broken off, presumably due to mechanical damage.

the lateral parts of the hypocyst.

Dimensions (µm, n=35): Min. (Mean) Max.
Length of cyst body (excl. processes): 54 (67) 82
Width of cyst body (excl. processes): 30 (46) 65
Height of paracingulum: 7 (8) 12
Length of processes: 1 (3) 15

The measured specimens are all from a sidewall core sample in Jabiru-10 well at 1790.00m.

Comments. Nannoceratopsis spinosus is the only species of this genus which is proximochorate. The small, relatively densely packed processes around the sagittal band and the prominent paracingulum, distinguish this taxon. The majority of the processes are parasutural and are typically centred around the sagittal band on the hypocyst, on or close to the paracingular parasutures and on the epicyst (Fig. 7). Because of the extremely small size of the epicyst, resolution of the precise location of the epicystal spines is difficult. The processes at the distal tips of the antapical horns are frequently up to 15µm, which is three times as long as the remaining spines. The majority of the processes are normally 2-4µm long. The parasutural crests developed on the hypocyst adjacent to the sagittal band are surmounted by processes. The processes surrounding the anterior paracingular parasuture in the epicyst have a radiating pattern and often appear to form a corona (Fig. 7E). The nontabular processes on the hypocyst vary in density but are normally sparse. The surfaces of the cingular paraplates may be devoid of processes but are commonly microgranulate, scabrate or smooth. The paracingulum is consistently prominent, broad and slopes antapically from dorsal to ventral in lateral view (Fig. 7A).

Comparison. Nannoceratopsis spinosus differs from all other species of the genus in having parasutural and nontabular processes.

Derivation of name. From the Latin *spinosus*, meaning thorny.

Holotype and type locality. Fig. 7I, CPC 35156, Jabiru-10 well, sidewall core sample at 1790.00m.

Stratigraphical distribution. See Appendix 1.

Nannoceratopsis sp. A (Figs 7G-H)

Description. A relatively elongate form of *Nannoceratopsis* which is characterised by small antapical horns which engender a weakly concave antapical margin. The dorsal and ventral sides are straight to weakly convex. These almost straight antapical, dorsal and ventral sides of the hypocyst, together with the apical side of the hypocyst, give this morphotype a characteristic rounded triangular outline in lateral view. The autophragm is scabrate or microscabrate.

Dimensions (µm, n=3): Min. (Mean) Max.
Length: 65 (70) 79
Width: 55 (56) 57

The measured specimens are all from sidewall core 2 in Jabiru-10 well at 1790.00m.

Comments. Insufficient material of this species has been recovered for a formal description.

Comparison. This morphotype is most similar to *Nannoceratopsis symmetrica* Bucefalo Palliani & Riding 2000. However, the latter is significantly smaller and has a more robust autophragm. *Nannoceratopsis* sp. A is similar to *Nannoceratopsis raunsgaardii* Poulsen 1996, however the latter is not longitudinally elongate and thus is much wider in lateral view than *Nannoceratopsis* sp. A. *Nannoceratopsis raunsgaardii* is also characterised by sharply distally pointed antapical horns; *Nannoceratopsis* sp. A, by contrast, has blunt, rounded terminations to the antapical horns. The relatively small, rounded *Nannoceratopsis evae* Prauss 1989 also has reduced antapical horns engendering a subrectangular lateral hypocystal outline. However, *N. evae* is characterised by a differentiated or coarsely reticulate autophragm. *Nannoceratopsis triangulata* Prauss 1987 is also similar in overall shape to *Nannoceratopsis* sp. A, but has pointed antapical horns and the ventral horn is reduced. Furthermore, *Nannoceratopsis* sp. A is markedly smaller than *Nannoceratopsis triangulata* and has significantly thicker autophragm.

Stratigraphical Distribution. See Appendix 1.

Skuadinium gen. nov.

Type Species. Skuadinium biturbinatum sp. nov.

Diagnosis. Acavate, proximate, biconical or subbiconical dinoflagellate cysts, intermediate in size with single apical and antapical horns. Subbiconical forms may be distorted by two hypocystal protuberances at and below the

paracingulum on the ventral side. Autophragm smooth, or with low-relief ornamentation; entire or reticulate. Ornamentation nontabular to occasionally partially tabular. Dark, subcircular accumulation bodies are generally present in the paracingular region. Paratabulation generally indicated by the paracingulum and parasulcus. Archaeopyle type uncertain, possibly epicystal.

Comparison. In outline, *Skuadinium* resembles several Triassic and Jurassic genera. *Kalyptea* Cookson & Eisenack 1960 has an anterior intercalary archaeopyle and is normally kalyptrate. The Early Jurassic *Liasidium* Drugg 1978 has a large single paraplate anterior intercalary archaeopyle and prominent shoulders on the epicyst and hypocyst. The archaeopyle of *Rhaetogonyaulax* Sarjeant 1966 emend. Harland *et al.* 1975 is a distinctive combination (apical/anterior intercalary) type and *Sverdrupiella* Bujak & Fisher 1976 is cavate.

Derivation of name. The genus *Skuadinium* is named after the Skua oilfield in the Timor Sea.

Skuadinium biturbinatum sp. nov. (Figs 8A-P)

Previous Australian usage
Skuadinium sp. – Helby.

Description. A species of *Skuadinium* which is longitudinally elongate and largely symmetrical about the paracingulum and parasulcus. Apical and antapical horns relatively short and broad with blunt or rounded distal terminations. Autophragm thin; smooth, microscabrate or microgranulate. The markedly laevorotatory paracingulum is indicated by low, smooth ridges. The parasulcus is indented. Discontinuous lineations of low-relief ornamentation sometimes present, generally on the apical and antapical horns. Archaeopyle type unknown, possibly epicystal.

Dimensions (μm, n=28): Min. (Mean) Max.
Length: 55 (74) 86
Width: 39 (54) 63

The measured specimens are from sidewall core samples in Jabiru-10 (1790.00m), Skua-5 (2646.00m), Skua-6 (2385.00m) and Skua-7A (2440.00m) wells.

Comments. The outline is variable because the thin autophragm readily folds and tears. Additionally, the cyst is not always dorsoventrally flattened and may present in different orientations. The paracingulum and parasulcus are usually the only indications of paratabulation, but short lineations, which may be paratabular, often occur close to the distal parts of the horns. A definite archaeopyle has not been observed; however, vague indications of an epicystal excystment aperture are present.

Comparison. Skuadinium biturbinatum differs from *S. asymmetricum* sp. nov. in being biconical and lacking reticulate surface features, and from *S. reticulatum* sp. nov. in lacking a reticulate autophragm.

Derivation of name. From the Latin prefix *bi-*, meaning two or double, and *turbinatus*, meaning conical or top-shaped.

Holotype and type locality. Fig. 8M, CPC 35177, Skua-6 well, sidewall core sample at 2385.00m.

Stratigraphical distribution. See Appendix 1 and Fig. 12.

Skuadinium asymmetricum sp. nov. (Figs 9A-I)

Previous Australian usage
Skuaceratopsis – Helby.

Description. Representatives of *Skuadinium* which have a reticulate to occasionally scabrate autophragm. The horns are highly variable; they range from relatively short to markedly elongate and may be pointed or rounded distally. In lateral view, the dorsal sides of the epicyst and hypocyst are convex. The ventral side of the epicyst is, however, generally highly concave, while the ventral side of the hypocyst is normally straight to convex, although concave close to the antapical horn. The main reason for the asymmetrical nature of this form in lateral view is that the ventral side of the cyst is inflated. The ventral precingular, and particularly the postcingular paraplates, are markedly inflated close to the paracingulum, resulting in the parasulcus being deeply indented. Most specimens have a relatively large, subcircular brown accumulation body within the cyst. The paracingulum may sometimes be faintly indicated by autophragmal folds. An epicystal archaeopyle is suggested by relatively consistent tearing along the anterior margin of the paracingulum.

Dimensions (μm, n=25): Min. (Mean) Max.
Length: 56 (72) 95
Width: 36 (50) 62

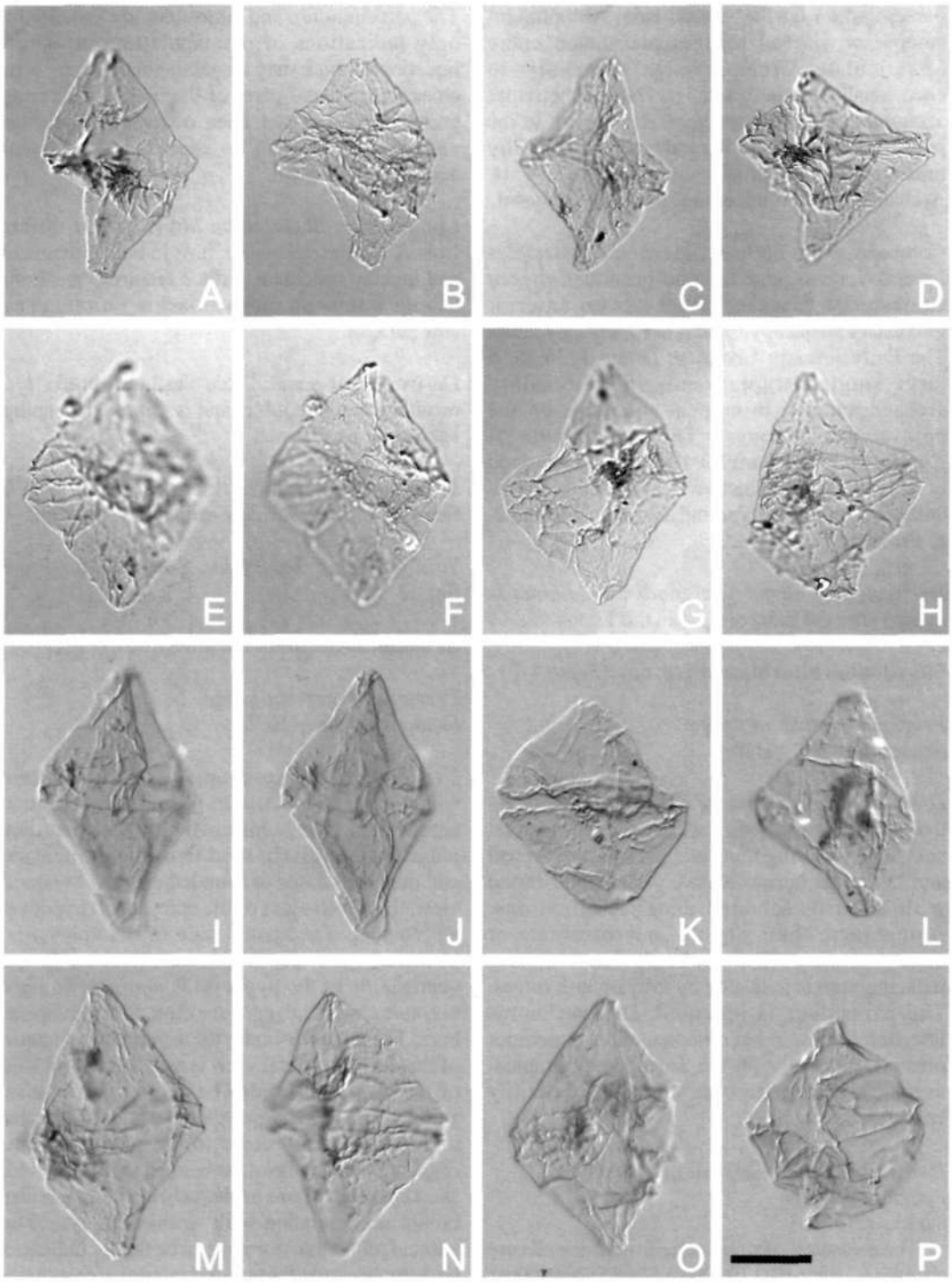

Fig. 8. Skuadinium biturbinatum sp. nov. The specimens are from sidewall cores in Jabiru-10 well at 1790.00m (Figs 8I-L), Skua-5 well at 2646.00m (Fig. 8P) and Skua-6 well at 2385.00m (Figs 8A-H, M-O). All photomicrographs were taken using Nomarski Interference Contrast. The scale bar in Fig. 8P refers to all the photomicrographs and represents 25µm. The holotype is Fig. 8M; the remainder are paratypes. Note the biconical shape, the blunt, rounded distal terminations of the apical and apical horns, the relatively thin, smooth autophragm and the apparent lack of a consistent archaeopyle. A - CPC 35167, paratype; dorsal view, high focus. B - CPC 35168, paratype; dorsal view, low focus. C - CPC 35169, paratype; (continued opposite)

Width of fenestrae: 1 (2) 5

The measured specimens are from sidewall core samples in Skua-6 (2385.00m) and Skua-7A (2440.00m) wells.

Comments. The asymmetry of the epicyst in lateral view, caused by extension of the ventral side is diagnostic of this species (Fig. 9). The shape of the epicyst, and often the hypocyst, in lateral view may impart a lateral outline superficially similar to a lateral view of *Nannoceratopsis* (see Piel & Evitt, 1980). However, the profound differences in paratabulation distinguish *Skuadinium asymmetricum* from species of *Nannoceratopsis*. A definite archaeopyle has not been observed, but incomplete splits immediately anterior of the paracingulum strongly suggest that the archaeopyle type is epicystal (Fig. 9F).

Comparison. *Skuadinium asymmetricum* differs from the other species of the genus in its distinctively asymmetrical outline in lateral view and its reticulate autophragm. It is most similar to *S. reticulatum* sp. nov., but lacks its symmetrical biconical shape, and has more variable ornament and commonly rounded horn extremities.

Derivation of name. From the marked asymmetry of the cyst in lateral view.

Holotype and type locality. Figs 9H-I, CPC 35166, Skua-6 well, sidewall core sample at 2385.00m.

Stratigraphical distribution. See Appendix 1 and Fig. 12.

Skuadinium reticulatum sp. nov. (Figs 10A-I)

Previous Australian usage
Skuadinium reticulatum – Helby.

Description. *Skuadinium* with a strongly reticulate autophragm. The apical and antapical horns are subequally developed and have pointed distal terminations. The fenestrae are frequently longitudinally elongate and appear to be arranged in apical-antapical lineations. A prominent accumulation body is normally present in the vicinity of the paracingulum. Paratabulation indicated only by the paracingulum and parasulcus. The former is marked in most specimens by prominent smooth ridges. A consistently developed archaeopyle has not been observed, but consistent tearing along the anterior surface of the paracingulum suggests that it is possibly epicystal.

Dimensions (μm, n=25): Min. (Mean) Max.
Length: 59 (81) 99
Width: 32 (50) 63
Diameter of fenestrae: 1 (3) 8

The measured specimens are from sidewall core samples at 2385.00m and 2391.50m in Skua-6 well.

Comments. The apical and antapical horns are sometimes slightly recurved (Fig. 10A).

Comparison. The prominent reticulation characterises *Skuadinium reticulatum*. It differs from *S. asymmetricum* in its spindle shape, and in lacking ventral inflations in the region of the paracingulum. It is similar to *Scriniocassis weberi* Gocht 1964 in its strongly reticulate autophragm. However, *S. weberi* is ovoidal in outline, has a thicker, differentiated autophragm and a consistently developed polyplacoid combination (apical/precingular) archaeopyle (Below, 1990).

Derivation of name. From the Latin *reticulatus* meaning netted or net-like.

Holotype and type locality. Figs 10G-H, CPC 35187, Skua-6 well, sidewall core sample at 2391.50m.

Stratigraphical distribution. See Appendix 1 and Fig. 12.

Susadinium Dörhöfer & Davies 1980

Type species. *Susadinium scrofoides* Dörhöfer & Davies 1980

Comments. The paratabulation pattern of *Facetodinium* Bjaerke (1980) and *Susadinium* by

oblique dorsal view, low focus. D - CPC 35170, paratype; ventral view, median focus. A relatively broad specimen. E, F - CPC 35171, paratype; dorsal view, high and low focus respectively. An almost perfectly biconical form. G - CPC 35172, paratype; ventral view, high focus. Note the prominent laevorotatory paracingulum. H - CPC 35173, paratype; oblique ventral view, median focus. I, J - CPC 35174, paratype; left lateral view, median and low focus respectively. An elongate example. K - CPC 35175, paratype; ventral view, low focus. This specimen is unusually squat. L - CPC 35176, paratype; ?oblique ventral view, median/low focus. M - CPC 35177, holotype; dorsal view, low focus. N - CPC 35178, paratype; oblique ventral view, median focus. O - CPC 35179, paratype; dorsal view, median focus. P - CPC 35180, paratype; left lateral view, median focus. Note the curved antapical horn and the prominent paracingulum.

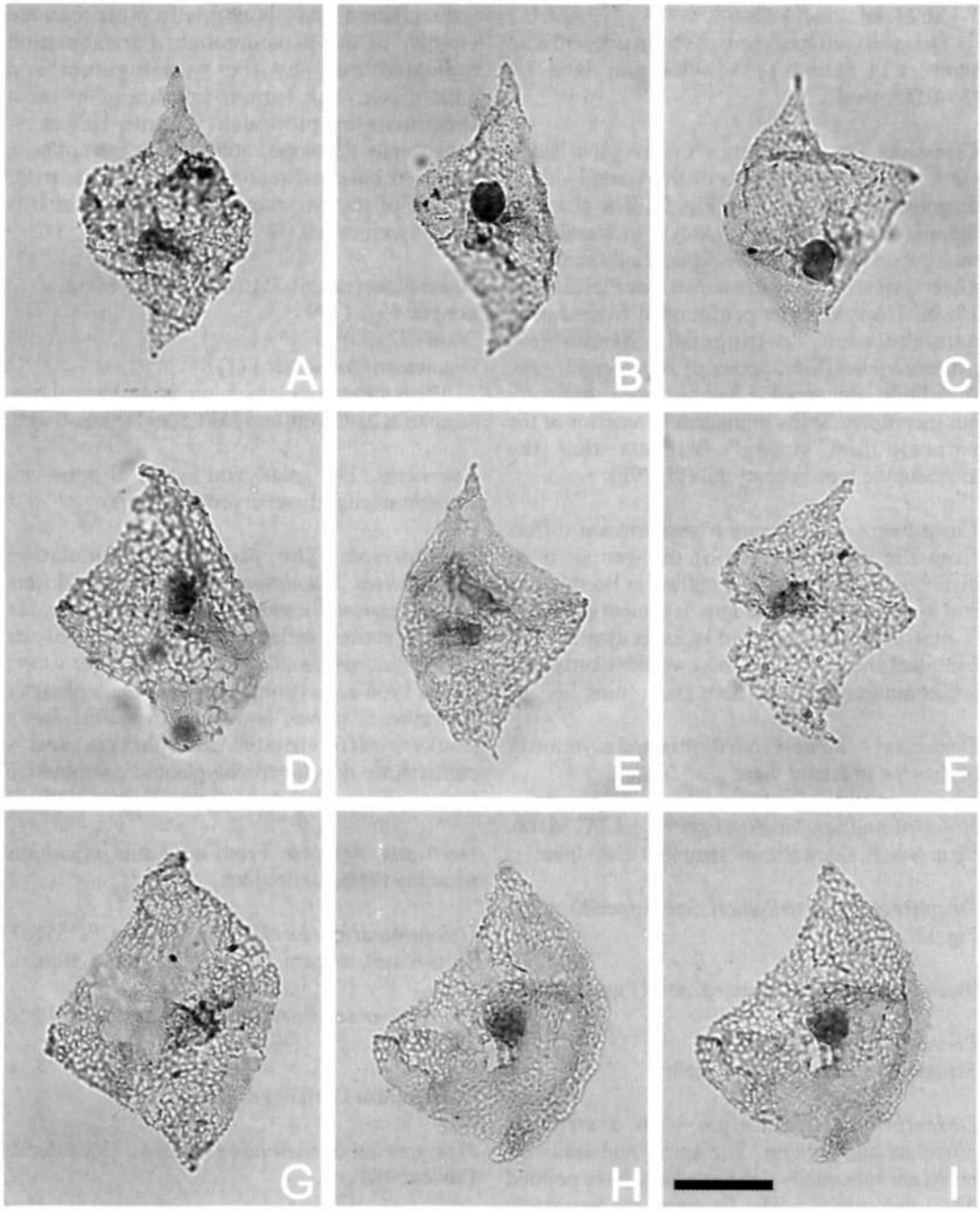

Fig. 9. Skuadinium asymmetricum sp. nov. Specimens are all from sidewall cores in Skua-6 well at 2385.00m (Figs 9A, D-I) and Skua-7A well at 2440.00m (Figs 9B-C). All photomicrographs were taken using plain transmitted light. The scale bar in Fig. 9I refers to all the photomicrographs and represents 25µm. Figs 9H-I are of the holotype; the remainder are paratypes. Note the asymmetrically biconical shape, the pointed distal terminations of the apical and apical horns, the finely reticulate autophragm, the prominent accumulation body within the cyst and the lack of a consistent archaeopyle. A - CPC 35159, paratype; right lateral view, low focus. B - CPC 35160, paratype; right lateral view, high focus. C - CPC 35161, paratype; left lateral view, low focus. D - CPC 35162, paratype; right lateral view, median focus. E - CPC 35163, paratype; left lateral view, median focus. F - CPC 35164, paratype; left lateral view, median focus. G - CPC 35165, paratype; right lateral view, median focus. H, I - CPC 35166, holotype; right lateral view, median and low focus respectively.

Below (1987) is accepted. However, the synonymy of *Susadinium* with *Dodekovia* proposed by Below (1987) is not followed here. The holotype of *Dodekovia syzygia* Dörhöfer & Davies 1980 is referable to *Apteodinium* (see Stover & Williams, 1987, p. 87).

Susadinium? australis sp. nov. (Figs 11A-P)

1987 *Susadinium* sp. A; Helby *et al.*, figs 9S-X.
1996 ?*Susadinium* sp. A of Helby *et al.* 1987; Burger, pl. 9, figs S-U.

Previous Australian usage
Susadinium sp. – Helby.

Description. Small, with a rounded pentagonal to subovoidal outline. Autophragm relatively thick, smooth, scabrate to microreticulate, frequently with low, smooth, anastomosing ridges. Prominent intratabular, rounded, commonly inflated protuberances are present in the precingular, postcingular and antapical paraplate series. These protuberances are surmounted by rounded to quadrate/rectangular periphragmal extensions which may be low ridges or relatively high and septate in form. The distal edges of the ridges are smooth to echinate and their height varies between specimens and also within individuals. There is a marked tendency for the protuberances and ridges/septa to be best developed in the precingular and postcingular paraplate series. Furthermore, they are typically located close to the paracingulum. Occasionally, low relief or negative ornamentation in the paracingulum partially indicate the paracingular paraplate boundaries. Parasulcus apparently not subdivided. Archaeopyle combination, apparently involving the apical and anterior intercalary paraplate series; compound operculum.

Dimensions (μm, n=31): Min. (Mean) Max.
Length incl. operculum: 38 (45) 53
Length excl. operculum: 31 (44) 53
Width: 31 (42) 56
Maximum height of protuberances: 2 (4) 7

The measured specimens are from sidewall core samples in Skua-3 (2402.50m) and Skua-4 (2366.00m) wells.

Comments. The most striking morphological feature of this species is the rounded, intratabular protuberances surmounted by ridges or septate periphragmal extensions. These are best developed in the precingular and postcingular paraplate series. However, low, reduced protuberances and ridges/septa may be present in the antapical series. These vary markedly in shape according to the size of the paraplate. In smaller paraplates, such as 1'', the protuberances may be suppressed. The apparent separation of the periphragm and endophragm where the ridges and/or septa emerge on the protuberances means that the protuberances are floored by autophragm proximally. Normally, the ridges/septa are echinate (and open) distally. However, they may also be distally smooth (Fig. 11). In the precingular and postcingular paraplate series, the protuberances and ridges/septa are present immediately adjacent to the paracingulum (Fig. 11). This leaves up to 50% of the paraplate entirely free of major ornamentation. Such eccentricity of intratabular features is extremely unusual among dinoflagellate cysts; normally features like these are located in the centres of paraplates. In the precingular paraplate series, the periphragmal extensions may be inserted close together, forming a row (Figs 11A-C). The ridges/septa vary in height within assemblages, specimens and in single paraplates, giving a dissected and incomplete appearance (Figs 11G-J). Frequently the side of the ridge/septal complex is reduced in height toward the paracingulum (Figs 11H-I, M). This feature is comparable to the septa which are open toward the paracingulum in *Amphorula* Dodekova 1969. However, this ridge/septal variability in *S? australis* is not as regular as in *Amphorula*. In some specimens of *S? australis*, the periphragmal extensions may be highest toward the paracingulum. The protuberance on the 2'''' paraplate may be significantly larger and more bulbous than the 1'''' paraplate, engendering an asymmetrical outline in dorsoventral view (Fensome *et al.*, 1993, fig 123). This prominent feature can often be a useful orientational criterion. Furthermore, a crack close to the 1''''/2'''' parasuture is often present (Figs 11H, L-O); this may be a result of mechanical damage along a line of weakness. The intratabular protuberances are largely parallel-sided in the Timor Sea specimens (Fig. 11) but are more rounded in the Carnarvon Basin specimens (Helby *et al*, 1987, figs 9S-X). Also, the latter appear to have aligned, coalescing low relief elements rather than complete ridges/septa.

Susadinium? australis is tentatively attributed to *Susadinium* because the archaeopyle is a combination, apparently involving the apical and anterior intercalary paraplate series. Unequivocal representatives of *Susadinium* have single

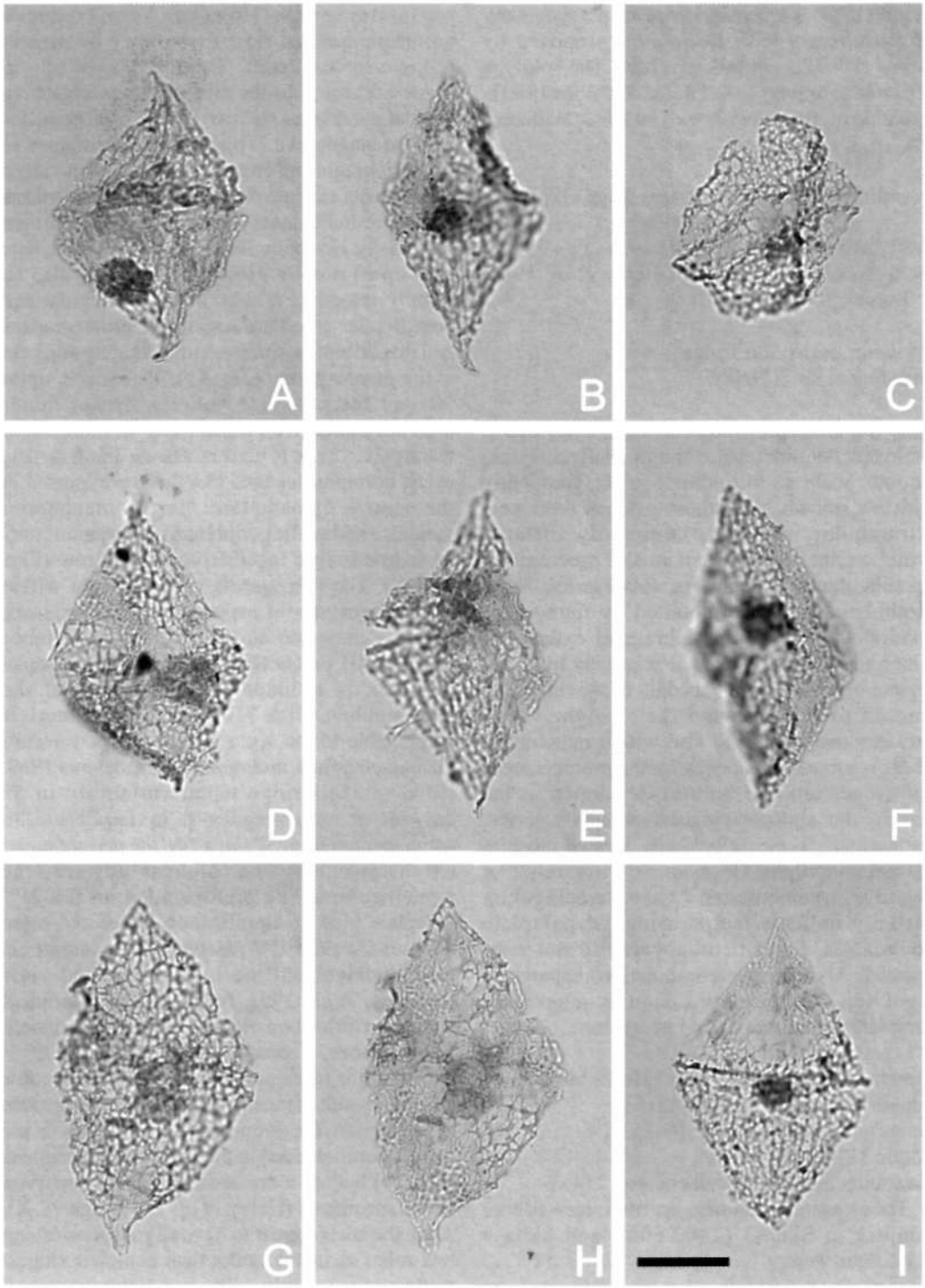

Fig. 10. Skuadinium reticulatum sp. nov. Specimens are all from sidewall cores in Skua-6 well at 2385.00m (Fig. 10I) and 2391.50m (Figs 10A-H). All photomicrographs were taken using plain transmitted light. The scale bar in Fig. 10I refers to all photomicrographs and represents 25µm. Figs 10G, H are the holotype; the remainder are paratypes. Note pointed terminations of apical and antapical horns, strongly reticulate autophragm and large accumulation bodies in the cysts. This species possibly has an epicystal archaeopyle (Figs 10C, E). A - CPC 35181, paratype; left lateral view, low focus. Note recurved nature of apical and antapical horns. B - CPC 35182, elongate paratype; ?ventral view, high focus. C - CPC 35183, unusually squat paratype; (continued opposite)

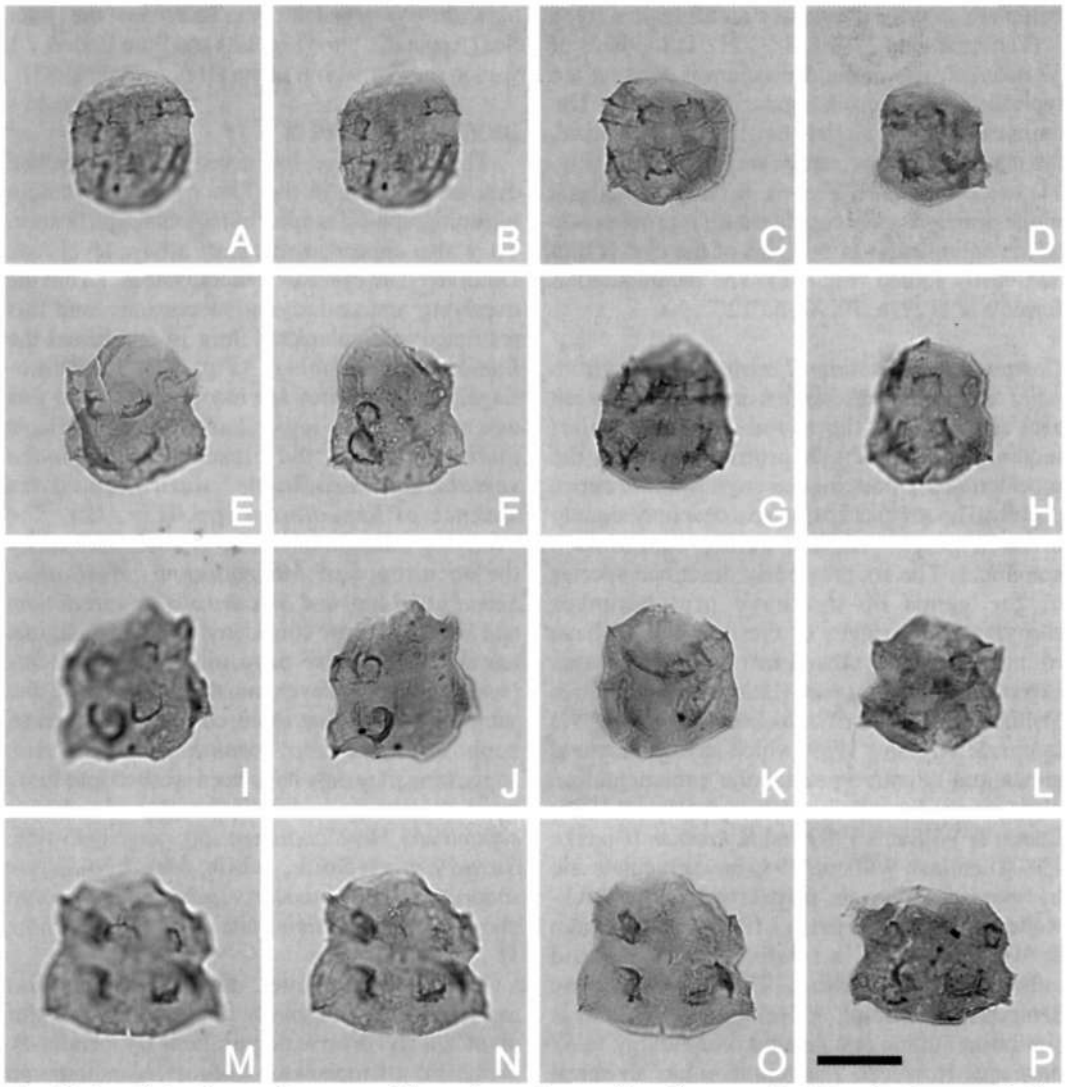

Fig. 11. Susadinium? australis sp. nov. All specimens from a sidewall core at 2366.00m in Skua-4 well. The photomicrographs were all taken using plain transmitted light. The scale bar in Fig. 11P refers to all the photomicrographs and represents 25µm. Figs 11M-O are the holotype; the remainder are paratypes. Note apparently apical intercalary archaeopyle and prominent intratabular protuberances in precingular and postcingular paraplate series. A, B - CPC 35189, paratype; dorsal view, median and low focus respectively. Unusually, this lacks an equatorial constriction and low intratabular protuberances. C - CPC 35190, paratype; ventral view, low focus. Subcircular form with low protuberances. D - CPC 35191, relatively elongate paratype; ventral view, median focus. E - CPC 35192, paratype; ventral view, low focus. Note prominent equatorial constriction. F - CPC 35193, paratype; ventral view, low focus. Elongate individual; note the antapical asymmetry. G - CPC 35317, paratype; dorsal view, median focus. This lacks clear antapical asymmetry. H - CPC 35318, paratype; ventral view, median focus. I, J - CPC 35319, paratype; dorsal view, high and low focus respectively. K - CPC 35320, paratype; ventral view, low focus. L - CPC 35321, paratype; ventral view, median focus. M, N, O - CPC 35322, holotype; dorsal view, high, median and low focus respectively. Well-preserved, with prominent protuberances and a strong paracingular concavity. Note the mid antapical crack in the autophragm. P - CPC 35323, relatively broad paratype; ventral view, median focus.

(continued from opposite) ?oblique dorsal view, median focus. D - CPC 35184, typical regularly biconical paratype; left lateral view, high focus. E - CPC 35185, paratype; left lateral view, median focus. F - CPC 35186, paratype; ?ventral view, median focus. G, H - CPC 35187, holotype; left lateral view, median and low focus respectively. Large, relatively broad, with a slightly recurved antapical horn. I - CPC 35188, paratype, dorsal view, low focus. Regularly biconical, with a sharply pointed apical horn.

paraplate anterior intercalary archaeopyles (type I) (Fensome *et al.*, 1993, fig. 123). Individuals of *S? australis* where the operculum is missing are typically rounded quadrangular (Figs 11A-C). The outline is normally slightly longitudinally elongate, but may be equant or, rarely, wider than long (Fig. 11; see *Dimensions*, above). A detailed analysis of the principal archaeopyle suture is problematic as the autophragm in this part of the cyst is thin and easily folded (Fig. 11). The paratabulation formula is ?5', ?3a, 7", Xc, 5"', 2"", Xs.

Comparison. Susadinium? australis differs from other species of *Susadinium* in its combination archaeopyle and the rounded quadrangular/ rectangular intratabular protruberances in the precingular and postcingular areas which are open distally. The antapical paraplates bear only slightly inflated protuberances, unlike *Susadinium scrofoides*. The six previously described species of the genus do not have protuberances surmounted by ridges or crests. They all have rounded, distally closed intratabular features except *Susadinium? pinna* (Below 1987) Lentin & Williams 1989 and *S? tabulatum* (Below 1987) Lentin & Williams 1989, which have parasutural crests and negative penitabular ornamentation respectively. *Susadinium delmense* (Below 1987) Lentin & Williams 1989 and *S. faustum* (Bjaerke 1980) Lentin & Williams 1985 have granulate and baculate autophragm respectively. The thick-walled *Susadinium knertense* (Below 1987) Lentin & Williams 1989 is relatively elongate and subangular in outline. The Late Jurassic *Tringadinium* Riding & Helby (this volume) is similar in outline and general morphology to *S? australis*. However, *Tringadinium* has an apical archaeopyle with a simple operculum and a different paratabulation pattern, with four apical, six precingular and six postcingular paraplates. *Horologinella* Cookson & Eisenack 1962 is similar to *S? australis* in shape and apparent archaeopyle style. However, *Horologinella* is much more deeply incised equatorially, its principal archaeopyle suture is circular, not angular (Backhouse, 1988, pl. 48, figs 2, 4) and it lacks intratabular protrusions.

Derivation of name. The specific name refers to the Southern Hemisphere location.

Holotype and type locality. Figs 11M-O, CPC 35322, Skua-4 well, sidewall core at 2366.00m.

Stratigraphical distribution. Susadinium? australis is recorded from the Toarcian of the Timor Sea (Appendix 1 and Fig. 12.) and from Enderby-1 well in the Carnarvon Basin (Helby *et al.*, 1987).

BIOSTRATIGRAPHY

These distinctive, low diversity, dinoflagellate cyst associations in the Timor Sea constitute a biostratigraphical marker of regional significance. They also appear to represent a base level rise. Dinoflagellate cysts are generally absent from the overlying and underlying successions, and this restricted microplankton flora is designated the *Luehndea* Assemblage (Fig. 12). Two dinoflagellate cyst suites are recognised within this assemblage. The lower *Susadinium*? Suite is distinguished by the presence of *Luehndea septata* and *Susadinium? australis* and the absence of *Skuadinium* spp. (Fig. 12). The overlying *Skuadinium* Suite is characterized by the occurrence of *Moorodinium tessellatum, Skuadinium* spp. and *S? australis*. *Moorodinium* and *Skuadinium* are considered to reflect marginal marine to lacustrine depositional environments (see below). However, most *Skuadinium* Suite samples also exhibit more cosmopolitan genera such as *Luehndea*, *Mendicodinium* etc., suggesting they may have been washed into more open marine palaeoenvironments. *Luehndea septata* and *Mendicodinium* spp. range below the *Susadinium?* Suite, while *Mendicodinium scabratum* and *Nannoceratopsis* spp. are present above the *Skuadinium* Suite (Fig. 12; Appendix 1).

These distinctive dinoflagellate cyst assemblages are normally minor components of abundant and diverse palynofloras (Appendix 1). Within the microplankton category, acanthomorph acritarchs are usually more prominent (up to 19% of total palynomorphs), with rare prasinophytes and relatively consistent occurrences of the freshwater alga *Botryococcus*. The *Luehndea* Assemblage is associated with the *Kekryphalospora distincta* (spore-pollen) Oppel Zone (Helby & Partridge, in prep). *Kekryphalospora distincta* Fenton & Riding 1987 is a locally stratigraphically diagnostic taxon and occurs most consistently in the *Susadinium?* Suite. The spore-pollen associations are dominated by *Corollina* spp., which increases in prominence down sequence (21.5%-86% of total palynomorphs). *Dictyophyllidites* spp. are also prominent and generally decrease in prominence down section; 66%-7%. However, there are several anomalous high counts of *Dictyophyllidites* spp, approximately corresponding with the top of the

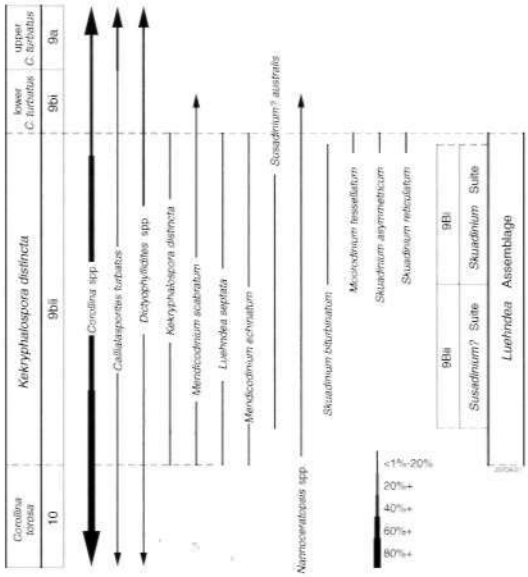

Fig. 12. Synthesis of ranges of selected palynomorph taxa in the *Luehndea* Assemblage and the *Susadinium?* and *Skuadinium* suites in the Timor Sea.

Susadinium? Suite. *Aratrisporites* spp. and *Callialasporites turbatus* (Balme 1957) Schulz 1967 occur as consistent background taxa, the former locally attaining 37% (Appendix 1).

CORRELATION AND AGE

Helby *et al.* (1987) invoked a correlation of the interval, which includes the *Luehndea* Assemblage, with the Toarcian of Europe on the basis of the occurrence of *Susadinium*? *australis* (as *Susadinium* sp. A), citing Bjaerke (1980). The latter is an important, largely taxonomic work which describes a closely related association of dinoflagellate cysts from the Toarcian of Spitsbergen. The range of *Susadinium* was subsequently determined to be early Toarcian to earliest Aalenian (Riding & Thomas, 1992; Riding, 1984a,b; Riding *et al.*, 1999). The questionable generic affinity of *Susadinium*? *australis* only marginally diminishes its correlative value as the similarity to the type, *Susadinium scrofoides*, is strong. The occurrence of *Luehndea septata*, together with *Susadinium*? *australis*, is also strongly indicative of the Toarcian Stage. In northwest Europe, the genotype, *Luehndea spinosa*, ranges from the late Pliensbachian to the earliest Toarcian (Morgenroth, 1970; Riding, 1987; Riding & Thomas, 1992). Furthermore, *Luehndea cirilliae* and *L. microreticulata* are also typical of the late Pliensbachian to early Toarcian in southern Europe (Bucefalo Palliani *et al.*, 1997a). Bucefalo Palliani *et al.* (1997b) reviewed the occurrence of *Mendicodinium* and Bucefalo Palliani & Mattioli (1998, fig.5) indicated that *Mendicodinium* is an important element in early Toarcian assemblages from the Tethyan Realm. Therefore, by comparison with northern and southern Europe, the overlapping ranges of the genera *Luehndea* (key range top) and *Susadinium*? (key range base), the *Luehndea* Assemblage is of early Toarcian age. It seems likely that the eustatic rise represented by this marine association reflects the early Toarcian global eustatic increase (Haq *et al.*, 1987). The records of *Susadinium* sp. A by Helby *et al.* (1987) from Enderby-1 well and by Burger (1996) from offshore Western Australia represent the only other published records of Toarcian to Aalenian dinoflagellate cysts from Australia.

The *Luehndea* Assemblage has been recorded from Coojong-1 well in the Carnarvon Basin at 1663.40m and 1652.50m. Howe (2000) interpreted the calcareous nannofossil assemblages from these samples as NJ5b/NJ6 and NJ6 respectively. He assigned an early Toarcian age on the basis of correlation with the Boreal nannofossil zonation of Bown *et al.* (1988).

Helby *et al.* (1987, p. 17, fig. 12) indicated that the boundary of the associated *Corollina torosa* and *Callialasporites turbatus* spore-pollen Oppel Zones (interval now represented by the *Kekryphalospora distincta* spore-pollen Oppel Zone) occurs within the Toarcian *Reinholdella* cf. *crebra* foraminiferal zone of Apthorpe & Heath (1981). The *Kekryphalospora distincta* Zone is distinguished by the occurrence of the index species and by a marked down-sequence increase in the proportion of *Corollina* spp. (Helby & Partridge, in prep.). In Europe, the range of *Kekryphalospora distincta* is late Pliensbachian to early Bajocian (Fenton & Riding, 1987). However, late Pliensbachian records of this spore are sparse, and its co-occurrences with *Luehndea* and *Susadinium*? support a correlation with the early Toarcian.

COMPARISONS WITH NORTHERN HEMISPHERE TOARCIAN PALYNOFLORAS

The *Luehndea* Assemblage differs fundamentally in species spectra from both the northwest European and North American provinces of Riding (1984b). The genera *Luehndea, Nannoceratopsis* and unequivocal *Susadinium* are all known from the Toarcian worldwide (Johnson & Hills, 1973; Morbey, 1978; Davies, 1983; 1985; Riding, 1984a, b; 1987; De

Vains, 1988; Feist-Burkhardt & Wille, 1992; Fauconnier, 1995; Riding *et al.*, 1999). The lower Toarcian strata of northwest Europe and Siberia are dominated by *Nannoceratopsis*; in upper Toarcian successions, the latter genus and *Parvocysta* and its relatives (including *Susadinium*) are predominant (Bjaerke, 1980; Riding, 1984b; Riding *et al.*, 1991; Riding & Thomas, 1992; Ilyina *et al.*, 1994). The lower Toarcian of southern Europe, by contrast, is dominated by *Mendicodinium* (Bucefalo Palliani & Riding, 1999). The *Parvocysta* complex of Riding (1984b) in the Northern Hemisphere becomes more diverse with increasing latitude (Thusu, 1978; Riding, 1984b; Riding *et al.*, 1991; 1999). It thus is possible that this association has a bipolar distribution. It is clear that *Susadinium* appears to be the most widely distributed member of this closely related plexus of genera. The Toarcian of Arctic Canada is relatively diverse (Dörhöfer & Davies, 1980; Davies, 1983, fig. 4). However, the only genera in common with the Australian assemblages are *Nannoceratopsis* and *Susadinium* in Zone B of Davies (1983).

PALAEOECOLOGY

The reason the Timor Sea assemblages are so unlike any other reported Toarcian dinoflagellate cyst associations may be due to the marginal marine depositional setting of the Lower Plover Formation. MacDaniel (1988a), Mory (1988) and Osborne (1990) reported that the Plover Formation is a heterolithic unit representing a fluvial regime. The formation passes upsection into deltaic and shallow marine depositional conditions, possibly with interbedded lacustrine sediments. This is supported by the consistently overwhelming dominance of spores and pollen, the presence of *Botryococcus* and the relatively rare and sporadic occurrence of dinoflagellate cysts (Appendix 1). The species *Skuadinium biturbinatum* and *Moorodinium tessellatum*, in particular, are relatively thin-walled. Both these taxa also have archaeopyles which are difficult to observe and to relate to paraplate equivalence. These are characteristic of species from freshwater, brackish or marginal marine regimes (e.g. Batten, 1985; Hunt *et al.*, 1985; Batten & Lister, 1988a,b). Furthermore, *Moorodinium* is a freshwater/brackish genus, originally described from near the Jurassic-Cretaceous boundary in the Perth Basin, Western Australia (Backhouse, 1988).

ACKNOWLEDGEMENTS

The authors are grateful to Dr Clinton B. Foster (AGSO) for promoting and facilitating this work and for his editorial guidance and advice. Christian Thun and Andrew Kelman (AGSO) provided much technical support with sample preparations and manipulation of digital images. BHP Petroleum Pty Ltd, Gulf Australia Resources Ltd and Newfield Exploration Australia Ltd kindly provided sample material on request. Laola Pty Ltd (Perth) gave support in the careful preparation of key samples. Ms Lindell Emerton (AGSO) drafted Figures 1, 2 and 12. Drs R. Bucefalo Palliani and J. E. Thomas are thanked for reviewing the manuscript. J. B. Riding publishes with the permission of the Chief Executive Officer, AGSO.

REFERENCES

APTHORPE, M.C. & HEATH, R.S., 1981. Late Triassic and Early to Middle Jurassic foraminifera from the North West Shelf, Australia. *Fifth Australian Geological Convention, Abstracts 3*, 66.

BACKHOUSE, J., 1988. Late Jurassic and Early Cretaceous palynology of the Perth Basin, Western Australia. *Geological Survey of Western Australia Bulletin 135*, 233 p.

BATTEN, D.J., 1985. Two new dinoflagellate cyst genera from the non-marine Lower Cretaceous of Southeast England. *Neues Jahrbuch für Geologie und Paläontologie Monatshefte, 1985(7)*, 427-437.

BATTEN, D.J. & LISTER, J.K., 1988a. Evidence of freshwater dinoflagellates and other algae in the English Wealden (Early Cretaceous). *Cretaceous Research 9*, 171-179.

BATTEN, D.J. & LISTER, J.K., 1988b. Early Cretaceous dinoflagellate cysts and chlorococcalean algae from freshwater and low salinity palynofacies in the English Wealden. *Cretaceous Research 9*, 337-367.

BELOW, R., 1987. Evolution und Systematik von Dinoflagellaten-Zysten aus der Ordnung Peridiniales. I. Allgemeine Grundlagen und Subfamilie Rhaetogonyaulacoideae (Familie Peridiniaceae). *Palaeontographica B 205*, 1-164.

BELOW, R., 1990. Evolution und Systematik von Dinoflagellaten-Zysten aus der Ordnung Peridiniales. III. Familie Pareodiniaceae. *Palaeontographica B 220*, 1-96.

BJAERKE, T., 1980. Mesozoic palynology of Svalbard IV. Toarcian dinoflagellates from Spitsbergen. *Palynology 4*, 57-77.

BOWN, P.R., COOPER, M.K.E., & LORD, A.R., 1988. A calcareous nannofossil biozonation scheme for the early to mid Mesozoic. *Newsletters on Stratigraphy 20*, 91-114.

BUCEFALO PALLIANI, R. & MATTIOLI, E., 1998. High resolution integrated microbiostratigraphy of

the Lower Jurassic (late Pliensbachian-early Toarcian) of central Italy. *Journal of Micropalaeontology 17,* 153-172.

BUCEFALO PALLIANI, R. & RIDING, J.B., 1997. *Umbriadinium mediterraneense* gen. et sp. nov. and *Valvaeodinium hirsutum* sp. nov.: two dinoflagellate cysts from the Lower Jurassic of the Tethyan Realm. *Palynology 21,* 197-206.

BUCEFALO PALLIANI, R. & RIDING, J.B., 1998. The influence of palaeoenvironmental change on dinoflagellate cyst distribution. An example from the Lower and Middle Jurassic of Quercy, southwest France. *Bulletin de Centres de Recherches Exploration-Production Elf-Aquitaine 21,* 107-123.

BUCEFALO PALLIANI, R. & RIDING, J. B., 1999. Early Jurassic (Pliensbachian-Toarcian) dinoflagellate migrations and cyst palaeoecology in the Boreal and Tethyan realms. *Micropaleontology 45,* 201-214.

BUCEFALO PALLIANI, R., RIDING, J.B. & TORRICELLI, S., 1997a. The dinoflagellate cyst *Luehndea* Morgenroth, 1970 emend. from the upper Pliensbachian (Lower Jurassic) of Hungary. *Review of Palaeobotany and Palynology 96,* 99-111.

BUCEFALO PALLIANI, R., RIDING, J.B. & TORRICELLI, S., 1997b. The dinoflagellate cyst *Mendicodinium* Morgenroth, 1970, emend. from the lower Toarcian (Jurassic) of central Italy. *Review of Palaeobotany and Palynology 96,* 99-111.

BURGER, D., 1996. Mesozoic palynomorphs from the North West Shelf, offshore Western Australia. *Palynology 20,* 49-103.

DAVIES E.H., 1983. The dinoflagellate Oppel-zonation of the Jurassic-Lower Cretaceous sequence in the Sverdrup Basin, Arctic Canada. *Geological Survey of Canada Bulletin No. 359,* 59 p.

DAVIES, E.H., 1985. The miospore and dinoflagellate cyst Oppel-zonation of the Lias of Portugal. *Palynology 9,* 105-132.

DEFLANDRE, G., 1939. Microplancton des mers Jurassiques conservé dans les marnes de Villers-sur-Mer (Calvados). Étude liminaire et considérations générales. *Travaux de la Station zoologique de Wimereux 13,* 147-200.

DE VAINS, G., 1988. Étude palynologique préliminaire de l'Hettangien à l'Aalénien du Quercy (France). *Bulletin des Centres de Recherches Exploration-Production Elf-Aquitaine 12,* 451-469.

DÖRHÖFER, G. & DAVIES, E.H., 1980. Evolution of archeopyle and tabulation in rhaetogonyaulacinean dinoflagellate cysts. *Miscellaneous Publication, Life Sciences Division, Royal Ontario Museum,* 91p.

EVITT, W.R., 1961. The dinoflagellate *Nannoceratopsis* Deflandre; morphology, affinities and intraspecific variability. *Micropaleontology 7,* 305-316.

EVITT, W.R., 1985. *Sporopollenin dinoflagellate cysts. Their morphology and interpretation.* American Association of Stratigraphic Palynologists Foundation, Dallas, 333 p.

FAUCONNIER, D., 1995. Jurassic palynology from a borehole in the Champagne area, France - correlation of the lower Callovian-middle Oxfordian using sequence stratigraphy. *Review of Palaeobotany and Palynology 87,* 15-26.

FENTON, J.P.G. & RIDING, J.B., 1987. *Kekryphalospora distincta* gen. et sp. nov., a trilete spore from the Middle Jurassic of north-west Europe. *Pollen et Spores 29,* 427-434.

FENSOME, R.A., TAYLOR, F.J.R., NORRIS, G., SARJEANT, W.A.S., WHARTON, D.I. & WILLIAMS, G.L., 1993. A classification of living and fossil dinoflagellates. *Micropaleontology Special Publication No. 7,* 351 p.

FEIST-BURKHARDT, S. & WILLE, W., 1992. Jurassic palynology in southwest Germany - state of the art. *Cahiers de Micropaléontologie, Nouvelle Serie 7,* 141-156.

FOSTER, C.B., this volume. Introduction.

HAQ, B.U., HARDENBOL. J. & VAIL, P.R., 1987. Chronology of fluctuating sea levels since the Triassic. *Science 235,* 1156-1169.

HELBY, R., MORGAN, R. & PARTRIDGE, A.D., 1987. A palynological zonation of the Australian Mesozoic. *Memoir of the Association of Australasian Palaeontologists 4,* 1-94.

HELBY, R. & PARTRIDGE, A.D., in prep. A palynological zonation of the Australian Mesozoic: an update.

HOWE, R.W., 2000. Jurassic calcareous nannofossil biostratigraphy of the North West Shelf and Timor Sea areas. *Minerals and Energy Institute of Western Australia (MERIWA) Project M319 report,* 154 p. (University of Western Australia, unpublished).

HUNT, C.O., ANDREWS, M.V. & GILBERTSON, D.D., 1985. Late Quaternary freshwater dinoflagellate cysts from the British Isles. *Journal of Micropalaeontology 4(2),* 101-109.

ILYINA, V.I., KULKOVA, I.A. & LEBEDEVA, N.K., 1994. Microphytofossils and detailed stratigraphy of marine Mesozoic and Cenozoic of Siberia. *United Institute of Geology, Geophysics and Mineralogy Transactions, Issue 818,* 192 p. (in Russian).

JOHNSON, C.D. & HILLS, L.V., 1973. Microplankton zones of the Savik Formation (Jurassic), Axel Heiberg and Ellesmere Islands, District of Franklin. *Bulletin of Canadian Petroleum Geology 21,* 178-218.

MACDANIEL, R.P., 1988a. The geological evolution and hydrocarbon potential of the western Timor Sea region. *Petroleum in Australia: The First*

Century. Australian Petroleum Exploration Association Publication, 270-284.

MACDANIEL, R.P., 1988b. Jabiru Oilfield. 439-440 in Purcell, P.G. & R.R., (eds). *The North West Shelf, Australia.* Petroleum Exploration Society Australia, Perth.

MORBEY, S.J., 1975. The palynostratigraphy of the Rhaetian Stage, Upper Triassic in the Kendelbach-graben, Austria. *Palaeontographica B 152,* 1-75.

MORBEY, S.J., 1978. Late Triassic and early Jurassic subsurface palynostratigraphy in northwestern Europe. *Palinologia número extraordinario 1.* 355-365.

MORY, A.J., 1988. Regional geology of the offshore Bonaparte Basin. 287-309 in Purcell, P.G. & R.R., (eds.), *The North West Shelf, Australia.* Petroleum Exploration Society Australia, Perth.

MORGENROTH, P., 1970. Dinoflagellate cysts from the Lias Delta of Lühnde/Germany. *Neues Jahrbuch für Geologie und Paläontologie Abhandlungen 136,* 345-359.

OSBORNE, M. O., 1990. The exploration and appraisal history of Skua Field, AC/P2 – Timor Sea. *APEA Journal 30,* 197-211.

PIEL, K.M. & EVITT, W.R., 1980. Paratabulation in the Jurassic dinoflagellate genus *Nannoceratopsis* and a comparison with modern taxa. *Palynology 4,* 79-104.

POULSEN, N.E., 1992. Jurassic dinoflagellate cyst biostratigraphy of the Danish Subbasin in relation to sequences in England and Poland: a preliminary review. *Review of Palaeobotany and Palynology 75,* 33-52.

PRAUSS, M., 1989. Dinozysten-stratigraphie und palynofazies im Oberen Lias und Dogger von NW-Deutschland. *Palaeontographica Abteilung B 214,* 1-124.

RIDING, J.B., 1984a. Dinoflagellate cyst range-top biostratigraphy of the uppermost Triassic to lowermost Cretaceous of northwest Europe. *Palynology 8,* 195-210.

RIDING, J.B., 1984b. A palynological investigation of Toarcian to early Aalenian strata from the Blea Wyke area, Ravenscar, North Yorkshire. *Proceedings of the Yorkshire Geological Society 45,* 109-122.

RIDING, J.B., 1987. Dinoflagellate cyst stratigraphy of the Nettleton Bottom Borehole (Jurassic: Hettangian to Kimmeridgian), Lincolnshire, England. *Proceedings of the Yorkshire Geological Society 46,* 231-266.

RIDING, J.B., FEDOROVA, V.A., & ILYINA, V.I., 1999. Jurassic and lowermost Cretaceous dinoflagellate cyst biostratigraphy of the Russian Platform and northern Siberia, Russia. *American Association of Stratigraphic Palynologists Contributions Series No. 36,* 179 p.

RIDING, J.B. & THOMAS, J.E., 1992. Dinoflagellate cysts of the Jurassic System. 7-97 in Powell, A.J. (ed.) *A stratigraphic index of dinoflagellate cysts,* Chapman and Hall, London.

RIDING, J.B., WALTON, W. & SHAW, D., 1991. Toarcian to Bathonian (Jurassic) palynology of the Inner Hebrides, northwest Scotland. *Palynology 15,* 115-179.

SARJEANT, W.A.S., 1982. Dinoflagellate cyst terminology: a discussion and proposals. *Canadian Journal of Botany 60,* 922-945.

STOVER, L.E. & EVITT, W.R., 1978. *Analyses of Pre-Pleistocene organic-walled dinoflagellates.* Stanford University Publications, Geological Sciences 15, 300p.

STOVER, L.E. & HELBY, R., 1987. Some Australian Mesozoic microplankton index species. *Memoir of the Association of Australasian Palaeontologists 4.* 101-134.

STOVER, L.E. & WILLIAMS, G.L., 1987. Analyses of Mesozoic and Cenozoic organic-walled dinoflagellates 1977-1985. *American Association of Stratigraphic Palynologists Contributions Series No. 18,* 243 p.

THUSU, B., 1978. Aptian to Toarcian dinoflagellate cysts from Arctic Norway. *Continental Shelf Institute (Trondheim, Norway), Publication 100,* 61-95.

WILLIAMS, G.L., LENTIN, J.K. & FENSOME, R.A., 1998. The Lentin and Williams Index of fossil dinoflagellates 1998 edition. *American Association of Stratigraphic Palynologists Contributions Series No. 34,* 817 p.

WOOLLAM, R. & RIDING, J.B., 1983. Dinoflagellate cyst zonation of the English Jurassic. *Institute of Geological Sciences Report No. 83/2,* 42 p.

APPENDIX 1: THE DISTRIBUTION OF *LUEHNDEA* ASSEMBLAGE TAXA AND OTHER PALYNOMORPHS IN SELECTED TIMOR SEA WELLS

Well	D (m)	Ms	Ls	Me	Su	Ns	Nu	Sb	Mt	Sa	Sr	Ot	Ph	Kd	Ac	Din	Ara	Ct	Cor	Dict
ARQUEBUS-1	2715.5	...	...	...	?	...	...	...	...	...	...	...	...	...	NC	NC	NC	NC	NC	NC
ARQUEBUS-1	2734.5	...	X	...	...	...	...	...	...	...	...	X	...	...	NC	NC	NC	NC	NC	NC
BARCOO-1	4249.5	...	...	...	X	...	X	...	...	...	...	X	...	...	NC	NC	NC	NC	NC	NC
BARCOO-1	4261	X	...	...	?	...	...	...	...	...	...	X	...	...	NC	NC	NC	NC	NC	NC
BARITA-1	2103	...	...	...	X	...	...	...	...	...	...	...	...	...	<1	X	...	<1	21.5	53
BARITA-1	2137	...	...	...	...	...	...	...	...	...	...	?	...	...	<1	X	...	3.5	73	8
BARITA-1	2166	...	...	...	...	...	...	...	...	...	...	?	...	X	<1	X	X	4	68	12
BARITA-1	2260.5	...	...	...	...	...	...	...	...	...	...	?	...	X	5+	X	2	<1	73	6.5
CYGNET-1	1925.3	...	...	...	X	...	...	...	...	...	...	...	...	...	X	0.5	...	2.5	78	11.5
CYGNET-1	1928.5	...	...	...	X	...	...	...	...	...	...	X	?	X	2+	4	X	3	75	10.5
CYGNET-1	1955	...	...	...	X	...	...	...	...	...	...	X	...	...	1.5+	X	...	2	68	10
ECLIPSE-1	2945	...	...	...	X	...	...	...	...	...	...	X	...	...	NC	NC	...	NC	NC	NC
JABIRU-1A	1610	...	...	...	X	...	...	...	...	...	...	...	...	X	3	X	...	7	31	37
JABIRU-1A	1619.5	...	...	...	X	...	...	...	...	...	...	...	...	X	3.5	X	...	1	72	11
JABIRU-2	1685.1	...	...	...	...	...	...	...	...	...	...	X	...	X	NC	NC	NC	NC	NC	NC
JABIRU-2	1690.5	...	...	...	...	...	...	...	...	...	...	X	...	X	NC	NC	NC	NC	NC	NC
JABIRU-2	1693.6	...	X	...	...	...	...	...	...	...	...	...	...	...	6	X	X	1	67	14
JABIRU-3	1691	X	...	...	...	...	?	...	...	...	...	X	X	X	1	X	1	4	37	31.5
JABIRU-3	1697.5	X	...	...	...	...	...	...	...	...	...	...	...	X	<1	X	0.5	2.5	59	13
JABIRU-3	1698.5	X	...	...	...	...	...	...	...	...	...	...	...	X	1	X	1.5	2	54	20
JABIRU-3	1708.3	...	...	...	...	...	...	...	...	...	...	...	...	...	18.5	X	4.5	0.5	49	15
JABIRU-4	1739	X	...	...	...	...	...	...	...	...	...	...	...	X	4.5	0.5	6	0.5	50	18
JABIRU-4	1746	...	...	...	...	...	...	?	...	...	...	X	...	...	0.5	X	...	0.5	69	9
JABIRU-6	1657.3	...	...	...	...	...	...	...	...	...	...	X	...	X	0.5	X	0.5	3	76	5
JABIRU-6	1662	X	...	...	...	...	X	...	...	...	...	X	X	X	1	0.5	0.5	2	65	15
JABIRU-6	1672.5	...	...	...	...	...	...	...	...	...	...	?	...	X	1.5	X	0.5	1	73.5	8
JABIRU-7	1756.2	?	...	...	...	...	...	...	...	...	...	...	...	...	<1	X	1.5	<1	65	28
JABIRU-8A ST1	1824	X	...	...	...	...	...	...	...	...	...	...	...	...	2	X	0.5	1	59	17
JABIRU-8A ST1	1851	...	...	...	...	...	...	X	...	...	...	...	...	...	1	X	2	1	61	15
JABIRU-9ST3	1780	?	...	...	X	...	...	...	...	...	...	...	...	...	NC	NC	NC	NC	NC	NC
JABIRU-10	1790	X	X	X	...	X	X	X	...	...	X	...	...	X	9.5	X	4.5	<1	49	16

Above and overleaf: Occurrence of *Luehndea* Assemblage taxa and other palynomorphs in selected Timor Sea wells. Abbreviations are: D (m), depth (metres); Ms, *Mendicodinium scabratum*; Ls, *Luehndea septata*; Me, *Mendicodinium echinatum*; Su, *Susadinium? australis*; Ns, *Nannoceratopsis spinosus*; Nu, undifferentiated species of *Nannoceratopsis*; Sb, *Skuadinium biturbinatum*; Mt, *Moorodinium tessellatum*; Sa, *Skuadinium asymmetricum*; Sr, *Skuadinium reticulatum*; Ot, unidentified dinoflagellate cysts; Ph, *Pareodinia halosa* (Filatoff 1975) Prauss 1989; Kd, *Kekryphalospora distincta* (pteridophyte spore); Ac, Total acritarchs (largely *Micrhystridium* and *Veryhachium*); Din, Total dinoflagellate cysts; Ara, *Aratrisporites* spp.; Ct, *Callialasporites turbatus*; Cor, *Corollina* spp.; Dict, *Dictyophyllidites* spp.; X, present; ?, questionable identification; ..., absent; NC, not counted. The numbers refer to percentages of the respective group/taxon

Well	D (m)	Ms	Ls	Me	Su	Ns	Nu	Sb	Mt	Sa	Sr	Ot	Ph	Kd	Ac	Din	Ara	Ct	Cor	Dict
JABIRU-12	1732.5	X	...	...	...	?	...	...	...	...	...	...	...	X	0.5	4	X	7	37	24
JABIRU-12	1740	X	...	...	X	...	...	X	...	...	...	...	...	X	X	X	1.5	1.5	45	16
LORIKEET-1	1779	...	...	...	...	...	...	...	...	...	...	X	X	X	X	X	2	0.5	32	54
LORIKEET-1	1811	X	...	...	X	...	...	X	...	...	...	...	X	X	X	X	41	0.5	37	X
LORIKEET-1	1848	...	...	...	X	...	X	X	...	...	...	...	...	X	3.5	X	1	2	61.5	14
OLIVER-1	3057	X	...	...	...	...	...	...	...	...	...	...	...	...	X	X	...	15	31	30
OLIVER-1	3094	X	...	...	...	...	...	...	...	...	...	...	...	X	0.5	X	1	3	49	15
OLIVER-1	3106	X	...	...	...	...	...	...	...	...	...	X	...	X	1	X	X	1	66	12
OLIVER-1	3123	...	...	...	?	...	...	...	...	...	...	...	...	...	X	X	X	0.5	78	9
OLIVER-1	3127	...	...	...	...	...	...	...	...	...	...	X	...	X	7.5	X	X	X	64	9
OLIVER-1	3134	...	X	...	?	...	...	...	...	...	...	...	...	...	X	X	0.5	...	74	10
SKUA-1	2786	...	?	...	...	...	...	...	...	...	...	...	...	...	NC	NC	NC	NC	NC	NC
SKUA-2	2342	...	...	...	X	...	...	...	...	...	...	X	?	...	NC	NC	NC	NC	NC	NC
SKUA-2	2349	...	...	...	X	...	...	X	...	...	...	X	...	X	NC	NC	NC	NC	NC	NC
SKUA-3	2394	...	...	...	X	...	...	...	...	...	...	X	...	X	9.5	1	X	1	69	11
SKUA-3	2395	...	...	...	X	...	...	...	...	...	...	X	...	...	5.5	0.5	X	1	65	8
SKUA-3	2395.9	...	...	...	X	...	...	...	...	...	...	X	...	X	5	X	X	0.5	76	9
SKUA-3	2397.1	...	...	...	X	...	...	...	...	...	...	X	...	X	12	0.5	...	0.5	69	13
SKUA-3	2401.9	...	...	...	X	...	...	...	...	...	...	X	...	X	3	X	X	...	75	11.5
SKUA-3	2402.5	...	...	...	X	...	?	...	...	...	...	X	...	X	8.5	1	1	...	66	17
SKUA-4	2302	...	...	...	X	...	...	...	...	...	...	...	...	...	...	X	...	...	...	...
SKUA-4	2304	...	...	...	?	...	...	...	...	...	...	...	...	X	X	X	...	2	80	11
SKUA-4	2321	...	...	...	...	...	...	...	...	...	...	X	...	...	1.5	X	...	0.5	78	11.5
SKUA-4	2322	X	...	...	X	...	...	...	...	...	...	X	...	...	1.5	1	...	1	68	23
SKUA-4	2323	...	...	...	...	...	...	...	...	...	...	X	...	...	X	0.5	X	X	71	23
SKUA-4	2324	...	...	...	X	...	...	...	...	...	...	...	...	...	1	X	...	1	74	10
SKUA-4	2366	...	...	...	X	...	...	...	...	...	...	...	...	X	4	2	0.5	X	76	14
SKUA-4	2375	...	...	...	...	...	...	...	...	...	...	X	...	X	X	X	3	X	84	9
SKUA-5	2612	X	...	X	...	...	...	...	...	...	...	X	...	X	6	2	6	7.5	43.5	22
SKUA-5	2624	...	...	...	...	...	...	...	...	...	...	X	...	...	...	X	X	1	28	66
SKUA-5	2633	...	...	...	...	...	...	...	...	...	...	...	...	...	7	X	3	2.5	64	9
SKUA-5	2646	X	...	X	...	...	...	X	...	...	...	X	...	X	4.5	X	X	1	47	38
SKUA-5	2654	X	...	X	...	...	...	X	...	...	...	...	...	X	3	X	X	12	46.5	26
SKUA-5	2659	...	X	...	...	...	...	...	...	...	?	X	...	X	X	X	X	X	36	22
SKUA-6	2385	X	X	X	...	...	...	X	X	X	X	X	X	X	7	3	1	0.5	48	18
SKUA-6	2391.5	X	X	X	...	...	...	X	...	X	X	...	...	X	0.5	32.5	...	X	40	8
SKUA-6	2412	...	...	X	...	...	...	...	...	...	...	...	...	...	11.5	...	1	X	45	15
SKUA-6	2440.5	...	...	X	...	...	...	...	...	...	...	...	...	...	2.5	X	1	X	47	17.5
SKUA-6	2460	?	...	...	X	...	...	...	...	...	...	...	...	...	1.5	0.5	...	...	37	45
SKUA-6	2470	...	...	...	X	...	...	X	...	...	...	X	...	...	8	X	0.5	X	49	14.5

Well	D (m)	Ms	Ls	Me	Su	Ns	Nu	Sb	Mt	Sa	Sr	Ot	Ph	Kd	Ac	Din	Ara	Ct	Cor	Dict
SKUA-6	2478	?	...	...	...	...	...	...	...	...	...	...	...	X	12.5	X	X	...	50	24
SKUA-6	2482	...	...	X	...	...	...	?	...	...	...	...	...	...	5	0.5	...	...	70	10
SKUA-6	2511	...	...	...	...	...	...	X	...	...	...	...	...	X	2.5	X	0.5	X	76	10
SKUA-6	2525	...	X	X	...	...	...	X	...	...	...	...	...	...	0.5	X	...	3	76	13
SKUA-6	2566	...	...	...	X	...	...	...	...	...	...	...	...	X	3	X	37	...	40	8.5
SKUA-7A	2344	?	X	...	...	...	...	...	...	...	...	...	...	...	12.5	X	X	X	67	20.5
SKUA-7A	2352	X	X	X	...	...	X	...	...	...	...	X	...	X	8.5	X	2	1	40	27.5
SKUA-7A	2379	X	X	X	...	...	...	X	...	...	...	X	X	...	1	X	X	10	45	19
SKUA-7A	2398	?	X	...	...	...	...	...	...	...	...	...	...	X	X	X	X	X	70	22
SKUA-7A	2428.5	...	X	?	...	...	?	...	...	...	...	X	X	X	3.5	X	7	1	64.5	15
SKUA-7A	2440	...	...	X	...	...	...	X	X	X	X	...	...	...	...	...	...	...	...	...
SKUA-7A	2458.5	...	...	...	X	...	...	?	...	...	...	X	X	X	6.5	X	X	X	74	14
SKUA-7A	2490	...	...	...	X	...	...	...	...	...	...	X	X	...	16	X	0.5	X	65	12
SKUA-7A	2501	X	...	...	X	...	...	...	...	...	...	X	X	...	4.5	X	4	X	60.5	26
SKUA-8	2315.8	...	...	...	X	...	...	...	...	...	...	...	...	X	6	X	0.5	2	75	10
SKUA-8	2316.1	...	...	X	X	...	...	...	...	...	...	...	...	X	9	1	0.5	1	69	10.5
SKUA-8	2325.4	...	...	...	X	...	...	...	...	...	...	X	...	...	9	X	9	X	69	11.5
SKUA-8	2330.5	...	X	...	?	...	...	...	...	...	...	X	X	...	2.5	X	1.5	1	83	10.5
SKUA-8	2333.2	X	...	?	X	...	...	...	...	...	...	X	X	X	6	X	0.5	X	74	13
SKUA-8	2343.4	...	...	...	X	...	?	...	...	...	...	X	...	X	19	X	9.5	X	54	14
SKUA-8	2344	X	...	...	X	...	...	...	...	...	...	X	...	...	...	...	...	...	...	...
SKUA-8	2344.6	...	...	...	...	...	...	...	...	...	...	X	...	X	1	X	37	X	43	15.5
SKUA-8	2349.1	...	...	...	X	...	...	...	...	...	...	...	...	X	X	X	4	...	73	15
SKUA-8	2349.4	...	...	...	...	...	...	...	...	...	...	?	...	X	X	X	7	...	82	10
SKUA-8	2386.5	...	...	X	...	...	...	...	...	...	...	X	X	X	1	X	3	...	86	4.5
SKUA-8	2440	X	X	X	...	...	...	X	...	...	...	X	X	X	1	0.5	0.5	X	64	28
SKUA-9	2355.8	X	X	X	...	...	...	X	...	...	...	...	...	...	X	3	...	...	34	62
SKUA-9	2362	X	X	X	...	...	...	X	...	...	...	X	...	...	X	2.5	X	8	39.5	18.5
SKUA-9	2365.4	...	X	X	...	...	X	X	...	...	...	X	X	...	X	X	...	3	70	16.5
SKUA-9	2385.1	X	...	X	?	...	X	X	...	...	...	...	...	X	2	0.5	1.5	1.5	63	14
SKUA-9	2386.3	X	X	...	X	...	...	X	...	...	...	X	...	X	2	0.5	X	1.5	64	17
SKUA-9	2395	...	...	...	X	?	...	...	...	...	...	X	...	X	3	2	X	1	66	18
SKUA-9	2399.8	...	X	...	X	...	...	...	...	...	...	X	...	X	X	1	...	0.5	75	14
SKUA-9	2400.1	...	X	X	X	...	...	...	...	...	...	X	X	X	X	X	...	0.5	72	12
SKUA-9	2406.1	...	...	...	X	...	...	...	...	...	...	X	...	...	4.5	X	...	1.5	67	17
SKUA-9	2413.6	...	...	...	X	...	...	...	...	...	...	...	...	...	X	0.5	...	X	37	40
SKUA-9	2425.6	...	...	...	X	...	X	?	...	...	...	X	...	X	1.5	X	6.5	X	68	19
SKUA-9ST	2315	...	...	X	...	...	...	...	...	...	...	...	...	...	X	X	X	...	69	16.5
SKUA-9ST	2333	...	...	?	...	...	...	...	...	...	...	?	...	X	2.5	X	1	2	65	13
SKUA-9ST	2340	...	...	...	X	...	...	...	...	...	...	X	...	X	3	X	...	X	64	21

Well	D (m)	Ms	Ls	Me	Su	Ns	Nu	Sb	Mt	Sa	Sr	Ot	Ph	Kd	Ac	Din	Ara	Ct	Cor	Dict
SKUA-9ST	2372	...	...	...	X	...	...	...	...	...	...	...	...	X	X	X	...	...	72	23.5
SKUA-9ST	2388	...	...	...	X	...	...	...	...	...	...	X	X	X	X	X	X	0.5	71	21
SKUA-9ST	2403	?	...	...	...	...	...	...	...	...	...	X	...	X	0.5	X	X	0.5	76	17
SKUA-9ST	2430	X	...	...	...	...	...	...	...	...	...	X	...	X	X	X	4	X	78	7
UNDAN-2	3382	?	...	...	...	...	...	...	...	...	...	X	...	X	0.5	?	...	9	39	15
UNDAN-2	3404	...	X	X	...	...	...	...	...	...	...	...	...	X	X	X	...	2	74	10

APPENDIX 2: LOCATIONS AND OPERATORS OF WELLS MENTIONED IN THE TEXT

Well Name and Number	Latitude	Longitude	Operator
ARQUEBUS-1	15° 18' 46.99"S	121° 29' 33.77"E	Amoco
BARCOO-1	15° 20' 32.00"S	120° 38' 16.70"E	Woodside
BARITA-1	11° 26' 30.92"S	125° 43' 45.93"E	Bond
COOJONG-1	20° 00' 65.26"S	116° 54' 93.92"E	Ampol
CYGNET-1	11° 53' 41.02"S	125° 56' 24.96"E	Bond
ECLIPSE-1	12° 16' 12.35"S	124° 37' 12.18"E	BHP
ENDERBY-1	20° 09' 25.50"S	116° 24' 24.30"E	BOC
JABIRU-1A	11° 55' 55.79"S	125° 00' 19.14"E	BHP
JABIRU-2	11° 56' 00.48"S	124° 59' 24.26"E	BHP
JABIRU-3	11° 55' 27.06"S	125° 00' 36.30"E	BHP
JABIRU-4	11° 55' 12.82"S	125° 01' 16.02"E	BHP
JABIRU-6	11° 55' 49.16"S	125° 00' 46.28"E	BHP
JABIRU-7	11° 55' 08.94"S	125° 01' 06.75"E	BHP
JABIRU-8A ST1	11° 56' 10.65"S	125° 00' 36.67"E	BHP
JABIRU-9 ST3	11° 57' 04.63"S	125° 58' 49.56"E	BHP
JABIRU-10	11° 55' 15.48"S	125° 01' 38.11"E	BHP
JABIRU-12	11° 54' 49.36"S	125° 00' 54.65"E	BHP
LORIKEET-1	11° 10' 20.77"S	125° 37' 08.89"E	BHP
OLIVER-1	11° 38' 36.27"S	125° 00' 36.14"E	BHP
SKUA-1	12° 30' 19.00"S	124° 25' 58.00"E	Arco
SKUA-2	12° 30' 29.22"S	124° 24' 20.10"E	BHP
SKUA-3	12° 30' 17.00"S	124° 24' 57.24"E	BHP
SKUA-4	12° 29' 30.35"S	124° 25' 37.99"E	BHP
SKUA-5	12° 28' 21.10"S	124° 26' 41.66"E	BHP
SKUA-6	12° 29' 10.84"S	124° 26' 23.30"E	BHP
SKUA-7A	12° 29' 19.55"S	124° 26' 04.40"E	BHP
SKUA-8	12° 30' 27.70"S	124° 24' 28.57"E	BHP
SKUA-9	12° 29' 47.93"S	124° 25' 16.34"E	BHP
SKUA-9ST	12° 29' 47.93"S	124° 25' 16.34"E	BHP
UNDAN-2	11° 04' 33.83"S	126° 34' 20.14"E	BHP

APPENDIX 3: REGISTER OF FIGURED SPECIMENS

All palynomorph specimens figured in this paper are listed here. The specimens are all curated in the Commonwealth Palaeontological Collection (CPC) of the Australian Geological Survey Organisation, Canberra. The dinoflagellate cyst genera and species are listed alphabetically and the location of the specimens on the microscope slides are all 'England-Finder' co-ordinates (EF). These were taken with the slide label to the left of the observer. The coding for types is as follows: H = holotype; P = paratype; T = topotype. All specimens of new taxa examined during this study contributed to the specific concepts, therefore all the figured specimens which are not holotypes are paratypes. SGM = single grain mount. The single grain mounts do not have unique numbers; they are numbered sequentially for each species within a particular sample. The specimens are all from sidewall core samples.

Species	Type	Figs	SGM/Slide No.	EF	Well (depth, m.)	CPC No.
L. septata	P	3A,B	SGM 100 (i)	M37/1	Skua-6 (2385.00)	35107
L. septata	P	3C	SGM 100 (iii)	N37	Skua-6 (2385.00)	35108
L. septata	P	3D	SGM 100 (ii)	N37	Skua-6 (2385.00)	35109
L. septata	P	3E,F	SGM 3 (ii)	O42	Skua-6 (2385.00)	35110
L. septata	P	3G	SGM 4 (i)	J32/4	Skua-6 (2385.00)	35111
L. septata	P	3H	SGM 4 (iii)	P26	Skua-7A (2440.00)	35112
L. septata	P	3I,J	SGM 4 (ii)	P26/1	Skua-7A (2440.00)	35113
L. septata	P	3K,L	SGM 5 (v)	L42	Skua-6 (2385.00)	35114
L. septata	P	3M,N	SGM 2	N37	Skua-6 (2385.00)	35115
L. septata	H	3O	SGM 4 (i)	P26/4	Skua-7A (2440.00)	35116
L. septata	P	3P	SGM 2 (ii)	O22/3	Skua-7A (2440.00)	35117
M. echinatum	P	4A	SGM 100	L39/1	Skua-6 (2385.00)	35118
M. echinatum	P	4B	SGM 101 (ii)	H41/4	Skua-6 (2385.00)	35119
M. echinatum	P	4C	SGM 13(iv)	N39	Skua-6 (2391.50)	35120
M. echinatum	P	4D	SGM 13 (ii)	N39/4	Skua-6 (2391.50)	35121
M. echinatum	P	4E	SGM 13 (iii)	N40	Skua-6 (2391.50)	35122
M. echinatum	P	4F	SGM H1 (i)	P33/3	Skua-6 (2385.00)	35123
M. echinatum	P	4G	SGM 14 (ii)	M34/3	Skua-6 (2391.50)	35124
M. echinatum	H	4H	SGM 11	H38/3	Skua-6 (2391.50)	35125
M. echinatum	P	4I	SGM 13 (i)	N40	Skua-6 (2391.50)	35126
M. echinatum	P	4J	SGM H1 (ii)	Q32/1	Skua-6 (2385.00)	35127
M. echinatum	P	4K	SGM 12	O42	Skua-6 (2391.50)	35128
M. echinatum	P	4L	SGM 101 (i)	H42	Skua-6 (2385.00)	35129
M. scabratum	P	5A-C	SGM 7(i)	O31/1	Skua-5 (2646.00)	35130
M. scabratum	H	5D-F	SGM 7(ii)	O31/2	Skua-5 (2646.00)	35131
M. scabratum	P	5G	SGM H1	P38	Skua-6 (2391.50)	35132
M. scabratum	P	5H	SGM H3 (i)	M34	Skua-6 (2391.50)	35133
M. scabratum	P	5I	SGM H2 (iii)	J30/2	Skua-6 (2391.50)	35134
M. tessellatum	P	6A,B	SGM 19	L36/1	Skua-6 (2385.00)	35135
M. tessellatum	P	6C	SGM 23	J40/1	Skua-6 (2385.00)	35136
M. tessellatum	P	6D	SGM 20	P39/4	Skua-6 (2385.00)	35137
M. tessellatum	P	6E	SGM 26	P42	Skua-6 (2385.00)	35138
M. tessellatum	P	6F	Slide 2	P33/3	Skua-6 (2385.00)	35139
M. tessellatum	P	6G	Slide 2	M8/2	Skua-6 (2385.00)	35140
M. tessellatum	P	6H	SGM H3	P39	Skua-6 (2385.00)	35141
M. tessellatum	P	6I	SGM 11	F34/4	Skua-6 (2385.00)	35142
M. tessellatum	H	6J	SGM 13	L37/4	Skua-6 (2385.00)	35143
M. tessellatum	P	6K	SGM H4	K37/4	Skua-6 (2385.00)	35144
M. tessellatum	P	6L	SGM H1(ii)	K28	Skua-6 (2385.00)	35145
M. tessellatum	P	6M	Slide 2	D46/2	Skua-6 (2385.00)	35146
M. tessellatum	P	6N	SGM H5	P32/2	Skua-6 (2385.00)	35147
M. tessellatum	P	6O	SGM H9	J36/3	Skua-6 (2385.00)	35148
M. tessellatum	P	6P	SGM H6	O30	Skua-6 (2385.00)	35149
N. spinosus	P	7A	SGM 16	N25/1	Jabiru-10 (1790.00)	35150
N. spinosus	P	7B	Slide 3	U45	Jabiru-10 (1790.00)	35151
N. spinosus	P	7C	SSM 9	S33/1	Jabiru-10 (1790.00)	35152
N. spinosus	P	7D	SGM 36	H31/3	Jabiru-10 (1790.00)	35153
N. spinosus	P	7E	SGM 26	Q34/3	Jabiru-10 (1790.00)	35154
N. spinosus	P	7F	Slide 3	R15/2	Jabiru-10 (1790.00)	35155
N. spinosus	H	7I	Slide 2	H43/2	Jabiru-10 (1790.00)	35156

Species	Type	Figs	SGM/Slide No.	EF	Well (depth, m.)	CPC No.
N. sp. A	n/a	7G	SGM 27	S25/4	Jabiru-10 (1790.00)	35157
N. sp. A	n/a	7H	SGM 28	O28/1	Jabiru-10 (1790.00)	35158
S. asymmetricum	P	9A	SGM H7	N38/3	Skua-6 (2385.00)	35159
S. asymmetricum	P	9B	SGM 11	L22	Skua-7A (2440.00)	35160
S. asymmetricum	P	9C	SGM 9	L27/1	Skua-7A (2440.00)	35161
S. asymmetricum	P	9D	SGM H8	L32	Skua-6 (2385.00)	35162
S. asymmetricum	P	9E	SGM 9	N40	Skua-6 (2385.00)	35163
S. asymmetricum	P	9F	Slide 2	W31/3	Skua-6 (2385.00)	35164
S. asymmetricum	P	9G	SGM H4	Q40/1	Skua-6 (2385.00)	35165
S. asymmetricum	H	9H,I	SGM 8	O36/1	Skua-6 (2385.00)	35166
S. biturbinatum	P	8A	SGM 100	O35/2	Skua-6 (2385.00)	35167
S. biturbinatum	P	8B	SGM 100	O37/3	Skua-6 (2385.00)	35168
S. biturbinatum	P	8C	SGM 101	N36	Skua-6 (2385.00)	35169
S. biturbinatum	P	8D	SGM 101	O36/4	Skua-6 (2385.00)	35170
S. biturbinatum	P	8E,F	SGM 101	O38	Skua-6 (2385.00)	35171
S. biturbinatum	P	8G	SGM 101	O35/4	Skua-6 (2385.00)	35172
S. biturbinatum	P	8H	SGM 100	N35	Skua-6 (2385.00)	35173
S. biturbinatum	P	8I,J	SGM 30	Q27/4	Jabiru-10 (1790.00)	35174
S. biturbinatum	P	8K	SGM 13	Q37/2	Jabiru-10 (1790.00)	35175
S. biturbinatum	P	8L	SGM 14	L20/4	Jabiru-10 (1790.00)	35176
S. biturbinatum	H	8M	SGM 25	J37/2	Skua-6 (2385.00)	35177
S. biturbinatum	P	8N	SGM 24 (ii)	P39	Skua-6 (2385.00)	35178
S. biturbinatum	P	8O	SGM 14 (i)	L40	Skua-6 (2385.00)	35179
S. biturbinatum	P	8P	SGM 13	L36/4	Skua-5 (2646.00)	35180
S. reticulatum	P	10A	SGM 6(iv)	O41	Skua-6 (2391.50)	35181
S. reticulatum	P	10B	SGM H4(ii)	S25/1	Skua-6 (2391.50)	35182
S. reticulatum	P	10C	SGM 7	J36/2	Skua-6 (2391.50)	35183
S. reticulatum	P	10D	SGM 6(ii)	P39	Skua-6 (2391.50)	35184
S. reticulatum	P	10E	SGM 6 (i)	Q40/2	Skua-6 (2391.50)	35185
S. reticulatum	P	10F	SGM H4 (i)	S25/1	Skua-6 (2391.50)	35186
S. reticulatum	H	10G,H	SGM 6(iii)	P41/1	Skua-6 (2391.50)	35187
S. reticulatum	P	10I	SGM 100	H35	Skua-6 (2385.00)	35188
S.? australis	P	11A-B	SGM 2 (i)	L37	Skua-4 (2366.00)	35189
S.? australis	P	11C	SGM H10	M35/2	Skua-4 (2366.00)	35190
S.? australis	P	11D	SGM 8	J36/1	Skua-4 (2366.00)	35191
S.? australis	P	11E	SGM 2 (v)	L38	Skua-4 (2366.00)	35192
S.? australis	P	11F	SGM 4	L33/1	Skua-4 (2366.00)	35193
S.? australis	P	11G	SGM H3	M34/1	Skua-4 (2366.00)	35317
S.? australis	P	11H	SGM H11	O29/2	Skua-4 (2366.00)	35318
S.? australis	P	11I,J	SGM H7	M33/3	Skua-4 (2366.00)	35319
S.? australis	P	11K	SGM H15	N38	Skua-4 (2366.00)	35320
S.? australis	P	11L	SGM H9	Q37	Skua-4 (2366.00)	35321
S.? australis	H	11M-O	SGM 10 (i)	K36	Skua-4 (2366.00)	35322
S.? australis	P	11P	SGM 12	M30/2	Skua-4 (2366.00)	35323

A selective reappraisal of *Wanaea* Cookson & Eisenack 1958 (Dinophyceae)

JAMES B. RIDING and ROBIN HELBY

RIDING, J. B. & HELBY, R., 2001:09:21. A selective reappraisal of *Wanaea* Cookson & Eisenack 1958 (Dinophyceae). *Memoir of the Association of Australasian Palaeontologists 24*, 33-58. ISSN 0810 8889.

Selected species of the dinoflagellate cyst genus *Wanaea* from Australasia and Europe have been restudied. The new species *Wanaea lacuna* from the late Bathonian of Australia demonstrates that the genus may be extensively cavate and the generic diagnosis has been emended. Other new species from the Bathonian and earliest Callovian of Australia include *Wanaea enoda* and *W. verrucosa*. *Wanaea enoda*, *W. lacuna* and *W. verrucosa* are all energlynioid forms which lack a prominent posterior paracingular flange. The European and sub-Mediterranean energlynioid species *Wanaea acollaris* Dodekova 1975 and *W. zoharensis* Conway 1978 have been redescribed and emended. *Wanaea zoharensis* may have a solid extension to the antapical horn or protuberance and the term antapicular structure is proposed for this feature. In Australia, the form originally described as *Epicephalopyxis spectabilis* Deflandre & Cookson 1955 has been subsequently misidentified. The species has a complex paracingular flange comprising three distinct zones; it is also stratigraphically important, being confined to the mid Oxfordian. It was transferred to *Wanaea* in 1958, however the figured specimen accompanying this transfer is not conspecific with the type. This specimen has a narrower flange comprising short, regular processes which are connected distally by a trabeculum. Subsequent identifications of *Wanaea spectabilis* have followed the latter specimen. The new species *Wanaea talea* is erected to accommodate these latter forms.

The more flamboyant species of this genus with lace-like paracingular flanges are consistently younger than the energlynioid species. Energlynioid species are largely confined to the Mid Jurassic (late Bajocian-Callovian) worldwide, and are most prominent in the Bathonian. However the presumably more evolved, flanged forms are confined to the mid Callovian to early Oxfordian in Europe and the mid Callovian to earliest Kimmeridgian in Australasia. Most species of *Wanaea* exhibit marked North-South provincialism and are currently known only from Europe and surrounding areas or the Indo-Pacific region. The exception to this is *Wanaea indotata* which is cosmopolitan and may be an intermediate between the energlynioid and flanged species.

James B. Riding, Australian Geological Survey Organisation, GPO Box 378, Canberra, ACT 2601, Australia (present address: British Geological Survey, Keyworth, Nottingham NG12 5GG, UK [e-mail: jbri@bgs.ac.uk]); Robin Helby (corresponding author), 356A Burns Bay Road, Lane Cove, NSW 2066, Australia (e-mail: rhelby@ozemail.com.au). 10 November 2000.

Keywords: dinoflagellate cysts, Middle and Late Jurassic, Australia, Europe, biostratigraphy, evolution, taxonomy

THE JURASSIC dinoflagellate cyst genus *Wanaea* Cookson & Eisenack 1958 comprises a conical hypocyst with an antapical horn and a flattened to slightly apically convex epicyst. It has an epicystal archaeopyle and, while the epicyst is commonly paratabulate (Figs 1C, 1D), the hypocyst rarely exhibits more than a partial paratabulation. Many representatives bear distinctive posterior paracingular flanges which are interrupted at the parasulcus. Some Bajocian-Bathonian representatives may exhibit minor, restricted and commonly delicate, crest development on the posterior paracingular suture but lack the prominent and relatively robust flange development of the mid Callovian and younger species. The Bajocian-Bathonian forms also commonly display convex epicysts. We refer, informally, to this group as the energlynioid species. In the flanged forms, the hypocyst is almost invariably smooth. *Wanaea indotata* Drugg 1978 is regarded as transitional between the two groups. Where present, the paratabulation is gonyaulacalean and is assumed to be a standard sexiform configuration (Sarjeant, 1966; Stover & Evitt, 1978). The epicystal archaeopyle style of the genus was first noted by Norris (1965).

Wanaea was proposed by Cookson & Eisenack (1958, p. 57), to accommodate forms originally described as *Epicephalopyxis spectabilis* Deflandre & Cookson 1955 and two new species,

Wanaea clathrata and *W. digitata,* from the Upper Jurassic of Australia and Papua New Guinea. Cookson & Eisenack (1958) were unsure as to the affinity of the genus and classified it as *Incertae Sedis*. Three years later, Evitt (1961) recognised that *Wanaea* is of unequivocal dinoflagellate affinity. Subsequently, Evitt (1963) stated that fossil dinoflagellates are dominantly of the cyst stage and this hypothesis was confirmed by experiments using modern dinoflagellates (for example, Wall & Dale, 1968). The type, *Wanaea spectabilis* from Papua New Guinea, was transferred to *Wanaea* from *Epicephalopyxis* Deflandre 1937 by Cookson & Eisenack (1958). However, in doing this Cookson & Eisenack (1958, pl. 9, fig. 1) illustrated a morphotype, which is different from the type specimens. This new form is named *Wanaea talea* sp. nov. herein. The first European species, *Wanaea fimbriata* was described by Sarjeant (1961), from the Lower Oxfordian of Yorkshire, northern England.

In 1975, Dodekova described *Wanaea acollaris* from the late Bathonian of north-east Bulgaria. This species lacks a posterior paracingular flange and is weakly paratabulate. Hence Dodekova (1975) informally modified the generic concept to include such forms. Shortly after, Sarjeant (1976) published *Energlynia kyrbasia* from the late Bathonian of the English Midlands. Sarjeant (1976) proposed a gonyaulacalean paratabulation pattern for this species which, like *W. acollaris*, lacks a paracingular flange. By establishing *Energlynia*, Sarjeant (1976) considered that the non-flanged forms should be distinguished from *Wanaea*. Sarjeant (1978) later stressed this by transferring *Wanaea acollaris* to *Energlynia*. However, in the same year, *Energlynia kyrbasia* was deemed to be a junior synonym of *Wanaea acollaris* by Fenton & Fisher (1978). This situation was effectively resolved by Riley & Fenton (1982) and Lentin & Williams (1993), who, in a broad consensus, listed *Energlynia* as a junior synonym of *Wanaea* (see also Drugg, 1978, p. 74). In 1978 two further species of *Wanaea* were proposed. These were *Wanaea indotata*, a form with a variable posterior paracingular flange, from the late Bajocian and mid Callovian of England and an energlynioid species, *Wanaea zoharensis* Conway 1978, from the late Bathonian of southern Israel. An energlynioid species with minor cavation, *Wanaea cornucavata* Feist Burkhardt & Pross 1998, was recently described from the early Bathonian of England, France and Germany.

A generic synopsis and modified description of *Wanaea* were given by Stover & Evitt (1978, p. 223) and this treatment was a *de facto* emendation. It stressed the possible paratabulation, archaeopyle style and the presence of accessory archaeopyle sutures on the epicyst.

Woollam (1980, p. 250) proposed that *Energlynia kyrbasia, Wanaea indotata* and *Wanaea zoharensis* are all junior synonyms of *Energlynia acollaris*. Subsequently, two papers on the genera *Energlynia* and *Wanaea* were published in the early 1980s. Fensome (1981) and Woollam (1982) reviewed the two genera and these authors chose to retain both *Energlynia* and *Wanaea*. These reviews agreed that *Energlynia* is difficult to speciate and Fensome (1981) followed Woollam (1980) in synonymising *Energlynia acollaris, E. kyrbasia* and *Wanaea zoharensis*. Fensome (1981, p. 51) also transferred *Wanaea indotata* to *Energlynia,* and inferred that the latter species may be conspecific with *E. acollaris*. Woollam (1982) did not formally describe species of *Energlynia*, however he illustrated *E. acollaris, "E. kyrbasia"* and *E. indotata*. A possible phylogenetic succession from the late Bajocian to mid Callovian genus *Energlynia* to the several Callovian-Kimmeridgian *Wanaea* species with their complex posterior paracingular flanges was presented by Fensome (1981, fig. 3). This approach was criticised by Woollam (1982) because of the clear provincialism between Europe and Australasia. Further, Woollam (1982) argued that the form which had been assigned to *Wanaea digitata* in the Northern Hemisphere (e.g. by Sarjeant, 1968, 1972; Fensome, 1979; Woollam, 1980) was significantly different from the Australasian form, and proposed *Wanaea thysanota* Woollam 1982.

This paper is one of a series designed to provide the taxonomic foundation that will allow the formal definition of some unpublished subdivisions of the Australian Mesozoic palynological zonation of Helby *et al.* (1987). That publication was the first attempt at an integrated, pan-Australian microplankton and spore-pollen zonation. Only the basic framework of the zonation was provided in anticipation that further contributions, particularly the documentation of new taxa, would be necessary as the zonation scheme evolved. Indeed, informal subdivisions of these zones have been recorded in Helby's unpublished reports to industry for over 20 years. These subzones have widespread currency within the hydrocarbon industry due to the legislative requirement for the release of technical data under the Petroleum (Submerged Lands) Act 1967. The informal subdivisions of the Helby *et al.* (1987) zonation

have been entered into the Australian Geological Survey Organisation (AGSO) STRATDAT database. A diagrammatic update of the Helby *et al.* (1987) zonal scheme is presented by Foster (this volume), and will be described fully by Helby & Partridge (in prep.). This taxonomic project is an initiative of the Petroleum and Marine Division of AGSO.

SYSTEMATIC PALYNOLOGY

In this section, the genus *Wanaea* and the species *W. acollaris, W. spectabilis* and *W. zoharensis* are emended. Four new species of *Wanaea, W. enoda, W. lacuna, W. talea* and *W. verrucosa*, are described from the Bathonian and Oxfordian of Australia. The locations of the offshore Australian wells are given by Foster (this volume). The dimensions quoted are all given in micrometres (µm). Herein, intermediate forms have a maximum dimension of between 50µm and 100µm and large cysts are over 100µm in size (Stover & Evitt, 1978, p. 5). Most of the morphological terminology for dinoflagellate cysts is that of Evitt (1985). References to author citations of taxa discussed may be found in the bibliography of Williams *et al.* (1998, p. 747-817). The synonymy lists are selective and mainly confined to illustrated specimens. Most figured specimens are deposited in the Commonwealth Palaeontological Collection (CPC) of AGSO, Canberra (Appendix 2).

This study has been conducted largely using single grain mounts (or mounts with multiple specimens) and the majority of the figured specimens are from these single species slides. Most samples are from outcrop, sidewall core or normal core material, however a small number of ditch cuttings samples were also used. The photomicrographs in Figs. 1-10 were all taken at AGSO using an Olympus DP10 digital camera system coupled to a Zeiss Axioskop photomicroscope. Some extraneous palynodebris, not adherent to the figured specimens, has been digitally removed in selected images.

The photomicrographs in this paper are from a database that contains many digital images. Sample details, key morphological data and measurements of each imaged specimen are held on open file spreadsheets. The image database may be accessed on the AGSO website (http://www.agso.gov.au).

The new taxa have been extensively used in unpublished reports, which are now in the public domain (open file). In order to maximise the utility of the species, the informal names and/or codes are listed, separate from any formal synonymy listing, under the heading 'Previous Australian usage'. To provide continuity, wherever practical, the informal name has been retained.

Dinoflagellate cysts

Wanaea Cookson & Eisenack 1958 emend.

1958 *Wanaea* Cookson & Eisenack, p. 57.
1976 *Energlynia* Sarjeant, p. 164-166.
1990 *Energlynia* Sarjeant; Dodekova, p. 43.

Type species. Wanaea spectabilis (Deflandre & Cookson 1955) Cookson & Eisenack 1958

Emended diagnosis. Proximate to proximochorate dinoflagellate cysts which may be cavate. Large or intermediate in size and subcircular in polar view. The hypocyst is relatively large and is strongly conical to subcircular in outline, with a prominent antapical horn having a blunt, rounded distal extremity. The antapical horn may be parallel to the polar axis or it may be slightly inclined; it may have a solid distal extension. By contrast, the epicyst is smaller and may be slightly to markedly apically convex. Endophragm and/or periphragm are smooth or may be ornamented with low-relief features, typically granules or spinules. Paratabulation is standard gonyaulacalean and is partially to fully indicated by parasutural elements. The posterior paracingular crest or flange can be prominent and may comprise radially arranged, solid, elements which may be interconnected radially. Alternatively, the flange may comprise a reticulate mesh lacking radial elements. Archaeopyle epicystal, the simple operculum is normally attached ventrally. The principal archaeopyle suture is immediately anterior of the paracingulum. The operculum may exhibit accessory archaeopyle sutures and may be detached mechanically. Paracingulum normally indicated by paired equatorial ridges or crests; the posterior one may be prominent. The parasulcus is marked by a midventral depression on the hypocyst, which may be flanked by parasutural ridges, and an interruption of the paracingulum.

Comments. The genus *Wanaea* is emended here to encompass cavate species and forms lacking a paracingulum. Feist-Burkhardt & Pross (1998) previously described *Wanaea cornucavata*, which is cornucavate to holocavate. However, these authors did not expand the generic diagnosis to

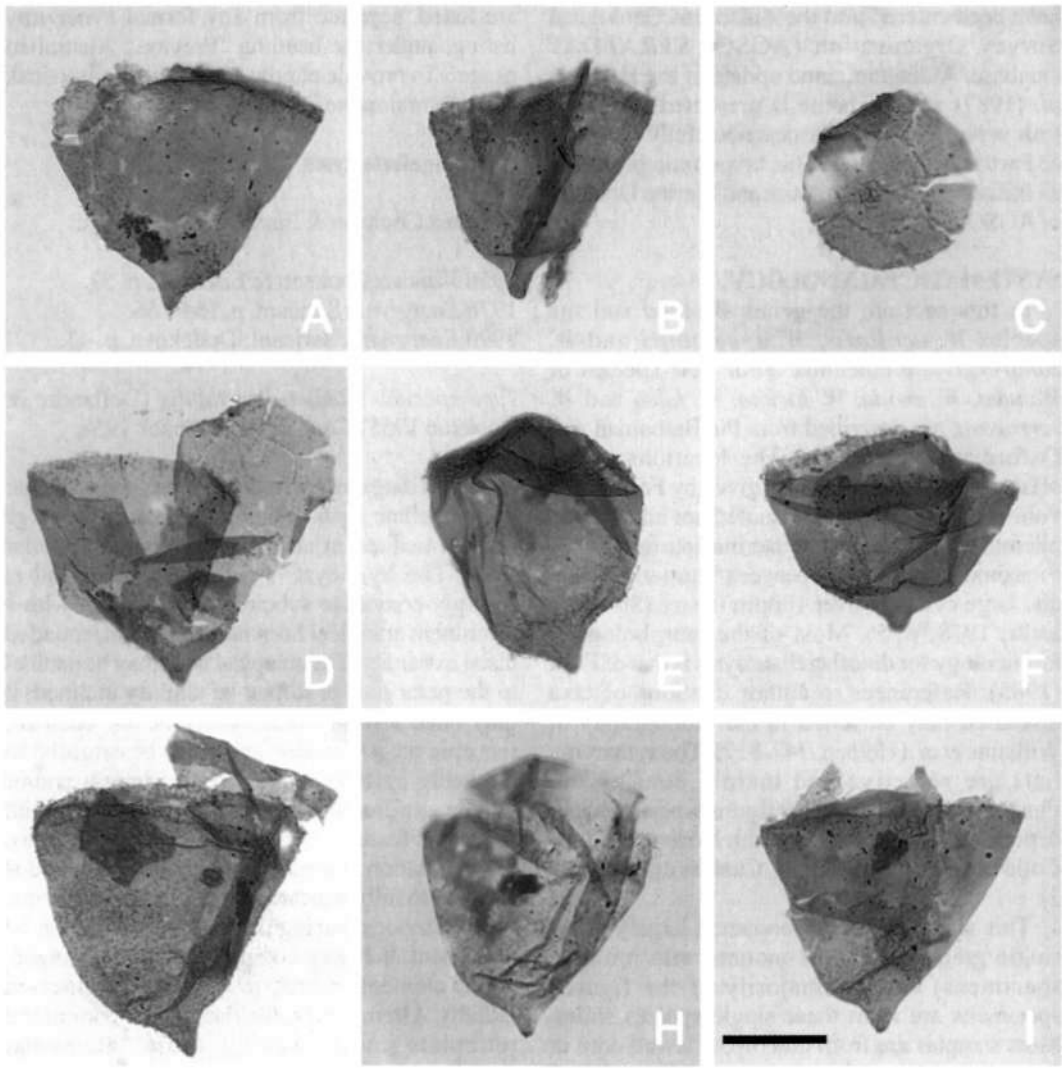

Fig. 1. Wanaea acollaris Dodekova 1975 emend. All specimens from Upper Bathonian Blisworth Limestone, Ketton Grange Quarry, Ketton, Lincolnshire, England U.K. (British Geological Survey micropalaeontological/ palynological sample MPA 15438). All photomicrographs taken using plain transmitted light. The scale bar is 25µm in Fig. 11 and refers to all the photomicrographs. All specimens are topotypes of *Energlynia kyrbasia* Sarjeant 1976, a junior synonym of *Wanaea acollaris*. Note acavate cyst organisation, relatively short antapical horn, flattened epicyst which may have accessory archaeopyle sutures, the smooth, scabrate, microgranulate to sparsely spinose autophragm and parasutural or penitabular nature of the spines (where developed), which may be trabeculate. A - hypocyst, right lateral view, high focus. Note short, slender spines in antapical region, highly incomplete hypocystal paratabulation, posterior paracingular ridge/crest. B - hypocyst, oblique lateral view, high focus. Note prominent nature of antapical horn. C - isolated epicyst, apical view, high focus. Note accessory archaeopyle sutures, consistent presence of low parasutural ridges. D - hypocyst with adherent epicyst, oblique left lateral view, high focus. Note disparity in paratabulation expression on the epicyst and hypocyst. E - entire cyst, left lateral view, high focus. Note slightly domed epicyst, trabeculate spinose ornamentation on the right side of hypocyst. F - relatively short, wide hypocyst with adherent operculum, lateral view, high/median focus. Note short antapical horn. G - large hypocyst with adherent epicyst, left lateral view, high/median focus. Note partial nature of hypocystal paratabulation. H - hypocyst and adjacent operculum, left lateral view, high/median focus. Note highly folded autophragm. I - hypocyst with adjacent, damaged operculum in oblique left lateral view, high/median focus. Specimen has relatively little ornamentation.

include cavate species. Species which lack a prominent posterior paracingular flange (energlynioid forms) are considered to be proximate, but species with a wide equatorial flange such as *Wanaea clathrata* Cookson & Eisenack 1958 are interpreted as proximochorate.

The synonymy of *Wanaea* and *Energlynia* was first validly accomplished by Dodekova (1990, p. 43). Operating at the species level, Riley & Fenton (1982, p. 200) had earlier relegated the genotype of *Energlynia, E. kyrbasia*, to *W. acollaris*. They suggested that *Energlynia* was therefore superfluous, but this was not supported by formal taxonomic procedures.

Wanaea acollaris Dodekova 1975 emend. (Figs 1A-I)

1975 *Wanaea acollaris*; Dodekova, p. 20-21, pl. 2, figs 9, 10, pl. 3, figs 1-7, 9.
1976 *Energlynia kyrbasia*; Sarjeant, p. 166-172, figs 1-16.
1978 *Energlynia acollaris* (Dodekova 1975); Sarjeant, p. 14.
1978 *Wanaea acollaris* Dodekova 1975 (=*Energlynia kyrbasia* Sarjeant 1976); Fenton & Fisher, p. 236.

Emended description. An acavate, intermediate sized species of *Wanaea* with a subconical hypocyst which bears an antapical horn. The epicyst is domed and varies in convexity from flat to slightly rounded. Accessory archaeopyle sutures are frequently developed on the epicyst. The antapical protuberance is closed, distally rounded and slightly variable in size; the horn may be relatively slender to somewhat squat and is straight or may be slightly inclined. The autophragm is moderately thick (0.5-1µm), smooth, scabrate, microgranulate to sparsely spinose. The low relief ornamentation, where developed, is extremely variable even within individual specimens. The scabrae and micrograna are nontabular, however the spines may be parasutural or penitabular. The spines are extremely slender (<0.5µm) and vary between 1 and 2µm in height. Occasionally parasutural spines may be joined distally by trabeculae, forming low, discontinuous crests, which are most common in the antapical and paracingular areas. Paratabulation may also be partially indicated by low (<0.5µm), smooth, irregular ridges, which may be surmounted by occasional spines, and are either parasutural or penitabular. The paratabulation is best expressed on the epicyst, where it is dominantly parasutural; typically the hypocyst has an incomplete paratabulation. Parasutural and penitabular ridges may occur on the hypocyst; both styles may rarely occur on the same specimen. The paracingular parasutures are marked by low ridges with occasional spines, which may be trabeculate or relatively long (c. 2µm), solid, simple processes which coalesce into crests. The parasulcus is indicated by a shallow concavity and the simple operculum is generally attached ventrally.

Dimensions (µm; n=17): Min. (Mean) Max.
Length of entire cyst: 65 (67) 71
Length of epicyst: 13 (17) 21
Length of hypocyst: 43 (55) 67
Equatorial width of hypocyst (in lateral view): 53 (62) 78
Length of antapical horn: 5 (7) 10
Width of antapical horn (at midpoint): 3 (5) 7

A single epicyst was observed in apical view, which measured 43µm x 42µm (Fig. 1C). These dimensions are similar to those of Dodekova (1975) except the width, which is significantly less than in the type material. The measured specimens are from the Blisworth Limestone (Upper Bathonian) of Ketton Grange Quarry, Ketton, Lincolnshire, U.K., the type locality of *Energlynia kyrbasia* Sarjeant 1976. The British Geological Survey (BGS) slides MPA 15438/1 and 2 were used in this study. These slides are in the palynological collections of the BGS, Nottingham, U.K.

Comments. This emendation of *Wanaea acollaris* is based upon the acceptance of the proposition by Fenton & Fisher (1978, p. 236), that it is a senior synonym of *Energlynia kyrbasia*. The original description of Dodekova (1975, p. 21) stressed the relative shortness of the epicyst to the hypocyst, i.e. that the epicyst is around 20% of the entire cyst length. However, fig. 2 of Dodekova (1975) is a line drawing of an idealised specimen which has a markedly inflated or 'domed' epicyst. Dodekova (1975) described the species as being 'proximo-chorate'; in fact it is proximate. The hypocysts of the Ketton Grange specimens are relatively narrow compared to other members of the genus and generally subtriangular in outline (Fig. 1). The paratabulation interpretations of Dodekova (1975, fig. 2) and Sarjeant (1976, figs 1-5) cannot be confirmed here because of the irregular and incomplete nature of the hypocystal paratabulation.

Comparison. Wanaea acollaris is most similar to *W. zoharensis* Conway 1978, distinguished mainly

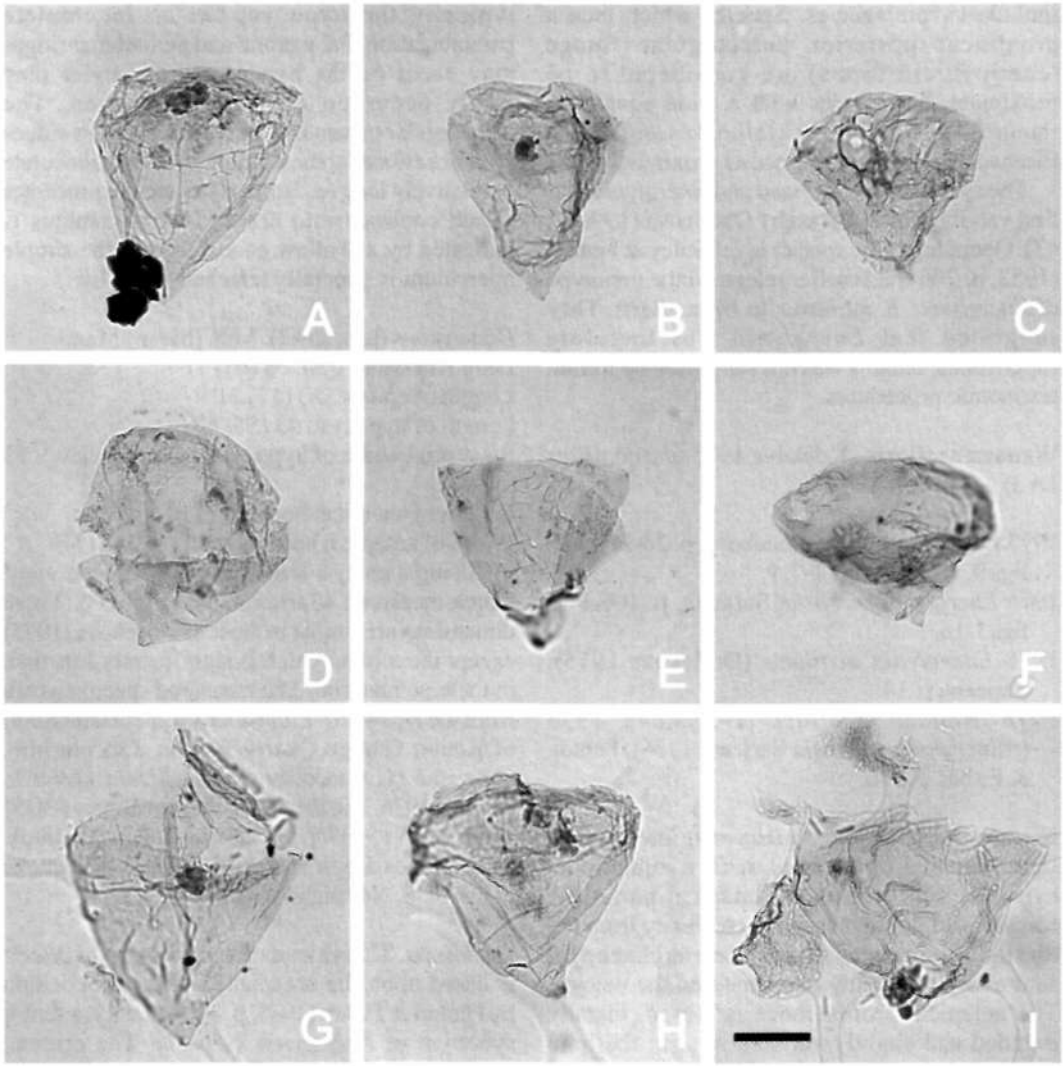

Fig. 2. Wanaea enoda sp. nov. All specimens from core in Magobu Island-1 well at 2266.02m. All photomicrographs taken using plain transmitted light. Scale bar of 25µm in Fig. 2I refers to all photomicrographs. Figure 2H is the holotype; the remainder, paratypes. Note thin, smooth to scabrate autophragm, acavate cyst organisation, lack of paracingular ornamentation and relatively small, distally rounded antapical horn. A - CPC 35841, complete specimen, right lateral view, high focus. Note slightly apically convex epicyst, smooth autophragm. B - CPC 35842, complete specimen, oblique lateral view, high focus. Note long hypocyst slightly indented immediately above the antapical region. C - CPC 35843, complete specimen, lateral view, high focus. Note small antapical horn, flattened operculum (epicyst). D - CPC 35844, complete specimen, lateral view, high focus. Note extremely small antapical horn, highly 'domed' epicyst. E - CPC 35845, hypocyst, lateral view, median focus. Note smooth autophragm, lack of paracingular ornamentation and antapical horn not well differentiated from hypocyst. F - CPC 35846, oblique apical view, high focus. Appears to be folding of autophragm in paracingular region. G - CPC 35847, left lateral view, median focus. Note adherent operculum, slightly ventrally inclined antapical horn. H - CPC 35848, left lateral view, median focus. Note smooth autophragm, relatively small antapical horn, lack of paracingular ornamentation. I - CPC 35849, lateral view, high focus. Relatively wide specimen.

by the denser, more variably distributed ornament of the latter. *Wanaea verrucosa* sp. nov. resembles *W. acollaris* in having granulate to verrucate ornament, but the former lacks parasutural ridges, crests and parasuturally aligned ornament. The latter also displays more strongly domed epicysts. *Wanaea cornucavata* is very similar but is distinguished by the cornucavate to holocavate cyst organization. *Wanaea enoda* sp. nov. is smooth, lacks a demonstrable paracingulum and

has a highly domed epicyst. The smooth hypocyst and the prominent 'fuzzy' posterior paracingular structure of *Wanaea indotata* Drugg 1978 distinguish it from *W. acollaris*. All remaining *Wanaea* species are distinguished by prominent posterior paracingular flanges.

Holotype and type locality. Slide 870-6 from 745.50m in Borehole C-32, Dolina, north-east Bulgaria (Dodekova, 1975). This horizon is within the Dobrich Formation and is Upper Bathonian. Material housed in the collections of the Geological Institute 'Str. Dimitrov', Sofia, Bulgaria.

Stratigraphical distribution. *Wanaea acollaris* extends from the latest early Bajocian to the early Oxfordian of north-west Europe (Fig. 12, Woollam & Riding, 1983; Riding, 1984; Gowland & Riding, 1991; Feist-Burkhardt & Wille, 1992; Riding & Thomas, 1992; 1997), but it is most prominent in the Bathonian (Riding *et al.*, 1985).

Wanaea enoda sp. nov. (Figs 2A-I)

Previous Australian usage
M.P. 491 – Helby.
Wanaea enoda – Helby.

Description. An intermediate sized, acavate species of *Wanaea* lacking demonstrable paracingular differentiation. Hypocyst subconical, subtriangular in dorsoventral and lateral views; sometimes with a rounded antapical horn which is sometimes slightly inclined. The epicyst is domed; the degree of convexity variable (see *Dimensions*, below). The autophragm is thin (c. 0.5µm thick) and generally smooth to irregularly scabrate. Ventrally, the parasulcus is marked by a narrow, shallow concavity. Simple operculum normally attached ventrally.

Dimensions (µm; n=26): Min. (Mean) Max.
Length of entire cyst: 61 (72) 82
Length of epicyst: 12 (22) 40
Length of hypocyst: 40 (59) 75
Equatorial width of hypocyst (in lateral view): 60 (75) 94
Length of antapical horn: 5 (8) 13
Width of antapical horn (at midpoint): 4 (7) 12

The measured specimens are from a conventional core sample at 2066.02m in Magobu Island-1 well.

Comments. The description above is based on a single sample (see above). Despite this limitation, the general morphology is accurately covered with the single exception that in other material the cyst wall may be slightly thicker (up to 1µm). The shape of the hypocyst is somewhat variable. Some specimens are relatively wide (Fig. 2I), whereas others are markedly elongate (Fig. 2B). In the Magobu Island-1 well specimens, the autophragm is thin and flimsy, however this species is surprisingly not especially susceptible to mechanical distortion. The development of an antapical horn is variable. Some individuals have a relatively distinct, short horn (Fig. 2D) and others have subtriangular hypocysts which lack a well differentiated antapical protrusion (Figs 2F, I). No accessory archaeopyle sutures have been observed on the epicyst.

Comparison. This distinctive species of *Wanaea* is characterised by its acavate organisation, the domed nature of the epicyst and its thin, smooth autophragm. *Wanaea enoda* differs from younger species of the genus by lacking a posterior paracingular flange. It is most similar to *Wanaea lacuna* sp. nov. in size, shape and autophragm morphology, however *W. enoda* is acavate. It differs from other acingulate *Wanaea* species such as *W. verrucosa* sp. nov. and *W. zoharensis* in possessing a smooth autophragm. The lack of a paracingular crest and partial paratabulation together with a domed epicyst differentiates *Wanaea enoda* from *W. acollaris*.

Derivation of name. From the Latin *enodis*, meaning free of knots and referring to the lack of ornamentation on the autophragm.

Holotype and type locality. Fig. 2H, CPC 35848, from a conventional core sample in Magobu Island-1 well at 2066.02m.

Stratigraphical distribution. *Wanaea enoda* ranges from the Bathonian base of the *Wanaea verrucosa* Zone (7ciaiii) to the Callovian basal *Wanaea digitata* Zone (7bi) (Figs 11, 12; Foster, this volume; Helby & Partridge, in prep.).

Wanaea lacuna sp. nov. (Figs 3A-L)

Previous Australian usage
M.P. 1016 – Helby.

Description. A smooth, cavate species of *Wanaea* intermediate in size and lacking a posterior paracingular flange and with a subconical hypocyst which has an antapical horn or

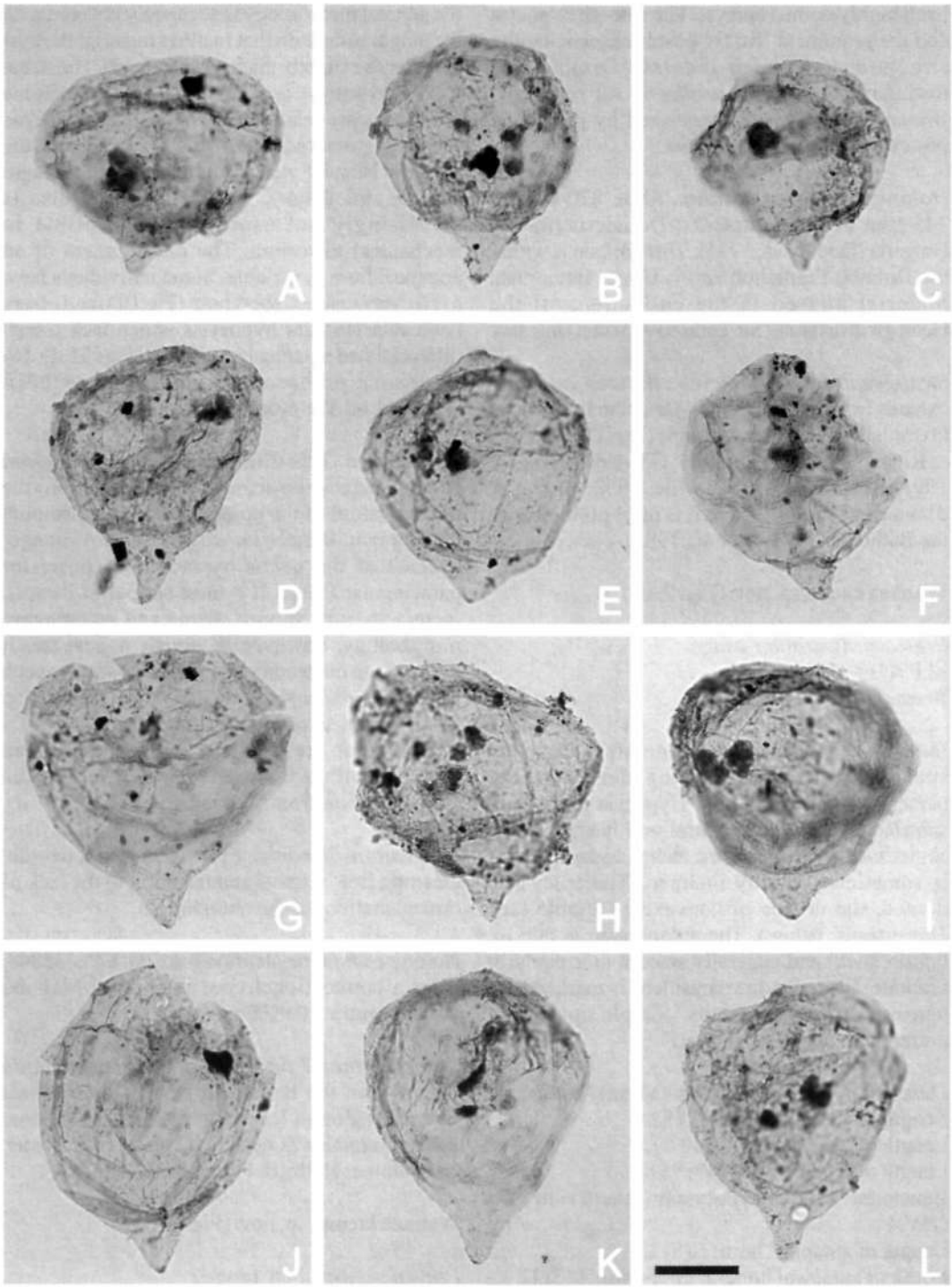

Fig. 3. Wanaea lacuna sp. nov. All from core in the Sunrise-2 well at 2122.33m (Figs 3B, D-F, H-I, K), 2122.25m (Figs 3E, G, J) and 2122.05m (Figs 3A, C, L). All photomicrographs taken using plain transmitted light. The scale bar of 25µm in Fig. 3L refers to all photomicrographs. Figures 3A, G-I are composite photomicrographs. Figure 3J is the holotype, the remainder are paratypes. Note subconical hypocyst lacking a posterior paracingular flange, hemispherical epicyst, antapical horn or protuberance, cavate cyst organisation and relatively thin endophragm and periphragm. A - CPC 35850, left lateral view, median focus (continued opposite)

protuberance. The short, broad antapical horn is slightly inclined and is blunt and rounded distally. A hemispherical epicyst is present. The endophragm is approximately 0.5µm thick; the periphragm is markedly thinner; both the cyst layers are irregularly smooth to microscabrate. This species is hypocavate to circumcavate; the two wall layers are consistently separated in the antapical region (Fig. 3). There is a distinct periphragmal antapical horn developed but no corresponding protuberance on the endocyst. Most specimens are cornucavate. Occasionally, the endophragm and periphragm are slightly separated in the lateral and apical areas, therefore ranging to bicavate and circumcavate organization. No unequivocal parasutural features are present. On the ventral side, the parasulcus is marked by a narrow, shallow concavity or depression. The smooth principal endoarchaeopyle and periarchaeopyle sutures are interpreted as being immediately anterior of the anterior paracingular parasuture; the simple operculum is generally attached ventrally.

Dimensions (µm; n=45): Min. (Mean) Max.
Length of entire cyst: 65 (80) 96
Length of epicyst: 12 (21) 40
Length of hypocyst (including paracingulum): 35 (61) 75
Equatorial width of hypocyst (in lateral view): 56 (70) 99
Length of antapical horn: 5 (9) 15
Width of antapical horn (at midpoint): 5 (9) 13
Length of pericoel at antapex: 5 (15) 23
Length of pericoel excluding at antapex: 1 (4) 13

The measured specimens are from conventional core samples in Sunrise-2 well at 2122.33m, 2122.25m and 2122.05m.

Comments. This species of *Wanaea* is distinguished by being cavate. The principal area where the endophragm is separated from the periphragm is at, and adjacent to, the antapical horn (Fig. 3). Most specimens are therefore hypocavate, however the cavation style is somewhat variable and bicavate, circumcavate and cornucavate forms have also been observed (Fig. 3). Wall separation in the lateral regions and in the epicyst is minor (see line drawing of a similar scenario in Sarjeant, 1982, fig. 4e).

No definite indications of paratabulation were observed, however occasional discontinuous low ridges which may represent parasutures are present. The fact that there is no ridge, crest or flange at the paracingulum is unusual for *Wanaea*, even the 'energlynioid' species such as *Wanaea acollaris* Dodekova 1975 have paracingular ridges or rims (Woollam, 1982, p. 47). The endophragm and periphragm are both susceptible to folding as a result of compression and this leads to the formation of arcuate folds (Figs 3G-L). The epicyst is distinctly hemispherical and lacks horns or protrusions (Figs 3B-C, J). Few specimens were observed where the epicyst is absent and many opercula were only slightly displaced. The lack of paracingular features and the frequent retention of the operculum in this species may make the differentiation of the epicyst and hypocyst difficult in some specimens.

Comparison. The only other species of this genus which is cavate is *Wanaea cornucavata*. However, that species is ornamented, has a trabeculate paracingular flange, is partially paratabulate and has a flat, lid-like epicyst (Feist-Burkhardt & Pross, 1998). *Wanaea enoda* is a closely similar, smooth-walled, acingulate, epicystally domed *Wanaea* but lacks cavate wall organization. *Wanaea indotata*, like *W. lacuna*, lacks parasutural features, however the former is acavate and has a prominent paracingular rim.

Derivation of name. From the Latin *lacuna*, meaning cavity or hollow and referring to the cavate cyst organisation of this species.

Holotype and type locality. Figure 3J, CPC 35859, from conventional core, Sunrise-2 well at 2122.25m.

Stratigraphical distribution. *Wanaea lacuna* is Bathonian, from the middle subzone (7ciaii) of the *Wanaea verrucosa* Zone (Figs 11, 12; Foster, this volume; Helby & Partridge, in prep).

Note cornucavate cyst organisation. B - CPC 35851, left lateral view, low focus. Note hemispherical epicyst. C - CPC 35852, left lateral view, high/median focus. D - CPC 35853, left lateral view, high/median focus. Relatively elongate specimen. E - CPC 35854, left lateral view, median focus. Note blunt distal part of antapical horn. F - CPC 35855, right lateral view, median focus. Note large, hemispherical epicyst. G - CPC 35856, right lateral view. Note damaged hemispherical epicyst. H - CPC 35857, left lateral view. Note folds in cyst wall. I - CPC 35858, right lateral view. Note wide antapical horn. J - CPC 35859, left lateral view, high/median focus. Note elongate nature of specimen. K - CPC 35860, left lateral view, median focus. Note cavation in antapical region. L - CPC 35861, left lateral view, median focus. Note adherent epicyst.

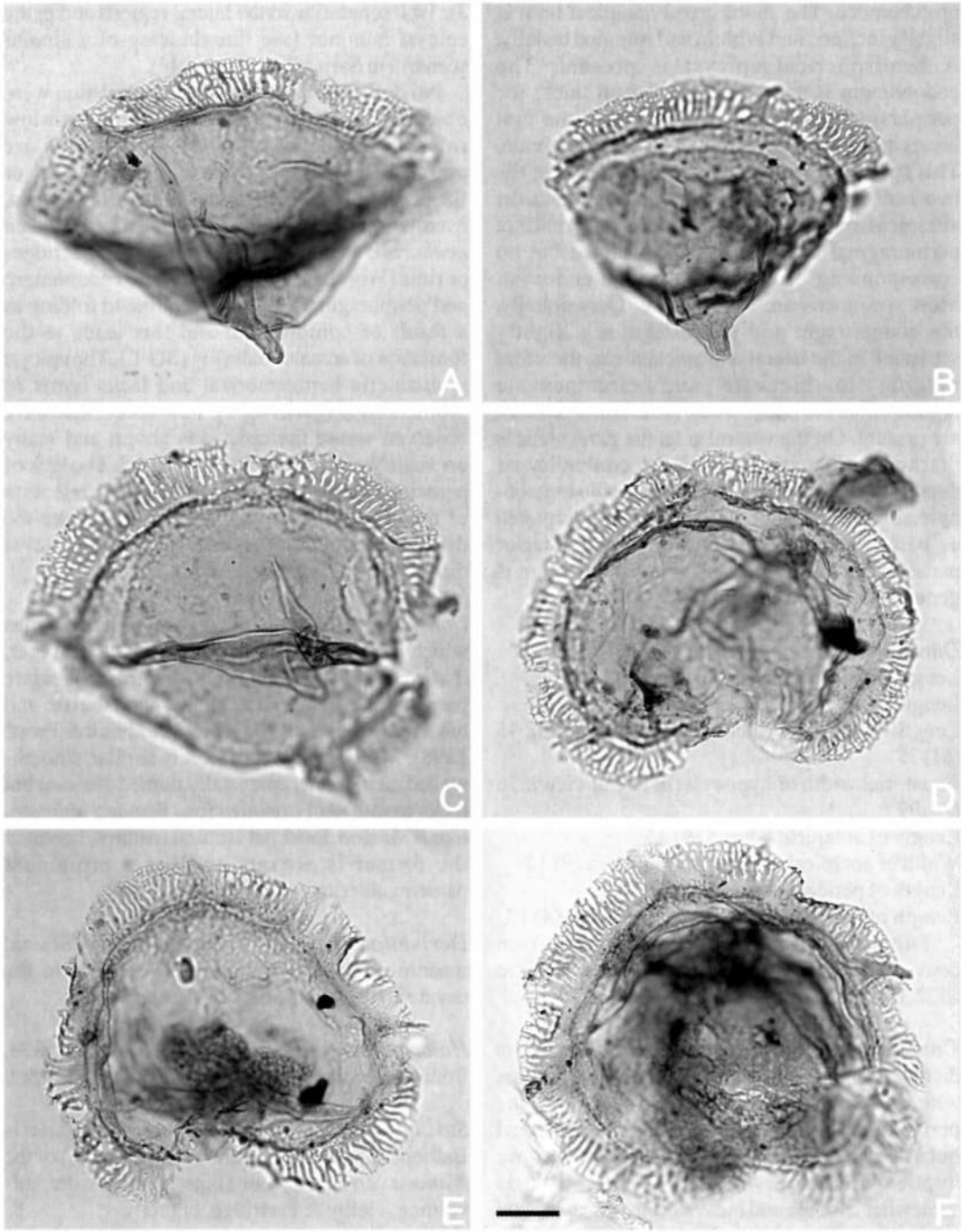

Fig. 4. Wanaea spectabilis (Deflandre & Cookson 1955) Cookson & Eisenack 1958 emend. All from Eclipse-2 well, sidewall core at 2477.00m. All photomicrographs taken using plain transmitted light. The scale bar of 18µm in Fig. 4F refers to all photomicrographs. Note broad, conical hypocyst with single antapical horn and broad, lace-like posterior paracingular flange. Flange complex and variable with long, radial processes arising from thin, largely entire, proximal area. Radial processes coalesce and branch distally, often distal to a distinct trabeculum. A - CPC 35862, hypocyst, oblique right lateral view, low focus. B - CPC 35863, right lateral view, low focus. Note epicyst within hypocyst. C - CPC 35864, hypocyst, oblique antapical view, low focus. D - CPC 35865, antapical view, median focus. Ventral side down. E - CPC 35866, hypocyst, apical view, median/low focus. Ventral side down. F - CPC 35867, antapical view, median/low focus. Ventral side down.

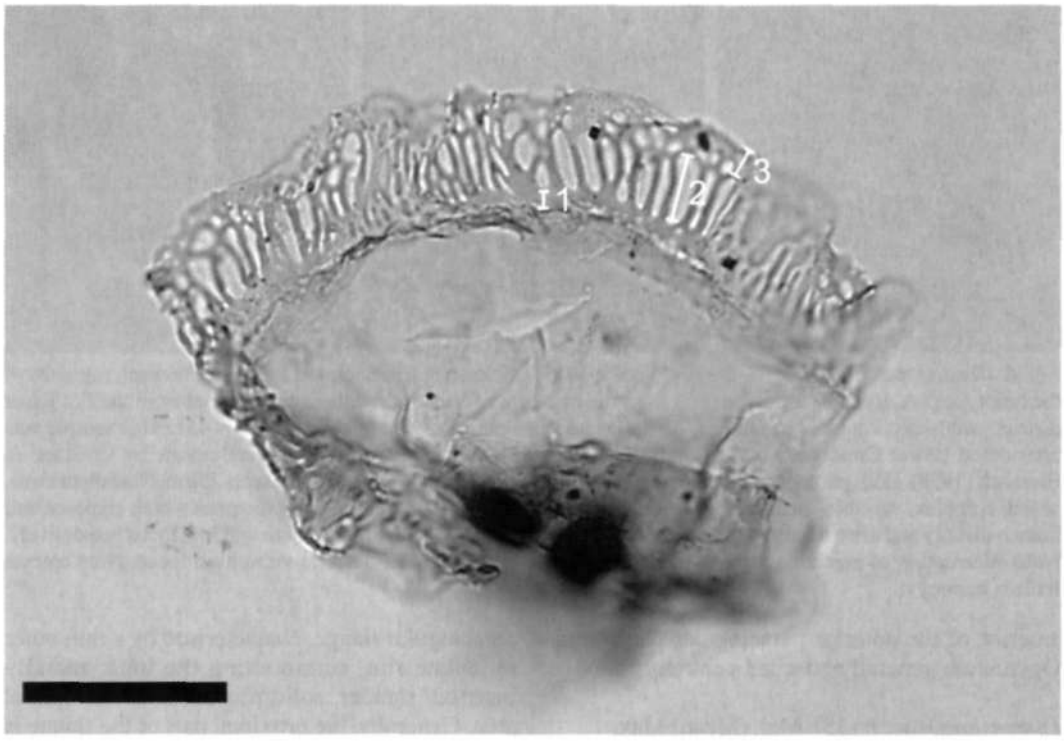

Fig. 5. Wanaea spectabilis (Deflandre & Cookson 1955) Cookson & Eisenack 1958 emend. Single specimen CPC 35868 from sidewall core at 1346.80m, Scafell-1 well. Photomicrograph taken using plain transmitted light. Scale bar represents 25µm. Hypocyst with well preserved posterior paracingular flange. Three zones of the flange are indicated. Zone 1 represents a thin, largely entire, proximal region, which may have small vacuoles irregularly developed. Zone 2 comprises relatively long, radial processes which are occasionally interconnected medially. The distal Zone 3 is a narrow, irregularly reticulate area, which is sometimes bounded distally and proximally, by a discontinuous trabeculum.

Wanaea spectabilis (Deflandre & Cookson 1955) Cookson & Eisenack 1958 emend. (Figs 4A-F, 5, 6A-C, 7B)

1955 *Epicephalopyxis spectabilis*; Deflandre & Cookson 1955, p. 293, pl. 3, figs 12-14.
1958 *Wanaea spectabilis* (Deflandre & Cookson 1955); Cookson & Eisenack, p. 57, non. pl. 9, fig 1.
1987 *Wanaea spectabilis auct. non* (Deflandre & Cookson 1955) Cookson & Eisenack; Davey, pl. 12, fig. 13.

Previous Australian usage
Wanaea clathtabilis – Helby.

Emended description. A large, acavate species of *Wanaea*, with a conical hypocyst and a short, distally rounded antapical horn which may point toward the ventral side. Autophragm smooth to scabrate. The epicyst is slightly apically convex to flattened and may show parasutural traces and re-entrants along the principal archaeopyle suture. Paratabulation is normally absent on the hypocyst, apart from a prominent, lace-like posterior paracingular flange, which is equatorial in position and interrupted at the indented parasulcus. This flange morphology comprises three distinct zones (Deflandre & Cookson, 1955, pl. 3, fig. 13; Figs 4, 5 and 7B). Zone 1 is a solid proximal area, which may be irregularly vacuolate or fenestrate. Zone 2 is the central, main body comprising radial processes. Zone 3 is the distal part of the flange which is irregularly reticulate and is bounded distally by a continuous trabeculum, whereas the inner boundary may be marked by a generally discontinuous trabeculum. The median zone 2 comprises long, radially arranged processes which may occasionally coalesce and branch. They are 10-16µm in length and 1-2µm wide. Generally, the processes are connected by a normally incomplete distal trabeculum, beyond which the zone 3 reticulation is developed. Principal archaeopyle suture generally smooth, located immediately

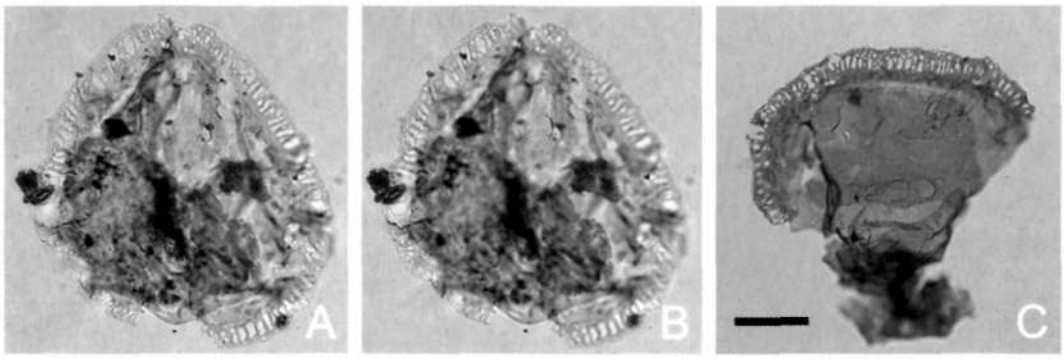

Fig. 6. Wanaea spectabilis (Deflandre & Cookson 1955) Cookson & Eisenack 1958 emend. Photomicrographs of the holotype (6A, B) and a topotype (6C) from the Museum of Victoria, Melbourne. Material from the Era River district, south-east Papua New Guinea, Australasian Petroleum Co. Wana Well sample W.451. This sample was considered Lower Cretaceous by Deflandre & Cookson (1955), but revised to Upper Jurassic by Cookson & Eisenack (1958). Both photographed using plain transmitted light. Scale bar in C represents 25µm. Note distinctive, broad, complex, variable, lace-like posterior paracingular flange with long, radial processes which coalesce and branch distally and arise from an entire proximal area. A-B - P.16235, polar view, high and low focus respectively. Note interruption of posterior paracingular flange ventrally. C - P.16234, lateral view, high focus. Note epicyst within hypocyst.

anterior of the anterior paracingular parasuture. Operculum generally attached ventrally.

Dimensions (µm; n=35): Min. (Mean) Max.
Length of hypocyst (excl. paracingular flange): 67 (73) 86
Length of antapical horn: 7 (13) 17
Width of cyst (incl. paracingular flange): 102 (120) 143
Width of cyst (excl. paracingular flange): 86 (96) 114
Width of paracingular flange: 10 (15) 20

The measured specimens are from sidewall core samples in Arunta-1 well at 1919.00m, Eclipse-2 well at 2477.00m and Krill-1 well at 3458.00m, 3470.00m and 3474.00m. Dimensions for holotype provided by Deflandre & Cookson (1955): 110µm x 84µm; paracingular flange c. 8µm.

Comments. Deflandre & Cookson (1955) figured three specimens of their new species *Epicephalopyxis spectabilis*. In their transfer of *E. spectabilis* to *Wanaea*, Cookson & Eisenack (1958) illustrated a morphotype which we consider to be a separate taxon (Cookson & Eisenack, 1958, pl. 9, fig. 1). Since then, the latter form has been widely, but erroneously, accepted as defining the concept of *W. spectabilis* (for example, Fensome, 1981, fig. 3; Helby *et al*, 1987, fig. 18A). Therefore, the specific description of *Wanaea spectabilis* is emended (see above), and the morphotype illustrated by Cookson & Eisenack (1958) is described separately as *Wanaea talea* sp. nov.

Wanaea spectabilis has a wide posterior paracingular flange, characterised by a thin outer reticulate rim, surmounting the long, radially inserted, slender, solid processes of the central area. Generally, the proximal part of the flange is largely entire and is sporadically interrupted by small, subcircular vacuoles which are normally inserted irregularly (Figs 4, 5, 7B). A trabeculum may occur 3 to 5µm from the distal rim connecting most of the radial processes (Figs 4A, E, 7B). This trabeculum is typically more slender than the radial elements of zone 2, which it delimits proximally. The trabeculum merges into the outer reticulate rim (Figs 4, 7B). In poorly preserved material, the outer rim of the flange (zone 3) may be absent due to mechanical damage. These damaged specimens may appear similar to *Wanaea digitata* Cookson & Eisenack 1958. However, damaged forms of *W. spectabilis* have long, irregular, anastomosing, processes and not the regular spines which characterise the outer flange of *W. digitata*.

The posterior paracingular flange of *Wanaea spectabilis* is considered to be intermediate in morphology between *Wanaea clathrata* Cookson & Eisenack 1958 and *W. talea*. It is similar to the flange in *W. talea*, however the latter is significantly narrower and has a smooth, trabeculate, distal rim (Figs 7C, 8). The flange in *Wanaea spectabilis* is most similar to that in *W. clathrata* in that it is wide and there is extensive coalescing of the lace-like elements, particularly in the distal region (Fig. 4). The paracingular flange in *W. clathrata*, despite the presence of some elongate fenestrae, is characterised by complex anastomosing elements throughout the flange

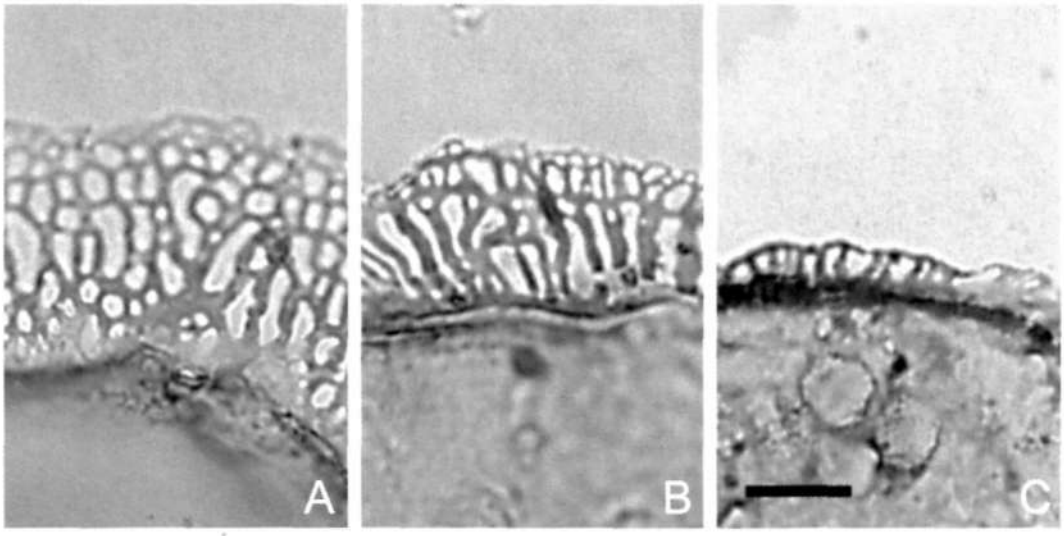

Fig. 7. Photomicrographs of the posterior paracingular flange of three species of *Wanaea*. All taken using plain transmitted light. Scale bar in Fig. 7C represents 10µm. A - *Wanaea clathrata* Cookson & Eisenack 1958. Unregistered outcrop sample from the Oxfordian of Sula, Indonesia (Sato *et al.*, 1978, fig. 8). Note the wide flange, comprising an anastomosing network of slender, solid processes and a largely entire distal edge. B - *Wanaea spectabilis* (Deflandre & Cookson 1955) Cookson & Eisenack 1958 emend. CPC 35862, from Eclipse-2 well at 2477.00m. Note that three zones of the posterior paracingular flange are developed; a thin, entire proximal region (Zone 1); long, radial processes (Zone 2); a distal, narrow, irregularly reticulate area, which is sometimes bounded, distally and proximally, by discontinuous trabeculae (Zone 3). C - *Wanaea talea* sp. nov. Holotype from Omati-1 well at 4285.54m-4288.59m, Museum of Victoria, P.17297. Note the relatively narrow posterior paracingular flange comprising radially arranged processes connected distally by a regular trabeculum.

often giving a relatively even reticulation pattern (Cookson & Eisenack, 1958, pl. 9, figs 7, 8; Helby *et al.*, 1987, fig. 18L; Fig. 7A). Furthermore, the distal edge of the flange in *W. clathrata* is relatively smooth (Fig. 7A).

Comparison. Wanaea spectabilis differs from other species of this genus due to the characteristic posterior paracingular flange (Fig. 7). It is most similar to *Wanaea clathrata* and *W. talea*. The other Australian species, *Wanaea digitata* has a posterior paracingular flange, which is two-layered. The inner layer is generally fenestrate, but may be less regular, defaulting to vacuolate. The outer layer comprises regular spines, although the length of the spines may vary considerably between specimens. *Wanaea spectabilis* also resembles the two European taxa *Wanaea thysanota* Woollam 1982 and *W. fimbriata* Sarjeant 1961. Indeed, damaged specimens with the outer rim entirely removed would be virtually indistinguishable from *W. thysanota*. Similarly, *W. fimbriata* resembles *W. spectabilis* from which the outer trabeculate rim has been stripped, although there is a greater tendency in the latter towards vacuolation than in the former.

Holotype and type locality. Figs 6A, B, Museum of Victoria specimen P.16235. Era River district, south-east Papua New Guinea, Australasian Petroleum Company Wana Well sample W.451. Sample originally considered Lower Cretaceous by Deflandre & Cookson (1955); this was revised to Upper Jurassic by Cookson & Eisenack (1958).

Stratigraphical distribution. Wanaea spectabilis occurs consistently through the Oxfordian, lower part of the upper *Wanaea spectabilis* Zone (subzones 6ciia/6cib) (Figs 11, 12; Foster, this volume; Helby & Partridge, in prep.). It ranges as an extremely rare component into the Oxfordian, lower *Wanaea clathrata* Zone (6bii) in the Timor Sea region but is slightly more prominent at this level in samples from the Sula Islands, Indonesia (from localities 8B & 9B in Sato *et al.*, 1978, fig. 8).

Wanaea talea sp. nov. (Figs 7C, 8A-I)

1958 *Wanaea spectabilis* (Deflandre & Cookson 1955); Cookson & Eisenack, p. 57, pl. 9, fig. 1.
1981 *Wanaea spectabilis* (Deflandre & Cookson 1955) Cookson & Eisenack 1958; Fensome, fig. 3.
1987 *Wanaea spectabilis* (Deflandre & Cookson

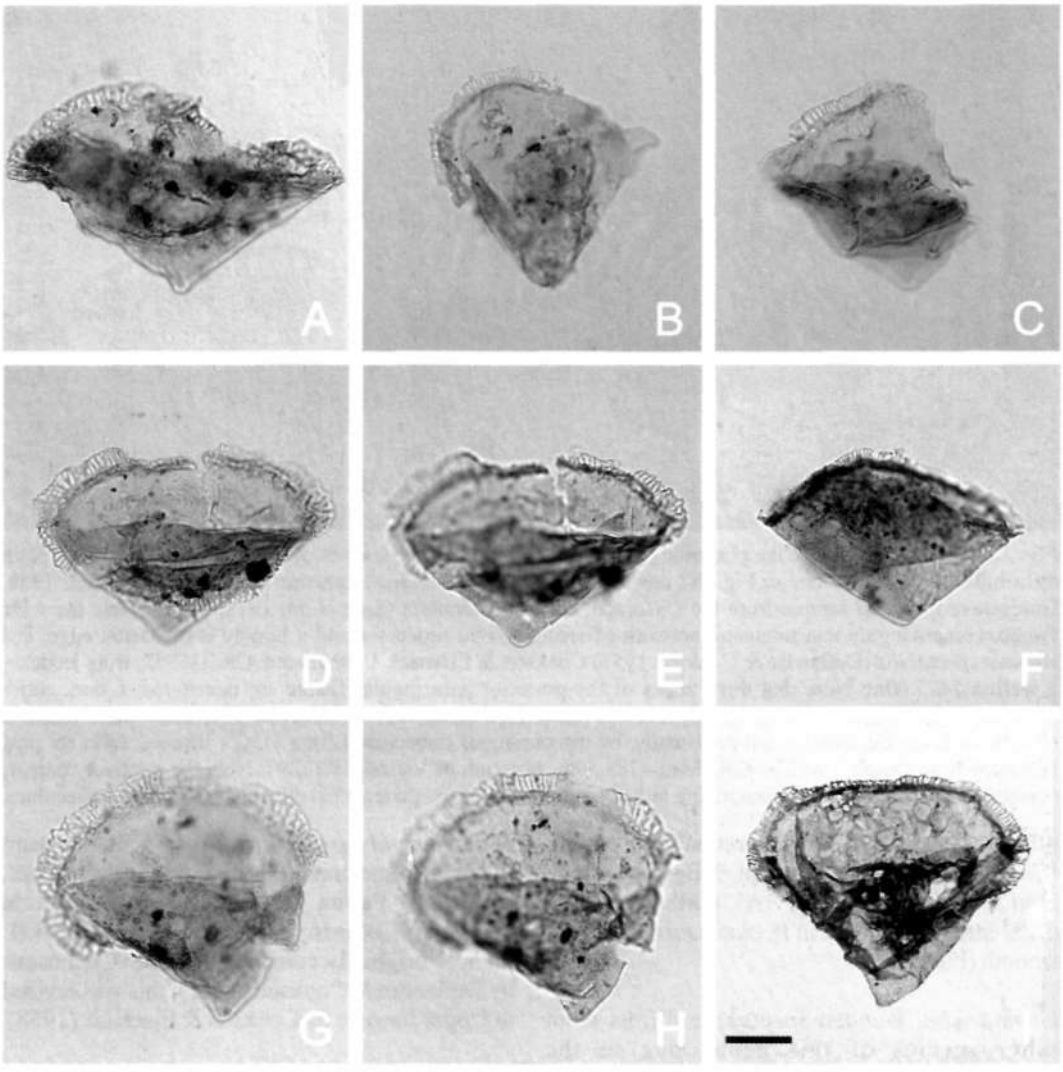

Fig. 8. Wanaea talea sp. nov. Specimens from sidewall cores from Buang-1 well at 3518.50m (Fig. 8A), Circinus-1 ST1 well at 3517.50m (Figs 8C, G-H), Crux-1 well at 3266.60m (Figs 8B, D-F) and ditch cuttings from Omati-1 well from 4285.54-4288.59m (Fig. 8I). All photomicrographs taken using plain transmitted light. The scale bar of 25µm in Fig. 8I refers to all photomicrographs. Figure 8I is the holotype, the remainder paratypes. Note conical hypocyst, presence or absence of short, rounded antapical horn, flattened epicyst, smooth autophragm and prominent posterior paracingular flange comprising a narrow proximal zone surmounted by slender trabeculate processes. A - CPC 35869, hypocyst, right lateral view, high focus. Relatively short, wide specimen. Note short antapical horn and smooth distal edge to posterior paracingular flange. B - CPC 35870, hypocyst, lateral view, median/low focus. Note susceptibility of the posterior paracingular flange to mechanical damage. C - CPC 35871, damaged hypocyst, lateral view, high/median focus. Note regular insertion of processes on the posterior paracingular flange. D, E - CPC 35872, hypocyst with adherent operculum, right lateral view, median and low focus respectively. Note relatively narrow posterior paracingular flange which may readily fold. F - CPC 35873, hypocyst with attached operculum, left lateral view, low focus. Specimen lacks antapical horn; small antapical protuberance barely differentiated from the hypocyst. G, H - CPC 35874, hypocyst with attached operculum, oblique right lateral view, high and low focus respectively. Note relatively prominent posterior paracingular flange. I - P.17297, hypocyst with adherent operculum, right lateral view, high focus. Well preserved specimen, note flattened epicyst and relatively narrow, regular posterior paracingular flange.

1955) Cookson & Eisenack 1958; Helby *et al.*, fig. 18A.

Previous Australian usage
Wanaea spectabilis – Ott (1970, pl. 8, figs 19, 20).
Wanaea spectabilis – Parker (1986, pl. 41, fig. 9).
Wanaea spectabilis – Helby.

Description. An acavate, intermediate to large species of *Wanaea* with a conical, hypocyst and with or without a short, distally blunt and rounded antapical horn which may be slightly inclined. The epicyst is essentially flat. Autophragm smooth. Paratabulation is absent on the hypocyst, apart from a prominent posterior paracingular flange; although accessory archaeopyle sutures are not uncommon on the epicyst. The paracingular flange is 5-11µm wide, equatorial in position and interrupted at the indented parasulcus. The flange comprises a short (1-4µm) proximal zone, which is entire to rarely irregularly vacuolate. This is surmounted by simple, slender (1-2µm wide), solid, processes which are linked distally by a continuous trabeculum. The processes vary from 3-9µm in length, however most are between 5 and 7µm. The trabeculum is c. 1µm in width, parallel sided and imparts a smooth distal margin to the flange. The processes are inserted densely and regularly at approximately every 1 to 2µm along the flange. The flange is not always perfectly regular and small, irregular areas where the processes appear to coalesce may occur. In these areas, the flange is usually solid or sparsely and irregularly vacuolate. Rarely, some processes bifurcate distally or are connected medially. Principal archaeopyle suture generally smooth, located immediately anterior of the anterior paracingular parasuture. The operculum is frequently attached ventrally.

Dimensions (µm; n=28): Min. (Mean) Max.
Length of hypocyst: 49 (62) 73
Width of cyst (incl. paracingular flange): 90 (107) 134
Width of cyst (excl. paracingular flange): 73 (92) 115
Width of paracingular flange: 5 (7) 11
Length of processes in paracingular flange: 3 (5) 9
Length of antapical horn: 5 (9) 18

The epicyst of this species is profoundly flattened and no epicysts were observed in lateral view. Therefore the length of the entire cyst is approximately equal to the length of the hypocyst. It proved difficult to accurately and consistently measure the antapical horn because a distinct protuberance on the hypocyst is not always developed.

The measured specimens are from sidewall cores in Circinus-1 ST1 well at 3517.50m, Crux-1 well at 3266.60m and Buang-1 well at 3518.50m and sample 40, ditch cuttings between 4285.54m and 4288.59m from Island Exploration Company Omati-1 well, south-east Papua New Guinea (Cookson & Eisenack, 1958, figs 1, 2).

Comments. The most characteristic feature of this species is the trabeculum which forms a distinct, regular, outer rim to the paracingular flange (Figs 7C, 8). The epicyst of *Wanaea talea* is flat (Fig. 8I), which is consistent with other species of *Wanaea* with prominent posterior paracingular flanges. Typically, the hypocyst is relatively low and wide, has a subtriangular outline, typically with no clearly differentiated antapical horn (Figs 8A, D-F). The postcingular flange is extremely characteristic, having a narrow, largely solid proximal zone surmounted by prominent parallel to subparallel, simple processes which are distally trabeculate (Figs 7C, 8I). The proximal zone of the flange is normally 2-3µm across, it is rarely reduced to 1µm. Restricted, irregularly vacuolate areas may occur in the flange (Fig. 8I). Rarely, some processes are distally bifurcate or medial connections are developed (Figs 8D, G-H).

Comparison. *Wanaea talea* is similar to other members of the genus with prominent posterior paracingular flanges. Of these, it is most similar to *Wanaea spectabilis*, with which it intergrades. However, the flange of *W. talea* is much more simple than that of *W. spectabilis*, having a short, entire proximal zone which is surmounted by simple processes which are distally connected at a single trabeculate strand. The flange of *W. spectabilis* is much wider, has longer, more complex processes and a thin outer reticulate to vacuolate rim (Figs 4, 5, 7B). The posterior paracingular flange of *W. clathrata* resembles that of *W. talea* in having a smooth distal margin. However, the flange of *W. clathrata* can be extremely wide and is vacuolate, comprising elements which form a relatively regular, complex pattern (Cookson & Eisenack, 1958, pl. 9, figs 7, 8; Fig. 7A). *Wanaea digitata* has a two-layered posterior paracingular flange, which lacks a distal trabeculum. The inner zone is fenestrate to vacuolate and is surmounted by spines (Cookson & Eisenack, 1958, pl. 9, figs 4, 5; Woollam, 1982, fig. 1Bi). *Wanaea talea* is also similar to *Wanaea thysanota* and *W. fimbriata*. The resemblance is

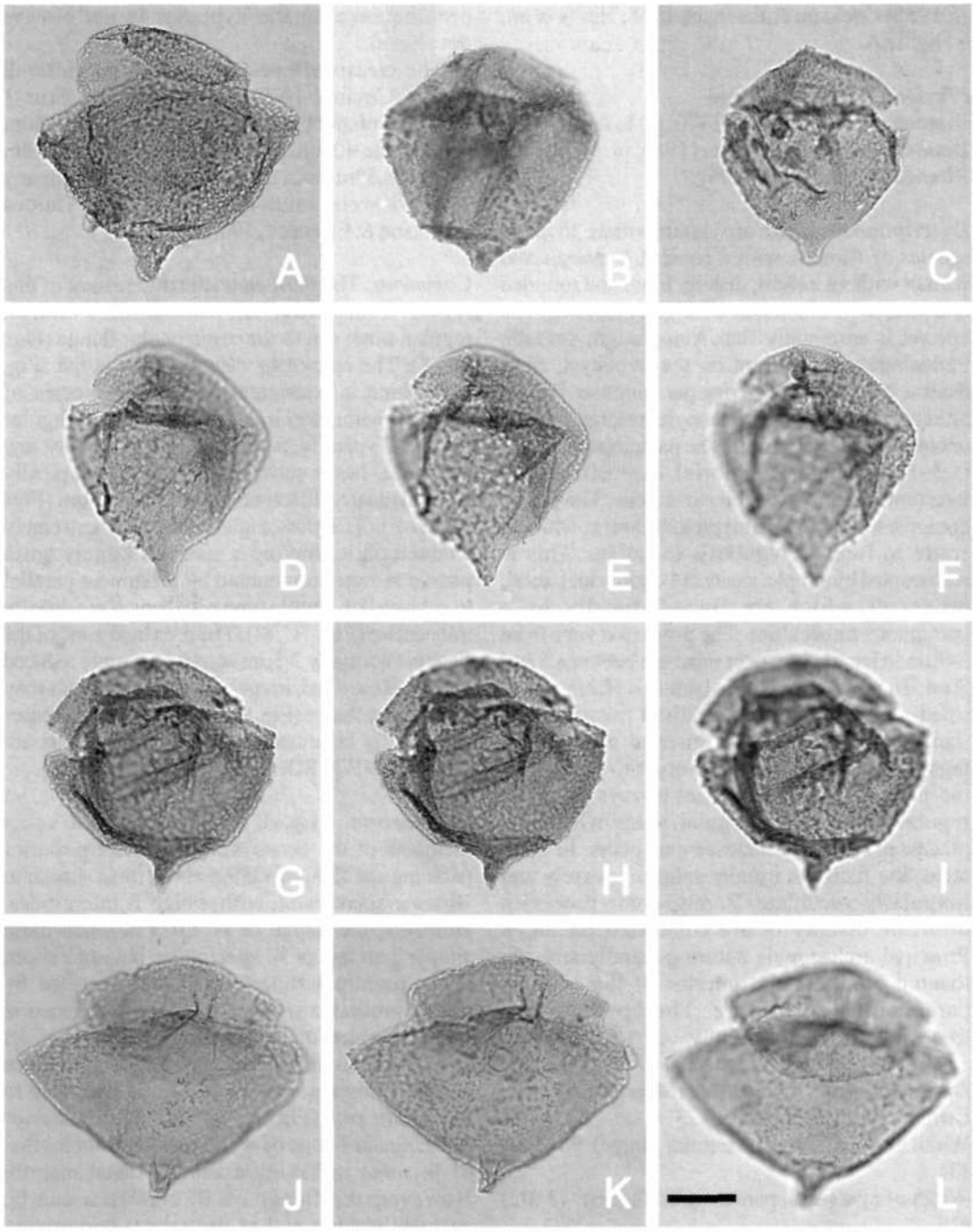

Fig. 9. Wanaea verrucosa sp. nov. From ditch cuttings at 800.00m in Stag-1 well (Fig. 9A) and AGSO dredge sample 96/DR014/5 from Rowley Terrace, offshore Western Australia (Figs 9B-L). All taken using plain transmitted light. The scale bar of 25µm in Fig. 9L refers to all images. Holotype is Fig. 9A, remainder paratypes. Note acavate cyst organisation, prominent antapical horn, broadly hemispherical nature of epicyst, robust autophragm ornamented by scabrae, grana, verrucae, baculae and occasionally pilae and virtual absence of paratabulation. A - CPC 35875, hypocyst and operculum, right lateral view, high focus. Note prominent antapical horn, dense, low-relief ornamentation. B - CPC 35876, entire specimen, right lateral view, high focus. Note domed nature of epicyst. C - CPC 35877, hypocyst and operculum, right lateral view, high focus. Note slightly angular nature of epicyst. D-F - CPC 35878, entire, elongate specimen, right lateral view, high to low focus sequence. G-I - CPC 35879, hypocyst and operculum, right lateral view, high to low focus sequence. Note dense, low-relief ornamentation and domed operculum. J-L - CPC 35880, wide hypocyst and adjacent operculum, right lateral view, high to low focus sequence.

closest in *W. thysanota*, which has simple, solid distal processes which are occasionally connected. However, the posterior paracingular flanges of both these species are irregular, and there is no consistent distal trabeculum (Woollam, 1982, figs 1Bii, 1Biv).

Derivation of name. From the Latin *talea*, meaning slender staff, rod or stick and referring to the distinctive, simple, rod-like trabeculum at the distal side of the posterior paracingular flange.

Holotype and type locality. Figures 7C, 8I, Museum of Victoria specimen P.17297, sample 40, ditch cuttings between 4285.54m and 4288.59m from Island Exploration Company Omati-1 well, south-east Papua New Guinea (Cookson & Eisenack, 1958, figs 1, 2).

Stratigraphical distribution. *Wanaea talea* is confined to the Oxfordian, upper part of the *Wanaea spectabilis* Zone (subzones 6cib-6cia) (Figs 11, 12; Foster, this volume; Helby & Partridge, in prep.). It is an inconsistent, relatively rare, component of the lower subzone (6cib), however, it may occur prominently in the upper part of the zone (subzone 6cia).

Wanaea verrucosa sp. nov. (Figs 9A-L)

1987 *Wanaea* sp. (granulate species); Helby *et al*., figs 17B, 17C.
1996 *Wanaea* sp. A "granulate species" of Helby *et al*. 1987; Burger, pl. 15, figs A, B, K-M.

Previous Australian usage
Wanaea verrucosa – Helby.

Description. An intermediate to occasionally large, acavate species of *Wanaea* which lacks a posterior paracingular flange. It has a subconical hypocyst with a prominent, wide, distally rounded antapical horn. The horn is closed distally and normally is inclined slightly towards the ventral side. The epicyst is also broadly domed, varies markedly in height and is either rounded apically or subangular. Short accessory archaeopyle sutures may be developed on the operculum only. The autophragm is robust, c. 1µm thick and is covered by nontabular low relief ornamentation. The ornamentation is relatively varied in concentration and morphology. Scabrae, grana, verrucae, baculae and occasionally pilae are present. These elements are normally 0.5-1µm in height, however occasionally the baculae and pilae may range up to 2.5µm high. Individual specimens may exhibit examples of more than one ornamentation type. The ornamentation may be slightly larger in the antapical region. In some specimens the mid-lateral areas may be relatively sparsely ornamented in comparison. Coalescence of the ornamentation into short, nontabular, sinuous lineations occurs. In some specimens there may be lineations of ornamentation at the posterior paracingular parasuture. On the hypocyst there are rare instances of possible, discontinuous parasutural ornamentation or a lack of ornamentation in pandasutural zones. Ventrally, the parasulcus is marked by a narrow, shallow concavity or depression and the simple operculum is generally attached ventrally.

Dimensions (µm; n=30): Min. (Mean) Max.
Length of entire cyst: 69 (81) 95
Length of epicyst: 11 (27) 35
Length of hypocyst (incl. paracingulum): 47 (62) 75
Equatorial width of hypocyst (in lateral view): 68 (83) 109
Length of antapical horn: 4 (11) 20
Width of antapical horn (at midpoint): 5 (9) 13

The measured specimens are from ditch cuttings at 800.00m in Stag-1 well, core at 2208.65m in Sunset-1 well and AGSO seafloor dredge sample 96/DR014/5 from the Rowley Terrace, offshore Western Australia (Burger, 1996).

Comments. This distinctive species of *Wanaea* is characterised by the 'domed' epicyst and the presence of varied, dominantly nontabular, low relief ornamentation. Most specimens are scabrate, granulate and/or verrucate. However, the ornamentation is extremely variable; some specimens may be scabrate and others densely granulate/verrucate. The apical angulation which is occasionally developed is not a horn/protuberance (Fig. 9C).

Comparison. *Wanaea verrucosa* differs from the other species of the genus by the lack of a posterior paracingular flange and the presence of consistent and normally dense, nontabular ornamentation. The Northern Hemisphere species *Wanaea acollaris* has a shorter epicyst and is partially paratabulate. *Wanaea zoharensis* also has nontabular ornamentation, but the elements are smaller than those on *W. verrucosa* and they are typically coalescing. Of the similar Southern Hemisphere species, *W. enoda* has thin autophragm which is largely smooth and *W.*

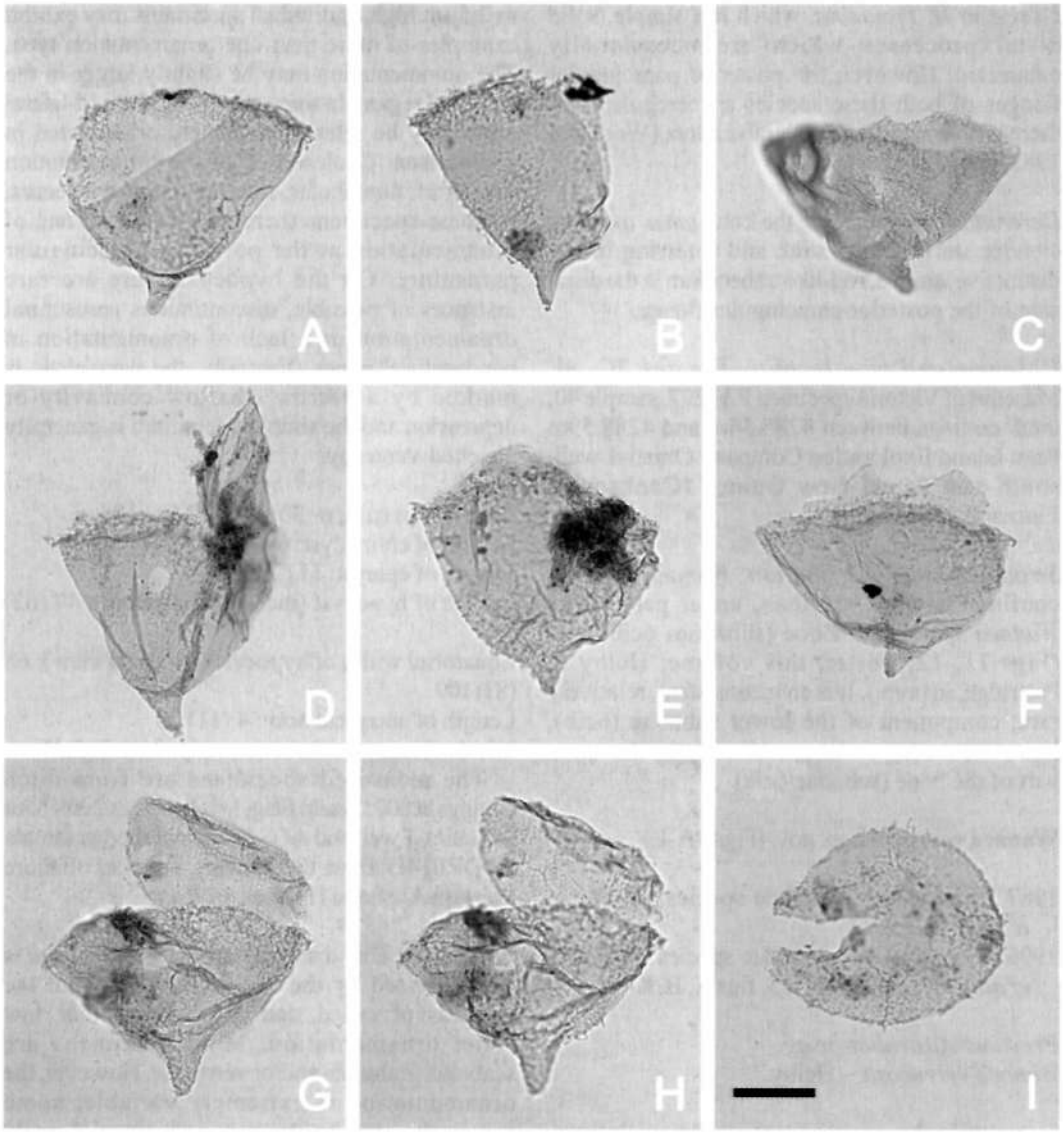

Fig. 10. Wanaea zoharensis Conway 1978 emend. All from core 9, at 1190.00-1197.00m in the Zohar-5 well, southern Israel (Conway, 1978), in University of Sheffield collection. All photomicrographs taken using plain transmitted light. The scale bar of 25µm in Fig. 10I refers to all photomicrographs. Figs 10G-H are the holotype, remainder, topotypes. Note acavate cyst organisation, prominent distally rounded antapical horn, flattened epicyst (operculum), relatively thick, scabrate/granulate to rugulate autophragm, low, irregular, commonly spinose, parasutural ridges and large intratabular areas devoid of ornamentation. A - ML 1459-M24, slightly damaged hypocyst, right lateral view, high focus. Note prominent antapical horn and lack of ornamentation in intratabular areas. B - ML 1459-O31, damaged hypocyst, left lateral view, high focus. Note short antapicular structure on antapical horn, relatively high ornamentation at paracingulum and parasutural lineation of ornamentation at left hand side. C - ML 1459-M27, hypocyst, left lateral view, high focus. Note inclined aspect of antapical horn. D - ML 1459-J14, specimen with attached operculum, left lateral view, high/median focus. Note small antapicular structure on antapical horn. E - ML 1459-M31, hypocyst with detached epicyst, left lateral view, high/median focus. Note relatively smooth autophragm in the intratabular regions. F - ML 1459-G29, specimen with detached operculum, right lateral view, high focus. Note apparent lack of parasutural features. G-H - ML 1459-B31, specimen with attached operculum, oblique left lateral view, high and low focus respectively. Note relatively large antapical horn and parasutural ornamentation on epicyst. I - ML 1459-L32, isolated epicyst, apical view, high focus. Note irregularly spinose nature of parasutural ridges.

lacuna is cavate. *Dissiliodinium caddaense* (Filatoff 1975) Stover & Helby 1987 is similar in overall morphology to *W. verrucosa*. The former species has a subconical hypocyst with an antapical horn/protuberance, a 'domed' epicyst and scabrate/granulate autophragm (Stover & Helby, 1987). However, *D. caddaense* has a compound, multiparaplate precingular (type 1P-5P, 'disintegration style') archaeopyle and is normally significantly larger than *W. verrucosa*. If the archaeopyle of *D. caddaense* has not started to open, the specimen may be identified as *W. verrucosa* (see Stover & Helby, 1987, fig. 4).

Derivation of name. From the Latin, *verruca*, meaning wart and referring to the characteristic verrucate ornamentation of this species.

Holotype and type locality. Fig. 9A, CPC 35875, ditch cuttings at 800.00m in Stag-1 well.

Stratigraphical distribution. *Wanaea verrucosa* is confined to the Bathonian *Wanaea verrucosa* Zone (subzones 7ciaiii-7ciai) (Figs 11, 12; Foster, this volume; Helby & Partridge, in prep.).

Wanaea zoharensis Conway 1978 emend. (Figs 10A-I).

1978 *Wanaea zoharensis*; Conway, p. 347, pl. 1, figs 7, 8, 10 (not figs 6-7, 9 as stated on p. 347).
1981 *Energlynia acollaris* (Dodekova 1975) Sarjeant 1978; Fensome, p. 50.

Emended description. An intermediate sized, acavate species of *Wanaea*. The hypocyst is subconical and appears subtriangular in outline. It has a prominent distally closed and rounded antapical horn. The antapical horn is somewhat variable but is normally relatively slender and is straight or may be slightly inclined ventrally or dorsally. A short (1-3µm), distally pointed, solid extension of the antapical horn may be present. The epicyst is a flattened dome shape, appears to vary considerably in height and is apically rounded to straight. Short accessory archaeopyle sutures and low, irregular parasutural ridges may be developed on the epicyst. The autophragm is moderately thick (0.5-1µm) and is scabrate/granulate to rugulate (c. 0.5µm high). The elements are scabrae and grana, which frequently coalesce into short, irregular, sinuous, nontabular to parasutural ridges. Where the ornamentation is densely packed and the elements merge/coalesce, it may appear to be pseudoreticulate. The distribution of this ornamentation is irregular to parasutural. Large intratabular areas which are free of ornamentation may be present. Paratabulation is partially indicated by irregular parasutural ridges which are occasionally surmounted by slender (c. 0.5µm wide), solid spines which are 0.5-1.5µm long. These spines may be present on the epicyst but are normally longest and most dense in the antapical region. Occasionally, the spines are connected distally by trabeculae. In some specimens, the parasutural ridges are suppressed and these are partially indicated by lineations of ornamentation. The paracingular parasutures are marked by relatively long (2-3µm) solid, simple processes, which frequently coalesce into crests. The parasulcus is indicated by a shallow concavity and the simple operculum is generally attached ventrally.

Dimensions (µm; n=15): Min. (Mean) Max.
Length of hypocyst: 56 (67) 77
Equatorial width of hypocyst (in lateral view): 74 (81) 95
Length of antapical horn: 8 (11) 18
Width of antapical horn (at midpoint): 4 (7) 10

No entire cysts were encountered. A single epicyst (operculum) was observed in lateral view which was 25µm long (high). Two epicysts were observed in polar view, these measured 57µm x 64µm and 63µm x 76µm (Fig. 10I). Based on the measurements here, Conway (1978, p. 347) appears to have transposed length and breadth. The measured specimens comprise topotypes and the holotype from the Zohar Formation in the Zohar-5 Borehole, southern Israel, sample 15, conventional core 9 at 1190.00m-1197.00m (Conway, 1978).

Comments. The contention of Fensome (1981, p. 50) that *Wanaea zoharensis* is a junior synonym of *Energlynia (Wanaea) acollaris* is rejected. Conway (1990) accepted Fensome's interpretation. However, following our reexamination of Conway's material we believe that *W. zoharensis* warrants continued separation. This species is a distinctive morphotype due to the ornamentation and does not appear to intergrade with any other representative of the genus. An emended description of this species is given in order to stress the partial and irregular nature of the paratabulation, that the overwhelming majority of the ornamentation is nontabular and that the ornamentation is best described as scabrate/granulate to rugulate (Fig. 10). Furthermore, large intratabular areas devoid of ornamentation may

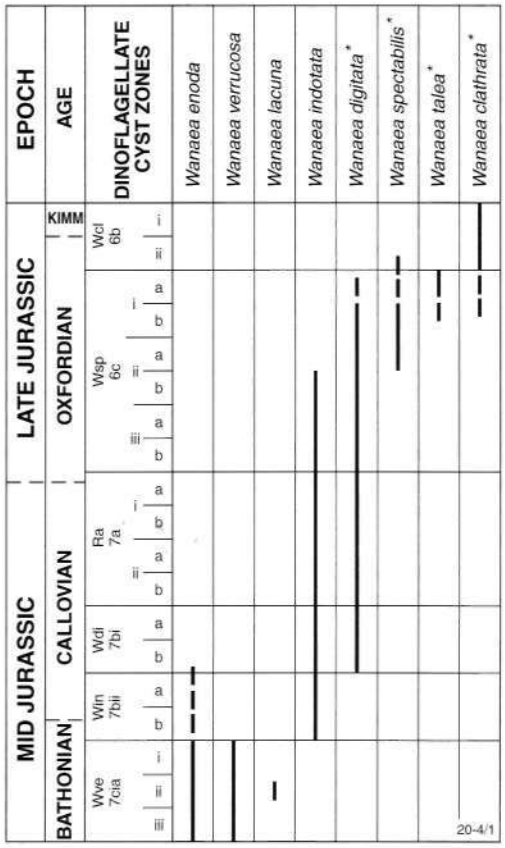

Fig. 11. Stratigraphical distribution of the eight species of *Wanaea* reported from the Mid and Late Jurassic of the Indo-Pacific region. Species with asterisks have posterior paracingular flanges. *Wanaea indotata* is envisaged as a possible intermediate species between the energlynioid forms and the species with distinct posterior paracingular flanges. The dinoflagellate cyst zones and subzones are from Foster (this volume) and Helby & Partridge (in prep.). The stage (age) correlations are based on those in Helby *et al.* (1987, figs 12, 19); it is not implied that these correlations to the European standard are precise. The abbreviations in the Australian dinoflagellate cyst zonation of Helby & Partridge (in prep.) are as for Fig. 12.

occur and parasutural ridges, which may be spinose and trabeculate, are sometimes present. It is clear from the original description that the author envisaged the hypocyst as the epicyst and *vice versa* (Conway, 1978, p. 347). The epicyst may be relatively short (Fig. 10D) or can exhibit a significant degree of 'doming' (Figs 10G-H). The short, solid extension of the antapical horn which is sporadically present (Figs 10B, D) would be termed an apicular structure if it were on an apical horn (Wiggins, 1975). We therefore propose the term antapicular structure for the solid extension to an antapical horn or protuberance.

Comparison. Wanaea zoharensis differs from some species of the genus in lacking a prominent, lace-like posterior paracingular flange, being acavate, having irregular scabrate/granulate to rugulate ornamentation and possibly being partially paratabulate. It is most similar to *Wanaea acollaris* and *W. indotata*. It differs from *W. acollaris* in having prominent scabrate/granulate to rugulate ornamentation. Furthermore, it does not exhibit parasutural ridges. The paracingular ornamentation of relatively long, simple processes which coalesce into crests in *W. zoharensis* is similar to the narrow 'fuzzy' posterior paracingular structure in *W. indotata* (see Drugg, 1978). However, the paracingular crests in *W. zoharensis* are longer than those in *W. indotata* and the latter is psilate or bears occasional nontabular grana or spines. *Wanaea enoda* has a thin, largely smooth, autophragm, *W. lacuna* is cavate and *W. verrucosa* has a relatively thick autophragm ornamented by nontabular scabrae, grana, verrucae and/or baculae.

Holotype and type locality. Figures 10G-H, specimen ML 1459, slide MS 2, England Finder coordinate B31/4, sample 15 (box 2 – top), from the late Bathonian Zohar Formation in the Zohar-5 Borehole, southern Israel, conventional core 9 between 1190.00m and 1197.00m (Conway, 1978). Material housed in the Centre for Palynology, University of Sheffield, Sheffield, U.K.

Stratigraphical distribution. Wanaea zoharensis has been recorded from the late Bathonian Zohar Formation of southern Israel (Fig. 12; Conway, 1978).

BIOSTRATIGRAPHY AND PROVINCIALISM

Wanaea is important in both hemispheres with several relatively short ranging species such as *W. talea* and *W. fimbriata* (Figs 11, 12). Figures 11 and 12 are range charts of the species of *Wanaea* which occur in the Indo-Pacific region and worldwide respectively. *Wanaea indotata* is the only species which is cosmopolitan; it apparently has a younger range in the Indo-Pacific region (Fig. 12). Records of Australasian ('Cookson') species in the Northern Hemisphere have subsequently been assigned to European species.

It is possible that a closer understanding of the species of *Wanaea*, and their evolution, will provide some key tie points for correlating Australian successions to the European standard.

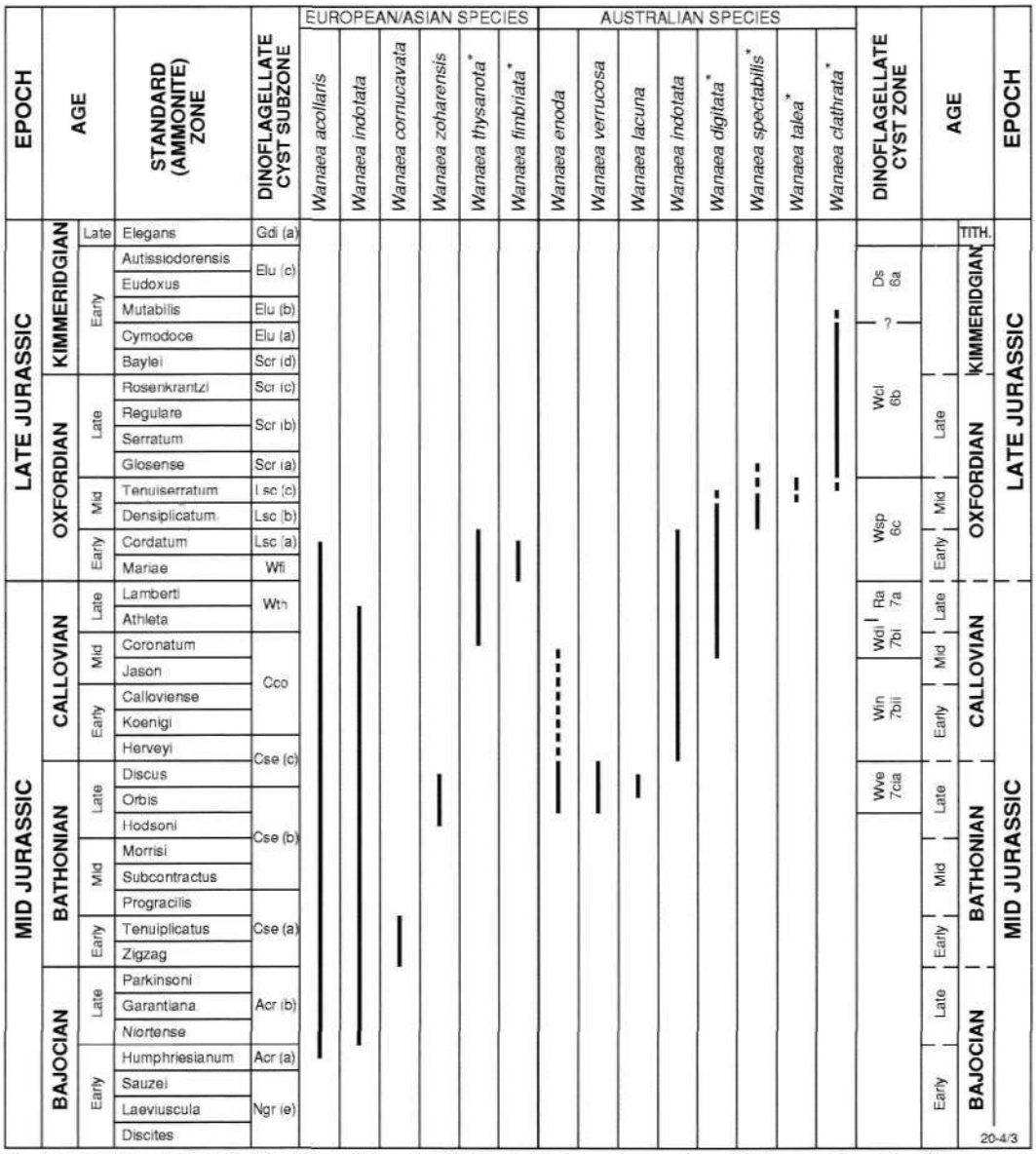

Fig 12. Stratigraphical distribution of the six Mid to Late Jurassic species of *Wanaea* found in Europe and western Asia (Israel), together with the eight species of *Wanaea* reported from the Indo-Pacific region. Species with asterisks have posterior paracingular flanges. *Wanaea indotata* is envisaged as a possible intermediate species between the energlynioid forms and the species with distinct posterior paracingular flanges. European dinoflagellate cyst subzones are from Riding & Thomas (1992); Australian dinoflagellate cyst zones and subzones are from Foster (this volume) and Helby & Partridge (in prep.). The stages/ages for the Australian dinoflagellate cyst zones and subzones are taken from Helby *et al*. (1987); it should be noted that the Australian ranges are consistently younger those in Europe. The abbreviations in the Australian dinoflagellate cyst zonation of Helby & Partridge (in prep.) are as follows: Ds – *Dingodinium swanense*; Wcl – *Wanaea clathrata*; Wsp – *Wanaea spectabilis*; Ra – *Rigaudella aemula*; Wdi - *Wanaea digitata*; Win – *Wanaea indotata*; Wve – *Wanaea verrucosa.*

One of these may be the oldest occurrence of abundant energlynioid species. In Europe, the report of *Wanaea acollaris* in the early Bajocian (Gowland & Riding, 1991) represents relatively few specimens and the range base of consistent, abundant *W. acollaris* is within the late Bathonian (Sarjeant, 1976; Conway, 1978; Riding *et al*., 1999). The oldest occurrences of *Wanaea* species in Australasia are considered to be late Bathonian (Fig. 12). These are all essentially energlynioid

taxa (Fig. 12). We consider that these bioevents are possibly coeval.

Wanaea indotata has a narrow paracingular 'fuzzy rim-like structure' (Drugg, 1978, p. 75). It is possible that this species represents an evolutionary intermediate between the older, energlynioid species and the younger flanged species. The range base of the oldest species with a posterior paracingular flange in both hemispheres appears to be a potentially correlatable bioevent. In the Southern Hemisphere this is the oldest occurrence of *Wanaea digitata* and is in the latest mid Callovian (Fig. 12). The oldest flanged representative of *Wanaea* in Europe is *W. thysanota*, which ranges from the latest mid Callovian to early Oxfordian (Riley & Fenton, 1982; Riding & Thomas, 1992). *Wanaea thysanota* was previously identified as *W. digitata* in Europe (Woollam, 1982). The base of '*Wanaea digitata*' in the latest mid Callovian of Europe in Riley & Fenton (1982, fig. 8) helped provide the age control for the base of the *W. digitata* Interval Zone (7bi-7aii) of Helby *et al.* (1987).

On the basis of currently available faunal information (Francis & Westermann, 1993), it is not unreasonable to suggest that the range top of *Wanaea spectabilis* is no older than latest mid Oxfordian. There are no European species which range above the early Oxfordian (Riding & Thomas, 1992). In Australia, *Wanaea clathrata* is the youngest species, and is considered to span the Oxfordian-Kimmeridgian transition (Helby *et al.*, 1987; Figs 11, 12).

ACKNOWLEDGEMENTS

The authors are grateful to Dr Clinton B. Foster (AGSO, Canberra) for promoting and facilitating this work and for editorial guidance and advice. Christian Thun and Andrew Kelman (AGSO, Canberra) provided invaluable help with preparations and the manipulation of digital images. Laola Pty. Ltd. (Perth) also gave support via the careful treatment of key samples in the preparatory process. Mr Eddie Resiak of the core and cuttings repository at AGSO, Canberra courteously provided access to sample material. BHP Petroleum Pty. Ltd., Esso Australia Ltd., Hadson Energy Ltd., Nippon Oil Exploration (Vulcan) Pty. Ltd. and Santos Ltd. generously provided material on request. We thank specifically Dr Neil G. Marshall (Woodside Energy Ltd.), Mr Peter Price (APG Consultants, Brisbane) and Mr Geoff Wood (Santos Ltd.) for the provision of sample material. Museum Victoria, Melbourne, are thanked for loaning the type and figured material of *Wanaea* in the Cookson & Eisenack and Deflandre & Cookson collections to JBR; the collection manager, Ms Elizabeth Thompson, kindly facilitated this loan. Professor Bernard Owens of the Centre for Palynology, University of Sheffield, U.K., kindly made the type material of *Wanaea zoharensis* available to JBR for a restudy. Sharma L. Gaponoff (Chevron Overseas Petroleum Incorporated, USA) is thanked for attempting to locate the type material of *Wanaea indotata* Drugg 1978. Drs J. Goodall and A. D. Partridge are thanked for reviewing the manuscript. J. B. Riding publishes with the permission of the Chief Executive Officer, AGSO.

REFERENCES

BURGER, D., 1996. Mesozoic palynomorphs from the North West Shelf, offshore Western Australia. *Palynology 20*, 49-103.

CONWAY, B.H., 1978. Microplankton from the Upper Bathonian of Zohar 5 and Yinnon 1 boreholes in southern Israel. *Review of Palaeobotany and Palynology 26*, 337-362.

CONWAY, B.H., 1990. Paleozoic-Mesozoic palynology of Israel. II. Palynostratigraphy of the Jurassic succession in the subsurface of Israel. *Geological Survey of Israel Bulletin 82*, p.39.

COOKSON, I.C. & EISENACK, A., 1958. Microplankton from Australian and New Guinea Upper Mesozoic sediments. *Proceedings of the Royal Society of Victoria (New Series) 70*, 19-79.

DAVEY, R.J., 1987. Palynological zonation of the Lower Cretaceous, Upper and uppermost Middle Jurassic in the northwestern Papuan Basin of Papua New Guinea. *Geological Survey of Papua New Guinea Memoir 13*, 77 p.

DEFLANDRE, G & COOKSON, I.C., 1955. Fossil microplankton from Australian Late Mesozoic and Tertiary sediments. *Australian Journal of Marine and Freshwater Research 6*, 242-313.

DODEKOVA, L., 1975. New Upper Bathonian dinoflagellate cysts from northeastern Bulgaria. *Bulgarska Akademiya na Naukite, Paleontologiya, Stratigrafiya i Litologiya 2*, 17-34.

DODEKOVA, L., 1990. Dinoflagellate cysts from the Bathonian-Tithonian (Jurassic) of North Bulgaria. I. Taxonomy of Bathonian and Callovian dinoflagellate cysts. *Geologica Balcanica 20*, 3-45.

DRUGG, W.S., 1978. Some Jurassic dinoflagellate cysts from England, France and Germany. *Palaeontographica Abteilung B 168*, 61-79.

EVITT, W.R., 1961. Observations on the morphology of fossil dinoflagellates. *Micropaleontology 7*, 385-420.

EVITT, W.R., 1963. A discussion and proposals

concerning fossil dinoflagellates, hystrichospheres and acritarchs, I and II. *Proceedings of the National Academy of Sciences, Washington 49*, 158-164 (I), 298-302 (II).

EVITT, W.R., 1985. *Sporopollenin dinoflagellate cysts. Their morphology and interpretation*. American Association of Stratigraphic Palynologists Foundation, Dallas, 333p.

FEIST-BURKHARDT, S. & PROSS, J. 1998. Morphological analysis and description of Middle Jurassic dinoflagellate cyst marker species using confocal laser scanning microscopy, digital optical microscopy, and conventional light microscopy. *Bulletin des Centres de Recherches Exploration-Production Elf-Aquitaine 22*, 103-145.

FEIST-BURKHARDT, S. & WILLE, W., 1992. Jurassic palynology in southwest Germany - state of the art. *Cahiers de Micropaléontologie, Nouvelle Serie 7*, 141-156.

FENSOME, R.A., 1979. Dinoflagellate cysts and acritarchs from the Middle and Upper Jurassic of Jameson Land, East Greenland. *Grønlands Geologiske Undersøgelse Bulletin 132*, 96 p.

FENSOME, R.A., 1981. The Jurassic dinoflagellate genera *Wanaea* and *Energlynia*: their morphology and evolution. *Neues Jahrbuch für Geologie und Paläontologie Abhandlungen 161*, 47-61.

FENTON, J.P.G. & FISHER, M.J., 1978. Regional distribution of marine microplankton in the Bajocian and Bathonian of northwest Europe. *Palinologia número extraordinario 1*, 233-243.

FOSTER, C.B., This volume. Introduction.

FRANCIS, G. & WESTERMANN, G.E.G., 1993. The Kimmeridgian problem in Papua New Guinea and other parts of the Indo-southwest Pacific. 75-93 in Carman, G.J & Carmen, Z. (eds). *Petroleum Exploration and Development in Papua New Guinea: Proceedings of the Second PNG Petroleum Convention, Port Moresby, 31st May-2nd June 1993.*

GOWLAND, S. & RIDING, J.B., 1991. Stratigraphy, sedimentology and palaeontology of the Scarborough Formation (Middle Jurassic) at Hundale Point, North Yorkshire. *Proceedings of the Yorkshire Geological Society 48*, 375-392.

HELBY, R. MORGAN, R. & PARTRIDGE, A.D., 1987. A palynological zonation of the Australian Mesozoic. *Memoir of the Association of Australasian Palaeontologists 4*, 1-94.

HELBY, R. & PARTRIDGE, A.D., in prep. A palynological zonation of the Australian Mesozoic: an update.

LENTIN, J.K. & WILLIAMS, G.L., 1993. Fossil dinoflagellates: index to genera and species. 1993 edition. *American Association of Stratigraphic Palynologists Contributions Series No. 28*, 856p.

NORRIS, G., 1965. Archaeopyle structures in Upper Jurassic dinoflagellates from southern England. *New Zealand Journal of Geology and Geophysics 8*, 792-806.

OTT, H.L., 1970. Palynological zonation of the Carnarvon Basin Jurassic-Miocene sequence. *Unpublished WAPET report*, 1-52.

PARKER, F.M., 1986. *Late Jurassic palynology of the Dampier Sub-Basin, Carnarvon Basin, Western Australia*. Unpublished PhD thesis, University of Western Australia, vol. 1; 334p., vol. 2; 63pls.

RIDING, J.B., 1984. Dinoflagellate range top biostratigraphy of the uppermost Triassic to lowermost Cretaceous of northwest Europe. *Palynology 8*, 195-210.

RIDING, J.B., FEDOROVA, V.A. & ILYINA, V.I., 1999. Jurassic and lowermost Cretaceous dinoflagellate cyst biostratigraphy of the Russian Platform and northern Siberia, Russia. *American Association of Stratigraphic Palynologists Contributions Series No. 36*, 179 p.

RIDING, J.B., PENN, I.E. & WOOLLAM, R., 1985. Dinoflagellate cysts from the type area of the Bathonian stage (Middle Jurassic; southwest England). *Review of Palaeobotany and Palynology 45*, 149-169.

RIDING, J.B. & THOMAS, J.E., 1992. Dinoflagellate cysts of the Jurassic System. 7-97 in Powell, A.J. (ed.). *A stratigraphic index of dinoflagellate cysts*. British Micropalaeontological Society Publications Series. Chapman and Hall, London.

RIDING, J.B. & THOMAS, J.E., 1997. Marine palynomorphs from the Staffin Bay and Staffin Shale formations (Middle-Upper Jurassic) of the Trotternish Peninsula, NW Skye. *Scottish Journal of Geology 33*, 59-74.

RILEY, L.A. & FENTON, J.P.G., 1982. A dinocyst zonation for the Callovian-Oxfordian succession of northwest Europe. *Palynology 6*, 193-202.

SARJEANT, W.A.S., 1961. Microplankton from the Kellaways Rock and Oxford Clay of Yorkshire. *Palaeontology 4*, 90-118.

SARJEANT, W.A.S., 1966. Dinoflagellate cysts with *Gonyaulax*-type tabulation. *Bulletin of the British Museum (Natural History), Geology, Supplement 3*, 107-156.

SARJEANT, W.A.S., 1968. Microplankton from the Upper Callovian and Lower Oxfordian of Normandy. *Revue de Micropaléontologie 10*, 221-242.

SARJEANT, W.A.S., 1972. Dinoflagellate cysts and acritarchs from the Upper Vardekløft Formation (Jurassic) of Jameson Land, East Greenland. *Kommissionen for Videnskabelige Undersøgelser i Grønland 195*, 69 p.

SARJEANT, W.A.S., 1976. *Energlynia*, new genus of dinoflagellate cysts from the Great Oolite Limestone (Middle Jurassic: Bathonian) of Lincolnshire, England. *Neues Jahrbuch für Geologie und Paläontolgie Monatshefte 1976(3)*, 163-173.

SARJEANT, W.A.S., 1978. A guide to the identification of Jurassic dinoflagellate cysts. *School of Geoscience, Louisiana State University, Miscellaneous Publication 78-1*, 107p.

SARJEANT, W.A.S., 1982. Dinoflagellate cyst terminology: a discussion and proposals. *Canadian Journal of Botany 60*, 922-945.

SATO, T., WESTERMANN, G.E.G., SKWARKO, S.K. & HASIBUAN, F., 1978. Jurassic biostratigraphy of the Sula Islands, Indonesia. *Geological Survey of Indonesia Bulletin 4*, 1-28.

STOVER, L.E. & EVITT, W.R., 1978. Analyses of Pre-Pleistocene organic-walled dinoflagellates. *Stanford University Publications, Geological Sciences 15*, 300p.

STOVER, L.E. & HELBY, R., 1987. Some Australian Mesozoic microplankton index species. *Memoir of the Association of Australasian Palaeontologists 4*, 101-134.

WALL, D. & DALE, B., 1968. Modern dinoflagellate cysts and the evolution of the Peridiniales. *Micropaleontology 14*, 265-304.

WIGGINS, V.D., 1975. The dinoflagellate Family Pareodiniaceae: a discussion. *Geoscience and Man 11*, 95-115.

WILLIAMS, G.L., LENTIN, J.K. & FENSOME, R.A., 1998. The Lentin and Williams Index of fossil dinoflagellates 1998 edition. *American Association of Stratigraphic Palynologists Contributions Series No. 34*, 817 p.

WOOLLAM, R., 1980. Jurassic dinocysts from shallow marine deposits of the East Midlands, England. *Journal of the University of Sheffield Geological Society 7.5*, 243-261.

WOOLLAM, R., 1982. Observations on the Jurassic dinocyst genera *Energlynia* and *Wanaea*. *Journal of Micropalaeontology 1*, 45-52.

WOOLLAM, R. & RIDING J.B., 1983. Dinoflagellate cyst zonation of the English Jurassic. *Institute of Geological Sciences Report 83/2*, 42p.

APPENDIX 1: SAMPLE DETAILS

1. Locations and operators of wells from which Australasian material has been studied

Well Name and Number	Latitude	Longitude	Operator
Buang-1	10° 35' 49.58"S	126° 04' 04.94"E	BHP
Circinus-1 ST1	12° 54' 44.97"S	124° 23' 23.89"E	Nippon Oil
Crux-1	12° 56' 38.49"S	124° 27' 09.32"E	Nippon Oil
Eclipse-2	12° 14' 13.30"S	124° 38' 41.44"E	BHP
Krill-1	10° 44' 54.52'S	126° 12' 06.74"E	BHP
*Magobu Island-1	08° 31' 47.39"S	143° 16' 31.18"E	Endeavour
*Omati-1	07° 26' 00.59"S	143° 57' 29.99"E	Island Exploration Co.
Scafell-1	21° 32' 43.79"S	114° 01' 08.02"E	BHP
Stag-1	20° 17' 13.78"S	116° 15' 28.71"E	Hadson
Sunrise-2	09° 29' 57.94"S	128° 06' 12.37"E	Woodside
Sunset-1	09° 38' 36.37"S	127° 58' 34.77"E	Shell

* - All listed wells are from Australia, except Magobu Island-1 and Omati-1 which are from Papua New Guinea.

2. Non-Australian and seafloor samples

Sample Number	Location	Age	Reference
2.1. Rowley Terrace, offshore Western Australia			
AGSO 96/DR014/5	16° 50' 01"S 117° 35' 13"E	Bajocian	Burger (1996)
2.2. Sula Islands, Indonesia			
8B	outcrop locality 8B	Oxfordian	Sato *et al.* (1978)
2.3. Zohar-5 borehole, southern Israel			
MS 2	West of the Dead Sea	Bathonian	Conway (1978)
2.4. Ketton Grange quarry, Ketton, Lincolnshire, U.K.			
MPA 15438	SK 4978 3062	Bathonian	Sarjeant (1976)

APPENDIX 2: REGISTER OF FIGURED SPECIMENS

All palynomorph specimens figured in this paper are listed here, together with essential details. The specimens are mainly curated in the Commonwealth Palaeontological Collection (CPC) of the Australian Geological Survey Organisation, Canberra. The species of *Wanaea* are listed alphabetically and the location (EF) of the specimens on the microscope slides are all 'England-Finder' co-ordinates. These were taken with the slide label to the left of the observer; the microscope stage opening toward the microscope user. The coding for types is as follows: H = holotype; P = paratype; T = topotype, where appropriate. All specimens of new taxa examined during this study contributed to the specific concepts described. Therefore, all the figured specimens which are not holotypes are paratypes. SGM = single grain mount. The single grain mounts do not have unique numbers; they are numbered sequentially for each species within a particular sample. The specimens are from outcrop, conventional core, sidewall core and ditch cutting samples.

Species	Fig(s)	Slide No.	EF.	Locality
W. acollaris	1A	MPA 15438/2*	T40/1	Ketton Grange Quarry, England, U.K.
W. acollaris	1B	MPA 15438/2*	G37/1	Ketton Grange Quarry, England, U.K.
W. acollaris	1C	MPA 15438/2*	D43/3	Ketton Grange Quarry, England, U.K.
W. acollaris	1D	MPA 15438/2*	U26/4	Ketton Grange Quarry, England, U.K.
W. acollaris	1E	MPA 15438/2*	H31/1	Ketton Grange Quarry, England, U.K.
W. acollaris	1F	MPA 15438/2*	E43/1	Ketton Grange Quarry, England, U.K.
W. acollaris	1G	MPA 15438/2*	N30	Ketton Grange Quarry, England, U.K.
W. acollaris	1H	MPA 15438/1*	M46/4	Ketton Grange Quarry, England, U.K.
W. acollaris	1I	MPA 15438/2*	N30	Ketton Grange Quarry, England, U.K.

* - collections of the British Geological Survey, Nottingham, UK.

Species	Type	Fig(s)	SGM/Slide No.	EF	Well (depth, m)	CPC No.
W. enoda	P	2A	Ass. sl. 3	P9	Magobu Island-1 (2266.02)	35841
W. enoda	P	2B	SGM 4 (i)	P23/1	Magobu Island-1 (2266.02)	35842
W. enoda	P	2C	SGM 4 (ii)	P22/1	Magobu Island-1 (2266.02)	35843
W. enoda	P	2D	SGM 6 (v)	M29	Magobu Island-1 (2266.02)	35844
W. enoda	P	2E	SGM 6 (iii)	O30/2	Magobu Island-1 (2266.02)	35845
W. enoda	P	2F	SGM2 (ii)	L30	Magobu Island-1 (2266.02)	35846
W. enoda	P	2G	Ass. sl. 3	K5/2	Magobu Island-1 (2266.02)	35847
W. enoda	H	2H	Ass. sl. 3	E20/1	Magobu Island-1 (2266.02)	35848
W. enoda	P	2I	Ass. sl. 3	N9	Magobu Island-1 (2266.02)	35849
W. lacuna	P	3A	SGM 1 (i)	L33	Sunrise-2 (2122.05)	35850
W. lacuna	P	3B	SGM 2 (iv)	M38/2	Sunrise-2 (2122.33)	35851
W. lacuna	P	3C	SGM 1 (iv)	K32/4	Sunrise-2 (2122.05)	35852
W. lacuna	P	3D	SGM 1 (i)	L40	Sunrise-2 (2122.33)	35853
W. lacuna	P	3E	SGM 1 (iii)	Q30/2	Sunrise-2 (2122.25)	35854
W. lacuna	P	3F	SGM 3 (v)	N35	Sunrise-2 (2122.33)	35855
W. lacuna	P	3G	SGM 2 (iii)	O38	Sunrise-2 (2122.25)	35856
W. lacuna	P	3H	SGM 4 (iv)	F33	Sunrise-2 (2122.33)	35857
W. lacuna	P	3I	SGM 4 (i)	H32	Sunrise-2 (2122.33)	35858
W. lacuna	H	3J	SGM 1 (i)	Q32/4	Sunrise-2 (2122.25)	35859
W. lacuna	P	3K	SGM 1 (vi)	J41/3	Sunrise-2 (2122.33)	35860
W. lacuna	P	3L	SGM 2 (iv)	N26/1	Sunrise-2 (2122.05)	35861
W. spectabilis		4A	SGM 4 (i)	M33/1	Eclipse-2 (2477.00)	35862
W. spectabilis		4B	SGM 1 (iv)	M36	Eclipse-2 (2477.00)	35863
W. spectabilis		4C	SGM 3 (i)	N27/1	Eclipse-2 (2477.00)	35864
W. spectabilis		4D	SGM 8 (ii)	J35/1	Eclipse-2 (2477.00)	35865
W. spectabilis		4E	SGM 4 (ii)	L31/2	Eclipse-2 (2477.00)	35866
W. spectabilis		4F	SGM 1 (i)	K36	Eclipse-2 (2477.00)	35867
W. spectabilis		5	Sl.k1	T9/1	Scafell-1 (1346.80)	35868

Species	Type	Fig(s)	SGM/Slide No.	EF	Well (depth, m)	CPC No.
W. spectabilis	H	6A,B	W.451/91	S42/4	outcrop, Era River, PNG	P.16235*
W. spectabilis	T	6C	W.451/93	P33/3	outcrop, Era River, PNG	P.16234*
*- Museum Victoria registration numbers						
W. clathrata		7A	K	F24	Sula, Indonesia unregistered outcrop sample	
W. spectabilis		7B	SGM 4 (i)	M33/1	Eclipse-2 (2477.00)	35862
W. talea	H	7C, 8I	P.17297*	F36	Omati-1 (4285.54**)	P.17297*
W. talea	P	8A	SGM 4 (ii)	S28/1	Buang-1 (3518.50)	35869
W. talea	P	8B	SGM 1 (i)	O32/1	Crux-1 (3266.60)	35870
W. talea	P	8C	SGM 2 (iii)	G31	Circinus-1 ST1 (3517.50)	35871
W. talea	P	8D,E	SGM 3 (i)	J39/2	Crux-1 (3266.60)	35872
W. talea	P	8F	SGM 3 (ii)	J39/1	Crux-1 (3266.60)	35873
W. talea	P	8G,H	SGM 1 (i)	Q38	Circinus-1 ST1 (3517.50)	35874
*- Museum Victoria registration number						
** - range depth of ditch cuttings: 4285.54m-4288.59m						
W. verrucosa	H	9A	SGM 2 (i)	Q21/2	Stag-1 (800.00)	35875
W. verrucosa	P	9B	SGM 1 (i)	Q24/4	AGSO 96/DR014/5 (seafloor)	35876
W. verrucosa	P	9C	SGM 4 (vi)	Q37/4	AGSO 96/DR014/5 (seafloor)	35877
W. verrucosa	P	9D-F	SGM 3 (iv)	M23/4	AGSO 96/DR014/5 (seafloor)	35878
W. verrucosa	P	9G-I	SGM 5 (i)	M30	AGSO 96/DR014/5 (seafloor)	35879
W. verrucosa	P	9J-L	SGM 4 (i)	S34	AGSO 96/DR014/5 (seafloor)	35880
W. zoharensis	T	10A	MS 2	M24/4	Zohar-5 (1190.00*)	ML 1459**
W. zoharensis	T	10B	MS 2	O31/4	Zohar-5 (1190.00*)	ML 1459**
W. zoharensis	T	10C	MS 2	M27/4	Zohar-5 (1190.00*)	ML 1459**
W. zoharensis	T	10D	MS 2	J14/4	Zohar-5 (1190.00*)	ML 1459**
W. zoharensis	T	10E	MS 2	M31	Zohar-5 (1190.00*)	ML 1459**
W. zoharensis	T	10F	MS 2	G29	Zohar-5 (1190.00*)	ML 1459**
W. zoharensis	H	10G,H	MS 2	B31/4	Zohar-5 (1190.00*)	ML 1459**
W. zoharensis	T	10I	MS 2	L32	Zohar-5 (1190.00*)	ML 1459**
*- range depth: 1190.00m-1197.00m						
**- Centre for Palynology, University of Sheffield, Sheffield, UK, type/figured slide collection registration number.						

Phallocysta granosa sp. nov., a Mid Jurassic (Bathonian) dinoflagellate cyst from the Timor Sea, Australia

JAMES B. RIDING and ROBIN HELBY

RIDING, J.B. & HELBY, R., 2001:09:21. *Phallocysta granosa* sp. nov., a Mid Jurassic (Bathonian) dinoflagellate cyst from the Timor Sea, Australia. *Memoir of the Association of Australasian Palaeontologists 24*, 59-63. ISSN 0810 8889.

Phallocysta granosa sp. nov. is described from the Timor Sea, Australia. This new dinoflagellate cyst has stratigraphical utility in the Bathonian (Mid Jurassic) *Caddasphaera halosa* and *Wanaea verrucosa* zones.

James B. Riding, Australian Geological Survey Organisation, GPO Box 378, Canberra, ACT 2601, Australia (present address: British Geological Survey, Keyworth, Nottingham NG12 5GG, UK [e-mail: jbri@bgs.ac.uk]); Robin Helby (corresponding author), 356A Burns Bay Road, Lane Cove, NSW 2066, Australia (e-mail: rhelby@ozemail.com.au). 10 November 2000.

Keywords: dinoflagellate cysts, Middle Jurassic, Australia, biostratigraphy, taxonomy

THE PALYNOLOGICAL zonation of the Australian Mesozoic published by Helby *et al.* (1987) was the first attempt to provide an integrated, pan-Australian microplankton and spore-pollen zonation. Only the basic framework of the zonation was provided in anticipation that further contributions, particularly the documentation of new taxa, would be necessary as the zonation scheme evolved. This paper is one of a series providing the taxonomic foundation necessary to formalise widely used unpublished subdivisions of these zones. These subzones have widespread currency within the hydrocarbon industry due to the legislative requirement for the release of technical data under the Petroleum (Submerged Lands) Act 1967. The informal subdivisions of the Helby *et al.* (1987) zonation have been entered into the Australian Geological Survey Organisation (AGSO) STRATDAT database. A diagrammatic update of the Helby *et al.* (1987) zonal scheme is presented by Foster (this volume), and will be described fully by Helby & Partridge (in prep.). This taxonomic project is an initiative of the Petroleum and Marine Division of AGSO.

This paper provides a formal description of *Phallocysta granosa* sp. nov. from a Mid Jurassic (Bathonian) dinoflagellate cyst assemblage in samples from the Timor Sea (Appendix 1). The new taxon has stratigraphical utility within the Bathonian *Caddasphaera halosa* and *Wanaea verrucosa* zones of Helby & Partridge (in prep.). The figured specimens in this paper are from the Bathonian part of the Plover Formation (Plover III sequence of Patillo & Nichols, 1990) in Sunrise 2 and Sunset 1 wells, offshore north-western Australia (Foster, this volume; Appendices 1, 2).

SYSTEMATIC PALYNOLOGY

Most of the morphological terminology for dinoflagellate cysts is from Evitt (1985). References to author citations of other taxa discussed are given in the bibliography of Williams *et al.*, 1998, p. 747-817). The figured specimens are housed in the Commonwealth Palaeontological Collection (CPC) of the Australian Geological Survey Organisation, Canberra, and the collection of Woodside Energy Ltd., Perth (Appendices 1, 2).

This study has been conducted using both single grain mounts (or mounts with multiple specimens) and strew mounts. All samples studied are from conventional cores. The photomicrographs in this paper were all taken using an Olympus DP10 digital camera system coupled to a Zeiss Axioskop photomicroscope, housed at AGSO. Some extraneous palynodebris, not adherent to the figured specimens, has been digitally removed in selected images.

The images illustrated in this paper are selected from a digital database that contains many more images than have been figured. The sample details, key morphological data and measurements of each specimen are held on open file spreadsheets. The image database may be accessed on the AGSO website (http://www.agso.gov.au).

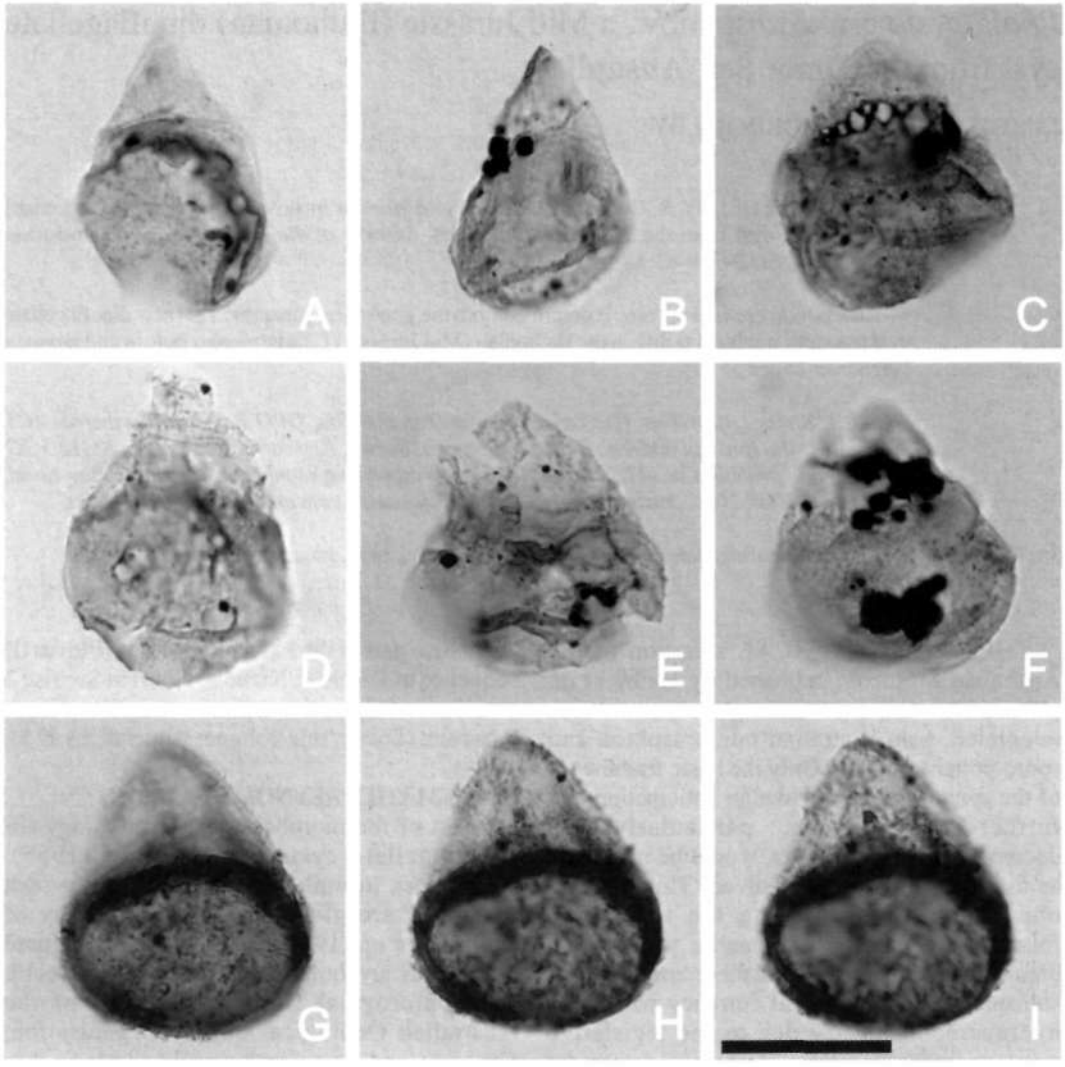

Fig. 1. Phallocysta granosa sp. nov. All from cores in Sunrise-2 well at 2122.25m (G-I) and Sunset-1 well at 2216.67m (C), 2216.66m (B, E-F), 2214.30m (A) and 2208.65m (D). All photomicrographs taken using plain transmitted light. The scale bar of 25µm in Fig. 1I refers to all photomicrographs. Figs A, C-E are composite photomicrographs. Figs G-I is the holotype; the remainder, paratypes. Note small size, elongate subconical outline, variable nature (rounded to pointed) of the apical extremity, lack of an apical horn, rounded antapex, ellipsoidal/subcircular endocyst and granulate-spinose periphragm. A - pale specimen with sharp apical extremity. B - note pyrite crystals, folding close to antapex and sharp apical extremity. C - CPC 35881, relatively wide, squat specimen with relatively large endocyst. Note granulate periphragm. D - note thin, diaphanous periphragm and randomly developed folds. E - highly folded, squat specimen. Note anterior intercalary archaeopyle. F - specimen with much growth of pyrite crystals. Note granulate periphragm. G-I - CPC 35882, well preserved specimen. Note folding of endocyst and granulose/spinose ornamentation of periphragm and archaeopyle in I.

This species has been used in unpublished reports, which are now in the public domain (on open file). To maximise the utility of this species, the informal 'M.P.' (microplankton) codes used are listed, separate from the formal synonymy listing, under the heading 'Previous Australian usage'.

Dinoflagellate cysts

Phallocysta Dörhöfer & Davies 1980 emend. Riding 1984

1994 *Andreedinium* Below 1987 Riding, p.13.

Type species. Phallocysta eumekes Dörhöfer &

Davies 1980 emend. Riding 1984

Phallocysta granosa sp. nov. (Figs 1A-I)

?1988 gen. et sp. indet. AR; Helby *et al.*, fig. 3B.

Previous Australian usage
M.P. 903 – Helby.
?M.P. 903B – Helby.

Description. A small to intermediate sized (Stover & Evitt, 1978, p. 5) species of *Phallocysta* with an elongate subconical outline. The pericyst is cone shaped, the distal extremity of the apical horn is blunt to sharply pointed and the antapex is rounded. The endocyst is ellipsoidal to subcircular in outline and fills most of the pericyst, apart from the apical part of the pericoel. The endophragm is relatively thick (c. 1µm) and microscabrate to microgranulate. By contrast, the periphragm is thinner (c. 0.5µm) and ornamented by granules and/or spinules. Where spinules are developed, they are irregular in density and short, simple and solid. They vary from 0.5 to 1µm in length and are c. 0.5µm in width at the base. Both the granules and spinules are nontabular and normally are of moderate density. Both cyst layers are susceptible to folding.

Dimensions (µm; n=20): Min. (Mean) Max.
Length of pericyst: 37 (43) 59
Length of pericoel: 8 (14) 20
Length of endocyst: 22 (30) 42
Equatorial width: 22 (32) 40

The measured specimens are from core from Sunrise-2 well at 2122.25m and Sunset-1 well at 2216.67m, 2216.66m, 2214.30m, 2208.65m and 2204.80m.

Comments. This species of *Phallocysta* has a densely granulate to spinose periphragm (Fig. 1). The ornamentational style is somewhat variable in that some forms have an irregular covering of short spinules and others are largely microgranulate (Fig. 1). The apical horn varies from being sharply-pointed (Figs 1A-B) to rounded (Figs 1E-I). Both cyst layers are closely appressed in the hypocyst; the species is consistently epicavate and the thin periphragm separates from the more robust endophragm above the equator. There is no manifestation of paratabulation apart from the anterior intercalary periarchaeopyle (Figs 1E, I).

Comparison. Phallocysta granosa differs from the other species of the genus by its relatively small size and the granulate/spinose ornamentation. *Phallocysta arctica* (Below 1987) Riding 1984 is more elongate than *P. granosa* (the holotype is 52µm long according to Below, 1987, p. 113), and the former is extremely densely granulate to microgranulate (Below, 1987). The Early-Mid Jurassic (latest Toarcian-early Bajocian) species *Phallocysta elongata* (Beju 1971) Riding 1994 is also more elongate than *P. granosa*, the former is also psilate to occasionally scabrate and is typically flask-shaped (Riding, 1994). *Phallocysta elongata* may be relatively sparsely ornamented and has a distinct apical horn. Rare late Toarcian to Aalenian specimens of *P. elongata* may be microgranulate; for example, those illustrated as *P. minuta* Prauss 1989 by Riding *et al.* (1991, pl. 2, figs 23-25). However, Lentin & Williams (1993) pointed out that *P. minuta* was invalid and proposed *P. subconica* as a substitute name. Subsequently, Riding (1994) synonymised *P. subconica* with *P. elongata.* The species *P. granosa* and *P. elongata* are clearly similar. However, the latter is generally smooth and rarely microgranulate, whereas the former is distinctly granulate to occasionally spinose and is generally more squat. The only other Australian species of *Phallocysta* is *P? erregulensis* (Filatoff 1975) Stover & Helby 1987. This species is larger than *P. granosa*, commonly antapically bilobate, may have a rounded apical extremity and has a smooth, granulate to spinose periphragm and rarely, a spinose endophragm (Stover & Helby, 1987, fig. 11). Furthermore, *Phallocysta? erregulensis* may be cavate or cornucavate. The cornucavate forms of *P? erregulensis* have a distinctive trilobate pericyst (Stover & Helby, 1987, fig. 10E). *Phallocysta eumekes* is significantly larger than *P. granosa*. The former also has a consistently smooth endophragm, frequently has a smooth periphragm, and has a distinct apical horn and a distinctly lobate hypocyst (Dörhöfer & Davies 1980; Riding 1984). *Phallocysta frommernensis* Below 1987 from the Aalenian of southern Germany is relatively small and squat. It also has a spongy, densely gemmate/verrucate periphragm (Below, 1987, pl. 22, figs 9-18). The Aalenian-Bajocian species *Phallocysta thomasii* Smelror 1991 is similar in size to *P. granosa* and has a spinose periphragm. However the former taxon has a strongly differentiated apical horn and is antapically bilobate.

Helby *et al.* (1988, fig. 3B) illustrated as "gen. et sp. indet. AR", a single specimen from the Callovian Oraka Sandstone of New Zealand which

closely resembles *Phallocysta granosa*.

Derivation of name. From the Latin *granosus*, meaning full of seeds or grains and referring to the distinctive granulate ornamentation of the periphragm in this species.

Holotype and type locality. Figures 1G-I, CPC 35882, from conventional core in Sunrise-2 well at 2122.25m.

Stratigraphical distribution. *Phallocysta granosa* ranges from the Bathonian, lower part of the *Caddasphaera halosa* Zone (subzone 7cii) to the middle part of the *Wanaea verrucosa* Zone (subzone 7ciaii) in Australia (Foster, this volume; Helby & Partridge, in prep.). The species has been tentatively identified in the Callovian Oraka Sandstone of New Zealand (Helby *et al.*, 1988).

ACKNOWLEDGEMENTS

The authors are grateful to Dr Clinton B. Foster (AGSO, Canberra) for promoting and facilitating this work and for editorial guidance and advice. Christian Thun and Andrew Kelman (AGSO, Canberra) provided invaluable help respectively with preparations and the manipulation of digital images. Mr Eddie Resiak of the core and cuttings repository at AGSO, Canberra courteously provided access to core material. Dr Neil G. Marshall (Woodside Energy Ltd., Perth) kindly provided slides on request. Drs J. Goodall and A. D. Partridge are thanked for reviewing the manuscript. J. B. Riding publishes with the permission of the Chief Executive Officer, AGSO.

REFERENCES

BELOW, R., 1987. Evolution und Systematik von Dinoflagellaten-Zysten aus der Ordnung Peridiniales. I. Allgemeine Grundlagen und Subfamilie Rhaetogonyaulacoideae (Familie Peridiniaceae). *Palaeontographica Abteilung B 205*, 1-164.

DÖRHÖFER, G. & DAVIES, E.H., 1980. Evolution of archeopyle and tabulation in rhaetogonyaulacinean dinoflagellate cysts. *Miscellaneous Publication of the Life Sciences Division, Royal Ontario Museum, Toronto*, 91p.

EVITT, W.R., 1985. *Sporopollenin dinoflagellate cysts. Their morphology and interpretation*. American Association of Stratigraphic Palynologists Foundation, Dallas, 333 p.

FOSTER, C.B., this volume. Introduction.

HELBY, R. MORGAN, R. & PARTRIDGE, A.D., 1987. A palynological zonation of the Australian Mesozoic. *Memoir of the Association of Australasian Palaeontologists 4*, 1-94.

HELBY, R. & PARTRIDGE, A.D., in prep. A palynological zonation of the Australian Mesozoic: an update.

HELBY, R., WILSON, G.J., & GRANT-MACKIE, J.A., 1988. A preliminary biostratigraphic study of Middle to Late Jurassic dinoflagellate assemblages from Kawhia, New Zealand. *Memoir of the Association of Australasian Palaeontologists 5*, 125-166.

PATILLO, J. & NICHOLS, P.J., 1990. A tectonostratigraphic framework for the Vulcan Graben, Timor Sea region. *APEA Journal 30*, 27-51.

RIDING, J.B., 1984. A palynological investigation of Toarcian to early Aalenian strata from the Blea Wyke area, Ravenscar, North Yorkshire. *Proceedings of the Yorkshire Geological Society 45*, 109-122.

RIDING, J.B., 1994. A taxonomic study of the Mesozoic dinoflagellate cysts *Phallocysta elongata* (Beju 1971) comb. nov., emend. nov. and *Wallodinium cylindricum* (Habib 1970) Duxbury 1983 emend. nov. *Palynology* 18, 11-22.

RIDING, J.B., WALTON, W. & SHAW, D., 1991. Toarcian to Bathonian (Jurassic) palynology of the Inner Hebrides, northwest Scotland. *Palynology 15*, 115-179.

STOVER, L.E. & EVITT, W.R., 1978. Analyses of Pre-Pleistocene organic-walled dinoflagellates. *Stanford University Publications, Geological Sciences 15*, iii + 300 p.

STOVER, L.E. & HELBY, R., 1987. Some Australian Mesozoic microplankton species. *Memoir of the Association of Australasian Palaeontologists 4*, 101-134.

WILLIAMS, G.L., LENTIN, J.K. & FENSOME, R.A., 1998. The Lentin and Williams Index of fossil dinoflagellates 1998 edition. *American Association of Stratigraphic Palynologists Contributions Series No. 34*, 817 p.

APPENDIX 1: LOCATIONS OF WELLS

Well Name/Number	Latitude	Longitude	Operator
Sunrise-2	09° 29' 57.94"S	128° 06' 12.37"E	Woodside
Sunset-1	09° 38' 36.37"S	127° 58' 34.77"E	Shell

APPENDIX 2: REGISTER OF FIGURED SPECIMENS

All figured specimens are listed here, together with essential details. The specimens are curated in the Commonwealth Palaeontological Collection (CPC) of the Australian Geological Survey Organisation, Canberra, and the collections of Woodside Energy Ltd., Perth. The location (EF) of the specimens on the microscope slides are all 'England-Finder' co-ordinates and were taken with the slide label to the left of the observer; the microscope stage opening toward the microscope user. The coding for types is as follows: H = holotype; P = paratype. SGM = single grain mount. The single grain mounts do not have unique numbers; they are numbered sequentially for each species within a particular sample. The specimens are all from conventional core samples.

Species	Type	Fig(s)	SGM/Slide No.	EF	Well (depth, m.)	CPC No.
P. granosa	P	1A	Ass. sl. 2	N12/4	Sunset-1 (2214.30)	*
P. granosa	P	1B	Ass. sl. 1	J20/3	Sunset-1 (2216.66)	*
P. granosa	P	1C	SGM 2 (i)	Q69	Sunset-1 (2216.67)	35881
P. granosa	P	1D	Ass. sl. 2	O36	Sunset-1 (2208.65)	*
P. granosa	P	1E	Ass. sl. 1	U23	Sunset-1 (2216.66)	*
P. granosa	P	1F	Ass. sl. 1	X35	Sunset-1 (2216.66)	*
P. granosa	H	1G-I	SGM 1 (i)	M27/4	Sunrise-2 (2122.25)	35882

* - Collections of Woodside Energy Ltd., Perth, Western Australia

Microplankton from the Mid Jurassic (late Callovian) *Rigaudella aemula* Zone in the Timor Sea, north-western Australia

JAMES B. RIDING and ROBIN HELBY

RIDING, J.B. & HELBY, R., 2001:09:21. Microplankton from the Mid Jurassic (late Callovian) *Rigaudella aemula* Zone in the Timor Sea, north-western Australia. *Memoir of the Association of Australasian Palaeontologists 24*, 65-110. ISSN 0810 8889.

A Mid Jurassic (late Callovian) suite of marine microplankton is documented from the Elang Formation and its equivalents in the Timor Sea, offshore north-western Australia. Two genera, *Voodooia* and *Woodinia* and eleven species of dinoflagellate cysts are described as new. The dinoflagellate cyst species are *Ctenidodinium ancorum, Ctenidodinium fuscibasilarum, Ctenidodinium planocristatum, Durotrigia magna, Fusiformacysta terniana, Lithodinia protothymosa, Meiourogonyaulax penitabulata, Meiourogonyaulax viriosa, Voodooia tabulata, Woodinia pedis* and *Yalkalpodinium elangiana*. *Nummus apiculus* is a new acritarch species.

The dinoflagellate cyst genus *Fusiformacysta* is emended to stress the 3P nature of the archaeopyle and the presence of at least one, small anterior intercalary paraplate. The genera *Lithodinia* and *Meiourogonyaulax* are maintained as separate, based on operculum character. *Tabulodinium* and its single species, *T. senarium*, are both emended in order to document a revised paratabulation pattern and the precise archaeopyle style (anterior intercalary, type 2I). The ornamentation of *T. senarium* is commonly destroyed by oxidation. The genus *Yalkalpodinium* is emended to accommodate the morphology of the new species *Y. elangiana*. All the newly described microplankton taxa have stratigraphical utility in the *Wanaea digitata* and *Rigaudella aemula* (Interval) Zones.

James B. Riding, Australian Geological Survey Organisation, GPO Box 378, Canberra, ACT 2601, Australia (present address: British Geological Survey, Keyworth, Nottingham NG12 5GG, UK [e-mail: jbri@bgs.ac.uk]); Robin Helby (corresponding author), 356A Burns Bay Road, Lane Cove, NSW 2066, Australia (e-mail: rhelby@ozemail.com.au). 10 November 2000.

Keywords: dinoflagellate cysts, acritarch, Middle Jurassic, Australia, biostratigraphy, taxonomy

THE PALYNOLOGICAL zonation of the Australian Mesozoic published by Helby *et al.* (1987) was the first attempt to provide an integrated, pan-Australian microplankton and spore-pollen zonation. Only the basic framework of the zonation was provided in anticipation that further contributions, particularly the documentation of new taxa, would be necessary as the zonation scheme evolved. This paper is one of a series providing the taxonomic foundation necessary to formalise the widely used unpublished subdivisions of these zones. These subzones have widespread currency within the hydrocarbon industry due to the legislative requirement for the release of technical data under the Petroleum (Submerged Lands) Act 1967. The informal subdivisions of the Helby *et al.* (1987) zonation have been entered into the Australian Geological Survey Organisation (AGSO) STRATDAT database. A diagrammatic update of the Helby *et al.* (1987) zonal scheme is presented by Foster (this volume), and will be fully described by Helby & Partridge (in prep.). This taxonomic project is an initiative of the Petroleum and Marine Division of AGSO.

This paper provides formal descriptions of previously undescribed marine microplankton taxa from Mid Jurassic (late Callovian) palynofloras recorded in samples from the Elang Formation and its equivalents in the Bayu-Undan gas field and the Challis oil field, Timor Sea, offshore north-western Australia (Figs 1, 2; Appendix 1). All the new taxa have stratigraphical utility within the *Wanaea digitata* and *Rigaudella aemula* (Interval) Zones of Helby *et al.* (1987). The figured specimens are from samples in the Broome-3 Town Bore, Challis-11-ST1, ST2, Investigator-1, Jabiru-2, Layang-1, Montebello-1, Rowan-1ST, Tamar-1, Tern-1, Tern-

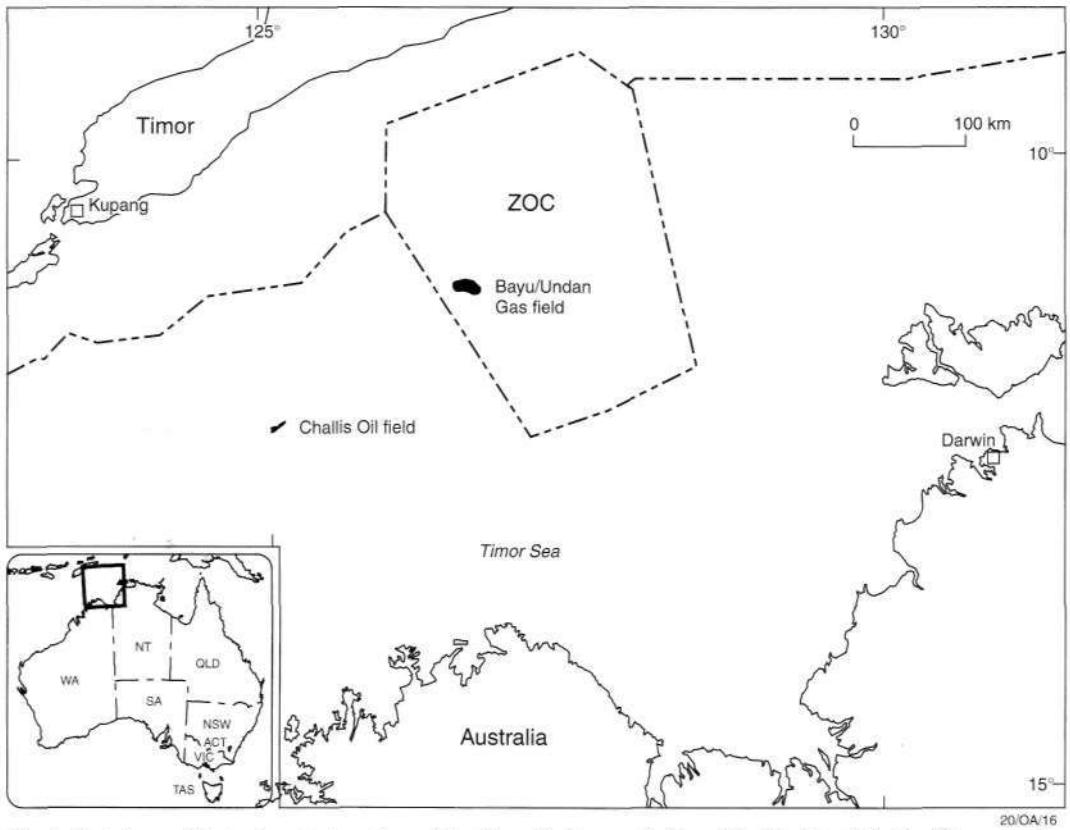

Fig. 1. Sketch map illustrating the locations of the Bayu/Undan gas field and the Challis oil field, offshore north-west Australia. The material in this contribution derives from the Upper Callovian strata from wells in these two fields. ZOC stands for the Zone of Cooperation. The inset map at the bottom left illustrates the location of the area depicted in the main map.

2, Undan-1, Undan-3 and Undan-4 wells (Foster, this volume; Appendices 1, 2).

Helby *et al.* (1987, p. 27) stated that their *Rigaudella aemula* Interval Zone is of late Callovian to earliest Oxfordian age based upon the intercalation of the zone between the mid Callovian and Oxfordian (Helby *et al.*, 1987, fig. 12). This evidence is from European palynological data (Riley & Fenton, 1982) and macrofauna, respectively (Arkell, unpublished reports to WAPET). Davey (1987, fig. 3), however, placed the zone entirely within the late Callovian, and assigned it to the lower part of his *Wanaea digitata* Zone. Francis & Westermann (1993, fig. 1b), also interpreted the age of the *Rigaudella aemula* Interval Zone to be late Callovian. However, these authors also suggested that it is most likely to be late Callovian to earliest Oxfordian as originally stated by Helby *et al.* (1987) (Francis & Westermann, 1993, fig. 7). The conclusions of Francis & Westermann (1993, fig. 7) were based on linking the Australasian molluscan faunas to north-west Europe by the several-order correlation of various ammonite faunal provinces. Burger (1996, fig. 2) assigned the *Rigaudella aemula* Interval Zone to the entire Callovian Stage, except the latest Callovian, within AGSO timeslice J-7. There is little direct evidence of Australian-European correlations within the Callovian.

SYSTEMATIC PALYNOLOGY

Here, two new genera and eleven new species of dinoflagellate cyst and one new species of acritarch are described. The genera are listed in alphabetical order within the two groups; for the dinoflagellate cysts, the recent suprageneric classification of Fensome *et al.* (1993) is not used. The dimensions are all given in micrometres (μm). For descriptive purposes, the cyst sizes, small, intermediate and large, are after Stover & Evitt (1978, p. 5). Therefore, intermediate size dinoflagellate cysts have a maximum dimension of between 50μm and 100μm. Small and large forms are less than 50μm and over 100μm respectively.

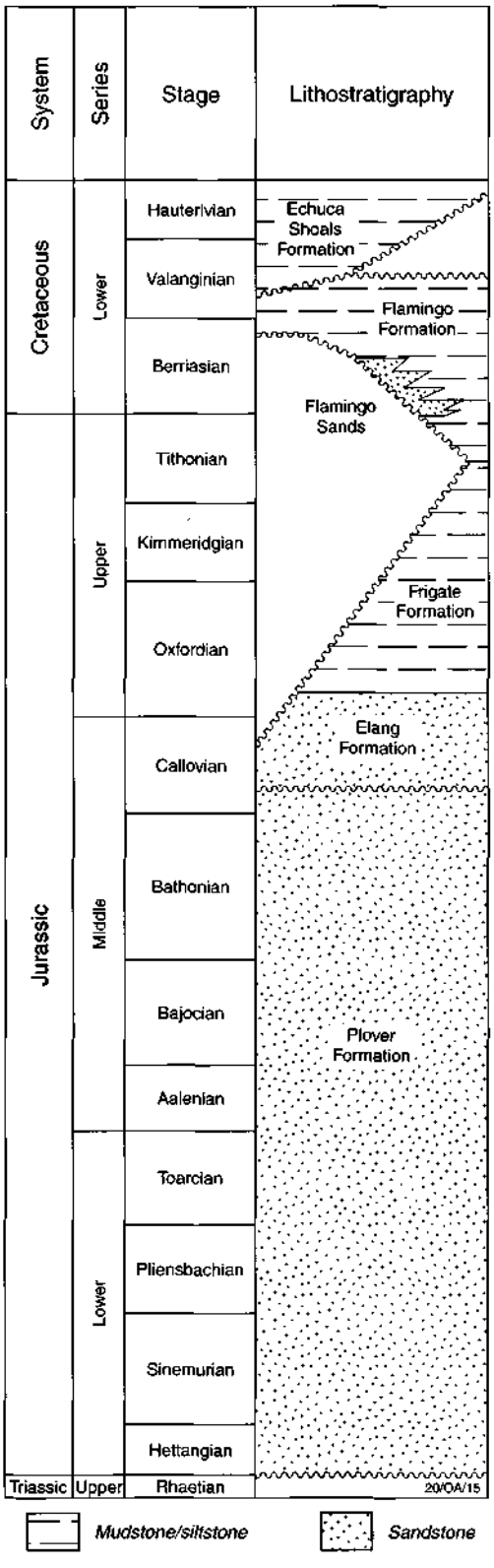

The majority of the morphological terminology for the dinoflagellate cysts are those used by Evitt (1985). However, the term loisthocyst refers to what remains of a dinoflagellate cyst after the operculum (or the separate opercular pieces) has (have) detached (Sarjeant *et al.*, 1987, p. 26, 27). Where appropriate, the dinoflagellate cyst paraplate notation system used throughout is Kofoidian, as opposed to the 'Taylor-Evitt' scheme of Evitt (1985). References to author citations of taxa discussed are not given here. These may be found in the bibliography of Williams *et al.*, 1998, p. 747-817). All figured specimens are housed in the Commonwealth Palaeontological Collection (CPC) of the Australian Geological Survey Organisation, Canberra (see Appendix 2).

This study has been conducted almost exclusively using single and multiple grain mounts and all the figured specimens, except for those of *Tabulodinium senarium* Dodekova 1990, are from these single species slides. The vast majority of the samples which were studied, are from conventional core and sidewall cores. However, a small number of ditch cuttings samples were also used. The photographs in the seventeen photomicrograph plates (Figs 3-13, 15, 16 and 18-21) were taken using an Olympus DP10 digital camera system coupled to a Zeiss Axioskop photomicroscope, housed at AGSO. Some extraneous palynodebris, which is not adherent to the figured specimens, has been digitally removed in selected images.

The specimen images herein are taken from a digital database containing many more images than have been figured. Sample details, morphological data and measurements of each specimen are held on open file spreadsheets. The image database may be accessed on the AGSO website (http://www.agso.gov.au).

Many of these new taxa have been extensively used in unpublished reports, which are now in the public domain (open file). In order to maximise the utility of the species, the informal names and/or codes are listed separate from any formal synonymy listing, under the heading 'Previous Australian usage'. To provide continuity,

Fig. 2. Regional Jurassic and Lower Cretaceous lithostratigraphy of the northern Bonaparte Basin, offshore north-west Australia; based on Brooks *et al.* (1996) and Whittam *et al.* (1996). The new microplankton described in this contribution are mainly from the Callovian part of the Elang Formation and its equivalents. Specimens from Investigator-1 and Montebello-1 are from the Carnarvon Basin, WA.

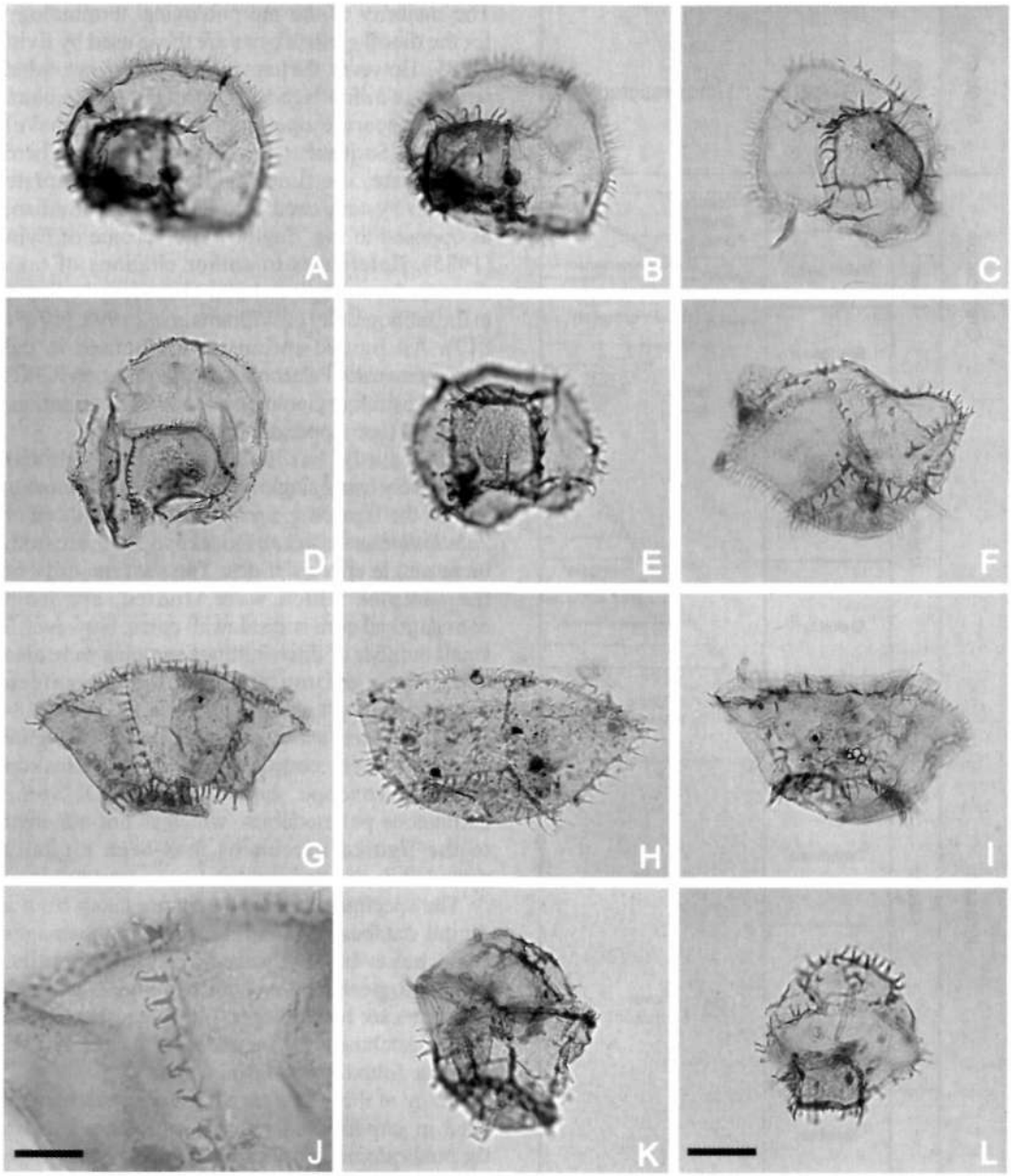

Fig. 3. Ctenidodinium ancorum sp. nov. The specimens are from a sidewall core in Rowan-1 well at 3183.00m (Figs 3G, 3J) and conventional core from Undan-1 well at 2996.15m (Figs 3D, H) and the Undan-4 well at 3135.24m (Figs 3A-C, E-F, I, K-L). The photomicrographs were all taken using plain transmitted light. The scale bar in Fig. 3L refers to all the photomicrographs, except Fig. 3J, and represents 25µm. Fig. 3J is a close-up to illustrate the detailed morphology of the parasutural processes; the scale bar represents 10µm. Figs 3G, J are the holotype; the remainder are paratypes. Note the relatively thin, microreticulate and/or microscabrate autophragm which may be slightly thicker and darker in the antapical (1'''' paraplate), the regular and typically distally bifid processes which surmount the parasutural ridges and the epicystal archaeopyle. A, B - CPC 35350, paratype; isolated hypocyst in apical view, median and low focus respectively. Note the irregularly thickened autophragm on the antapical (1'''') paraplate. C - CPC 35351, paratype; isolated hypocyst in apical view, low focus. Note that the longest processes are those around the antapical (1'''') paraplate. D - CPC 35352, paratype; isolated hypocyst in antapical view, low focus. A specimen with relatively short processes. E - CPC 35353, paratype; isolated hypocyst in antapical view, high focus. F - CPC 35354, paratype; (continued opposite)

wherever practical, the informal name has been retained.

Dinoflagellate cysts

Ctenidodinium Deflandre 1939 emend. Benson 1985

Type species. Ctenidodinium ornatum (Eisenack 1935) Deflandre 1939

Ctenidodinium ancorum sp. nov. (Figs 3A-L)

1996 *Ctenidodinium tenellum auct. non* Deflandre 1939; Burger, pl. 5, fig. R.

Previous Australian usage
M.P. 501 – Helby.
Ctenidodinium sp. 501 – Helby.
Ctenidodinium tenellum (pars.) – Morgan.

Description. A species of *Ctenidodinium* subhexagonal in dorsoventral outline, lacking an apical protuberance or horn. Autophragm thin, smooth to microscabrate and irregularly microreticulate. The antapical paraplate may have a thicker and thus marginally darker autophragm. Paratabulation fully indicated by parasutural ridges, which are regularly surmounted by processes. The processes are consistently solid, but otherwise are variable in form, being acuminate, bifid, conical/subconical or slender; distal terminations are bifurcate, blunt or sharp. Typically many processes are bifurcate with recurved terminations. At the distal end of the processes, immediately below the bifid tip there is a characteristic narrow, neck-like constriction which constitutes a natural break-point. Individual specimens may exhibit processes of varying morphologies. The longest processes are those in gonal positions around the antapical paraplate. Dark, subcircular accumulation bodies may be present.

Dimensions (µm; n=38): Min. (Mean) Max.
Length of cyst excl. spines: 57 (73) 86
Length of epicyst excl. spines: 16 (28) 40
Length of hypocyst excl. spines: 36 (53) 66
Width of cyst excl. spines: 57 (77) 106
Length of spines: 2 (5) 10
Height of parasutural ridges: 1 (2) 4

The measured specimens are from conventional core samples from Undan-1 and Undan-4 wells at 2996.15m and 3135.24m respectively and sidewall core samples from Challis-11 ST1 well at 1552.50m and Rowan-1ST well at 3183.00m.

Comments. The most characteristic feature in *Ctenidodinium ancorum* are the processes which surmount the parasutural ridges. Typically, the distal terminations are bifurcate, with recurved furcae (Fig. 3J). The processes may be bent distally at the tips so that they and the process shafts may be at different focal levels at high magnifications. Trifid tips on the gonal processes, or elsewhere, were not observed. These grapnel or anchor-shaped process endings are reminiscent of the glochidia in the microspore massulae of the Late Cretaceous to Holocene water fern genus *Azolla sensu lato* (see Collinson, 1980). It is possible that these hooked processes evolved in order that this cyst species could attach itself to other individuals or to other sedimentary particles. The ornamentational elements, which have blunt or sharp distal terminations, may represent processes which have been damaged, the bifid tips breaking off during sedimentation and/or processing. This seems likely as the 'necks' of the processes, immediately below the recurved bifid tip are extremely slender (Fig. 3J). Furthermore, individual specimens have both bifid and sharp processes, thereby supporting the contention that the process terminations may be randomly damaged. Isolated tips were not seen in the residues, being close to the limit of optical resolution and also possibly removed by sieving during processing. The processes are longest around the antapex, being 5µm and above (Fig. 3C). They become progressively shorter in an apical direction, typically being around 4µm and 3µm in the postcingular and paracingular series respectively. The species is relatively variable in size (see *Dimensions*, above); this factor is

isolated hypocyst in oblique right lateral view, low focus. G, J - CPC 35355, holotype; isolated hypocyst in ventral view, low focus. G - the full specimen. J - a closeup of a postcingular parasuture illustrating the bifid and recurved distal nature of the parasutural processes. Note the narrow constriction on each process immediately below the distal termination. H - CPC 35356, paratype; isolated hypocyst in ventral view, low focus. I - CPC 35357, paratype; isolated hypocyst in left lateral view, median focus. K - CPC 35358, paratype; entire cyst in oblique left lateral view, median focus. Note that the epicyst is relatively long. L - CPC 35359, paratype; entire cyst in dorsal/antapical view, median focus. Note the prominent parasutural processes on the epicyst.

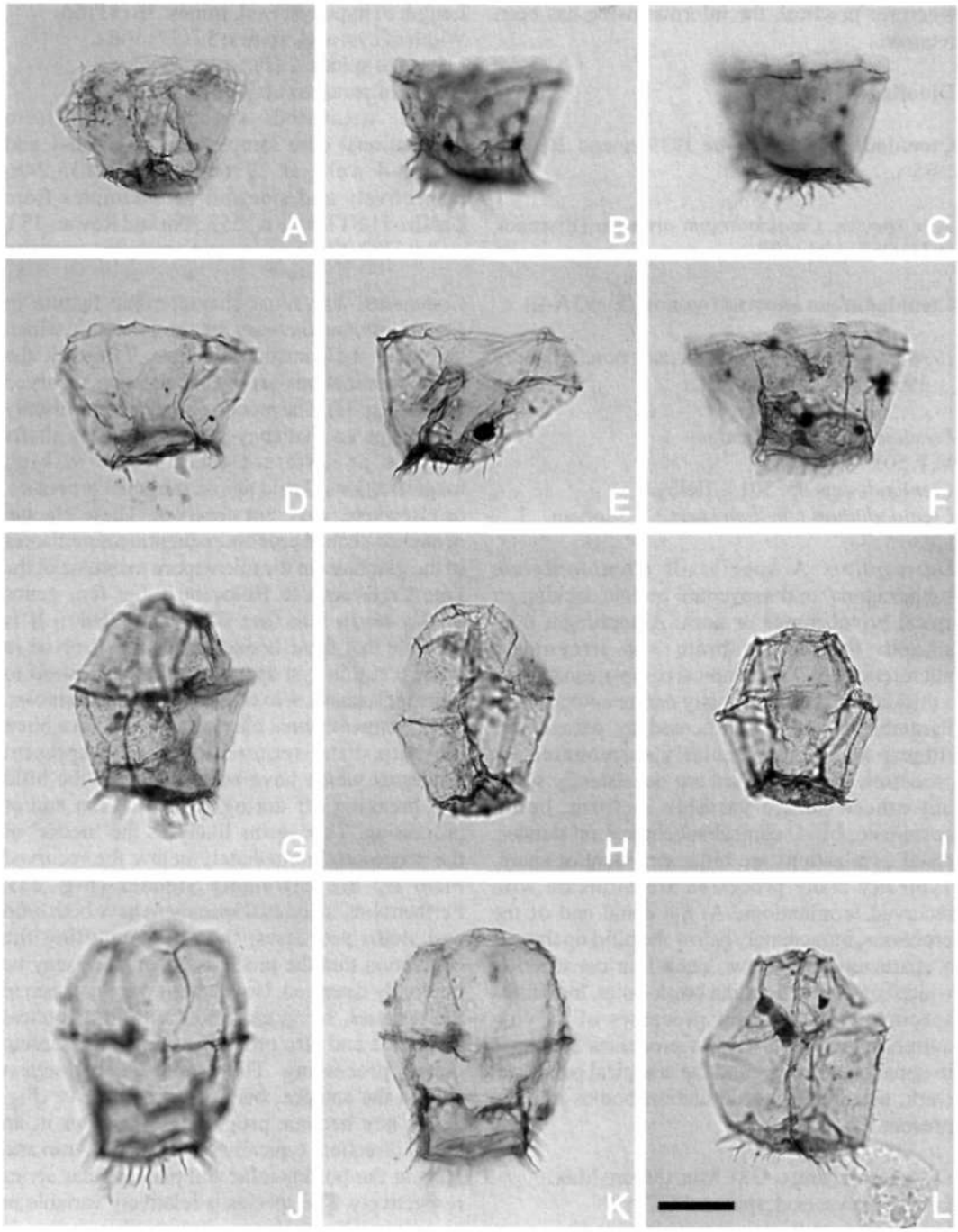

Fig. 4. Ctenidodinium fuscibasilarum sp. nov. All specimens are from conventional core samples in the Undan-3 well at 3048.00m (Figs 4A, 4D, 4E and 4H) and 3057.00m (Figs 4B, 4C, 4F, 4G and 4I-4L). The photomicrographs were all taken using plain transmitted light. The scale bar in Fig. 4L refers to all the photomicrographs and represents 25µm. Figs 4J and 4K are of the holotype, the remainder are paratypes (see Appendix 2). The antapical (1'''') paraplate is characterised by relatively thick and darker autophragm. Note also the elongate nature of this species, the epicystal archaeopyle and the low parasutural ridges surmounted by short spines or denticles, which are longer and more densely inserted around the antapex. A - CPC 35360, paratype; isolated hypocyst in oblique dorsal view, low focus. A specimen with short, sparse parasutural denticles; note the prominent parasulcus. B, C - CPC 35361, paratype; isolated hypocyst in ventral view, (continued opposite)

probably due to the variable compressions and preservational style.

Comparison. Ctenidodinium ancorum most closely resembles *Ctenidodinium fuscibasilarum* sp. nov., both having thicker and darker 1'''' paraplates, although in the latter the development is more extreme. In addition, *C. ancorum* has bifid processes surmounting the parasutural ridges over the entire cyst. *Ctenidodinium* aff. *tenellum* Deflandre 1939, particularly, "Form B", of Gocht (1970, pl. 42, figs. 7-8, pl. 32, figs 18a,b) is the European form most similar to *C. ancorum* in process distribution and style, but is substantially smaller, has a conical epicyst, and appears to lack the thickening of the 1'''' paraplate. The Mid Jurassic *C. sellwoodii* (Sarjeant 1975) Stover & Evitt 1978 may closely resemble *C. ancorum* in general morphology apart from the bifid process tips. The most common Mid Jurassic representatives of the genus in northwest Europe are *C. combazii, C. continuum, C. ornatum* and *C. sellwoodii* (Woollam & Riding, 1983). *Ctenidodinium combazii* has a small antapical paraplate and long, distally elaborate processes (Riding *et al.*, 1985, pl. 1). The parasutural crests of *C. continuum* and *C. ornatum* are relatively high and surmounted by densely inserted denticles or processes, lacking tip furcation.

If observations of *C. ancorum* are gathered using low power objectives the bifid nature of the processes may not be apparent. In these cases the forms would possibly be identified as *C. sellwoodii* or *C. tenellum.*

Derivation of name. After the Latin *ancora*, meaning anchor and referring to the typically anchor-like process terminations.

Holotype and type locality. Figures 3G, J, CPC 35355, Rowan-1ST well, sidewall core sample at 3183.00m.

Stratigraphical distribution. Ctenidodinium ancorum has been recorded from the uppermost Bathonian to the Callovian of the Timor Sea area, ranging from the upper *Wanaea verrucosa* Zone (7ciai) to the *Rigaudella aemula* Zone (7ai) (Foster, this volume; Helby & Partridge, in prep.).

Ctenidodinium fuscibasilarum sp. nov. (Figs 4A-L)

Previous Australian usage
M.P. 833 – Helby.
Ctenidodinium sp. 833 – Helby.
M.P. 1044 – Helby.
Ctenidodinium sp. 1044 – Helby.

Description. A species of *Ctenidodinium,* which is elongate subhexagonal in dorsoventral outline and with or without a small apical protuberance. Autophragm thin, smooth to occasionally microscabrate except the antapical paraplate, which has significantly thicker and darker autophragm. Paratabulation fully indicated by low parasutural ridges, which may be surmounted by short, solid, slender spines or denticles. The spines and/or denticles are sharply pointed or bifurcate. Gonal spines are consistently present on the antapical paraplate, which normally is also characterised by closely inserted intergonal spines. Elsewhere on the cyst, particularly on paraplates of the precingular and postcingular series, spines are sparse, irregularly developed and/or commonly absent.

Dimensions (µm; n=37): Min. (Mean) Max.
Length of cyst excl. spines: 61 (73) 86
Width of cyst body at paracingulum: 54 (70) 94
Width of antapical paraplate excl. spines: 19 (33) 44
Length of parasutural spines (mainly on 1''''): 3 (7) 16

The measured specimens are from conventional core samples in Undan-3 well at 3048.00m and 3057.00m.

Comments. The most characteristic feature of *Ctenidodinium fuscibasilarum* is the relatively

high and low focus respectively. Note the large antapical (1'''') paraplate. D - CPC 35362, paratype; isolated hypocyst in oblique ventral view, low focus. The antapical (1'''') paraplate has relatively large gonal spines. E - CPC 35363, paratype; isolated hypocyst in dorsal view, median focus. F - CPC 35364, paratype; isolated hypocyst in dorsal view, median focus. G - CPC 35365, paratype; entire cyst in oblique ventral view, high/median focus. Note that the most prominent parasutural spines/denticles are around the antapical region. H - CPC 35366, paratype; entire cyst in oblique ventral view, high/median focus. I - CPC 35367, paratype; entire cyst in dorsal view, median focus. A specimen with relatively short parasutural denticles. J, K - CPC 35368, holotype; entire cyst in dorsal view, high and low focus respectively. The antapical parasutural spines are distally bifurcate. L - CPC 35369, paratype; entire cyst in oblique ventral view, high/median focus.

dark, thickened antapical (1'''') paraplate which is normally surrounded by spines or processes (Fig. 4). The preferential thickening of a single paraplate is extremely unusual among dinoflagellate cysts and was hitherto unknown in this genus. The spines are longer and more numerous closer to the antapex and the gonal spines around the 1'''' paraplate are the longest. This lengthening is typical of *Ctenidodinium* and other gonyaulacalean genera. The spines/denticles other than around the 1'''' paraplate are irregular and short (up to 2µm-5µm, when present). The parasutural ridges are highest around the paracingulum (1µm-2µm) and lowest in the apical area. Around the apical series, they may occasionally be discontinuous. The species is normally elongate, however the outline is somewhat variable and forms which are wider than long have been occasionally observed. Most forms have the paracingulum inserted equatorially, but in some forms the hypocyst is longer than the epicyst. The paratabulation pattern is consistent with the configuration determined for the genus by Woollam (1983) and Benson (1985). Two small anterior intercalary paraplates are present.

Comparison. Ctenidodinium fuscibasilarum most closely resembles *C. ancorum* (as discussed above). *Ctenidodinium fuscibasilarum* differs from all other species of *Ctenidodinium* by the characteristically large, dark, thickened antapical paraplate with spinose parasutures. The Mid Jurassic species *C. sellwoodii* may closely resemble *C. fuscibasilarum* in general morphology aside from the dark 1'''' paraplate. *Ctenidodinium sellwoodii* is a variable form and can have few, irregularly inserted short parasutural processes like *C. fuscibasilarum* (see Woollam, 1983). Isolated, more spinose epicysts of *C. fuscibasilarum* may be difficult to distinguish from those of *C. sellwoodii*. Many other species of this genus have parasutures which are surmounted by regularly inserted and relatively dense processes and thus differ profoundly from *Ctenidodinium fuscibasilarum*. These comprise *Ctenidodinium capitatum* Wheeler & Sarjeant 1990 ex Wheeler & Sarjeant 1992, *C. combazii* Dupin 1968, *C. complanatum* Harding 1990, *C. continuum* Gocht 1970, *C. cornigerum* (Valensi 1953) Jan du Chêne *et al.* 1985, *C. elegantulum* Millioud 1969, *C. ornatum* (Eisenack 1935) Deflandre 1939, *C? rotundum* Dodekova 1975, *C? scissum* McIntyre & Brideaux 1980, *C. tenellum* and *C? thulium* (Davies 1983) Jan du Chêne *et al.* 1986. *Ctenidodinium coronatum* Prauss 1989 is characterised by prominent, distally smooth parasutural crests. The Late Jurassic species *Ctenidodinium chondrum* Drugg 1978 and *C? schizoblatum* (Norris 1965) Lentin & Williams 1973 exhibit low, smooth parasutural crests.

The most common Mid Jurassic representatives of *Ctenidodinium* in northwest Europe are *C. combazii, C. continuum, C. ornatum* and *C. sellwoodii* (Woollam & Riding, 1983). *Ctenidodinium combazii* has a small antapical paraplate and long, distally furcate processes (Riding *et al.*, 1985, pl. 1). The parasutural crests of *C. continuum* and *C. ornatum* are relatively high and surmounted by densely-inserted denticles or processes lacking bifid terminations.

Derivation of name. From the Latin *fuscus* meaning dark or swarthy and *basilaris* meaning at the base. This refers to the prominent dark, thickened antapical (1'''') paraplate.

Holotype and type locality. Figures 4J-K, CPC 35368, Undan-3 well, conventional core sample at 3057.00m.

Stratigraphical distribution. Ctenidodinium fuscibasilarum has been recorded from Middle to Upper Callovian strata of the Timor Sea region. It ranges from the *Wanaea digitata* Zone (7bi) to the middle *Rigaudella aemula* Zone (7aiiaii) (Foster, this volume; Helby & Partridge, in prep.).

Ctenidodinium planocristatum sp. nov. (Figs 5A-O)

Previous Australian usage
M.P. 753B – Helby.
Ctenidodinium sp. 753B – Helby.
Ctenidodinium cf. *gochtii* – Morgan.

Description. A species of *Ctenidodinium*, subspherical in outline and with or without a small apical protuberance. Autophragm relatively thin, smooth, microgranulate and/or irregularly microreticulate. Paratabulation fully indicated by low parasutural ridges and/or crests which are dominantly distally smooth and even in height. The parasutural ridges/crests may occasionally be fenestrate. Rarely the fenestrae may be reduced, thereby producing irregularly denticulate parasutural crests. When developed, the denticles are short, solid and distally pointed.

Dimensions (µm; n=32): Min. (Mean) Max.
Length of cyst: 69 (79) 93

Width of cyst: 67 (78) 96
Height of parasutural ridges/crests: 1 (2) 4

The measured specimens are all from conventional core from Undan-4 well at 3135.24m.

Comments. Ctenidodinium planocristatum is characterised by its equant, subspherical outline and the mainly distally smooth parasutural ridges or crests. These ridges/crests are occasionally irregularly fenestrate. The distal parts of the fenestrate crests may be lost, thereby producing an irregular denticulate ornament. However the overall impression is that of a species devoid of larger ornamentational elements. The parasutural crests surrounding the paracingulum are normally the most prominent.

Comparison. Ctenidodinium planocristatum differs from the other species of *Ctenidodinium* by the low, largely smooth, parasutural ridges or crests. The majority of other representatives of the genus have ornamentation in the form of processes or denticles surmounting the parasutures and inserted relatively densely (Woollam, 1983; Benson, 1985; see *Comparison* section for *Ctenidodinium fuscibasilarum* above). *Ctenidodinium coronatum* exhibits high, distally smooth parasutural crests, thus is comparable to *C. planocristatum*. The crests of *C. coronatum* are confined to the hypocyst and are significantly higher and more prominent than the parasutural ornament of *C. planocristatum* (see Prauss, 1989, fig. 12). *Ctenidodinium? schizoblatum* has parasutural crests devoid of processes, yet is smaller than *C. planocristatum* and has parasutural crests which are serrated and split (Norris, 1965). The Late Jurassic *Ctenidodinium chondrum* also has low, smooth parasutural crests, but is markedly shorter, although almost as wide as *C. planocristatum*, and is granulate. Furthermore, *C. planocristatum* never bears processes. Representatives of *Korystocysta* Woollam 1983, such as *K. gochtii* (Sarjeant 1976) Woollam 1983 and *K. kettonensis* (Sarjeant 1976) Woollam 1983, differ from *C. planocristatum* in lacking fenestrate ridges/crests. However, Sarjeant (1976, fig. 3) suggested that the parasutural features on *K. kettonensis* may bear denticles/ small "spinelets" in the antapical area.

Derivation of name. From the Latin *planus*, meaning smooth or even, and *cristatus*, meaning crested. This refers to the largely smooth, low, parasutural ridges/crests of this species.

Holotype and type locality. Figure 5J, CPC 35379, Undan-4 well, conventional core sample at 3135.24m.

Stratigraphical distribution. Ctenidodinium planocristatum has been recorded from the Middle-Upper Callovian strata of the Timor Sea region. It ranges from the *Wanaea digitata* Zone (7bi) to the middle *Rigaudella aemula* Zone (7aiia) and is most prominent, providing biostratigraphically useful acmes, in the middle *Rigaudella aemula* Zone (7aiiaii) (Foster, this volume; Helby & Partridge, in prep.).

Durotrigia Bailey 1987

Type species. Durotrigia daveyi Bailey 1987

Durotrigia magna sp. nov. (Figs 6A-F)

Previous Australian usage
M.P. 831 – Helby.
Durotrigia sp. 831 – Helby.

Description. An intermediate to large species of *Durotrigia,* subcircular to ellipsoidal in outline. The species is slightly distally flattened. Autophragm robust, relatively thick and readily folded; it is microscabrate and/or microreticulate. Continuous or discontinuous low parasutural ridges are developed which may occasionally be irregularly denticulate. The denticles, where developed, are short, slender, solid and distally pointed. Ridges bordering the paracingulum are consistently developed and represent the highest parasutural ornament (c. 1µm). A relatively small, solid, distally foliate apical horn is present. The parasulcus is relatively narrow, not surrounded by high ridges or subdivided and is slightly indented. Archaeopyle compound, most commonly formed by loss of three precingular paraplates.

Dimensions (µm; n=38): Min. (Mean) Max.
Length of cyst excl. apical horn: 89 (105) 126
Width of cyst at paracingulum: 82 (105) 124
Length of apical horn: 5 (10) 16

All measured specimens are from conventional core in Undan-3 well at 3057.00m.

Comments. Durotrigia magna is a relatively large species, which is normally equant/subequant in terms of cyst body length and width (Fig. 6). An apical horn is developed which is very small and spongeous to solid; it varies in colour from light

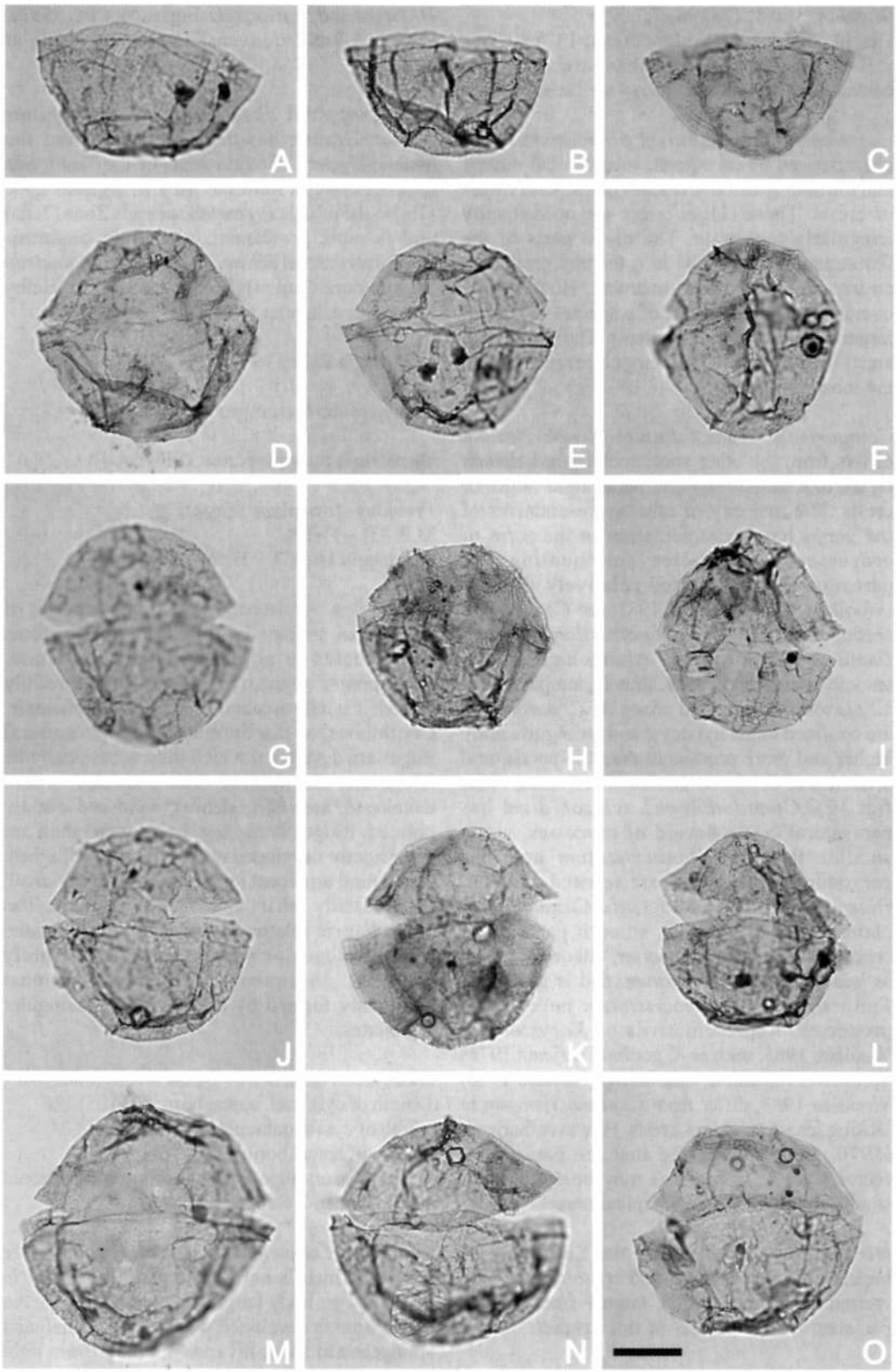
A
B
C
D
E
F
G
H
I
J
K
L
M
N
O

to extremely dark; the foliate distal tip is distinctive (Fig. 6D). The large, multi-paraplate precingular archaeopyle (up to 5P, but generally no more than 3P) means that individuals may be compressed to such an extent that the dorsoventral flattening is exaggerated (Fig. 6E). Largely longitudinal folds readily develop on the autophragm.

Comparison. The other five species of *Durotrigia*, described from the Mid Jurassic (Bajocian-earliest Callovian) of northwest Europe (Williams *et al*., 1998, p. 205, 206), are all significantly smaller than *D. magna*. It is by far the largest species in the genus and is most similar to *Durotrigia aspera* Bailey & Partington 1991, which has irregular parasutural ridges and a thick autophragm. However, *D. aspera* is smaller than *D. magna* and has coarsely granulate autophragm. *Durotrigia asketa* Bailey 1990 has distinctive fenestrate/distally denticulate parasutural crests and tuberculate/verrucate intratabular ornament (Bailey, 1990, fig. 3). The parasutural ridges of *Durotrigia daveyi* are consistently and relatively densely denticulate. *Durotrigia filapicata* (Gocht 1970) Riding & Bailey 1991 is covered by a dense, low relief ornament and the parasutural ridges are surmounted by trabeculate denticles. The autophragm of *Durotrigia vesiculata* Bailey 1990 is differentiated and extremely thick (Bailey, 1990, pl. 1).

Derivation of name. From the Latin *magnus* meaning large or great.

Holotype and type locality. Figure 6B, CPC 35386, Undan-3 well, conventional core sample at 3057.00m.

Stratigraphical distribution. *Durotrigia magna* has been recorded from the Upper Callovian strata of the Timor Sea region. It ranges from the upper part of the *Wanaea digitata* Zone (7bi) to the lower part of the *Rigaudella aemula* Zone (7aiibii) (Foster, this volume; Helby & Partridge, in prep.). In the Bayu-Undan Gas Field it occurs as an acme (bioevent 7aiibiib) which is commonly associated with maximum flooding surface 2 of Arditto (1996, figs 2-4).

Fusiformacysta Morgan 1975 emend.

1975 *Fusiformacysta* Morgan, p. 161.

Type species. *Fusiformacysta salasii* Morgan 1975

Emended diagnosis. Proximate, acavate dinoflagellate cysts, intermediate to large in size; subspherical to fusiform in shape, with or without apical and antapical horns. Polar horn development is extremely variable. Archaeopyle precingular, type 3P, involving paraplates 2", 3" and 4". A small, quadrate anterior intercalary paraplate (K of Evitt, 1985, fig. 5.16), inserted between paraplates 3" and 4" may be developed. Autophragm smooth, microreticulate or with low relief positive ornamentation. Paracingulum may be indicated by a lineation of ornament; the parasulcus not indicated.

Comments. The original generic diagnosis of *Fusiformacysta* by Morgan (1975, p. 161) outlined an elongate, acavate, proximate cyst with a compound precingular archaeopyle, type 2P to ?5P. The genotype, *F. salasii*, has an unequivocal type 3P archaeopyle and expansion of this to 4P or 5P is deemed to be the result of mechanical damage. This can also remove the apical paraplate series. Representatives of *Fusiformacysta* and related morphotypes are present, often prominently, in the Mid Jurassic to Early

Fig. 5. Ctenidodinium planocristatum sp. nov. All specimens are from a conventional core sample in the Undan-4 well at 3135.24m. The photomicrographs were taken using plain transmitted light. The scale bar in Fig. 5O refers to all the photomicrographs and represents 25µm. Fig. 5J is the holotype, the remainder are paratypes. Note the subspherical outline, the low, mostly smooth, parasutural ridges, the relatively thin autophragm and the epicystal archaeopyle. A - CPC 35370, paratype; isolated hypocyst in ventral view, high/median focus. B - CPC 35371, paratype; isolated hypocyst in ventral view, high focus. C - CPC 35372, paratype; isolated hypocyst in ventral view, median/low focus. Note the rare, small denticles surmounting the parasutural ridges. D - CPC 35373, paratype; entire cyst in ventral view, low focus. E - CPC 35374, paratype; entire cyst in ventral view, low focus. F - CPC 35375, paratype; entire cyst in ventral view, median focus. G - CPC 35376, paratype; entire cyst in ventral view, high focus. An unusually elongate specimen. H - CPC 35377, paratype; entire cyst in ventral view, median/low focus. I - CPC 35378, paratype; entire cyst in dorsal view, low focus. A form with a small apical protuberance. J - CPC 35379, paratype; entire cyst in dorsal view, median focus. K - CPC 35380, paratype; entire cyst in dorsal view, low focus. Note the relatively high, fenestrate parasutural ridges/crests in the apical region. L - CPC 35381, paratype; entire cyst in dorsal view, median focus. M - CPC 35382, paratype; entire cyst in dorsal view, low focus. N - CPC 35383, paratype; entire cyst in dorsal view, median focus. O - CPC 35384, paratype; entire cyst in dorsal view, median focus.

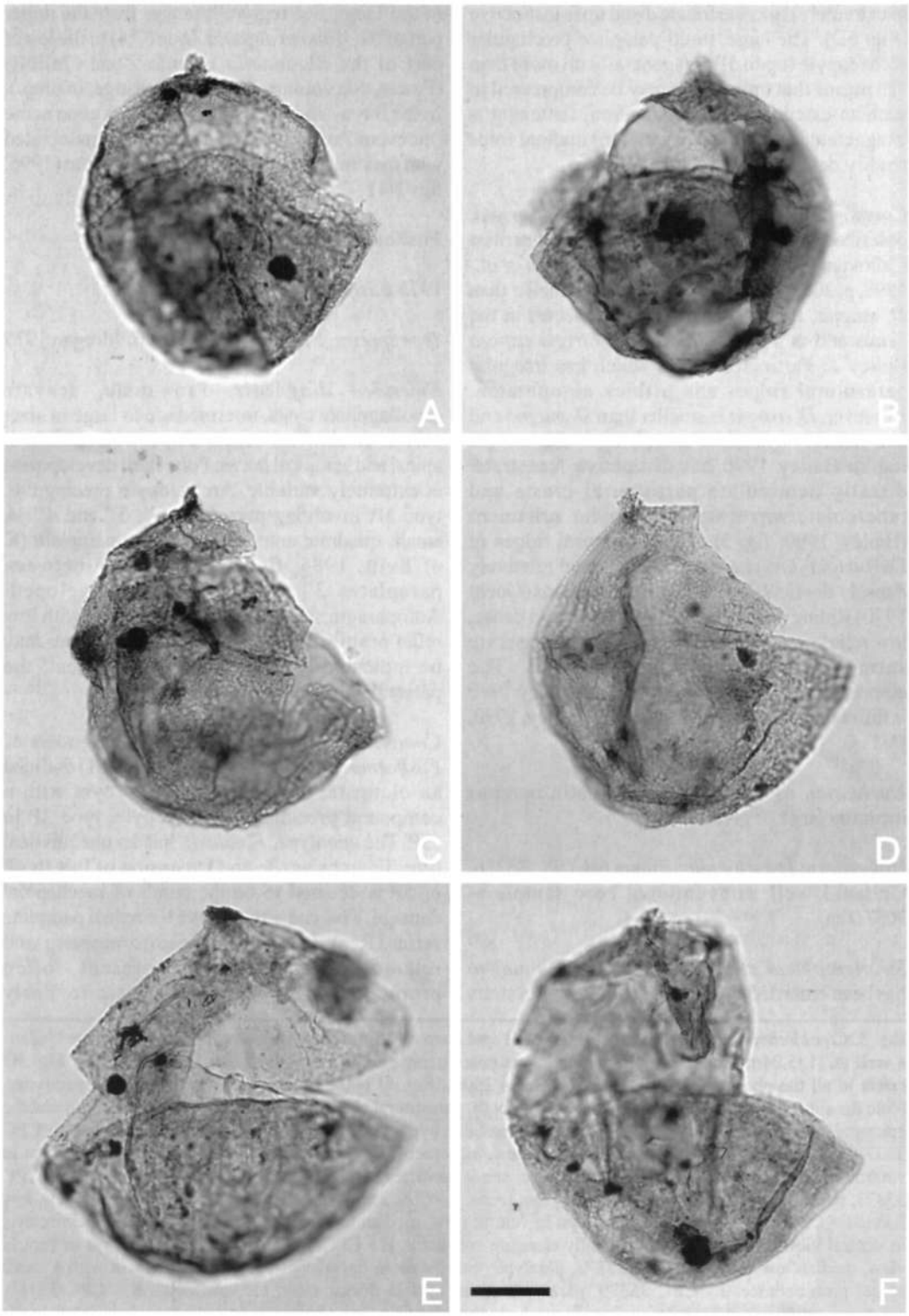
A
B
C
D
E
F

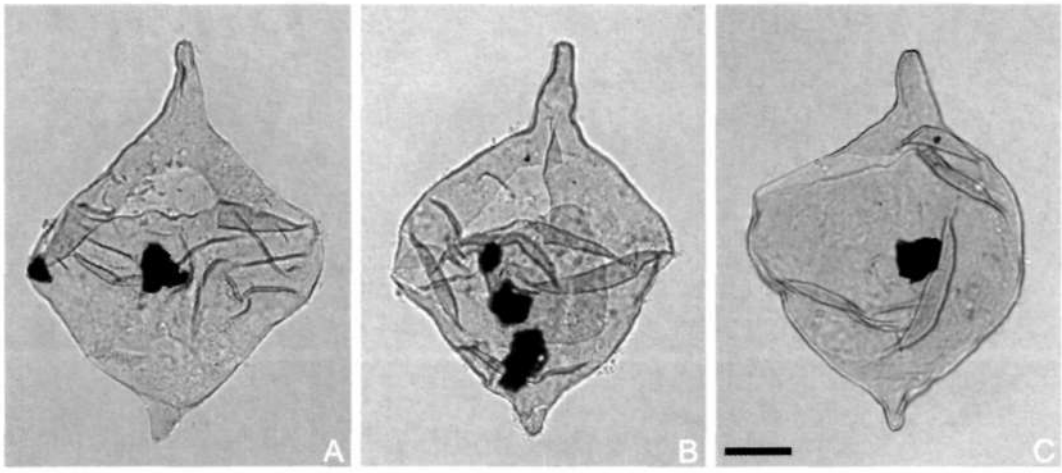

Fig. 7. Komewuia glabra Cookson & Eisenack 1960. Three topotype specimens from the Tithonian Jarlemai Siltstone (upper portion) of the Broome-3 Town Bore (an artesian borehole), Western Australia at between 305.11m and 317.60m (ditch cuttings). The photomicrographs were taken using plain transmitted light. The scale bar in Fig. 7C refers to all the photomicrographs and represents 25µm. Note the biconical outline, the markedly longer apical horn, the tendency of the autophragm to fold and the large, single paraplate, precingular archaeopyle. A - CPC 35405; ventral view, low focus. Note the intense folding in the equatorial area. B - CPC 35406; dorsal view, high focus. Note the operculum (the 3" paraplate) inside the loisthocyst. C - CPC 35407; oblique dorsal view, median focus.

Cretaceous of Australia. Morgan (1975) and Backhouse (1988) noted that this genus is indicative of restricted marine or non-marine depositional regimes. We have noted extreme variation in shape and polar horn development, especially in *F. terniana* sp. nov., and consider that the fundamental feature of this group of cysts is the type 3P precingular archaeopyle.

The possibility of emending the diagnosis of *Komewuia* Cookson & Eisenack 1960 to encompass forms with type 3P archaeopyles was considered. *Komewuia* has a single paraplate, type P, precingular archaeopyle (Chen, 1982). This putative emendation of *Komewuia* would have been principally to accommodate *F. terniana* sp. nov. and *F. challisiana* Riding & Helby (this volume). However, the morphological and stratigraphical coherence of *Komewuia* would be have been significantly diminished by such an expansion. *Komewuia* has an extremely distinctive, large precingular archaeopyle, with the middorsal paraplate (3") comprising the operculum, and is characteristic of the Kimmeridgian and Tithonian of the Southern Hemisphere (Chen, 1982, fig. 3). This large, type P archaeopyle is well illustrated in the genotype, *Komewuia glabra* Cookson & Eisenack 1960 (see Cookson & Eisenack 1960, pl. 39, fig. 8). The phenomenon is also shown herein; Figure 7 comprises three topotype specimens of *K. glabra*, all of which show the large single paraplate precingular archaeopyle.

Fusiformacysta terniana sp. nov. (Figs 8A-L, 9A-D)

Previous Australian usage
Apteodinium sp. – Lister.
Komewuia sp. 555 (smooth) – Helby.

Fig. 6 (opposite). *Durotrigia magna* sp. nov. All specimens are from conventional core in Undan-3 well at 3057.00m. All photomicrographs taken using plain transmitted light. The scale bar in Fig. 6F refers to all images and represents 25µm. Figure 6B is the holotype, the remainder are paratypes. Note the large size of this species, the small, distally foliate apical horn and the multi-paraplate precingular archaeopyle. A - CPC 35385, paratype; slightly oblique right lateral view, median focus. A specimen with a regular ellipsoidal outline; note the short apical horn. B - CPC 35386, holotype; ventral view, low focus. Note the large archaeopyle. C - CPC 35387, paratype; oblique dorsal view, low focus. Note the irregular, microscabrate/microreticulate autophragm. D - CPC 35388, paratype; right lateral view, low focus. Note the foliate nature of the apical horn. E - CPC 35389, paratype; right lateral view, high focus. The removal of two or three precingular paraplates during archaeopyle formation has caused the partial (mechanical) rupture of the anterior paracingular parasuture. F - CPC 35390, paratype; right lateral view, median focus. A large specimen; note the large multi-paraplate precingular archaeopyle.

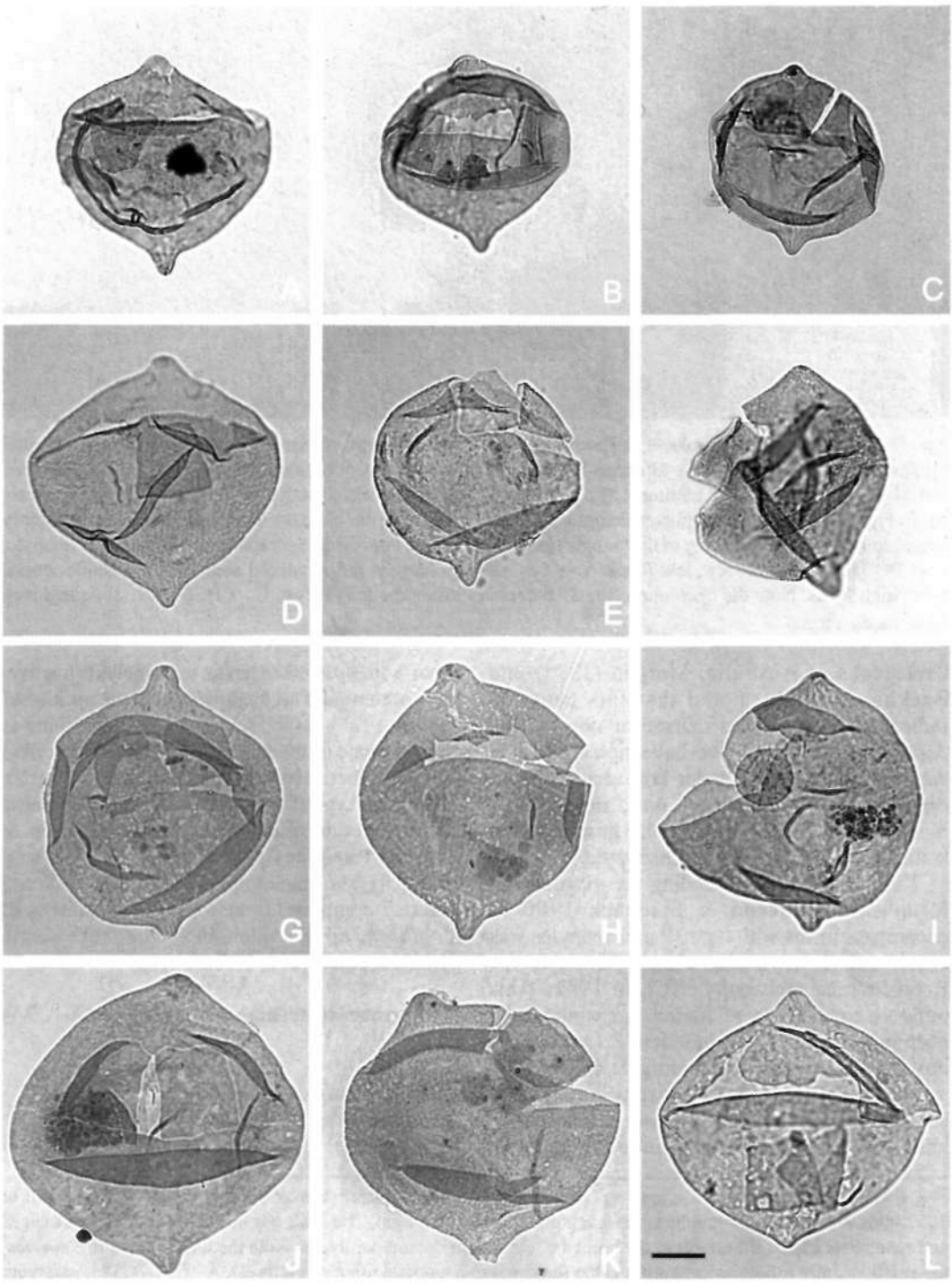

Fig. 8. Fusiformacysta terniana sp. nov. All specimens from a sidewall core at 1528.28m (Figs 8D-E, G-L) and ditch cuttings between 1530.11m-1536.21m (Figs 8A-C, F) in Tern-1 well. All photomicrographs taken using plain transmitted light. The scale bar in Fig. 8L refers to all photomicrographs and represents 25µm. Fig. 8J is the holotype, the remainder are paratypes. Note the biconical outline, the short, blunt apical and antapical horns and the precingular, type 3P archaeopyle. A - CPC 35391, paratype; dorsal view, high focus. Note the opercular piece in the interior of the cyst and the relatively short apical horn. B - CPC 35392, paratype; dorsal view, high focus. A relatively small specimen with a well developed 3P archaeopyle. (continued opposite)

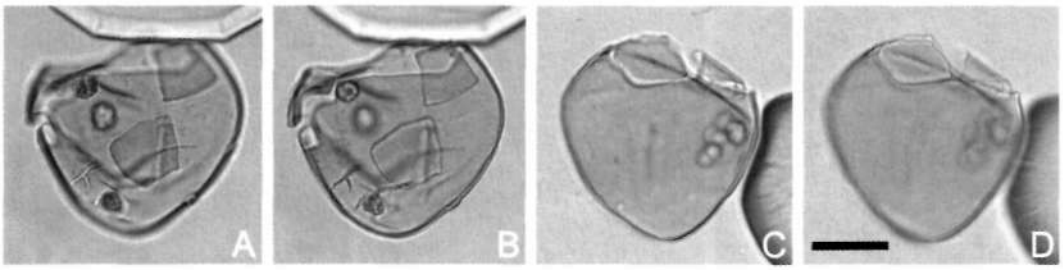

Fig. 9. Fusiformacysta terniana sp. nov. All specimens from a sidewall core at 1552.50m from the Challis-11 ST1 well. Photomicrographs taken in plain transmitted light. The scale bar in Fig. 9D refers to all the photomicrographs and represents 25µm. Note the precingular, type 3P, archaeopyle, the psilate autophragm and the lack of polar horns. A, B - CPC 35403, paratype; ventral view, high and median focus respectively. Note the ellipsoidal outline and the two opercular pieces, which have fallen back into the loisthocyst. C, D - CPC 35404, paratype; oblique dorsal/right lateral view, median and low focus respectively. Note the lack of apical or antapical horns and the precingular archaeopyle.

Mancodinium sp. "555" – Morgan.
Helbycysta psilata – Morgan.

Description. A species of *Fusiformacysta* with a type 3P archaeopyle, which is biconical or ellipsoidal in outline, with or without relatively short, blunt, distally rounded, apical and antapical horns. Where horns are developed, the antapical horn is normally the longest and occasionally the apical horn may be reduced or entirely suppressed. Generally the species is elongate, but it may also be wider than long or subequant. The only indication of paratabulation is the type 3P archaeopyle. Isolated opercula are frequently present within the loisthocyst. Dark brown accumulation bodies may be present in the cyst. The autophragm is mainly smooth, but may be partially microgranulate or microreticulate.

Dimensions. Two morphotypes of *F. terniana* were observed. Specimens from a sidewall core in Challis-11 ST1 well at 1552.50m are relatively small, have ellipsoidal outlines and lack polar horns (Fig. 9). However, material from Tern-1 well (sidewall core sample at 1528.28m and ditch cuttings between 1530.11m and 1536.21m) are larger than the Challis-11 ST1 forms and are typically biconical in outline due to the development of apical and antapical horns (Fig. 8).

The measurements of five specimens of the small, ellipsoidal forms from Challis-11 ST1, sidewall core sample at 1552.50m are as follows:
Dimensions (µm; n=5): Min. (Mean) Max.
Maximum length of cyst: 65 (72) 82
Width of cyst at paracingulum: 62 (69) 79
(Horns are absent in this morphotype, see Fig. 9).

The dimensions of 29 specimens from Tern-1 well, sidewall core sample at 1528.28m and a ditch cuttings sample between 1530.11m and 1536.21m are given below:
Dimensions (µm; n=29): Min. (Mean) Max.
Maximum length of cyst: 72 (94) 122
Width of cyst at paracingulum: 67 (89) 115
Length of apical horn: 0 (6) 11
Length of antapical horn: 3 (8) 14

The data for the length and width of both the Challis-11 ST1 well and Tern-1 well morphotypes, a total of 34 specimens, is as follows:
Dimensions (µm; n=34): Min. (Mean) Max.
Maximum length of cyst: 65 (90) 122
Width of cyst at paracingulum: 62 (86) 115

Note that horn measurements are not given in this table because the Challis-11 ST1 forms lack apical and antapical horns/protrusions.

Comments. In most specimens from Tern-1 well, the antapical horn is longer (see Fig. 8 and *Dimensions*, above). However, horn lengths are variable and the apical horn may be longer than the antapical protuberance (Figs 8G, L). In several

C - CPC 35393, paratype, oblique right lateral view, median focus. D - CPC 35394, paratype; ventral view, high focus. Note the single opercular piece immediately below the archaeopyle. E - CPC 35395, paratype; oblique dorsal view, median focus. Note the absence of an apical horn; he opercular pieces have detached but are still close to the loisthocyst. F - CPC 35396, paratype; left lateral view, median focus. G - CPC 35397, paratype; dorsal view, high focus. H - CPC 35398, paratype; dorsal view, high focus. I - CPC 35399, paratype; left lateral view, median focus. Note the longitudinal striations on the apical and antapical horns. J - CPC 35400, holotype; dorsal view, high focus. Note the incipient archaeopyle formation. K - CPC 35401, paratype; right lateral view, high focus. A specimen with a damaged antapical horn. L - CPC 35402, paratype; dorsal view, high/median focus.

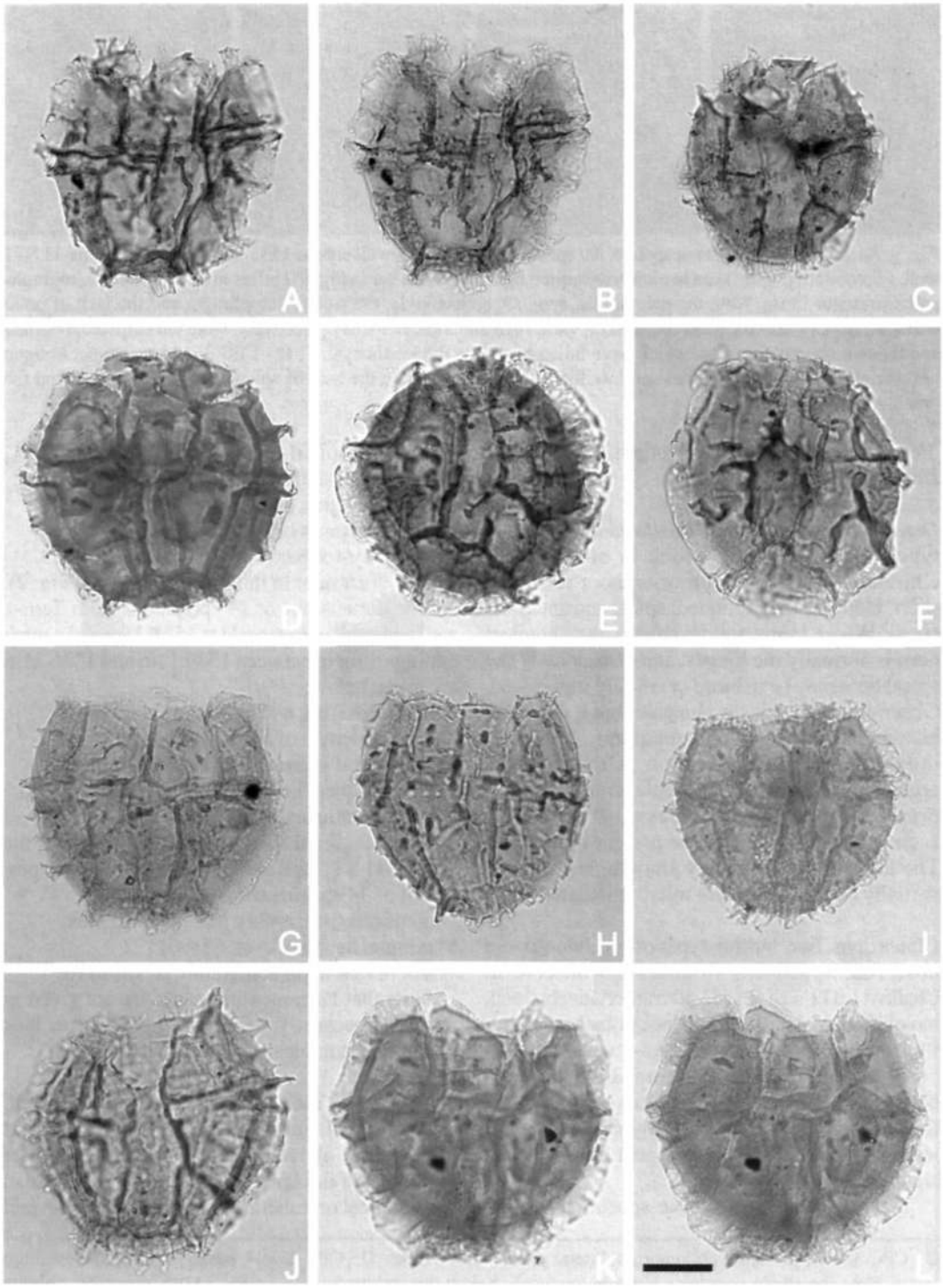

Fig. 10. Lithodinia protothymosa sp. nov. All specimens from sidewall core samples from Investigator-1 well at 3260.00m (Figs 10D-F, H, J), an unnamed well (Figs 10A-C) and Tern-2 well at 1459.20m (Fig. 10I) and 1457.30m (Figs 10G, K, L). The photomicrographs were taken using plain transmitted light. The scale bar in Fig. 10L refers to all photomicrographs and represents 25µm. Fig. 10D is the holotype, the remainder are paratypes. Note the ellipsoidal outline, the apical archaeopyle with a compound archaeopyle, the prominent parasutural crests or ridges with low-relief ornamentation, the intratabular ridges and (continued opposite)

specimens, the area around the antapical horn is micropunctate (Fig. 8H). Analyses of the shape of the anterior margins of the opercula and the principal archaeopyle suture, indicates the presence of a small anterior intercalary paraplate (Fig. 8J). The biconical shape is reduced to a more ellipsoidal shape in some of the older associations, such as the material from Challis-11 ST1 well (see Fig. 9 and *Dimensions*, above).

Comparison. *Fusiformacysta terniana* differs from *K. challisiana* Riding & Helby (this volume) by the absence of a verrucate and/or reticulate autophragm. The genotype, *F. salasii* Morgan 1975, is much more slender and has markedly longer apical and antapical horns than *F. terniana*. *Fusiformacysta tumida* Backhouse 1988 is also narrower than *F. terniana* and is granulate.

Derivation of name. From Tern-1 well, from which the holotype was selected.

Holotype and type locality. Figure 8J, CPC 35400, Tern-1 well, sidewall core sample at 1528.28m.

Stratigraphical distribution. *Fusiformacysta terniana* is present in the Bathonian to Callovian throughout the Timor Sea region. It ranges from the *Wanaea verrucosa* Zone (7cia) to the *Rigaudella aemula* Zone (7ai) (Foster, this volume; Helby & Partridge, in prep.).

Lithodinia Eisenack 1935 emend. Gocht 1975 (modified by Stover & Evitt, 1978)

Type species. *Lithodinia jurassica* Eisenack 1935

Comments. We prefer to retain both *Lithodinia* and *Meiourogonyaulax* Sarjeant 1966 on the basis of the demonstrable presence of compound and simple opercula, respectively (Stover & Evitt, 1978, p. 62-63). Williams *et al.* (1993, 53-57) have comprehensively outlined the historical background to this long running debate concerning the status of these genera. We disagree with the conclusions of Williams *et al.* (1993) that *Meiourogonyaulax* is a junior synonym of *Lithodinia* on the basis that "the separation of these genera based on whether the apical opercula are contiguous or disarticulated is unrealistic and impractical". However, we recognise problems with the original description of *Meiourogonyaulax*, particularly relating to the nature of the operculum; implicitly discussed as a compound operculum with a single plate still attached but not shown in the illustration (Sarjeant, 1966, p. 144, fig. 37). However, one of us (JBR) has examined many specimens of *M. valensii* Sarjeant 1966 from the Middle Jurassic of Europe and confirms that the apical paraplates remain contiguous in a simple operculum upon archaeopyle formation. Residues containing *M. valensii* yield common simple opercula derived from this species. Furthermore, isolated simple opercula of *Meiourogonyaulax penitabulata* sp. nov. are illustrated herein (Figs 11A-11D). Both *Lithodinia jurassica* and *L. protothymosa* sp. nov. are Callovian, therefore unequivocal representatives of this genus may be stratigraphically significant.

Lithodinia protothymosa sp. nov. (Figs. 10A-L)

Previous Australian usage
Lithodinia jurassica - Ott (1970, pl. 8, figs 29-32).
M.P. 179A – Helby.
Meiourogonyaulax protothymosa – Helby.
Lithodinia australica – Morgan.

Description. An ellipsoidal to rounded subrectangular species of *Lithodinia*. The length and breadth are frequently subequal, especially in specimens where the archaeopyle has operated. Paratabulation indicated by parasutural ridges, crests and processes. Gonal points are marked by relatively prominent short, solid processes which may be distally bifid, buccinate, recurved or

---

the robust autophragm. A, B - CPC 35408, paratype; dorsal view, high/median and low focus respectively. Note the compound operculum. C - CPC 35409, paratype; dorsal view, median/low focus. A relatively small morphotype, note the compound operculum. D - CPC 35410, holotype; dorsal view, median/low focus. Note the robust, smooth autophragm and the apical archaeopyle with an unequivocally compound operculum. E - CPC 35411, paratype; dorsal view, median focus. Note the relatively narrow, straight parasulcus and the incipient principal archaeopyle sutures. F - CPC 35412, paratype; dorsal view, median/low focus. Note the prominent parasutural crests on the hypocyst and the incipient principal archaeopyle sutures. G - CPC 35413, paratype; ventral view, low focus. Note the variable nature of the parasutural ornament. H - CPC 35414, paratype; ventral view, median/low focus. Note the intratabular ornamentation. I - CPC 35415, paratype; dorsal view, median/low focus. Note the apical archaeopyle and the irregularly microreticulate autophragm. J - CPC 35416, paratype; dorsal view, low focus. Note the prominent parasutural notch. K, L - CPC 35417, paratype; ventral view, median and low focus respectively. A relatively wide loisthocyst; note the prominent parasutural crests.

subconical. The gonal processes are joined by low, smooth parasutural ridges which may or may not be surmounted by prominent, distally smooth to finely denticulate parasutural crests. Parasutural ridges may be surmounted by short, buccinate or bifid processes. The parasutural crests may also be fenestrate. Intratabular ridges and/or processes may also be present; these are normally nontabular in position. The intratabular ridges are low and smooth and the processes are solid and usually bifid. The paracingulum and parasulcus lack intratabular ornamentation and are not subdivided into paraplates. Autophragm relatively thick, smooth to occasionally microscabrate or microreticulate. Archaeopyle apical, tends to gape; operculum compound with individual paraplates only rarely retained inside the loisthocyst.

Dimensions (µm; n=30): Min. (Mean) Max.
Length of cyst incl. operculum: 74 (87) 96
Length of cyst excl. operculum: 71 (83) 98
Width of cyst: 71 (83) 99
Height of parasutural crests: 2 (7) 15

The measured specimens are from sidewall core samples in Investigator-1 well at 3260.00m and Tern-2 well at 1459.20m and 1457.30m.

Comments. This species is characterised by its prominent and variable mixture of parasutural and intratabular ornamentation. It often has relatively large gonal processes, which are connected by parasutural ridges and crests, and a thick, smooth autophragm (Fig. 10). It is also significantly larger than most species of *Meiourogonyaulax*. Individual specimens may have parasutural crests surmounting each parasutural ridge. However, some crests may be reduced or suppressed. In particular, the crest between the 2''' and the 1c paraplates is often reduced or absent. Where the ridges are not surmounted by crests, short processes may be developed, implying that the crests may be the result of coalesced processes. The crests are higher and more consistently developed on the hypocyst, and especially close to the antapical region. These parasutural features are more commonly entire but often fenestrate. They are usually distally smooth, but can be finely denticulate. Intratabular ornamentation is also commonly developed as ridges, which may represent growth structures *sensu* Gocht (1979; 1984), and/or processes and are nontabular. The ridges may be short, curved or angular and rarely appear to approach a penitabular distribution. The operculum is unequivocally compound (Figs 10A-F). The opercular pieces are normally lost and the loisthocysts are usually not longitudinally elongate; they may be equant and are frequently wider than long (e.g. Figs 10K, L). The autophragm is thick and normally smooth, but is occasionally microscabrate or microreticulate. This species tends to be strongly dorsoventrally flattened.

Comparison. *Lithodinia protothymosa* is most similar to *Lithodinia jurassica* Eisenack 1935 subsp. *reburrosa* Quattrocchio & Sarjeant 1992, which has parasutural processes, the bases of which coalesce to form parasutural ridges, in addition to intratabular processes (Quattrocchio & Sarjeant, 1992, fig. 3). Furthermore, prominent gonal processes, which are distally acuminate to bifurcate, are present. However, this subspecies is smaller than *Lithodinia protothymosa* and lacks the parasutural crests and intratabular ridges characteristic of this species. It is distinguished from the genotype, *Lithodinia jurassica* subsp. *jurassica* by its much larger size and more varied and robust sculptural elements (see Gocht, 1970, pl. 35, figs 13-22; Gocht, 1975, figs 2-7). Except for the difference in operculum configuration, species of *Meiourogonyaulax* lack the combination of parasutural and intratabular features seen in *L. protothymosa*. *Meiourogonyaulax penitabulata* sp. nov. exhibits penitabular ridges and crests except around the paracingulum and the parasutural ridges in *M. viriosa* sp. nov. are normally distally smooth.

Other species of *Meiourogonyaulax* which are superficially similar to *L. protothymosa* include *Meiourogonyaulax valensii* Sarjeant 1966 which has high parasutural crests which connect largely gonal processes. The small *Meiourogonyaulax? rioultii* Sarjeant 1965 ex Sarjeant 1968 has distally bifurcate gonal spines but has thin, smooth autophragm and low, smooth parasutural ridges. *Meiourogonyaulax araneosa* Muir & Sarjeant 1978 also has low parasutural crests surmounted by short processes. However the latter species entirely lacks intratabular ornamentation and is also significantly smaller than *L. protothymosa*. Irregular process-bearing or trabeculate parasutural ridges characterise *M. callomonii* Sarjeant 1972, however this species lacks parasutural crests, intratabular ornamentation and gonal processes. *Meiourogonyaulax strongyla* Sarjeant 1972 has a combination of low, denticulate parasutural ridges and nontabular granules. Thus, it lacks the intratabular features characteristic of *L. protothymosa*. The nature of the opercula in these taxa is not clear from the original descriptions

and illustrations.

Derivation of name. From '*Meiourogonyaulax? thymosa*', a widely used manuscript name of A.D. Partridge, for a Berriasian morphotype and the Greek *protos*, meaning first.

Holotype and type locality. Figure 10D, CPC 35410, Investigator-1 well, sidewall core sample at 3260.00m.

Stratigraphical distribution. *Lithodinia protothymosa* has been recorded from the Callovian strata of the Timor Sea region, ranging from the upper *Wanaea indotata* Zone (7bii) to the lowermost *Rigaudella aemula* Zone (7aiibii) (Foster, this volume; Helby & Partridge, in prep.).

Meiourogonyaulax Sarjeant 1966

Type species. *Meiourogonyaulax valensii* Sarjeant 1966

Comments. See discussion relating to *Lithodinia* (above). Furthermore, despite the clear difference in opercula, Gocht (1976, p. 353) and Williams *et al.* (1993, p. 54) stated that *Meiourogonyaulax* is a junior synonym of *Lithodinia* by priority. However, most workers have used *Meiourogonyaulax* rather than *Lithodinia* and the vast majority of species of assigned to *Lithodinia* by Williams *et al.* (1998) were originally attributed to *Meiourogonyaulax*. Moreover, *Meiourogonyaulax* is a diverse genus, which includes many well established and biostratigraphically important forms. Therefore, the conservation of *Meiourogonyaulax* due to its long and almost universal acceptance and usage would be justified even if the opercula in these two genera were identical.

Meiourogonyaulax penitabulata sp. nov. (Figs 11A-M, 12A-I)

Previous Australian usage
M.P. 745 – Helby.
Meiourogonyaulax sp. 745 – Helby.
Meiourogonyaulax 'penitabular' – Morgan.

Description. An ellipsoidal species of *Meiourogonyaulax*. The major paraplate series on the loisthocyst bear prominent, low penitabular ridges or crests. The ridges or crests on the apical series (the operculum) are, however, parasutural (Figs 11A-D). The forms with low, broad, robust ridges have short, solid denticles or spines surmounting the ridges (Fig. 12). These elements are irregularly distributed and may be subconical, distally bifid or buccinate and may be joined by slender trabeculae. These trabeculate denticles/spines, when regularly inserted, may appear to be a fenestrate crest. The sporadic nature and variability of this ornamentation engenders an irregular outline. Individuals bearing entire or perforate crests have a more regular outline as the crests are smooth distally (Fig. 11). The crests are normally narrow and may appear to have formed via the coalescing of densely inserted processes, which surmount a penitabular ridge. Normally the crests are perforate to occasionally fenestrate, giving them a spongeous appearance. The parasulcus is devoid of ornamentation and the ridges/crests bordering the paracingulum may frequently be parasutural, not penitabular (Figs 11F-G, 12A-I). Autophragm relatively thick, microreticulate to occasionally microgranulate. One or two dark, subspherical accumulation bodies are often present inside the cyst. Apical archaeopyle; free, simple opercula common.

Dimensions (µm; n=42): Min. (Mean) Max.
Length of cyst incl. operculum: 66 (74) 85
Length of cyst excl. operculum: 48 (64) 76
Width of cyst: 50 (67) 85
Height of penitabular ridges/crests: 2 (4) 8

The average dimensions of several isolated opercula observed are 30µm x 35µm

The measured specimens are from sidewall core samples in Challis-11 ST1 well at 1552.50m, Challis-11 ST2 well at 1842.00m and Rowan-1ST well at 3181.00m and 3183.00m.

Comments. *Meiourogonyaulax penitabulata* is an extremely distinctive taxon due to the prominent penitabular crests and/or ridges on all the major paraplate series on the loisthocyst. The ridges and/or crests on the apical paraplate series, however, are parasutural (Figs 11A-D). These features clearly indicate a standard gonyaulacalean paratabulation pattern. A preapical paraplate is present (Figs 11A-D). Penitabular elements are relatively rare in the Mid Jurassic, being much more common in the Late Jurassic, Cretaceous and Palaeogene. The morphology of the penitabular ornamentation is somewhat variable. It varies from having regular, entire/perforate, distally smooth, relatively narrow crests (the 'spongy' morphotype; Fig. 11), to somewhat discontinuous robust ridges which are irregularly surmounted by short, bifid, buccinate,

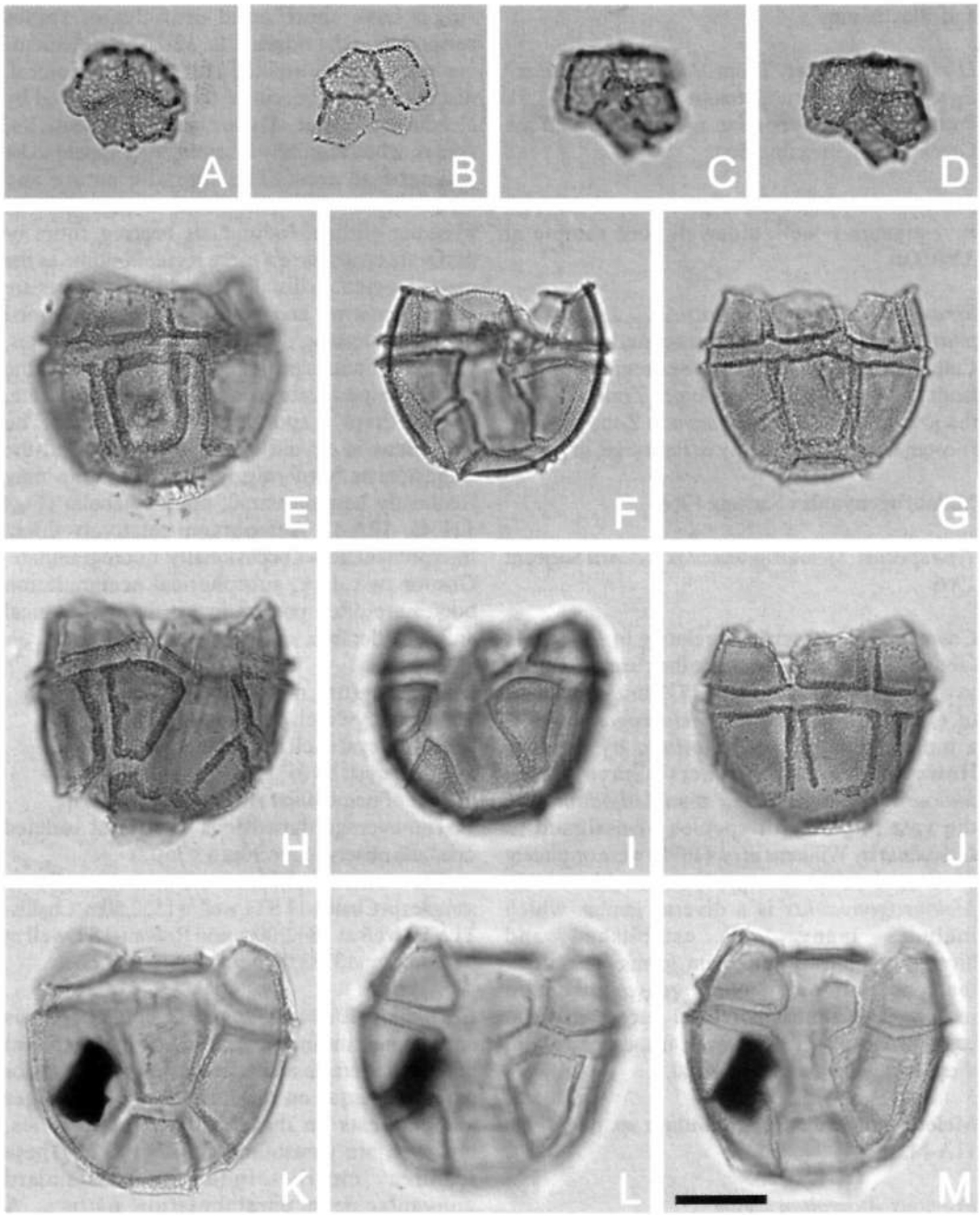

Fig. 11. Meiourogonyaulax penitabulata sp. nov. All specimens from sidewall cores in Challis-11 ST1 well at 1552.50m (Figs 11B, E-G, I-M), Challis-11 ST2 well at 1842.00m (Fig. 11H) and Rowan-1ST well at 3181.00m (Figs 11A, C-D). The photomicrographs were taken using plain transmitted light. The scale bar in Fig. 11M refers to all the photomicrographs and represents 25µm. Figs 11I, ♂ are the holotype, the remainder are paratypes. Note the ellipsoidal outline, the thick, microreticulate autophragm and the apical archaeopyle. This figure only illustrates forms with prominent penitabular crests, which are regular, entire or perforate, distally smooth and relatively narrow. These morphotypes are informally known as the 'spongy' form of this species. A - CPC 35418, paratype; an isolated operculum in low focus. Note the prominently microreticulate autophragm. B - CPC 35419, paratype; an isolated operculum in low focus. Note that the crests are parasutural, not penitabular. C, D - CPC 35420, paratype; an isolated operculum, high and low focus respectively. Note preapical paraplate and the parasutural crests. E - CPC 35421, paratype; ventral view, low focus. (continued opposite)

subconical or trabeculate processes (the 'irregular' morphotype; Fig. 12). The crests may appear to be formed by the dense coalescing of processes and they are occasionally fenestrate or, in extreme cases, somewhat trabeculate. The crests and the ridges/processes are markedly higher on the antapical (1''') paraplate (Fig. 11E). Both the distinctive 'irregular' and 'spongy' forms of *Meiourogonyaulax penitabulata* have exactly the same stratigraphical range, being present in the late Callovian of the Timor Sea area. Moreover, they commonly occur together, often in approximately similar relative proportions. Therefore, they are considered to be a single species and are not formally subdivided into subspecies or varieties here.

The paracingulum is apparently not subdivided into paraplates and is the only major paraplate series on the loisthocyst which has parasutural, as opposed to penitabular, ridges or crests (Figs 11F-G, 12A-I). The parasutural nature of the paracingular crests/ridges is far more common in the 'irregular' morphotype (Fig. 12). The parasulcus is not subdivided. The penitabular nature of the ornamentation on the ventral paraplates makes the parasulcal area appear anomalously wide (Figs 11H-I, L). The operculum is normally lost and the loisthocysts are usually not markedly elongate. They may be equant and are frequently wider than long (Figs 11, 12). The autophragm is thick and microreticulate and/or occasionally microgranulate. The species is slightly dorsoventrally flattened.

Comparison. Meiourogonyaulax penitabulata differs from most other species of *Meiourogonyaulax* and *Lithodinia* in having penitabular crests or ridges in the major paraplate series. Some Tithonian specimens of *M. bulloidea* (Cookson & Eisenack 1960) Sarjeant 1969 emend. Riding & Helby (this volume) exhibit intratabular ridges and bosses, which have a resemblance to *M. penitabulata,* but differ in lacking consistent penitabular ridges/crests. *Meiourogonyaulax viriosa* sp. nov. lacks intratabular and penitabular ridges, while *Lithodinia protothymosa* exhibits randomly inserted intratabular elements, but lacks penitabular ridges. *Meiourogonyaulax penitabulata* is also relatively large for the genus; the majority of the validly published species are significantly smaller than this new species.

The Bathonian *Meiourogonyaulax insulofigurata* Dodekova 1975 is the most similar in morphology, albeit superficially. It has thick, spongy autophragm in the intratabular areas and immediately adjacent to the parasutures (Dodekova, 1975, fig. 3). However, *M. insulofigurata* is smaller than *M. penitabulata* and appears to have parasutural ornamentation. The majority of the previously published species of this characteristically Middle Jurassic genus have paratabular ornamentation. Several species have parasutural crests similar in form to the penitabular crests of *Meiourogonyaulax penitabulata.* These include, *M. amlasis* Below 1981, *M. borealis* Sarjeant 1980, *M. bulloidea, M. caytonensis* (Sarjeant 1959) Sarjeant 1969, *M. cristulata* (Sarjeant 1959) Sarjeant 1969, *M. ghermanii* Beju 1971, *M. pertusa, M. planoseptata* Riding 1987 and *M. stoveri.* In particular, the specimens of *M. bulloidea* illustrated by Backhouse (1988, fig. 28, pl. 32, fig. 2) resemble *Meiourogonyaulax penitabulata* in that the relatively high parasutural crests appear in some cases to be penitabular.

Meiourogonyaulax penitabulata is also similar to *Atlantodinium jurassicum* Zotto *et al.* 1987, however the latter is fully penitabular and has penitabular crests in all six paracingular paraplates (Zotto *et al.*, 1987, fig. 6). Likewise, all species of the characteristically Tethyan Jurassic genera *Amphorula* and *Histiophora* are fully penitabular and lack any parasutural features.

Derivation of name. From the characteristic penitabular crests and ridges.

Holotype and type locality. Figures 11I-J, CPC 35424, Challis-11 ST1 well, sidewall core sample at 1552.50m.

Stratigraphical distribution. Meiourogonyaulax penitabulata has been recorded from the late Callovian strata of the Timor Sea region, Australia, where it is confined to the lower *Rigaudella aemula* Zone (subzones 7aiib-7aiia)

Note the perforate, spongeous nature of the penitabular crests. F, G - CPC 35422, paratype; ventral view, high and low focus respectively. Note that the crests around the paracingulum appear to be parasutural, not penitabular. H - CPC 35423, paratype; oblique dorsal view, low focus. Note relatively wide parasulcus. I, J - CPC 35424, holotype; ventral view, high and low focus respectively. Note the relatively wide parasulcus and how the postcingular penitabular crests in Fig. 12J diverge antapically. K-M - CPC 35425, paratype; dorsal view, high to low focus sequence. Note relatively wide parasulcus.

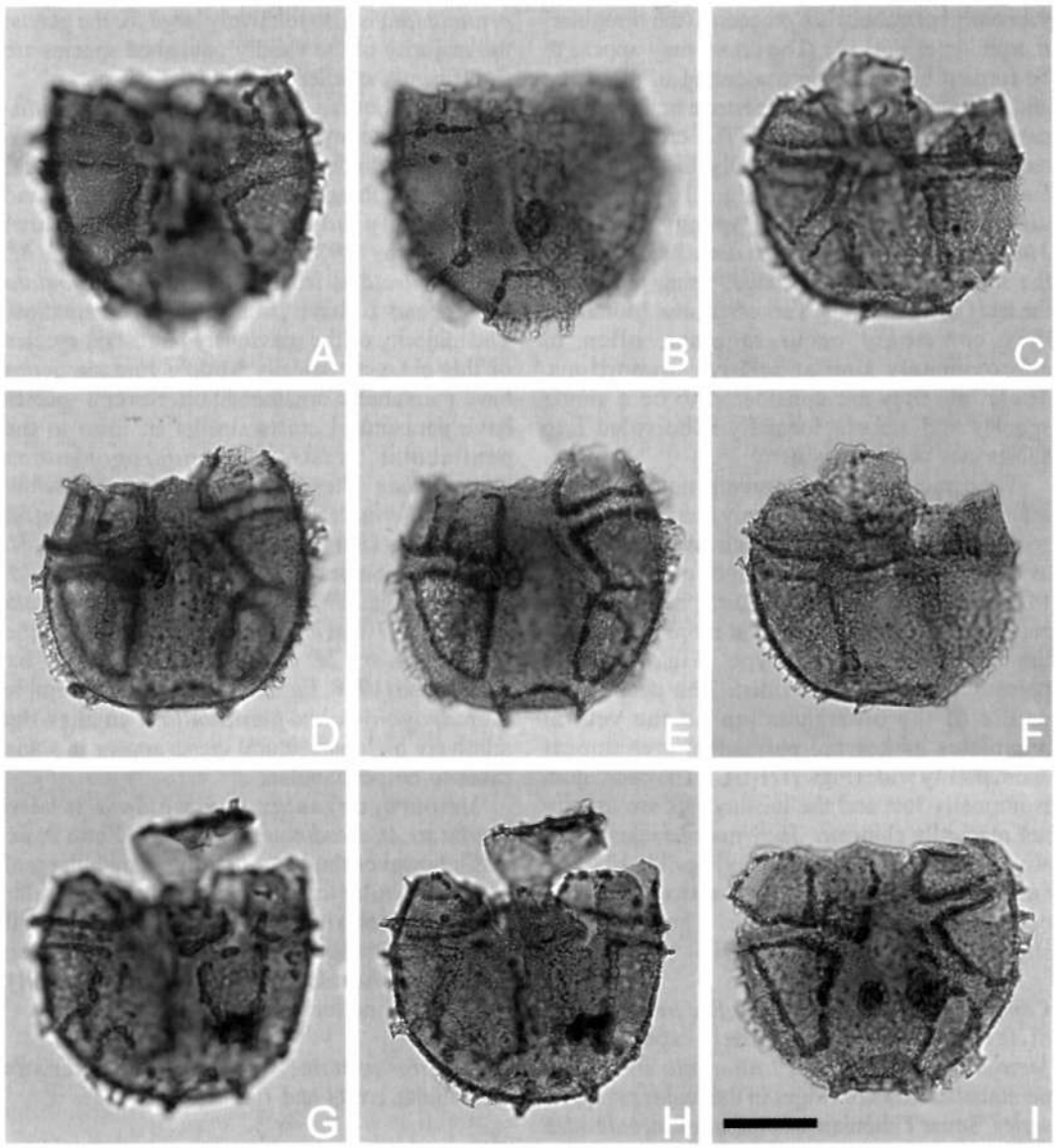

Fig. 12. Meiourogonyaulax penitabulata sp. nov. All specimens are paratypes from a sidewall core at 3181.00m in the Rowan-1ST well. The photomicrographs were taken using plain transmitted light. The scale bar in Fig. 12I refers to all the photomicrographs and represents 25µm. Note the squat ellipsoidal outline of the loisthocysts, the robust, strongly microreticulate autophragm and the apical archaeopyle. Figure 12 illustrates forms with low penitabular ridges surmounted by irregularly distributed, short, solid denticles or spines. The ornamentational elements may be trabeculate or may coalesce into fenestrate crests. These forms are informally known as the ' irregular' morphotype of this species. A, B - CPC 35426, paratype; ventral view, high/median and low focus respectively. Note the irregular outline caused by the sporadically coalescing penitabular ornamentation. C, F - CPC 35427, paratype; ventral view, high/median and low focus respectively. A form with relatively delicate penitabular denticles. D, E - CPC 35428, paratype; dorsal view, median and low focus respectively. Note the extremely wide parasulcus. G, H - CPC 35429, paratype; ventral view, high and median focus respectively. Note the highly irregular insertion of the penitabular ornamentation. I - CPC 35430, paratype; dorsal view, low focus. Note the wide parasulcus in the hypocyst.

(Foster, this volume; Helby & Partridge, in prep.). It is most prominent in, and characteristic of, subzones 7aiibia to 7aiiaii.

Meiourogonyaulax viriosa sp. nov. (Figs 13A-L)

Previous Australian usage
M.P. 70 – Helby.
Meiourogonyaulax sp. 70 – Helby.
Meiourogonyaulax bulloidea (pars.) – Morgan.

Description. A species of *Meiourogonyaulax*, ellipsoidal to subcircular in dorsoventral outline. A small, rounded, solid apical boss-like protuberance may be present on the operculum. Paratabulation fully indicated by low parasutural crests which are normally distally smooth. The parasutural crests are slender to relatively wide. They are continuous and generally entire, however slim, fenestrate crests are present and rarely these may be irregularly denticulate distally. The crests are highest at gonal points where they may be thickened into short projections. The paracingulum is not subdivided into paraplates, however the antapical end of the strongly indented parasulcus may occasionally exhibit internal parasutural crests. Autophragm thick, robust, microreticulate; occasionally partially microgranulate and/or microscabrate. One or more dark, subcircular accumulation bodies are normally present inside the cyst body.

Dimensions (μm; n=37) including crests where appropriate: Min. (Mean) Max.
Length of cyst incl. operculum: 62 (74) 99
Length of cyst excl. operculum: 46 (64) 79
Width of cyst: 47 (67) 93
Height of parasutural crests: 1 (2.5) 5

The measured specimens are from sidewall core samples in Challis-11 ST2 well (1842.00m), Rowan-1ST well (3181.00m and 3183.00m), Tern-1 well (1528.28m and 1529.50m) and Tern-2 well (1459.20m), a conventional core sample at 1642.50m from Jabiru-2 well and ditch cuttings between 1530.11m and 1536.21m in Tern-2 well.

Comments. *Meiourogonyaulax viriosa* is variable in outline; it may be elongate (Fig. 13D), however, many specimens are wide and squat (Figs 13A, E-F, L). Furthermore, the apical protuberance, when developed, helps to impart a flat cone shape to the operculum (Fig. 13K). The apical boss or protuberance is solid and typically low in height (1μm-3μm) and broad (up to 6μm). A characteristic feature of this taxon is the thick autophragm, which is consistently microreticulate and occasionally partially microgranulate and/or microscabrate. The fenestrae are normally less than 1μm in diameter, however occasionally some attain 1μm in width. The autophragm does not bear intratabular ornamentation, apart from the small fenestrae and microgranules/microscabrae, and varies between 1and 2μm in thickness. Because of the robust nature of the autophragm, the species does not tend to fold. However, mechanical damage may cause the autophragm to break, normally along parasutures, and damaged (crushed) specimens may be anomalously wide because of this (Fig. 13G). The parasutural ornamentation is also somewhat variable, but typically comprises slender (<1μm) to relatively broad (up to 3μm), continuous crests which are normally smooth distally. The rare, thin, fenestrate and occasionally distally irregularly denticulate parasutural crests suggest that the parasutural ornamentation may be formed from a dense network of coalescing processes. The parasutural crests are highest at gonal points and around the antapical (1'''') paraplate and lowest in the apical region. As indicated in *Dimensions* above, there is considerable variation in size.

Comparison. *Meiourogonyaulax viriosa* closely resembles *M. bulloidea* but differs in not being granulate and in lacking the intratabular ridges and the distinctive intratabular bosses that characterise the type material of the latter (Riding & Helby, this volume). *Meiourogonyaulax viriosa* also shows similarities to *M. penitabulata* and *Lithodinia protothymosa,* with which it co-occurs and is presumably closely related. However, *M. viriosa* lacks penitabular ornamentation and major intratabular elements. This new form is also similar to several previously described species with distally smooth parasutural crest or ridges. These include *M. bulloidea*, *M. pertusa*, *M. planoseptata* and *M. stoveri*. However, these taxa all lack the variable parasutural crests which are characteristic of *M. viriosa*.

Derivation of name. From the Latin *viriosus*, meaning robust or strong, and referring to the thick autophragm of this species.

Holotype and type locality. Fig. 13K, CPC 35439, Tern-1 well, sidewall core sample at 1528.28m

Stratigraphical distribution. *Meiourogonyaulax viriosa* has been recorded from the late Callovian strata of the Timor Sea region, occurring

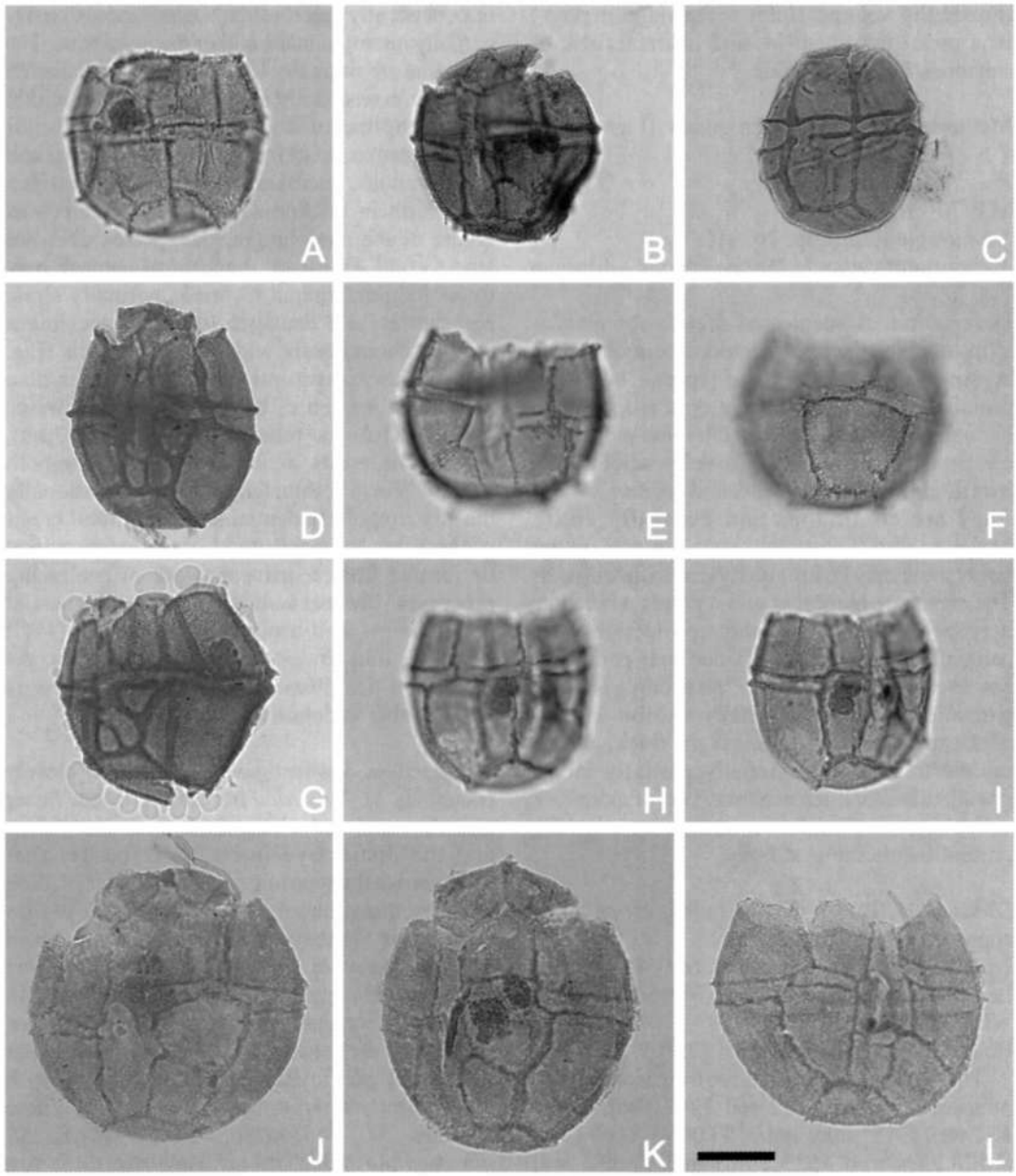

Fig. 13. Meiourogonyaulax viriosa sp. nov. Figures 13C-D, G are from conventional core at 1642.50m in Jabiru-2 well. The remainder of the specimens are from sidewall core samples from Challis-11 ST2 well at 1842.00 (Figs 13A, E-F, H-I), Rowan-1ST well at 3181.00m (Fig. 13B) and the Tern-1 well at 1528.28m (Figs 13J-L). All photomicrographs taken using plain transmitted light. Scale bar in Fig. 13L refers to all the photomicrographs and represents 25µm. Fig 13K is the holotype, the remainder are paratypes. Note the ellipsoidal to subcircular outline, the apical archaeopyle, the low, distally smooth parasutural crests, the frequent presence of accumulation bodies and the robust, microreticulate autophragm. A - CPC 35431, paratype; oblique ventral view, low focus. Note the low parasutural crests and the single accumulation body. B - CPC 35432, paratype; dorsal view, low focus. Note the low apical boss on the attached, simple operculum and the straight, narrow parasulcus, which includes some low, discontinuous parasutures on the hypocyst. C - CPC 35433, paratype; left lateral view, low focus. A relatively small specimen; note the relatively wide parasutural crests. D - CPC 35434, paratype; dorsal view, low focus. An elongate specimen; note the parasulcal parasutures on the hypocyst. E, F - CPC 35435, paratype; ventral view, high and low focus respectively. A wide specimen; note the strongly microreticulate autophragm and the apical archaeopyle. G - CPC 35436, paratype; slightly oblique (continued opposite)

sporadically in the *Wanaea digitata* Zone (7bi) and consistently throughout the *Rigaudella aemula* Zone (7a) (Foster, this volume; Helby & Partridge, in prep.).

Tabulodinium Dodekova 1990 emend.

1990 *Tabulodinium* Dodekova, p. 23-24.

Type species. Tabulodinium senarium Dodekova 1990

Emended diagnosis. Cavate, proximate dinoflagellate cysts intermediate in size, elongate ovoidal in outline and having a single, prominent apical horn. Periphragm, smooth, thin, easily folded and damaged. Endophragm relatively robust and ornamented by low-relief features except in the pandasutural areas. A pareodinioid paratabulation pattern is indicated by absence of ornamentation on the endophragm in the pandasutural areas; the paratabulation formula is: ?pr, 3', 2a, 6", 6c, 6"', 2'"", 5s. Paracingulum and parasulcus both relatively broad and fully paratabulate. Archaeopyle anterior intercalary (type 2I), operculum compound and free.

Comments. Dodekova (1990, p. 23, 24) stated that this genus would require emendation upon the discovery of more material. The abundant, well-preserved specimens of *Tabulodinium senarium* from the Elang Formation in this study allow a full revision. *Tabulodinium* is emended here in order to include a revised paratabulation pattern and the precise archaeopyle style. Furthermore, the 'kalyptra', or possible ectophragm, of Dodekova (1990) is here designated as thin periphragm. Dodekova (1990, p. 25) stated that the outer wall of this species is more like an ectophragm than a kalyptra. This outer wall cannot be an ectophragm, however, as the genus is not holocavate (Evitt, 1985, fig. 4.1). No ornamentation was observed on the periphragm; Dodekova (1990), however, reported a coarse reticulation and parasutural ridges.

The paratabulation pattern of *Tabulodinium senarium* is in accord with that of members of the Subfamily Pareodinioideae of Fensome *et al.* (1993), due to the presence of two anterior intercalary paraplates (Fig. 14). Fensome *et al.* (1993, p. 79) recognised that *Tabulodinium* belongs in the Family Pareodiniaceae, but assigned it to 'subfamily uncertain' due to the fact that Dodekova (1990, p. 25) was unsure of the paratabulation of the upper part of the epicyst. Dodekova (1990) questionably interpreted three anterior intercalary paraplates. The genus appears to be an evolutionary offshoot of *Pareodinia* Deflandre 1947 (see Below, 1990, fig. 1).

Tabulodinium senarium Dodekova 1990 emend. (Figs 14A-B, 15A-P, 16A-P)

1990 *Tabulodinium senarium*; Dodekova, p. 24, pl. 4, figs 4-10, pl. 9, figs 3-5, 9, 10.

Previous Australian usage
Pareodinia tamarense – Ingram.
Pareodinia tamarense – Helby.
Tabulodinium senarium – Helby.

Emended description. A species of *Tabulodinium* with a relatively short apical horn, which is blunt and rounded distally. The pericoel is narrow, the flimsy periphragm is normally damaged and may frequently be partially or wholly absent. Endophragm covered by dark brown to black, short (c. 1µm), solid, densely inserted elements except in the pandasutural areas. The boundaries of the ornamented areas are relatively regular and penitabular in position; they thus give a precise indication of the number and shape of the paraplates. The short processes are normally expanded distally and may be buccinate, bulbous or capitate. The density and small size of the processes gives an appearance of differentiated autophragm and it is possible that some of the elements are linked medially or distally. The narrow pandasutural bands are smooth or microscabrate. The paracingulum divides the cyst body equally in half, however in some specimens the epicyst is slightly longer than the hypocyst. The paracingulum is laevorotatory and is displaced by approximately its height ventrally.

Dimensions (µm; n=58) all measurements exclude periphragm: Min. (Mean) Max.
Length of cyst: 62 (78) 94

dorsal view, low focus. An angular, damaged specimen; note parasutural parasutures on the hypocyst. H, I - CPC 35437, paratype; dorsal view, high and median focus respectively. Note the irregularly microreticulate autophragm and the apical archaeopyle. J - CPC 35438, paratype; slightly oblique ventral view, high/median focus. Note the subcircular outline and the well developed paratabulation pattern K - CPC 35439, holotype; dorsal view, low focus. Note the apical boss and the two prominent accumulation bodies. L - CPC 35440, paratype; dorsal view, low focus. Note the strongly microreticulate autophragm.

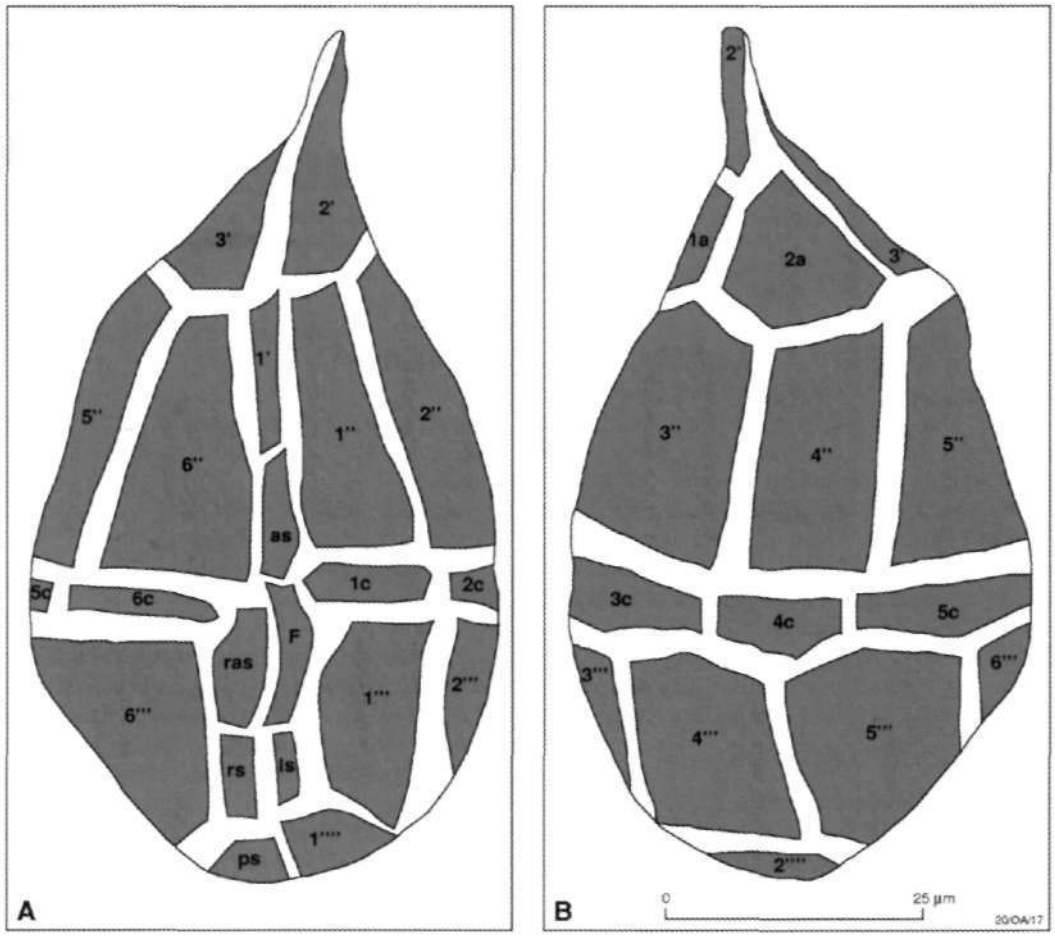

Fig. 14. Line drawings of an idealised specimen of *Tabulodinium senarium* Dodekova 1990 emend., illustrating the Kofoidian paratabulation pattern as indicated by the dark, ornamented penitabular areas. A - specimen in ventral view; B - specimen in dorsal view. F = reflected flagellar scar.

Width of cyst: 33 (44) 56
Length of apical horn: 7 (13) 20

The measured specimens are from sidewall core samples in Challis-11 ST1 well (1548.00m and 1552.50m), Challis-11 ST2 well (1842.00m) and Rowan-1 ST well (3181.00m and 3183.00m).

Comments. *Tabulodinium senarium* has a full paratabulation pattern, which is indicated by the narrow, straight pandasutural bands, which are devoid of the dense ornamentation of short processes. This characteristic pattern of pandasutural bands devoid of the dense, dark, low-relief intratabular ornamentation was termed areolate by Williams *et al*. (1978, fig. 115). Figure 14 illustrates the pareodinioid paratabulation pattern and therefore represents a revision of fig. 3 of Dodekova (1990). The penitabular ornamentation in the apical paraplate series may be lower and paler than elsewhere on the cyst. Frequently, some variations are observed in the precise shape of some of the penitabular areas. For example, the paracingular paraplates may be quadrangular or pentangular, with an angular

Fig. 15 (opposite). *Tabulodinium senarium* Dodekova 1990 emend. The specimens are all from sidewall core samples from Challis-11 ST1 well at 1548.00m (Fig. 15M) and 1552.50m (Figs 15A-G, I-K, N, O), Challis-11 ST2 well at 1842.00m (Figs 15H, L) and Rowan-1 ST well at 3138.00m (Fig. 15P). All photomicrographs taken using plain transmitted light. The scale bar in Fig. 15P refers to all photomicrographs and represents 25µm. Note the prominent apical horn, the anterior intercalary (type 2I) archaeopyle and the thin, flimsy periphragm, which is susceptible to mechanical damage. A complete pareodinioid paratabulation is indicated on the endophragm by narrow pandasutural bands, which are devoid of the distinctive dark ornamentation. (continued opposite)

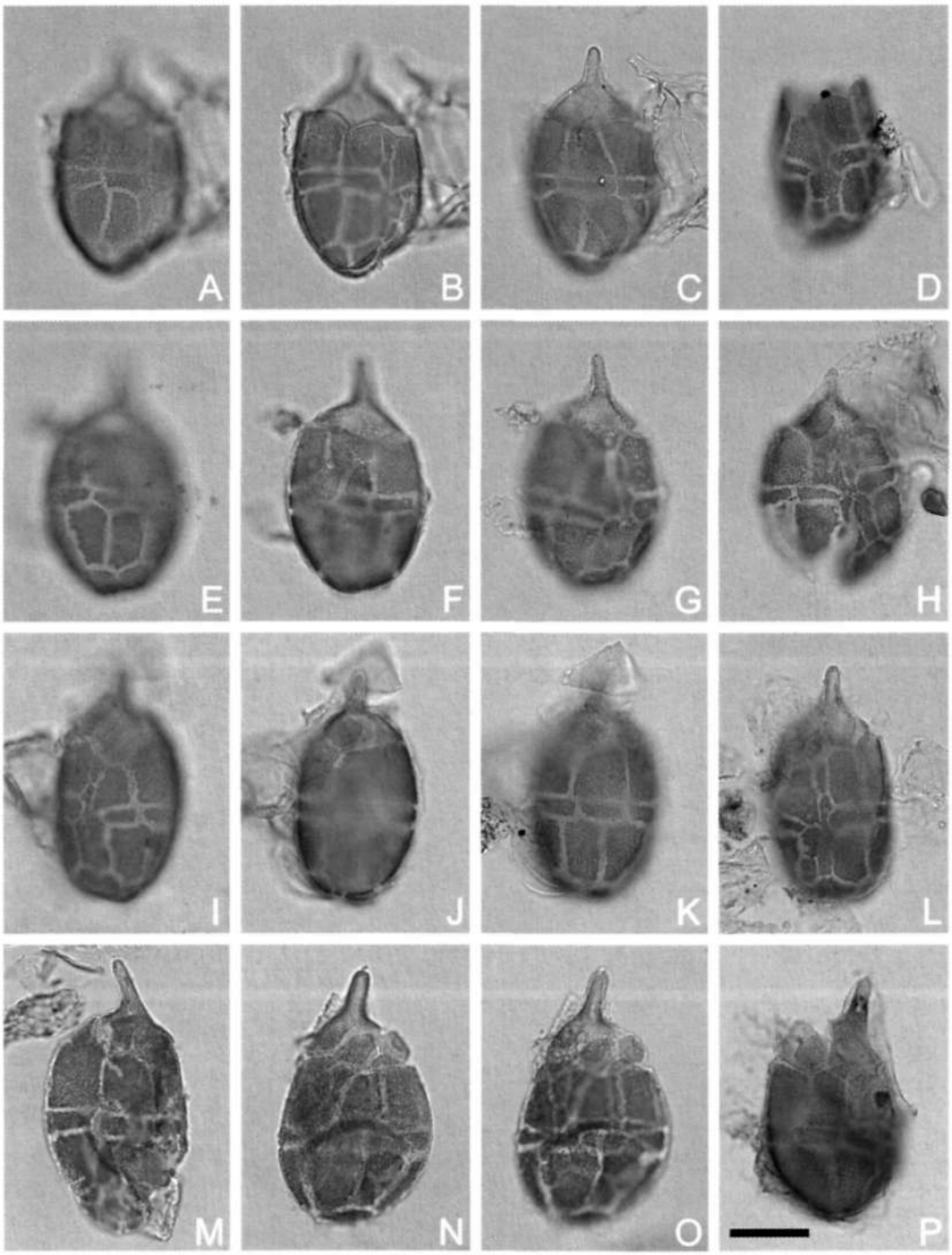

A-C - CPC 35457; oblique ventral view, high to low focus sequence. D - CPC 35458; dorsal view, low focus. The apical paraplate series have been lost by mechanical damage. Note the laevorotatory paracingulum and the ventral paratabulation. E-G - CPC 35459; slightly oblique dorsal view, high to low focus sequence. H - CPC 35460; dorsal view, low focus. I-K - CPC 35461; oblique ventral view, high to low focus sequence. Note the type 2I archaeopyle. L - CPC 35462; dorsal view, low focus. Note the complex ventral paratabulation pattern. M - CPC 35463; ventral view, low focus. Note the recurved nature of the apical horn. N, O - CPC 35464; right lateral view, high and low focus respectively. Note the anterior intercalary (type 2I) archaeopyle. P - CPC 35465; left lateral view, median/low focus. Note the prominent periphragm and the anterior intercalary (type 2I) archaeopyle.

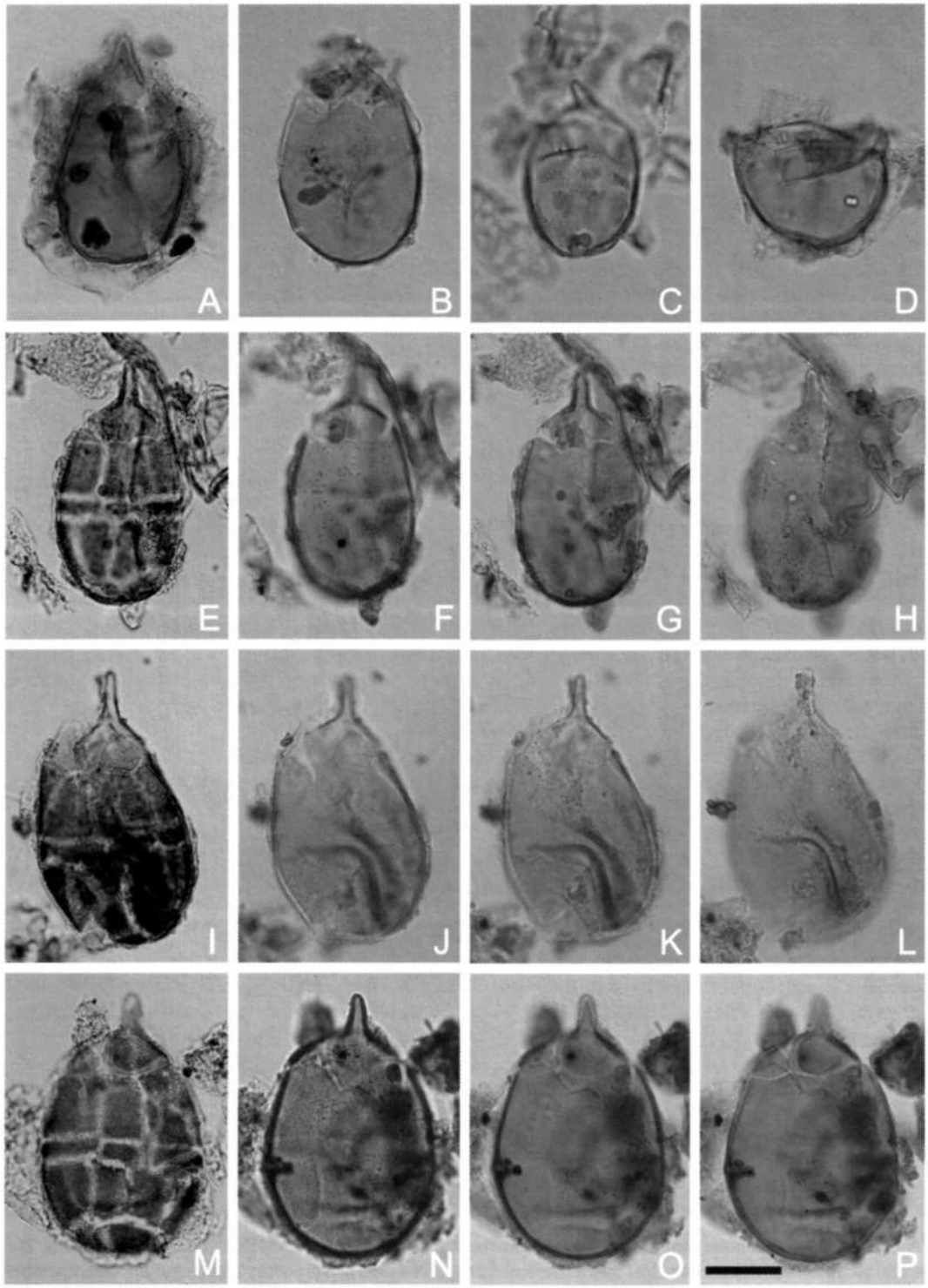

Fig. 16. Tabulodinium senarium Dodekova 1990 emend. The specimens are all from sidewall core samples from Challis-11 ST1 well at 1548.00m (Fig. 16C), Rowan-1 ST well at 3183.00m (Fig. 16A) and Tamar-1 well at 2183.00m (Figs 16B, D-P). All photomicrographs were taken using plain transmitted light. The scale bar in Fig. 16P refers to all the photomicrographs and represents 25µm. Note the apical horn, the anterior intercalary (type 2I) archaeopyle. This photomicrograph plate illustrates 'faded' forms of *T. senarium* (continued opposite)

posterior boundary (Figs 15B, E). The detailed parasutural paratabulation pattern may be difficult to resolve because in some specimens, the ornamented regions representing the 1', as, flagellar mark and ls appear to be joined. This gives the impression of a single, slender dark area over much of the midventral area (Figs 15D, H, L).

The exposure of specimens of *Tabulodinium senarium* to an oxidising environment has the effect of destroying the ornamentation of dark, dense, short processes in the central areas of the paraplates. However, the endophragm forming the cyst wall is not affected. In specimens which have been subject to heat, e.g. by an electric hot plate during the production of single grain mounts, the processes lose their dark colouration (e.g. Fig. 16A). This degradation of the dark intratabular orna-mentation can occur within hours given an excess of free oxygen. Therefore, the majority of the undegraded specimens of *T. senarium* which were studied are from strew mounts (Fig. 15). Chemical oxidation during sample processing also tends to promote a similar loss of ornamentation. This fading appears to be arrested when the residue is sealed in a permanent mount (i.e. deprived of free oxygen). Most specimens of *T. senarium* on strew mount slides from a sidewall core at 2183.00m in Tamar-1 well (completed early 1979) have lost their penitabular ornamentation (Figs 16B, D-P). By contrast, the majority of specimens on slides from Challis-11 ST1 well (completed 1992) show no reduction (Figs 15A-G, I-K, M-O). It is likely that the chemistry of the sporopollenin which forms the processes in this species is somehow significantly more susceptible to oxidation than the endophragm and periphragm. In faded specimens, the periphragm tends to lose integrity and may significantly expand and/or take on a kalyptrate appearance (Figs 16A, D). The implications of this are that specimens of *Tabulodinium senarium* in samples which have been subject to oxidation via pre- or post-diagenetic weathering may not be recognisable. Such oxidised specimens may resemble species of *Pareodinia* or *Kalyptea monoceras* Cookson & Eisenack 1960 (Figs 16B, C).

Stratigraphical distribution. The species was originally reported from the Upper Bathonian and Lower Callovian Dobric Formation of northern Bulgaria by Dodekova (1990). It has also been recorded from the Lower Callovian Brora Roof Bed of Brora, north-east Scotland (unpublished data). The Brora Roof Bed is the lowermost unit of the Brora Shale Member (Brora Argillaceous Formation) and belongs to the *Proplanulites koenigi* Ammonite Zone (Sykes, 1975). *Tabulodinium senarium* has been recorded from the late Callovian strata of the Timor Sea region, and is confined to the *Rigaudella aemula* Zone (7ai) (Foster, this volume; Helby & Partridge, in prep.). It is a distinctive, relatively consistent, minor component of dinoflagellate cyst associations from subzones 7aiia to 7aib.

Voodooia gen. nov.

Type species. Voodooia tabulata sp. nov.

Diagnosis. Proximate, acavate, longitudinally elongate ellipsoidal cysts with a single, long apical horn and two shorter antapical horns. Intermediate to large in size. Epicyst significantly longer than hypocyst. Paratabulation indicated by low relief ornamentational features and of pareodinioid style; paratabulation formula: 3', 2a, 6", 7c, 6"', 2"", 5s. Archaeopyle anterior intercalary, probably one or two-paraplate (type I or 2I). Operculum probably compound, attached or free.

---

which have been oxidised and largely lost the distinctive dark ornamentation in the penitabular areas. Figs 16E, I, M were taken by RH in the early 1980s and illustrate the respective specimens 'unfaded', i.e. unoxidised. Figs F-H, J-L, N-P were taken by JBR during June 2000 and illustrate directly how these three individual specimens have gradually lost the dark penitabular ornamentation. A - CPC 35466; ventral view, low focus. A form with a 'kalyptrate' periphragm. The periphragm has expanded over time and become significantly more amorphous. B - CPC 35467; ventral view, low focus. A faded form which has lost the apex and much of the periphragm through mechanical and chemical damage respectively. C - CPC 35468; dorsal view, high focus. Note the peripheral loss of much of the dark ornamentation in the penitabular areas. However, some faint ornamentation toward the centres of the paraplates remains. D - CPC 35469; ?dorsal view, median focus. Note the loss of the apex and the expansion of the periphragm. E-H - CPC 35470; specimen in dorsal view. Fig. E taken in the early 1980s. Figs F-H are recent photomicrographs, high to low focus sequence. Note the loss of the dark penitabular ornamentation. I-L - CPC 35471; specimen in dorsal view. Fig. I taken in the early 1980s. Figs J-L are recent photomicrographs, high to low focus sequence. Note the loss of the dark penitabular ornamentation. M-P - CPC 35472; specimen in slightly oblique ventral view. Fig. M taken in the early 1980s. Figs N-P are recent photomicrographs, high to low focus sequence. Note the loss of the dark penitabular ornamentation.

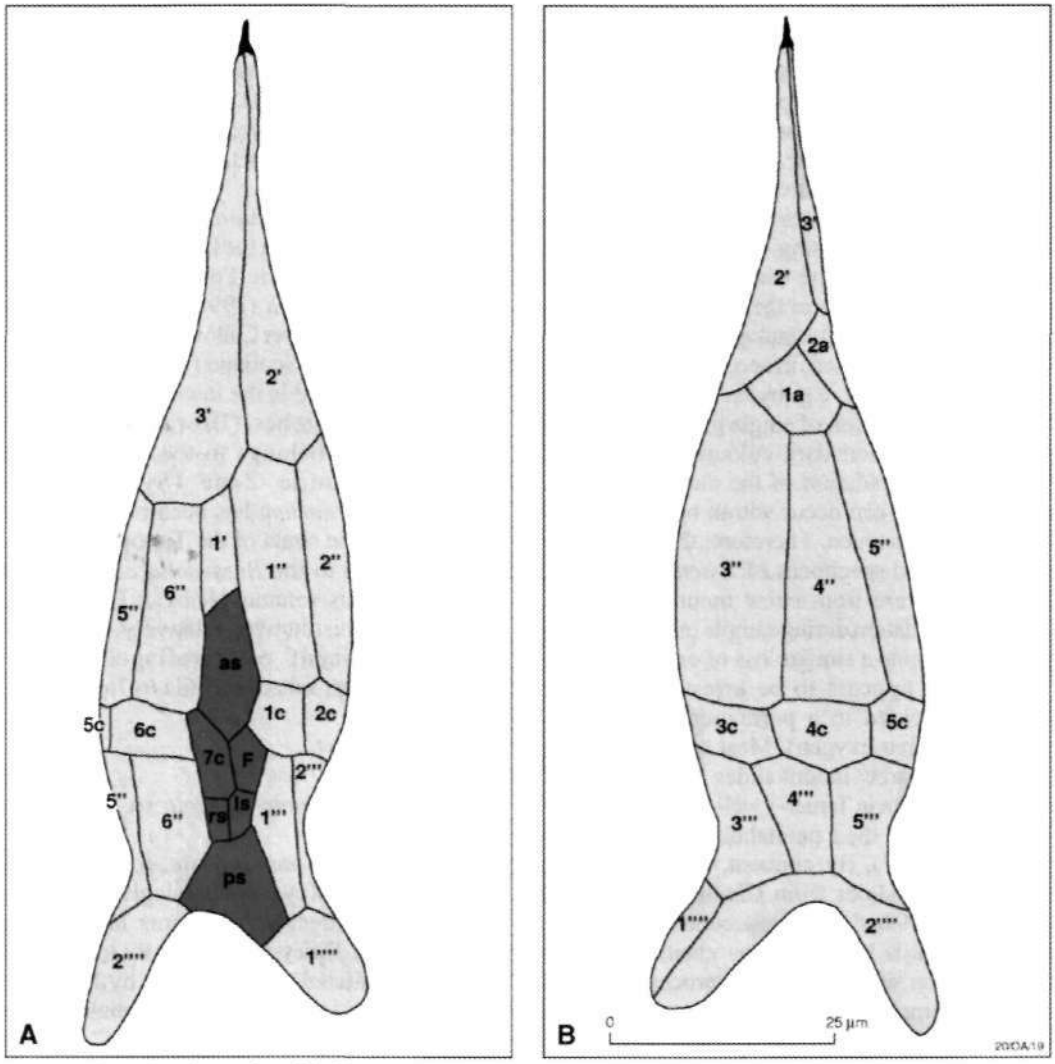

Fig. 17. Line drawings of an idealised specimen of *Voodooia tabulata* sp. nov., illustrating the Kofoidian paratabulation pattern. A - specimen in ventral view, note that the parasulcal area is shaded in a darker ornament. F = reflected flagellar scar. B - specimen in dorsal view.

Comments. *Voodooia* gen. nov. is a pareodinioid genus with two anterior intercalary paraplates which may be lost in archaeopyle formation (Fig. 17). The precise archaeopyle style, however, has not been determined. The genotype, *Voodooia tabulata* sp. nov., appears to exhibit paraplate dehiscence in the anterior intercalary series. However, whether one or two paraplates are lost and if these are attached or free, is not clear.

Comparison. *Voodooia* is similar to some other elongate pareodinioid genera, specifically *Batioladinium* Brideaux 1975 and *Broomea* Cookson & Eisenack 1958. *Batioladinium* is not normally fully paratabulate (but see Below, 1990, fig. 15). Similarly, *Aprobolocysta* Duxbury 1977 is distinguished from *Voodooia* by the apical archaeopyle, variable cavation and the lack of a long apical horn (Duxbury, 1977, p.52; Backhouse, 1987). *Broomea* Cookson & Eisenack 1958 is also similar to *Voodooia*, but is variably paratabulate and has an unequivocal one- or two-paraplate anterior intercalary archaeopyle (type I or 2I). The genotype, *Broomea ramosa* Cookson & Eisenack 1958, is also characterised by two groups of bunched antapical appendages (Cookson & Eisenack, 1958, pl. 6, figs 6, 7). *Voodooia* has some similarities to *Gresslyodinium* Below 1990, but this has a single antapical horn or protrusion. *Cantulodinium* Alberti 1961 differs from

Voodooia in being pear-shaped, nontabulate and having a three paraplate (type 3I) anterior intercalary archaeopyle. Furthermore, it may have several relatively small, thorn-like antapical horns or appendages (Van Helden, 1986). Other broomeoid and pareodinioid genera such as *Gochteodinia* Norris 1978, *Paraevansia* Below 1990 and *Pareodinia* Deflandre 1947 lack antapical horns and *Kalyptea* Cookson & Eisenack 1960 is typically kalyptrate. *Protobatioladinium* Nøhr-Hansen 1986 has a combination apical-intercalary, type (tA) + (2I), archaeopyle and lacks paired antapical horns (Nøhr-Hansen, 1986).

Derivation of name. From the resemblance in shape to a voodoo doll.

Voodooia tabulata sp. nov. (Figs 17A-B, 18A-O)

1996 *Pareodinia* spp.; Burger, pl. 8, figs S, T.

Previous Australian usage
Broomea tabulata - Ott (1970, pl. 9, figs 4-6).
Imbatodinium sp. - Lister/Burmah (BOC).
M.P. 707 – Helby.
Voodooia tabulata – Helby.
Samsonia tabulata – Morgan.

Description. A species of *Voodooia* which is not primarily dorsoventrally compressed and has microgranulate to occasionally microscabrate autophragm. The widest part of the cyst is at, or anterior of, the prominent paracingulum. Apart from the tapering apical horn, the narrowest part of the cyst is posterior to the paracingulum, where a distinct 'waist' is developed close to the level of the antapical margin of the 4''' paraplate. The dorsal side of the cyst is frequently slightly inflated. The three horns are rounded distally and are of variable length, especially the paired antapical horns. A small capitate structure may be developed on the distal part of the apical horn and rarely, small, solid spinules are developed on the antapical horns (Fig. 18D). The apical horn is generally distinct, and the rest of the epicyst is cone-shaped. Paratabulation is indicated by low, smooth parasutural ridges, which are most prominent at, and adjacent to, the paracingulum. The parasulcus is indented. Generally the paratabulation is fully indicated, however the parasutural ridges may be suppressed, especially in the apical and antapical regions.

Dimensions (µm; n=35): Min. (Mean) Max.
Length of cyst body incl. horns: 84 (105) 136
Length of cyst body excl. horns: 52 (63) 80
Length of epicyst incl. apical horn: 53 (67) 94
Length of hypocyst incl. antapical horns: 21 (32) 43
Length (height) of paracingulum: 5 (8) 10
Width of cyst body: 25 (36) 44
Length of apical horn: 17 (28) 45
Length of antapical horns: 4 (16) 30

The measured specimens are from a conventional core sample at 3221.47m in Layang-1 well and from sidewall core samples in Challis-11 ST1 well at 1552.50m, Challis-11 ST2 well at 1842.00m and Montebello-1 well at 2575.00m.

Comments. *Voodooia tabulata* is a distinctive, elongate species. The precingular paraplates, in particular, are extremely long (Fig. 17), however the degree of elongation is extremely variable (Fig. 18). The species appears to be either slightly squat in outline (Figs 18A-E, I-J) or markedly slender and elongate (Figs. 18F-H, K-O). Most specimens are large in size, but a minority are intermediate. In lateral view, this species is commonly asymmetrical; this is caused by the inflation of the dorsal side (Fig. 18B). This feature can often be a useful orientational criterion. Note that the average length of the hypocyst, including the antapical horns, is over half the length of the epicyst including the apical horn (see *Dimensions* above and Figs 17, 18). Many specimens were observed in oblique lateral views, indicating that this species is not primarily dorsoventrally compressed (Fig. 18). The species is often damaged, presumably mechanically, and it seems to split along parasutures. Dark, subspherical accumulation bodies are commonly present within the cyst. Some definite disruption of the anterior intercalary paraplate series was noted, which is interpreted as being related to archaeopyle formation (Figs 18A, I, L; see also Burger, 1996, pl. 8, figs S, T). The precise paraplate equivalence and whether the opercular piece(s) are adnate or free, however, is not clear. Some specimens do not appear to exhibit an excystment aperture (Fig. 18).

Derivation of name. From the fact that this cyst is fully paratabulate.

Holotype and type locality. Figure 18M, CPC 35484, Challis-11 ST1 well, sidewall core sample at 1552.50m

Stratigraphical distribution. *Voodooia tabulata* occurs in the lower part of the late Callovian

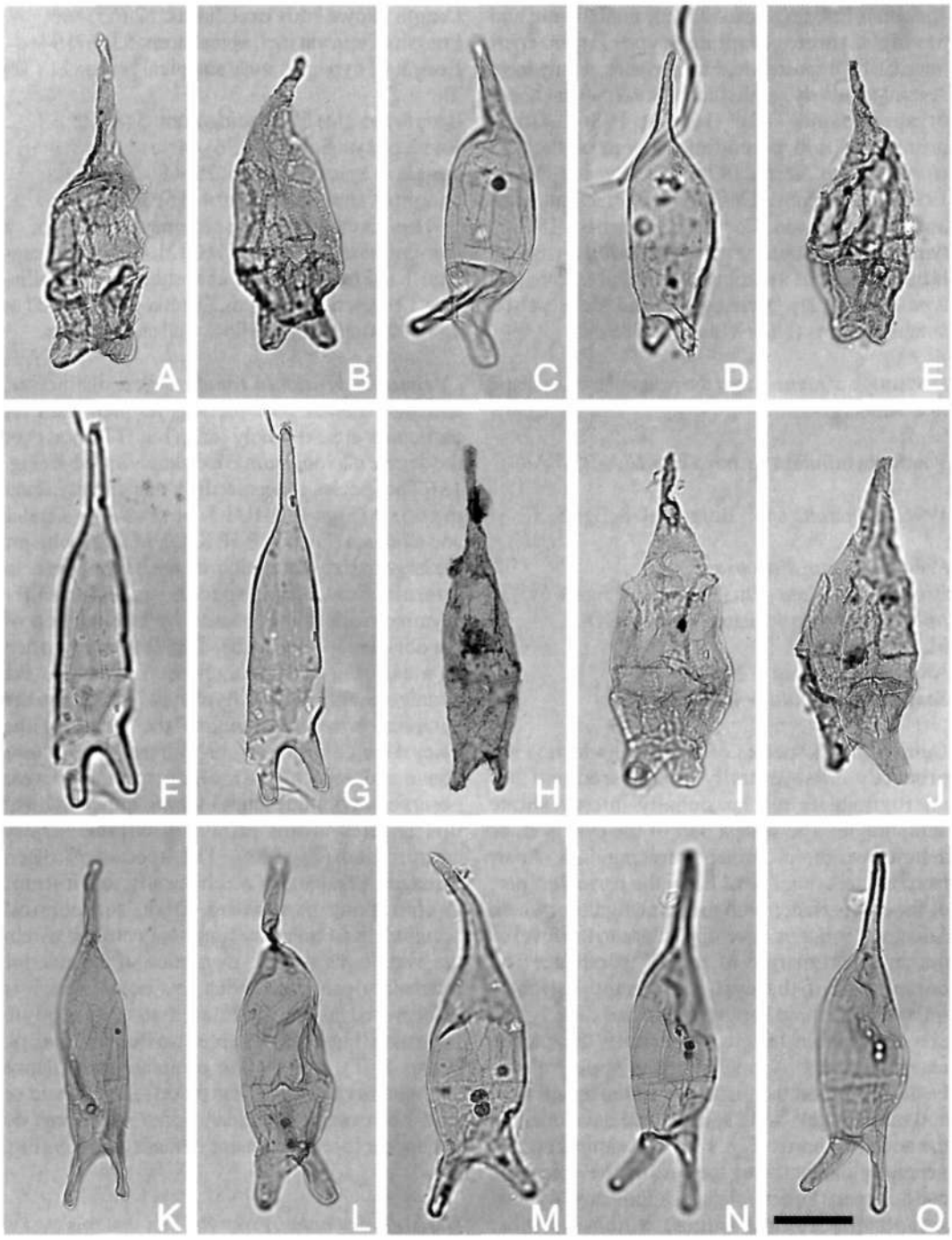

Fig. 18. Voodooia tabulata sp. nov. The specimens are from conventional core in Layang-1 well at 3221.47m (Fig. 18H) and sidewall cores from Challis-11 ST1 well at 1552.50m (Figs 18C-D, F-G, M), Challis-11 ST2 well at 1842.00m (Figs 18K-L, N-O) and Montebello-1 well at 2575.00m (Figs 18A-B, E, I-J). All photomicrographs taken using plain transmitted light. Scale bar in Fig. 18O refers to all photomicrographs and represents 25µm. Fig. 18M is the holotype; remainder are paratypes. Note slender, elongate ellipsoidal cyst body, the three horns (of which the apical horn is consistently longest), the discontinuous low parasutural ridges indicating pareodinioid paratabulation and lack of a distinct archaeopyle. Figs 18A-E, I-J are relatively squat, whereas Figs. 18F-H, K-O are long and slender. A - CPC 35473, paratype; ventral view, median/low focus. (continued opposite)

Rigaudella aemula Zone (7ai) in the Timor Sea region (Foster, this volume; Helby & Partridge, in prep.). The species is confined to subzones 7aiibia-7aiia in the Bayu-Undan Gas Field.

Woodinia gen. nov.

Type species. Woodinia pedis sp. nov.

Diagnosis. Small, proximate, acavate, elongate, flask-shaped dinoflagellate cysts which are normally dorsoventrally flattened. Outline varies from rounded subrectangular to subtriangular. The widest part of the cyst is normally the antapex and the antapical lateral areas are typically extended into lobes or protuberances. Intratabular areas of differentiated autophragm or discrete, less dense, low relief ornamentation may be developed on the apical, precingular, postcingular and antapical paraplate series. Elsewhere the autophragm may be microgranulate, granulate, microreticulate, scabrate or smooth. The intratabular ornamentation, where developed, suggests a gonyaulacalean paratabulation; the formula being X', 6", Xc, 6'", 2"", Xs. The postcingular paraplates are markedly elongate. Paracingulum undivided and located high on the cyst, may be prominent and indented. Parasulcus midventral and indented. Archaeopyle apical; operculum simple, attached or free.

Comments. The two lateral antapical lobes developed in this genus are considered to probably represent paired antapical paraplates. This suggests a relationship to *Microdinium* Cookson & Eisenack 1960 and other partiform genera but this cannot be demonstrated unequivocally.

Comparison. *Woodinia* gen. nov. resembles *Dissimulidinium* May *et al.* 1987 in shape, particularly in the presence of prominent paired antapical lobes (May *et al.*, 1987, figs 2-4). However, *Dissimulidinium* is significantly larger than *Woodinia*, is laterally compressed, proximochorate and has nontabular, penitabular and possibly parasutural ornamentation. Similarly, *Woodinia* also resembles the latest Jurassic-Early Cretaceous restricted marine genus *Tetrachacysta* Backhouse 1988. The latter is, by contrast, a quadrilobate form with a pair of lateral protuberances on both the epicyst and hypocyst (Backhouse, 1988, fig. 32). The type material of *Kylindrocysta* Fenton *et al.* 1980 is, like *Woodinia*, a flask-shaped Jurassic genus, but is parallel-sided and lacks indications of paratabulation aside of the archaeopyle (Stover & Williams, 1987, fig. 49). Other flask-like or egg-shaped Jurassic dinoflagellate cyst genera with apical archaeopyles such as *Lanterna* Dodekova 1969 and *Meiourogonyaulax* Sarjeant 1966 differ from *Woodinia* in having sexiform gonyaulacalean paratabulation patterns. *Stenopyxinium* Deflandre 1968 has spinose antapical protrusions and possibly an epicystal archaeopyle, but otherwise is similar in overall shape to *Woodinia*. Certain members of the Early-Mid Jurassic '*Parvocysta* suite' of Riding (1984) bear superficial resemblance to *Woodinia*, but normally have anterior intercalary archaeopyles and most are significantly less elongate. These include *Mikrocysta* Bjaerke 1980, *Parvocysta* Bjaerke 1980 and *Susadinium* Dörhöfer & Davies 1980. The closely related genus *Phallocysta* Dörhöfer & Davies 1980 is, like *Woodinia*, flask-shaped and antapically wide, tapering toward the apex. *Phallocysta*, however, has an interior intercalary archaeopyle and is epicavate (Riding, 1984).

Derivation of name. *Woodinia* is named in honour

A - CPC 35473, paratype; ventral view, median/low focus. Note the short, stubby antapical horns. B - CPC 35474, paratype; oblique lateral/dorsal view, median focus. Note the recurved apical horn and the faint parasutural ridges. C - CPC 35475, paratype; oblique ventral view, median/low focus. Note the prominent paracingulum, located relatively close to the antapex and the small accumulation body. D - CPC 35476, paratype; oblique ventral view, high focus. Note the short denticles on the distal part of the antapical horn. E - CPC 35477, paratype; oblique dorsal view, high/median focus. A specimen with relatively short horns. F, G - CPC 35478, paratype; dorsal view, high and median focus respectively. An extremely elongate form; note the incipient crack at the paracingulum. H - CPC 35479, paratype; dorsal view; a composite photomicrograph. A relatively small, elongate morphotype. I - CPC 35480, paratype; ventral view, median focus. Note the wide, stubby antapical horns and the possible anterior intercalary archaeopyle. J - CPC 35481, paratype; oblique right lateral view, median focus. Note the prominent paracingulum. K - CPC 35482, paratype; dorsal view, low focus. A specimen with relatively smooth autophragm. L - CPC 35483, paratype; dorsal view, median focus. Note the distorted apical horn and the relatively wide antapical horns. M - CPC 35484, holotype; dorsal view, median focus. Note the prominent paracingulum and small accumulation bodies. N, O - CPC 35485, paratype; dorsal view, median and low focus respectively. Note the slightly distally tapering apical horn and the relatively long antapical horns.

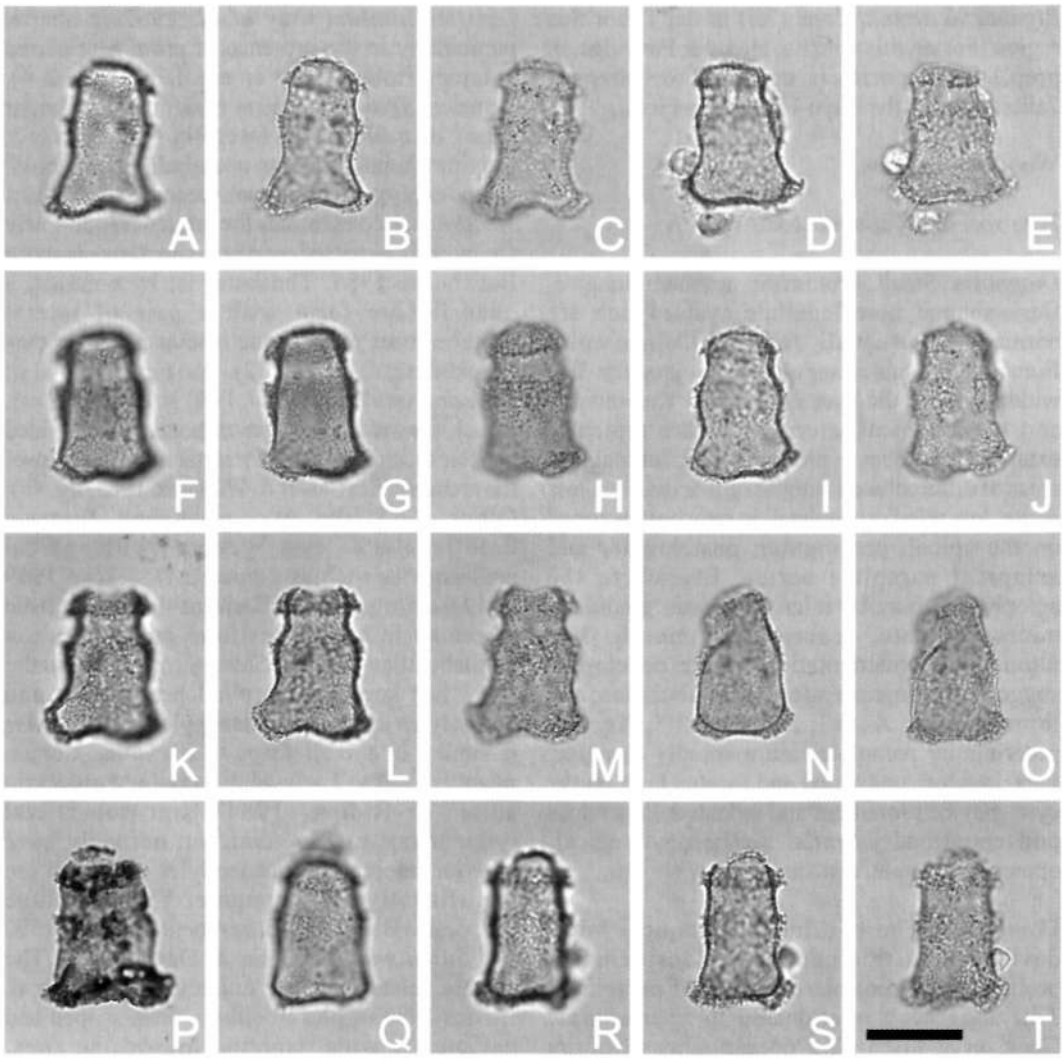

Fig. 19. Woodinia pedis sp. nov. The specimens are from sidewall cores from Challis-11 ST1 well at 1552.50m (Figs 19A-E, I-J) and Challis-11 ST2 well (Figs 19F-H, K-O, Q-T), except Fig. 19P, which is from conventional core at 3124.87m in Undan-4 well. All photomicrographs were taken using plain transmitted light. The scale bar in Fig. 19T refers to all photomicrographs and represents 25µm. Figs 19K-M are of the holotype and the remainder are paratypes. Note the small, subrectangular cyst body, the apical archaeopyle, the prominent, high, paracingulum, the long postcingular paraplate series and the antapical lateral lobes with their prominent ornamentation (or 'pedestals'). A-C - CPC 35486, paratype; dorsal view, high to low focus sequence. Note the distinct antapical concavity and that the low, virtually flat, operculum is in place. D, E - CPC 35487, paratype; ventral view, median and low focus respectively. F-H - CPC 35488, paratype; ventral view, high to low focus sequence. Note the intratabular areas of differentiated autophragm. I, J - CPC 35489, paratype; dorsal view, median and low focus respectively. K-M - CPC 35490, holotype; ventral view, high to low focus sequence. Note the apical archaeopyle and the intratabular areas of differentiated autophragm or 'pads'. N, O - CPC 35491, paratype; ventral view, median and low focus respectively. A specimen with a flask-shaped cyst body. Note the prominent ornamentation on the antapical lateral lobes. P - CPC 35492, paratype; dorsal view, high focus. Note the archaeopyle has operated, but the operculum remains attached. Q - CPC 35493, paratype; dorsal view, high focus. Note the subrectangular outline and the prominent paracingulum. R-T - CPC 35494, paratype; dorsal view, high to low focus sequence. A slender, relatively elongate form.

of Gordon D. Wood.

Woodinia pedis sp. nov. (Figs 19A-T)

Previous Australian usage
M.P. 618 (Challis) – Helby.

Description. A subrectangular to rounded subtriangular species of *Woodinia*. Two small lateral antapical protuberances are normally developed, imparting a slight antapical concavity. Rounded subquadrate or subrectangular, intratabular pad-like areas of differentiated autophragm in which short, slender, solid, dense, trabeculate processes are developed. These processes may coalesce to form anastomosing crests. The antapical processes/crests are the longest and extend laterally to form pedestal-like features. The ornamentation on the apical paraplate series may appear to be merged. The 'pads' on the elongate postcingular paraplate series are inserted close to the prominent, indented, paracingulum, which is close to the apex. 'Pads' occupy the majority of the small precingular paraplate series. The paracingulum and parasulcus are emphasised by the adjacent precingular and postcingular 'pads'. The very small parasulcal notch is close to mid ventral in position. Autophragm is microgranulate to occasionally microreticulate. The apical paraplate series (the operculum) is flat and very small.

Dimensions (μm; n=32): Min. (Mean) Max.
Length of cyst body (excl. operculum): 30 (34) 40
Width of cyst body at antapex: 16 (22) 27
Width of cyst body at equator (postcingulars): 12 (19) 26
Width of cyst body at apex (archaeopyle suture): 11 (15) 20
Length of processes/crests: 1 (2) 4

The measured specimens are all from a sidewall core sample in Challis-11 ST1 well at 1552.50m.

Comments. This species is a distinctly subrectangular/subtriangular form of *Woodinia*. The distribution of the ornamentation gives a characteristic profile in lateral or dorsoventral view. The cyst has a banded appearance, reflecting the development of differentiated autophragmal 'pads' on the precingular, postcingular and antapical paraplate series (Fig. 19).

Comparison. *Woodinia pedis* is similar in overall morphology to the Oxfordian species *W. bensonii* Riding & Helby (this volume). *Woodinia bensonii*, however, is rounded subtriangular in dorsoventral outline, having prominent lateral antapical protuberances which frequently impart a significant antapical concavity. The latter species also only has regular intratabular 'pads' of differentiated autophragm on the precingular paraplate series. This contrasts markedly with the thicker, more regular intratabular ornamentation, particularly in the postcingular paraplate series, of *W. pedis* (Fig. 19). *Woodinia bensonii* also lacks the skirt-like flange to the antapex, formed by the relatively prominent antapical ornamentation, characteristic of *W. pedis* (Fig. 19).

Derivation of name. From the Latin *pedis* meaning foot and referring to the prominent, foot-like or pedestal-like antapical differentiated autophragmal protuberances.

Holotype and type locality. Figures 19K-M, CPC 35490, Challis-11 ST2, sidewall core sample at 1842.00m.

Stratigraphical distribution. *Woodinia pedis* has been recorded from the late Callovian strata of the Timor Sea region and is confined to the lower *Rigaudella aemula* Zone (subzones 7aiib to 7aiia) (Foster, this volume; Helby & Partridge, in prep.). It is most prominent and characteristic of subzones 7aiibia-7aiiaii.

Yalkalpodinium Morgan 1980 emend.

1980 *Yalkalpodinium* Morgan, p. 34.

Type species. *Yalkalpodinium scutum* Morgan 1980

Emended diagnosis. The generic circumscription is emended here to exclude the presence of paracingular projections of the periphragm as a generic criterion (Morgan, 1980; Stover & Williams, 1987). Furthermore, this emendation includes forms which are intermediate in size, may have processes on the endophragm and have simple or compound opercula. The paratabulation pattern is standard sexiform gonyaulacalean with a longitudinal (L-type) parasulcus and is indicated by low folds or ridges on the periphragm, which may be microreticulate and/or microscabrate.

Comments. The diagnosis has been emended to accommodate *Yalkalpodinium elangiana* sp. nov. This species is not subpentagonal in outline as it lacks periphragmal paracingular projections.

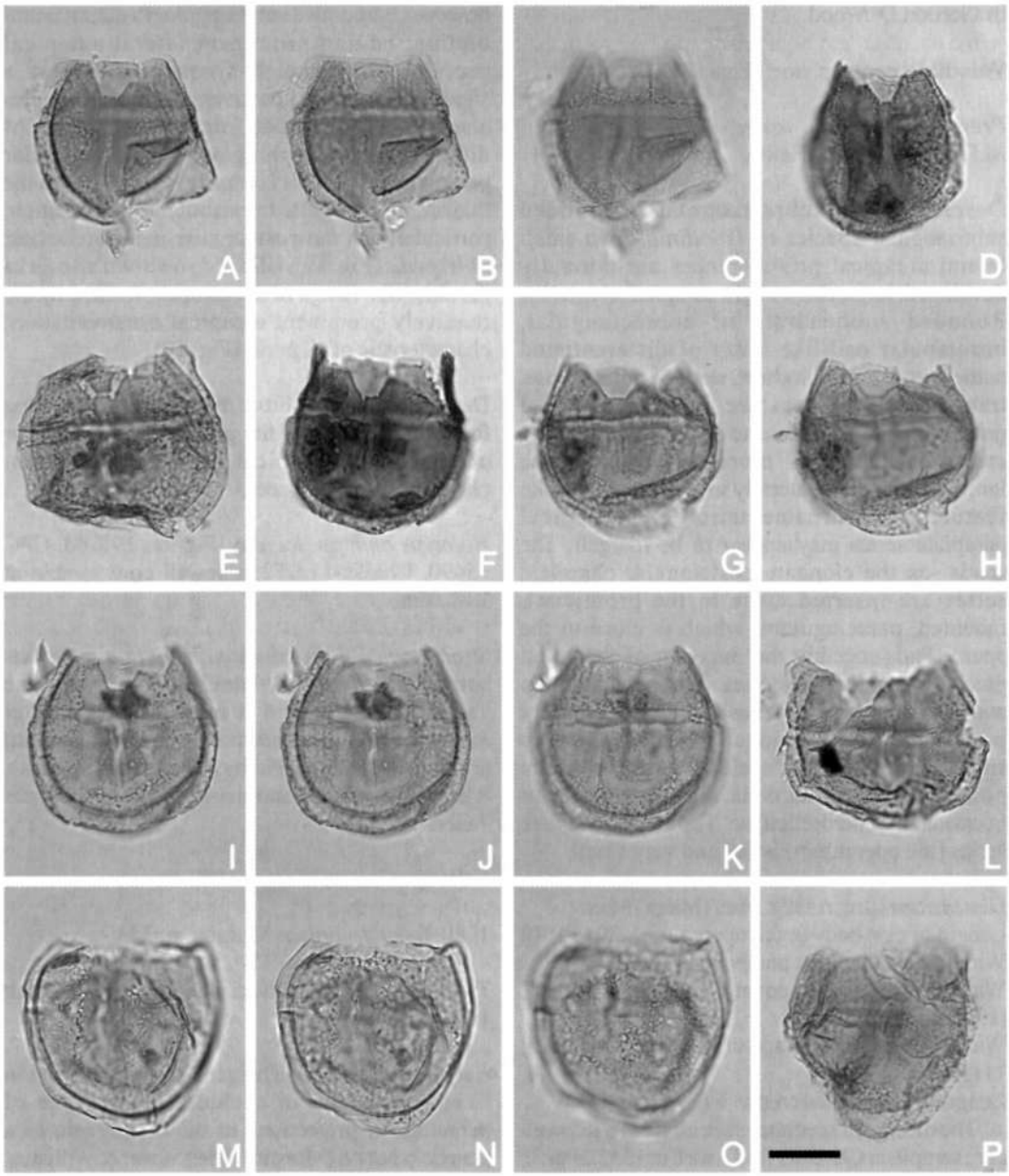

Fig. 20. Yalkalpodinium elangiana sp. nov. The specimens are from sidewall core samples from Challis-11 ST1 well at 1552.50m (Figs 20I-K, M-O), Challis-11 ST2 well at 1842.00m (Figs 20A-C, E, G-H, L, P) and Rowan-1ST well at 3183.00m (Figs 20D, F). All photomicrographs were taken using plain transmitted light. The scale bar in Fig. 20P refers to all photomicrographs and represents 25µm. Figs 20I-K are of the holotype; the remainder are paratypes. Note the circumcavate cyst organisation, the apical archaeopyle, the relatively thick endophragm and the thinner, microgranulate and/or microreticulate periphragm. A-C - CPC 35495, paratype; ventral view, high, median and low focus sequence. The hypocystal periphragm has been damaged; note the prominent parasulcal notch in Fig. 20A. D - CPC 35496, paratype; dorsal view, low focus. Note the mid-ventral parasulcal notch. E - CPC 35497, paratype; ventral view, low focus. Note the parasulcal notch and the parasulcal tongue, the latter formed by paraplate 1', which has detached. F - CPC 35498, paratype; ventral view, high/median focus. A relatively darkened specimen. G, H - CPC 35499, paratype; ventral view, high/median focus. Note that the microreticulation on the periphragm is concentrated at the periphery of the cyst. I-K - CPC 35500, holotype; ventral view, high, median and low focus sequence. Well-preserved specimen; note the hypocystal paratabulation and the prominent paracingulum in Fig. 20K. L - CPC 35501, paratype; ventral view, (continued opposite)

Additionally it may exhibit occasional processes on the endophragm, is paratabulate via low ridges on the microreticulate to occasionally microscabrate periphragm and is intermediate in size. Frequently, the opercula of this species are observed to be compound, therefore both simple and compound opercula are accommodated in this emendation. The paratabulation formula of *Yalkalpodinium elangiana* is interpreted as being 4", 6", Xc, 6"', 1p, 1"", Xs.

The genera most similar to *Yalkalpodinium* are *Ambonosphaera* Fensome 1979, *Sirmiodiniopsis* Drugg 1978 and *Sirmiodinium* Warren 1973 because they are all subcircular, cavate forms with gonyaulacalean paratabulation. *Ambonosphaera* is typically camocavate to bicavate with a consistently entire periphragm (Stover & Williams, 1987; Poulsen & Riding, 1992). The characteristic feature of *Sirmiodiniopsis* is a pair of hypocystal claustra bordering an antapical protuberance (Drugg, 1978, pl. 7, fig.11). *Sirmiodinium* has a combination, type (tA)a+Pa, archaeopyle. The prominent midventral parasulcus of *Yalkalpodinium* indicates a clear difference with lenticular genera such as *Senoniasphaera* Clarke & Verdier 1967.

Yalkalpodinium elangiana sp. nov. (Figs 20A-P)

Previous Australian usage
Yalkalpodinium elangiana – Helby.

Description. A species of *Yalkalpodinium*, which is slightly dorsoventrally flattened, intermediate in size and ellipsoidal to subcircular in outline. Endophragm relatively thick, psilate, occasionally sporadically granulate to baculate where the endophragm and periphragm are separated. The endophragm may or may not bear rare slender, solid processes which connect to the interior of the periphragm at the cyst periphery. Periphragm thin, microreticulate; rarely microscabrate. One or two ovoidal claustra may be present in the periphragm at the antapex. Standard sexiform gonyaulacalean paratabulation indicated by low smooth folds or ridges in the periphragm. The periphragm at the paracingulum is sometimes indented and the longitudinal parasulcus is narrow and deeply indented. The operculum is compound.

Dimensions (µm; n=38): Min. (Mean) Max.
Length of pericyst (incl. operculum): 67 (73) 80
Length of pericyst (excl. operculum): 56 (66) 75
Length of endocyst (incl. operculum): 63 (67) 74
Length of endocyst (excl. operculum): 46 (58) 68
Width of pericyst: 56 (68) 79
Width of endocyst: 47 (60) 72

The measured specimens are from a conventional core sample in Undan-1 well (3124.87m) and sidewall core samples from Challis-11 ST1 (1552.50m), Challis-11 ST2 (1842.00m) and Rowan-1ST (3183.00m) wells.

Comments. The apical archaeopyle in this species has normally operated and the resulting prominent midventral parasulcal notch, formed by the loss of the relatively large 1' paraplate, is a characteristic feature (Fig. 20). The operculum appears to be compound; the 1' paraplate frequently is observed detached from both the loisthocyst and the other apical paraplates (Fig. 20E). Specimens of *Yalkalpodinium elangiana* may rarely have thin, solid processes inserted between the cyst wall layers in the peripheral regions in both hemispheres. These processes are not consistently and/or extensively developed and therefore the species is deemed to be circumcavate and not holocavate (Evitt, 1985). The periphragm is microreticulate to occasionally microscabrate; it encloses a pericoel which is usually best developed on the hypocyst and is typically 5-6µm wide (Fig. 20). The lacunae in the periphragm have widely differing concentrations, for example they are often relatively sparse in the middorsal and midventral areas (Fig. 20A). They are also virtually absent in the paracingulum and parasulcus. By contrast, they may be relatively densely inserted in the peripheral areas of the cyst (Fig. 20G). The lacunae are normally between 1 and 2µm in diameter. One, occasionally two, ovoidal claustra may penetrate the periphragm at the antapex (Fig. 20M). Claustra are also present in the genotype, *Yalkalpodinium scutum* (see Morgan, 1980, pl. 31, figs 15-18). The two cyst layers are in contact over most of the dorsal and ventral areas, and there is a distinct border marking wall separation approaching the cyst periphery (Fig. 20). The species may exhibit one or more dark, subspherical accumulation bodies within the endocoel of the cyst, normally close to the paracingular area (Figs 20I-J). The paracingulum

high/median focus. A loisthocyst which is unusually squat. M-O - CPC 35502, paratype; ventral view, high, median and low focus sequence. Note the prominently microreticulate periphragm. P - CPC 35503, paratype; dorsal view, low focus. Note the extremely narrow lateral pericoels.

is essentially equatorial in position, however the hypocyst may be slightly longer than the epicyst.

Comparison. *Yalkalpodinium elangiana* differs from the genotype, *Y. scutum* Morgan 1980, in not exhibiting paracingular protrusions and in having sporadically ornamented endophragm, microreticulate periphragm, being paratabulate, of intermediate size and having a compound operculum. *Yalkalpodinium indicum* (Jain & Taugourdeau-Lanz 1973) Morgan 1980 is similar in morphology to *Y. scutum*, but has a small apical horn. The species *Ambonosphaera hemicavata* Prauss 1989 is similar in overall morphology and size to *Yalkalpodinium elangiana*. However, *A. hemicavata* is bicavate and significantly more longitudinally elongate (Prauss, 1989, pl. 10, figs 8, 12-15). The parasulcus in *A. hemicavata* is relatively wide and prominent, with several small claustra inserted around the antapical parasulcal paraplate (Prauss, 1989, fig. 9). Furthermore, Prauss (1989) described the endophragm of *A. hemicavata* as being 'fossulate, alveolate as well as rugulate to baculate' (translation). The endophragm of *Y. elangiana* is never fossulate (grooved) or alveolate (punctoreticulate).

Morgan (1980) transferred the Tithonian *Cyclonephelium areolatum* Cookson & Eisenack 1960 to *Yalkalpodinium*. However, this was rejected by Stover & Williams (1987, p. 231) as, in their opinion, this taxon is questionably cavate and lenticular. We disagree with Stover & Williams (1987) as the holotype and our topotype material show indisputable cavation. However, we suggest a provisional transfer to *Yalkalpodinium* on the basis that we have seen no evidence of claustra. Furthermore, in *Y? areolatum* the endophragm bears many more periphragm support structures than in *Y. elangiana*, and the condition approaches holocavation. The other two unequivocal species of *Yalkalpodinium*, *Y. indicum* (Jain & Taugourdeau-Lantz 1973) Morgan 1980 and *Y. scutum* Morgan 1980 are both Early Cretaceous (Neocomian-Albian) Indo-Pacific species and may be conspecific (Morgan, 1980).

Derivation of name. From the Elang Formation.

Holotype and type locality. Figs 20I-K, CPC 35500, Challis-11 ST1 well, sidewall core at 1552.50m.

Stratigraphical distribution. *Yalkalpodinium elangiana* is known from the late Callovian to Oxfordian of the Timor Sea region, ranging from the lower *Rigaudella aemula* Zone (7aiib) to the lower *Wanaea spectabilis* Zone (6ciii) (Foster, this volume; Helby & Partridge, in prep.). It is most characteristic of subzones 7aiibia to 7aiiaii.

Acritarch

Nummus Morgan 1975

Type species. *Nummus monoculatus* Morgan 1975

Nummus apiculus sp. nov. (Figs 21A-P)

Previous Australian usage
M.P. 556 – Helby.
Nummus sp. 556 – Helby.
Nummus ambitomegasimilis – Morgan.

Description. A species of *Nummus* ellipsoidal in dorsoventral view. Vesicle normally longer than broad. The vesicle wall is thick and robust, the external surface is smooth and may be sparsely and irregularly microreticulate. Occasionally the wall is also microscabrate. The pylome is located in an apical position and frequently has a thickened rim. A detached plug is occasionally present within the pylome. The thin ventral wall is often entirely absent, however small fragments may be preserved. A thickened rim surrounds the ventral part of the vesicle, which has the thinned vesicle wall; this rim is ovoidal in outline.

Dimensions (µm; n=41): Min. (Mean) Max.
Length: 60 (81) 105

Fig. 21. Nummus apiculus sp. nov. The specimens are from conventional core in Undan-3 well at 3057.00m (Figs 21A, C-D, F-H, J, L-P) and Undan-4 well at 3135.24m (Figs 21B, E, I, K). Photomicrographs taken using plain transmitted light, except Fig. 21J, which was taken using Nomarski Interference Contrast. The scale bar in Fig. 21P refers to all photomicrographs and represents 20µm. Fig. 21K is the holotype, and the remainder are paratypes. Note ellipsoidal outline, the apical pylome, and the thin ventral wall, which is normally wholly or partially absent. A - CPC 35441, paratype; slightly oblique dorsal view, median/low focus. Note the prominent thickened rim surrounding the ventral thin-walled area. B - CPC 35442, paratype; ventral view, high focus. A specimen with an equatorial fold. C - CPC 35443, paratype; ventral view, median focus. A subcircular specimen. D - CPC 35444, paratype; oblique dorsal view, low focus. A relatively elongate specimen. E - CPC 35445, paratype; dorsal view, median focus. F - CPC 35446, paratype; ventral view, low focus. Note the small, subcircular apical pylome. G - CPC 35447, paratype; ventral view, a composite (continued opposite)

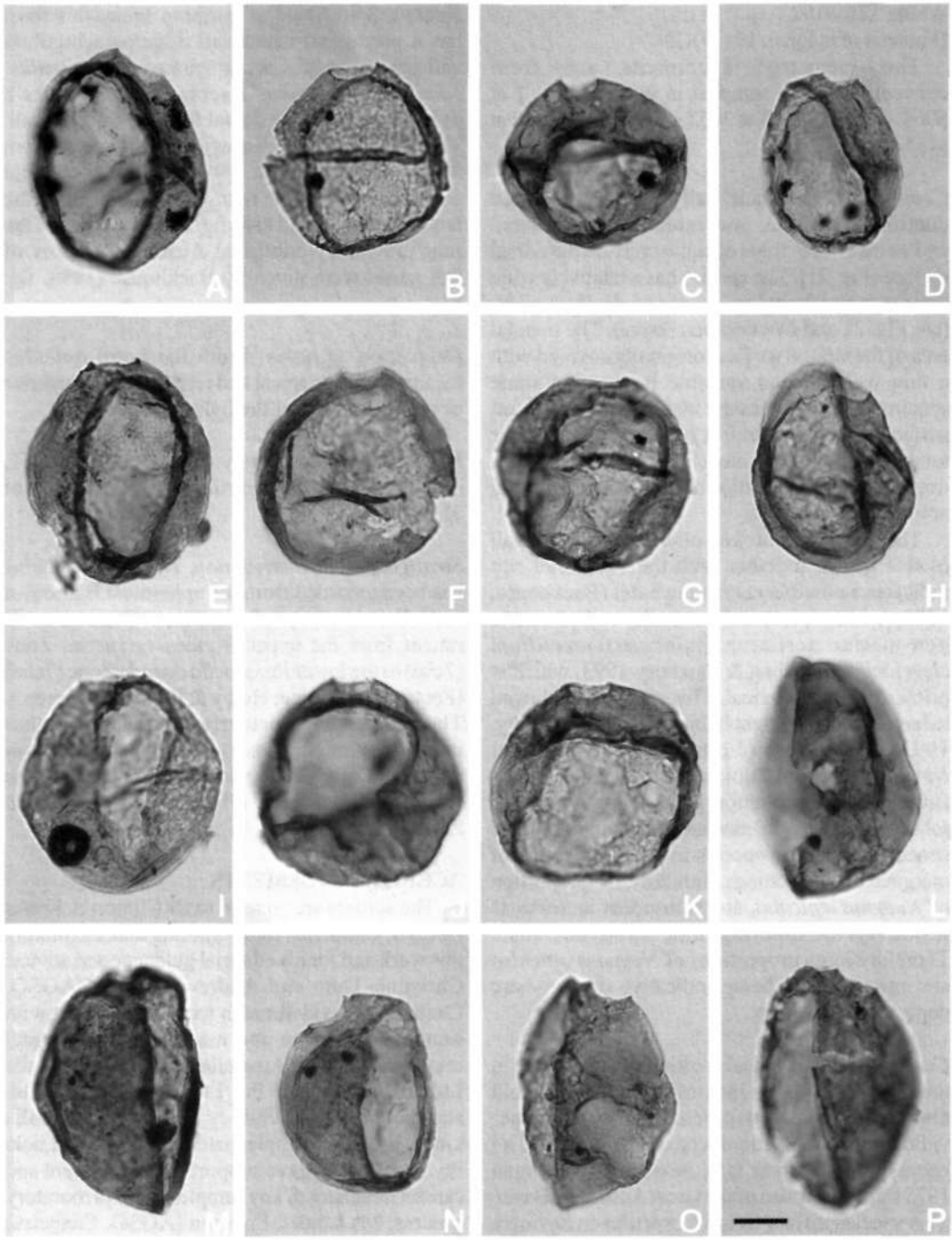

photomicrograph. A specimen with a relatively large pylome. H- CPC 35448, paratype; ventral view, median focus. I - CPC 35449, paratype; ventral view, high focus. J - CPC 35450, paratype; oblique ventral view, median focus. K - CPC 35451, holotype; oblique ventral view, a composite photomicrograph. A well-preserved subcircular specimen. L - CPC 35452, paratype; antapical view, low focus. Note the pylome. M - CPC 35453, paratype; left lateral view, median focus. N - CPC 35454, paratype; oblique left lateral view, high/median focus. In this specimen, the relatively large pylome is slightly offset toward the dorsal side. O - CPC 35455, paratype; right lateral view, median focus. Note that the pylome is close to the equatorial region. P - CPC 35456, paratype; oblique right lateral view, high focus.

Width: 52 (68) 92
Diameter of pylome: 10 (17) 28

The measured specimens are from conventional core samples in wells Undan-1 at 3063.18m, Undan-3 at 3057.00m and Undan-4 at 3135.24m.

Comments. The vesicle wall is frequently folded due to compaction, and extensive longitudinal and/or transverse folds occur, largely on the dorsal surface (Fig. 21). The species has a relatively wide size range and the pylome varies markedly in width (see Fig. 21 and *Dimensions*, above). The ovoidal area of the ventral surface, originally covered with a thin wall, is also variable in area. In some specimens, it occupies the majority of the ventral surface (Fig. 21A) and in others it accounts for around 50% of the venter (Fig. 21C). The sparse, irregular microreticulation may be a preservational artefact.

The thin, often broken or absent, ventral wall of this genus, together with the equatorial rim indicates a possible encrusting habit (Backhouse, 1988, p. 112). It is therefore similar to the Jurassic non-marine acritarch *Truncatisphaeridium clevelandense* Riding & Duxbury 1993, which is primarily hemispherical. This species is believed to have had an adherent habit (Riding & Duxbury, 1993). Backhouse (1988, p. 113) noted that *Nummus similis* (Cookson & Eisenack 1960) Burger 1980 is common in horizons which are relatively sparse in marine microplankton and speculated that the species may be indicative of marginal marine settings. Similarly, the proportion of *Nummus apiculus* and miospores increase as the levels of dinoflagellate cysts decrease. Therefore large proportions of *Nummus apiculus* are interpreted as being indicative of nearshore depositional regimes.

Comparison. The apical position of the pylome in this species and the lack of an equatorial fold distinguish *Nummus apiculus* from the other validly described members of the genus. The genotype of *Nummus* is *N. monoculatus* Morgan 1975 from the Aptian of the Great Australian Basin. This species differs from *N. apiculus* in having a relatively large pylome, which is located between the apex and the equator, in an 'intercalary' position (Morgan, 1975, p. 163) and also being smaller. *Nummus apiculus* differs from *N. similis* (Cookson & Eisenack 1960) Burger 1980 in lacking a prominent equatorial ridge, which may represent a paracingulum. Jain & Garg (in Jain *et al*., 1984) described *N. mallajoharensis* from the Late Jurassic Spiti Shale of northern India; this form has a prominent equatorial ridge/paracingulum and appears to be a junior synonym of *N. similis*. *Nummus pentagonus* Backhouse 1988 lacks a pylome and has five dorsal folds in the cell wall. The features which distinguish *N. apiculus* from *N. parvus* Backhouse 1988 are the equatorial constrictions and the relatively small size of the latter (Backhouse, 1988, fig. 33). Sketches of the four previously published Australian species of this genus were given by Backhouse (1988, fig. 33).

Derivation of name. From the Latin *apiculus* meaning apex or apical and referring to the anterior or apical position of the pylome.

Holotype and type locality. Fig. 21K, CPC 35451, Undan-4 well, conventional core sample at 3135.24m.

Stratigraphical distribution. *Nummus apiculus* has been recorded from the uppermost Bathonian to Callovian strata of the Timor Sea region. It ranges from the upper *Wanaea verrucosa* Zone (7ciai) to the lower *Rigaudella aemula* Zone (7aiia) (Foster, this volume; Helby & Partridge, in prep.). The species is particularly prominent (i.e. has intermittent minor acmes) possibly in the *Wanaea indotata* Zone (7bii) and unequivocally in the *Wanaea digitata* Zone (7bi) and basal *R. aemula* Zone (7aiib).

ACKNOWLEDGEMENTS

The authors are grateful to Dr Clinton B. Foster (AGSO, Canberra) for promoting and facilitating this work and for his editorial guidance and advice. Christian Thun and Andrew Kelman (AGSO, Canberra) provided much technical support with sample preparation and manipulation of digital images. Aquitaine Australia Ltd., Arco Australia Ltd., BHP Petroleum Pty. Ltd, Esso Australia Ltd. and the Geological Survey of Western Australia kindly provided sample material on request. Laola Pty. Ltd. (Perth) gave support in their diligent and careful treatment of key samples in the preparatory process. Ms Lindell Emerton (AGSO, Canberra) skilfully drafted Figures 1, 2, 15 and 17. Drs A. J. Powell and R. Woollam are thanked for reviewing the manuscript. J. B. Riding publishes with the permission of the Chief Executive Officer, AGSO.

REFERENCES

ARDITTO, P.A., 1996. A sequence stratigraphic study of the Callovian fluvio-deltaic to marine succession

within the ZOCA region. *APPEA Journal 36*, 269-283.

BACKHOUSE, J., 1987. Microplankton zonation of the Lower Cretaceous Warnbro Group, Perth Basin, Western Australia. *Memoir of the Association of Australasian Palaeontologists 4*, 205-226.

BACKHOUSE, J., 1988. Late Jurassic and Early Cretaceous palynology of the Perth Basin, Western Australia. *Geological Survey of Western Australia Bulletin 135*, 233 p.

BAILEY, D.A., 1990. Some dinoflagellate cysts from latest Bajocian and Bathonian sediments in southern England. *Palynology 14*, 135-144.

BELOW, R., 1990. Evolution und Systematik von Dinoflagellaten-Zysten aus der Ordnung Peridiniales. III. Familie Pareodiniaceae. *Palaeontographica Abteilung B 220*, 1-96.

BENSON, D.G. Jr., 1985. Observations and recommendations on the fossil dinocyst genera *Ctenidodinium, Dichadogonyaulax,* and *Korystocysta*. *Tulane Studies in Geology and Paleontology 18*, 145-155.

BROOKS, D.M., GOODY, A.K., O'REILLY, J.B. & MCCARTY, K.L., 1996. Bayu/Undan gas-condensate discovery: western Timor gap zone of cooperation, area A. *The APPEA Journal 1996 36*, 142-160.

BURGER, D., 1996. Mesozoic palynomorphs from the North West Shelf, offshore Western Australia. *Palynology 20*, 49-103.

CHEN, Y., 1982. Recognition of the dinocyst genus *Komewuia* with assignable species from Madagascar. *Micropaleontology 28*, 31-42.

COLLINSON, M.E., 1980. A new multiple-floated *Azolla* from the Eocene of Britain with a brief review of the genus. *Palaeontology 23*, 213-229.

COOKSON, I.C. & EISENACK, A., 1958. Microplankton from Australian and New Guinea Upper Mesozoic sediments. *Proceedings of the Royal Society of Victoria (New Series) 70*, 19-79.

COOKSON, I.C. & EISENACK, A., 1960. Upper Mesozoic microplankton from Australia and New Guinea. *Palaeontology 2*, 243-261.

DAVEY, R.J., 1987. Palynological zonation of the Lower Cretaceous, Upper and uppermost Middle Jurassic in the northwestern Papuan Basin of Papua New Guinea. *Geological Survey of Papua New Guinea Memoir 13*, 77 p.

DODEKOVA, L., 1975. New Upper Bathonian dinoflagellate cysts from northeastern Bulgaria. *Bulgarska Akademiya na Naukite, Paleontologiya, Stratigrafiya i Litologiya 2*, 17-32.

DODEKOVA, L., 1990. Dinoflagellate cysts from the Bathonian-Tithonian (Jurassic) of North Bulgaria. I. Taxonomy of Bathonian and Callovian dinoflagellate cysts. *Geologica Balcanica 20*, 3-45.

DRUGG, W.S., 1978. Some Jurassic dinoflagellate cysts from England, France and Germany. *Palaeontographica Abteilung B 168*, 61-79.

DUXBURY, S., 1977. A palynostratigraphy of the Berriasian to Barremian of the Speeton Clay of Speeton, England. *Palaeontographica Abteilung B 160*, 17-67.

EVITT, W.R., 1985. *Sporopollenin dinoflagellate cysts. Their morphology and interpretation*. American Association of Stratigraphic Palynologists Foundation, Dallas, xv + 333 p.

FENSOME, R.A., TAYLOR, F.J.R., NORRIS, G., SARJEANT, W.A.S., WHARTON, D.I. & WILLIAMS, G.L., 1993. A classification of living and fossil dinoflagellates. *Micropaleontology Special Publication No. 7*, viii + 351 p.

FOSTER, C.B., this volume. Introduction.

FRANCIS, G. & WESTERMANN, G.E.G., 1993. The Kimmeridgian problem in Papua New Guinea and other parts of the Indo-southwest Pacific. In: Carman, G.J & Carmen, Z. (eds). *Petroleum Exploration and Development in Papua New Guinea: Proceedings of the Second PNG Petroleum Convention, Port Moresby, 31st May-2nd June 1993*, 75-93.

GOCHT, H., 1970. Dinoflagellaten-zysten aus dem Bathonium des Erdölfeldes Aldorf (NW-Deutschland. *Palaeontographica Abteilung B 129*, 125-165.

GOCHT, H., 1975. Morphologie und Wandstruktur von *Lithodinia jurassica* Eisenack 1935 (Dinoflagellata, Oberjura). *Neues Jahrbuch für Geologie und Paläontologie, Monatshefte 1975(6)*, 343-359.

GOCHT, H., 1976. *Hystrichosphaeropsis quasicribrata* (O. Wetzel), ein Dinoflagellat aus dem Maastricht Nordeuropas. Mit einem nomenklatorischen Nachtrag zur Gattung *Lithodinia* Eis. *Neues Jahrbuch für Geologie und Paläontologie, Monatshefte 1976(6)*, 331-336.

GOCHT, H., 1979. Korrelation von Überlappungssystem und Wachstum bei fossilen Dinoflagellaten (*Gonyaulax*-Gruppe) *Neues Jahrbuch für Geologie und Paläontologie, Abhandlungen 157*, 344-365.

GOCHT, H., 1984. Intratabulare Strukturen bei *Ctenidodinium* (Dinoflagellata, Jura). *Neues Jahrbuch für Geologie und Paläontologie, Monatshefte 1984(6)*, 341-359.

HELBY, R. MORGAN, R. & PARTRIDGE, A.D., 1987. A palynological zonation of the Australian Mesozoic. *Memoir of the Association of Australasian Palaeontologists 4*, 1-94.

HELBY, R. & PARTRIDGE, A.D., in prep. A palynological zonation of the Australian Mesozoic

– an update.

JAIN, K.P., GARG, R., KUMAR, S. & SINGH, I.B., 1984. Upper Jurassic dinoflagellate biostratigraphy of Spiti Shale (Formation), Malla Johar area, Tethys Himalaya, India. *Journal of the Palaeontological Society of India 29*, 67-83.

MAY, F.E., STEVENS, J. & PARTRIDGE, A.D., 1987. The Early Cretaceous dinoflagellate, *Dissimulidinium lobispinosum* gen. et sp. nov. from Western Australia. *Memoir of the Association of Australasian Palaeontologists 4*, 199-204.

MORGAN, R., 1975. Some Early Cretaceous organic-walled microplankton from the Great Australian Basin, Australia. *Journal and Proceedings of the Royal Society of New South Wales 108*, 157-167.

MORGAN, R., 1980. Palynostratigraphy of the Australian Early and Middle Cretaceous. *Memoirs of the Geological Survey of New South Wales. Palaeontology 18*, 153 p.

NØHR-HANSEN, H., 1986. Dinocyst stratigraphy of the Lower Kimmeridge Clay, Westbury, Wiltshire, England. *Bulletin of the Geological Society of Denmark 35*, 31-51.

NORRIS, G., 1965. Archeopyle structures in Upper Jurassic dinoflagellates from southern England. *New Zealand Journal of Geology and Geophysics 8*, 792-806.

OTT, H.L., 1970. Palynological zonation of the Carnarvon Basin Jurassic-Miocene sequence. *Unpublished WAPET report*, 1-52.

POULSEN, N.E. & RIDING, J.B., 1992. A revision of the Late Jurassic dinoflagellate cysts *Ambonosphaera? staffinensis* (Gitmez 1970) comb. nov., and *Senoniasphaera jurassica* (Gitmez & Sarjeant 1972) Lentin & Williams 1976. *Palynology 16*, 25-34.

PRAUSS, M., 1989. Dinozysten-stratigraphie und palynofazies im Oberen Lias und Dogger von NW-Deutschland. *Palaeontographica Abteilung B 214*, 1-124.

QUATTROCCHIO, M. & SARJEANT, W.A.S., 1992. Dinoflagellate cysts and acritarchs from the Middle and Upper Jurassic of the Neuquen Basin, Argentina. *Revista Española Micropaleontologia 24*, 67-118.

RIDING, J.B., 1984. A palynological investigation of Toarcian to early Aalenian strata from the Blea Wyke area, Ravenscar, North Yorkshire. *Proceedings of the Yorkshire Geological Society 45*, 109-122.

RIDING, J.B. & DUXBURY, S., 1993. A new non-marine acritarch from the Middle Jurassic of Britain. *Special Papers in Palaeontology No. 48*, 57-66.

RIDING, J.B., & HELBY, R., this volume. Marine microplankton from the Late Jurassic (Tithonian) of the north-west Australian region.

RIDING, J.B., PENN, I.E. & WOOLLAM, R., 1985. Dinoflagellate cysts from the type area of the Bathonian stage (Middle Jurassic; southwest England). *Review of Palaeobotany and Palynology 45*, 149-169.

RILEY, L.A. & FENTON, J.P.G., 1982. A dinocyst zonation for the Callovian-Oxfordian succession of northwest Europe. *Palynology 6*, 193-202.

SARJEANT, W.A.S., 1966. Dinoflagellate cysts with *Gonyaulax*-type tabulation. In Davey, R.J., Downie, C., Sarjeant, W.A.S. & Williams, G.L. Studies on Mesozoic and Cainozoic dinoflagellate cysts. *Bulletin of the British Museum (Natural History), Geology, Supplement 3*, 107-156.

SARJEANT, W.A.S., 1976. Dinoflagellate cysts and acritarchs from the Great Oolite Limestone (Jurassic: Bathonian) of Lincolnshire, England. *Géobios 9*, 5-46.

SARJEANT, W.A.S., LACALLI, T. & GAINES, G., 1987. The cysts and skeletal elements of dinoflagellates: speculations on the ecological causes for their morphology and development. *Micropaleontology 33*, 1-36.

STOVER, L.E. & EVITT, W.R., 1978. Analyses of Pre-Pleistocene organic-walled dinoflagellates. *Stanford University Publications, Geological Sciences 15*, 300 p.

STOVER, L.E. & WILLIAMS, G.L., 1987. Analyses of Mesozoic and Cenozoic organic-walled dinoflagellates 1977-1985. *American Association of Stratigraphic Palynologists Contributions Series No. 18*, 243 p.

SYKES, R.M., 1975. The stratigraphy of the Callovian and Oxfordian stages (Middle-Upper Jurassic) in northern Scotland. *Scottish Journal of Geology 11*, 51-78.

VAN HELDEN, B.G.T., 1986. Dinoflagellate cysts at the Jurassic-Cretaceous boundary, offshore Newfoundland, Canada. *Palynology 10*, 181-199.

WHITTAM, D.B., NORVICK, M.S. & MCINTYRE, C.L., 1996. Mesozoic and Cainozoic tectonostratigraphy of western Zoca and adjacent areas. *The APPEA Journal 36*, 209-232.

WILLIAMS, G.L., LENTIN, J.K. & FENSOME, R.A., 1998. The Lentin and Williams Index of fossil dinoflagellates 1998 edition. *American Association of Stratigraphic Palynologists Contributions Series No. 34*, 817 p.

WILLIAMS, G.L., SARJEANT, W.A.S. & KIDSON, E.J., 1978. A glossary of the terminology applied to dinoflagellate amphiesmae and cysts and acritarchs. *American Association of Stratigraphic Palynologists Contributions Series No. 2A*, 121 p.

WILLIAMS, G.L., STOVER, L.E. & KIDSON, E.J., 1993. Morphology and stratigraphic ranges of

selected Mesozoic-Cenozoic dinoflagellate taxa in the Northern Hemisphere. *Geological Survey of Canada Paper No. 92-10*, 137 p.

WOOLLAM, R., 1983. A review of the Jurassic dinocyst genera *Ctenidodinium* Deflandre 1938 and *Dichadogonyaulax* Sarjeant 1966. *Palynology 7*, 183-196.

WOOLLAM, R. & RIDING, J.B., 1983. Dinoflagellate cyst zonation of the English Jurassic. *Institute of Geological Sciences Report 83/2*, 42 p.

ZOTTO, M., DRUGG, W.S. & HABIB, D., 1987. Kimmeridgian dinoflagellate stratigraphy in the southwestern North Atlantic. *Micropaleontology 33*, 193-213.

APPENDIX 1: LOCATIONS AND OPERATORS OF WELLS AND BORES FROM WHICH MATERIAL HAS BEEN STUDIED

Well Name and Number	Latitude	Longitude	Operator
Broome-3 Town Bore	17° 57' 31"S	122° 14' 20"E	WAMD*
Challis-11 ST1 and ST2	12° 05' 51.90"S	125° 03' 20.81"E	BHP
Investigator-1	20° 21' 02.27"S	112° 58' 19.56"E	Esso
Jabiru-2	11° 56' 00.48"S	124° 59' 24.26"E	BHP
Layang-1	10° 50' 59.70"S	126° 25' 21.50"E	BHP
Montebello-1	20° 05' 15.95"S	116° 17' 28.25"E	BHP
Rowan-1ST	12° 29' 48.51"S	124° 23' 41.42"E	BHP
Tamar-1	11° 52' 10.26"S	126° 12' 44.53"E	Getty
Tern-1	13° 13' 09.99"S	128° 03' 57.00"E	Arco
Tern-2	13° 16' 37.90"S	128° 08' 02.45"E	Aquitaine
Undan-1	11° 02' 34.80"S	126° 36' 16.50"E	BHP
Undan-3	11° 04' 33.83"S	126° 34' 20.14"E	BHP
Undan-4	11° 02' 44.47"S	126° 21' 55.23"E	BHP

Well completion reports on all the offshore wells listed are publicly available five years after completion.
*WAMD – Department of Mines, Western Australia

APPENDIX 2: REGISTER OF FIGURED SPECIMENS

All palynomorph specimens figured in this paper are listed here, together with essential details. The specimens are all curated in the Commonwealth Palaeontological Collection (CPC) of the Australian Geological Survey Organisation, Canberra. The marine microplankton genera and species are listed alphabetically and the location of the specimens on the microscope slides are all 'England-Finder' co-ordinates. These were taken with the slide label to the left of the observer; the microscope stage opening toward the microscope user. The coding for types is as follows: H = holotype; P = paratype; T = topotype. All specimens of new taxa examined during this study contributed to the specific concepts described. Therefore, all figured specimens, which are not holotypes are paratypes. SGM = single grain mount. The single grain mounts do not have unique numbers; they are numbered sequentially for each species within a particular sample. The specimens are from conventional core, sidewall core and ditch cutting samples.

Species	Type	Figs	SGM/Slide No.	EF	Well (depth, m.)	CPC No.
C. ancorum	P	3A-B	SGM H4 (iii)	K34/1	Undan-4 (3135.24)	35350
C. ancorum	P	3C	SGM H5 (ii)	O34	Undan-4 (3135.24)	35351
C. ancorum	P	3D	SGM 3	N28/4	Undan-1 (2996.15)	35352
C. ancorum	P	3E	SGM H4 (ii)	K33/2	Undan-4 (3135.24)	35353
C. ancorum	P	3F	SGM H5 (iii)	O34/2	Undan-4 (3135.24)	35354
C. ancorum	H	3G,J	SGM H1	O34/3	Rowan-1ST (3183.00)	35355
C. ancorum	P	3H	SGM 5	N33/4	Undan-1 (2996.15)	35356
C. ancorum	P	3I	SGM H1	N32/4	Undan-4 (3135.24)	35357
C. ancorum	P	3K	SGM H5 (i)	P34	Undan-4 (3135.24)	35358
C. ancorum	P	3L	SGM H2	R32	Undan-4 (3135.24)	35359
C. fuscibasilarum	P	4A	SGM H2 (ii)	L36/3	Undan-3 (3048.00)	35360

Species	Type	Figs	SGM/Slide No.	EF	Well (depth, m.)	CPC No.
C. fuscibasilarum	P	4B,C	SGM 2 (i)	P33/1	Undan-3 (3057.00)	35361
C. fuscibasilarum	P	4D	SGM H2 (iv)	K36/2	Undan-3 (3048.00)	35362
C. fuscibasilarum	P	4E	SGM H2 (v)	J35/4	Undan-3 (3048.00)	35363
C. fuscibasilarum	P	4F	SGM H5 (ii)	K28	Undan-3 (3057.00)	35364
C. fuscibasilarum	P	4G	SGM 2 (iii)	P35/2	Undan-3 (3057.00)	35365
C. fuscibasilarum	P	4H	SGM H1 (vi)	L34/3	Undan-3 (3048.00)	35366
C. fuscibasilarum	P	4I	SGM 2 (iv)	O35/4	Undan-3 (3057.00)	35367
C. fuscibasilarum	H	4J,K	SGM 2 (ii)	P33/2	Undan-3 (3057.00)	35368
C. fuscibasilarum	P	4L	SGM H5 (i)	K29/4	Undan-3 (3057.00)	35369
C. planocristatum	P	5A	SGM H1 (iii)	O35/3	Undan-4 (3135.24)	35370
C. planocristatum	P	5B	SGM H4 (v)	M36/3	Undan-4 (3135.24)	35371
C. planocristatum	P	5C	SGM H3 (ii)	P24/4	Undan-4 (3135.24)	35372
C. planocristatum	P	5D	SGM H6 (vi)	Q37	Undan-4 (3135.24)	35373
C. planocristatum	P	5E	SGM H1 (ii)	P33	Undan-4 (3135.24)	35374
C. planocristatum	P	5F	SGM H5 (iv)	Q38/3	Undan-4 (3135.24)	35375
C. planocristatum	P	5G	SGM H1 (i)	P34	Undan-4 (3135.24)	35376
C. planocristatum	P	5H	SGM H6 (iii)	R37/4	Undan-4 (3135.24)	35377
C. planocristatum	P	5I	SGM H2 (ii)	O33/4	Undan-4 (3135.24)	35378
C. planocristatum	H	5J	SGM H2 (iv)	O32/4	Undan-4 (3135.24)	35379
C. planocristatum	P	5K	SGM H1 (iv)	N34/3	Undan-4 (3135.24)	35380
C. planocristatum	P	5L	SGM H6 (i)	S36/1	Undan-4 (3135.24)	35381
C. planocristatum	P	5M	SGM H2 (i)	P34/4	Undan-4 (3135.24)	35382
C. planocristatum	P	5N	SGM H3 (iii)	P24	Undan-4 (3135.24)	35383
C. planocristatum	P	5O	SGM H4 (i)	P36/3	Undan-4 (3135.24)	35384
D. magna	P	6A	SGM H4 (ii)	P33/2	Undan-3 (3057.00)	35385
D. magna	H	6B	SGM H4 (i)	P26	Undan-3 (3057.00)	35386
D. magna	P	6C	SGM H4 (vi)	L15	Undan-3 (3057.00)	35387
D. magna	P	6D	SGM H1 (iii)	P29	Undan-3 (3057.00)	35388
D. magna	P	6E	SGM H5 (iii)	L36/1	Undan-3 (3057.00)	35389
D. magna	P	6F	SGM H5 (vii)	K35/1	Undan-3 (3057.00)	35390
F. terniana	P	8A	SGM 1 (ii)	N33/2	Tern-1 (1530.11*)	35391
F. terniana	P	8B	SGM 2 (iv)	T25	Tern-1 (1530.11*)	35392
F. terniana	P	8C	SGM 1 (i)	M34	Tern-1 (1530.11*)	35393
F. terniana	P	8D	SGM SS12 (i)	M39/3	Tern-1 (1528.28)	35394
F. terniana	P	8E	SGM 14 (vii)	O35/3	Tern-1 (1528.28)	35395
F. terniana	P	8F	SGM 2 (ii)	S26/1	Tern-1 (1530.11*)	35396
F. terniana	P	8G	SGM SS13 (ii)	O33	Tern-1 (1528.28)	35397
F. terniana	P	8H	SGM SS11 (iii)	M38/3	Tern-1 (1528.28)	35398
F. terniana	P	8I	SGM SS12 (iii)	N41/3	Tern-1 (1528.28)	35399
F. terniana	H	8J	SGM SS13 (iv)	P30/4	Tern-1 (1528.28)	35400
F. terniana	P	8K	SGM SS11 (v)	P40	Tern-1 (1528.28)	35401
F. terniana	P	8L	SGM 14 (iii)	N34	Tern-1 (1528.28)	35402
F. terniana	P	9A,B	SGM 52	K39	Challis-11 ST1 (1552.50)	35403
F. terniana	P	9C,D	SGM 124	Q33	Challis-11 ST1 (1552.50)	35404
K. glabra	T	7A	SGM 26	O29	Broome-3 (305.11**)	35405
K. glabra	T	7B	SGM 41	N36	Broome-3 (305.11**)	35406
K. glabra	T	7C	SGM 27	M31/1	Broome-3 (305.11**)	35407

*depth range: 1530.11m-1536.21m

**ditch cuttings, depth range: 305.11m-317.60m

Species	Type	Figs	SGM/Slide No.	EF	Well (depth, m.)	CPC No.
L. protothymosa	P	10A,B	SGM 4 (i)	N28/2	unregistered sample	35408
L. protothymosa	P	10C	SGM 4 (v)	P27/4	unregistered sample	35409
L. protothymosa	H	10D	SGM SS31	N37/1	Investigator-1 (3260.00)	35410
L. protothymosa	P	10E	SGM SS83	N29	Investigator-1 (3260.00)	35411
L. protothymosa	P	10F	SGM SS84 (i)	N39/1	Investigator-1 (3260.00)	35412
L. protothymosa	P	10G	SGM SS16 (ii)	O17	Tern-2 (1457.30)	35413
L. protothymosa	P	10H	SGM SS84 (ii)	N37/1	Investigator-1 (3260.00)	35414
L. protothymosa	P	10I	SGM SS8	N42/1	Tern-2 (1459.20)	35415
L. protothymosa	P	10J	SGM SS84 (iii)	Q37/2	Investigator-1 (3260.00)	35416
L. protothymosa	P	10K,L	SGM SS16	Q20	Tern-2 (1457.30)	35417
M. penitabulata	P	11A	SGM 4	Q32/2	Rowan-1ST (3181.00)	35418
M. penitabulata	P	11B	SGM 100	O33/2	Challis-11 ST1 (1552.50)	35419
M. penitabulata	P	11C,D	SGM H3	Q44/2	Rowan-1ST (3181.00)	35420
M. penitabulata	P	11E	SGM 119	M35/3	Challis-11 ST1 (1552.50)	35421
M. penitabulata	P	11F,G	SGM 38	N36/4	Challis-11 ST1 (1552.50)	35422
M. penitabulata	P	11H	SGM H1	H38/2	Challis-11 ST2 (1842.00)	35423
M. penitabulata	H	11I,J	SGM 36	J36	Challis-11 ST1 (1552.50)	35424
M. penitabulata	P	11K-M	SGM 118	N17/1	Challis-11 ST1 (1552.50)	35425
M. penitabulata	P	12A,B	SGM H9	P31	Rowan-1ST (3181.00)	35426
M. penitabulata	P	12C,F	SGM H5	Q41/1	Rowan-1ST (3181.00)	35427
M. penitabulata	P	12D,E	SGM 4 (iii)	P33/4	Rowan-1ST (3181.00)	35428
M. penitabulata	P	12G,H	SGM H6	O31/1	Rowan-1ST (3181.00)	35429
M. penitabulata	P	12I	SGM 5 (iii)	M37/2	Rowan-1ST (3181.00)	35430
M. viriosa	P	13A	SGM 2	P34/1	Challis-11 ST2 (1842.00)	35431
M. viriosa	P	13B	SGM 7	M36/1	Rowan-1ST (3181.00)	35432
M. viriosa	P	13C	SGM 25 (i)	N31	Jabiru-2 (1642.50)	35433
M. viriosa	P	13D	SGM 25 (iii)	P33/1	Jabiru-2 (1642.50)	35434
M. viriosa	P	13E,F	SGM 4 (ii)	Q33/3	Challis-11 ST2 (1842.00)	35435
M. viriosa	P	13G	SGM 25 (ii)	O32/1	Jabiru-2 (1642.50)	35436
M. viriosa	P	13H,I	SGM 3	R26/2	Challis-11 ST2 (1842.00)	35437
M. viriosa	P	13J	SGM SS1 (iii)	K35/1	Tern-1 (1528.28)	35438
M. viriosa	H	13K	SGM SS1 (i)	M34	Tern-1 (1528.28)	35439
M. viriosa	P	13L	SGM SS1 (ii)	K36	Tern-1 (1528.28)	35440
N. apiculus	P	21A	SGM H4 (iv)	M33/2	Undan-3 (3057.00)	35441
N. apiculus	P	21B	SGM H2 (iv)	L37/3	Undan-4 (3135.24)	35442
N. apiculus	P	21C	SGM H6 (i)	P38	Undan-3 (3057.00)	35443
N. apiculus	P	21D	SGM H3 (iv)	M37	Undan-3 (3057.00)	35444
N. apiculus	P	21E	SGM H2 (iii)	M36/4	Undan-4 (3135.24)	35445
N. apiculus	P	21F	SGM H5 (iii)	N36	Undan-3 (3057.00)	35446
N. apiculus	P	21G	SGM H5 (vi)	L35/3	Undan-3 (3057.00)	35447
N. apiculus	P	21H	SGM H5 (iv)	M35/4	Undan-3 (3057.00)	35448
N. apiculus	P	21I	SGM H1 (ii)	P34/1	Undan-4 (3135.24)	35449
N. apiculus	P	21J	SGM H5 (v)	M36	Undan-3 (3057.00)	35450
N. apiculus	H	21K	SGM H1 (iii)	O34/2	Undan-4 (3135.24)	35451
N. apiculus	P	21L	SGM 1 (iv)	K23/1	Undan-3 (3057.00)	35452
N. apiculus	P	21M	SGM H5 (i)	O35/1	Undan-3 (3057.00)	35453
N. apiculus	P	21N	SGM 1 (ii)	K24/2	Undan-3 (3057.00)	35454
N. apiculus	P	21O	SGM H6 (iv)	O38/1	Undan-3 (3057.00)	35455
N. apiculus	P	21P	SGM1 (i)	K23/4	Undan-3 (3057.00)	35456
T. senarium		15A-C	AGSO slide 2	W39/1	Challis-11 ST1 (1552.50)	35457

Species	Type	Figs	SGM/Slide No.	EF	Well (depth, m.)	CPC No.
T. senarium		15D	Slide 2	U22/1	Challis-11 ST1 (1552.50)	35458
T. senarium		15E-G	Slide 3	D28/1	Challis-11 ST1 (1552.50)	35459
T. senarium		15H	Slide 2	L23/3	Challis-11 ST2 (1842.00)	35460
T. senarium		15I-K	Slide 3	R23/1	Challis-11 ST1 (1552.50)	35461
T. senarium		15L	Slide 3	O9/4	Challis-11 ST2 (1842.00)	35462
T. senarium		15M	Slide 3	L39	Challis-11 ST1 (1548.00)	35463
T. senarium		15N,O	AGSO slide 2	Q9/1	Challis-11 ST1 (1552.50)	35464
T. senarium		15P	Slide 2	W33/3	Rowan-1ST (3183.00)	35465
T. senarium		16A	SGM H1 (I)	N31/4	Rowan-1ST (3183.00)	35466
T. senarium		16B	Slide 1	R38/2	Tamar-1 (2138.00)	35467
T. senarium		16C	Slide 3	E18/2	Challis-11 ST1 (1548.00)	35468
T. senarium		16D	Slide 1	V37	Tamar-1 (2138.00)	35469
T senarium		16E-H	Slide 1	R40/3	Tamar-1 (2138.00)	35470
T. senarium		16I-L	Slide 1	Y43/2	Tamar-1 (2138.00)	35471
T. senarium		16M-P	Slide 1	F33/1	Tamar-1 (2138.00)	35472
V. tabulata	P	18A	SGM 5	O32/4	Montebello-1 (2575.00)	35473
V. tabulata	P	18B	SGM 8	N33/2	Montebello-1 (2575.00)	35474
V. tabulata	P	18C	SGM 70	L30/3	Challis-11 ST1 (1552.50)	35475
V. tabulata	P	18D	SGM 67 (i)	N33	Challis-11 ST1 (1552.50)	35476
V. tabulata	P	18E	SGM 12	P31/3	Montebello-1 (2575.00)	35477
V. tabulata	P	18F,G	SGM 67 (ii)	N33/2	Challis-11 ST1 (1552.50)	35478
V. tabulata	P	18H	SGM 1	J35/3	Layang-1 (3221.47)	35479
V. tabulata	P	18I	SGM 4	P27/1	Montebello-1 (2575.00)	35480
V. tabulata	P	18J	SGM 11	L33/3	Montebello-1 (2575.00)	35481
V. tabulata	P	18K	SGM 100	F36/1	Challis-11 ST2 (1842.00)	35482
V. tabulata	P	18L	SGM 101	N40/4	Challis-11 ST2 (1842.00)	35483
V. tabulata	H	18M	SGM 66	J30	Challis-11 ST1 (1552.50)	35484
V. tabulata	P	18N,O	SGM 103	L33	Challis-11 ST2 (1842.00)	35485
W. pedis	P	19A-C	SGM 2 (i)	N35/1	Challis-11 ST1 (1552.50)	35486
W. pedis	P	19D,E	SGM 2 (ii)	N34/4	Challis-11 ST1 (1552.50)	35487
W. pedis	P	19F-H	SGM H4	Q38	Challis-11 ST2 (1842.00)	35488
W. pedis	P	19I,J	SGM 2 (iii)	O34	Challis-11 ST1 (1552.50)	35489
W. pedis	H	19K-M	SGM H1 (i)	R32/2	Challis-11 ST2 (1842.00)	35490
W. pedis	P	19N,O	SGM H3	K34/2	Challis-11 ST2 (1842.00)	35491
W. pedis	P	19P	SGM H1	Q35	Undan-4 (3124.87)	35492
W. pedis	P	19Q	SGM H2	N27/4	Challis-11 ST2 (1842.00)	35493
W. pedis	P	19R-T	SGM H1 (ii)	P30/3	Challis-11 ST2 (1842.00)	35494
Y. elangiana	P	20A-C	SGM H2 (i)	L30/1	Challis-11 ST2 (1842.00)	35495
Y. elangiana	P	20D	SGM 15	L39	Rowan-1ST (3183.00)	35496
Y. elangiana	P	20E	SGM H5 (iv)	L32/3	Challis-11 ST2 (1842.00)	35497
Y. elangiana	P	20F	SGM H10 (I)	G37/3	Rowan-1ST (3183.00)	35498
Y. elangiana	P	20G,H	SGM H5 (ii)	N31	Challis-11 ST2 (1842.00)	35499
Y. elangiana	H	20I-K	SGM 33	O32/2	Challis-11 ST1 (1552.50)	35500
Y. elangiana	P	20L	SGM H2 (ii)	K29/4	Challis-11 ST2 (1842.00)	35501
Y. elangiana	P	20M-O	SGM 20	G36	Challis-11 ST1 (1552.50)	35502
Y. elangiana	P	20P	SGM H4 (iv)	M36/2	Challis-11 ST2 (1842.00)	35503

Dinoflagellate cysts from the Late Jurassic (Oxfordian) *Wanaea spectabilis* Zone in the Timor Sea region

JAMES B. RIDING and ROBIN HELBY

RIDING, J.B. & HELBY, R., 2001:09:21. Dinoflagellate cysts from the Late Jurassic (Oxfordian) *Wanaea spectabilis* Zone in the Timor Sea region. *Memoir of the Association of Australasian Palaeontologists 24*, 111-140. ISSN 0810 8889.

A suite of hitherto unpublished Late Jurassic (Oxfordian) dinoflagellate cysts which have restricted stratigraphical ranges has been recorded from offshore exploration wells in the Timor Sea region. Three genera and eight species of dinoflagellate cysts are formally described as new. The genera are *Cygnusicysta*, *Fosteria* and *Tringadinium*; the species are *Cygnusicysta taltarniana*, *Fosteria eclipsiana*, *Fusiformacysta challisiana*, *Microdinium jurassicum*, *Systematophora geminus*, *Tringadinium bjaerkei*, *T. comptum* and *Woodinia bensonii*. The dinoflagellate cyst genus *Systematophora* is emended to include forms with paired, slender solid processes within the paracingulum, in order to accommodate *S. geminus*. With the exception of *Tringadinium bjaerkei*, which ranges from late Callovian to Tithonian-Berriasian, all these new dinoflagellate cyst taxa have stratigraphical utility in the Oxfordian *Wanaea spectabilis* Zone of the north-western Australian region.

James B. Riding, Australian Geological Survey Organisation, GPO Box 378, Canberra, ACT 2601, Australia (present address: British Geological Survey, Keyworth, Nottingham NG12 5GG, UK [e-mail: jbri@bgs.ac.uk]); Robin Helby (corresponding author), 356A Burns Bay Road, Lane Cove, NSW 2066, Australia (e-mail: rhelby@ozemail.com.au). 10 November 2000.

Keywords: dinoflagellate cysts, Late Jurassic, Australia, biostratigraphy, taxonomy

THE PALYNOLOGICAL zonation of the Australian Mesozoic published by Helby *et al.* (1987) was the first attempt to provide an integrated, pan-Australian microplankton and spore-pollen zonation. Only the basic framework of the zonation was provided in anticipation that further contributions, particularly the documentation of new taxa, would be necessary as the zonation scheme evolved. This paper is one of a series providing the taxonomic foundation necessary to formalise the widely used unpublished subdivisions of these zones. These subzones have widespread currency within the hydrocarbon industry due to the legislative requirement for the release of technical data under the Petroleum (Submerged Lands) Act 1967. The informal subdivisions of the Helby *et al.* (1987) zonation have been entered into the Australian Geological Survey Organisation (AGSO) STRATDAT database. A diagrammatic update of the Helby *et al.* (1987) zonal scheme is presented by Foster (this volume), and will be fully described by Helby & Partridge (in prep.). This taxonomic project is an initiative of the Petroleum and Marine Division of AGSO.

This paper provides formal descriptions of previously undescribed dinoflagellate cyst taxa from Oxfordian (Late Jurassic) palynofloras recorded in samples from the Frigate Shale and lower Vulcan Formation and equivalent strata in the Timor Sea region. All the new taxa have stratigraphical utility within the *Wanaea spectabilis* Interval Zone of Helby *et al.* (1987) and Helby & Partridge (in prep.). The figured specimens in this paper from the north-western Australian region are from the Frigate Shale and lower Vulcan Formation and coeval strata from twelve wells (Foster, this volume; Appendices 1, 2). The Polda-1 well is from onshore South Australia. Specimens from Polda-1 are illustrated specifically to demonstrate morphological variation in the genus *Fusiformacysta* Morgan 1975 emend. The Polda sample contains a restricted dinoflagellate cyst assemblage, which cannot be assigned to the *Wanaea spectabilis* Zone.

Helby *et al.* (1987, p. 29) stated that their *Wanaea spectabilis* Interval Zone is of early to mid Oxfordian age. This correlation was based on

evidence from ammonites and belemnites (Arkell, 1956; Balme, 1957; Wiseman, 1980). Davey (1987, fig. 3), however, concluded that this zone lies entirely within the early Oxfordian. Francis & Westermann (1993, fig. 1b), further interpreted the age of this zone to be possibly as old as late Callovian, but most likely to be early-mid Oxfordian (fig. 7). The conclusions of Francis & Westermann (1993, fig. 7) were based on linking the Australasian faunas to northwest Europe by the correlation indirectly across several ammonite faunal provinces. The interpretations of Francis & Westermann (1993) were adapted by Davey (1999), who stated that the top of the *Wanaea spectabilis* Zone cannot be younger than intra-mid Oxfordian and that the base is within the late Callovian. Burger (1996, fig. 2) suggested that the *Wanaea spectabilis* Zone ranged from the latest Callovian to the mid Oxfordian, within AGSO timeslice J-8, based on AGSO datum point 5. He pointed out the lack of direct evidence of correlations to Europe within the Late Jurassic *Wanaea spectabilis* to *Cribroperidinium perforans* zones. The AGSO datum point 5 in Burger (1996, fig. 2), within the *Wanaea spectabilis* Zone, is based on the correlation of early and mid Oxfordian ammonites occurring together with *Wanaea spectabilis* Zone dinoflagellate cyst floras in the Sula Islands, Indonesia (Burger, 1996, p. 74). Burger (1996) further argued for a latest Callovian to mid Oxfordian age for the *Wanaea spectabilis* Zone, based on the Callovian age of the preceding *Rigaudella aemula* Zone according to Davey (1987) and Burger (1995) and the mid-late Oxfordian age of the succeeding *Wanaea clathrata* Zone.

SYSTEMATIC PALYNOLOGY

In this section, three new genera and eight new species of dinoflagellate cyst are described. Additionally, the genus *Systematophora* is emended. The new taxa are from the Frigate Shale, lower Vulcan Formation and equivalent strata in twelve offshore north western Australian exploration wells (Foster, this volume) as well as two Tithonian outcrop samples from the Lelinta Formation of Misool, eastern Indonesia (Appendices 1, 2). The genera are listed in alphabetical order; the recent suprageneric classification of Fensome *et al.* (1993) is not used here. The dimensions quoted are all given in micrometres (µm). For descriptive purposes, the cyst sizes, small, intermediate and large, are after Stover & Evitt (1978, p. 5). These parameters are such that intermediate size dinoflagellate cysts have a maximum dimension of between 50µm and 100µm. Small and large forms are less than 50µm and over 100µm, respectively. The majority of the morphological terminology for dinoflagellate cysts are those used by Evitt (1985). However, the term loisthocyst refers to a dinoflagellate cyst in which the operculum (or the separate opercular pieces) has (have) detached and is therefore the part that remains (Sarjeant *et al.*, 1987, p. 26, 27). Where appropriate, the dinoflagellate cyst paraplate notation system used throughout is Kofoidian, as opposed to the 'Taylor-Evitt' scheme of Evitt (1985). References to author citations of taxa discussed are not given here. These may be found in the bibliography in Williams *et al.*, 1998, p. 747-817). The synonymy lists given here are selective and are mainly confined to illustrated specimens. All of the figured specimens are housed in the Commonwealth Palaeontological Collection (CPC) of the Australian Geological Survey Organisation, Canberra (see Appendix 2).

This study has almost exclusively used single grain mounts (or mounts with multiple specimens of a single species) and most figured specimens are from these slides. The vast majority of the samples are from conventional core and sidewall cores, but a single ditch cuttings sample was also examined. The photomicrographs in the eleven plates (Figs. 1, 3-6 and 8-13) were all taken using an Olympus DP10 digital camera system on a Zeiss Axioskop photomicroscope, housed at AGSO. Some extraneous palynodebris not adherent to the figured specimens has been digitally removed in selected images. The images in Figs 1, 3-6 and 8-13 herein are from a digital database containing many more images than have been figured. Sample details, morphological data and measurements of each specimen are on open file spreadsheets. The image database may be accessed on the AGSO website (http://www.agso.gov.au).

Many of these new taxa have been extensively used in unpublished reports, which are now in the public domain (open file). In order to maximise their utility, the informal names and/or codes are listed separate from any formal synonymy listing under the heading 'Previous Australian usage'. To provide continuity, wherever practical, the informal names have been retained.

Dinoflagellate cysts

Cygnusicysta gen. nov.

Type species. Cygnusicysta taltarniana sp. nov.

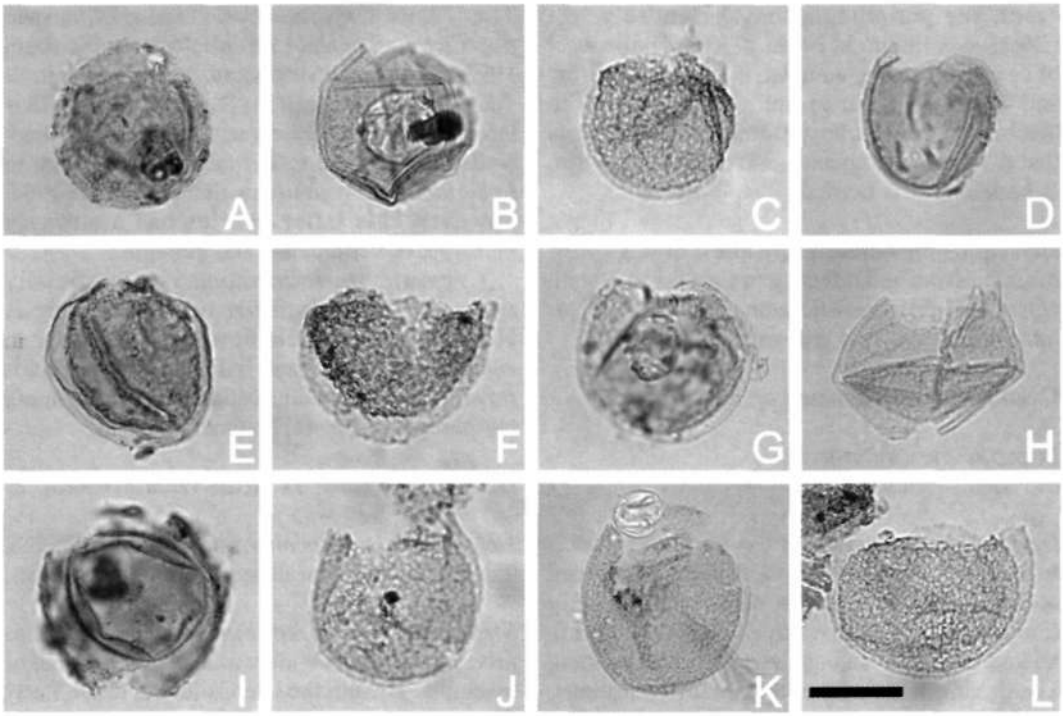

Fig. 1. Cygnusicysta taltarniana sp. nov. All from sidewall core at 2820.00m in Taltarni-1 well. All photomicrographs taken using plain transmitted light except Figs 1H, J, L, which were taken using Nomarski Interference Contrast. Scale bar in Fig. 1L refers to all photomicrographs and is 25µm. Fig. 1L is the holotype, the remainder, paratypes. Note circumcavate cyst organisation with narrow pericoel; subcircular outline; variability of endophragmal ornamentation; and apical archaeopyle. A - CPC 35517, paratype; median focus. Note adherent operculum and accumulation bodies. B - CPC 35518, paratype; median focus. Note extremely narrow pericoel. C - CPC 35519, paratype; median focus. Note endophragm is microreticulate. D - CPC 35520, paratype; median focus. Note apical archaeopyle and virtually psilate endophragm. E - CPC 35521, paratype; low focus. Note relatively prominent periphragm and long, arcuate fold. F - CPC 35522, paratype; median focus. Compressed with mechanically expanded archaeopyle. G - CPC 35523, paratype; median focus. Note large accumulation body. H - CPC 35524, paratype; median focus. Folded and compressed specimen. I - CPC 35525, paratype; median focus. Note unusually wide, almost kalyptrate, pericoel. J - CPC 35526, paratype; median focus. Note microreticulate endophragm and narrow pericoel. K - CPC 35527, paratype; a composite photomicrograph. Note narrow pericoel and apical archaeopyle with distinctively angular principal archaeopyle suture and accessory archaeopyle sutures. L - CPC 35528, holotype; median focus. Note microreticulate endophragm, narrow pericoel and apical archaeopyle.

Diagnosis. Proximate, circumcavate dinoflagellate cysts, small to intermediate in size and compressed subspherical in shape. Periphragm and endophragm smooth or having low relief ornamentation. Indications of paratabulation lacking apart from the principal and accessory archaeopyle sutures. Paratabulation apparently gonyaulacalean. Paracingulum not indicated, parasulcus indicated by parasulcal notch. Archaeopyle apical, operculum free, simple.

Comments. The principal archaeopyle suture of the type, *Cygnusicysta taltarniana,* is angular and indicates the presence of six precingular paraplates, sometimes marked by short accessory archaeopyle sutures. Furthermore, isolated opercula of the type indicate that four apical paraplates are present. *Cygnusicysta taltarniana* was regarded as an acritarch until the archaeopyle was recognised.

Comparison. This new genus is similar to *Leberidocysta* Stover & Evitt 1978 in that both are cavate and have apical archaeopyles. However, the endocyst of the genotype, *Leberidocysta chlamydata* (Cookson & Eisenack 1962) Stover & Evitt 1978, is characteristically elongate ellipsoidal in outline and verrucate. Furthermore, the pericyst is irregular in outline due to intense folding and damage of the periphragm. In some

cases, the periphragm may be entirely lost (Cookson & Eisenack, 1962a, p. 496). The pericoel of *Cygnusicysta*, by contrast, is relatively narrow and the periphragm in not generally prone to mechanical damage, apart from folding. It appears that a restudy of species currently assigned to *Leberidocysta* is needed.

Derivation of name. From the Latin *cygnus*, meaning swan and referring to East Swan-1 well, where the characteristic acme of *Cygnusicysta taltarniana* was first recognised.

Cygnusicysta taltarniana sp. nov. (Figs 1A-L).

Previous Australian usage
M.P. 620 – Helby.

Description. A species of *Cygnusicysta*, that is subcircular in dorsoventral view. Generally equant in overall length and width, occasionally slightly elongate. Endophragm relatively thick (up to 2µm), microreticulate or having low relief ornamentation. The ornament may be microgranulate, scabrate, or rugulate. Periphragm thinner, microgranulate to smooth (0.5-1.5µm). Pericoel normally relatively narrow (generally 2-5µm wide). The operculum is normally free. Accumulation bodies are frequently present inside the cyst.

Dimensions (µm; n=40): Min. (Mean) Max.
Length of pericyst (incl. operculum): 37 (48) 64
Length of pericyst (excl. operculum): 34 (44) 60
Length of endocyst (incl. operculum): 36 (42) 59
Length of endocyst (excl. operculum): 31 (40) 52
Width of pericyst: 32 (45) 68
Width of endocyst: 30 (40) 53
Maximum separation of wall layers: 1 (4) 13

The measured specimens are all from a sidewall core sample at 2820.00m in Taltarni-1 well.

Comments. Specimens are often crushed and this can increase the overall length, and width as well as the width of the pericoel (Fig. 2).

Comparison. Although *Cygnusicysta* is a monospecific genus, *C. taltarniana* is similar to some species assigned to *Leberidocysta*. In particular, *Leberidocysta? pergamentacea* (Burger 1980) Burger 1980 is an Early Cretaceous species which is not unequivocally cavate (Burger, 1980, p. 88). If cavation is developed, it may be sporadic and the pericoel is extremely thin. *Leberidocysta defloccata* (Davey & Verdier 1973) Stover & Evitt 1978 has an extremely wide pericoel. The Late Cretaceous *Leberidocysta? flagellichnia* Schiøler 1993 is holocavate (Schiøler, 1993, p. 110). *Leberidocysta? scabrata* Jain & Taugourdeau-Lantz 1973) Stover & Evitt 1978 is larger than *C. taltarniana* and has a thick, spongy wall. *Cygnusicysta taltarniana* is also similar to *Leberidocysta? verrucosa* Schiøler *et al.* 1997, however, this latter species has a strongly verrucate or vermiculate endophragm.

Cygnusicysta taltarniana is superficially similar to *Craspedodinium swanense* Riding & Helby (this volume); however, the latter is significantly larger, and has periphragmal folds reflecting paratabulation and essentially smooth periphragm and endophragm.

Derivation of name. From the Taltarni-1 well.

Holotype and type locality. Figure 1L, CPC 35528, Taltarni-1 well, sidewall core sample at 2820.00m.

Stratigraphical distribution. *Cygnusicysta taltarniana* ranges widely as a rare component of assemblages from the late Callovian to the Early Cretaceous. However, it occurs as a stratigraphically significant acme in the Oxfordian, lower part of the middle *Wanaea spectabilis* Zone (6ciib) in wells in the Montara Field and in the adjacent Vulcan Sub-Basin in the Timor Sea (Foster, this volume; Helby & Partridge, in prep.).

Fosteria gen. nov.

Type species: Fosteria eclipsiana sp. nov.

Diagnosis. Small, proximate to proximochorate, acavate cysts, rounded subquadrate to subpolygonal in dorsoventral outline, with a prominent, incised paracingular region. Autophragm smooth or with low relief ornamentation. A gonyaulacalean paratabulation is indicated partially or fully by low parasutural ridges or crests. These indicate a paratabulation formula of ?4', 6", ?6c, 6"', 1p, 1"", Xs and may be surmounted by relatively short ornamentational elements. Paracingulum indicated by both the incised equatorial region and by ridges/crests bordering the precingular, postcingular paraplate series and occasional, inconsistent intra-paracingular plate boundaries. Parasulcus delimited by parasulcal ridges or crests, not obviously subdivided. Archaeopyle apical, assumed to be type 4A; operculum free, simple. Accumulation bodies may be present.

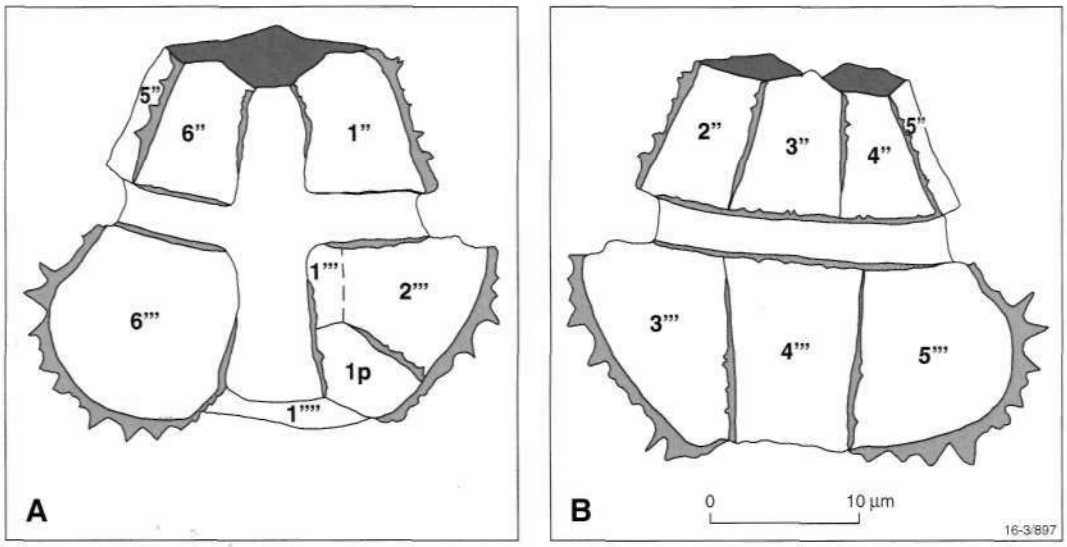

Fig. 2. Line drawings of an idealised specimen of *Fosteria eclipsiana* sp. nov. illustrating the interpreted Kofoidian paratabulation pattern. A - specimen in ventral view; B - specimen in dorsal view. For clarity, the accumulation body is not illustrated; therefore, the central area of the cyst has been left blank. Note how the midventral and middorsal parasutural ridges become higher toward the periphery of the cyst.

Comments. This distinctive new gonyaulacalean genus normally exhibits a full paratabulation, however the paracingulum and parasulcus are not obviously subdivided. This genus ostensibly appears to be of cladopyxiacean affinity in terms of its size, shape and general appearance. However, the 1p/1'''' parasuture is considerably off centre (Figs 2, 3), which suggests it is not standard partiform *sensu* Evitt (1985, p. 112-116), although it has features in common with the partiform species *Glyphanodinium facetum* Drugg 1964 (see Evitt, 1985, fig. 5.18.A). Detail of the central parasulcal region in *Fosteria* is unclear (Figs 2, 3).

Comparison. *Fosteria* is similar in morphology, size, shape and wall relationships to the Jurassic *Reutlingia* Drugg 1978 emend. Below 1987 and its relatives, for example *Parvocysta* Bjaerke 1980 and *Susadinium* Dörhöfer & Davies 1980 (see Riding, 1984). However members of this *Parvocysta* suite (Riding, 1984) all have intercalary archaeopyles and paratabulation patterns differing from *Fosteria* (see Below, 1987a). *Mikrocysta* Bjaerke 1980 emend. Below 1987 differs from *Fosteria* in having a type 2A apical archaeopyle and is essentially partiform, with a strong mid antapical 1''''/2'''' parasuture and an inverted omegaform ps paraplate (Below, 1987b, pl. 2, 3). The schematic paratabulation diagram of the hypocyst of *Mikrocysta bjaerkei* of Below (1987b, fig. 3b) closely resembles paratabulation on the hypocyst of *F. eclipsiana*. We note that the shape of the ps paraplate and the location of the 1'''/2'''' parasutural boundary in the latter diagram does not accord with the specimens of *M. bjaerkei* illustrated by Below (1987b, pl. 2, 3). *Mikrocysta bjaerkei* is distinguished from *Fosteria* in losing only two, rather than four, apical paraplates during excystment, in addition to having an unequivocally partiform paratabulation pattern. *Fosteria* is also morphologically similar to *Horologinella* Cookson & Eisenack 1962 emend. Backhouse 1988 and *Dollidinium* Helby & Stover 1987. These are both distinguished from *Fosteria* by their paratabulation patterns, their apical type 2A (3'/4') archaeopyles. *Horologinella* may have an enlarged type A (4') archaeopyle which can impinge on paraplates 3' and 5' (Backhouse, 1988, p. 90, fig. 26). *Dollidinium*, *Horologinella* and *Mikrocysta* also lack denticulate crests. *Dollidinium* is further distinguished by the occurrence of apical and antapical lobes.

Derivation of name. Named for Dr. Clinton Foster.

Fosteria eclipsiana sp. nov. (Figs 2, 3A-P)

Previous Australian usage
Horologinella eclipsiana – Helby.

Description. Cysts having a rounded subpentangular to subquadrate dorsoventral outline with a deeply incised paracingulum. They are strongly dorsoventrally compressed.

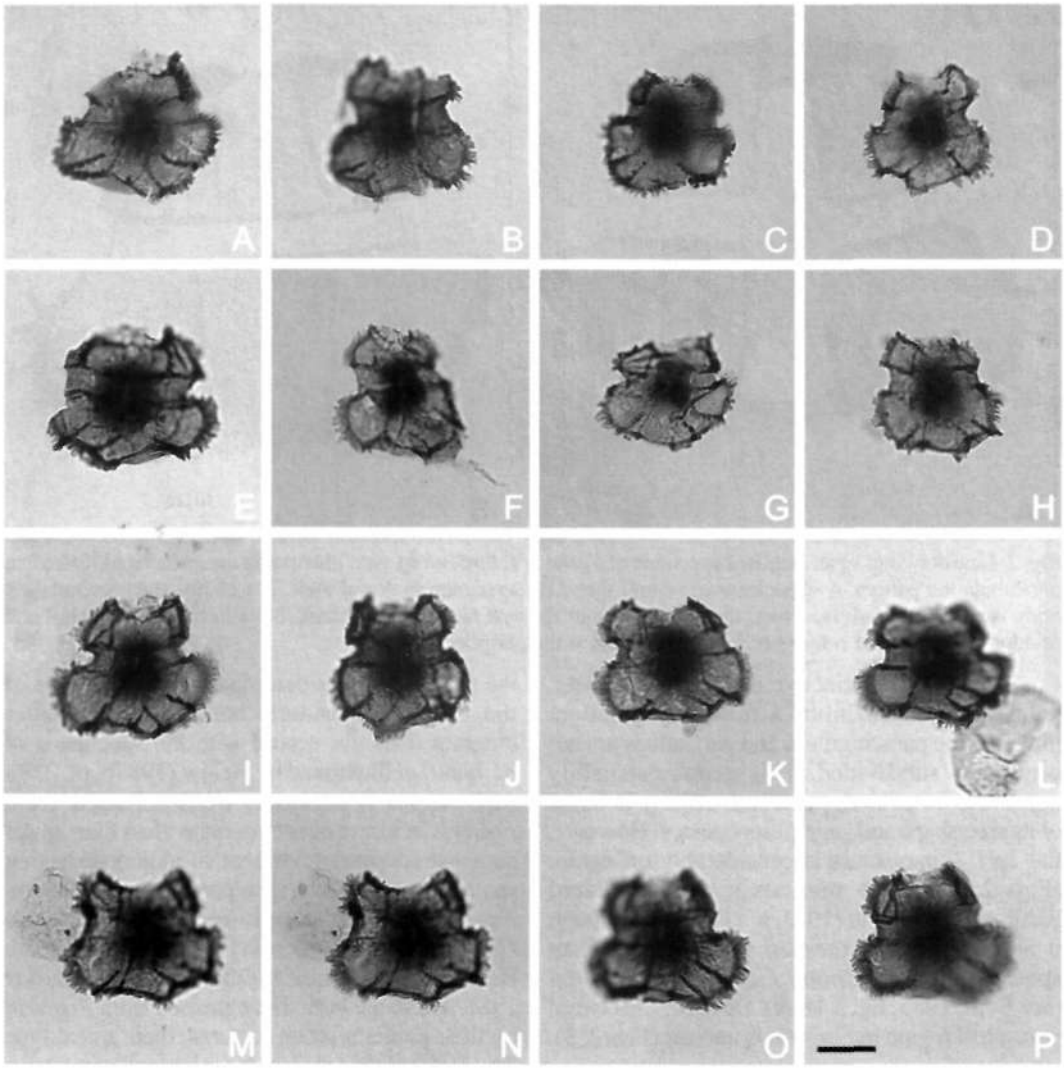

Fig. 3. Fosteria eclipsiana sp. nov. All from conventional core at 3221.47m in Layang-1 well. All photomicrographs taken using plain transmitted light. Scale bar in Fig. 3P refers to all photomicrographs and is 12µm. Fig. 3I is the holotype, the remainder, paratypes. Note robust, dark autophragm; rounded subpentangular/subquadrate outline; prominent, deeply-incised paracingulum; denticulate parasutural crests; apical archaeopyle; and large accumulation body. A - CPC 35529, paratype; dorsal view, low focus. Note amorphous nature of large, dark, centrally-located accumulation body. B - CPC 35530, paratype; ventral view, low focus. Note densely denticulate parasutural crests. C - CPC 35531, paratype; ventral view, median focus. Angular specimen; note prominent posterior intercalary (1p) paraplate at bottom left. D - CPC 35532, paratype; ventral view, median focus. Small specimen. E - CPC 35533, paratype; ventral view, median focus. Large specimen. F - CPC 35534, paratype; dorsal view, median focus. Elongate specimen. G - CPC 35535, paratype; dorsal view, median focus. Squat morphotype. H - CPC 35536, paratype; dorsal view, median/low focus. Note variable nature of parasutural denticles. I - CPC 35537, holotype; dorsal view, median focus. Note well-defined standard gonyaulacalean paratabulation pattern. J - CPC 35538, paratype; ventral view, median focus. Note apical archaeopyle. K - CPC 35539, paratype; dorsal view, median focus. L - CPC 35540, paratype; dorsal view, median focus. Note diffuse nature of periphery of accumulation body. M, N - CPC 35541, paratype; dorsal view, median and low focus respectively. Note large accumulation body. O, P - CPC 35542, paratype; dorsal view, low and high focus respectively. The 1p paraplate is to bottom right in Fig. 3O; note blunt nature of majority of parasutural denticles.

Autophragm relatively thick; smooth to microgranulate, occasionally irregularly microreticulate. Paratabulation indicated by low parasutural ridges or low crests, which are surmounted by denticles and/or spines. The parasutural ridges become gradually higher and slightly broader laterally. Lateral parasutural denticles are solid, sharp or blunt distally, and are longest on the hypocyst; the density of insertion is also variable. The epicyst is shorter than the hypocyst. Hypocyst is slightly asymmetrical in that the left lateral side is slightly more angular due to the presence of the 1p paraplate. The parasulcus is wide and located mid-ventrally. Similarly, the paracingulum is relatively high and is only slightly laevorotatory. A large, dark accumulation body is consistently present in the centre of the cyst.

Dimensions (μm; n=34, all loisthocysts), including spines/denticles: Min. (Mean) Max.
Length of loisthocyst: 26 (30) 35
Length of epicyst (i.e. precingular series): 7 (10) 13
Length of hypocyst: 12 (16) 20
Height of paracingulum: 4 (5) 7
Width of epicyst: 20 (24) 32
Width at paracingulum: 15 (21) 28
Width of hypocyst: 25 (31) 39
Length of accumulation body: 10 (14) 17
Width of accumulation body: 8 (12) 15
Length of denticles/spines: 1 (1.5) 7

The measured specimens are from sidewall core at 3221.57m and 3223.20m from Layang-1 Well.

Comments. *Fosteria eclipsiana* is a distinctive small species, and is equant in terms of length and width. The posterior intercalary (1p) paraplate of *F. eclipsiana* is particularly slender and is located close to the left lateral side. Its presence makes this side straighter, or more angular than the right lateral side (Figs 2, 3). The species is dorsoventrally flattened. The relatively thick autophragm, which is normally smooth to microgranulate, imparts a dark body colour (Fig. 3). Parasutural ridges emerge in the central area of the cyst, close to the edge of the accumulation body. These ridges become more robust, higher and slightly wider, and the surmounting denticles/spines increase in size proportionally (Figs 2, 3). The denticles are normally evenly inserted, generally taper distally to a sharp point and are most prominent on the hypocyst (Figs 2, 3). However, specimens have been observed where the denticles are relatively sparse and/or are either blunt or extremely wide distally, i.e. crenellate or stauromate (Figs 3O, P). In extreme cases, some specimens are virtually devoid of denticles (Fig. 3K). All the specimens observed have a large, dark accumulation body in the centre of the cyst (Fig. 3). These accumulation bodies frequently lack sharp edges, having a diffuse, vaguely-defined periphery. The paracingulum is only slightly laevorotatory, relatively high and is deeply incised; it is located high on the cyst, normally making the epicyst significantly shorter than the hypocyst. The wide, mid-ventral parasulcus is not obviously subdivided. The archaeopyle represents the loss of the entire apical paraplate series. The operculum is free and no isolated opercula were observed, possibly indicating that it is compound. No attached opercula wer found; only loisthocysts were recovered (Fig. 3).

Comparison. Some species of *Horologinella* are smaller, have poorly defined paratabulation, and have more deeply incised paracingular regions than *F. eclipsiana*. These taxa include *Horologinella angulata* De Coninck 1985 and *H. tenuissima* He 1984. However, *Horologinella? obliqua* Cookson & Eisenack 1962 and *H. scabrosa* He 1984 are larger than *F. eclipsiana*, and entirely lack indications of paratabulation.

Derivation of name. From Eclipse-1 well, where we first encountered this species.

Holotype and type locality. Figure 3I, CPC 35537, Layang-1 well, conventional core at 3221.47m.

Stratigraphical distribution. *Fosteria eclipsiana* ranges from the Callovian *Wanaea digitata* Zone (7bi) to the Oxfordian mid *Wanaea spectabilis* Zone (6cii) in the Timor Sea region. It is most prominent in the lower *Rigaudella aemula* Zone (7aiia) to lower *W. spectabilis* Zone (6ciii), but is usually a minor, although distinctive, background component of these dinoflagellate cyst suites (Foster, this volume; Helby & Partridge, in prep.).

Fusiformacysta Morgan 1975 emend. Riding & Helby this volume

Type species: Fusiformacysta salasii Morgan 1975

Fusiformacysta challisiana sp. nov. (Figs 4A-L)

Previous Australian usage
Komewuia sp. 555 (verrucate) – Helby.
Dissiliodinium verrucate '555' – Morgan.

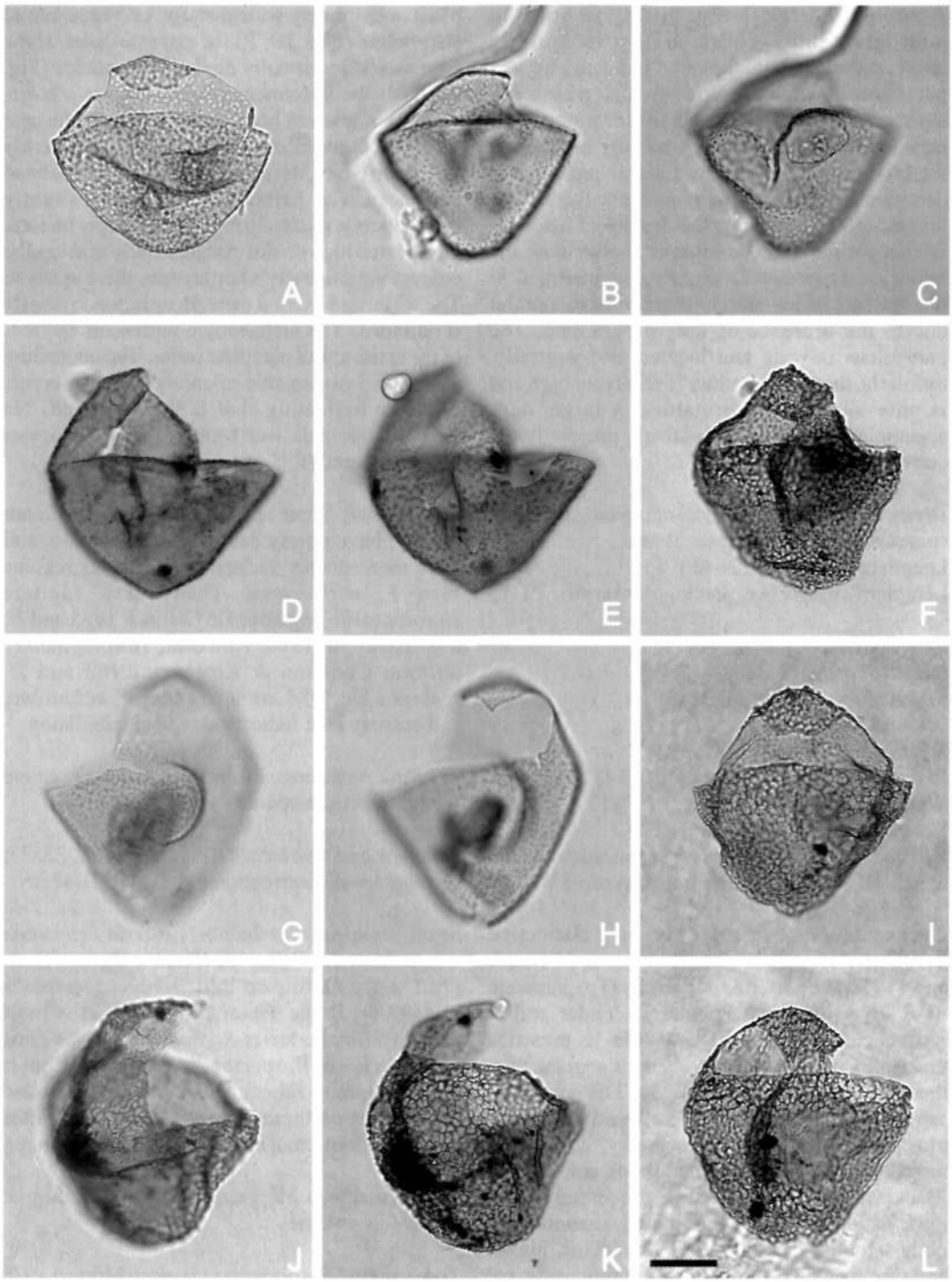

Fig. 4. Fusiformacysta challisiana sp. nov. All from sidewall core in Arunta-1 well at 1805.00m (Figs 4F, I-L), Challis-11 ST1 well at 1552.50m (Figs 4A-C, G, F) and Rowan-1 well at 3183.00m (Figs 4D-E). All photomicrographs taken using plain transmitted light. Scale bar in Fig. 4L refers to all photomicrographs and is 25µm. Fig. 4A is the holotype, the remainder, paratypes. Note biconical outline, precingular (type 3P) archaeopyle, occasional presence of accumulation body and verrucate to occasionally reticulate autophragm. A - CPC 35543, holotype; squat, verrucate specimen in ventral view, low focus. Note precingular (type 3P) archaeopyle; opercular piece visible inside the cyst. B, C - CPC 35544, paratype; entirely verrucate specimen (continued opposite)

Helbycysta verrucosa – Morgan.
Komewuia challisiana – Helby.

Description. A species of *Fusiformacysta* with a type 3P archaeopyle and a biconical outline, with or without an apical horn or protuberance. Specimens vary from those with a rounded apical extremity to occasional forms with small apical horns or protuberances. The antapical region is rounded to almost flat. Most commonly, the species is elongate, but may also be subequant or wider than long. Indications of paratabulation comprise the type 3P archaeopyle and a lineation of ornamentation along the posterior margin of the paracingulum. Isolated opercular paraplates are common in the loisthocyst. A regular shaped, dark brown accumulation body may be present in the cyst. The relatively robust autophragm bears verrucae and/or a reticulum. The entirely verrucate forms are relatively densely covered in low-relief (0.5-1µm high) verrucae or grana, which are variable in shape. These elements are normally ovoidal, although rarely some coalescence of verrucae result in irregularly shaped, rounded vermiculae. The width of verrucae or grana varies from 0.5 to 6µm. Forms which are verrucate and reticulate both are generally reticulate in the vicinity of the paracingulum, with fenestrae varying in width from 1 to 5µm, the average being 2µm.

Dimensions (µm n=24): Min. (Mean) Max.
Maximum length of cyst: 71 (89) 103
Width of cyst at paracingulum: 67 (82) 96

The measured specimens are from sidewall cores in Arunta-1 well at 1805.00m, Challis-11 ST1 well at 1552.50m and Rowan-1 well at 3183.00m.

Comments. *Fusiformacysta challisiana* is a large form which has a distinctive ornamentation. It may be either verrucate or, occasionally, verrucate and reticulate. In the partially reticulate forms, the reticulum is best developed in the equatorial area (Figs 4J-L). This variability in ornamentational style is unusual. In some specimens the presence of a small anterior intercalary paraplate (K paraplate of Evitt, 1985) is suggested by angulation of the principal archaeopyle suture.

Comparison. *Fusiformacysta challisiana* differs from *F. terniana* Riding & Helby (this volume) in the typical lack of apical and antapical horns and the presence of a largely verrucate autophragm. *Fusiformacysta salasii* is significantly more elongate than *F. challisiana*, with extremely long polar horns and smooth autophragm. The Tithonian to Berriasian species *F. tumida* Backhouse 1988 is also more slender than *F. challisiana* and is ornamented by small (<1µm wide), nontabular grana. *Fusiformacysta* sp. cf. *F. tumida* from the Late Jurassic Polda Formation of the Eyre Peninsula, South Australia closely resembles *F. challisiana*, but generally has more prominent polar horns (Figs 5A-C). Like the type material from the Perth Basin (Backhouse, 1988), these Polda specimens were recovered from a paralic succession (Gatehouse & Cooper, 1982).

Derivation of name. From Challis-11 ST1 well, from which material of this species was first recovered.

Holotype and type locality. Figure 4A, CPC 35543, Challis-11 ST1 well, sidewall core at 1552.50m.

Stratigraphical distribution. *Fusiformacysta challisiana* ranges from the Callovian *Rigaudella aemula* Zone (7aii) to the Oxfordian *Wanaea clathrata* Zone (6b) of the Timor Sea (Foster, this volume; Helby & Partridge, in prep.). It is generally a background component and is most consistent between the upper part of the lower *Rigaudella aemula* Zone (7aiia) to the lower *Wanaea spectabilis* Zone (6ciiia).

Microdinium Cookson & Eisenack 1960 emend. Slimani 1994

Type species. *Microdinium ornatum* Cookson & Eisenack 1960

---

in dorsal view, high/median and low focus respectively. Note precingular (type 3P) archaeopyle; two opercular pieces present in hypocyst (Fig. 4C). D, E - CPC 35545, paratype; oblique dorsal/right lateral view, median and low focus respectively. Entirely verrucate specimen; note large archaeopyle. F - CPC 35546, paratype; ventral view, low focus. Entirely verrucate specimen with small apical protuberance. G, H - CPC 35547, paratype; ventral view, high and low focus respectively. Verrucate specimen; note precingular (type 3P) archaeopyle. I - CPC 35548, paratype; ventral view, low focus. Entirely verrucate specimen; note precingular (type 3P) archaeopyle. J, K - CPC 35549, paratype; right lateral view, high and low focus respectively. Note strong reticulate ornamentation in equatorial region and verrucae in area around antapex. L - CPC 35550, paratype; ventral view, low focus. Note lack of apical horn and precingular (type 3P) archaeopyle. Specimen largely verrucate, however reticulate ornamentation is developed at, and near paracingulum.

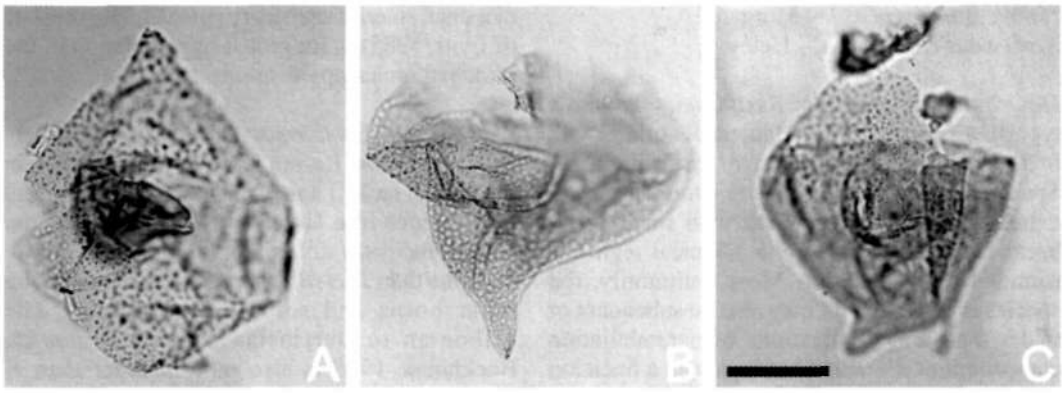

Fig. 5. Fusiformacysta sp. cf. *F. tumida* Backhouse 1988. These are illustrated for comparison with *F. challisiana*. All from conventional core in Polda-1 well at 116.43m. All taken using plain transmitted light. Scale bar in Fig. 5C refers to all photomicrographs and is 25µm. Note biconical outline; nontabular grana comprising the autophragmal ornamentation; and prominent polar horns. A - CPC 35551; ventral view, median focus. Note biconical shape. B - CPC 35552; ventral view, high focus. Note relatively long, distally pointed antapical horn. C - CPC 35553; dorsal view, median focus. Note short antapical horn and prominent nontabular grana.

Microdinium jurassicum sp. nov. (Figs 6A-T)

1988 *Microdinium* sp. A (M.P. 619); Helby *et al.*, fig. 10G-H.
1996 *Microdinium ornatum auct. non* Cookson & Eisenack 1960; Burger, pl. 7, figs O-Q.

Previous Australian usage
Microdinium oxfordensis – Ott (1970, pl. 8, figs 26-28).
M.P. 619 – Helby.
Microdinium jurassicum – Helby.

Description. A small species of *Microdinium*, elongate ellipsoidal to rounded subquadrangular/subpentagonal in dorsoventral or lateral view and may be slightly dorsoventrally flattened. Autophragm relatively thick (1-2µm), microreticulate. The fenestrae of the microreticulum are subcircular to irregularly subovoidal, narrow (<0.5-1µm in maximum diameter) and of variable density. They are normally more densely spaced close to the parasutures. Occasionally, one, rarely two, large (up to 2.5µm high and 1µm wide) intratabular tubercles are present on the precingular and postcingular paraplates. A similar tubercle or protuberance may be present at the apex of the cyst. Parasutures marked by prominent (1-2µm high), distally-smooth to slightly undulate parasutural crests which may also be irregularly microreticulate. Apical archaeopyle, operculum simple, generally free.

Dimensions (µm n=49): Min. (Mean) Max.
Overall length of entire cyst: 25 (37) 49
Overall length of loisthocyst: 27 (36) 49
Overall width of cyst body: 20 (33) 47

The measured specimens are from conventional cores from Jabiru-2 well at 1642.50m and Jabiru-3 well at 1604.0m to 1604.13m. and sidewall cores from Arunta-1 well at 2135.00m, Challis-11 ST1 well at 1552.50m, Challis-11 ST2 well at 1842.00m, Rowan-1ST well at 3181.00m and Taltarni-1 well at 2950.00m.

Microdinium jurassicum has a wide size range

Fig 6. (opposite) *Microdinium jurassicum* sp. nov. All from sidewall cores from Arunta-1 well at 2135.00m (Figs 6D, H), Rowan-1ST well at 3181.00m (Figs 6E-G, K-L) and Taltarni-1 well at 2950.00m (Figs 6A-C, I-J, M-P, T), except Figs 6Q-S, which are from conventional core in Jabiru-2 well at 1642.50m. All photomicrographs taken using plain transmitted light. Scale bar in Fig. 6T refers to all photomicrographs and is 25µm. Figures 6M-O are the holotype, the remainder, paratypes. Note elongate ellipsoidal to rounded subquadrangular/subpentagonal outline, robust, microreticulate autophragm, occasional intratabular tubercles, distally smooth, slightly undulate parasutural crests, and apical archaeopyle. A-C - CPC 35554, paratype; dorsal view, high to low focus sequence. Note prominent paracingulum and broad parasulcus in Fig. 6C. D - CPC 35555, paratype; ventral view, low focus. Note apical archaeopyle. E-G - CPC 35556, paratype; slightly oblique dorsal view, high to low focus sequence. Small morphotype, note thick autophragm and intratabular tubercles in postcingular paraplate series. H - CPC 35557, paratype; right lateral view, high focus. Note angular base of median paracingular paraplate. I, J - CPC 35558, paratype; dorsal view, high and low focus respectively. Note apical archaeopyle and typically partiform ventral paratabulation pattern in Fig. 6J (see Evitte, 1985, figs 5.18A-C). (continued opposite)

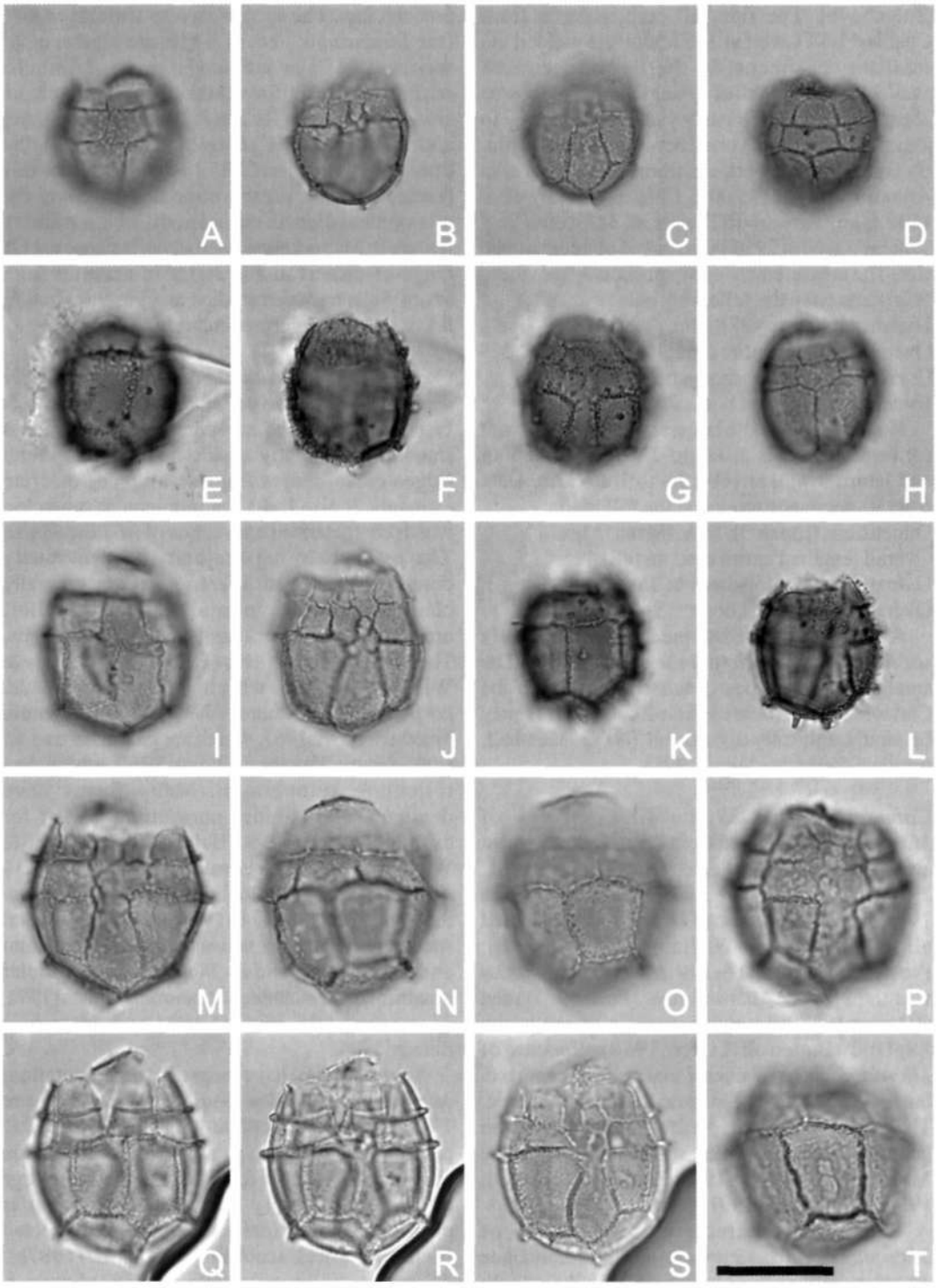

K, L - CPC 35559, paratype; slightly oblique dorsal view, high to low focus sequence. M-O - CPC 35560, holotype; dorsal view, high and media/low focus respectively. Note thick autophragm, intratabular tubercles and denticulate parasutural crests in Fig. 6L. P, T - CPC 35561, paratype; ventral view, high and low focus respectively. Note suppression of small, central parasulcal paraplates and strongly microreticulate autophragm. Q-S - CPC 35562, paratype; dorsal view, high to low focus sequence. Note concentration of microreticulation around the postcingular parasutures and apical archaeopyle.

(see above). The sidewall core material from Challis-11 ST1 well at 1552.50m has yielded the smallest specimens. In the three specimens available, the height of a single entire cyst was 25µm, the height of loisthocysts varied from 27 to 28µm and the width varied between 20 and 22µm. By contrast, the specimens from sidewall cores in Arunta-1 well at 2135.00m, Challis-11 ST2 well at 1842.00m, Rowan-1ST well at 3181.00m and Taltarni-1 well at 2950.00m proved of intermediate size. The measurement of 37 specimens from these four wells gave the following data:

Dimensions (µm n=37): Min. (Mean) Max.
Overall length of entire cyst: 30 (36) 41
Overall length of loisthocyst: 28 (34) 42
Overall width of cyst body: 20 (31) 42

However, by far the largest material came from conventional cores in Jabiru-2 well at 1642.50m and Jabiru-3 well at 1604.0m to 1604.13m. Data from 9 specimens produced the following:

Dimensions (µm n=9): Min. (Mean) Max.
Overall length of entire cyst: 46 (48) 49
Overall length of loisthocyst: 36 (42) 49
Overall width of cyst body: 35 (40) 47

All the material examined is unequivocally considered to be *Microdinium jurassicum*. The smallest morphotypes consistently occur in the Callovian *Rigaudella aemula* Zone and this may be stratigraphically significant (N. G. Marshall, personal communication, 1998).

Comments. This is the first species of *Microdinium* described from Jurassic strata: most are Cretaceous and/or Palaeogene (Williams *et al.*, 1998, p.399-404). *Microdinium? ovatum* Horowitz 1975, from the Triassic of Israel, was considered allochthonous by Williams *et al.* (1998). Previously, the oldest *in situ* material of this genus was the spinose *Microdinium? fibratum* Batten & Lister 1988 from the Barremian of south-east England (Batten & Lister, 1988). Species of *Microdinium* have occasionally been reported, but not convincingly illustrated, from the Jurassic. The principal Jurassic partiform gonyaulacalean genus is *Jansonia,* which seems confined to the Mid Jurassic (Pocock, 1972; Rauscher & Schmitt, 1990; Riding *et al.*, 1991; Martínez *et al.*, 1999).

The most characteristic features of *Microdinium jurassicum* are the microreticulate autophragm and the prominent, distally smooth to slightly irregular (undulate) parasutural crests, which may also be microreticulate (Fig. 6). In rare cases, the crests may be denticulate (Fig. 6L). The precingular paraplate series is extremely short and the paracingulum is normally higher than the precingulars. The species is very variable in size (see *Dimensions*, above). There are several other species in the Callovian and Oxfordian of Australia with microreticulate autophragm, such as *Durotrigia magna* Riding & Helby (this volume) and *Yalkalpodinium elangiana* Riding & Helby (this volume). Therefore, it is possible that this feature may be preservational. However, the microreticulation is considered to be a primary feature in *Microdinium jurassicum* because a wide range of preservational styles in material from seven wells has been studied and the autophragm is consistently microreticulate.

Comparison. Microdinium jurassicum closely resembles the genotype, *M. ornatum* Cookson & Eisenack 1960. The autophragm of the latter is smooth, it is slightly smaller and its parasutural ridges/crests may comprise aligned, discrete elements. It also lacks the intratabular tubercles, which characterise some suites of *M. jurassicum*. The overwhelming majority of previously described species of *Microdinium* are generally characterised by nontabular, low relief, ornamentation, rather than being microreticulate. These include *M. balteus* (Below 1987) Lentin & Williams 1989, which is verrucate, *M. carpentieriae* Slimani 1994 and *M. dentatum* Vozzhennikova 1967, which are granulate, and *M. reticulatum* Vozzhennikova 1967 which has reticulate autophragm. Many forms have denticulate or spinose parasutural crests, for example *M. angulare* (Below 1987) Lentin & Williams 1989, *M. carpentierae* Slimani 1994, *M. dentatum* Vozzhennikova 1967 and *M. setosum* Sarjeant 1966. Slimani (1994) described several species from the Campanian to Danian of Belgium and The Netherlands which have penitabular ornamentation, including *M. bensonii* Slimani 1994, *M. marheineckii* Slimani 1994 and *M. mariae* Slimani 1994.

Some species have negative ornamentation; *Microdinium? alatum* Conrad 1941 ex Sarjeant 1967 is densely areolate and has high, striate parasutural crests. The paraplates of *M. carinatum* (Below 1987) Lentin & Williams 1989 have large perforations largely arranged in penitabular positions; the perforations represent reflected trichocyst pores according to Below (1987b). *Microdinium? horridum* (Below 1987) Lentin & Williams 1989 has an autophragm which is irregularly perforate (Below, 1987b, pl. 17, figs 1-6). This form is readily distinguished from *M. jurassicum* in having extremely prominent gonal spines formed by extensions of the parasutural

crests. The autophragm in *Microdinium? reteinvolvatum* (Below 1987) Lentin & Williams 1989 is densely and widely perforate. In addition to this form having larger and more dense perforations than *M. jurassicum*, it also has low parasutural ridges.

Derivation of name. From the occurrence of this species in the Jurassic.

Holotype and type locality. Figures 6M-O, CPC 35560, Taltarni-1 well, sidewall core at 2950.00m.

Stratigraphical distribution. *Microdinium jurassicum* ranges from the Callovian lower *Rigaudella aemula* Zone (7aiibi) to the Oxfordian lower part of the upper *Wanaea spectabilis* Zone (6cib) in the Timor Sea region (Foster, this volume; Helby & Partridge, in prep.). The species occurs consistently from the upper part of the lower *Rigaudella aemula* Zone (7aiia) to the mid *Wanaea spectabilis* Zone (6ciib).

Systematophora Klement 1960 emend.

1960 *Systematophora* Klement; p. 61, 62.
?non. 1988 *Systematophora* Klement 1960 emend. Brenner; p. 83.
1990 *Systematophora* Klement 1960 emend. Stancliffe & Sarjeant; p. 207, 208.
(see Williams *et al.*, 1998, p. 595, 596 for further detail).

Type species. *Systematophora areolata* Klement 1960

Emended diagnosis. The original generic diagnosis of Klement (1960) and the emended diagnosis of Stancliffe & Sarjeant (1990) are accepted. This emended diagnosis allows for the presence of two, paired process groups in each of the plates in the paracingular series and low relief elements occurring within the circular area defined by the major paraplate process groups.

Comments. We do not follow the emendation proposed by Brenner (1988) as we consider that each paraplate in the apical series bears an essentially complete process group, although admitting that the proximal ridge may be open, to varying degrees, towards the apex (Brenner, 1988, fig. 23C). However, these diagnoses do not allow for the presence of two, paired process groups in each of the plates in the paracingular series (contrast Klement, 1960, figs 32, 33). The exact location of these processes on the paracingulum (and also surrounding the parasulcus) is uncertain. They are close to, or on the parasutures; however, process group style in *Systematophora* suggests that they are likely to be intratabular rather than parasutural. Hence, the generic diagnosis is here modified to allow for two sets of paired processes on each paracingular paraplate (Figs 7, 8H). Furthermore, short intratabular processes or other low relief elements may occur within the circular area defined by major process groups (Fig. 8C). Similarly, low relief elements, occurring within the circular area defined by the major paraplate process groups, have not been recorded previously.

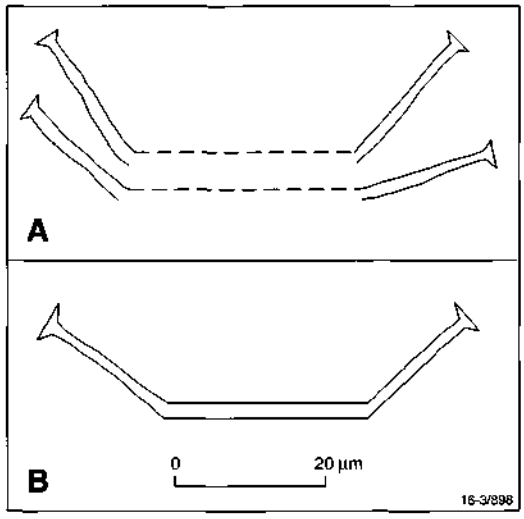

Fig. 7. Line drawings of middorsal paracingular processes in *Systematophora geminus* sp. nov. (A) and *Systematophora areolata* Klement 1960 (B). Note two pairs of processes on each paracingular paraplate in *Systematophora geminus*, which are not joined by low ridges and the single set which are commonly connected by a low ridge in *S. areolata*.

Systematophora geminus sp. nov. (Figs 7A, 8A-I, 9A-I)

Previous Australian usage
Systematophora? sp. A – Helby.
Systematophora areolata (pars) – Morgan.

Description. A species of *Systematophora* with a subspherical cyst body, the autophragm of which is microreticulate to scabrate. Slender, solid processes, which may branch both proximally and distally, emerge from subcircular to subquadrangular annulate penitabular process groups in the major transverse paraplate series. The processes are joined proximally by low,

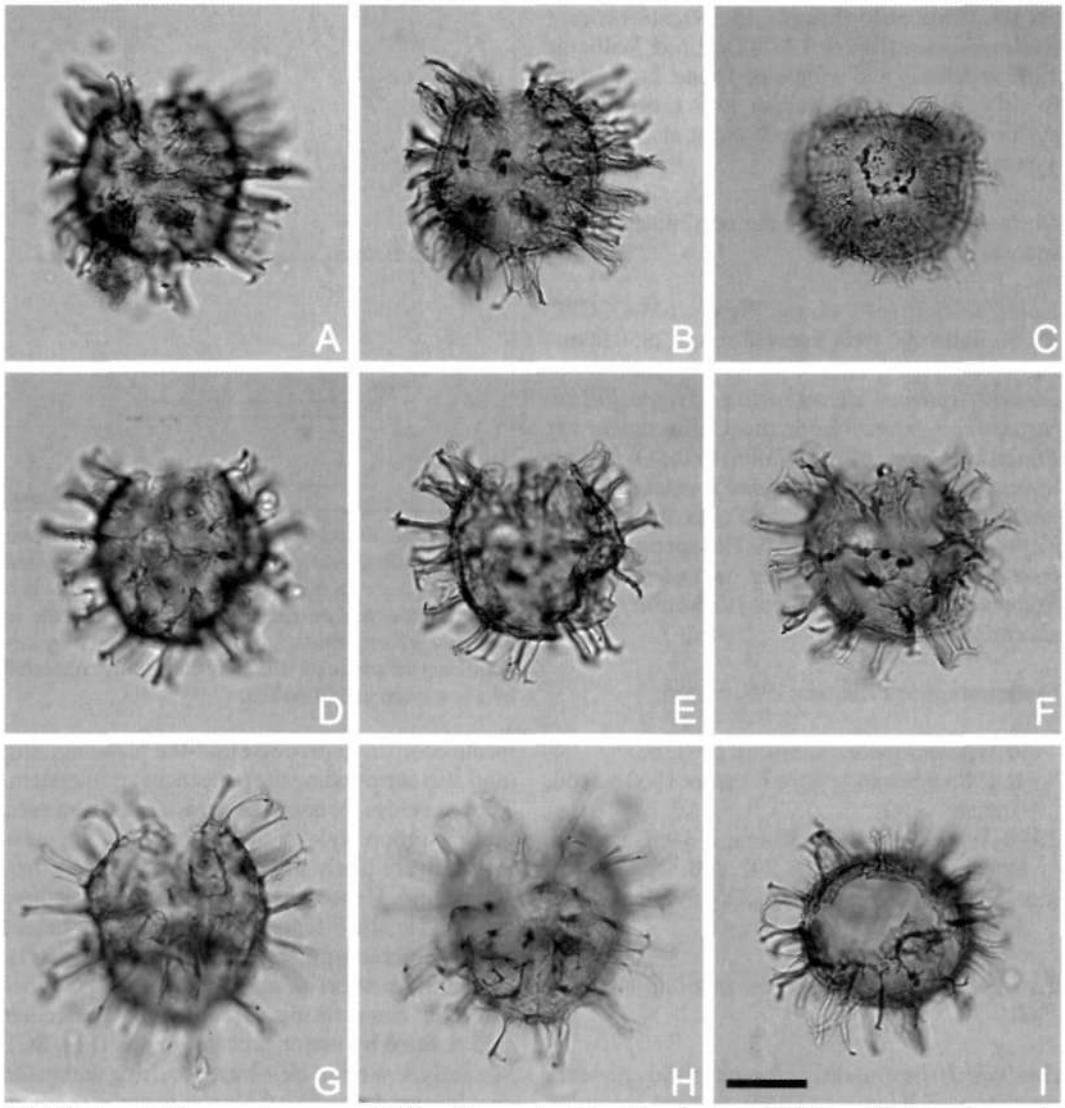

Fig. 8. Systematophora geminus sp. nov. All from Bogong-1 well, a sidewall core at 3530.00m. All photomicrographs taken using plain transmitted light. 25µm scale bar in Fig. 8I refers to all photomicrographs. Figs D-F are the holotype; the remainder, paratypes. Note subspherical cyst body, microreticulate to scabrate autophragm, slender, solid processes which may branch, arranged in annulate, penitabular groups and paired paracingular processes. These are the typical morphotype, lacking distal trabeculae connecting the processes. A, B - CPC 35563, paratype; dorsal view, high and low focus respectively. Note apical archaeopyle and paired paracingular processes. C - CPC 35564, paratype; ventral view, low focus. Note short low-relief elements within process groups. D-F - CPC 35565, holotype; dorsal view, high to low focus sequence. Note apical archaeopyle, microreticulate autophragm and distally bifurcate processes. G, H - CPC 35566, paratype; dorsal view, high and low focus respectively. Note paired paracingular processes, especially in Fig. H. I - CPC 35567, paratype; oblique antapical view, low focus. Note apical archaeopyle, proximal connecting ridges of annulate, penitabular process groups and microreticulate autophragm.

smooth penitabular ridges; the distal terminations may be joined by trabeculae. Typically, the distal process endings are bifid, however they also may be branched or multifurcate and frequently form continuous distal trabecular rings, which may be joined by trabecular filaments. Two pairs of solid, slender, distally bifid, processes are present within each paracingular paraplate (Fig. 7A). Low relief elements, which range to short processes, are present within and close to the boundary of the parasulcus. Short, solid, simple processes or low relief elements may be present within the areas

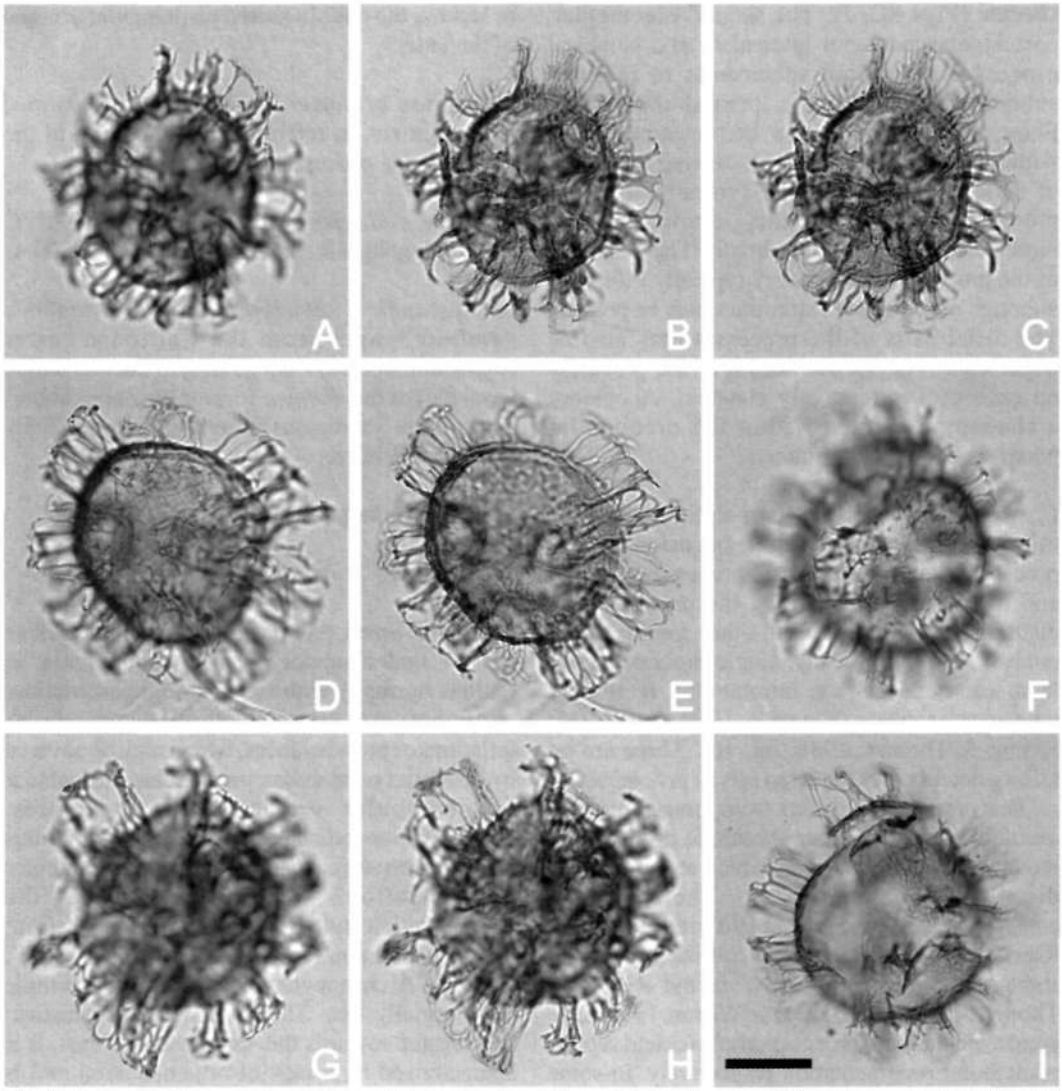

Fig.9. Systematophora geminus sp. nov. All are paratypes from Bogong-1 well, a sidewall core at 3530.00m. All photomicrographs were taken using plain transmitted light. Scale bar in Fig. 9I refers to all photomicrographs and is 25µm. These specimens are morphotypes in which the processes are connected by distal trabeculae. A-C - CPC 35568, paratype; oblique dorsal view, high to low focus sequence. Note occasional distal trabeculae. D, E - CPC 35569, paratype; oblique ventral view, high and median/low focus respectively. Strongly trabeculate specimen, note apical archaeopyle. F, I - CPC 35570, paratype; oblique dorsal view, high and low focus respectively. Slightly damaged specimen showing significant development of distal trabeculae. G, H - CPC 35571, paratype; oblique dorsal view, high and median focus respectively. Note extensive development of distal trabeculae connecting the processes.

defined by the major process complexes.

Dimensions (µm n=34, loisthocysts only): Min. (Mean) Max.
Length of cyst incl. processes: 55 (77) 97
Length of cyst body (excl. processes): 35 (54) 67
Width of cyst incl. processes: 56 (79) 97
Width of cyst body (excl. processes): 39 (57) 74
Length of processes: 7 (14) 23

A single cyst with operculum attached was measured at 97µm overall length with a cyst body 63µm long. The measured specimens are from sidewall core samples from Arunta-1 well at 2135.00m and Bogong-1 well at 3530.00m.

Comments. The thin, solid processes in *Systematophora geminus* vary in morphology and length; they are generally shorter than in other

species (Figs 8C, I). The apical, precingular, postcingular, posterior intercalary and antapical processes arise from subcircular to rounded subrectangular, annulate, penitabular ridges. Short, simple processes or denticles may arise within the process complexes, causing darkening of these areas (Figs 8A-C). Typically, the main processes are branched, this occurring distally more consistently than proximally. The distal tips of the processes/branches are typically bifurcate, although multifurcate extremities may be present. The distal parts of the processes may also be trabeculate (Fig. 9). The length of the processes on each cyst is relatively constant. Accessory archaeopyle sutures within the precingular paraplate series are common.

Comparison. The presence of a relatively thick, microreticulate autophragm, occasional short processes within the annulate process complexes and paired processes within the paracingulum distinguish *S. geminus* from other species of the genus (Fig. 7). Typically, single processes arise from each end of low, intratabular, rectilinear paracingular crests (Klement, 1960, figs 32-33; Riding & Thomas, 1988, fig. 10). There are no known occurrences of paired sets as in *S. geminus*.

This new species differs from the genotype, *S. areolata* and many other species of the genus in having branched processes, which are sometimes distally trabeculate (Fig. 9). The species *S. complicata* Neale & Sarjeant 1962 and *S. orbifera* Klement 1960 are, by contrast, consistently distally trabeculate. *Systematophora daveyi* Riding & Thomas 1988 and *S. septata* Wilson 1988 have arcuate penitabular process complexes and septate penitabular ornamentation respectively. In some suites, the distal trabeculation results in distinct ring trabeculae which may in turn be joined by interconnecting trabecular filaments. *Polystephanephorus* Sarjeant 1961 emend. Stancliffe & Sarjeant 1990 includes forms which have distally connected trabeculae sometimes joined by trabeculate filaments (Stancliffe & Sarjeant 1990, figs 1, 2). These are distinguished from *S. geminus* in lacking the double-paired paracingular process of the latter.

Derivation of name. From the Latin *geminus*, meaning twin, in reference to the pairing of the paracingular processes.

Holotype and type locality. Figures 8D-F, CPC 35565, Bogong-1 well, sidewall core at 3530.00m.

Stratigraphical distribution. *Systematophora geminus* ranges from the Callovian lower *Rigaudella aemula* Zone (7aiib) to the Oxfordian basal part of the *Wanaea spectabilis* Zone (6ciiib) in the Timor Sea region (Foster, this volume; Helby & Partridge, in prep.).

Tringadinium gen. nov.

Type species. *Tringadinium bjaerkei* sp. nov.

Diagnosis. Small, proximate, acavate dinoflagellate cysts, rounded subpolygonal to subtriangular in outline, normally with an equatorial constriction. Autophragm generally exhibits intratabular inflations or protuberances, which may be covered by low relief paratabular, penitabular, intratabular or nontabular ornamentational features. Paratabulation indicated by intratabular inflations and/or parasutural, penitabular and intratabular ornamentation. Where developed, the paratabulation style is partiform gonyaulacalean; the paratabulation formula is: 4', ?a, 6", Xc, 6'", 2"", Xs. Archaeopyle apical, operculum simple and normally free. The paracingulum is distinct and located towards the anterior of the cyst. It is characterised by a lack of ornamentation and is not obviously subdivided into paraplates. A marked constriction is generally present in the paracingular area. Parasulcus situated midventrally and indicated by a lack of ornamentation and a concavity; not obviously subdivided.

Comments. *Tringadinium* is a small partiform

Fig. 10. Tringadinium bjaerkei sp. nov. All are Tithonian, from ditch cuttings in Peak-1 well at 1493.54m-1496.59m (Fig. 10P), a sidewall core from Sandpiper-1 well at 658.38m (Figs 10Q-T) and Misool, eastern Indonesia (Figs 10A-O). All photomicrographs taken using plain transmitted light. Scale bar in Fig. 10T refers to all photomicrographs and is 25µm. Figures 10Q-S are the holotype; the remainder, paratypes. Note apical archaeopyle, variable, rounded subpentagonal outline, relatively small epicyst, prominent intratabular protuberances with their subcircular/subquadrangular rims, and variable ornamentation on autophragm. A-D - CPC 35572, paratype; slightly oblique ventral view, high to low focus sequence. Note large, rounded intratabular inflations/protuberances and prominent, high paracingulum. E-H - CPC 35573, paratype; ventral view, high to low focus sequence. Elongate specimen; note apical archaeopyle. I-K - CPC 35574, paratype; dorsal view, high to low focus sequence. Note deeply incised paracingulum and apical archaeopyle. (continued opposite)

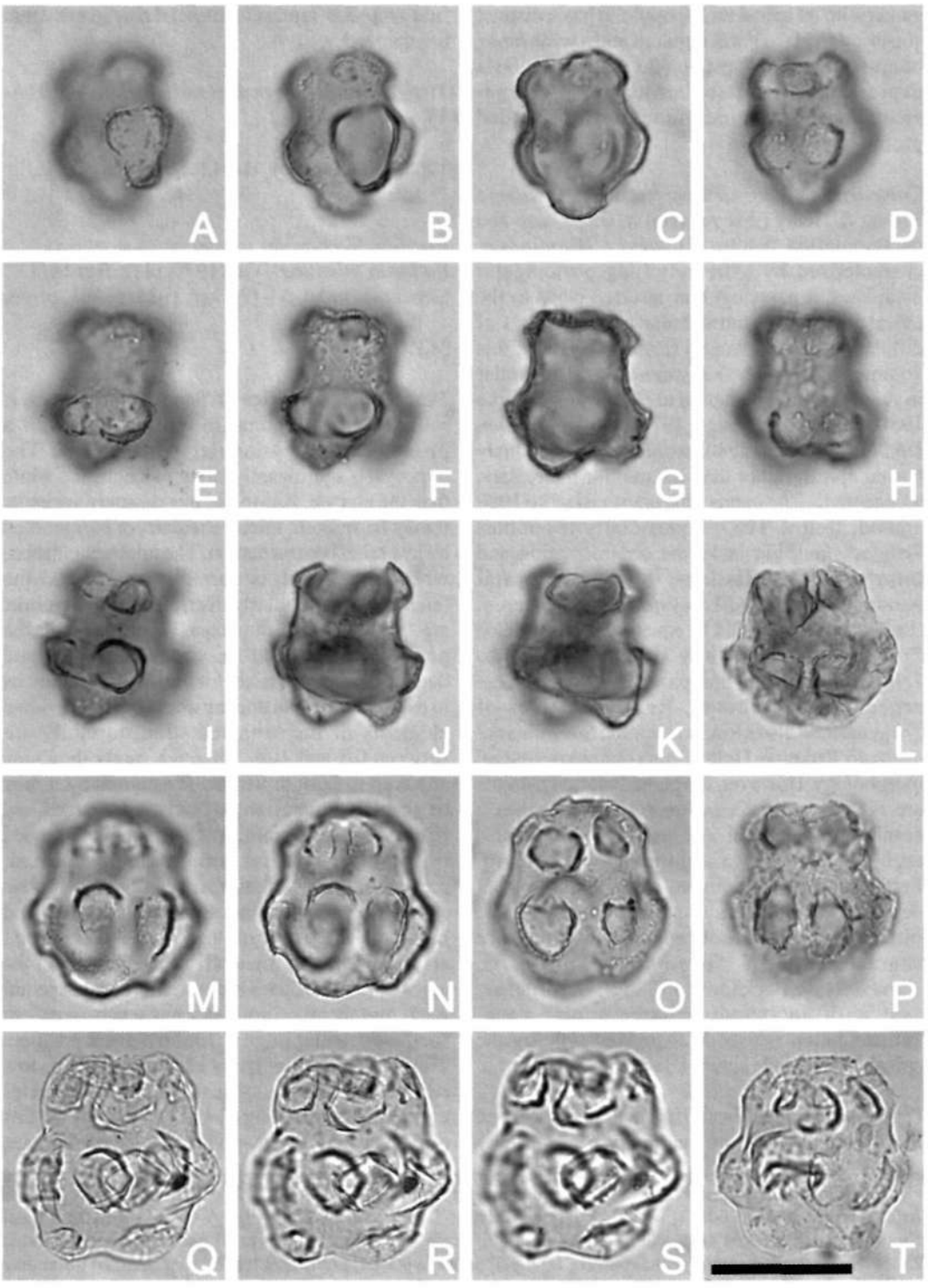

L - CPC 35575, paratype; ventral view, high focus. Squat, pyriform specimen; note that rims on intratabular protrusions are subquadrangular. M-O - CPC 35576, paratype; dorsal view, high to low focus sequence. Note that paracingulum is not deeply incised. P - CPC 35577, paratype; dorsal view, high/median focus. The rims on intratabular protrusions are elongate. Q-S - CPC 35578, holotype; dorsal view, high to low focus sequence. Well preserved specimen, note two antapical paraplates and apical archaeopyle. T - CPC 35579, paratype; ventral view, median focus. Note detached operculum of apical archaeopyle, still adherent to loisthocyst.

genus with an apical archaeopyle. It has a distinct constriction at the paracingulum and a wide range of ornamentation. Typically, the paratabulation is expressed by penitabular/intratabular ornamentation or prominent intratabular rounded protuberances.

Comparison. Tringadinium resembles *Woodinia* Riding & Helby (this volume) in shape, size and paratabulation pattern. However, *Woodinia* is characterised by extremely long postcingular paraplates, a paracingulum inserted close to the apical region and intratabular areas ('pads') of differentiated autophragm (Riding & Helby, this volume). The genus *Tringadinium* is also similar in shape and ornamentation to *Parvocysta* Bjaerke 1980, *Reutlingia* Drugg 1978 and *Susadinium* Dörhöfer & Davies 1980, except that *Tringadinium* has an apical, rather than an anterior intercalary, archaeopyle. The genus *Mikrocysta* Bjaerke 1980 emend. Below 1987 superficially resembles *Tringadinium*, but lacks the ornamentation and intratabular inflations. The epicystal paratabulation of *Mikrocysta* is also different (Below, 1987b, fig. 4). The equatorially constricted *Fosteria* is superficially similar in shape to *Tringadinium*, but has parasutural denticles/processes (see above). Representatives of *Tringadinium* also closely resemble *Susadinium? australis* Riding & Helby (this volume) in general morphology. However, the paratabulation patterns are different and *Susadinium? australis* has a combination, apical and anterior intercalary, archaeopyle with a compound operculum. Furthermore, *Tringadinium* lacks the consistent development of ridges or septa surmounting the intratabular protuberances, which are characteristic of *Susadinium? australis*. *Tetrachacysta* Backhouse 1988 is a quadrilobate cyst with an indented paracingular zone. Paratabulation is usually expressed only by the apical archaeopyle suture (Backhouse, 1988).

Derivation of name. From *Tringa*, the generic name for most of the common sandpiper species. Helby first recorded representatives of this genus from Sandpiper-1 well.

Tringadinium bjaerkei sp. nov. (Figs 10A-T, 11A-T)

1988 Gen. et sp. nov. B (M.P. 36); Helby *et al.*, fig. 15L.

Previous Australian usage

Bulbosia tithonica – Ott (1970, pl. 7, figs 10, 11).
Gen. et sp. indet. A – (Parker, 1986, p. 191, pl. 44, fig. 3).
M.P. 36 – Helby.

Description. A species of *Tringadinium* which is rounded subpolygonal in outline, and with a pronounced paracingular constriction. The hypocyst is significantly larger in length and width than the epicyst. Autophragm extremely variable; it may be smooth, microreticulate, or surmounted by low relief ornamentation. The microreticulation, where developed, is normally sparse and the fenestrae are irregularly distributed; the fenestrae are 0.5 to 1µm in diameter. Where present, the positive ornamentation varies in height and density, and it is possible for individual specimens to exhibit more than one ornament type. Individual elements of the ornamentation normally are between 0.5 and 1µm, although rarely they may attain up to 2µm in height. The autophragm may be scabrate, granulate or, rarely, tuberculate and is extended into prominent intratabular rounded inflations or protuberances in the apical, precingular, postcingular and antapical paraplate series. These protuberances are usually wider and higher on the hypocyst than on the epicyst and are distally flat to rounded. The inflations on the apical paraplate series are extremely low in relief. Each protuberance normally has a subcircular to subquadrangular ridge or rim in a distal position. The rims are low and may be surmounted by low relief ornamentation, typically denticles, tubercles or pila up to 1µm long. Some coalescence of this ornament may occur, giving rise to continuous,

Fig. 11. Tringadinium bjaerkei sp. nov. All are paratypes from the *W. spectabilis* Zone, from sidewall cores in Arunta-1 well at 2135.00m (Figs D, H, L) and Taltarni-1 well at 2950.00m (Figs A-C, E-G, I-K, M-T). All photomicrographs taken using plain transmitted light. Scale bar in Fig. T refers to all photomicrographs and is 25µm. Note rounded subpolygonal outline, relatively large hypocyst, prominent intratabular rounded inflations/protuberances with their subcircular/subquadrangular rims and variable ornamentation on autophragm. A-C - CPC 35580, paratype; lateral view, high to low focus sequence. Note subquadrangular rims on intratabular protuberances and irregular granulate ornamentation. D, H, L - CPC 35581, paratype; lateral view, high to low focus sequence. Note subcircular rims on intratabular protuberances and apical archaeopyle. E-G - CPC 35582, paratype; ventral view, high to low focus sequence. Note granulate ornamentation. I-K - CPC 35583, paratype; slightly oblique ventral view, high to low focus sequence. Elongate form; rims on the intratabular protuberances are correspondingly ellipsoidal. Note paired antapical intratabular protuberances (continued opposite)

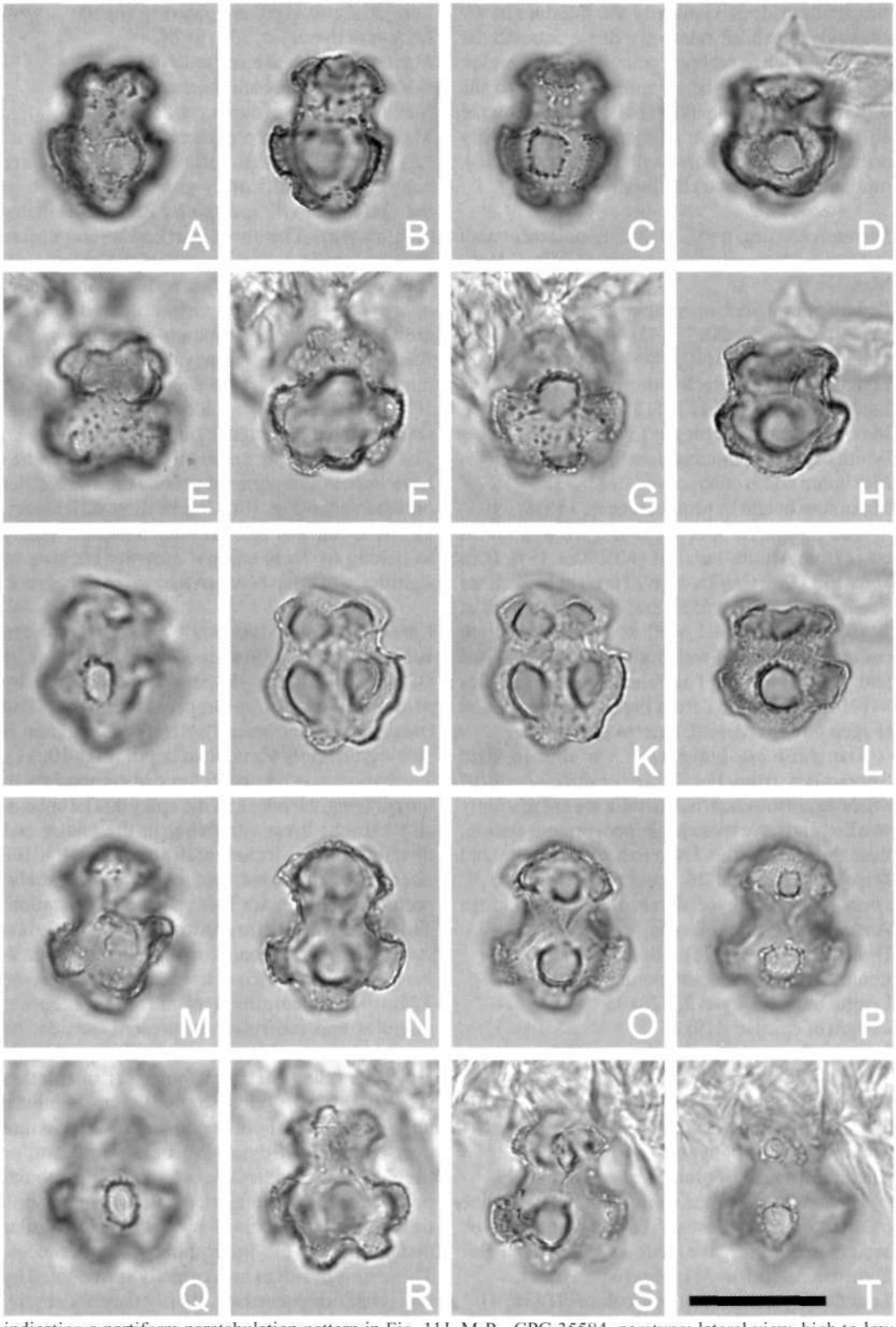

indicating a partiform paratabulation pattern in Fig. 11J. M-P - CPC 35584, paratype; lateral view, high to low focus sequence. Note deeply-incised paracingulum and that archaeopyle has not developed. Q-T - CPC 35585, paratype; dorsal view, high to low focus sequence. Note deeply-incised paracingulum.

subcircular ridges. Generally the interiors of the rims/ridges exhibit relatively dense intratabular ornament such as scabrae, granules and tubercles. The hypocyst may be asymmetrical due to the differing sizes of the intratabular inflation on the antapical paraplates. This species is slightly primarily flattened dorsoventrally and the wide, midventral parasulcus is slightly indented.

Dimensions (µm, n=62, including ornament and/or protuberances where appropriate): Min. (Mean) Max.
Length of cyst, incl. operculum: 25 (33) 41
Length of loisthocyst: 23 (32) 40
Length of epicyst: 6 (10) 18
Length of cyst at paracingulum: 3 (6) 10
Length of hypocyst: 11 (17) 25
Maximum width of epicyst: 15 (23) 34
Width of cyst at paracingulum: 12 (20) 32
Maximum width of hypocyst: 21 (28) 38
Maximum height of protuberances: 3 (5) 9

The measured specimens are from sidewall cores from Arunta-1 well at 1805.00m, 1919.00m and 2135.00m; Challis-11 ST1 well at 1552.50m; Sandpiper-1 well at 658.38m; Serrurier-1 well at 1440.00m; Taltarni-1 well at 2950.00m; ditch cuttings from Peak-1 well from between 1493.54m and 1496.59m and Tithonian outcrop samples 81FH05 and 81FH11 from the Lelinta Formation (Fageo Group) Misool, eastern Indonesia.

Tringadinium bjaerkei is variable in size. Specimens from the *W. spectabilis* Zone of offshore north-western Australia are significantly smaller, and have more prominent ornamentation, than those from the Tithonian of Australia and Misool, Indonesia. 26 specimens from the *W. spectabilis* Zone of offshore north-western Australia gave the following data:
Dimensions, (µm n=26): Min. (Mean) Max.
Length of cyst incl. operculum: 25 (30) 33
Length of loisthocyst: 23 (28) 35
Length of epicyst: 6 (9) 14
Length of cyst at paracingulum: 4 (6) 8
Length of hypocyst: 11 (15) 20
Maximum width of epicyst: 16 (20) 23
Width of cyst at paracingulum: 12 (17) 22
Maximum width of hypocyst: 21 (25) 30
Maximum height of protuberances: 3 (4.5) 7

By contrast, 36 specimens from the Tithonian of offshore north-western Australia and Misool, eastern Indonesia, gave the following size ranges:
Dimensions, (µm n=36): Min. (Mean) Max.
Length of cyst including operculum: 31 (36) 41
Length of loisthocyst: 29 (34) 40
Length of epicyst: 7 (11) 18
Length of cyst at paracingulum: 3 (6) 10
Length of hypocyst: 15 (19) 25
Maximum width of epicyst: 18 (24) 34
Width of cyst at paracingulum: 14 (22) 32
Maximum width of hypocyst: 25 (31) 38
Maximum height of protuberances: 3 (5) 9

The sizes of the Tithonian material are consistently significantly greater than those of the Oxfordian (*W. spectabilis* Zone) specimens (see above). The most marked average size differences are in the lengths of the entire cyst, the length of the loisthocyst and the width of the hypocyst. The size differences observed between the Oxfordian and Tithonian of north-western Australia and Indonesia may represent a potential morphostratigraphical lineage (Monteil, 1990; 1991). Furthermore, the older, Oxfordian material tends to have a granulate autophragm (Fig. 11). The Tithonian specimens, by contrast, tend to have smooth autophragms outside the intratabular protuberances (Fig. 10). Despite these differences, all the specimens are considered unequivocally to belong to *Tringadinium bjaerkei* because of significant overlap between the two morphotypes.

Comments. *Tringadinium bjaerkei* is rounded subpolygonal in outline. Frequently it is subhexagonal, the shape being distorted by prominent intratabular protuberances. The constriction at the apically offset paracingulum is also significantly variable in depth (Figs 10, 11). The hypocyst is relatively large in comparison to the paracingular area and the epicyst. The species also exhibits great variability in the nature and distribution of ornamentation. Typically, the interiors of the distal rims on each intratabular protuberance contain low relief ornamentation. This feature is similar to the penitabular/intratabular ornamentational distribution in *T. comptum* sp. nov. (see below). However, in some Tithonian specimens, nontabular scabrae, granules and tubercles are present outside the intratabular areas. These are normally significantly less dense than the intratabular ornamentation (Fig. 10). Most Oxfordian specimens exhibit a uniform density of ornamentation over the entire cyst (Fig. 11). Some may be smooth and/or irregularly microreticulate outside the intratabular protuberences. The majority of the ornamentation lies inside the subcircular to subquadrangular distal rims on the intratabular protuberances. These rims or ridges are normally surmounted by low relief ornamentation. Rarely they are absent, their positions indicated only by vague rings of intratabular granules. The two antapical

protuberances may be equal in size (Figs 10Q-S); however, frequently one is significantly larger than the other (Figs 10E-H).

Comparison. Tringadinium bjaerkei differs from *T. comptum* sp. nov. in the consistent occurrence of prominent intratabular protuberances/ inflations. The intratabular features, together with the size and shape, make *T. bjaerkei* significantly similar in appearance to the Early-Mid Jurassic taxon *Susadinium scrofoides* Dörhöfer & Davies 1980. However, *S. scrofoides*, and the other members of the *Parvocysta* suite (Riding, 1984) have a different paratabulation pattern and single paraplate anterior intercalary, type I, archaeopyles. *Susadinium scrofoides* has five apical, three anterior intercalary, seven precingular, seven paracingular and five postcingular paraplates (Bjaerke, 1980; Evitt, 1985, fig. 12.3; Below, 1987a). The involvement of the apical paraplates in the archaeopyle and the intratabular protuberances make *Susadinium? australis* Riding & Helby (this volume) similar in overall appearance to *T. bjaerkei.* However, the paratabulation pattern of *S? australis* conforms to that of *Susadinium* (see above) and *S? australis* lacks the smaller ornamentational features which are typical of *T. bjaerkei.* Furthermore, *S? australis* appears to have a combination (apical and anterior intercalary) archaeopyle.

Derivation of name. In honour of Dr. Tor Bjaerke.

Holotype and type locality. Figures 10Q-S, CPC 35578, Sandpiper-1 well, sidewall core sample at 658.38m.

Stratigraphical distribution. Tringadinium bjaerkei ranges from the Callovian, lower *Rigaudella aemula* Zone (7aiibi) to the Tithonian-Berriasian, *Pseudoceratium iehiense* Zone (4ci) on the North West Shelf of Australia (Foster, this volume; Helby & Partridge, in prep.). It has also been recorded from the Tithonian Lelinta Formation (Fageo Group) of Misool, eastern Indonesia (Helby & Hasibuan, 1988). In New Zealand, it is recorded from the Kimmeridgian Waikutakuta Siltstone to the Tithonian Puti Siltstone (Helby *et al.*, 1988).

Tringadinium comptum sp. nov. (Figs 12A-T)

1988 Gen. et sp. nov. G (M.P. 618D); Helby *et al.*, fig. 3F,G

Previous Australian usage
M.P. 618D – Helby.

Description. A species of *Tringadinium* that is rounded subtriangular in outline; a deep equatorial constriction in the paracingular area is commonly developed, imparting an hour-glass shape to the cyst. The hypocyst is relatively large and the paracingulum, by contrast, is prominent. The epicyst, however, is relatively small. The autophragm is microgranulate, scabrate and may also be irregularly microreticulate. Fenestrae, where developed, are subcircular to ellipsoidal and 0.5-1µm in diameter. The autophragm is further surmounted by ornament of low relief, which may be bacula, clava, large granules, pila or tubercles. Sculptural elements are mainly intratabular, although some appear to be penitabular. These ornamentational elements are highly variable in form, density and arrangement, but they typically comprise penitabular tubercles and/or clava. Some of the postcingular and antapical paraplates may have circular arrangements of ornamentation in penitabular areas. In forms where the ornamentation is densely inserted, there may be some coalescence of the elements. The ornamentation is usually longest and densest on the hypocyst. A slight medial concavity and/or break in ornament may be developed at the antapex, reflecting a partiform gonyaulacalean paratabulation pattern. The cyst is slightly primarily dorsoventrally flattened and the wide, midventral parasulcus is slightly indented.

Dimensions (µm n=54 including ornament where appropriate): Min. (Mean) Max.
Length of cyst including operculum: 23 (30) 40
Length of loisthocyst: 22 (29) 37
Length of epicyst: 5 (7) 11
Length of cyst at paracingulum: 5 (7) 11
Length of hypocyst: 10 (15) 20
Maximum width of epicyst: 15 (19) 27
Width of cyst at paracingulum: 11 (16) 24
Maximum width of hypocyst: 19 (24) 31
Length of ornamentational elements: 1 (1.5) 3

The measured specimens are from sidewall cores from Arunta-1 well at 2135.00m; Challis-11 ST1 well at 1552.50m; Challis-11 ST2 well at 1670.70m and 1842.00m and Taltarni-1 well at 2950.00m.

Marked differences in the development of the paracingular constriction were observed. For example, at 1670.70m in Challis-11 ST2 well, the specimens had consistently weakly developed equatorial concavities (Figs 12N-O, T). At this

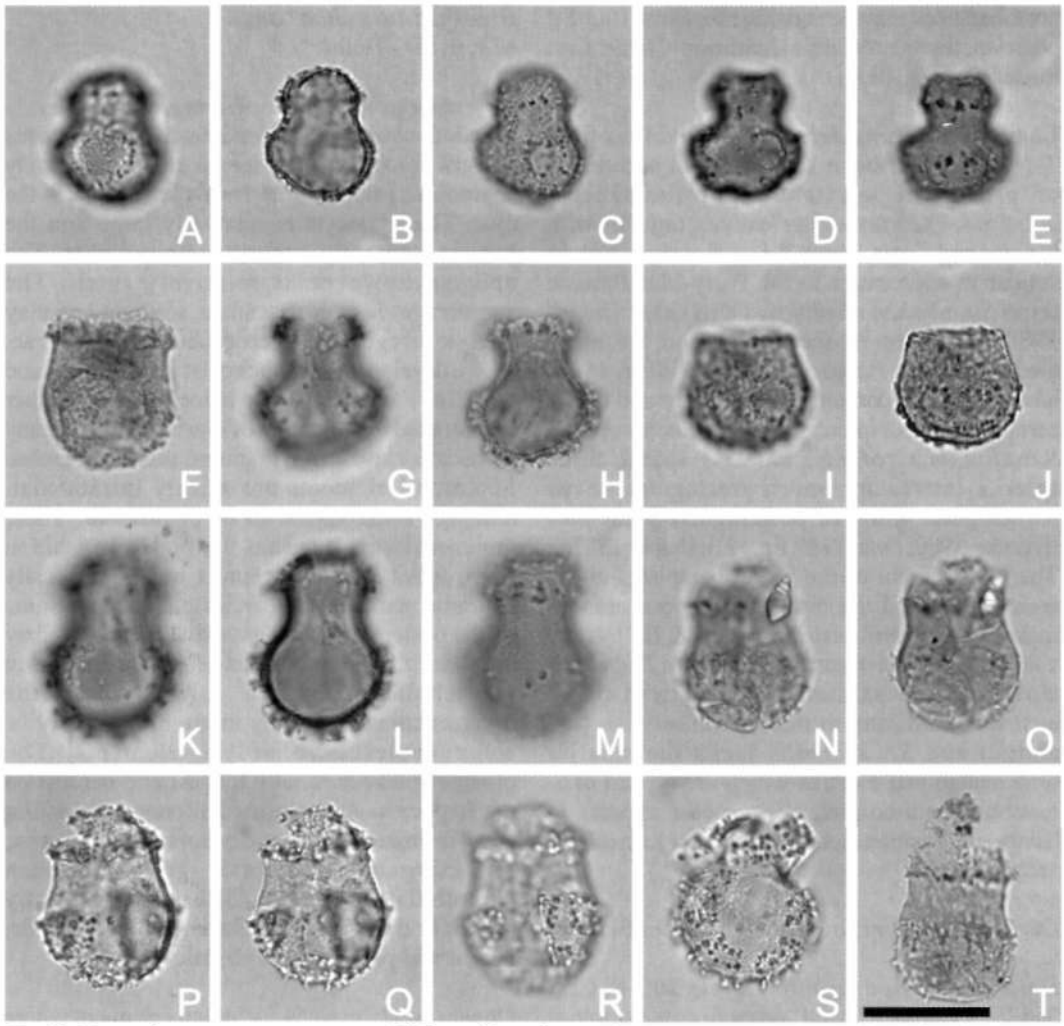

Fig.12. Tringadinium comptum sp. nov. All from sidewall cores in Arunta-1 well at 2135.00m (Figs 12D-E, I-J), Challis-11 ST1 well at 1552.50m (Figs 12P-R), Challis-11 ST2 at 1670.70m (Figs 12N-O, T) and 1842.00m (Figs 12F-H, K-M), and Taltarni-1 well at 2950.00m (Figs 12A-C). All photomicrographs taken using plain transmitted light. Scale bar in Fig. 12T refers to all photomicrographs and is 25µm. Figs 12P-R are the holotype; the remainder, paratypes. Note rounded subtriangular outline, relatively large hypocyst, normally deeply indented, prominent paracingulum, microreticulate autophragm which normally has penitabular ornamentation, and apical archaeopyle. A-C - CPC 35586, paratype; ventral view, high to low focus sequence. Small specimen with adherent operculum. D, E - CPC 35587, paratype; ventral view, high/median and low focus respectively. Note deeply incised paracingular region, relatively small overall size and apical archaeopyle. F - CPC 35588, paratype; ventral view, median focus. Note lack of significant paracingular incision. G, H - CPC 35589, paratype; ventral view, high and low focus respectively. Note prominent ornamentation, especially on hypocyst. I, J - CPC 35590, paratype; ventral view, high and low focus respectively. Note lack of incised paracingulum. K-M - CPC 35591, paratype; ventral view, high to low focus sequence. Note hour-glass shape and prominent, largely penitabular ornamentation. N, O - CPC 35592, paratype; dorsal view, high/median and low focus respectively. Note lack of ornamentation in paracingular area and apical archaeopyle. P-R - CPC 35593, holotype; dorsal view, median to low focus sequence. Note prominent, unornamented paracingulum and parasulcus, penitabular arrangement of ornamentation and apical archaeopyle. S - CPC 35594, paratype; slightly oblique dorsal view, a composite photomicrograph. Note clear penitabular arrangement of ornament on hypocyst. T - CPC 35595, paratype; dorsal view, median focus. Elongate specimen; note prominent paracingulum and adherent operculum.

horizon, the average width of the cyst at the paracingulum was 18µm. By contrast, in the remainder of the samples studied, the average paracingular width was 15µm.

Comments. The epicyst and paracingulum are approximately as long as the remainder of the cyst (see *Dimensions* above). Both the precingular and apical paraplate series are relatively short in height. On average, the epicyst is only 23% of the overall cyst length. The low, nearly flat, operculum is normally free, but specimens with attached opercula have been observed (e.g. Figs 12A-C, N-R, T). An equatorial constriction may be entirely absent or extremely deep with all intermediate conditions between these extremes (Fig. 12). This constriction is at the paracingulum, which is relatively long and a distinctive feature of this species. It is possible that post-depositional flattening of the cyst affects the depth of the equatorial constriction. For example, it was noted that specimens which have been post diagenetically flattened tend to have more strongly developed 'waists'. The parasulcus is relatively wide and expands markedly antapically (Figs 12P-R). This is typical of the partiform paratabulation style. The cyst is widest across the postcingular paraplate series (Fig. 12).

The ornamentation of the species is also highly variable and comprises penitabular or penitabular/intratabular elements, which may attain 3µm in length. In the majority of forms, the paratabulation is indicated by penitabular and/or intratabular tubercles and/or clava. Different ornamentational elements may be present on a single specimen, for example forms with bacula, clava and tubercles have been observed. Furthermore, the density and position of the ornamentation is highly variable from extremely sparse to relatively dense and from strictly penitabular to virtually nontabular (Fig. 12). Some coalescence of the ornamentation may occur, giving rise to crest-like features, especially in median view. The general variability of the penitabular nature of the ornamentation means that there is a marked variability in the development of the paratabulation (Fig. 12). Thus, the slight medial concavity and/or break in ornament at the antapex may represent the 1''''/2'''' parasuture. The autophragmal fenestrae vary in the density within the specimens studied. Occasionally, the fenestrae may be arranged in lineations, which may be parasutural or penitabular.

Comparison. *Tringadinium comptum* differs from *T. bjaerkei* in lacking intratabular inflations or protuberances and having a rounded subtriangular outline. This species also resembles *Woodinia bensonii* sp. nov. and *Woodinia pedis* Riding & Helby (this volume). However, *T. comptum* lacks the extremely elongate postcingular paraplates and intratabular 'pads' of differentiated autophragm which characterise *Woodinia*. The size and shape of *Tringadinium comptum* are similar to many members of the Early-earliest Mid Jurassic *Parvocysta* 'complex' of Riding (1984). The most similar species being *Susadinium faustum* (Bjaerke 1980) Lentin & Williams 1985, with its intratabular bacula (Bjaerke, 1980). The *Parvocysta* 'complex', however, all have anterior intercalary archaeopyles (Riding *et al.*, 1991).

Derivation of name. From the Latin *comptus* meaning ornamented and referring to the low-relief ornamentation elements, which characterise this form.

Holotype and type locality. Figures 12P-R, CPC 35593, Challis-11 ST1 well, sidewall core sample at 1552.50m.

Stratigraphical distribution. *Tringadinium comptum* ranges from the Callovian, lower *Rigaudella aemula* Zone (7aiib) to the Oxfordian, mid *Wanaea spectabilis* Zone (6cii) in the Timor Sea region (Foster, this volume; Helby & Partridge, in prep.). In New Zealand, this species has been recorded from the Callovian to Oxfordian Oraka Sandstone (Helby *et al.*, 1988, fig. 23).

Woodinia Riding & Helby this volume

Type species. *Woodinia pedis* Riding & Helby this volume

Woodinia bensonii sp. nov. (Figs 13A-T)

1988 Gen. et sp. indet. AO (M.P. 618R); Helby *et al.*, fig. 5D.
1996 *Dissimulidinium lobispinosum auct. non* May *et al.* 1987; Burger, pl. 5, fig DD.

Previous Australian usage
M.P. 618 (triangular) – Helby.
M.P. 618R – Helby.
Taltarnia spp. – Morgan.

Description. A rounded subtriangular species of *Woodinia* with two lateral antapical protuberances which often give rise to a prominent antapical concavity. The cyst normally tapers gently

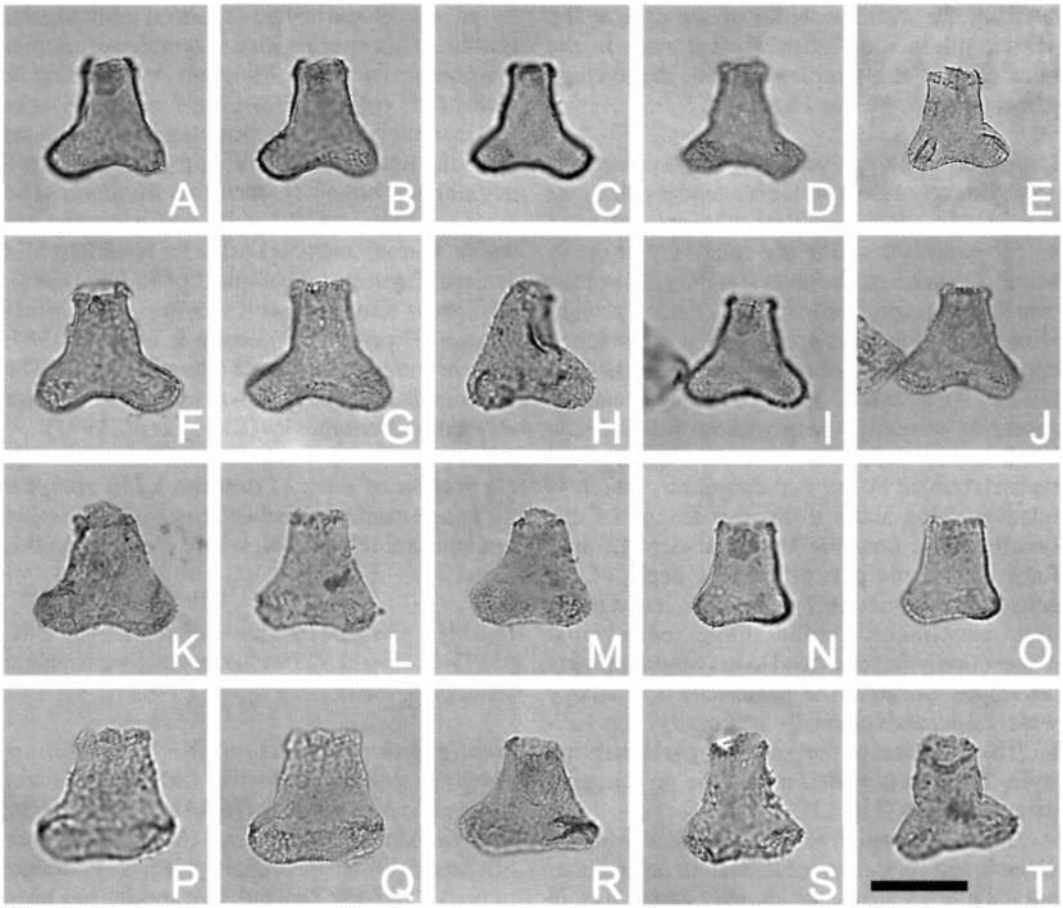

Fig. 13. Woodinia bensonii sp. nov. Specimens from sidewall cores from Arunta-1 well at 1805.00m (Figs 13H, K-M, P-R, T) and 1991.00m (Fig. 13S), Challis-11 ST2 well at 1670.70m (Figs 13N-O) and Taltarni-1 well at 2950.00m (Figs 13A-G, I-J). All photomicrographs taken using plain transmitted light. Scale bar in Fig. 13T refers to all photomicrographs and is 25µm. Figs 13A-B are the holotype, and the remainder, paratypes. Note rounded subtriangular outline with two lateral antapical protuberances and intervening antapical concavity, apical archaeopyle and intratabular areas of low-relief ornamentation. A, B - CPC 35596, holotype; ventral view, high and low focus respectively. Note prominent antapical concavity and apical archaeopyle with adherent operculum which has been folded back down into loisthocyst. C, D - CPC 35597, paratype; dorsal view, high and low focus respectively. Note apical archaeopyle and low-relief ornamentation on prominent lateral antapical protuberances. E - CPC 35598, paratype; dorsal view, high focus. Note high paracingulum which is located high on the cyst as a result of extremely high postcingular paraplate series. F - CPC 35599, paratype; dorsal view, low focus. Squat form with especially prominent antapical concavity. G - CPC 35600, paratype; dorsal view, low focus. This specimen is extremely wide antapically and tapers dramatically apically. Note small 'pads' of differentiated autophragm in precingular paraplate series, close to principal archaeopyle suture. H - CPC 35601, paratype; ventral view, high focus. Note archaeopyle has not formed. I, J - CPC 35602, paratype; ventral view, high/median and low focus respectively. Note operculum has been folded into the loisthocyst. K - CPC 35603, paratype; dorsal view, median focus. Note operculum of apical archaeopyle is still attached ventrally. L - CPC 35604, paratype; dorsal view, median focus. Note small quadrangular 'pads' of differentiated autophragm in precingular paraplate series. M - CPC 35605, paratype; ventral view, median focus. Note adherent operculum and small antapical concavity. N, O - CPC 35606, paratype; dorsal view, median and low focus respectively. A well preserved specimen, narrow antapically with prominent attached operculum within loisthocyst. P, Q - CPC 35607, paratype; dorsal view, high and low focus respectively. Note angular principal archaeopyle suture and flat antapical margin. R - CPC 35608, paratype; ventral view, median focus. Note attached operculum inside loisthocyst and flat antapical margin. S - CPC 35609, paratype; ventral view, median focus. Elongate specimen with prominent paracingulum. T - CPC 35610, paratype; dorsal view, high focus. Small specimen with slight antapical concavity.

apically. Autophragm microreticulate, scabrate or granulate. Intratabular areas of low relief ornamentation are variably developed. In some specimens, extremely low relief ornamentation is present in the apical paraplate series. In the short precingular paraplate series, the intratabular ornamentation comprises subrectangular areas ('pads') of differentiated autophragm comprising dense, short, solid processes which may be interconnected by trabeculae. These subrectangular 'pads' of ornamentation occur close to the principal archaeopyle suture, i.e. near to the apex of the cyst. The elongate postcingular paraplate series may also have areas of differentiated autophragm developed. However, most specimens lack positive ornamentation in this area and short, simple, slender, solid spines may occur, somewhat sparsely and irregularly, in the equatorial region of the cyst, i.e. posterior of the paracingulum. The antapical paraplates are characterised by a subcircular or irregularly shaped cover of short processes in the intratabular areas. The style of ornamentation is similar to that developed within the precingular paraplates, i.e. comprising densely inserted short filaments or processes. However, the density of elements is normally markedly less on the antapical paraplates. These elements may coalesce distally, thereby frequently producing a raised reticulum. The paracingulum and the centre of the antapical area are devoid of positive ornamentation, but may be scabrate or granulate. The paracingulum may be indented. A narrow midventral indented area may be present and represents the parasulcus. The operculum is relatively flat to slightly domed and is frequently attached ventrally and folded back inside the epicyst.

Dimensions (μm n=35): Min. (Mean) Max.
Length of cyst body incl. operculum: 29 (36) 44
Length of cyst body excl. operculum: 28 (33) 38
Width of cyst body at antapex: 25 (33) 44
Width of cyst body at equator: 13 (18) 25
Width of cyst body at apex: 11 (15) 22
Length of ornamentation: <0.5 (1) 2

The measured specimens are from sidewall cores from Arunta-1 well at 1805.00m, 1919.00m and 2135.00m; Challis-11 ST-2 well at 1670.70m; Eclipse-1 well at 2477.00m and Taltarni-1 well at 2950.00m.

Comments. *Woodinia bensonii* is characterised by its rounded subtriangular dorsoventral outline and an often well developed antapical concavity (Fig. 13). The overall length of the cyst is normally close to the maximum width (see *Dimensions*, above). The length and shape of the lateral antapical protuberances are variable (Fig. 13). The consistent presence of regular subrectangular areas ('pads') of differentiated autophragm in intratabular precingular positions, close to the apical series is also diagnostic. These relatively small 'pads' commonly form an interrupted ring around the principal archaeopyle suture. This is the only area where the intratabular ornamentation is consistent and regular. The elongate postcingular paraplates are normally surmounted by relatively sparsely occurring short, slender, simple processes equatorially. Differentiated autophragm is also present on the paired antapical paraplates. This ornamentation is often less dense than that developed on the precingular paraplates and frequently has a microreticulate appearance (Fig. 13). The antapical ornamentation may coalesce extensively. It is typically concentrated on the distal parts of the lateral antapical lobes and the central antapical area, close to the 1''''/2'''' paraplate junction and is normally devoid of positive ornamentation (Fig. 13). Individual elements of ornamentation at the antapical region may be relatively variable in thickness.

Some significant variation in terms of the development of the antapical concavity was observed. Specimens from Taltarni-1 well at 2950.00m are relatively wide antapically, with a consistent prominent antapical concavity (Figs 13A-G, I-J). Material from Arunta-1 well between 1805.00m and 2135.00m and Challis-11 ST2 well at 1670.70m, however, includes relatively high proportions of specimens which lack a marked antapical concavity (e.g. Figs 13M-S).

Comparison. *Woodinia pedis* is subrectangular and distinctly flask-shaped, lacking the prominent, large lateral antapical protuberances and the antapical concavity of *Woodinia bensonii*. The former species also has thicker and more regular intratabular ornamentation, particularly prominent 'pads' of differentiated autophragm in the postcingular paraplate series immediately posterior of the paracingulum. Furthermore, the antapical ornamentation of *Woodinia pedis* is more prominent than that in *W. bensonii* and is normally contiguous, forming a skirt-like flange to the antapex. Some forms of *Woodinia bensonii* may be superficially similar in outline to representatives of the Late Cretaceous-Palaeogene acritarch genus *Paucilobimorpha* de Coninck 1986; for example *Paucilobimorpha triradiata* de Coninck 1986. However, this genus

of small acritarchs lacks any indications of paratabulation and an archaeopyle.

Derivation of name. Named for Dr. Don G. Benson

Holotype and type locality. Figures 13A-B, CPC 35596, Taltarni-1 well, sidewall core sample at 2950.00m.

Stratigraphical distribution. A notable acme of *Woodinia bensonii* distinguishes the Oxfordian, upper part of the mid *Wanaea spectabilis* Zone (6ciia) in wells in the Montara Field and the adjacent Vulcan Subbasin. Rare occurrences are recorded in the lower part of the upper *Wanaea spectabilis* Zone (6cib) and the species occurs consistently and is intermittently prominent through the remainder of the *Wanaea spectabilis* Zone (subzones 6ciiib-6ciia) (Foster, this volume; Helby & Partridge, in prep.).

ACKNOWLEDGEMENTS

The authors are grateful to Dr Clinton B. Foster (AGSO, Canberra) for promoting and facilitating this work and for his editorial guidance and advice. Mr Eddie Resiak of the core and cuttings repository at AGSO, Canberra, courteously provided access to sample material. Invaluable technical support, largely sample preparations and manipulation of digital images was provided by Christian Thun and Andrew Kelman (AGSO, Canberra). Laola Pty. Ltd. (Perth) gave support in their diligent and careful treatment of key samples in the preparatory process. Arco Australia Ltd., BHP Petroleum Pty. Ltd and Esso Australia Ltd. kindly provided sample material on request. Dr Fauzie Hasibuan of the Geological Research and Development Center, Bandung, Indonesia supplied the sample material from Misool, eastern Indonesia. Ms Lindell Emerton (AGSO, Canberra) skilfully drafted Figs 2 and 6. Drs R. A. Fensome and N. E. Poulsen are thanked for reviewing the manuscript. J. B. Riding publishes with the permission of the Chief Executive Officer, AGSO.

REFERENCES

ARKELL, W.J., 1956. *Jurassic geology of the World*. Oliver & Boyd, Edinburgh, 806 p.

BACKHOUSE, J., 1988. Late Jurassic and Early Cretaceous palynology of the Perth Basin, Western Australia. *Geological Survey of Western Australia Bulletin 135*, 233 p.

BALME, B.E., 1957. Spores and pollen grains from the Mesozoic of Western Australia. *Commonwealth Scientific and Industrial Research Organisation of Australia, Coal Research Section, T.C. 25*, 1-48.

BATTEN, D.J. & LISTER, J.K., 1988. Early Cretaceous dinoflagellate cysts and chlorococcalean algae from freshwater and low salinity palynofacies in the English Wealden. *Cretaceous Research 9*, 337-367.

BELOW, R., 1987a. Evolution und Systematik von Dinoflagellaten-Zysten aus der Ordnung Peridiniales. I. Allgemeine Grundlagen und Subfamilie Rhaetogonyaulacoideae (Familie Peridiniaceae). *Palaeontographica Abteilung B 205*, 1-164.

BELOW, R., 1987b. Evolution und Systematik von Dinoflagellaten-Zysten aus der Ordnung Peridiniales. II. Cladopyxiaceae und Valvaeodiniaceae. *Palaeontographica Abteilung B 206*. 1-115.

BJAERKE, T., 1980. Mesozoic palynology of Svalbard IV. Toarcian dinoflagellates from Spitsbergen. *Palynology 4*, 57-77.

BRENNER, W., 1988. Dinoflagellaten aus dem Unteren Malm (Oberer Jura) von Süddeutschland; Morphologie, Ökologie, Stratigraphie. *Tübinger Mikropaläontologische Mitteilungen Nr.6*. 115 p.

BURGER, D., 1980. Palynological studies in the Lower Cretaceous of the Surat Basin, Australia. *Bureau of Mineral Resources, Geology and Geophysics Bulletin 189*, 106 p.

BURGER, D., 1995. Australian Phanerozoic Timescales: 8 Jurassic. Geochronological charts and explanatory notes. Second edition. *Australian Geological Survey Organisation Record 1995/37*, 30 p.

BURGER, D., 1996. Mesozoic palynomorphs from the North West Shelf, offshore Western Australia. *Palynology 20*, 49-103.

CHEN, Y., 1982. Recognition of the dinocyst genus *Komewuia*, with assignable species from Madagascar. *Micropaleontology 28*, 31-42.

COOKSON, I.C. & EISENACK, A., 1960. Upper Mesozoic microplankton from Australia and New Guinea. *Palaeontology 2*, 243-261.

COOKSON, I.C. & EISENACK, A., 1962a. Additional microplankton from Australian Cretaceous sediments. *Micropaleontology 8*, 485-507.

COOKSON, I.C. & EISENACK, A., 1962b. Some Cretaceous and Tertiary microfossils from Western Australia. *Proceedings of the Royal Society of Victoria 75*, 269-273.

COOKSON, I.C. & EISENACK, A., 1974. Mikroplankton aus australischen mesozoischen und tertiären Sedimenten. *Palaeontographica Abteilung B 148*, 44-93.

DAVEY, R.J., 1987. Palynological zonation of the Lower Cretaceous, Upper and uppermost Middle Jurassic in the northwestern Papuan Basin of Papua New Guinea. *Geological Survey of Papua New Guinea*

Memoir 13, 77 p.

DAVEY, R.J., 1999. Revised palynological zonation for the Late Cretaceous, Early Cretaceous and Late Jurassic of Papua New Guinea. *Geological Survey of Papua New Guinea Memoir 17*, 51 p.

DODEKOVA, L., 1975. New Upper Bathonian dinoflagellate cysts from northeastern Bulgaria. *Bulgarska Akademiya na Naukite, Paleontologiya, Stratigrafiya i Litologiya 2*, 17-34.

EVITT, W.R., 1985. *Sporopollenin dinoflagellate cysts. Their morphology and interpretation*. American Association of Stratigraphic Palynologists Foundation, Dallas, 333 p.

FENSOME, R.A., TAYLOR, F.J.R., NORRIS, G., SARJEANT, W.A.S., WHARTON, D.I. & WILLIAMS, G.L., 1993. A classification of living and fossil dinoflagellates. *Micropaleontology Special Publication No. 7*, 351 p.

FOSTER, C.B., this volume. Introduction.

FRANCIS, G. & WESTERMANN, G.E.G., 1993. The Kimmeridgian problem in Papua New Guinea and other parts of the Indo-southwest Pacific. In: Carman, G.J & Carmen, Z. (eds). *Petroleum Exploration and Development in Papua New Guinea: Proceedings of the Second PNG Petroleum Convention, Port Moresby, 31st May-2nd June 1993*, 75-93.

GATEHOUSE, C.G. & COOPER, B.J., 1982. The Late Jurassic Polda Formation, Eyre Peninsula. *Geological Survey of South Australia Quarterly Geological Notes No. 81*, 13-16.

HASIBUAN, F., 1990. *Mesozoic stratigraphy and paleontology of Misool Archipelago, Indonesia*. Unpublished Ph.D. thesis, University of Auckland, 384p., 22pl.

HELBY, R. & HASIBUAN, F., 1988. A Jurassic dinoflagellate sequence from Misool, Indonesia. *7th International Palynological Congress, Brisbane, Abstracts Volume*, p. 69.

HELBY, R. MORGAN, R. & PARTRIDGE, A.D., 1987. A palynological zonation of the Australian Mesozoic. *Memoir of the Association of Australasian Palaeontologists 4*, 1-94.

HELBY, R. & PARTRIDGE, A.D., in prep. A palynological zonation of the Australian Mesozoic: an update.

HELBY, R., WILSON, G.J. & GRANT-MACKIE, J.A., 1988. A preliminary biostratigraphic study of Mid to Late Jurassic dinoflagellate assemblages from Kawhia, New Zealand. *Memoir of the Association of Australasian Palaeontologists 5*, 125-166.

KLEMENT, K., 1960. Dinoflagellaten und Hystrichosphaerideen aus dem unteren und mittleren Malm Südwestdeutschlands. *Palaeontographica Abteilung A 114*, 1-104.

MARTÍNEZ, M.A., QUATTROCCHIO, M. & SARJEANT, W.A.S., 1999. *Jansonia psilata* n. sp., a Middle Jurassic dinoflagellate from the Neuquén Basin, Argentina. *Revista Española de Micropaleontología 31*, 255-263.

MONTEIL, E., 1990. Revision and emendation of dinocyst genus *Amphorula* Dodekova 1969. The concept of morphostratigraphy. *Bulletin des Centres de Recherches Exploration-Production Elf-Aquitaine 14*, 597-609.

MONTEIL, E., 1991. Morphology and systematics of the ceratioid group: a new morphographic approach. Revision and emendation of the genus *Muderongia* Cookson and Eisenack 1958. *Bulletin des Centres de Recherches Exploration-Production Elf-Aquitaine 15*, 461-505.

MORGAN, R., 1975. Some Early Cretaceous organic-walled microplankton from the Great Australian Basin, Australia. *Journal and Proceedings of the Royal Society of New South Wales 108*, 157-167.

MORGAN, R., 1980. Palynostratigraphy of the Australian Early and Middle Cretaceous. *Memoirs of the Geological Survey of New South Wales, Palaeontology No. 18*, 153 p.

NORVICK, M.S., 1973. The microplankton genus *Disphaeria* Cookson and Eisenack emend. *Bureau of Mineral Resources, Geology and Geophysics, Bulletin 140*, 45-46.

OTT, H.L., 1970. Palynological zonation of the Carnarvon Basin Jurassic-Miocene sequence. *Unpublished WAPET report*, 1-52.

PARKER, F.M., 1986. *Late Jurassic palynology of the Dampier Sub-Basin, Carnarvon Basin, Western Australia*. Unpublished PhD thesis, University of Western Australia, 2 Vols.

POCOCK, S.A.J., 1972. Palynology of the Jurassic sediments of Western Canada. Part 2. Marine species. *Palaeontographica Abteilung B 137*, 85-153.

RAUSCHER, R. & SCHMITT J.-P., 1990. Recherches palynologiques dans le Jurassique d'Alsace (France). *Review of Palaeobotany and Palynology 62*, 107-156.

RIDING, J.B., 1984. A palynological investigation of Toarcian to early Aalenian strata from the Blea Wyke area, Ravenscar, North Yorkshire. *Proceedings of the Yorkshire Geological Society 45*, 109-122.

RIDING, J.B. & HELBY, R., this volume. Microplankton from the Mid Jurassic (late Callovian) *Rigaudella aemula* Zone in the Timor Sea, north-western Australia.

RIDING, J.B. & THOMAS, J.E., 1988. Dinoflagellate cyst stratigraphy of the Kimmeridge Clay (Upper Jurassic) from the Dorset coast, southern England. *Palynology 12*, 65-88.

RIDING, J.B., WALTON, W. & SHAW, D., 1991. Toarcian to Bathonian (Jurassic) palynology of the Inner Hebrides, northwest Scotland. *Palynology 15*, 115-179.

SARJEANT, W.A.S., 1961. Microplankton from the Kellaways Rock and Oxford Clay of Yorkshire. *Palaeontology 4*, 90-118.

SARJEANT, W.A.S., LACALLI, T. & GAINES, G., 1987. The cysts and skeletal elements of dinoflagellates: speculations on the ecological causes for their morphology and development. *Micropaleontology 33*, 1-36.

SCHIØLER, P., 1993. New species of dinoflagellate cysts from Maastrichtian-Danian chalks of the Danish North Sea. *Journal of Micropalaeontology 12*, 99-112.

SLIMANI, H., 1994. Les dinokystes des Craies du Campanien au Danien a Halembaye, Turnhout (Belgique) et a Beutenaken (Pays-Bas). *Mémoires pour servir à l'Explication des Cartes Géologiques et Minières de la Belgique No. 37*, 173 p.

STANCLIFFE, R.P.W. & SARJEANT, W.A.S., 1990. The complex chorate dinoflagellate cysts of the Bathonian to Oxfordian (Jurassic): Their taxonomy and stratigraphic significance. *Micropaleontology 36*, 197-228.

STOVER, L.E. & EVITT, W.R., 1978. Analyses of Pre-Pleistocene organic-walled dinoflagellates. *Stanford University Publications, Geological Sciences 15*, 300 p.

WILLIAMS, G.L., LENTIN, J.K. & FENSOME, R.A., 1998. The Lentin and Williams Index of fossil dinoflagellates 1998 edition. *American Association of Stratigraphic Palynologists Contributions Series No. 34*, 817 p.

WISEMAN, J.F., 1980. Palynostratigraphy near the 'Jurassic-Cretaceous Boundary' in the Carnarvon Basin, Western Australia. *Fourth International Palynological Conference, Lucknow (1976-1977) Proceedings 2*, 330-349.

APPENDIX 1: SAMPLE DETAILS

1 Locations and operators of wells from which material has been studied

Well Name and Number	Latitude	Longitude	Operator
Arunta-1	11° 58' 26.58"S	124° 57' 11.06"E	BHP
Bogong-1	10° 43' 59.35"S	126° 05' 25.22"E	BHP
Challis-11 ST1 & ST2	12° 05' 51.90"S	125° 03' 20.81"E	BHP
Eclipse-1	12° 16' 12.35"S	124° 37' 12.18"E	BHP
Jabiru-2	11° 56' 00.48"S	124° 59' 24.26"E	BHP
Jabiru-3	11° 55' 27.06"S	125° 00' 36.30"E	BHP
Layang-1	10° 50' 59.70"S	126° 25' 21.50"E	BHP
Peak-1	21° 36' 16.99"S	114° 30' 21.99"E	WAPET
Polda-1	33° 31' 19.11"S	135° 19' 40.06"E	SADME*
Rowan-1ST	12° 29' 48.51"S	124° 23' 41.42"E	BHP
Sandpiper-1	13° 18' 47.99"S	127° 58' 39.00"E	Arco
Serrurier-1	21° 34' 39.54"S	114° 42' 08.84"E	Esso
Taltarni-1	12° 36' 35.56"S	124° 34' 50.76"E	BHP

*SADME – South Australian Department of Mines and Energy

Well completion reports on all the offshore wells listed are publicly available five years after completion.

2 Outcrop material from Misool, Eastern Indonesia

Sample Number	Lithostratigraphy	Age	Reference
81FH05	Lelinta Formation (Fageo Group)	Tithonian	Hasibuan (1990)
81FH11	Lelinta Formation (Fageo Group)	Tithonian	Hasibuan (1990)

APPENDIX 2: REGISTER OF FIGURED SPECIMENS

All palynomorph specimens figured in this paper are listed here, together with essential details. The specimens are all curated in the Commonwealth Palaeontological Collection (CPC) of the Australian Geological Survey Organisation, Canberra. The dinoflagellate cyst genera and species are listed alphabetically and the location of the specimens on the microscope slides are all 'England-Finder' co-ordinates. These were taken with the slide label to the left of the observer; the microscope stage opening toward the microscope user. The coding for types is as follows: H = holotype; P = paratype; T = topotype. All specimens of new taxa examined during this study contributed to the specific concepts described. Therefore all the figured specimens, which are not holotypes are

paratypes. SGM = single grain mount. The single grain mounts do not have unique numbers; they are numbered sequentially for each species within a particular sample. The specimens are from conventional cores and sidewall cores, except for Peak-1 at 1493.54m-1496.59m, which is a sample of ditch cuttings.

Species	Type	Fig(s)	SGM/Slide No.	EF	Well (depth, m)	CPC No.
C. taltarniana	P	1A	SGM 3 (i)	H38/3	Taltarni-1 (2820.00)	35517
C. taltarniana	P	1B	SGM 4 (vi)	M35/2	Taltarni-1 (2820.00)	35518
C. taltarniana	P	1C	Sl. 3	M27/1	Taltarni-1 (2820.00)	35519
C. taltarniana	P	1D	SGM 5 (ii)	K30	Taltarni-1 (2820.00)	35520
C. taltarniana	P	1E	SGM 3 (ii)	J40/4	Taltarni-1 (2820.00)	35521
C. taltarniana	P	1F	Sl. 3	M32/3	Taltarni-1 (2820.00)	35522
C. taltarniana	P	1G	SGM 6 (iii)	O29/2	Taltarni-1 (2820.00)	35523
C. taltarniana	P	1H	SGM 4 (ii)	L34/2	Taltarni-1 (2820.00)	35524
C. taltarniana	P	1I	SGM 1 (ii)	S29/3	Taltarni-1 (2820.00)	35525
C. taltarniana	P	1J	Sl 3	Q33/1	Taltarni-1 (2820.00)	35526
C. taltarniana	P	1K	SGM 7 (iv)	O40/1	Taltarni-1 (2820.00)	35527
C. taltarniana	H	1L	Sl. 2	P15	Taltarni-1 (2820.00)	35528
F. eclipsiana	P	3A	SGM 7 (i)	H37/4	Layang-1 (3221.47)	35529
F. eclipsiana	P	3B	SGM 5 (iv)	O34/1	Layang-1 (3221.47)	35530
F. eclipsiana	P	3C	SGM 3 (i)	P29/2	Layang-1 (3221.47)	35531
F. eclipsiana	P	3D	SGM 7 (vii)	L38/1	Layang-1 (3221.47)	35532
F. eclipsiana	P	3E	SGM 5 (v)	O32	Layang-1 (3221.47)	35533
F. eclipsiana	P	3F	SGM 4 (i)	M35/3	Layang-1 (3221.47)	35534
F. eclipsiana	P	3G	SGM 2 (i)	M34/3	Layang-1 (3221.47)	35535
F. eclipsiana	P	3H	SGM 7 (iii)	J39/3	Layang-1 (3221.47)	35536
F. eclipsiana	H	3I	SGM 7 (iv)	K37	Layang-1 (3221.47)	35537
F. eclipsiana	P	3J	SGM 4 (iii)	O33	Layang-1 (3221.47)	35538
F. eclipsiana	P	3K	SGM 6 (iv)	P35/4	Layang-1 (3221.47)	35539
F. eclipsiana	P	3L	SGM 2 (iv)	N36/3	Layang-1 (3221.47)	35540
F. eclipsiana	P	3M,N	SGM 3 (ii)	P29/4	Layang-1 (3221.47)	35541
F. eclipsiana	P	3O,P	SGM 4 (ii)	N34/3	Layang-1 (3221.47)	35542
F. challisiana	H	4A	SGM 56	O35/1	Challis-11 ST1 (1552.50)	35543
F. challisiana	P	4B,C	SGM 131	Q36/1	Challis-11 ST1 (1552.50)	35544
F. challisiana	P	4D,E	SGM 22	O38/3	Rowan-1ST (3183.00)	35545
F. challisiana	P	4F	SGM 1 (v)	G36/3	Arunta-1 (1805.00)	35546
F. challisiana	P	4G,H	SGM 58	M38/2	Challis-11 ST1 (1552.50)	35547
F. challisiana	P	4I	SGM 2 (iv)	N33	Arunta-1 (1805.00)	35548
F. challisiana	P	4J,K	SGM 3 (i)	J36/1	Arunta-1 (1805.00)	35549
F. challisiana	P	4L	SGM 2 (v)	N33/4	Arunta-1 (1805.00)	35550
F. sp. cf. *tumida*		5A	Ass. sl. 1	C25/3	Polda-1 (116.43)	35551
F. sp. cf. *tumida*		5B	Ass. sl. 1	H18	Polda-1 (116.43)	35552
F. sp. cf. *tumida*		5C	Ass. sl. 1	U40	Polda-1 (116.43)	35553
M. jurassicum	P	6A-C	SGM 4 (ii)	L29	Taltarni-1 (2950.00)	35554
M. jurassicum	P	6D	SGM 4	N30	Arunta-1 (2135.00)	35555
M. jurassicum	P	6E-G	SGM 17	K35/3	Rowan-1ST (3181.00)	35556
M. jurassicum	P	6H	SGM 5	S34/3	Arunta-1 (2135.00)	35557
M. jurassicum	P	6I,J	SSM 6 (i)	O37	Taltarni-1 (2950.00)	35558
M. jurassicum	P	6K,L	SGM 6	N31/4	Rowan-1ST (3181.00)	35559
M. jurassicum	H	6M-O	SGM 1	G25	Taltarni-1 (2950.00)	35560
M. jurassicum	P	6P,T	SGM 5	K29/1	Taltarni-1 (2950.00)	35561
M. jurassicum	P	6Q-S	SGM 4	Q28/4	Jabiru-2 (1642.50)	35562

Species	Type	Fig(s)	SGM/Slide No.	EF	Well (depth, m)	CPC No.
S. geminus	P	8A,B	SGM 4 (iv)	Q30	Bogong-1 (3530.00)	35563
S. geminus	P	8C	SGM 3 (i)	J36/2	Bogong-1 (3530.00)	35564
S. geminus	H	8D-F	SGM 4 (i)	Q31	Bogong-1 (3530.00)	35565
S. geminus	P	8G,H	SGM 2 (v)	O34	Bogong-1 (3530.00)	35566
S. geminus	P	8I	SGM 4 (i)	P31	Bogong-1 (3530.00)	35567
S. geminus	P	9A-C	SGM 2 (ii)	N34/1	Bogong-1 (3530.00)	35568
S. geminus	P	9D,E	SGM 2 (i)	M34/3	Bogong-1 (3530.00)	35569
S. geminus	P	9F,I	SGM 3 (vi)	H37	Bogong-1 (3530.00)	35570
S. geminus	P	9G,H	SGM 1 (iv)	N34/1	Bogong-1 (3530.00)	35571
T. bjaerkei	P	10A-D	SGM 101 (ii)	P31/2	Misool 81FH11 (outcr.)	35572
T. bjaerkei	P	10E-H	SGM 102 (ii)	O33/4	Misool 81FH11 (outcr.)	35573
T. bjaerkei	P	10I-K	SGM 103 (ii)	J27	Misool 81FH11 (outcr.)	35574
T. bjaerkei	P	10L	SGM 100 (i)	O35/2	Misool 81FH11 (outcr.)	35575
T. bjaerkei	P	10M-O	SSM 6 (ii)	M25/2	Misool 81FH11 (outcr.)	35576
T. bjaerkei	P	10P	SGM 1 (i)	R30/2	Peak-1 (1493.54*)	35577
T. bjaerkei	H	10Q-S	Ass. sl. P/A	V35/4	Sandpiper-1 (658.38)	35578
T. bjaerkei	P	10T	Ass. sl. P/2	U53/4	Sandpiper-1 (658.38)	35579
T. bjaerkei	P	11A-C	SGM 3 (iii)	O22/4	Taltarni-1 (2950.00)	35580
T. bjaerkei	P	11D,H,L	SGM 1(i)	K35	Arunta-1 (2135.00)	35581
T. bjaerkei	P	11E-G	SGM 3 (i)	O21/2	Taltarni-1 (2950.00)	35582
T. bjaerkei	P	11I-K	SGM 2 (iv)	L33	Taltarni-1 (2950.00)	35583
T. bjaerkei	P	11M-P	SGM 3 (iii)	O22/4	Taltarni-1 (2950.00)	35584
T. bjaerkei	P	11Q-T	SGM 3 (ii)	O22	Taltarni-1 (2950.00)	35585
* - ditch cuttings sample, range depth 1493.54m-1496.59m						
T. comptum	P	12A-C	SGM 3 (vi)	N35/3	Taltarni-1 (2950.00)	35586
T. comptum	P	12D,E	SGM 1	N37/3	Arunta-1 (2135.00)	35587
T. comptum	P	12F	SGM 4 (i)	M32/1	Challis-11 ST2 (1842.00)	35588
T. comptum	P	12G,H	SGM 4 (ii)	N31	Challis-11 ST2 (1842.00)	35589
T. comptum	P	12I,J	SGM 3 (i)	P35/2	Arunta-1 (2135.00)	35590
T. comptum	P	12K-M	SGM 2 (i)	L31/2	Challis-11 ST2 (1842.00)	35591
T. comptum	P	12N,O	SGM 4 (iv)	M28/2	Challis-11 ST2 (1670.70)	35592
T. comptum	H	12P-R	SGM 5	L37	Challis-11 ST1 (1552.50)	35593
T. comptum	P	12S	SGM 12	N38/3	Challis-11 ST1 (1552.50)	35594
T. comptum	P	12T	SGM 1 (iii)	M25	Challis-11 ST2 (1670.70)	35595
W. bensonii	H	13A,B	SGM 10	N37/3	Taltarni-1 (2950.00)	35596
W. bensonii	P	13C,D	SGM 9	N27/4	Taltarni-1 (2950.00)	35597
W. bensonii	P	13E	SSM 1	Q33/1	Taltarni-1 (2950.00)	35598
W. bensonii	P	13F	SGM 6	P34	Taltarni-1 (2950.00)	35599
W. bensonii	P	13G	SSM 2	K33	Taltarni-1 (2950.00)	35600
W. bensonii	P	13H	SGM 1 (ii)	G34/3&4	Arunta-1 (1805.00)	35601
W. bensonii	P	13I,J	Ass. sl. 2	N21/4	Taltarni-1 (2950.00)	35602
W. bensonii	P	13K	SGM 2 (iv)	Q27/2	Arunta-1 (1805.00)	35603
W. bensonii	P	13L	SGM 2 (iii)	P34/3	Arunta-1 (1805.00)	35604
W. bensonii	P	13M	SGM 4 (i)	J27/1	Arunta-1 (1805.00)	35605
W. bensonii	P	13N,O	SGM 2 (i)	N21	Challis-11 ST2 (1670.70)	35606
W. bensonii	P	13P,Q	SGM 3 (i)	M27/3	Arunta-1 (1805.00)	35607
W. bensonii	P	13R	SGM 2 (i)	O33/3	Arunta-1 (1805.00)	35608
W. bensonii	P	13S	SGM 2 (ii)	Q33/3	Arunta-1 (1919.00)	35609
W. bensonii	P	13T	SGM 5 (i)	O34/3	Arunta-1 (1805.00)	35610

Dinoflagellate cysts from the Late Jurassic (Kimmeridgian) *Dingodinium swanense* Zone in the North-West Shelf and Timor Sea, Australia

JAMES B. RIDING and ROBIN HELBY

RIDING, J.B. & HELBY, R., 2001:09:21. Dinoflagellate cysts from the Late Jurassic (Kimmeridgian) *Dingodinium swanense* Zone in the North-West Shelf and Timor Sea, Australia. *Memoir of the Association of Australasian Palaeontologists 24*, 141-176. ISSN 0810 8889.

Late Jurassic (Kimmeridgian) dinoflagellate cysts from the Timor Sea, offshore north-western Australia, include several undescribed forms. Of these, three genera, *Hadriana*, *Mombasadinium* and *Striatodinium*, and seven species are described as new. The new dinoflagellate cyst species are *Craspedodinium swanense*, *Cribroperidinium corrugatum*, *Gonyaulacysta fenestrata*, *Hadriana cincta*, *Oligosphaeridium swanense*, *Striatodinium lineatum* and *Striatodinium ottii*. The genus *Craspedodinium* and the species *Indodinium khariense* are emended. The species formerly known as *Indodinium? parvelatum* is transferred to the new genus *Mombasadinium* and is also emended. All these dinoflagellate cyst taxa have stratigraphical utility in the Kimmeridgian *Dingodinium swanense* Zone of Australia.

James B. Riding, Australian Geological Survey Organisation, GPO Box 378, Canberra, ACT 2601, Australia (present address: British Geological Survey, Keyworth, Nottingham NG12 5GG, UK [e-mail: jbri@bgs.ac.uk]); Robin Helby (corresponding author), 356A Burns Bay Road, Lane Cove, NSW 2066, Australia (e-mail: rhelby@ozemail.com.au). *10 November 2000.*

Keywords: dinoflagellate cysts, Late Jurassic, Australia, biostratigraphy, taxonomy

THE PALYNOLOGICAL zonation of the Australian Mesozoic published by Helby *et al.* (1987) was the first attempt to provide an integrated, pan-Australian microplankton and spore-pollen zonation. Only the basic framework of the zonation was provided in anticipation that further contributions, particularly the documentation of new taxa, would be necessary as the zonation scheme evolved. This paper is one of a series providing the taxonomic foundation necessary to formalise the widely used unpublished subdivisions of these zones. These subzones have widespread currency within the hydrocarbon industry due to the legislative requirement for the release of technical data under the Petroleum (Submerged Lands) Act 1967. The informal subdivisions of the Helby *et al.* (1987) zonation have been entered into the Australian Geological Survey Organisation (AGSO) STRATDAT database. A diagrammatic update of the Helby *et al.* (1987) zonal scheme is presented by Foster (this volume), and will be fully described by Helby & Partridge (in prep.). This taxonomic project is an initiative of the Petroleum and Marine Division of AGSO.

This paper provides formal descriptions of previously undescribed taxa from a Late Jurassic (mainly Kimmeridgian) dinoflagellate cyst assemblage recorded in samples from the North-West Shelf and the Timor Sea (Appendix 1). All these new taxa have stratigraphical utility within the *Dingodinium swanense* Interval Zone of Helby *et al.* (1987). The figured specimens in this paper from offshore north-western Australia are from Alaria-1, Buang-1, Cockell-1, Frigate-1, Hadrian-1, Jabiru-8A, Jurabi-1, Macedon-5, Octavius-2, Peak-1, Scafell-1, Swan-1, Tenacious-1 and Tenacious West-1 wells (Foster, this volume; Appendix 1). Additional material from outcrops in Misool, eastern Indonesia, Scotland, Kenya and New Zealand was also studied and some specimens figured (Appendices 1, 2).

Helby *et al.* (1987, p. 29) stated that their *Dingodinium swanense* Interval Zone is of mid to late Kimmeridgian age based upon evidence from ammonites and belemnites (Arkell, 1956; Balme, 1957; Wiseman, 1980). Davey (1987, fig. 3), however, concluded that the equivalent of this zone, the lower part of the *Cribroperidinium perforans* Zone of Davey (1987), lies entirely within the late Oxfordian. Francis & Westermann (1993, fig. 1b), further interpreted the age of this zone to be possibly as old as mid Oxfordian. However, these authors went on to suggest that

it is most likely to be early Kimmeridgian (Francis & Westermann, 1993, fig. 7). The conclusions of Francis & Westermann (1993, fig. 7) were based on linking the Australasian molluscan faunas to north-west Europe by indirect correlation via various ammonite faunal provinces. The early Kimmeridgian interpretation of Francis & Westermann (1993) was, however, not accepted by Davey (1999, figs 8, 9), who indicated that the *Dingodinium swanense* Interval Zone is entirely within the late Oxfordian. Burger (1996, fig. 2) also assigned the *Dingodinium swanense* Interval Zone to the Oxfordian, within AGSO timeslice J-8. This author highlighted the lack of direct evidence of correlations to Europe within the Oxfordian and much of the Kimmeridgian.

SYSTEMATIC PALYNOLOGY

In this section, three new genera and seven new species of dinoflagellate cyst are described from the Upper Jurassic Lower Vulcan Formation and equivalent strata on the North-West Shelf and in the Timor Sea. The material is from the *Dingodinium swanense* Zone of Helby *et al.* (1987). The type material of one of these species, *Striatodinium ottii* sp. nov., is from New Zealand. Additionally, one dinoflagellate cyst species is emended and another is emended and recombined. The genera are listed in alphabetical order; the recent suprageneric classification of Fensome *et al.* (1993) is not used here. The dimensions quoted are all given in micrometres (µm). For descriptive purposes, the cyst sizes, small, intermediate and large are after Stover & Evitt (1978, p. 5). These parameters are such that intermediate size dinoflagellate cysts have a maximum dimension of between 50 and 100µm. Small and large forms are less than 50µm and above 100µm respectively. The majority of the morphological terminology for the dinoflagellate cysts are those used by Evitt (1985). However, the term loisthocyst refers to a dinoflagellate cyst in which the operculum (or separate opercular pieces) has (have) detached and is therefore the part that remains (Sarjeant *et al.*, 1987, p. 26, 27). Where appropriate, the dinoflagellate cyst paraplate notation system used throughout is Kofoidian, as opposed to the 'Taylor-Evitt' scheme of Evitt (1985). References to author citations of taxa discussed are not given here. These may be found in the bibliography in Williams *et al.*, 1998, p. 747-817). The synonymy lists given here are selective and mainly confined to illustrated specimens. The majority of the figured specimens are housed in the Commonwealth Palaeontological Collection (CPC) of the Australian Geological Survey Organisation (AGSO), Canberra (Appendix 2).

This study has been conducted almost exclusively using single grain mounts (or mounts with multiple specimens) and the majority of the figured specimens are from these single species slides. Most of the samples studied are from sidewall core or conventional core material, however a small number of ditch cuttings samples were also used. The photomicrographs in Figs 1-15 were all taken at AGSO using an Olympus DP10 digital camera system coupled to a Zeiss Axioskop photomicroscope. Extraneous palynodebris, which is not adherent to the figured specimens, has been digitally removed in selected images.

The images in Figs 1 to 15 in this paper are taken from a digital database. Many more digital images exist than have been figured. The sample details, key morphological data and measurements of each imaged specimen are held digitally on open file spreadsheets. The image database may be accessed on the AGSO website (http://www.agso.gov.au).

Many of these new taxa have been extensively used in unpublished reports, which are now in the public domain (open file). In order to maximise the utility of the species, the informal names and/or codes are listed, separate from any formal synonymy listing, under the heading 'Previous Australian usage'. To provide continuity, wherever practical, the informal name has been retained.

Dinoflagellate cysts

Craspedodinium Cookson & Eisenack 1974 emend.

1974 *Craspedodinium* Cookson & Eisenack; p. 75.

1978 *Craspedodinium* Cookson & Eisenack 1974; Stover & Evitt, p. 34.

Type species. Craspedodinium indistinctum Cookson & Eisenack 1974 emend. Riding & Helby this volume

Emended diagnosis. The original generic diagnosis of Cookson & Eisenack (1974) and the synopsis and modified description given by Stover & Evitt (1978) are all accepted. However, the generic concept is further expanded to include the partial indication of a gonyaulacalean paratabulation (formula: 4', 6", Xc, 6"', ?1p, 1"", Xs), including the paracingulum and parasulcus,

by low relief ornamentation of the periphragm, the presence of short, parasutural processes on the endophragm and/or the outline of the operculum. These endophragmal processes may be trabeculate. Furthermore, the archaeopyle type of this genus is confirmed as being apical with a simple operculum which is free.

Comments. This emendation to include a standard gonyaulacalean paratabulation is based on observations of the type, *Craspedodinium indistinctum* (see Morgan, 1980, pl. 8, figs 3-6 and Riding & Helby, this volume, a), and *C. swanense* sp. nov. (see below). *Craspedodinium indistinctum* has irregular parasutural periphragmal folds and parasulcal ornamentation on the hypocyst (Morgan, 1980, pl. 8, fig. 5; Riding & Helby, this volume, a). The archaeopyle type of *Craspedodinium* is apical, as stated by Cookson & Eisenack (1974), Stover & Evitt (1978, p. 34) and Wilson & Clowes 1981, p. 31). Helenes (1983, p. 257) interpreted the evidence for the archaeopyle type of this genus as inconclusive, based largely on interpretations by Lentin & Williams (1976, p. 157). Helenes' (1983) contention that *Craspedodinium* is possibly related to *Ascodinium* Cookson & Eisenack 1960 and *Ovoidinium* Davey 1970 emend. Duxbury 1983 was based on the possibility of *Craspedodinium* having a combination apical-anterior intercalary archaeopyle.

Craspedodinium swanense sp. nov. (Figs 1A-L, 2A-H)

Previous Australian usage
Craspedodinium swanense – Helby.

Description. A species of *Craspedodinium*, ovoidal in outline and dorsoventrally flattened. A low, wide, solid apical protuberance or boss is developed on the endophragm and the periphragm mirrors the outline of this feature. Circumcavate or bicavate in cyst organisation. The endophragm is relatively thick (1-2µm) and smooth, scabrate, rugulate and/or microreticulate; generally not folded. Periphragm thin (<0.5µm), diaphanous, smooth and may be folded. These low, distally smooth periphragmal folds may partially reflect a gonyaulacalean paratabulation, especially around the paracingulum and the hypocyst. Epicyst and hypocyst normally subequal in length; the hypocyst, however, may be slightly longer. Accessory archaeopyle sutures may be developed.

Dimensions. The specimens of *Craspedodinium swanense* studied are from sidewall core samples in Buang-1 well at 3504.00m and 3505.20m and Jabiru-8A well at 1842.50m. The dimensions of material from both wells are given here separately, to effect comparisons. Note that secondary dorsoventral flattening may have distorted some of the specimens. In particular, some specimens are anomalously wide due to severe compression.

Measurements of specimens from 3504.00m and 3505.20m in Buang-1 well (µm; n=27): Min. (Mean) Max.
Length of pericyst incl. operculum: 85 (99) 110
Length of pericyst excl. operculum: 80 (105) 123
Length of endocyst incl. operculum: 80 (93) 100
Length of endocyst excl. operculum: 70 (95) 112
Width of pericyst at paracingulum: 81 (99) 118
Width of endocyst at paracingulum: 79 (96) 111
Maximum width of pericoel: 3 (6) 10
Width of operculum in dorsoventral view: 35 (46) 57
Depth of operculum in dorsoventral view: 47 (55) 61
Height of apical protuberance: 3 (4.5) 5
Width of apical protuberance: 7 (10) 11

Note that only 4 entire cysts were measured, out of an assemblage of 27 specimens. This disparity has given rise to the apparently anomalous average and maximum lengths of the pericyst and endocyst.

Measurements of specimens from 1842.50m in Jabiru-8A well (µm; n=24): Min. (Mean) Max.
Length of pericyst incl. operculum: 77 (92) 100
Length of pericyst excl. operculum: 67 (84) 100
Length of endocyst incl. operculum: 76 (90) 98
Length of endocyst excl. operculum: 58 (77) 89
Width of pericyst at paracingulum: 75 (93) 111
Width of endocyst at paracingulum: 70 (88) 105
Maximum width of pericoel: 2 (5) 12
Width of operculum, dorsoventral view: 37 (47) 56
Depth of operculum, dorsoventral view: 53 (58) 67
Height of apical protuberance: 3 (4) 5
Width of apical protuberance: 5 (8) 12

Note that only 5 entire cysts were measured, out of an assemblage of 24 specimens. This disparity has given rise to the apparently anomalous average and maximum lengths of the pericyst and endocyst in both the entire cyst and the loisthocyst.

It is clear from the above data that the Buang-1 well material is consistently slightly larger than the specimens from Jabiru-8A well.

Comments. Specimens of *Craspedodinium swanense* may be elongate or wider than long (Fig.

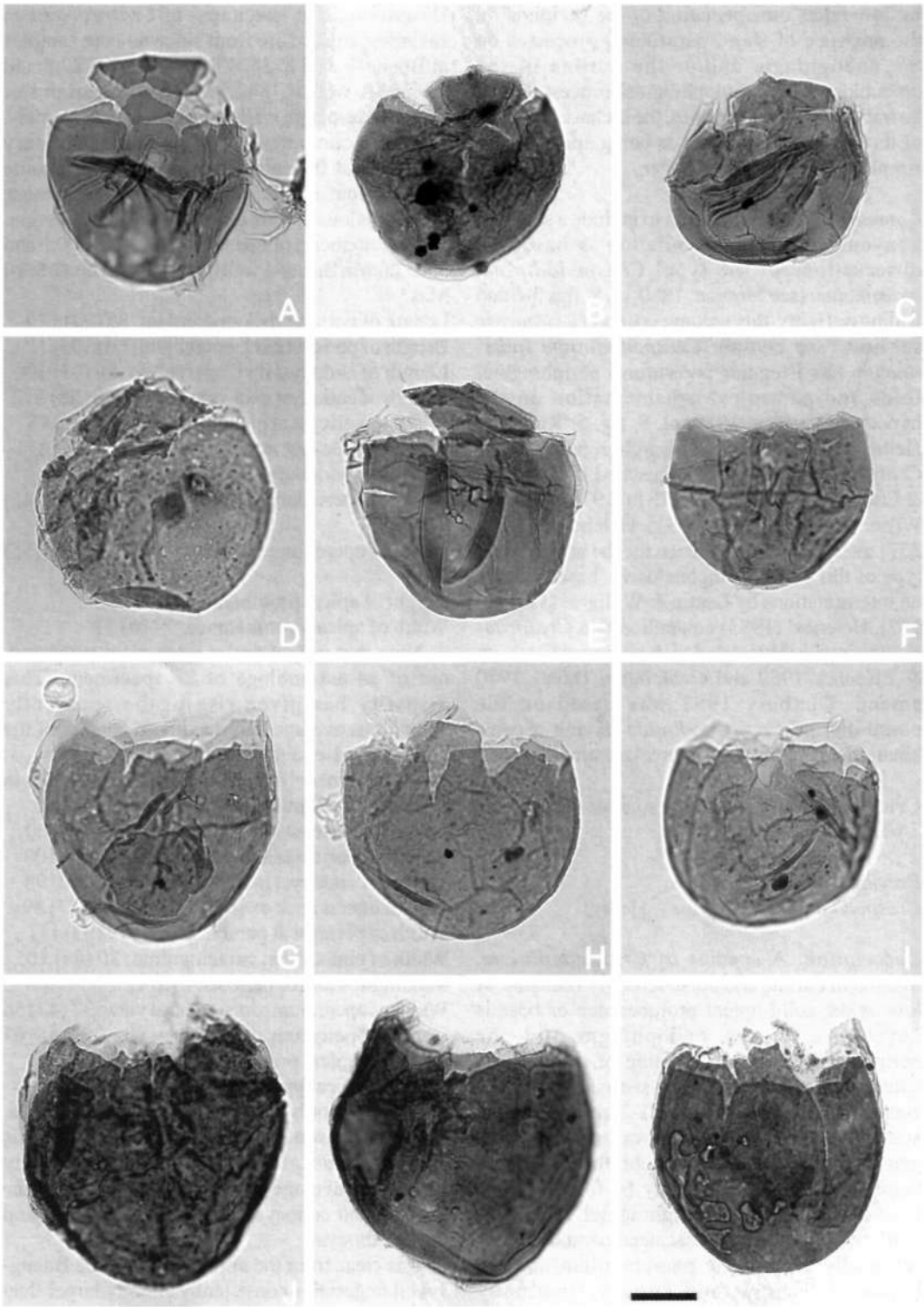

Fig. 1. Craspedodinium swanense sp. nov. From sidewall cores in Buang-1 well at 3505.20m (Figs 1J-K) and 3504.00m (Figs 1B, L) and Jabiru-8A well at 1842.50m (Figs 1A, C-I). All photomicrographs taken using plain transmitted light. Scale bar in Fig. 1L refers to all photomicrographs and is 25µm. Fig. 1L is the holotype; the remainder, paratypes. Note ovoidal outline, cavate cyst organisation, thick endophragm, thin, diaphanous periphragm and apical archaeopyle. A - CPC 35645, paratype; oblique ventral view, (continued opposite)

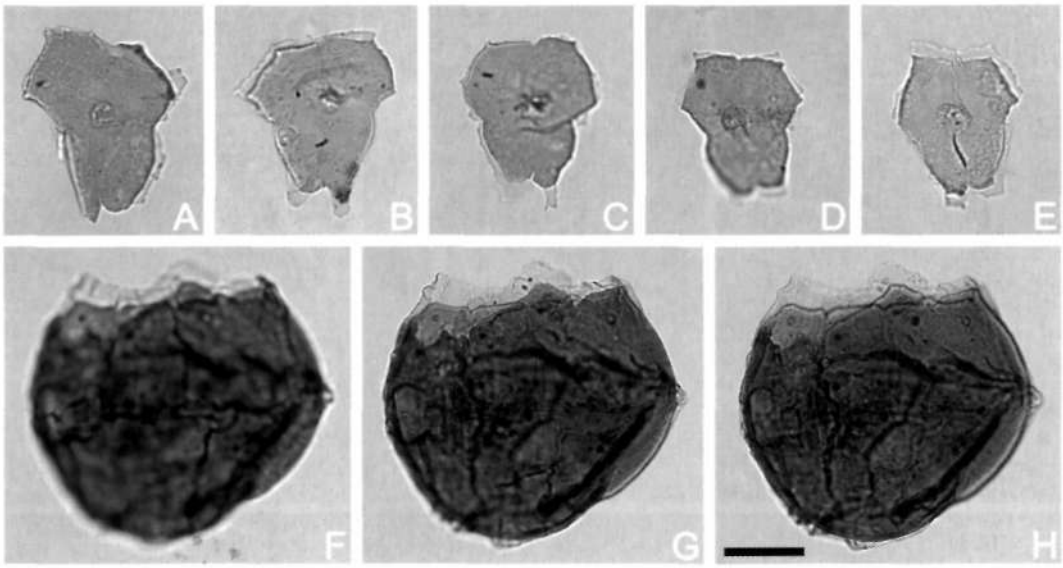

Fig. 2. Craspedodinium swanense sp. nov. All are paratypes from sidewall cores in Buang-1 well at 3505.20m (Figs 2F-H) and Jabiru-8A well at 1842.50m (Figs 2A-E; all isolated opercula). All photomicrographs taken using plain transmitted light. Scale bar in Fig. 2H refers to all photomicrographs and is 25µm. Note ovoidal outline, cavate nature, thick endophragm and apical archaeopyle. A - CPC 35657, paratype; internal view, low focus. Note apical boss and parasulcal tongue. B - CPC 35658, paratype; external view, low focus. Note two cyst layers. C - CPC 35659, paratype; external view, high focus. Note clear parasulcal tongue. D - CPC 35660, paratype; internal view, high focus. Note apical boss. E - CPC 35661, paratype; internal view, low focus. Note parasutural folds on periphragm and apical boss. F-H - CPC 35662, paratype; dorsal view, high to low focus sequence. Note apical archaeopyle and parasutural folds in periphragm.

1). The pericoel is normally best developed at the antapex, where it can approach, but rarely exceed, 10µm. This cavity, where developed, is normally 1-2µm wide in the equatorial regions. However, the two cyst layers are frequently closely appressed in the midlateral areas (Fig. 1). Occasionally, the periphragm may be missing, probably removed by mechanical damage. The outline of the operculum and the accessory archaeopyle sutures indicates the presence of four apical and six precingular paraplates (Figs 1, 2). Furthermore, the low folds in the periphragm may partially indicate the paracingulum and, more rarely, a hypocystal paratabulation of six postcingulars and a single antapical paraplate (Figs 2F-H). Folds indicating the precingular paraplates are relatively rare. This paratabulation is clearly gonyaulacalean, with a formula of 4', 6", Xc, 6"', ?1p, 1"", Xs. A similar paratabulation pattern is evident from the specimens of the genotype, *Craspedodinium indistinctum* (see Morgan, 1980, pl. 8, figs 3-6 and Riding & Helby, this volume, a). Accessory archaeopyle sutures may form deep splits between the precingular paraplates of the endophragm (Fig. 1L). The robust endophragm exhibits significant variation in ornamentation. Material from the Buang-1 well is scabrate to rugulate and furthermore the rugulate forms may also be irregularly microreticulate (Fig. 1J). By contrast, the endophragm in the specimens from the Jabiru-8A well is smooth (Figs 1A, C-I).

(from opposite) median focus. Note small apical boss on endocyst and small accessory endoarchaeopyle sutures. B - CPC 35646, paratype; dorsal view, median focus. Note apical boss and bicavate cyst organisation. C - CPC 35647, paratype; ventral view, median focus. Squat specimen. D - CPC 35648, paratype; ventral view, median focus. Note folding of endophragm, and apical boss. E - CPC 35649, paratype; ventral view, median focus. Note circumcavate nature and small apical boss. F - CPC 35650, paratype; ventral view, median focus. Loisthocyst; note parasutural folds on periphragm. G - CPC 35651, paratype; dorsal view, median focus. Note operculum, fallen into loisthocyst. H - CPC 35652, paratype; dorsal view, median focus. Note prominent accessory archaeopyle sutures in endophragm. I - CPC 35653, paratype; oblique dorsal view, median focus. Note thin periphragm and apical archaeopyle. J - CPC 35654, paratype; dorsal view, median/low focus. Note vague parasutural folds on periphragm. K - CPC 35655, paratype; dorsal view, median focus. Note narrow pericoel. L - CPC 35656, holotype; ventral view, median focus. Note prominent accessory archaeopyle sutures on endophragm.

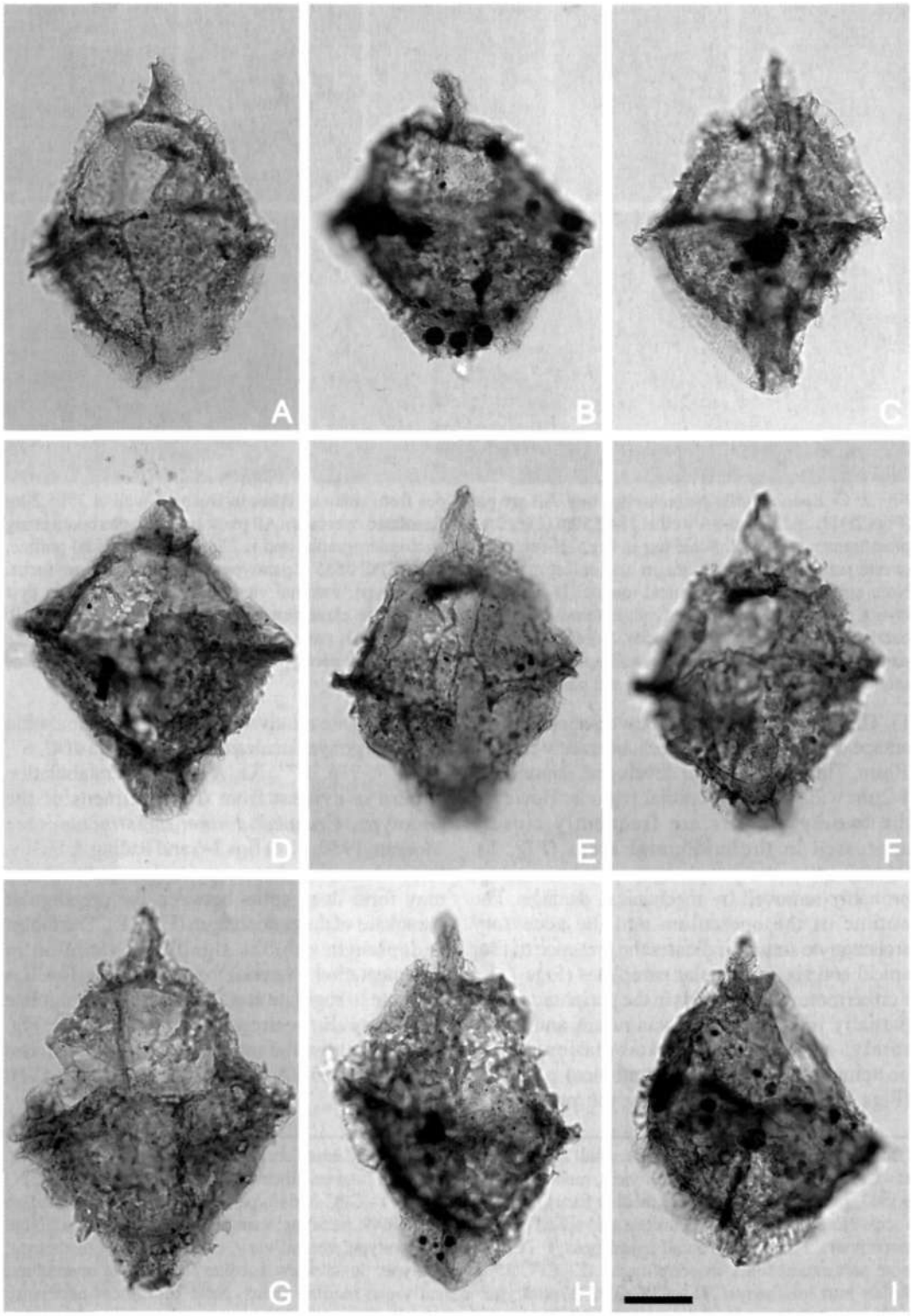

Fig. 3. Cribroperidinium corrugatum sp. nov. Specimens from conventional core in Alaria-1 well at 3315.95m (Figs 3B, D-H) and 3318.58m (Figs 3A, C, I). All photomicrographs taken using plain transmitted light. Scale bar in Fig. 3I refers to all photomicrographs and is 25µm. Fig. 3A is the holotype; the remainder, paratypes. Note large size, prominent apical horn, small antapical (1'''') paraplate which imparts a (continued opposite)

Comparison. The genotype, *Craspedodinium indistinctum*, differs from *C. swanense* in lacking an apical boss/protuberance on the endocyst and having trabeculate endophragmal processes at the cyst periphery and the apical paraplate series (Morgan, 1980, pl. 8, figs 3-6; Riding & Helby, this volume, a). *Craspedodinium americanum* Habib 1970 is subcircular in outline, not paratabulate and much smaller than *C. swanense*. The Late Cretaceous species *Craspedodinium turonicum* Prössl 1990 is also significantly smaller than *C. swanense*. Furthermore, it has an antapical constriction and a strongly reticulate periphragm (Prössl, 1990). In addition, the three other species of *Craspedodinium* lack apical protuberances formed by the endophragm.

Cygnusicysta taltarniana Riding & Helby (this volume) is consistently circumcavate and significantly smaller than *Craspedodinium swanense*. Furthermore, apart from the principal archaeopyle suture, *C. taltarniana* lacks any indication of paratabulation. *Craspedodinium* is similar to other cavate genera with apical archaeopyles such as *Leberidocysta* Stover & Evitt 1978. However, *Leberidocysta* has delicate periphragm which is extremely susceptible to mechanical damage (Cookson & Eisenack, 1962).

Derivation of name. From the *Dingodinium swanense* Zone, to which this species is confined.

Holotype and type locality. Figure 1L, CPC 35656, Buang-1 well, sidewall core at 3504.00m.

Stratigraphical distribution. *Craspedodinium swanense* is confined to the Kimmeridgian *Dingodinium swanense* Zone (6aiia-6aib) of the Timor Sea region (Foster, this volume; Helby & Partridge, in prep.).

Cribroperidinium Neale & Sarjeant 1962 emend. Helenes 1984

Type species. *Cribroperidinium sepimentum* Neale & Sarjeant 1962

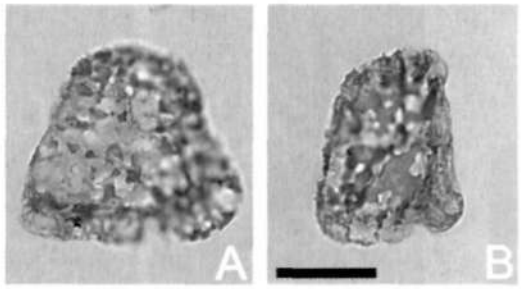

Fig. 4. Cribroperidinium corrugatum sp. nov. Both are paratype isolated opercula from conventional core in Alaria-1 well at 3315.95m (Fig. 4B) and 3319.95m (Fig. 4A). Both taken using plain transmitted light. Scale bar in Fig. 4B refers to both photomicrographs and is 25µm. Note thick, irregular corrugate autophragm which sometimes forms a partial, crude reticulum. A - CPC 35671, paratype; high focus. Note large size of 3'' paraplate. B - CPC 35672, paratype; median focus. Note irregular corrugate ornamentation.

Cribroperidinium corrugatum sp. nov. (Figs 3A-I, 4A-B)

Previous Australian usage
Cribroperidinium sp. (corrugate) – Helby.

Description. A large species of *Cribroperidinium* with a prominent apical horn. The species is slightly dorsoventrally flattened and is elongate subquadrangular in dorsoventral or lateral view. The subquadrangular outline is due to the relatively small diameter of the antapical (1'''') paraplate. The autophragm is thick (1.5-2.5µm), with a strong corrugate ornamentation. Parasutures, indicating a sexiform gonyaulacalean paratabulation pattern, are marked by slender, perforate crests of variable height (2-20µm), which may be reduced to aligned, distally trabeculate short processes and are highest at the hypocystal periphery and particularly at the antapex. The corrugate ornament is arranged as irregular ridges, which vary from 2 to 5µm in width. They are

subquadrangular outline, thick corrugate autophragm and slender parasutural crests. A - CPC 35663, holotype; dorsal view, high/median focus. Note corrugate autophragm, typically cribroperidinoid dorsal paratabulation pattern (Helenes, 1984), high parasutural crests, precingular archaeopyle and prominent apical horn. Parasutural crests in apical region strongly suggests an A/B apical paraplate configuration of Helenes (1984). B - CPC 35664, paratype; dorsal view, median focus. Note well preserved corrugate autophragm on hypocyst. C - CPC 35665, paratype; ventral view, median focus. Elongate specimen, note small antapical (1'''') paraplate. D - CPC 35666, paratype; oblique ventral view, median focus. Note prominently corrugate autophragm and distinctly subquadrangular dorsoventral outline. E, F - CPC 35667, paratype; ventral view, high and low focus respectively. Note extremely prominent apical horn and well expressed midventral paratabulation in Fig. 3E. G - CPC 35668, paratype; dorsal view, high focus. Large specimen, note corrugate autophragm. H - CPC 35669, paratype; oblique dorsal view, low focus. Slender; note high parasutural crests and large apical horn. I - CPC 35670, paratype; oblique right lateral view, median focus. Note trabeculate parasutural crests on hypocyst.

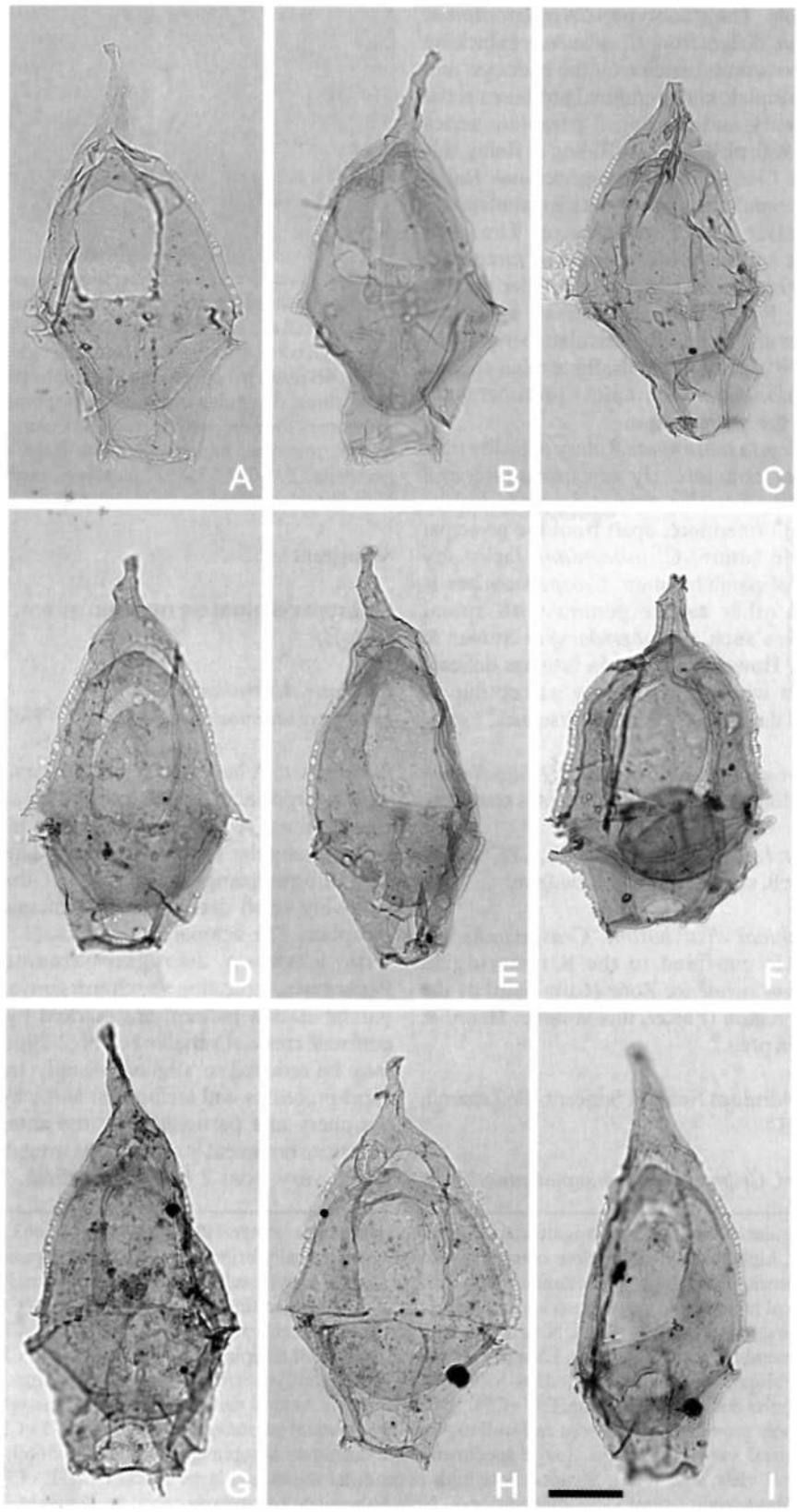
A
B
C
D
E
F
G
H
I

rounded and random in orientation and often coalesce freely. The anastomosing nature and the density of insertion of the ridges is extremely variable. Some are entirely random and in other specimens, a crude reticulation may be present. The paracingulum is indicated by relatively thick parasutural ridges and is relatively narrow for such a large cyst. Parasulcus indicated by crests or ridges, not subdivided.

Dimensions (µm; n=32) inclusive of parasutural crests where appropriate: Min. (Mean) Max.
Length of cyst incl. apical horn: 102 (130) 175
Length of epicyst incl. apical horn: 40 (63) 87
Length (height) of paracingulum: 4 (6) 9
Length of hypocyst: 44 (62) 85
Length of apical horn: 12 (23) 36
Equatorial width of cyst: 90 (102) 117
Height of parasutural crests: 2 (7) 20

The measured specimens are from cores in Alaria-1 well at 3319.95m, 3318.58m and 3315.95m and a sidewall core at 1842.50m in Jabiru-8A well.

Comments. This large and characteristic species is variable in size (see *Dimensions*, above) and outline (Fig. 3). It appears to lack intratabular growth ridges. *Cribroperidinium corrugatum* is distinguished by the distinctive corrugate ornamentation, as defined by Tappan & Loeblich (1971, p. 387). The thick autophragm is covered by rounded ridges, which are variable in width, density of insertion and the degree of coalescence within individual specimens and populations (Figs 3, 4). In some specimens, the corrugate ridges are best developed on the hypocyst (Fig. 3B). Where the ridges are inserted relatively sparsely, the cysts may appear to be somewhat degraded (Fig. 4B). The ridges are rarely discontinuous; this phenomenon may be due to preservational effects. Both the apical horn and the parasutural crests are variable in size and morphology (Fig. 3). They appear to be formed entirely of periphragm. Some parasutural crests are entire, however, most are reticulate with subcircular to ellipsoidal fenestrae, which vary from 2 to 5µm in diameter. The fenestrae may expand such that the crests become rows of trabeculate short spines (Figs 3C, I).

Comparison. *Cribroperidinium corrugatum* is distinguished from the other species of this genus by the characteristic corrugate ornamentation. The majority of the species of *Cribroperidinium* have smooth, scabrate or microreticulate autophragms. *Cribroperidinium janinae* Górka 1982 and *C? muderongense* (Cookson & Eisenack 1958) Davey 1969 have a granulate autophragm, but entirely lack any corrugate ornamentation.

This species appears to lack intratabular growth ridges, which are typical of most Cretaceous and Palaeogene *Cribroperidinium*. However this does not preclude assignment to *Cribroperidinium* (Helenes, 1984). The antapical paraplate (1'''') is extremely small (Fig. 3). This genus typically comprises species with relatively large antapical paraplates (Helenes, 1984). Gonyaulacalean genera may exhibit such size variations at the antapex. *Ctenidodinium* Deflandre 1939 emend. Benson 1985 normally has a relatively large 1'''' paraplate. The Mid Jurassic species *Ctenidodinium combazii* Dupin 1968 is similar to *C. corrugatum* in that it has a small antapical paraplate (Riding *et al*., 1985, pl. 1).

Derivation of name. From the Latin *corrugatus* meaning ridged or wrinkled and referring to the characteristic corrugate ornament.

Holotype and type locality. Figure 3A, CPC 35663,

Fig. 5. Gonyaulacysta fenestrata sp. nov. Specimens from sidewall cores in Buang-1 well at 3504.00m (Figs 5D-E, I) and 3505.20m (Fig 5G), Frigate-1 well at 1233.00m (Figs 5A-B) and Jabiru-8A well at 1842.50m (Fig. 5C), conventional core in Alaria-1 well at 3315.95m (Fig. 5H) and outcrop material from Misool, eastern Indonesia (Fig. 5F). All photomicrographs taken using plain transmitted light. Scale bar in Fig. 5I refers to all the photomicrographs and is 25µm. Figs 5D, I are composite photomicrographs. Fig. 5D is the holotype; the remainder, paratypes. Note elongate, cavate nature, prominent apical horn, fenestrate parasutural crests with small fenestrae close to distal margin, claustrum close to antapex and precingular archaeopyle. A - CPC 35673, paratype; ventral view, median focus. Note elongate, slender apical horn, claustrum and laterally fenestrate parasutural crests. B - CPC 35674, paratype; dorsal view, low focus. Note elongate apical horn and wide parasutural crests. C - CPC 35675 (see also Fig. 6A) paratype; dorsal view, median focus. Note relatively short apical horn, claustrum and fenestrate parasutural crests in lateral regions. D - CPC 35676, holotype; dorsal view. Note detached endoperculum, claustrum and fenestrate parasutural crests. E - CPC 35677 (see also Fig. 6B) paratype; dorsal view, high focus. Slender, elongate specimen, note precingular archaeopyle and ellipsoidal fenestrae on lateral parasutural crest. F - CPC 35678, paratype; ventral view, median/low focus. Note relatively short apical horn. G - CPC 35679, paratype; dorsal view, high focus. Note long, sinuous apical horn, short apical protuberance on endocyst and prominent claustrum. H - CPC 35680, paratype; dorsal view, high focus. Wide specimen. I - CPC 35681, paratype; ventral view. Slender, elongate specimen.

Fig. 6. Enlargements of parasutural crests of various forms of *Gonyaulacysta*. All photomicrographs taken using plain transmitted light. Scale bar in Fig. 6E refers to all photomicrographs and is 25µm. A - *Gonyaulacysta fenestrata* sp. nov. CPC 35675 (see also Fig. 5C); paratype; dorsal view, median focus. Note distinctively trabeculate nature of this parasutural crest. Fenestrae are enlarged and parasutural crest appears to be of short processes linked distally by trabeculae. B - *Gonyaulacysta fenestrata* sp. nov. CPC 35677 (see also Fig. 5E); paratype; dorsal view, high focus. Note ellipsoidal nature and irregular insertion of fenestrae on this lateral parasutural crest. C - *Gonyaulacysta* sp. cf. *G. fenestrata* sp. nov. CPC 35684 (see also Fig. 7E); ventral view, median focus. Note denticles surmounting this midlateral parasutural crest. D - *Gonyaulacysta dualis*. CPC 35682; ventral view, high focus. Note smooth to undulose distal margin of this lateral parasutural crest. E - *Gonyaulacysta jurassica* subsp. *adecta* Sarjeant 1982. MPA 15496/1; dorsal view high focus. Note denticulate nature of this antapical parasutural crest. The specimen is from the Lower Callovian Brora Roof Bed of Brora, NE Scotland. This is the lowermost unit of the Brora Shale Member (Brora Argillaceous Formation) and belongs to the *Proplanulites koenigi* Ammonite Zone (Sykes, 1975).

Alaria-1 well, conventional core sample at 3318.58m.

Stratigraphical distribution. Cribroperidinium corrugatum is confined to the Kimmeridgian middle to upper *Dingodinium swanense* Zone (6ai/6aii) in the Timor Sea region (Foster, this volume; Helby & Partridge, in prep.).

Gonyaulacysta Deflandre 1964 emend. Helenes & Lucas-Clark 1997

Type species. Gonyaulacysta jurassica (Deflandre 1939) Norris & Sarjeant 1965

Comments. The latest emendation of this important Jurassic genus by Helenes & Lucas-Clark (1997) is accepted, together with the redefinitions of Stover & Evitt (1978), Sarjeant (1982) and Jan du Chene *et al.* (1986).

Gonyaulacysta fenestrata sp. nov. (Figs 5A-I, 6A-B)

1980 *Gonyaulacysta jurassica* (Deflandre 1939) Norris & Sarjeant 1965 *auct. non.*; Wiseman, pl. 2, fig. 49 (no description).
1987 *Gonyaulacysta jurassica* (Deflandre 1939) Norris & Sarjeant 1965 *auct. non.*; Stevens, fig. 5K (reworked into the Early Cretaceous).

Previous Australian usage
Gonyaulacysta oligodentata (pars) – Helby.

Description. A large, elongate species of *Gonyaulacysta* with a long, distally-blunt, slender apical horn. The cyst is primarily dorsoventrally flattened. The pericyst, excluding the apical horn, is elongate subellipsoidal to subpolygonal and is antapically truncate. The endocyst is elongate ellipsoidal, normally with a prominent apical protuberance. Bicavate cyst organisation; the epicyst may be epicavate or cornucavate. Paratabulation partially indicated by parasutural crests which are generally smooth distally and fenestrate. The fenestrae are subcircular, ellipsoidal or rectangular; normally they are best developed in the midlateral and antapical areas and inserted close to the distal margin of the crest. Occasionally, the parasutural crests may be distally irregular or undulose. Parasutural features are generally entirely lacking, or profoundly reduced, midventrally in the parasulcal area and the middorsal hypocystal area. A prominent subcircular claustrum is present in the antapical parasulcal paraplate. Periphragm is smooth to microscabrate and may be irregularly microreticulate. The endophragm is markedly thicker than the periphragm and smooth. The perioperculum is absent; the large endoperculum is frequently displaced and visible. Both the periarchaeopyle and the endoarchaeopyle is occasionally slightly enlarged posteriorly, at the 3''/3c-4c paraplate boundary.

Dimensions (µm; n=35): Min. (Mean) Max.
Length of pericyst: 113 (133) 158
Length of apical horn: 14 (24) 31
Length of epipericyst (excl. paracingulum)*: 69 (82) 100
Length (height) of paracingulum: 3 (5) 8
Length of hypopericyst (excl. paracingulum): 34 (45) 55
Length of endocyst: 71 (86) 103
Width of pericyst at paracingulum**: 55 (70) 86
Width of endocyst at paracingulum: 48 (62) 79
Height of parasutural crests***: 1 (3) 7
Diameter of fenestrae: 1 (1.5) 3

*- including the apical horn
**- includes the parasutural crests at the paracingulum
*** - measured midlaterally, within the precingular paraplate series

The measured specimens are from sidewall core samples in Buang-1 well at 3504.00m and 3505.20m, Frigate-1 well at 1233.00m and Tenacious-1 well at 3002.00m and a ditch cuttings sample from Hadrian-1 well between 3285.00m and 3300.00m.

Comments. Gonyaulacysta fenestrata is a unique species, being large and elongate with fenestrate parasutural crests. The subcircular to ellipsoidal fenestrae on the parasutural crests are diagnostic. These characteristic perforations exhibit some variability in their density of insertion (Fig. 5). In some specimens the fenestrae are rectangular, separated by distinct rods or short processes (Figs 5C, H, I). They are normally present in the midlateral and antapical areas of the cyst, closely adjacent to the distal margin of the crests. The antapical parasutural crest appears to be susceptible to mechanical damage. This may affect the distal part of the parasutural crest, giving rise to an irregularly denticulate margin due to 'bursting' of the fenestrae. Normally, the parasutural crests are distally smooth, but in occasional specimens, they may be slightly undulose distally. The lateral parasutural crests are the most prominent and consequently these may be the only crests to exhibit significant fenestrae. The pericyst is elongate subellipsoidal in outline with a truncated antapex and the parasutural crests are interrupted at the paracingulum, thereby imparting a distinctive equatorial profile. The relatively thin apical horn is highly variable in length (see *Dimensions* above). It is blunt distally due to the presence of the first preapical paraplate (1pr/P of Helenes & Lucas-Clark, 1997). A porichnon (Evitt, 1985) is present on the ventral side of the apical horn, at the 2pr/1'/4' paraplate triple junction. The hypopericoel is consistently prominent, with a relatively large cavity developed both antapically and laterally in the hypocyst. By contrast, the epipericoel is generally smaller and more variable, with occasional forms having small pericoels and being merely cornucavate (Fig. 5F). The endocyst is ellipsoidal and normally has an apical protuberance which may closely approach the apical horn in the pericyst. Occasionally, a slight antapical protuberance is present in the endocyst.

The paratabulation of the species appears to be precisely that determined for *G. dualis* (Brideaux & Fisher 1976) Stover & Evitt 1978 by Helenes & Lucas-Clark (1997). However, the midventral paratabulation is not known in detail due to the significant suppression of parasutures around the parasulcus. This phenomenon was also noted in *Gonyaulacysta jurassica* by Stover & Evitt (1978, p. 277). The material studied is strongly dorsoventrally flattened and the orientation, dorsal or ventral, may appear difficult to determine. This scenario is exacerbated by the suppression of the midventral parasutural crests. However, using the ventral claustrum in the antapical parasulcal paraplate and the dorsal archaeopyle, the orientation can be readily determined. This is a gonyaulacalean species where the absence of the perioperculum is clearly demonstrable (Eaton, 1984). However, the large endoperculum is frequently displaced and retained within the cyst (Figs 5D, F-I). The two archaeopyles may be slightly enlarged along the paracingulum.

Gonyaulacysta fenestrata is similar in overall morphology to *G. jurassica* (see *Comparison* below), differing only in size and the presence of fenestrate, largely smooth parasutural crests. Therefore, given that *G. jurassica* is currently separated into 3 subspecies (Williams *et al.*, 1998, p.251, 252), the possibility of giving *fenestrata* subspecific status within *G. jurassica* was considered. However, *G. fenestrata* is arguably more similar to *G. dualis*, and this is maintained as a separate species. We consider *G jurassica* has far too many subspecific and varietal subdivisions and the most important stratigraphical morphotypes should be elevated to specific status.

Comparison. Gonyaulacysta fenestrata is similar in morphology, and identical in paratabulation, to *G. dentata* (Raynaud 1978) Lentin & Vozzhennikova 1990, *G. dualis*, *G. eisenackii* (Deflandre 1939) Dodekova 1967 and *G. jurassica* subsp. *jurassica*. It may have an enlarged archaeopyle at the paracingulum like *G. jurassica* (see Williams *et al.*, 1978, fig. 33). The unusually long epicyst (with respect to the hypocyst) in *G. fenestrata, G. dualis* and *G. jurassica* is especially striking. However, the criterion distinguishing this species from all species in this important genus are the characteristic fenestrate parasutural crests. *Gonyaulacysta fenestrata* is most similar in size to *G. dentata* and *G. dualis*, and furthermore the parasutural crests in the latter species are typically smooth (Fig. 6D). However the crests in *G. dualis* are not fenestrate and may also be relatively sparsely denticulate or spinose (Brideaux & Fisher, 1976). *Gonyaulacysta dentata* (Raynaud

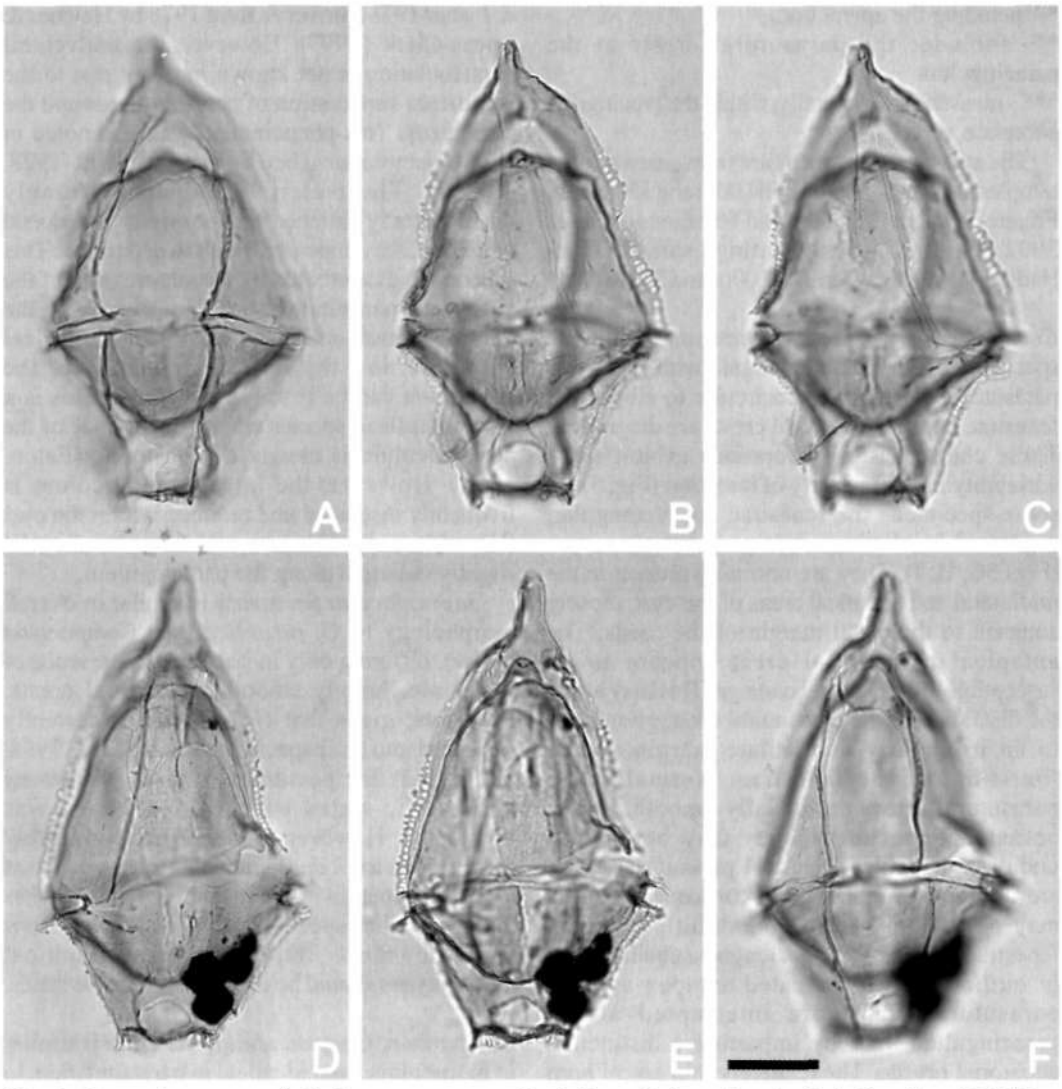

Fig. 7. Gonyaulacysta sp. cf. *G. fenestrata* sp. nov. Both from ditch cuttings in Peak-1 well at 1463.06m-1466.10m. All photomicrographs taken using plain transmitted light. Scale bar in Fig. 7F refers to all photomicrographs and is 25µm. Note short, solid denticles surmounting the fenestrate parasutural crests, best developed in the midlateral areas. A-C - CPC 35683; dorsal view, high to low focus sequence. Note bicavate cyst organisation, close resemblance to *Gonyaulacysta fenestrata* and small denticles on distal part of midlateral parasutural crests. The denticles are best seen in Figs 7B-C. D-F - CPC 35684 (see also Fig. 6C); ventral view, high to low focus sequence. Note pyrite crystals in hypocyst and denticles surmounting midlateral parasutural crests. The denticles are best seen in Figs 7D-E.

1978) Lentin & Vozzhennikova 1990 and *G. eisenackii* (Deflandre 1939) Górka 1965 have epicysts and hypocysts of approximately equal length and denticulate parasutural crests. For the same reasons, *G. fenestrata* differs from *G. jurassica* subsp. *jurassica* which also lacks fenestrate parasutural crests. The latter Late Jurassic subspecies, with densely denticulate parasutural crests, has smaller epipericoels and hypopericoels and is significantly smaller in overall size than *G. fenestrata* (see Deflandre, 1939). In terms of overall size and epicystal morphology, the variety of *G. jurassica* which is closest to *G. fenestrata* is *G. jurassica* subsp. *adecta* Sarjeant 1982 var. *longicornis* (Deflandre 1938) Downie & Sarjeant 1965. This large, elongate morphotype is characteristic of the mid Oxfordian in Europe (Riding & Thomas, 1997, figs 3, 5h, 5k), but is epicavate and has strongly denticulate parasutural crests. An example of a denticulate parasutural

crest of *G. jurassica* subsp. *adecta* is figured as Fig. 6E.

Gonyaulacysta fenestrata differs from *G.* sp. cf. *fenestrata* (see below) in having smooth distal margins to the parasutural crests. Figure 6 illustrates the differences in the parasutural crest morphology of *G. fenestrata*, *G.* sp. cf. *G. fenestrata*, *G. dualis* and *G. jurassica* subsp. *adecta*.

Derivation of name. From the Latin *fenestra*, meaning window, and referring to the window-like holes or perforations in the distal parts of the parasutural crests in this species.

Holotype and type locality. Figure 5D, CPC 35676, Buang-1 well, sidewall core sample at 3504.00m.

Stratigraphical distribution. *Gonyaulacysta fenestrata* ranges from the Kimmeridgian mid *Dingodinium swanense* Zone (6aiia) to the Tithonian *Cribroperidinium perforans* Zone (5d) in the Timor Sea region (Foster, this volume; Helby & Partridge, in prep.). Identical forms were illustrated as *G. dualis* from the Chichali and Sembar formations of Pakistan (Beju, 1979, pl. 1, figs 6, 7; 1980).

Gonyaulacysta sp. cf. G. fenestrata Riding & Helby (Figs 6C, 7A-F)

1978 *Gonyaulacysta jurassica* (Deflandre 1939) Norris & Sarjeant 1965; Chen, fig. 16-1-7.
1987 *Gonyaulacysta jurassica* (Deflandre 1939) Norris & Sarjeant 1965; Davey, pl. 4, figs 14, 15.

Previous Australian usage
Gonyaulacysta oligodentata (pars) – Helby.

Description. This morphotype has the same morphology as *Gonyaulacysta fenestrata*, except that the distal parts of the parasutural crests are wholly or partially ornamented by short (1μm), solid denticles.

Dimensions (μm; n=2):
Length of pericyst: 135, 136
Length of apical horn: 11, 20
Length of epipericyst (excl. paracingulum)*: 78, 85
Length (height) of paracingulum: 5, 5
Length of hypopericyst (excl. paracingulum): 52, 46
Length of endocyst: 80, 93
Width of pericyst at paracingulum**: 80, 81
Width of endocyst at paracingulum: 70, 70
Height of parasutural crests***: 2, 3; 4, 5
Diameter of fenestrae: 0.5-2.0
Length of distal denticles: 1
*- including the apical horn
**- includes the parasutural crests at the paracingulum
***- measured midlaterally, within the precingular paraplate series

The measured specimens are from a ditch cuttings sample from Peak-1 well between 4800.00m and 4810.00m.

Comments. *Gonyaulacysta* sp. cf. *G. fenestrata* can be misidentified as *G. fenestrata* because the denticles surmounting the parasutural crests are small and they may be developed only on parts of some of the crests. Figures 6C and 7 illustrate the differences in the crest morphology of this morphotype. Insufficient material exists to erect this form as a species, subspecies or variety. This morphotype is similar in all dimensions to *Gonyaulacysta fenestrata* (see above).

Stratigraphical distribution. *Gonyaulacysta* sp. cf. *G. fenestrata* is known from the Kimmeridgian, mid *Dingodinium swanense* Zone (6aiia) to the Tithonian, *Cribroperidinium perforans* Zone (5d) in the Timor Sea region (Foster, this volume; Helby & Partridge, in prep.). It was recorded by Davey (1987) as *Gonyaulacysta jurassica* from the Imburu Mudstone of Papua New Guinea (late Oxfordian to early Kimmeridgian *Cribroperidinium perforans* Zone to *Omatia montgomeryi* Zone). Identical forms were recorded as *G. jurassica* (Fig. 16, 1-7) from Late Jurassic ditch cuttings in the Ankamotra-1 well in western Madagascar (Chen, 1978).

Hadriana gen. nov.

Type species. *Hadriana cincta* sp. nov.

Diagnosis. Large dinoflagellate cysts which comprise a subspherical to ellipsoidal cyst body. A prominent ectophragm, which is perforate to trabeculate and is open antapically, emerges in the lower part of the precingular paraplate series and extends below the cyst body. The ectophragm may be connected to the cyst body by paracingular (?) and postcingular processes. The ectophragm and autophragm are closely appressed in the apical paraplate series. The paratabulation is gonyaulacalean, indicated by the intratabular processes, where developed, and the

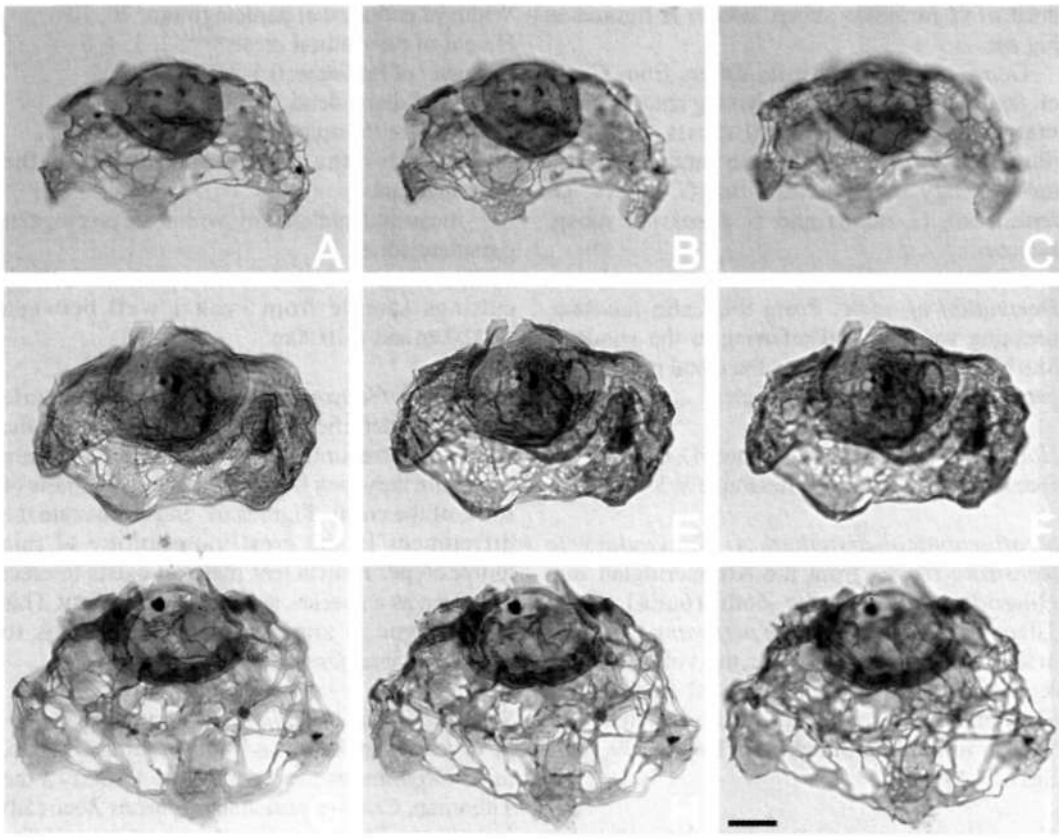

Fig. 8. Hadriana cincta sp. nov. All from ditch cuttings in Hadrian-1 well at 3285.00m-3300.00m. All photomicrographs taken using plain transmitted light. Scale bar in Fig. 8I refers to all photomicrographs and represents 25µm. Figs 8G-I are the holotype; the remainder (Figs 8A-F), paratypes. All in dorsoventral view. Note wide, ellipsoidal cyst body, prominent broad, variably perforate, trabeculate ectophragmal girdle which emerges from equatorial part of cyst body, and intratabular paracingular and precingular processes. A-C - CPC 35685; ventral view, high to low focus sequence. Note characteristically undulating antapical margin of ectophragmal girdle, due to five polygonal areas of ectophragm relatively free of perforations reflecting postcingular paraplates. D-F - CPC 35686; dorsal view, high to low focus sequence. Note apical archaeopyle and variably perforate ectophragmal girdle. G-I - CPC 35687; ventral view, high to low focus sequence. Note trabeculate, rather than perforate, ectophragm. Note how ectophragmal girdle emerges equatorially on cyst body and prominent polygonal areas of ectophragm reflecting postcingular paraplates.

principal archaeopyle suture. Apical archaeopyle; operculum free. The parasulcus is flat to slightly indented.

Comments. *Hadriana* is a large, morphologically complicated, variable and extremely distinctive genus. It is similar in many respects to *Belowia* Riding & Helby (this volume) and it seems likely that the Tithonian *Belowia* may have evolved from *Hadriana* (Riding & Helby, this volume, b). Both *Belowia* and *Hadriana* are thought to be related to *Rigaudella* Below 1982 (see *Comparison* of *Hadriana cincta*, below). The ectophragm is highly variable, from perforate to trabeculate and it may be connected to the autophragm of the cyst body by intratabular processes in the paracingular (?) and postcingular paraplate series. A large, subcircular to ellipsoidal, antapical hole is generally present in the ectophragm, which separates from the autophragm close to the base of the precingular paraplate series. Therefore, the ectophragm forms an extensive belt or girdle, surrounding all of the hypocystal autophragm.

Comparison. The Tithonian *Belowia* Riding & Helby (this volume) is closely related to *Hadriana*. They share a small, essentially smooth epicyst, devoid of processes and the fact that wall separation occurs close to the base of the precingular paraplates. Although there are marked hypocystal differences, these genera both display major ectophragmal development at and below

the paracingulum. However, *Hadriana* lacks the paracingular tunnel, which characterises all morphotypes of *Belowia*; it does not display large processes and the ectophragm is widely open antapically (around twice diameter of autocyst).

Eatonicysta Stover & Evitt 1978 emend. Stover & Williams 1995 is reminiscent of *Hadriana* in having an apical archaeopyle and a large ectophragmal covering supported by intratabular processes in all the major paraplate series. However, *Hadriana* is larger, oblate and lacks epicystal processes and reduced hypocystal processes. The ectophragm in *Hadriana* is generally open antapically. *Reticulatosphaera* Matsuoka 1983 is also similar in morphology to *Hadriana*, however the former is smaller, has a precingular archaeopyle and has about 26, apparently intratabular processes. The periphragm of *Disphaeria* Cookson & Eisenack 1960 emend. Norvick 1973 has a large dorsal opening, and this genus has a precingular archaeopyle. *Hadriana* differs from trabeculate complex chorate dinoflagellate cyst genera such as *Adnatosphaeridium* Williams & Downie 1966, *Hapsidaulax* Sarjeant 1975, *Hystrichosphaerina* Alberti 1961, *Polystephanephorus* Sarjeant 1961 and *Rigaudella* Deflandre emend. Below 1982, in lacking large intratabular processes or process complexes representing the major epicystal paraplate series and in having a dense equatorial trabeculum. In *Hadriana*, the paracingular and postcingular processes are largely subsumed into the ectophragm. The Palaeogene genus *Riculacysta* Stover 1977, like *Hadriana*, has a trabeculate ectophragm especially well developed on the hypocyst and an apical archaeopyle (Stover, 1977). *Riculacysta*, however, is a distinctly chorate form, which bears solid processes on the ventrolateral and lateral surfaces.

Derivation of name. After Hadrian-1 well, where the type material was recovered.

Hadriana cincta sp. nov. (Figs 8A-I, 9A-L)

1978 *Adnatosphaeridium* sp.; Chen, p. 78, fig. 55-431.

Previous Australian usage
MP 528 – Helby.
?*Rigaudella* sp. A – Parker (1986, pl. 22, figs 1, 2).

Description. A species of *Hadriana* which is slightly dorsoventrally flattened and flat to slightly indented at the parasulcus. It has an ellipsoidal cyst body, which is consistently wider than long. The autophragm is smooth to microscabrate and 1-1.5µm thick. The prominent perforate to trabeculate ectophragm is also significantly wider than long, imparting a squat shape to many specimens; it is smooth and 0.5-1µm thick. For the most part the epicystal wall is generally not obviously layered. However, an ectocoel opens near the base of the precingular paraplate series and spreads, girdle-like, posteriorly from the paracingular region and generally leaving a wide polar opening. The ectophragm is connected to the cyst body by short postcingular and paracingular processes which may be intratabular in location. The processes are solid and expand proximally. They also expand distally where they are subsumed into the ectophragm. There is a characteristic gap, which is widest in the interprocess areas, between the top of the ectophragm and the cyst body in polar view. The trabecular girdle is widest close to the base of the autophragm, narrowing marginally antapically. The antapical hole in the ectophragm is large and ellipsoidal in shape; it is located well below the antapex of the autocyst. The margin is interrupted by five distinctive polygonal areas of ectophragm which are relatively free of perforations, or have small (<1µm in diameter) lacunae. These reflect the postcingular paraplates. The ectophragm is highly variable in morphology. It may be perforate with subcircular/ellipsoidal lacunae from 1 to 8µm in diameter. Alternatively, many specimens are largely trabeculate with a network of anastomosing solid, slender, ribbon-like elements. These elements are normally between 1.5 and 4µm, but occasionally may attain 10µm in width. Rarely, individuals are partially perforate and partially trabeculate.

Dimensions (µm; n=40): Min. (Mean) Max.
Length of ectocyst (excl. operculum): 84 (106) 140
Length of autocyst (excl. operculum): 46 (61) 79
Dorsoventral width of ectocyst: 114 (141) 181
Dorsoventral width of autocyst: 57 (72) 93
Lateral width of ectocyst: 101 (112) 145
Lateral width of autocyst: 58 (65) 75
Width of ectocoel at antapex: 12 (36) 76
Width of ectocoel in the postcingular series: 30 (45) 73
Height of postcingular processes: 7 (14) 22

The measured specimens are from a ditch cuttings sample in Hadrian-1 well between 3285.00m and 3300.00m and a sidewall core sample at 3087.00m from Cockell-1 well.

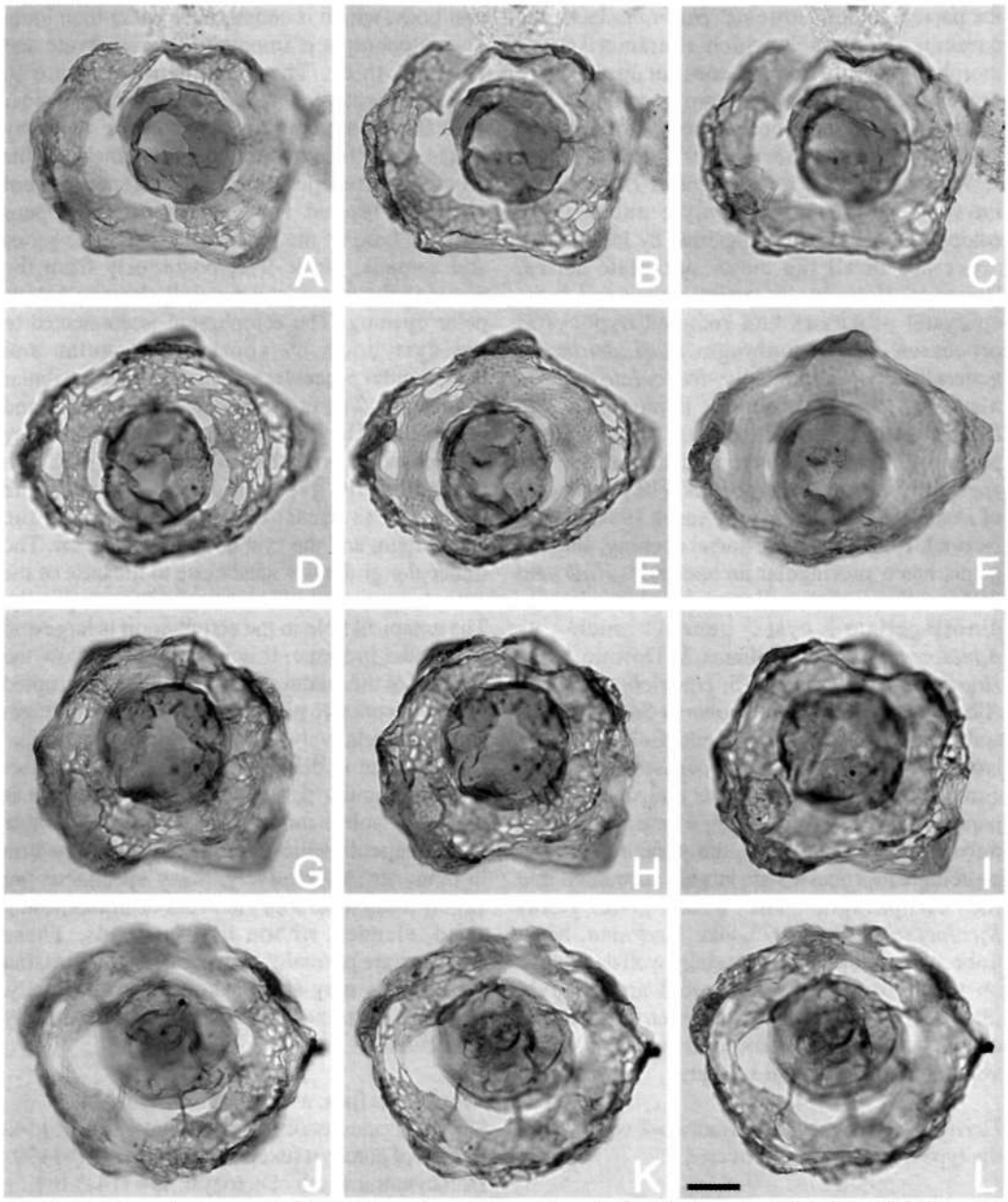

Fig. 9. Hadriana cincta sp. nov. All paratypes from ditch cuttings in Hadrian-1 well at 3285.00m-3300.00m. All photomicrographs taken using plain transmitted light. Scale bar in Fig. 9L refers to all photomicrographs and is 25µm. Note subcircular outline of cyst body, prominent broad, ellipsoidal to polygonal, perforate/trabeculate ectophragmal girdle, large antapical hole in ectophragm and intratabular paracingular and precingular processes. All in polar view. Figs 9A-I appear to have a precingular, type 3P, endoarchaeopyle due to folding of principal endoarchaeopyle suture so it appears subquadrangular. This is a preservational artefact; this genus has an apical archaeopyle. A-C - CPC 35688; apical view, high to low focus sequence. Note apical archaeopyle, slightly, indented ventral (parasulcal) area and solid intratabular processes which connect autophragm to ectophragm. D-F - CPC 35689; antapical view, low to high focus sequence. Note antapical hole in ectophragm, variably perforate ectophragm and polygonal areas of ectophragm reflecting postcingular paraplates located on antapical margin of ectophragm. G-I - CPC 35690; apical view, high to low focus sequence. Note distinctly perforate, rather than trabeculate, ectophragm, prominently indented parasulcus and solid intratabular processes emerging from cyst body. J-L - CPC 35691; apical view, high to low focus sequence. Note good intratabular process development and large antapical hole in ectophragm.

Comments. Most of the material studied are loisthocysts (Figs 8, 9). The longitudinal flattening of the cyst body is consistent and is a good recognitional criterion in poorly preserved material. The most characteristic feature of this species is the prominent and variable girdle-like ectophragm, which emerges close to the base of the precingular paraplate series. This ectophragm overlies the hypocystal autophragm and is open antapically. The antapical margin of the ectophragm in dorsoventral view is characteristically interrupted due to the occurrence of the postcingular 'nodes' (Fig. 8). The paracingular and postcingular processes are variable. The majority are solid; but a few appear to be funnel-like. There is a tendency for the solid processes to break. The processes are best observed in polar view (Fig. 9).

Comparison. Hadriana cincta is broadly similar to *Belowia baltea* Riding & Helby (this volume) in size and overall morphology. However, *B. baltea* is generally compressed in polar view, has a paracingular protuberance and commonly, a solid antapical girdle. It is distinguished from large chorate cysts with apical archaeopyles in lacking large intratabular processes and process complexes. Because of the general morphological similarities in *Belowia, Hadriana* and *Rigaudella*, it is suggested that they are closely related and probably form part of a phylogenetic lineage. The rootstock is envisioned to be *Rigaudella*, which then evolved into the Kimmeridgian genus *Hadriana*, which gave rise to *Belowia* in the Tithonian (Riding & Helby, this volume, b).

Derivation of name. From the Latin *cinctum* meaning girdle, or zone, and referring to the characteristic, extensive, skirt-like development of ectophragm which emerges on the epicyst and extends beyond the antapex of the cyst body.

Holotype and type locality. Figs 8G-I, CPC 35687, Hadrian-1 well, ditch cuttings between 3285.00m and 3300.00m.

Stratigraphical distribution. Hadriana cincta has been recorded from the Kimmeridgian *Dingodinium swanense* Zone (6aiia) to the Tithonian *Cribroperidinium perforans* Zone (5d) in Australia and Papua New Guinea (Foster, this volume; Helby & Partridge, in prep.). It is recorded as *Adnatosphaeridium* sp. from Late Jurassic ditch cuttings in the Ankamotra-1 well in western Madagascar (Chen, 1978). It is also recorded as *Thalassiphora* sp. from the Sembar Formation of Pakistan (Beju, 1979, pl. 32, figs 4-6; 1980).

Indodinium Kumar 1986

Type species. Indodinium khariense Kumar 1986

Indodinium khariense Kumar 1986 emend. (Figs. 10A-P)

1978 *Hexagonifera* sp. 3; Chen, p. 57, fig. 43-287-293.
1986 *Indodinium khariense*; Kumar, p. 389-391, figs 5A-B, pl. 4, figs 2,3.
1987 *Indodinium kharensis* Kumar; Garg *et al.*, p.256.
1988 *Indodinium* sp. A; Helby *et al.*, figs 6B, 15U, 15V, 18F.
1992 *?Indodinium khariense* Kumar; Jiang *et al.*, p. 83, 84, pl. 2, figs 7, 9, 13.

Previous Australian usage
Diplotesta nodosus - Ott (1970, pl. 17, fig. 40).
MP 727 – Helby.
Indodinium sp. 727 – Helby.

Emended description. A species of *Indodinium*, intermediate in size, which is dorsoventrally flattened. It has a thin (<0.5µm), smooth to microscabrate periphragm, which may exhibit a partial gonyaulacalean paratabulation pattern by discontinuous low, smooth ridges or folds. The paracingulum is frequently indicated by ridges or folds and is positioned close to the centre of the cyst. The parasulcus, precingular and postcingular paraplates may also be partially indicated. An apical horn is present. The endophragmal horn usually comprises a low pyramidal apical series, which passes into a solid, slender apical extension. The periphragmal horn is considerably larger, does not mirror the shape of the endophragmal horn and the pericoel is particularly wide in this region. The pericoel is narrowest at the antapex or the two cyst wall layers may be closely appressed in this region. Endophragm relatively thick (1-1.5µm), smooth, scabrate granulate, verrucate or baculate. It may also be partially echinate with short (2-3µm), solid, distally pointed spinules occasionally developed at the antapex, the apex and the principal endoarchaeopyle suture. These spinules may be aligned along parasutures on the endophragm. The antapical portion of the endophragm is rarely baculate or may have densely inserted ornamentation which forms a corona. Prominent accessory archaeopyle sutures

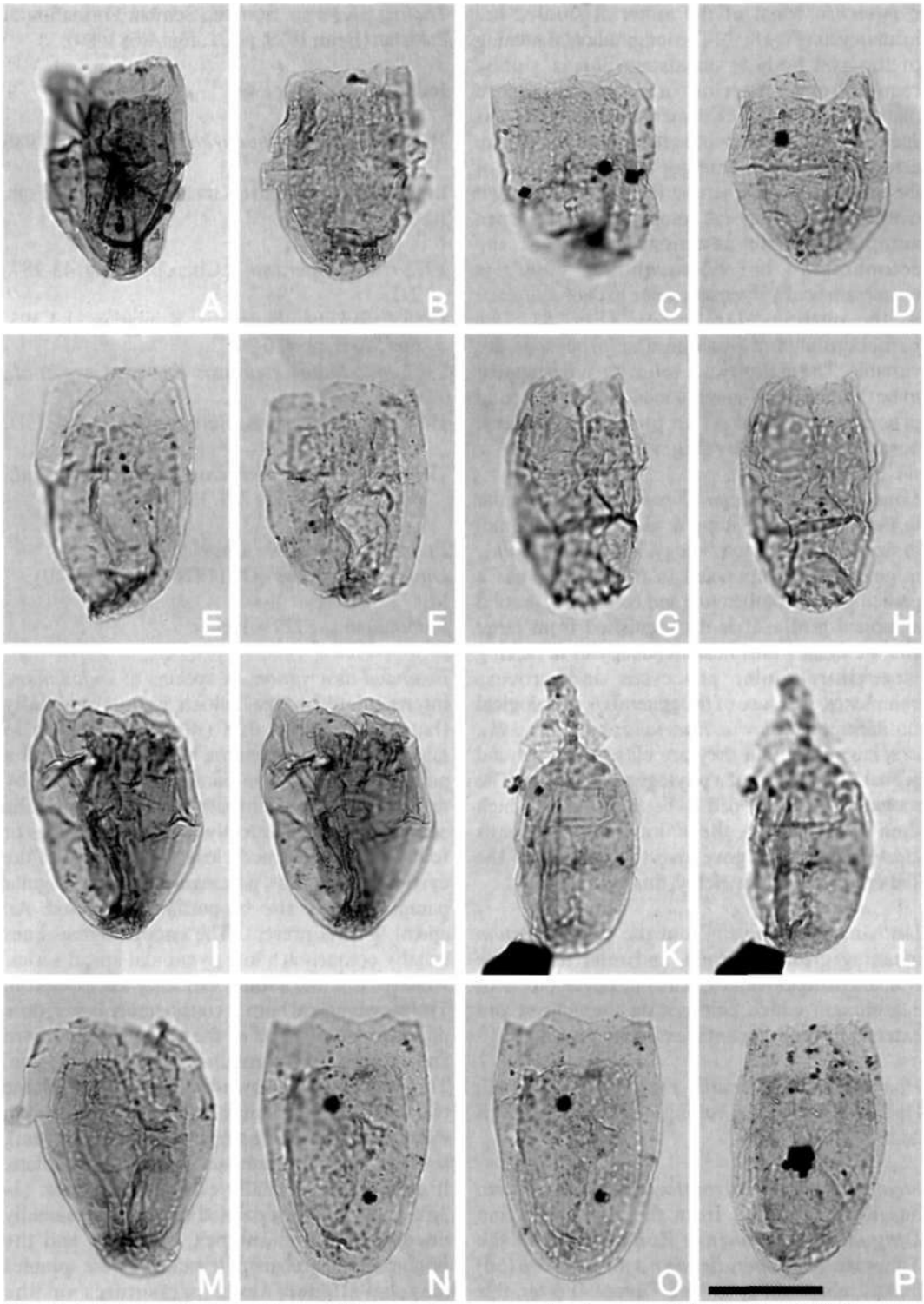

Fig. 10. Indodinium khariense Kumar 1986 emend. From conventional core in Alaria-1 well at 3315.95m (Figs 10B-D, G-H, P), 3317.26m (Figs 10F, K-L) and 3318.58m (Figs 10E, N-O), sidewall core in Buang-1 well at 3504.00m and outcrop material from Misool, eastern Indonesia (Figs 10A, I-J). All photomicrographs taken using plain transmitted light. Fig. 10F is a composite photomicrograph. The scale bar in Fig. 10P refers to all photomicrographs and is 25µm. Note elongate nature, apical archaeopyle, partially (continued opposite)

may be developed in the endophragm. The principal periarchaeopyle suture is consistently higher than the principal endoarchaeopyle suture, typically by approximately 5µm.

Dimensions (µm; n=25): Min. (Mean) Max.
Length of pericyst excl. operculum: 40 (55) 65
Length of endocyst excl. operculum: 34 (45) 56
Width of pericyst at paracingulum: 30 (36) 44
Width of endocyst at paracingulum: 22 (28) 38
Maximum width of lateral pericoel: 3 (5) 10

A single specimen with an attached operculum was encountered (Figs 10K-L). The entire pericyst of this specimen from conventional core in Alaria-1 well at 3317.26m is 72µm long and the full endocyst 65µm in length.

The measured specimens are from conventional core samples from Alaria-1 well at 3318.58m, 3317.26m and 3315.95m, sidewall core samples from Buang-1 and Tenacious-1 wells at 3504.00m and 3002.00m respectively and outcrop material from the lower part of the Lelinta Formation of Misool, eastern Indonesia.

Comments. The specific description of *Indodinium khariense* is emended here in order to note several features. These are the apical horn, the prominent accessory endoarchaeopyle sutures, the characteristic substantial displacement of the two archaeopyle sutures and the presence and variability of the endophragmal ornamentation. The antapical displacement of the endocyst (Fig. 10) suggests that there is no ventral contact between the two wall layers. Kumar (1986) did not mention these features in the type material from the Jhuran Formation (Lower Kimmeridgian-Tithonian) of Kachchh, western India. The apical horn formed by the endophragm may be up to 15µm long and was also illustrated by Jiang *et al.* (1992, pl. 2, fig. 13). Commonly, the endophragm is sparsely granulate; however, the ornamentation is variable in both morphology and density of insertion (Fig. 10). Strongly granulate or verrucate forms tend not to be echinate. The antapical portion of the endophragm is frequently strongly ornamented. It may be baculate (Figs 10B, N-O), or may have dense ornamentation, forming a corona (Figs 10G-H). The marked separation of the two principal archaeopyle sutures in this form is a valuable diagnostic criterion and the profound dorsoventral flattening of this species often makes orientation difficult.

Comparison. Indodinium khariense differs from *Mombasadinium parvelatum* (Jiang in Jiang *et al.* 1992) comb. nov., emend. (see below) in having a prominent apical horn. The latter is also slightly wider than *I. khariense*. Jiang (in Jiang *et al.* 1992, p. 85) stated that *I? parvelatum* may exhibit solid processes, which may be parasutural, surmounting the endophragm, commonly at the antapex. Such processes may be present in *I. khariense*, but Jiang (in Jiang *et al.* 1992, pl. 2, fig. 10) did not convincingly illustrate this feature.

Stratigraphical distribution. Indodinium khariense has been recorded from the Oxfordian *Wanaea clathrata* Zone (6b) to the Tithonian *Cribroperidinium perforans* Zone (5d) in the Timor Sea region and Misool, eastern Indonesia (Foster, this volume; Helby & Partridge, in prep.). Chen (1978, figs 43, 287-293) illustrated identical forms as *Hexagonifera* sp. 3. from Late Jurassic ditch cuttings in the Ankamotra-1 well in western Madagascar. Kumar (1986) reported the species from the Middle Member of the Jhuran Formation of western India and it has been recorded from the Oxfordian to Tithonian Ohineruru Siltstone, Kinohaku Siltstone and Puti Siltstone of New Zealand (Helby *et al.*, 1988).

Mombasadinium gen. nov.

Type species. Mombasadinium parvelatum (Jiang

---

paratabulate nature, narrow antapical pericoel and that principal periarchaeopyle suture is significantly higher than principal endoarchaeopyle suture. A - CPC 35692; dorsal view, median focus. Note wide pericoel at antapex. B - CPC 35693; ventral view, median focus. Note wide equatorial part of cyst. C - CPC 35694; dorsal view, high/median focus. Note distinctly echinate nature of endophragm in top left corner. D - CPC 35695; dorsal view, low focus. Note rounded elongate outline. E - CPC 35696; ventral view, median focus. Note marked difference in positions of principal periarchaeopyle suture and principal endoarchaeopyle suture. F - CPC 35697; ventral view. Note the relatively wide pericoel. G, H - CPC 35698; ventral view, median and low focus respectively. Elongate; note antapical ornamentation. I, J - CPC 35699; dorsal view, median and low focus respectively. Note narrow pericoel at antapex. K, L - Woodside Petroleum collections, Perth, WA; dorsal view, high and median/low focus respectively. Note prominent apical horn. M - CPC 35700; ventral view, median focus. Note echinate nature of endophragm in top left corner. N, O - CPC 35701; ventral view, high and low focus respectively. Note wide pericoel and significant difference in positions of the principal periarchaeopyle suture and principal endoarchaeopyle suture. P - CPC 35702; ventral view, median focus. Note narrow pericoel.

in Jiang *et al.* 1992) comb. nov., emend.

Diagnosis. Proximate, circumcavate dinoflagellate cysts, elongate ellipsoidal in outline, lacking polar horns and being intermediate in size. Periphragm smooth, endophragm smooth or bearing low relief ornamentation. Standard gonyaulacalean paratabulation partially to fully indicated by periphragmal folds. Paracingulum and parasulcus may be indicated by folds in the periphragm. Archaeopyle apical; operculum simple, free.

Comments. The genotype was originally described as *?Indodinium parvelatum* Jiang (in Jiang *et al.* 1992). A re-examination of the type material and the study of new material from offshore northwestern Australia and Misool, eastern Indonesia has indicated that this species does not belong to *Indodinium* (see below).

Comparison. *Mombasadinium* closely resembles *Indodinium* in shape and size, but the latter has an apical horn and an endophragm which is typically ornamented and may be echinate, having parasutural spinules. Additionally, in loisthocysts of *Indodinium khariense*, the endocyst is significantly shorter than the pericyst due to the principal periarchaeopyle suture being consistently significantly higher than the principal endoarchaeopyle suture (see above, Fig. 10 and Jiang *et al*, 1992, pl. 2, fig. 7). Additionally, this new genus is similar to *Craspedodinium* in morphology. However, *Craspedodinium* is not elongate and may be large in size. This new genus is broadly similar to *Belodinium* Cookson & Eisenack 1960 emend. Stover & Helby 1987, but *Mombasadinium* lacks the prominent endophragmal processes, the prominent apical horn and the diagnostic claustrum representing the antapical paraplate, which characterise the former. *Boreocysta* Stover & Evitt 1978 emend. Århus 1992 is superficially similar, but is holocavate, has no paratabulation apart from the principal archaeopyle suture and exhibits a prominent apical horn. The holocavate genus *Gardodinium* Alberti 1961 emend. Harding 1996 resembles *Mombasadinium*, but has an apical horn. *Wallodinium* Loeblich & Loeblich 1968 emend. Riding 1994 is elongate, lacks polar horns, has an apical archaeopyle and may be circumcavate. However, unlike *Mombasadinium*, most species of *Wallodinium* are bicavate and have no parasutural features other than relating to the archaeopyle. *Lagenadinium* Piel 1985 is a Jurassic genus which is slightly elongate and has an apical archaeopyle. It differs from *Mombasadinium* by being holocavate, lacking parasutural features and having hypocystal coronas. The Cretaceous *Carpodinium* Cookson & Eisenack 1962 emend. Leffingwell & Morgan 1977 is, like *Mombasadinium*, elongate with prominent periphragmal folds, but has a precingular archaeopyle and may be suturocavate.

Fig. 11. Mombasadinium parvelatum (Jiang in Jiang *et al.* 1992) comb. nov. From conventional core in Peak-1 well at 4302.00m (Figs 11A-B, H, K-N, S, W-Y) and sidewall cores in Macedon-5 well at 1350.00m (Fig. 11O) and Scafell-1 well at 1365.00m (Fig. 11J). Figs 11G, I, T-V are from outcrop sample 81FH66, Misool, eastern Indonesia (Hasibuan, 1990). Figs 11P-Q (the holotype) and Figs 11C-F, R (topotypes) are from Mto Panga Quarry, Kenya. All photomicrographs taken using plain transmitted light. Scale bar in Fig. 11Y refers to all photomicrographs and is 25µm. Note thick endophragm, thin, diaphanous, folded periphragm, narrow pericoel, occasional parasutural periphragmal folds and apical archaeopyle. A, B - CPC 35703; dorsal view, high and low focus respectively. Note angular principal archaeopyle suture, clearly indicating a gonyaulacalean paratabulation pattern. C - University of Sheffield ML 2155-J21/1, topotype; dorsal view, high focus. Note narrow pericoel and sparse antapical processes or thickenings within periphragmal folds. D - University of Sheffield ML 2155-R23, topotype; ventral view, median focus. Note longitudinal periphragmal folds. E - University of Sheffield ML 2155-J27, topotype; oblique ventral view, median focus. Note parasutural folds in periphragm. F - University of Sheffield ML 2155-L39, topotype; ventral view, high/median focus. Note parasulcal notch. G - CPC 35704; dorsal view, median focus. Note lack of periphragm, possibly due to chemico-mechanical damage. H - CPC 35705; ventral view, low focus. Note processes or thickenings within periphragmal folds on hypocyst. I - CPC 35706; ventral view, median focus. Note narrow pericoel. J - CPC 35707; dorsal view, median focus. Note smooth endophragm. K - CPC 35708; ventral view, high focus. Note apparently paracingular folds on periphragm. L, M - CPC 35709; slightly oblique dorsal view, high and median focus respectively. Note short, dark processes or thickenings within periphragmal folds on hypocyst. N - CPC 35710; dorsal view, median focus. Note relatively wide pericoel on right hand side. O - CPC 35711; dorsal view, median focus. Short; note parasutural folds. P, Q - University of Sheffield ML 2155-V60/1, holotype; dorsal view, high and median focus respectively. Note adherent operculum and wide pericoel. R - University of Sheffield ML 2155-D35, topotype; ventral view, median focus. Note dark nature and apparent lack of periphragm in midlateral areas. S - CPC 35712; ventral view, high focus. Note prominent, long periphragmal fold which appears not to be parasutural. T - CPC 35713; ventral view, median focus. Note discontinuous periphragmal folds. U - CPC 35714; dorsal view, (continued opposite)

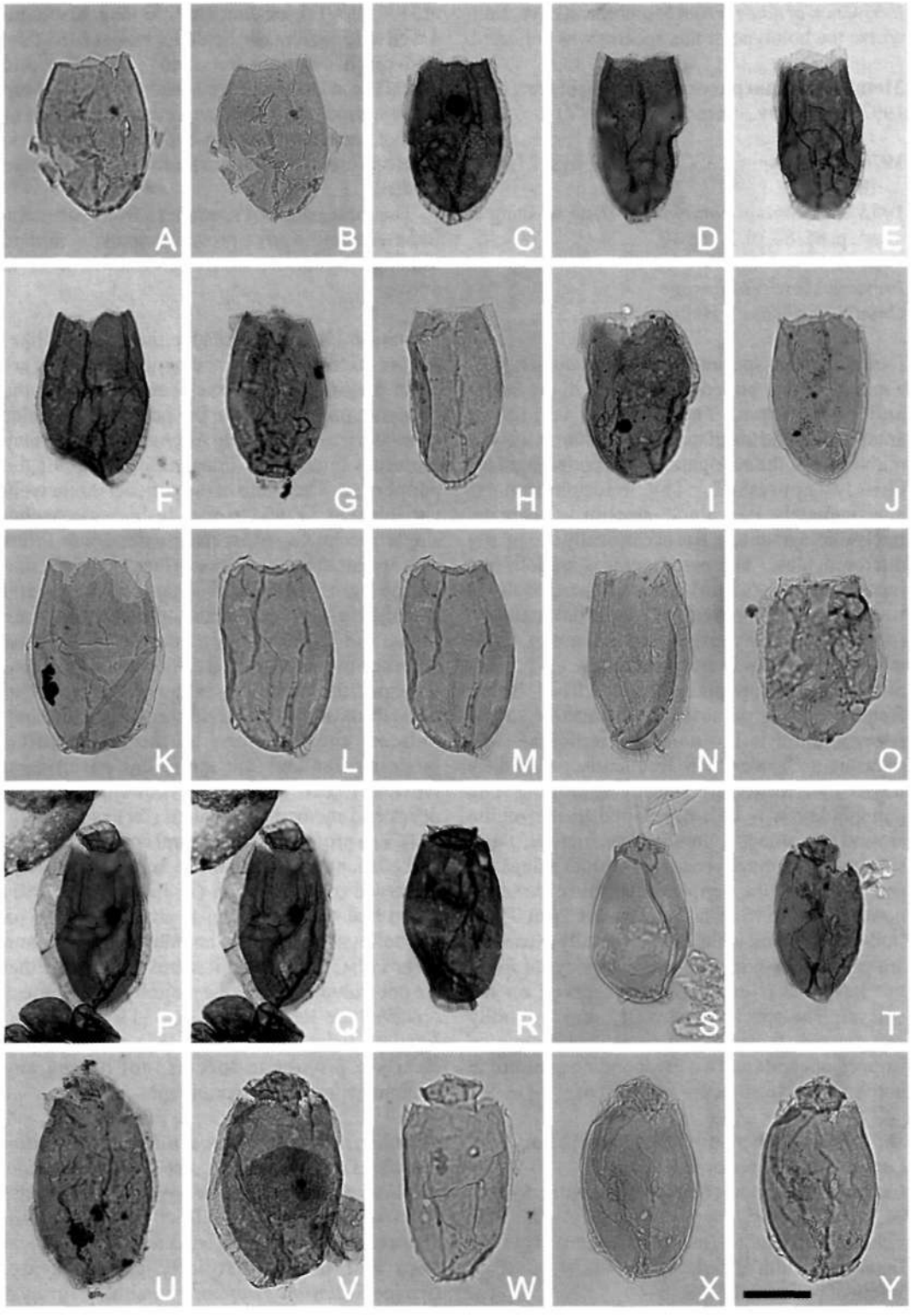

high focus. Large specimen. V - CPC 35715; ventral view, high focus. Note well preserved, adherent operculum. W - CPC 35716; ventral view, median focus. Unusually elongate. X, Y - CPC 35717; dorsal view, high and median focus respectively. Note short processes or thickenings within periphragmal folds on hypocyst.

Derivation of name. From Mombasa, Kenya, from where the holotype of this species was collected.

Mombasadinium parvelatum (Jiang in Jiang *et al.* 1992) comb. nov., emend. (Figs 11A-Y)

1978 *Belodinium* sp. 3; Chen, p. 31, figs. 27 – 98-100.
1992 ?*Indodinium parvelatum*; Jiang in Jiang *et al.*, p. 85, 87, pl. 2, fig. 10.

Previous Australian usage
Omatia jurabiana – Helby.

Description. A species of *Mombasadinium* with a relatively thin pericoel developed in the lateral and polar areas. The pericoel is highest antapically and midlaterally. Middorsally and midventrally, the endophragm and periphragm are closely appressed. The endophragm is approximately 1µm thick, smooth to scabrate, rarely microgranulate; it is occasionally irregularly microreticulate. The periphragm is smooth and much thinner (<0.5µm) and also occasionally is irregularly microreticulate. A partial standard (presumed sexiform) gonyaulacalean paratabulation pattern is marked by low (1-2.5µm), distally smooth, periphragmal folds. The folds are frequently low or absent equatorially so the paracingulum is not normally indicated. The parasulcus, however, is frequently marked by these low folds in the periphragm. The paratabulation is best developed in the region around the antapex. In some specimens, dark, slender, parasutural processes or thickenings are present within the periphragmal folds; these are normally c.1µm wide, but may attain c.2µm. These 'rod-like' features, which may be distally expanded, are particularly common in the hypocystal folds, but have occasionally been observed on the epicyst. The species is strongly dorsoventrally compressed. A prominent parasulcal tongue on isolated opercula and a corresponding parasutural notch on the loisthocyst are present.

Dimensions (µm; n=80): Min. (Mean) Max.
Length of entire pericyst: 60 (77) 90
Length of loisthocyst (incl. periphragm): 53 (70) 90
Length of operculum (incl. periphragm): 8 (13) 19
Equatorial width of pericyst: 33 (43) 54
Width of pericoel: 1 (3) 8

The measured specimens are from core samples from Alaria-1 well at 3315.95m and Peak-1 well at 4302.00m, sidewall core samples from Buang-1 well at 3504.00m, Frigate-1 well at 1233.00m, Macedon-5 well at 1350.00m and Scafell-1 well at 1365.00m and ditch cuttings between 3295.00m and 3300.00m in Hadrian-1 well. Additionally, outcrop material from the Tithonian Lelinta Formation of Misool, eastern Indonesia and the holotype and nineteen topotypes from Mombasa, Kenya were studied.

The dimensions of specimens from Australia, Indonesia and Kenya proved extremely similar, therefore the data has been aggregated in the table above.

Comments. It seems probable that the 'rod-like' features which occur in the hypocystal folds are short parasutural processes emerging from the endophragm, which have the periphragmal folds closely draped over them. Alternatively, they may represent interrupted linear thickenings of the periphragm. The width of the pericoel is relatively variable (Fig. 11) and frequently this varies within single specimens. In extreme cases some forms may appear to be camocavate (Fig. 11N). The thin periphragm has been mechanically torn and damaged in some specimens and in extremely rare cases, the entire pericyst may be torn away. Another parameter where there is significant intraspecific variability is the development of paratabulation. The periphragmal folds may indicate the positions of the precingular, postcingular and the antapical paraplates. However, the folds are frequently poorly developed and/or discontinuous (for example, Fig. 11J). The profound dorsoventral compression can make orientation difficult in relatively poorly-preserved material. Jiang (in Jiang *et al.*, 1992) stated that the operculum is attached, based on the holotype which has an adherent operculum (Figs 11P-Q). However, it seems more likely that the operculum is free as the majority of specimens observed are loisthocysts (Fig. 11). Contrary to Jiang (in Jiang *et al.*, 1992, p. 87), this species is clearly a proximate species, not having any ornamentation on the periphragm.

Comparison. *Mombasadinium parvelatum* resembles *Belodinium* spp., especially *B. nereidis* Stephens & Helby 1987 in having periphragmal folds which partially reflect paratabulation. However, *M. parvelatum* lacks an elongate apical horn and is not distinctly circumcavate. *Craspedodinium swanense* is similar in cyst organisation. However, *C. swanense* may be bicavate, is significantly larger than *Mombasadinium parvelatum*, is not elongate, has

an apical protuberance or boss, often exhibits accessory archaeopyle sutures and has a paracingulum indicated by periphragmal ornament (see above). *Indodinium khariense* has a distinct apical horn and frequently exhibits a paracingulum (see also *Comparison* relating to *Mombasadinium* above).

Fistulacysta simplex Davey 1987 closely resembles *Mombasadinium parvelatum* in morphology and dimensions. The two species also have the same stratigraphical ranges. Especially noteworthy are the similarities between the low, pre- and postcingular parasutural crests developed on the autophragm of *F. simplex* and the low parasutural folds on the periphragm of *M. parvelatum*. It seems likely that the crests of *F. simplex* are made of periphragm, which further strengthens the likeness. *Fistulacysta*, however, is an acavate genus and no separation of endophragm and periphragm is present. Despite this, it is possible that *Fistulacysta* is closely related to *Mombasadinium*.

Holotype and type locality. Figured specimen ML 2155-V60/1 on Slide MP26 (iv) (also marked 15804), 'England Finder' coordinate V60/1 of Jiang (in Jiang *et al*., 1992, pl. 2, fig. 10). Figured here as Figs 11P-Q. Housed in the type collection of the Centre for Palynology, University of Sheffield, Sheffield, U.K. From the Changamwe Shale Formation, Mto Panga Quarry, Bamburi Portland Cement Works, Freretown, near Mombasa, Kenya. The upper part of the Changamwe Shale Formation, which was sampled by Jiang *et al.* (1992), is late Kimmeridgian-early Tithonian (*Hybonoticeras beckeri* and *Hybonoticeras hybonotum* Tethyan ammonite zones) on ammonite evidence according to Verma & Westermann (1984). Jiang *et al.* (1992) reported this species to be confined to their Zone III(a), which they correlated to the late Kimmeridgian (*sensu anglico*) *Pectinatites elegans* ammonite zone, hence is close to the Kimmeridgian-Tithonian transition of Australia.

Stratigraphical distribution. *Mombasadinium parvelatum* has been recorded from the Kimmeridgian mid *Dingodinium swanense* Zone (6aii) to the Tithonian lower *Cribroperidinium perforans* Zone (5d) of Australia and Misool, eastern Indonesia (Foster, this volume; Helby & Partridge, in prep.). Identical forms were illustrated as *Belodinium* sp. 3 (fig. 27 – 98-100) from Late Jurassic ditch cuttings in Ankamotra-1 well in western Madagascar by Chen (1978) and *Sembaridinium sembari* from the Sembar Formation of Pakistan (Beju, 1979, pl. 22, figs 1-4; 1980). The species was originally described from the late Kimmeridgian-early Tithonian of Kenya (see *Holotype and type locality*, above).

Oligosphaeridium Davey & Williams 1966 emend. Davey 1982

Type species. *Oligosphaeridium complex* (White 1842) Davey & Williams 1966

Oligosphaeridium swanense sp. nov. (Figs 12A-F, 13A-C)

Previous Australian usage
M.P. 171 pars – Helby.
Oligosphaeridium swanense – Helby.

Description. A large species of *Oligosphaeridium* with long, tubiform intratabular (paraplate-centered) processes. The processes are formed by the periphragm only, vary considerably in width, are open distally and are deeply indented as a result of branching of up to three times. Branching typically first occurs at the mid-point of the process, where the tubular process bifurcates, or occasionally trifurcates. The resultant branches further bifurcate in a distal direction and there may be a final bifurcation at the distal extremities. The distal parts of the processes are sharply pointed and simple; trabeculation is not developed. This branching causes the distal portion of the processes to be significantly expanded. The long, rounded subtriangular notches caused by the branching may be deeper on the hypocyst than on the epicyst. Epicystal processes are also generally slightly smaller and possibly more slender, however the variation of process length on individual specimens is minor. The width of the processes varies significantly however; the majority of these elements are between 5 and 11µm. The processes are also slightly expanded proximally, where they are thickened, markedly striate and fibrous. Occasionally, processes are entirely longitudinally striated. Parasulcal processes are not normally developed. The autophragm, which comprises closely appressed periphragm and endophragm, on the cyst body is relatively robust, microscabrate to smooth, occasionally irregularly microreticulate. Accessory archaeopyle sutures may be developed, which deeply subdivide the precingular paraplates.

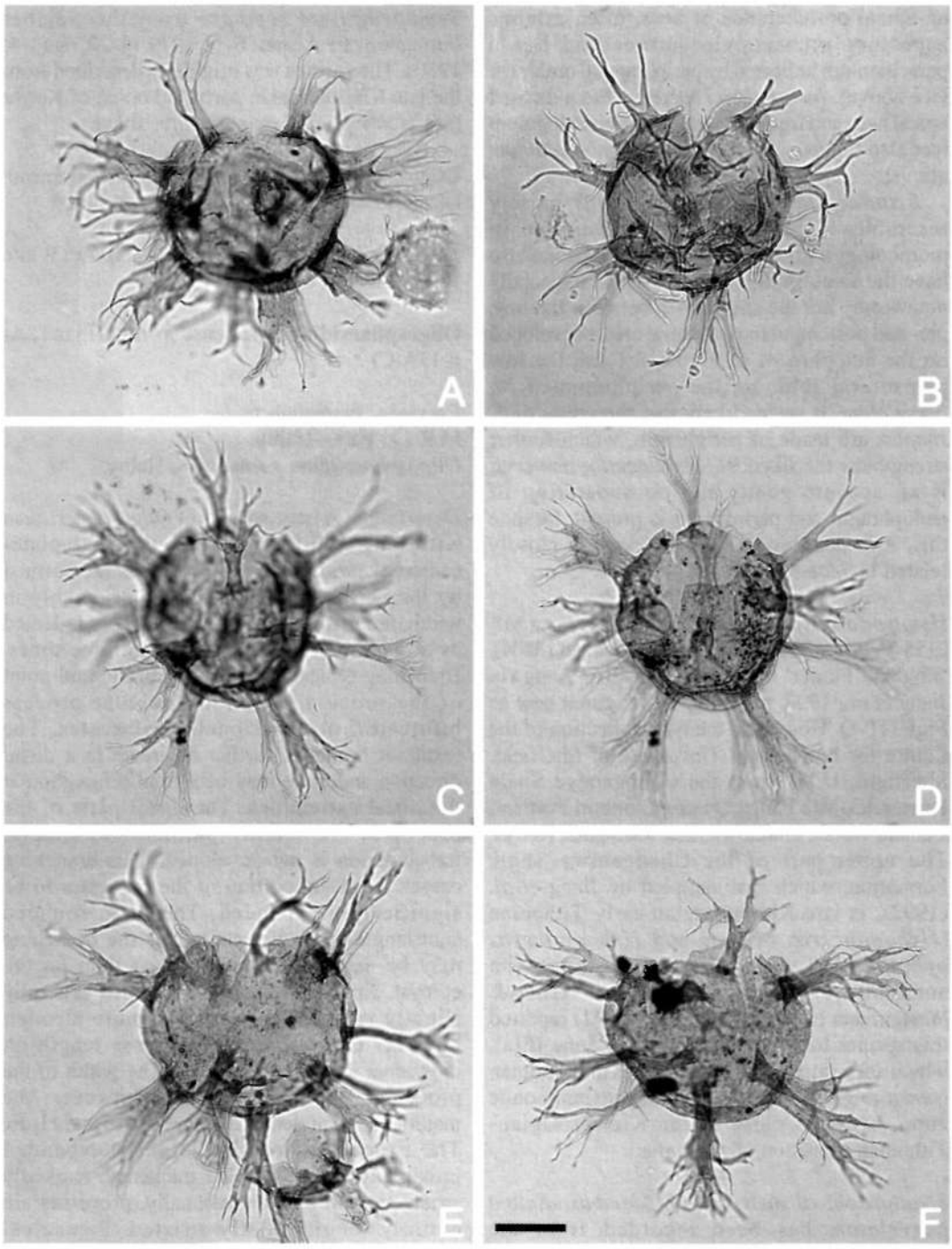

Fig. 12. Oligosphaeridium swanense sp. nov. From conventional core in Alaria-1 well at 3319.95m (A, C-F) and sidewall core in Jabiru-8A well at 1842.50m (B). All images taken using plain transmitted light. Scale bar in Fig. 12F refers to all images and is 25µm. Fig. 12E is the holotype; the remainder, paratypes. Note large size, wide intratabular processes indented and expanded distally, and apical archaeopyle. Processes branch up to three times distally. A - CPC 35718, paratype; dorsal view, median focus. Note very wide, hollow intratabular processes which branch medially. B - CPC 35719, paratype; ventral view, median focus. Note deeply incised process at top left. C, D - CPC 35720, paratype; oblique dorsal view, high and median focus respectively. Note principal and accessory archaeopyle sutures in Fig. 12D. E - CPC 35721, holotype; ventral view, median focus. Note detached operculum to bottom right. F - CPC 35722, paratype; oblique ventral view, high focus. Note lack of paracingular processes, and apical archaeopyle.

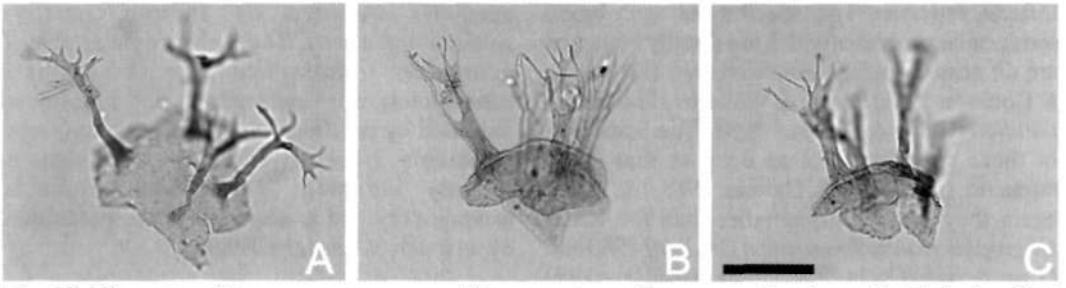

Fig. 13. Oligosphaeridium swanense sp. nov. All are paratypes from conventional core in Alaria-1 well at 3319.95m. All images taken using plain transmitted light. Scale bar in Fig. 13C refers to all images and is 25µm. Note four intratabular processes and prominent parasulcal tongue. A - CPC 35723, paratype; external/ventral view, median/low focus. Note prominent parasulcal tongue and relatively slender intratabular processes. B - CPC 35724, paratype; external/ventral view, low focus. Note four hollow intratabular apical processes. C - CPC 35725, paratype; external/oblique ventral view, median focus. Note parasulcal tongue.

Dimensions (µm; n=31): Min. (Mean) Max.
Length of entire cyst incl. processes: 107 (131) 153
Length of entire cyst excl. processes: 48 (62) 72
Length of loisthocyst incl. processes: 87 (130) 163
Length of loisthocyst excl. processes: 40 (63) 86
Width of cyst incl. processes: 103 (129) 168
Width of cyst excl. processes: 48 (63) 84
Length of processes: 28 (43) 60
Width of processes: 3 (6) 18

The measured specimens are from conventional core samples at 3315.95m and 3319.95m from Alaria-1 well and sidewall core samples from Buang-1 well at 3505.20m and Tenacious-1 well at 3002.00m.

Comments. The processes, particularly their branching, in *Oligosphaeridium swanense* are highly distinctive. Normally each process branches three times, the initial furcation generally occurring close to the central portion, although this is relatively variable (Fig. 12). The final branching is close to the distal extremity and the median furcation being approximately intermediate in position. This species is distinctive in comparison to others in the genus because the initial, most proximal, branching is relatively close to the cyst body, within the median portion of the process. In some cases, the first furcation is only one third the distance from the cyst body to the distal tip of the process (Fig. 12). In a very small number of forms, which may be transitional to other taxa, there is some re-connection of the distal elements of the processes. The majority of the processes are largely subparallel, but are expanded both proximally and distally. Occasionally the processes may be irregularly microreticulate, although the cyst wall is generally microscabrate. Their length is normally relatively constant in an individual specimen, however the width varies significantly (Fig. 12). The apical processes are consistently the narrowest (Fig. 13). Orientation is generally straightforward to interpret due to both the archaeopyle and the wide equatorial region, which is devoid of processes. The cyst is slightly dorsoventrally flattened. The operculum is consistently free and accessory archaeopyle sutures are often present, causing the precingular paraplates to be separated along their longitudinal sides. The accessory archaeopyle sutures are typically relatively deep and chemical/mechanical damage to the precingular paraplate series may loosen individual paraplates (Figs 12A-B, F).

Representatives of other species of the genus occur in the same samples as *Oligosphaeridium swanense*, although as minor components.

Comparison. Oligosphaeridium swanense differs from the other 37 validly published species of *Oligosphaeridium* (see Williams *et al*., 1998, p. 434-438) in its large size and the extremely deep branching of the intratabular processes. Normally species of *Oligosphaeridium* are less than 100µm in maximum diameter and any branching, or the insertion of narrow distal elements, occurs close to the distal end of the processes. The Early Cretaceous species *Oligosphaeridium diluculum* Davey 1982 and *O. dividuum* Williams 1978 also have relatively deeply furcate, tubiform processes. However, both of these are smaller than *O. swanense*, have slender processes, the distal branching of which is not as deep as in the latter. *Oligosphaeridium porosum* Lentin & Williams 1981, from the Albian of southern India, resembles *O. swanense* in having broad processes which branch deeply. However, *Oligosphaeridium swanense* has longer processes which vary considerably in width and it is significantly larger

than *O. porosum*. Two species also with broad intratabular processes which are distally branched are *Oligosphaeridium pulcherrimum* (Deflandre & Cookson 1955) Davey & Williams 1966 and *O. patulum* Riding & Thomas 1988. The branching in these species is not as deep as that in *O. swanense* (see Riding & Thomas, 1988, fig. 9) and again they are slightly smaller than the latter. *Oligosphaeridium fenestratum* Duxbury 1980 and *O. perforatum* (Gocht 1959) Davey & Williams 1969 have processes which branch relatively deeply distally. Both these Early Cretaceous forms, however, are smaller than *O. swanense* and have fenestrae in the distal portions of the processes. Furthermore, *Oligosphaeridium perforatum* has an entire distal rim. The large, annulate processes of *Systematophora palmula* Davey 1982 are similar in that they may be deeply branched (Davey, 1982, pl. 1, figs 1-3).

Derivation of name. From the *Dingodinium swanense* Zone.

Holotype and type locality. Figure 12E, CPC 35721, Alaria-1 well, conventional core at 3319.95m.

Stratigraphical distribution. *Oligosphaeridium swanense* ranges from the Oxfordian *Wanaea spectabilis* Zone (6c) to the Kimmeridgian upper *Dingodinium swanense* Zone (6aiia) (Foster, this volume; Helby & Partridge, in prep.).

Striatodinium gen. nov.

Type species. *Striatodinium ottii* sp. nov.

Diagnosis. Small to intermediate, proximate, acavate dinoflagellate cysts, which are elongate ellipsoidal in outline. The autophragm is smooth or has low relief, non-parasutural ornamentation. The autophragm also bears numerous, prominent, largely longitudinal ridges or crests, which may be nontabular or penitabular. These nontabular elements may be discontinuous. The paratabulation is gonyaulacalean. Paraplates are normally outlined by smooth, narrow, pandasutural bands. The archaeopyle is apical; operculum simple and free. Parasutures surrounding the paracingulum and parasulcus indicated by the absence of ornamentation or by penitabular ridges or crests; the parasulcus is slightly indented. The paracingulum is laevorotatory and is displaced at the parasulcus by as much as its entire height.

Comments. *Striatodinium* is a small, distinctive genus. The longitudinal alignment of the nontabular or penitabular ridges or crests, coupled with the elongate shape of this genus, are characteristic. In forms with penitabular ornamentation, lateral features are present, for example on the paracingular paraplates. However, in the markedly more elongate precingular and postcingular paraplate series, the apical and antapical sides of the penitabular fields are particularly narrow. Nontabular elements commonly occur within the fields marked by the penitabular ridges; the dominant lineation of these elements is longitudinal.

Comparison. *Dinogymnium* Evitt *et al.* 1967 and *Ellipsodinium* Clarke & Verdier 1967 both have longitudinal ornamentation and thus resemble *Striatodinium*. However, *Dinogymnium* is biconical, has an extremely small, apical archaeopyle and a unique wall structure (May, 1976; Evitt, 1985). *Ellipsodinium* lacks parasutural features and has a precingular archaeopyle. *Hemiplacophora* Cookson & Eisenack 1965 has penitabular ornamentation, but these elements are incomplete and polar in position. *Alisocysta* Stover & Evitt 1978 is subspherical and penitabular crests or septa are consistently present. *Lanterna* Dodekova 1969 is ellipsoidal, has an apical archaeopyle and penitabular ornamentation. However, this Jurassic genus completely lacks longitudinal ornamentation characteristic of *Striatodinium*. The genera *Eisenackia* Deflandre & Cookson 1955 and *Cassidium* Drugg 1967 have linear parasutural features, but these are

Fig. 14. Striatodinium lineatum sp. nov. All from outcrop sample 81FH63, from Misool, eastern Indonesia (Hasibuan, 1990). All photomicrographs taken using plain transmitted light. Scale bar in Fig. 14P refers to all photomicrographs and is 25µm. Figs 14A-B are the holotype; the remainder, paratypes (Figs 14C-P). Note apical archaeopyle, elongate outline, low, smooth, subparallel nontabular ridges which are sometimes discontinuous and sinuous. Rarely these nontabular ridges may coalesce; paratabulation indicated by absence of ridges. A, B - CPC 35726, holotype; left lateral view, high and low focus respectively. Note well defined gonyaulacalean paratabulation pattern indicated by absence of longitudinal ridges, and prominent fold close to antapex. C - CPC 35727, paratype; ventral view, low focus. Note discontinuous nature of some longitudinal ridges. D - CPC 35728, paratype; oblique ventral view, low focus. Squat specimen with well developed dorsal paratabulation. E, F - CPC 35729, paratype; ventral view, high and low focus respectively. Note parasulcus (continued opposite)

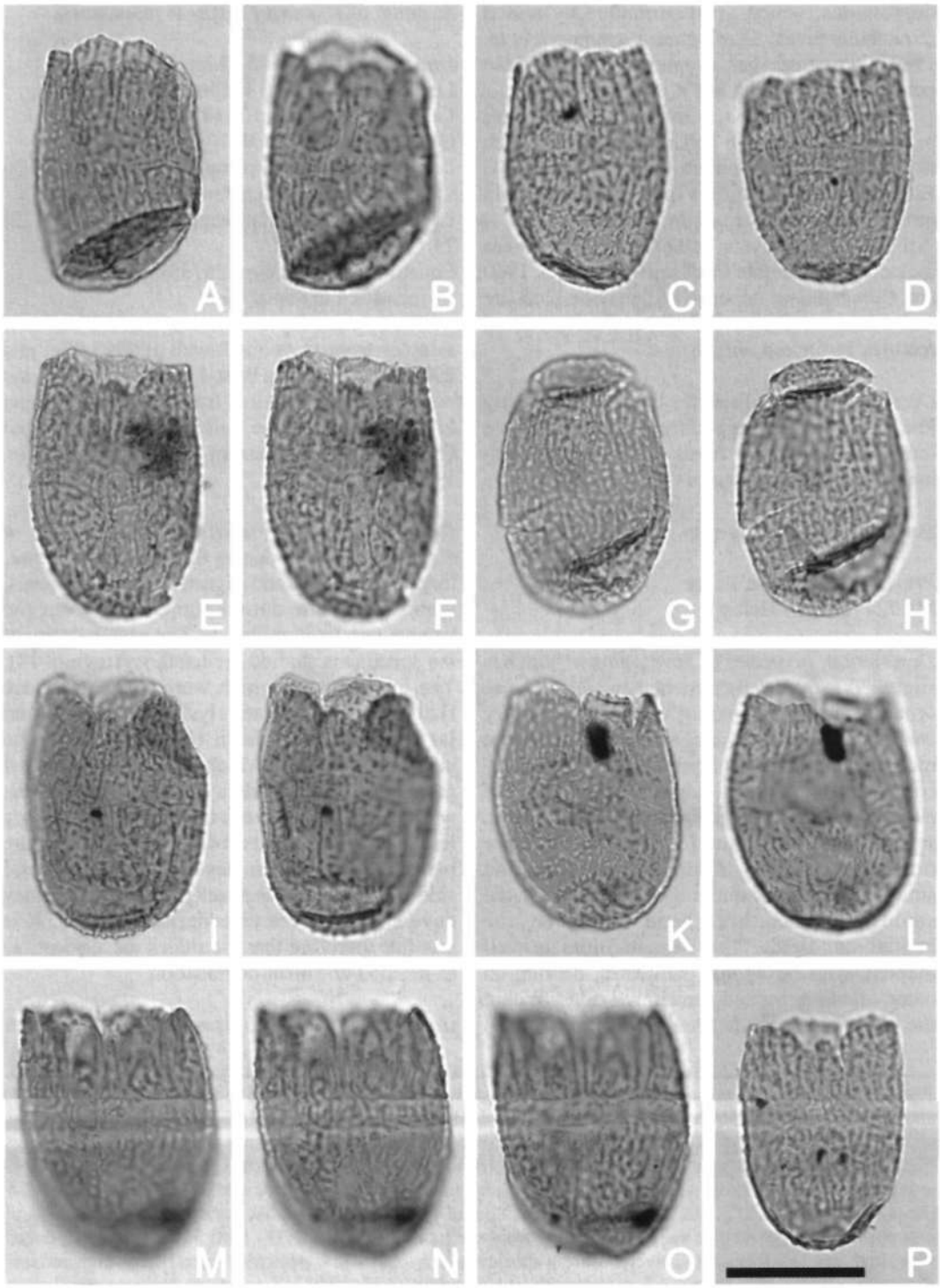

and parasulcal notch in Fig. 14E. G, H - CPC 35730, paratype; ventral view, high and low focus respectively. Note adherent operculum lacking an apical horn. I, J - CPC 35731, paratype; ventral view, high and median focus respectively. Note prominent parasulcal notch. K, L - CPC 35732, paratype; dorsal view, high and low focus respectively. Note low, well spaced longitudinal ridges. M-O - CPC 35733, paratype; ventral view, high to low focus sequence. Note gonyaulacalean paratabulation pattern indicated by absence of positive ornamentation. P - CPC 35734, paratype; dorsal view, median/low focus. Small; note apical archaeopyle and parasulcal notch.

depressions, which are surrounded by raised intratabular areas. *Gerdiocysta* Liengjarern *et al.* 1980 is proximate, has an apical archaeopyle and penitabular ornament, but it is holocavate.

This new genus resembles several other proximate genera with apical archaeopyles such as *Ellipsoidictyum* Klement 1960 and *Valensiella* Eisenack 1963, but differs in its penitabular and pandasutural paraplate delineation.

Isolated endocysts of some cavate genera including *Belodinium* Cookson & Eisenack 1960 and *Gardodinium* Alberti 1961 may be elongate and exhibit similar penitabular and pandasutural features to *Striatodinium*.

Derivation of name. From the Latin *stria*, meaning line or furrow, referring to the numerous prominent longitudinal ridges or crests of this genus which impart a striate appearance.

Striatodinium lineatum sp. nov. (Figs 14A-P)

Previous Australian usage
MP 724 (gran.) – Helby.

Description. A species of *Striatodinium* which is slightly dorsoventrally flattened and has a dense ornamentation, consisting of outer, generally continuous, penitabular ridges, within which there may be numerous subparallel, occasionally coalescing, longitudinal ridges or aligned rows of elements. The ridges are low, 0.5-1µm in height, smooth distally and narrow (c. 1µm in width). These ridges may be long, short, discontinuous and sinuous. The paratabulation is marked by the smooth pandasutural bands between the penitabular fields. The paracingulum is well marked, with hexagonal paraplates, bearing an outer, often interrupted penitabular ridge. Within the penitabular fields the overall longitudinal lineation of accessory ridges is maintained.

Dimensions (µm; n=43): Min. (Mean) Max.
Length of entire cyst: 41 (46) 54
Length of loisthocyst: 33 (42) 50
Length of operculum: 9 (10) 11
Length of precingular paraplate series*: 14 (17) 20
Length of paracingulum*: 4 (5) 6
Length of postcingular paraplate series*: 20 (22) 25
Equatorial width of cyst: 26 (30) 35
* - measured in dorsal view

The measured specimens are from sidewall core samples from Octavius-2 well at 2905.00m and 2907.00m, Tenacious West-1 well at 3040.00m and outcrop sample 81FH63, from the Kimmeridgian lowermost part of the Lelinta Formation (Fageo Group) of Misool, eastern Indonesia (Hasibuan, 1990).

Comments. *Striatodinium lineatum* is a distinctive species due to the prominent, dense, longitudinal ridges and aligned low relief elements, which cover the autophragm, apart from the smooth pandasutural bands. The vast majority of the specimens studied are loisthocysts (Fig. 14). The few opercula which were encountered are flattened cones, relatively low in height, and lacking an apical horn (Figs 14G-H). The pandasutural bands, which define the individual paraplates, are not always clearly developed, particularly in specimens in which the ridges are less prominent (Figs 14K-L). Normally the paratabulation is best developed on the dorsal side (Fig. 14O). The less well preserved forms may have sparser, more discontinuous ridges. It is possible therefore that the ridges are susceptible to physico-chemical degradation.

Comparison. *Striatodinium lineatum* is smaller

Fig. 15. *Striatodinium ottii* sp. nov. From ditch cuttings from 1493.54m-1496.59m in Peak-1 well (Figs 15A-D) and outcrop sample f8556 from Kawhia, New Zealand (Helby *et al.*, 1988) (Figs 15E-P). All photomicrographs taken using plain transmitted light. Scale bar in Fig. 15P refers to all photomicrographs and represents 25µm. Figs 15O-P are the holotype; the remainder, topotypes (Figs 15E-N) and paratypes (Figs 15A-D). Note smooth autophragm, the markedly elongate outline and prominent, slender, straight, distally-smooth, penitabular periphragmal crests. A, B - CPC 35735, paratype; ventral view, high and low focus respectively. Widening of cyst at principal archaeopyle suture is probably from mechanical damage. C, D - CPC 35736, paratype; dorsal view, high and low focus respectively. Narrow specimen. E, F - SM 4757, topotype; ventral view, high and low focus respectively. Note short (i.e. low in height) paracingulum. G, H - SM 4758, topotype; oblique ventral view, high and low focus respectively. Narrow; note flat, small antapical (paraplate 1'''') area. I - SM 4759, topotype; ventral view, median focus. Note rounded antapex. J, K - SM 4759, topotype; ventral view, high and low focus respectively. Note offset of parasulcus in ventral focus (Fig. 15J). L - SM 4760, topotype; oblique ventral view, high focus. Unusually small. M, N - SM 4761, topotype; ventral view, high and low focus respectively. Large; note penitabular crests on paracingular paraplates in Fig. 15N. O, P - SM 4762, holotype; dorsal view, high and low focus respectively. Note penitabular crests in paracingular paraplates.

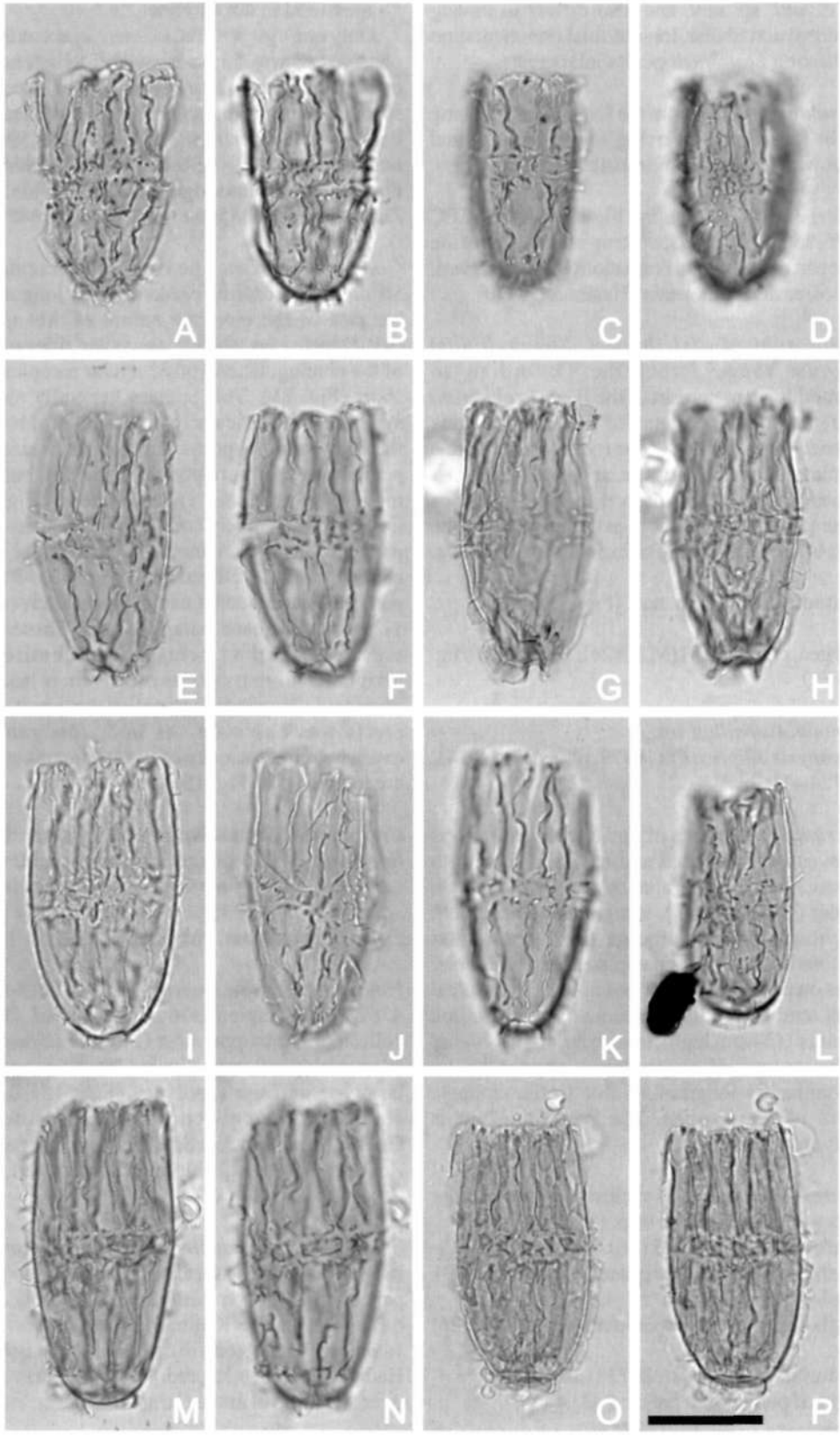
A
B
C
D
E
F
G
H
I
J
K
L
M
N
O
P

than *S. ottii* sp. nov. and also differs in having additional nontabular, longitudinal ornamentation and lacking prominent penitabular crests.

Derivation of name. From the Latin *linea*, meaning line or thread and referring to the longitudinal ridges which impart a linear pattern to this species.

Holotype and type locality. Figures 14A-B, CPC 35726, sample 81FH63, outcrop material from the lower part of the Lelinta Formation (Kimmeridgian), Misool, eastern Indonesia (Hasibuan, 1990).

Stratigraphical distribution. Striatodinium lineatum ranges from the Oxfordian to Kimmeridgian upper part of the *Wanaea clathrata* Zone (6bi) to the basal part of the Kimmeridgian *Dingodinium swanense* Zone (6aiiib) (Foster, this volume; Helby & Partridge, in prep.). It occurs consistently over this interval in the Timor Sea region (and Misool), but is extremely rare to the south in the Carnarvon Basin, Western Australia.

Striatodinium ottii sp. nov. (Figs 15A-P)

1988 gen. et sp. nov. H (M.P. 724); Helby *et al*., fig. 8H, Q.

Previous Australian usage
Dictyopyxis elliptica Ott (1970, pl. 8, figs 11-14). MP 724 – Helby.

Description. A species of *Striatodinium* which is dorsoventrally flattened and having a smooth to microscabrate autophragm which is 1µm thick. Slender (<0.5µm thick), straight, distally smooth periphragmal crests emerge from penitabular positions on each major paraplate. The penitabular ridges on paracingular and possibly the parasulcal plates tend to be discontinuous. The crests are prominent (2-4µm high), tend to be slightly higher in the antapical region and appear to be predominantly longitudinal due to the elongate nature of the species. The paracingulum is relatively narrow.

Dimensions (µm; n=41) exclusive of penitabular crests where applicable: Min. (Mean) Max.
Length of loisthocyst: 45 (56) 68
Length of precingular paraplate series*: 18 (25) 31
Length of paracingulum*: 3 (4.5) 6
Length of postcingular paraplate series*: 20 (26) 30
Equatorial width of cyst: 20 (28) 34
Height of penitabular crests: 2 (3) 4

* - measured in dorsal view

Only one cyst with an adherent operculum was observed; it was 53µm in overall length and the operculum was 7µm long. The measured specimens are from a ditch cuttings sample from Peak-1 well between 1493.54m and 1496.59m and outcrop material from the uppermost Ohineruru Formation (Kimmeridgian) from Kawhia, New Zealand (sample f8556 of Helby *et al*., 1988).

Comments. The penitabular crests of *Striatodinium ottii* are predominantly longitudinal because of the elongate nature of this species (see *Dimensions*, above); the polar sides of each of the precingular and postcingular paraplates are short (Fig. 15). This species generally appears symmetrical, particularly in dorsal view, because the epicyst and hypocyst are similar in size. The penitabular crests are normally straight, but there may be some minor crest sinuosity (Fig. 15). Despite the relatively small paraplate areas in the parasulcus and paracingulum, penitabular crests are normally developed (e.g. Figs 15N-P). The penitabular crests emerge from immediately (within 1-2µm) inside each paraplate area. These crests are interpreted as being formed entirely of periphragmal extensions; no cavation has been observed. No degradation of the penitabular crests was observed. As in *S. lineatum*, the overwhelming majority of the specimens studied are loisthocysts (Fig. 15).

Comparison. Striatodinium ottii is larger than *S. lineatum*; it also differs in having penitabular crests and lacking nontabular ornamentation.

Derivation of name. For Hank L. Ott.

Holotype and type locality. Figures 15O-P, SM 4762, from sample f8556 of Helby *et al*. (1988), collected in the uppermost Ohineruru Formation (Kimmeridgian) from Kawhia, New Zealand. The holotype and the topotypes (Figs 15E-N) are curated in the collections of the Institute of Geological and Nuclear Sciences (formerly the New Zealand Geological Survey), Lower Hutt, New Zealand.

Stratigraphical distribution. Striatodinium otii ranges from the Oxfordian-Kimmeridgian upper part of the *Wanaea clathrata* Zone (6bi) to the basal part of the Kimmeridgian *Dingodinium swanense* Zone (6aiiib) (Foster, this volume; Helby & Partridge, in prep.). It occurs consistently over this interval in the Carnarvon Basin, Western

Australia but is extremely rare to the north in the Timor Sea region. It has not been recorded in Misool. The species is also present in the Kimmeridgian uppermost Ohineruru Formation of Kawhia, New Zealand (Helby *et al.*, 1988).

ACKNOWLEDGEMENTS

The authors are grateful to Dr C.B. Foster (AGSO, Canberra) for promoting and facilitating this work and for editorial guidance and advice. Christian Thun and Andrew Kelman (AGSO, Canberra) provided invaluable help with preparations and the manipulation of digital images. Mr Eddie Resiak of the core and cuttings repository at AGSO, Canberra courteously provided access to sample material. Arco Australia Ltd., BHP Petroleum Pty. Ltd, Cultus Petroleum N.L., Esso Australia Ltd., WAPET, Western Mining Co. and Woodside kindly provided sample material on request. Dr Fauzie Hasibuan of the Geological Research and Development Center, Bandung, Indonesia supplied the sample material from Misool, eastern Indonesia. Laola Pty. Ltd. (Perth) gave support via the careful treatment of key samples in the preparatory process. Professor Bernard Owens of the Centre for Palynology, University of Sheffield, UK kindly made the type material of ?*Indodinium* (now *Mombasadinium*) *parvelatum* to JBR for a restudy. Drs D. G. Benson Jr. and J. Helenes are thanked for reviewing the manuscript. J. B. Riding publishes with the permission of the Chief Executive Officer, AGSO.

REFERENCES

ARKELL, W.J., 1956. *Jurassic geology of the World.* Oliver & Boyd, Edinburgh, 806p.

BALME, B.E., 1957. Spores and pollen grains from the Mesozoic of Western Australia. *Commonwealth Scientific and Industrial Research Organisation of Australia, Coal Research Section, T.C. 25*, 1-48.

BEJU, D., 1979. Middle and Upper Jurassic dinoflagellate assemblages from the Alozai, Sembar and Chichali formations of Pakistan. *Unpublished report prepared for presentation at the 5th International Palynological Conference, Cambridge 1980*, 2 volumes.

BEJU, D., 1980. Middle and Upper Jurassic dinoflagellate assemblages from the Alozai, Sembar and Chichali formations of Pakistan. *Abstracts volume, 5th International Palynological Conference, Cambridge 1980*, 35.

BELOW, R., 1982, *Rigaudella*, eine neues Genus von Dinoflagellaten-Zysten. *Neues Jahrbuch für Geologie und Paläontologie Monatshefte 1982/3*, 137-150.

BRIDEAUX, W.W. & FISHER, M.J., 1976. Upper Jurassic-Lower Cretaceous dinoflagellate assemblages from Arctic Canada. *Geological Survey of Canada Bulletin 259*, 53p.

BURGER, D., 1996. Mesozoic palynomorphs from the North West Shelf, offshore Western Australia. *Palynology 20*, 49-103.

CHEN, Y.-Y., 1978. *Jurassic and Cretaceous palynostratigraphy of a Madagascar well.* Unpublished PhD thesis, University of Arizona, Tucson, Arizona, 264p.

COOKSON, I.C. & EISENACK, A., 1962. Additional microplankton from Australian Cretaceous sediments. *Micropaleontology 8*, 485-507.

COOKSON, I.C. & EISENACK, A., 1974. Mikroplankton aus australischen mesozoischen und tertiären Sedimenten. *Palaeontographica Abteilung B 148*, 44-93.

DAVEY, R.J., 1982. Dinocyst stratigraphy of the latest Jurassic to Early Cretaceous of the Haldager No. 1 borehole, Denmark. *Danmarks Geologiske Undersøgelse Serie B Nr. 6*, 57p.

DAVEY, R.J., 1987. Palynological zonation of the Lower Cretaceous, Upper and uppermost Middle Jurassic in the northwestern Papuan Basin of Papua New Guinea. *Geological Survey of Papua New Guinea Memoir 13*, 77p.

DAVEY, R.J., 1999. Revised palynological zonation for the Late Cretaceous, Early Cretaceous and Late Jurassic of Papua New Guinea. *Geological Survey of Papua New Guinea Memoir 17*, 51p.

DEFLANDRE, G., 1939. Microplancton des mers Jurassiques conservé dans les marnes de Villers-sur-Mer (Calvados). Étude liminaire et considérations générales. *Travaux de la Station zoologique de Wimereux 13*, 147-200.

EATON, G.L., 1984. Structure and encystment in some fossil cavate dinoflagellate cysts. *Journal of Micropalaeontology 3(2)*, 53-64.

EVITT, W.R., 1985. *Sporopollenin dinoflagellate cysts. Their morphology and interpretation.* American Association of Stratigraphic Palynologists Foundation, Dallas, 333p.

FENSOME, R.A., TAYLOR, F.J.R., NORRIS, G., SARJEANT, W.A.S., WHARTON, D.I. & WILLIAMS, G.L., 1993. A classification of living and fossil dinoflagellates. *Micropaleontology Special Publication No. 7*, 351p.

FOSTER, C.B., this volume. Introduction.

FRANCIS, G. & WESTERMANN, G.E.G., 1993. The Kimmeridgian problem in Papua New Guinea and other parts of the Indo-southwest Pacific. In: Carman, G.J & Carmen, Z. (eds). *Petroleum Exploration and Development in Papua New Guinea: Proceedings of the Second PNG Petroleum*

Convention, Port Moresby, 31st May-2nd June 1993, 75-93.

GARG, R., KHOWAJA-ATEEQUZZAMAN & JAIN, K.P., 1987. Jurassic and Lower Cretaceous dinoflagellate cysts from India with some remarks on the concept of Upper Gondwana. *The Palaeobotanist 36*, 254-267.

HASIBUAN, F., 1990. *Mesozoic stratigraphy and paleontology of Misool Archipelago, Indonesia.* Unpublished Ph. D. thesis, University of Auckland, 384p., 22pl.

HELBY, R., MORGAN, R. & PARTRIDGE, A.D., 1987. A palynological zonation of the Australian Mesozoic. *Memoir of the Association of Australasian Palaeontologists 4*, 1-94.

HELBY, R. & PARTRIDGE, A.D., in prep. A palynological zonation of the Australian Mesozoic – an update.

HELBY, R., WILSON, G.J., & GRANT-MACKIE, J.A., 1988. A preliminary biostratigraphic study of Middle to Late Jurassic dinoflagellate assemblages from Kawhia, New Zealand. *Memoir of the Association of Australasian Palaeontologists 5*, 125-166.

HELENES, J., 1983. Evaluation of Jurassic-Cretaceous dinoflagellates in the *Ascodinium-Ovoidinium* complex. *Micropaleontology 29*, 255-266.

HELENES, J., 1984. Morphological analysis of Mesozoic-Cenozoic *Cribroperidinium* (Dinophyceae), and taxonomic implications. *Palynology 8*, 107-137.

HELENES, J. & LUCAS-CLARK, J., 1997. Morphological variations among species of the fossil dinoflagellate genus *Gonyaulacysta*. *Palynology 21*, 173-196.

JAN DU CHÊNE, R., MASURE, E., BECHELER, I., BIFFI, U., DE VAINS, G., FAUCONNIER, D., FERRARIO, R., FOUCHER, J.-C., GAILLARD, M., HOCHULI, P., LACHKAR, G., MICHOUX, D., MONTEIL, E., MORON, J.-M., RAUSCHER, R., RAYNAUD, J.-F., TAUGOURDEAU, J. & TURON, J.-L. 1986. Guide pratique pour la détermination de kystes de dinoflagellés fossiles. Le complexe *Gonyaulacysta*. *Bulletin des Centres de Recherches Exploration-Production Elf-Aquitaine, Mémoir 12*, 479p.

JIANG, Q., MUNGAI, M.W., DOWNIE, C. & NEVES, R., 1992. Late Jurassic dinoflagellate assemblages of the Mto Panga Quarry, Mombasa, Kenya. *Review of Palaeobotany and Palynology 74*, 77-100.

KUMAR, A., 1986. A dinocyst assemblage from the Middle Member (Lower Kimmeridgian-Tithonian) of the Jhuran Formation, Kachchh, India. *Review of Palaeobotany and Palynology 48*, 377-407.

LENTIN, J.K. & WILLIAMS, G.L., 1976. A monograph of fossil peridinioid dinoflagellate cysts. *Bedford Institute of Oceanography Report Series No. BI-R-75-16*, 237p.

MAY, F.E., 1976. Dinoflagellates: fossil motile stage tests from the Upper Cretaceous of the northern New Jersey Coastal Plain. *Science 193*, 1128-1130.

MONTEIL, E., 1990. Revision and emendation of dinocyst genus *Amphorula* Dodekova 1969. The concept of morphostratigraphy. *Bulletin des Centres de Recherches Exploration-Production Elf-Aquitaine 14*, 597-609.

MONTEIL, E., 1991. Morphology and systematics of the ceratioid group: a new morphographic approach. Revision and emendation of the genus *Muderongia* Cookson and Eisenack 1958. *Bulletin des Centres de Recherches Exploration-Production Elf-Aquitaine 15*, 461-505.

MORGAN, R., 1980. Palynostratigraphy of the Australian Early and Middle Cretaceous. *Memoirs of the Geological Survey of New South Wales, Palaeontology No. 18*, 153p.

OTT, H.L., 1970. Palynological zonation of the Carnarvon Basin Jurassic-Miocene sequence. *Unpublished WAPET report*, 1-52.

PARKER, F.M., 1986. *Late Jurassic palynology of the Dampier Sub-Basin, Carnarvon Basin, Western Australia.* Unpublished PhD thesis, University of Western Australia, vol. 1: 334p; vol. 2: pl. 1-63.

PRÖSSL, K.F., 1990. Dinoflagellaten der Kreide – Unter-Hauterive bis Ober-Turon – im niedersächsischen Becken. Stratigraphie und Fazies in der Kernbohrung Konrad 101 sowie einiger anderer Bohrungen in Nordwestdeutschland. *Palaeontographica Abteilung B 218*, 93-191.

RAYNAUD, J.-F., 1978. Principaux dinoflagellés caractéristiques du Jurassique Supérieur d'Europe du nord. *Palinologia número extraordinario 1*, 387-405.

RIDING, J.B. & HELBY, R., this volume, a. Some stratigraphically significant dinoflagellate cysts from the Early Cretaceous (Aptian and Albian) of Australia.

RIDING, J.B. & HELBY, R., this volume, b. Marine microplankton from the Late Jurassic (Tithonian) of the north-west Australian region.

RIDING, J.B., PENN, I.E. & WOOLLAM, R., 1985. Dinoflagellate cysts from the type area of the Bathonian stage (Middle Jurassic; southwest England). *Review of Palaeobotany and Palynology 45*, 149-169.

RIDING, J.B. & THOMAS, J.E., 1988. Dinoflagellate cyst stratigraphy of the Kimmeridge Clay (Upper Jurassic) from the Dorset coast, southern England. *Palynology 12*, 65-88.

RIDING, J.B. & THOMAS, J.E., 1997. Marine

palynomorphs from the Staffin Bay and Staffin Shale formations (Middle-Upper Jurassic) of the Trotternish Peninsula, NW Skye. *Scottish Journal of Geology 33*, 59-74.

SARJEANT, W.A.S., 1982. The dinoflagellate cysts of the *Gonyaulacysta* group: a morphological and taxonomic restudy. *American Association of Stratigraphic Palynologists Contributions Series No. 9*, 81p.

SARJEANT, W.A.S., LACALLI, T. & GAINES, G., 1987. The cysts and skeletal elements of dinoflagellates: speculations on the ecological causes for their morphology and development. *Micropaleontology 33*, 1-36.

STEVENS, J., 1987. Some Early Cretaceous dinoflagellates from the *Cassiculosphaeridia delicata* Zone on the Exmouth Plateau, Western Australia. *Memoir of the Association of Australasian Palaeontologists 4*, 185-197.

STOVER, L.E., 1977. Oligocene and Early Miocene dinoflagellates from Atlantic Corehole 5/5B, Blake Plateau. *American Association of Stratigraphic Palynologists Contributions Series No. 5A*, 66-89.

STOVER, L.E. & EVITT, W.R., 1978. Analyses of Pre-Pleistocene organic-walled dinoflagellates. *Stanford University Publications, Geological Sciences 15*, 300 p.

SYKES, R.M., 1975. The stratigraphy of the Callovian and Oxfordian stages (Middle-Upper Jurassic) in northern Scotland. *Scottish Journal of Geology 11*, 51-78.

TAPPAN, H. & LOEBLICH, A.R., 1971. Surface sculpture of the wall in Lower Palaeozoic acritarchs. *Micropaleontology 17*, 385-410.

VERMA, H.M. & WESTERMANN, G.E.G., 1984. Ammonoid fauna of the Kimmeridgian-Tithonian boundary beds of Mombasa, Kenya. *Life Sciences Contributions of the Royal Ontario Museum 135*, 124 p.

WILLIAMS, G.L., LENTIN, J.K. & FENSOME, R.A., 1998. The Lentin and Williams Index of fossil dinoflagellates 1998 edition. *American Association of Stratigraphic Palynologists Contributions Series No. 34*, 817p.

WILLIAMS, G.L., SARJEANT, W.A.S. & KIDSON, E.J., 1978. A glossary of the terminology applied to dinoflagellate amphiesmae and cysts and acritarchs. *American Association of Stratigraphic Palynologists Contributions Series No. 2A*, 121p.

WILSON, G.J. & CLOWES, C.D., 1981. A concise catalogue of organic-walled fossil dinoflagellate genera. *New Zealand Geological Survey Report 92*, 199p.

WISEMAN, J.F., 1980. Palynostratigraphy near the 'Jurassic-Cretaceous Boundary' in the Carnarvon Basin, Western Australia. *Fourth International Palynological Conference, Lucknow (1976-1977) Proceedings 2*, 330-349.

APPENDIX 1: SAMPLE DETAILS

1. LOCATIONS AND OPERATORS OF WELLS FROM WHICH MATERIAL HAS BEEN STUDIED

Well Name/Number	Latitude	Longitude	Operator
Alaria-1	10° 36' 38.43"S	125° 55' 30.55"E	Woodside
Buang-1	10° 35' 49.58"S	126° 04' 04.94"E	BHP
Cockell-1	11° 39' 57.21"S	125° 02' 25.68"E	BHP
Frigate-1	13° 10' 42.99"S	127° 55' 29.00"E	Arco Australia
Hadrian-1	11° 40' 24.10"S	124° 59' 16.87"E	Western Mining Co.
Jabiru-8A	11° 56' 05.62"S	125° 00' 41.12"E	BHP
Jurabi-1	21° 37' 07.30"S	114° 11' 59.81"E	Esso
Macedon-5	21° 33' 22.50"S	114° 15' 19.00"E	BHP
Octavius-2	11° 51' 38.55"S	124° 54' 24.86"E	Western Mining Co.
Peak-1	21° 36' 16.99"S	114° 30' 21.99"E	WAPET
Scafell-1	21° 32' 43.79"S	114° 01' 08.02"E	BHP
Swan-1	12° 11' 12.39"S	124° 29' 38.69"S	Arco Australia
Tenacious-1	11° 51' 34.09"S	124° 54' 04.32"E	Cultus
Tenacious West-1	11° 51' 46.32"S	124° 53' 44.23"E	Woodside

Well completion reports on all the offshore wells listed are publicly available five years after completion.

2. OUTCROP MATERIAL

2.1. MISOOL, EASTERN INDONESIA

Sample Number	Lithostratigraphy	Age	Reference
81FH63	Lelinta Formation (Fageo Group)	Kimmeridgian	Hasibuan (1990)
81FH66	Lelinta Formation (Fageo Group)	Tithonian	Hasibuan (1990)

2.2. BRORA, NORTH-EAST SCOTLAND, UK

MPA 15496	Brora Roof Bed (Brora Argillaceous Fm.)	Callovian	Sykes (1975)

2.3. MTO PANGA QUARRY, FRERETOWN, KENYA

*MP*26	Uppermost Changamwe Shale Formation	Kimm./Tith.	Jiang *et al.* (1992)

2.4. KAWHIA, NEW ZEALAND

f8556	Uppermost Ohineruru Formation	Kimmeridgian	Helby *et al.* (1988)

APPENDIX 2: REGISTER OF FIGURED SPECIMENS

All palynomorph specimens figured in this paper are listed here, together with essential details. The specimens are mainly curated in the Commonwealth Palaeontological Collection (CPC) of the Australian Geological Survey Organisation, Canberra. Eight specimens of *Striatodinium ottii*, however, are curated with the New Zealand Geological Survey, Lower Hutt, New Zealand. The holotype and topotypes specimens of *Mombasadinium parvelatum* are housed in the type collections of the Centre for Palynology, University of Sheffield, UK. Furthermore, a single specimen of *Indodinium khariense* figured herein is curated in the collections of Woodside Petroleum, Perth.

The dinoflagellate cyst genera and species are listed alphabetically and the location of the specimens on the microscope slides are all 'England-Finder' co-ordinates. These were taken with the slide label to the left of the observer; the microscope stage opening toward the microscope user. The coding for types is as follows: H = holotype; P = paratype; T = topotype. All specimens of new taxa examined during this study contributed to the specific concepts described. Therefore all figured specimens which are not holotypes are paratypes. SGM = single grain mount. The single grain mounts do not have unique numbers; they are numbered sequentially for each species within a particular sample. The specimens are from conventional core, sidewall core and ditch cutting samples.

Species	Type	Fig(S)	SGM/Slide No.	EF	Well (depth, m.)	CPC No.
C. swanense	P	1A	SGM 31 (i)	L26/2	Jabiru-8A (1842.50)	35645
C. swanense	P	1B	SGM 1 (ii)	N30	Buang-1 (3504.00)	35646
C. swanense	P	1C	SGM 32 (ii)	E29/3	Jabiru-8A (1842.50)	35647
C. swanense	P	1D	SGM 7 (i)	H33/2	Jabiru-8A (1842.50)	35648
C. swanense	P	1E	SGM 32 (iii)	F29/2	Jabiru-8A (1842.50)	35649
C. swanense	P	1F	SGM 32 (i)	E29	Jabiru-8A (1842.50)	35650
C. swanense	P	1G	SGM 33 (i)	L26/4	Jabiru-8A (1842.50)	35651
C. swanense	P	1H	SGM 32 (iv)	F28/2&4	Jabiru-8A (1842.50)	35652
C. swanense	P	1I	SGM 31 (iii)	L26	Jabiru-8A (1842.50)	35653
C. swanense	P	1J	SGM 1 (i)	L19/2	Buang-1 (3505.20)	35654
C. swanense	P	1K	SGM 2 (i)	Q23/3&4	Buang-1 (3505.20)	35655
C. swanense	H	1L	SGM 1(i)	M32/2	Buang-1 (3504.00)	35656
C. swanense	P	2A	SGM 34 (i)	O35	Jabiru-8A (1842.50)	35657
C. swanense	P	2B	SGM 34 (ii)	O35	Jabiru-8A (1842.50)	35658
C. swanense	P	2C	SGM 34 (iv)	P36/3	Jabiru-8A (1842.50)	35659
C. swanense	P	2D	SGM 34 (vi)	Q36/1[T]	Jabiru-8A (1842.50)	35660
C. swanense	P	2E	SGM 6 (iv)	N32/4	Jabiru-8A (1842.50)	35661
C. swanense	P	2F-2G	SGM 6 (i)	J37	Buang-1 (3505.20)	35662
C. corrugatum	H	3A	SGM 1 (iv)	P25/4	Alaria-1 (3318.58)	35663
C. corrugatum	P	3B	SGM 1 (v)	N27	Alaria-1 (3315.95)	35664
C. corrugatum	P	3C	SGM 1 (i)	Q26/3	Alaria-1 (3318.58)	35665

Species	Type	Fig(S)	SGM/Slide No.	EF	Well (depth, m.)	CPC No.
C. corrugatum	P	3D	SGM 4 (iii)	N36/4	Alaria-1 (3315.95)	35666
C. corrugatum	P	3E, F	SGM 1 (iii)	N27/3	Alaria-1 (3315.95)	35667
C. corrugatum	P	3G	SGM 4 (vii)	M37	Alaria-1 (3315.95)	35668
C. corrugatum	P	3H	SGM 1 (i)	N27/3	Alaria-1 (3315.95)	35669
C. corrugatum	P	3I	SGM 1 (vi)	P24/4	Alaria-1 (3318.58)	35670
C. corrugatum	P	4A	SGM 1 (iii)	B19/4	Alaria-1 (3319.95)	35671
C. corrugatum	P	4B	SGM 2 (vi)	L23	Alaria-1 (3315.95)	35672
G. fenestrata	P	5A	SGM 2 (iii)	J30	Frigate-1 (1233.00)	35673
G. fenestrata	P	5B	SGM 2 (ii)	H32/3	Frigate-1 (1233.00)	35674
G. fenestrata	P	5C,6A	SGM 1 (i)	L36	Jabiru-8A (1842.50)	35675
G. fenestrata	H	5D	SGM 5 (i)	P33	Buang-1 (3504.00)	35676
G. fenestrata	P	5E,6B	SGM 2 (ii)	N25/1	Buang-1 (3504.00)	35677
G. fenestrata	P	5F	SSM 1 (i)	N19	Misool, 81FH66	35678
G. fenestrata	P	5G	SGM 1 (ii)	O32/2	Buang-1 (3505.20)	35679
G. fenestrata	P	5H	SGM 2 (ii)	Q27	Alaria-1 (3315.95)	35680
G. fenestrata	P	5I	SGM 5 (i)	Q33/1&2	Buang-1 (3504.00)	35681
G. dualis		6D	SGM 102	H36	Misool, 81FH63	35682
G. jurassica adecta		6E	MPA 15496/1**	S42/2	Brora, Scotland	
G. cf. *fenestrata*		7A-C	SGM 1 (i)	L29	Peak-1 (1463.06*)	35683
G. cf. *fenestrata*		7D-F	SGM 1 (ii)	L28/2	Peak-1 (1463.06*)	35684

*ditch cuttings sample, range depth: 1463.06m-1466.10m

** - collections of the British Geological Survey, Nottingham, UK.

H. cincta	P	8A-C	SGM 10 (i)	K29/4	Hadrian-1 (3285.00*)	35685
H. cincta	P	8D-8F	SGM 2 (i)	L27/3	Hadrian-1 (3285.00*)	35686
H. cincta	H	8G-8I	SGM 3 (ii)	O21	Hadrian-1 (3285.00*)	35687
H. cincta	P	9A-9C	SGM 7 (i)	K19	Hadrian-1 (3285.00*)	35688
H. cincta	P	9D-9F	SGM 10 (v)	J30/4	Hadrian-1 (3285.00*)	35689
H. cincta	P	9G-9I	SGM 9 (iii)	R30/4	Hadrian-1 (3285.00*)	35690
H. cincta	P	9J-9L	SGM 7 (iv)	H20/3	Hadrian-1 (3285.00*)	35691

*ditch cuttings sample, range depth: 3285.00m-3300.00m

I. khariense	10A	SGM 1 (i)	P34	Misool, 81FH66	35692
I. khariense	10B	SGM 1 (i)	M17/3	Alaria-1 (3315.95)	35693
I. khariense	10C	SGM 2 (vi)	N19	Alaria-1 (3315.95)	35694
I. khariense	10D	SGM 3 (i)	K21	Alaria-1 (3315.95)	35695
I. khariense	10E	SGM 1 (i)	O31/1	Alaria-1 (3318.58)	35696
I. khariense	10F	SGM 1 (i)	Q28	Alaria-1 (3317.26)	35697
I. khariense	10G-H	SGM 3 (iv)	M21/3	Alaria-1 (3315.95)	35698
I. khariense	10I-J	SGM 2 (i)	M24/2	Misool, 81FH66	35699
I. khariense	10K-L	Ass, sl. 3	K35	Alaria-1 (3317.26)	*
I. khariense	10M	SGM 1 (i)	S22	Buang-1 (3504.00)	35700
I. khariense	10N-O	SGM 1 (ii)	O30/4	Alaria-1 (3318.58)	35701
I. khariense	10P	SGM 1 (iii)	O18	Alaria-1 (3315.95)	35702

*Collection of Woodside Petroleum, Perth, WA

M. parvelatum		11A-B	SGM 2 (ii)	N30/3	Peak-1 (4302.00)	35703
M. parvelatum	T	11C	Ass. sl. *MP* 26 (iv)	J21/1	Mto Panga Quarry	ML 2155*
M. parvelatum	T	11D	Ass. sl. *MP* 26 (iv)	R23	Mto Panga Quarry	ML 2155*
M. parvelatum	T	11E	Ass. sl. *MP* 26 (iv)	J27	Mto Panga Quarry	ML 2155*
M. parvelatum	T	11F	Ass. sl. *MP* 26 (iv)	L39	Mto Panga Quarry	ML 2155*
M. parvelatum		11G	SGM 2 (vi)	M16/4	Misool, 81FH66	35704
M. parvelatum		11H	SGM 4 (ii)	N40/3	Peak-1 (4302.00)	35705

Species	Type	Fig(S)	SGM/Slide No.	EF	Well (depth, m.)	CPC No.
M. parvelatum		11I	SGM 2 (iv)	M16/4	Misool, 81FH66	35706
M. parvelatum		11J	Ass sl. 3	J18/3	Seafell-1 (1365.00)	35707
M. parvelatum		11K	SGM 4 (i)	O36/2	Peak-1 (4302.00)	35708
M. parvelatum		11L-M	SGM 2 (iv)	M29/2	Peak-1 (4302.00)	35709
M. parvelatum		11N	SGM 1 (i)	Q28/4	Peak-1 (4302.00)	35710
M. parvelatum		11O	SGM 2 (v)	H31/4	Macedon-5 (1350.00)	35711
M. parvelatum	H	11P-Q	Ass. sl. *MP* 26 (iv)	V60/1	Mto Panga Quarry	ML 2155*
M. parvelatum	T	11R	Ass. sl. *MP* 26 (iv)	D35	Mto Panga Quarry	ML 2155*
M. parvelatum		11S	SGM 1 (ii)	T32/1	Peak-1 (4302.00)	35712
M. parvelatum		11T	SGM 5 (iii)	Q21/2	Misool, 81FH66	35713
M. parvelatum		11U	SGM 5 (i)	N19/4	Misool, 81FH66	35714
M. parvelatum		11V	SSM 34	Q36/4	Misool, 81FH66	35715
M. parvelatum		11W	SGM 2 (i)	P28	Peak-1 (4302.00)	35716
M. parvelatum		11X-Y	SGM 2 (v)	L29/4	Peak-1 (4302.00)	35717
O. swanense	P	12A	SGM 1 (ii)	M22/1	Alaria-1 (3319.95)	35718
O. swanense	P	12B	SGM 100 (i)	N34/1	Jabiru-8A (1842.50)	35719
O. swanense	P	12C-D	SGM 2 (iii)	P23/1	Alaria-1 (3319.95)	35720
O. swanense	H	12E	SGM 1 (i)	L22	Alaria-1 (3319.95)	35721
O. swanense	P	12F	SGM 2 (i)	N23/1	Alaria-1 (3319.95)	35722
O. swanense	P	13A	SGM 2 (i)	O23/2	Alaria-1 (3315.95)	35723
O. swanense	P	13B	SGM 1 (i)	K25/3	Alaria-1 (3315.95)	35724
O. swanense	P	13C	SGM 2 (iv)	P23	Alaria-1 (3319.95)	35725
S. lineatum	H	14A-B	SGM 102 (i)	J35/4	Misool, 81FH63	35726
S. lineatum	P	14C	SGM 10 (ii)	M30/4	Misool, 81FH63	35727
S. lineatum	P	14D	SGM 100 (i)	Q39/3	Misool, 81FH63	35728
S. lineatum	P	14E-F	SGM 102 (vi)	H35/2	Misool, 81FH63	35729
S. lineatum	P	14G-H	SGM 10 (iii)	M30/4	Misool, 81FH63	35730
S. lineatum	P	14I-J	SGM 100 (ii)	P39/4	Misool, 81FH63	35731
S. lineatum	P	14K-L	SGM 101 (iii)	D39/1	Misool, 81FH63	35732
S. lineatum	P	14M-O	SGM 7 (ii)	M37/1	Misool, 81FH63	35733
S. lineatum	P	15P	SGM 4 (iii)	N14	Misool, 81FH63	35734
S. ottii	P	15A-B	SGM 2 (iii)	P25	Peak-1 (1493.54*)	35735
S. ottii	P	15C-D	SGM 1 (ii)	N33/3	Peak-1 (1493.54*)	35736
S. ottii	P	15E-F	SGM 6 (iii)	K20/3	New Zealand, f8556	SM 4757**
S. ottii	P	15G-H	SGM 10 (ii)	M24	New Zealand, f8556	SM 4758**
S. ottii	P	15I	SGM 8 (i)	L24/2	New Zealand, f8556	SM 4759**
S. ottii	P	15J-K	SGM 8 (iii)	K25/1	New Zealand, f8556	SM 4759**
S. ottii	P	15L	SGM 9 (iv)	O19/4	New Zealand, f8556	SM 4760**
S. ottii	P	15M-N	SGM 4 (iii)	N19/1	New Zealand, f8556	SM 4761**
S. ottii	H	15O-P	SGM 2 (ii)	J34	New Zealand, f8556	SM 4762**

* - Centre for Palynology, University of Sheffield, UK: type/figured slide collection registration number.

*ditch cuttings sample, range depth: 1493.54m-1496.59m

**Institute of Geological and Nuclear Sciences (formerly New Zealand Geological Survey) figured specimen numbers

Marine microplankton from the Late Jurassic (Tithonian) of the north-west Australian region

JAMES B. RIDING and ROBIN HELBY

RIDING, J.B. & HELBY, R., 2001:09:21. Marine microplankton from the Late Jurassic (Tithonian) of the north-west Australian region. *Memoir of the Association of Australasian Palaeontologists 24*, 177-220. ISSN 0810 8889.

A Late Jurassic (Tithonian) suite of marine microplankton is present in the Flamingo Formation and its equivalents in the Timor Sea, offshore north-western Australia and adjacent regions. It includes three new dinoflagellate cyst genera, *Aidelocysta*, *Ampulladinium* and *Belowia*, and ten species of dinoflagellate cysts, *Aidelocysta clavata*, *Ampulladinium variabile*, *Balcattia cheleusis*, *Batioladinium paeminosum*, *Belowia balteus*, *Biorbifera ferox*, *Cassiculosphaeridia solida*, *Dissimulidinium purattense*, *Gardodinium angustum* and *Pseudoceratium robustum*, are described as new. An additional morphotype of *Belowia*, *B.* sp. A. is informally described. The genera *Balcattia*, *Biorbifera* and *Dissimulidinium* and the species *Meiourogonyaulax bulloidea* are emended to note key morphological features observed in the material studied. *Stanfordella granulosa* is reported from the Southern Hemisphere for the first time. A new acritarch species, *Nummus tithonicus*, is also described. These microplankton taxa have stratigraphical utility in the Tithonian *Cribroperidinium perforans* Zone to the upper *Pseudoceratium iehiense* Zone.

James B. Riding, Australian Geological Survey Organisation, GPO Box 378, Canberra, ACT 2601, Australia (present address: British Geological Survey, Keyworth, Nottingham NG12 5GG, UK [e-mail: jbri@bgs.ac.uk]); Robin Helby (corresponding author), 356A Burns Bay Road, Lane Cove, NSW 2066, Australia (e-mail: rhelby@ozemail.com.au). *10 November 2000.*

Keywords: acritarchs, dinoflagellate cysts, Late Jurassic, Australia, biostratigraphy, taxonomy

THE PALYNOLOGICAL zonation of the Australian Mesozoic published by Helby *et al.* (1987) was the first attempt to provide an integrated, pan-Australian microplankton and spore-pollen zonation. Only the basic framework of the zonation was provided in anticipation that further contributions, particularly the documentation of new taxa, would be necessary as the zonation scheme evolved. This paper is one of a series providing the taxonomic foundation necessary to formalise the widely used unpublished subdivisions of these zones. These subzones have widespread currency within the hydrocarbon industry due to the legislative requirement for the release of technical data under the Petroleum (Submerged Lands) Act 1967. The informal subdivisions of the Helby *et al.* (1987) zonation have been entered into the Australian Geological Survey Organisation (AGSO) STRATDAT database. A diagrammatic update of the Helby *et al.* (1987) zonal scheme is presented by Foster (this volume), and will be fully described by Helby & Partridge (in prep.). This taxonomic project is an initiative of the Petroleum and Marine Division of AGSO.

This paper provides formal descriptions of previously undescribed marine microplankton taxa from Late Jurassic (Tithonian) palynofloras recorded in samples mainly from the Flamingo Formation and its equivalents in the Timor Sea, and equivalents elsewhere off north-western Australia (Whittam *et al.*, 1996, fig. 5) (see Appendices 1 and 2). The new taxa have stratigraphical utility within the Tithonian *Cribroperidinium perforans* Zone (5d) to the upper *Pseudoceratium iehiense* Zone (4ci) zones (Foster, this volume; Helby & Partridge, in prep.).

SYSTEMATIC PALYNOLOGY

In this section, three new genera and ten new species of dinoflagellate cyst and one new acritarch species are described. Additionally, *Meiourogonyaulax bulloidea* Cookson & Eisenack 1960 is emended. The genera are listed in alphabetical order within the two palynomorph groups; for the dinoflagellate cysts, the recent suprageneric classification of Fensome *et al.* (1993) is not formally used, but new genera are compared

with that scheme. The dimensions quoted are all given in micrometres (µm). For descriptive purposes, the cyst sizes, small, intermediate and large, follow Stover & Evitt (1978, p. 5). These parameters are such that intermediate size dinoflagellate cysts have a maximum dimension of between 50 and 100µm. Small and large forms are less than 50µm and above 100µm respectively. The majority of the morphological terminology for the dinoflagellate cysts are those used by Evitt (1985). However, the term loisthocyst refers to a dinoflagellate cyst in which the operculum (or the separate opercular pieces) has (have) detached and is therefore the part that remains (Sarjeant *et al.*, 1987, p. 26, 27). Where appropriate, the dinoflagellate cyst paraplate notation system used throughout is Kofoidian, as opposed to the 'Taylor-Evitt' scheme of Evitt (1985). References to author citations of taxa discussed are not given here. These may be found in the bibliography in Williams *et al.*, 1998, p. 747-817). The vast majority of specimens are housed in the Commonwealth Palaeontological Collection (CPC) of the Australian Geological Survey Organisation (AGSO), Canberra. Two specimens, previously illustrated by Bint & Marshall (1994), are housed in the collections of the Geological Survey of Western Australia, Perth (see Appendix 2).

This study has been conducted almost exclusively using single and multiple grain mounts and all the figured specimens, except for the Bint & Marshall (1994) material, are from these single species slides. The majority of the samples which were studied, are from conventional core and sidewall cores. However, some ditch cuttings and outcrop samples were also used. The photographs in the eighteen photomicrograph plates were all taken using an Olympus DP10 digital camera system coupled to a Zeiss Axioskop photomicroscope, all equipment being housed at AGSO. Some extraneous palynodebris, which is not adherent to the figured specimens, has been digitally removed in selected images.

The specimen images herein are taken from a digital database containing many more than have been figured. The sample details, morphological data and measurements of each imaged specimen are held on open file spreadsheets. The image database may be accessed on the AGSO website (http://www.agso.gov.au).

Some of the illustrated specimens (Figs 9Q-S, 14B-C, G-I), from older slides, have become quite transparent and have lost much of the natural colour and contrast evident in contemporaneous photomicrographs. Although the illustrations are "muddy", the specimens display features not shown adequately by other specimens.

Many of these new taxa have been extensively used in unpublished reports, which are now in the public domain (open file). In order to maximise the utility of the species, the informal names and/or codes are listed separate from any formal synonymy listing, under the heading 'Previous Australian usage'. To provide continuity, where practical, the informal name has been retained.

An unpublished manuscript which included some of the taxa described herein was prepared by Jill Stevens during the early 1980s (Stevens & Helby, unpublished). The manuscript names proposed by Stevens have been retained and she is included in the authorship of these taxa. These species are *Aidelocysta clavata*, *Balcattia cheleusis* and *Gardodinium angustum*. Similarly, the new genus *Ampulladinium* was originally proposed by Frances M. Parker (see Parker, 1986) and she is also included as an author of this genus and the species *A. variabile*. However, neither the specimens studied, nor the descriptions by Stevens and Parker have been used in this paper.

Dinoflagellate cysts

Aidelocysta Riding, Helby & Stevens gen. nov.

Type species. Aidelocysta clavata Riding, Helby & Stevens sp. nov.

Diagnosis. Small, acavate to holocavate, proximate, quadrilobate, dorsoventrally flattened dinoflagellate cysts with an equatorial constriction. The hypocyst and epicyst each comprise two prominent rounded lobes or protuberances in dorsoventral view. The cysts are elongate ellipsoidal in lateral view. The autophragm bears predominantly nontabular low relief ornamentation, which may be distally connected to form an ectophragm. The autophragm may also be differentiated. Occasionally, short, discontinuous lineations of ornamentation may be parasutural or penitabular. Archaeopyle anterior intercalary, type I (2a), eurydeltaform in shape; the operculum is normally free. The archaeopyle is situated close to the apex (i.e. subpolar). The hexagonal outline of the principal archaeopyle suture may be distorted into an ellipsoidal shape. Paratabulation not developed except at the principal archaeopyle suture, and occasional alignment of ornament. Paracingulum indicated by the equatorial constriction and possibly a lack of ornamentation. The parasulcus

is marked by a narrow, midventral, linear depression and by reduced ornamentation.

Comments. *Aidelocysta* is a distinctive, small, quadrilobate genus with a subpolar, anterior intercalary archaeopyle. Distortion may alter the outline of the archaeopyle from hexagonal to ellipsoidal. Due to the high position of the archaeopyle on the epicyst, the hexagonal shape may not be observable in poorly preserved or oriented material. The shape of the archaeopyle is hexagonal and is eury-deltaform of Bujak & Davies (1983). This genus is, therefore, peridiniacean and *Aidelocysta* appears to be one of the oldest representatives of the suborder Peridiniineae (order Peridiniales) of Fensome *et al*. (1993). Previously, the oldest known peridiniacean was the Tithonian calcareous dinoflagellate cyst *Pirumella multistrata* (Pflaumann & Krasheninnikov 1978) Lentin & Williams 1993 forma *carteri* (Bolli 1974) Williams *et al*. 1998. However, the oldest unequivocal dinosporin peridinacean species is *Subtilisphaera terrula* (Davey 1974) Lentin & Williams 1976, the earliest occurrence of which is Hauterivian (Duxbury, 1977, fig. 21). *Pyxidiella pandora* Cookson & Eisenack 1958, from the Upper Jurassic (Tithonian) Dingo Siltstone of Western Australia (Cookson & Eisenack, 1958) is older (Callovian to Berriasian), but its anterior intercalary archaeopyle appears to be seven-sided, suggesting an affinity with the Family Heterocapsaceae. There are also two possible species of *Subtilisphaera*; *S? inaffecta* (Drugg 1978) Bujak & Davies 1983 and *S? paeminosa* (Drugg 1978) Bujak & Davies 1983, in the Late Jurassic (Kimmeridgian) of Europe. However, the peridiniacean affinities of these species are uncertain (Riding & Thomas, 1988). *Aidelocysta* is unusual among peridinioid genera in lacking polar horns and not being cavate.

Comparison. *Aidelocysta* resembles several other small proximate genera, but is the only quadrilobate genus to have an anterior intercalary archaeopyle of peridiniacean type. *Hexagonifera* Cookson & Eisenack 1961 emend. Stover & Evitt 1978 resembles *Aidelocysta* in being an acavate peridiniineacean genus which lacks polar horns and has a subpolar type I archaeopyle. However, *Hexagonifera* is subspherical to ellipsoidal in outline, is not holocavate and lacks an equatorial constriction. *Pyxidiella* Cookson & Eisenack 1958 differs from *Aidelocysta* in being elongate ellipsoidal, exclusively acavate, paratabulate and not constricted in the paracingular region.

Members of the '*Parvocysta* suite' of Riding (1984) resemble *Aidelocysta* in having lobate epicysts and hypocysts. This complex includes *Parvocysta* Bjaerke 1980, *Reutlingia* Drugg 1978 emend. Below 1987 and *Susadinium* Dörhöfer & Davies. However, members of the '*Parvocysta* suite' usually have apical horns and therefore are subpentagonal in outline. Moreover, the anterior intercalary archaeopyles are longitudinally elongate and have geniculate anterior and posterior margins. *Stenopyxinium* Deflandre 1968 is a lobate genus, but is extremely small, spinose and probably has a epicystal rather than an intercalary archaeopyle.

Of the genera with apical archaeopyles, the most similar to *Aidelocysta* are the quadrilobate forms *Horologinella* Cookson & Eisenack 1962 emend. Backhouse 1988 and *Tetrachacysta* Backhouse 1988. However, *Horologinella* has an unusual paratabulation indicated by parasutural ridges and an apical archaeopyle with a subcircular principal archaeopyle suture (Backhouse, 1988). *Tetrachacysta* is small, quadrilobate, has no indications of paratabulation other than the angular, apical principal archaeopyle suture (Backhouse, 1988, fig. 32) and accessory archaeopyle sutures.

Ampulladinium gen. nov. varies from being acavate to holocavate and sometimes has a differentiated autophragm. However, *Ampulladinium* is trilobate and has an apical archaeopyle. *Tringadinium* Riding & Helby (this volume) and *Woodinia* Riding & Helby (this volume) are also somewhat similar to *Aidelocysta*. *Tringadinium* is lobate and has an equatorial constriction, but is exclusively acavate and has a gonyaulacalean paratabulation indicated by intratabular protuberances. *Woodinia* is elongate, sometimes trilobate, has intratabular ornamentation and an extremely small epicyst. Both *Tringadinium* and *Woodinia* have apical archaeopyles.

Derivation of name. From the Greek, *aidelos*, meaning unseen or obscure, referring to the intercalary archaeopyle.

Aidelocysta clavata Riding, Helby & Stevens sp. nov. (Figs 1A-P)

1994 *Tetrachacysta* sp. A; Bint & Marshall, figs 5.13-5.14.

Previous Australian usage
Aidelocysta clavata Stevens & Helby (manuscript name).

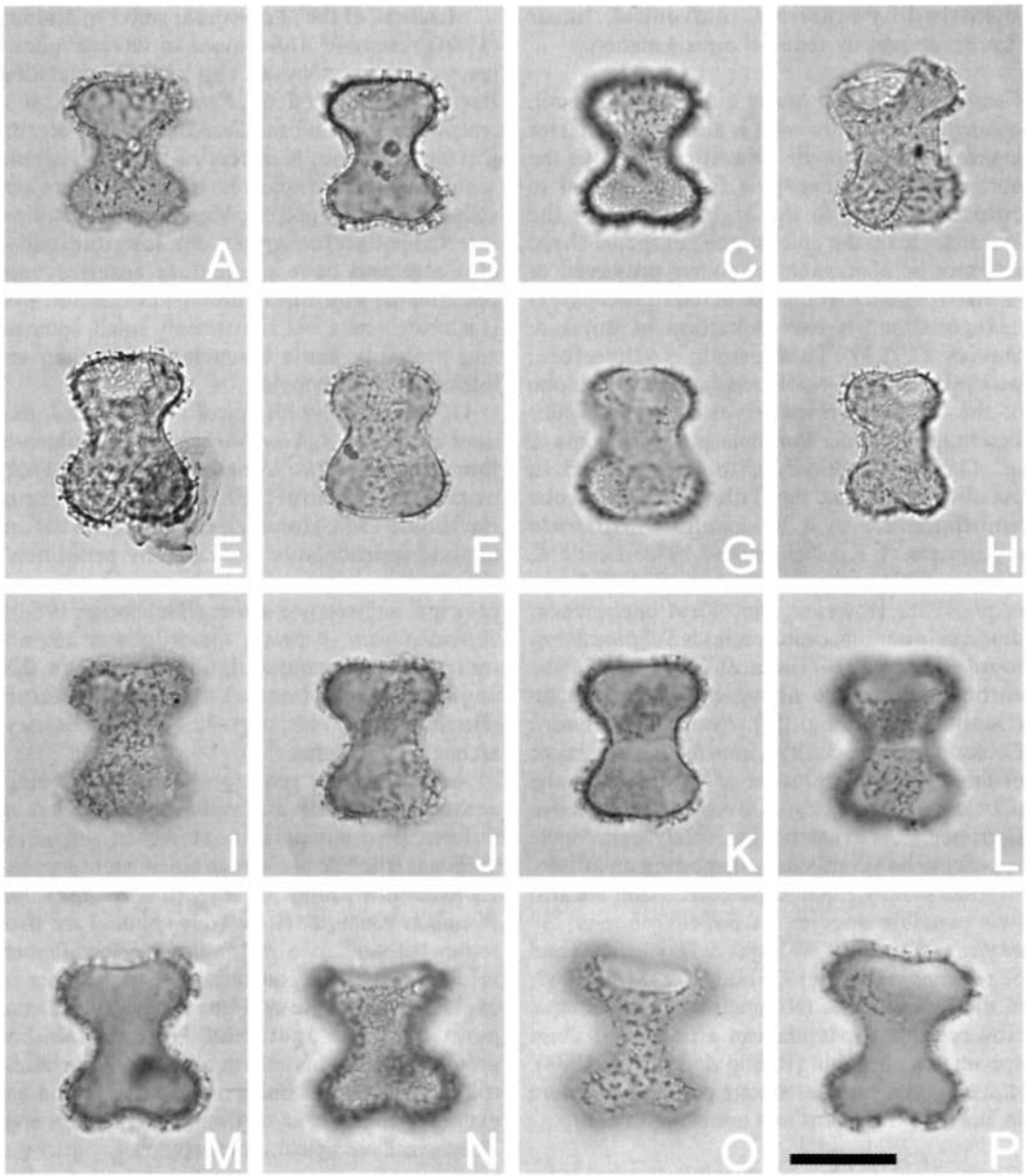

Fig. 1. Aidelocysta clavata Riding, Helby & Stevens sp. nov. All from conventional core in Lorikeet-1 well at 1759.10m (Figs 1A-C, F-G), Wanaea-2 well at 3375.34m (Fig. 1D), 2880.50m (Figs 1I-L) and 2875.30m (Figs 1E, H) and a sidewall core from Avocet-1A well at 1771.50m (Figs 1M-P). All photomicrographs taken using plain transmitted light. The scale bar in Fig. 1P refers to all photomicrographs and is 25µm. Figures 1I-L are the holotype; the remainder paratypes. Note small size, quadrilobate outline with marked paracingular constriction, short, dense processes which may be connected distally by an ectophragm, and anterior intercalary archaeopyle. A-C - CPC 35883, paratype; ventral view, high to low focus sequence. Note dense cover of short processes and partial development of an ectophragm. D - CPC 35884, paratype; dorsal view, median focus. Note prominent anterior intercalary archaeopyle. E - CPC 35885, paratype; dorsal view, median focus. Note short processes, some of which are connected distally, and anterior intercalary archaeopyle. F, G - CPC 35886, paratype; ventral view, high and low focus respectively. Note extremely short processes. H - CPC 35887, paratype; oblique dorsal view, median focus. Note strongly quadrilobate nature of species and anterior intercalary archaeopyle. I-L - CPC 35888, holotype; ventral view, high to low focus sequence. Note extremely dense cover of short processes and displaced operculum in Figs 1J-K. M, N - CPC 35889, paratype; ventral view, median and low focus respectively. Note highly constricted equatorial region. O, P - CPC 35890, paratype; dorsal view, high and median focus respectively. Note even cover of processes and anterior intercalary archaeopyle.

Vespadinia clavata Parker (1986, p. 176, 177, pl. 40, figs 5, 6).

Description. A species of *Aidelocysta* which may be acavate to holocavate. Four prominent rounded lobes or protuberances are present, two on the epicyst and two on the hypocyst. The lobes are virtually identical in size and shape, imparting longitudinal symmetry to the cyst. However the lobes in the epicyst may be larger than the lobes of the hypocyst and *vice versa*; the species is rarely symmetrical about the equator (Fig. 1). The autophragm is about 1µm thick and covered by dominantly nontabular, short, solid processes which are distally truncate, buccinate or capitate. The processes are between 0.5 and 1µm in width and vary between being isolated, up to 2.5µm apart, to extremely closely spaced. In forms with densely packed processes, individual elements are connected distally forming an ectophragm. Holocavate specimens may have a microreticulate appearance due to the network formed by distally-expanded process tips beneath the ectophragm. Typically the width of the archaeopyle is twice the height (see dimensions, below). Some short, discontinuous lineations of processes appear to be parasutural or penitabular. The paracingulum and parasulcus are marked by a deep equatorial constriction and a narrow depression respectively and generally lack processes.

Dimensions (µm, n=25) including ornamentation where appropriate: Min. (Mean) Max.
Length of cyst: 34 (40) 49
Maximum width of hypocyst: 24 (30) 36
Equatorial (paracingular) width: 16 (19) 28
Maximum width of epicyst: 26 (31) 36
Height of archaeopyle: 6 (8) 10
Width of archaeopyle: 12 (15) 20
Height of processes: 1 (2) 4

The measured specimens are from conventional core samples in Lambert-2 well at 3101.00m, Lorikeet-1 well at 1759.10m and Wanaea-2 well at 3375.34m, 2880.50m and 2875.30m, a sidewall core sample from Jurabi-1 well at 1140.00m and ditch cuttings from Broome-3 Town Bore between 305.11m and 317.61m.

Comments. This species of *Aidelocysta* does not vary significantly in size. The shape, however, varies in that the epicyst or the hypocyst may be the widest part of the cyst (Fig. 1). Specimens where the epicystal and hypocystal lobes are similar in size are relatively rare. It also exhibits considerable variability in ornament type, length and density (Fig. 1). The short processes may be distally truncate, buccinate or most commonly capitate. They are also sparsely to densely spaced, with occasional specimens having differentiated autophragm. Forms with dense processes are frequently holocavate (e.g. Figs 1I-L). Occasionally, some areas of this species may have discontinuous lineations of processes which are either parasutural or penitabular. A full paratabulation pattern, however, has not been observed. Compression of the autophragm distorts the shape of the archaeopyle to ellipsoidal in some specimens.

Comparison. This species is distinguished by its quadrilobate shape, lack of polar horns and subpolar, peridiniacean style, anterior intercalary archaeopyle. *Aidelocysta* is currently monotypic and therefore generic comparisons (see above) also apply here. Species of *Tetrachacysta* such as *T. allenii* Backhouse 1988, *T. baculata* Backhouse 1988 and *T. spinosigibberosa* (Brideaux & Fisher 1976) Backhouse 1988 closely resemble *A. clavata*, but are distinguished by their apical archaeopyles.

Derivation of name. An adjective derived from the Latin *clava*, meaning club or cudgel, referring to the distally flared nature of the processes.

Holotype and type locality. Figures 1I-L, CPC 35888, from a conventional core sample in Wanaea-2 well at 2880.50m.

Stratigraphical distribution. *Aidelocysta clavata* ranges from the Tithonian upper *Dingodinium jurassicum* Zone (5aii) to the Berriasian *Kalyptea wisemaniae* Zone (4biii) (Foster, this volume; Helby & Partridge, in prep.).

Ampulladinium Riding, Helby & Parker gen. nov.

Type species. *Ampulladinium variabile* Riding, Helby & Parker sp. nov.

Diagnosis. Small to intermediate sized, rounded triangular dinoflagellate cysts, that are acavate to holocavate, proximate to proximochorate, and exhibit some dorsoventral flattening. The widest part of the cyst is at the antapex, and the antapical lateral areas are extended into prominent lobes or protuberances. The apex is much narrower. Ornamentation is nontabular and of low relief; the autophragm may be differentiated. Archaeopyle apical, operculum simple, normally free. The

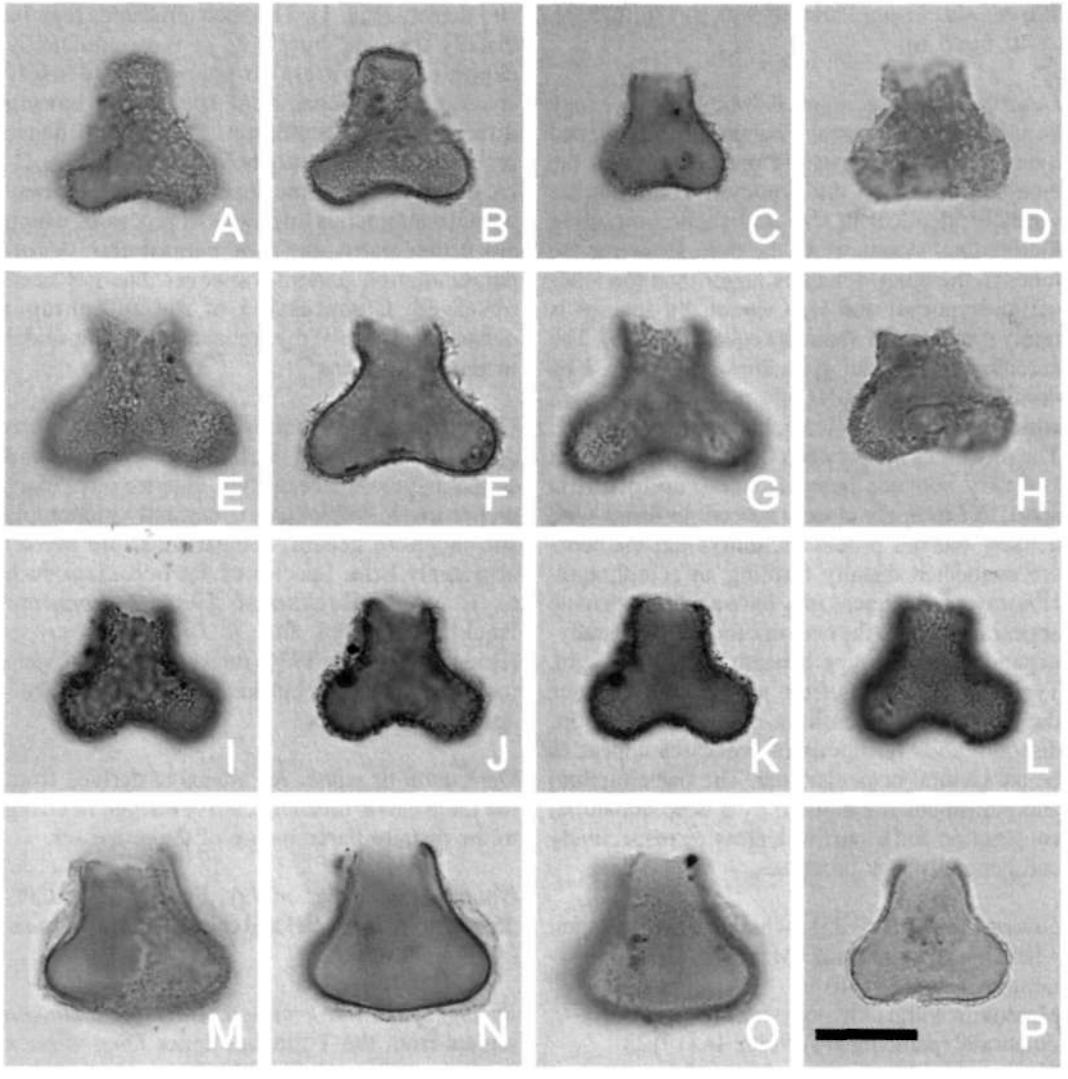

Fig. 2. Ampulladinium variabile Riding, Helby & Parker sp. nov. All from conventional core samples from Lorikeet-1 well at 1759.10m (Figs 2A-C) and 1756.70m (Figs 2E-F) and Mutineer-1B well at 3132.25m (Figs 2D, H), a sidewall core sample from Jurabi-1 well at 1140.00m (Fig. 2P) and ditch cuttings from Avocet-1A well between 1775.00m and 1780.00m (Figs 2I-L) and Peak-1 well between 1493.54m and 1496.59m (Figs 2M-O). All photomicrographs taken using plain transmitted light. The scale bar in Fig. 2P refers to all the photomicrographs and is 25µm. Figs 2I-L are the holotype; the remainder paratypes. Note trilobate/subtriangular outline, variable development of an antapical constriction between lateral/antapical lobes, variably holocavate cyst organisation and apical archaeopyle. A, B - CPC 35891, paratype; dorsal view, high and median focus respectively. Note flattened nature of the operculum, which is in place. C - CPC 35892, paratype; dorsal view, median focus. Note partial holocavate cyst organisation and apical archaeopyle. D - CPC 35893, paratype; dorsal view, median focus. Note that ectophragm and the processes have been removed in this poorly preserved specimen. E-F - CPC 35894, paratype; ventral view, high to low focus sequence. Note prominent antapical concavity and processes; the majority of the thin ectophragm has been lost. H - CPC 35895, paratype; dorsal view, high focus. Note that ectophragm and processes have been lost. I-L - CPC 35896, holotype; oblique ventral view, high to low focus sequence. Note angular nature of the principal archaeopyle suture, trilobate outline, holocavate cyst organisation and apical archaeopyle. M-O - CPC 35897, paratype; right lateral view, high to low focus sequence. Note relatively wide ectocoel and lack of an antapical concavity. P - CPC 35898, paratype; dorsal view, high/median focus. Note narrow ectocoel and apical archaeopyle.

principal archaeopyle suture has a prominent midventral parasulcal notch and is consistent with a gonyaulacalean paratabulation pattern. Accessory archaeopyle sutures may be developed. Except for the archaeopyle, paratabulation is not evident.

Comments. *Ampulladinium* has a distinctive rounded triangular outline. The autophragm forms two antapical lateral lobes, while the apex is subspherical. The genus is typically holocavate with a narrow ectocoel, however, in the type, *A. variabile,* the ectophragm appears susceptible to physico-chemical degradation.

Comparison. This new genus is similar in size and shape to *Woodinia* Riding & Helby (this volume). However *Woodinia* is not holocavate and has intratabular areas of ornamentation differentiated on the major paraplate series, which indicate gonyaulacacean paratabulation. Furthermore, the paracingulum of *Woodinia* is high on the cyst due to the unusually long postcingular paraplates. *Ampulladinium* also resembles *Dissimulidinium* May *et al.* 1987 in having paired antapical lobes, but the latter is laterally compressed, consistently proximochorate and may have parasutural ornamentation. The Late Cretaceous *Dorocysta* Davey 1970 has longer processes and lacks the trilobate shape of *Ampulladinium*. *Phallocysta* Dörhöfer & Davies 1980 is, like *Ampulladinium*, flask-shaped, trilobate and widest at the antapex, but has an anterior intercalary archaeopyle and is epicavate (Riding, 1984; 1994). Members of the Early-Mid Jurassic '*Parvocysta* suite' of Riding (1984) also bear a superficial resemblance to *Ampulladinium*, but these taxa have an anterior intercalary archaeopyle. *Stenopyxinium* Deflandre 1968 is similar in shape to *Ampulladinium,* but is distinguished by its spinose antapical protrusions and possible combination (apical/precingular) or epicystal archaeopyle. *Tetrachacysta* Backhouse 1988 is a quadrilobate genus with a pair of lateral protuberances on both the epicyst and hypocyst (Backhouse, 1988, fig. 32).

Derivation of name. From the Latin, *ampulla* meaning flask or bottle, referring to the cyst shape.

Ampulladinium variabile Riding, Helby & Parker sp. nov. (Figs 2A-P)

Previous Australian usage
Ampulladinium minutispinosum – Parker (1986, p. 30, 31, fig. 5.2, pl. 1, figs 4-6).
M.P. 766 (pars) – Helby.

Description. A holocavate species of *Ampulladinium* which is slightly dorsoventrally-compressed. It is trilobate and subtriangular in outline; a slight antapical concavity may be present between the hypocystal lobes. The autophragm is about 1 to 1.5µm thick and overlain by a thin (<0.5µm), finely but irregularly reticulate ectophragm. Short (1-5µm), solid, slender processes support the outer layer of the ectophragm. Where this outer layer is missing, the processes may be thorn-shaped and appear to taper to sharp points distally. The density of these elements varies from relatively sparse to extremely dense, although they have not been observed on the parasulcus. The density of the processes tends to be greatest in the peripheral areas of the cyst, especially on the antapical-lateral lobes. The ectophragm may be absent in poorly-preserved material, suggesting that it may be susceptible to physico-chemical degradation. In extreme cases, the processes may also be degraded. The operculum is small, flattened and short accessory archaeopyle sutures are normally developed.

Dimensions (µm, n=25): Min. (Mean) Max.
Length of entire cyst: 37 (43) 52
Length of loisthocyst: 32 (39) 50
Width of epicyst incl. ornament*: 14 (21) 31
Width of hypocyst incl. ornament**: 34 (44) 59
Length of processes/height of ectocoel: 1 (2) 5
* - measured at the principal archaeopyle suture
** - measured at the antapex

The measured specimens are from conventional core samples in Lorikeet-1 well at 1759.10m and 1756.70m and Mutineer-1B well at 3132.25m, sidewall core samples from Jurabi-1 well at 1140.00m and Scafell-1 well at 1418.00m and ditch cuttings from Avocet-1A well between 1775.00m and 1780.00m, Broome-1 Bore at 297.79m and Peak-1 well between 1493.54m and 1496.59m.

Comments. This species is highly variable in morphology due to the apparent susceptibility of the ectophragm to physico-chemical degradation. In well-preserved material, a continuous ectophragm is supported by numerous processes (Figs 2M-O). However, the ectophragm is frequently incomplete (e.g. Figs 2E-G). In poorly-preserved material, both the processes/spines and ectophragm are missing (Figs 2D, H). Most specimens of *A. variabile* are small and the

majority loisthocysts. The ectocoel is normally narrow; from 1-5µm across. In some specimens, the processes are longest at the antapical-lateral lobes, broadening the ectocoel in those areas.

Comparison. *Ampulladinium variabile* closely resembles *Woodinia bensonii* Riding & Helby (this volume) in morphology. However, the latter is significantly smaller, frequently more elongate and antapically concave. Furthermore, *W. bensonii* is not holocavate and is characterised by intratabular areas of ornamentation or differentiated autophragm on the major paraplate series.

Derivation of name. From the Latin, *variabilis* meaning different or changeable and referring to the varied wall structure and ornamentational styles of this species.

Holotype and type locality. Figures 2I-L, CPC 35896, from a ditch cuttings sample in Avocet-1A well between 1775.00m and 1780.00m.

Stratigraphical distribution. *Ampulladinium variabile* ranges from the Tithonian upper *Dingodinium jurassicum* Zone (5aii) to the lower *Pseudoceratium iehiense* Zone (4ciia) (Foster, this volume; Helby & Partridge, in prep.).

Balcattia Cookson & Eisenack 1974 emend. Riding, Helby & Stevens

Type species. *Balcattia cirrifera* Cookson & Eisenack 1974

Emended diagnosis. Intermediate to large, acavate, chorate dinoflagellate cysts. Autophragm smooth or with low-relief ornamentation; low parasutural ridges and short, nontabular elements may occur. Cyst body subspherical to elongate ellipsoidal, bearing long, solid or hollow processes, which may be distally connected by trabeculae. The intratabular processes are confined to the polar regions and may be present on each of the antapical, posterior intercalary, postcingular, precingular and apical paraplates. The processes (and the parasutural ridges where developed) indicate a gonyaulacalean paratabulation pattern. Archaeopyle apical; operculum simple and free. Paracingulum not indicated; parasulcus only indicated by the parasulcal notch.

Comments. The generic concept is emended above to accommodate our observations of the illustrations of *Balcattia cheleusis* Riding, Helby & Stevens sp. nov. and *Balcattia* sp. A of Helby *et al*. (1987, figs 27I-27K). The generic synthesis of Stover & Evitt (1978, p. 20) closely followed the original diagnosis of Cookson & Eisenack (1974, p. 78) and Stover & Evitt concluded that the posterior structure is '...formed of indistinct longitudinal strands joined antapically and loosely connected laterally'. We consider that the topotype of Cookson & Eisenack (1974, pl. 28, fig. 16) clearly exhibits separate, distally trabeculate processes, in contradistinction to the Stover & Evitt interpretation. The holotype also exhibits antapical processes, although they are not as clearly defined as those on the topotype. Distally trabeculate, apical processes are also distinct on the specimen of *B. cirrifera* illustrated by Morgan (1980, pl. 2, figs 6, 7). Where postcingular and precingular processes occur, they are migrated to the polar margins of their respective paraplates. The polar disposition of the processes on *B. cheleusis*, particularly the antapical processes, parallels the migration of the major processes on *B. cirrifera*. This concept of process migration is also encountered in *Belowia* Riding & Helby (see below) and *Hadriana* Riding & Helby (this volume). While the anterior process groups on *B. cirrifera* are on the apical paraplates, the anterior processes on *B. cheleusis* are located close to the apical margins of the precingular paraplates. Although these differences are significant, other similarities suggest that a separate genus is not warranted. *Balcattia* sp. A of Helby *et al*. (1987) has low, smooth parasutural ridges.

Balcattia cheleusis Riding, Helby & Stevens sp. nov. (Figs 3A-P)

1994 *Rigaudella* sp. B; Bint & Marshall, fig. 5.15.

Previous Australian usage

Emmetrocysta cheleusis Stevens & Helby (manuscript name).

Rigaudella separata – Parker (1986, p. 99-100, fig. 5.41, pl. 21, figs 3-6).

Rigaudella separata – Helby.

MP 346 – Helby.

Description. A species of *Balcattia* with a large, elongate ovoidal to subquadrangular cyst body. A small antapical protuberance may be present and the paracingular area is occasionally indented. The autophragm is moderately thin (0.5-1µm), smooth to occasionally shagreenate or irregularly microscabrate. Intratabular processes, which are

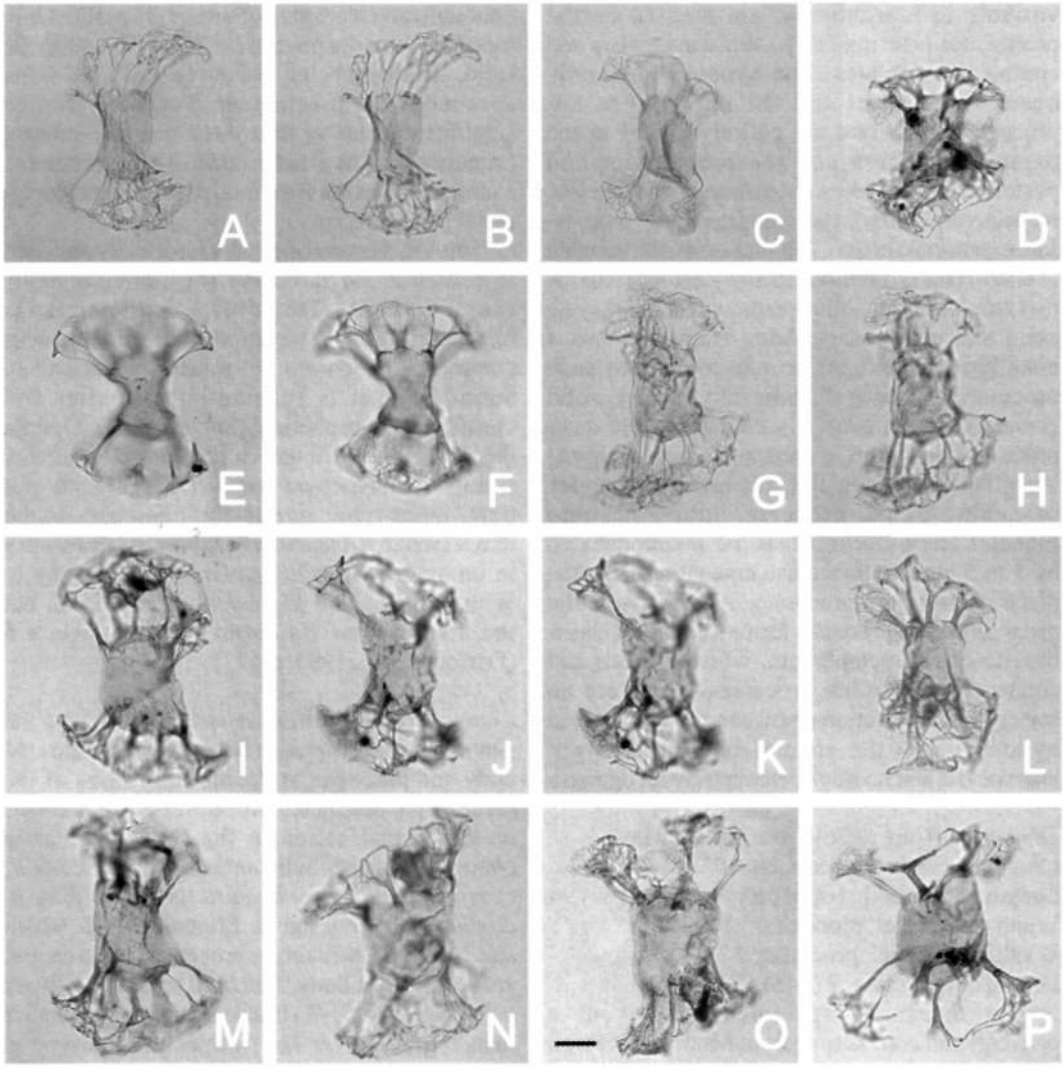

Fig. 3. Balcattia cheleusis Riding, Helby & Stevens sp. nov. Specimens from sidewall core samples in Nancar-1 well at 3240.00m (Fig. 3O), Scafell-1 well at 1421.00m (Figs 3A-C, L) and 1418.00m (Figs 3G-H, N), Wanaea-3 well at 2964.00m (Figs 3E-F) and ditch cuttings from Mindil-1 well between 3150.00m and 3155.00m (Figs 3D, I-K, M, P). All photomicrographs taken using plain transmitted light. The scale bar in Fig. 3O refers to all photomicrographs and is 25µm. Figures 3E-F are the holotype; remainder are paratypes. Note elongate ovoidal cyst body, 12-13 distally expanded, trabeculate intratabular processes inserted close to poles (i.e. have migrated), and apical archaeopyle. A, B - CPC 35899, paratype; dorsal view, high and median focus respectively. Note smooth autophragm of the cyst body and how subpolar processes branch medially. C - CPC 35900, paratype; oblique ventral view, high focus. Note wide equatorial area devoid of processes. D - CPC 35901, paratype; oblique dorsal view, high/median focus. Note strongly distally trabeculate nature of the subpolar processes. E, F - F.49309, holotype; ventral view, high and median/low focus respectively. Note strong equatorial constriction of cyst body and parasulcal notch in E. G, H - CPC 35902, paratype; ventral view, high/median and low focus respectively. Note elongate cyst body and small antapical protuberance surmounted by the 1'''' process. I - CPC 35903, paratype; dorsal view, low focus. Note regular nature of intratabular processes. J, K - CPC 35904, paratype; dorsal view, median and low focus respectively. Note small antapical protuberance with its intratabular process. L - CPC 35905, paratype; dorsal view, median focus. Note largely hollow nature of processes. M - CPC 35906, paratype; dorsal view, median focus. Note antapical part of cyst body is relatively wide in this specimen. N - CPC 35907, paratype; ventral view, low focus. Specimen with relatively squat cyst body. O - CPC 35908, paratype; dorsal view, median focus. Form with relatively wide processes. P - CPC 35909, paratype; oblique ventral view, median focus. Distal trabeculum in this specimen is damaged.

variable in morphology, are present on the precingular, postcingular, posterior intercalary and antapical paraplates. The hypocyst generally bears 7 processes and the epicyst has 5-6 processes. Processes are entirely absent in the paracingular area and the precingular and postcingular processes are inserted high and low respectively. This factor highlights the process-free equatorial region. The processes are variable in length (see dimensions, below), slender to wide (3-12µm), mostly hollow, although some may be solid and others vacuolate. They are always distally expanded. At around midlength each process subdivides distally into slender, solid elements, which generally connect to the other processes and form a trabeculate ectophragmal layer. This expansion normally involves complex branching of the processes into fenestrate funnels. The processes may be interconnected by 1 to 5 slender trabeculae emanating from the distal parts of the processes. Alternatively, the distal part of the processes forms a complex, sheet-like, fenestrate ectophragm, which extends and connects to the other processes. There are no trabeculate connections between the epicyst and hypocyst. All the specimens studied were loisthocysts and no free opercula were recognised.

Dimensions (µm, n=26): Min. (Mean) Max.
Length of cyst incl. processes: 105 (141) 170
Length of cyst body (excl. processes): 56 (69) 94
Width of cyst incl. processes: 73 (104) 135
Width of cyst excl. processes: 37 (54) 78
Length of processes: 27 (45) 66

The measured specimens are from a conventional core sample from Mutineer-1B well at 3147.60m, sidewall core samples from Nancar-1 well at 3240.00m, Puratte-1 well at 172.00m, Scafell-1 well at 1421.00m and Wanaea-3 well at 2964.00m and ditch cuttings from Broome-1 Bore at 297.79m and Mindil-1 well between 3150.00m and 3155.00m.

Comments. This distinctive species of *Balcattia* is large, and the size range is considerable. The processes have a bipolar distribution and are positioned high on the precingular paraplate series and low on the postcingular paraplate series (Fig. 3). All of the specimens studied were loisthocysts, and these were oriented by the position of the archaeopyle and the occasional presence of a small antapical protuberance. Where present, this protuberance bears the 1'''' process. The processes are somewhat variable in morphology. Most are relatively long and slender (e.g. Figs 3A, 3B); however, short and wide processes, although rare, were also observed (Fig. 3D). Only especially slender processes (1-2µm in width) are solid, all others being hollow (Fig. 3). On some specimens the precingular processes may be significantly shorter than those near the antapex (specimens not illustrated). The specimens examined from the Broome-1 Bore do not exhibit distal trabeculation.

This species was originally informally assigned to *Emmetrocysta* Stover 1975 by Stevens & Helby (unpublished). However, that genus is characterised by paraplate-centred process complexes which are not joined by trabeculate strands and it is substantially smaller and consistently subspherical (Stover, 1975). Despite the substantial differences between *B. cheleusis* and the genotype, we consider the erection of a new, monotypic genus for *cheleusis* to be unwarranted. *B. cheleusis* has some major features in common with *Oligosphaeridium* Davey & Williams 1966 and *Rigaudella* Below 1982, but the affinities of *Balcattia* remain uncertain (Fensome *et al.*, 1993, p. 117).

Comparison. Balcattia cheleusis differs from the genotype, *B. cirrifera*, in having an elongate cyst body and processes at the apical margins of the precingular paraplates, as opposed to processes on the apical series in the latter. *Balcattia cheleusis* is also substantially larger than *B. cirrifera*. *Balcattia cheleusis* is larger than *B. cirribarbata* Cookson & Eisenack 1982, which also has short, nontabular processes in the central area of the cyst body. *Balcattia* sp. A of Helby *et al.* (1987, figs 27I-K) is also significantly smaller than *B. cheleusis*. The former morphotype is paratabulate and lacks precingular processes.

Derivation of name. From the Greek, *cheleusis* meaning a netting and referring to the complex distal trabeculation of this species.

Holotype and type locality. Figures 3E-F, Geological Survey of Western Australia specimen F.49309, sidewall core sample from Wanaea-3 well at 2964.00m. This specimen was figured as *Rigaudella* sp. B by Bint & Marshall (1994, fig. 5.15).

Stratigraphical distribution. Balcattia cheleusis is confined to the Tithonian and ranges from the upper *Dingodinium jurassicum* Zone (5ai) to the lower *Pseudoceratium iehiense* Zone (4ciiib) (Foster, this volume; Helby & Partridge, in prep.).

Batioladinium Brideaux 1975

Type species. Batioladinium jaegeri (Alberti 1961) Brideaux 1975 emend. Below 1990

Comments. Pourtoy (1988, p. 390) proposed the inclusion of forms without polar horns from *Batioladinium*. We concur with Lentin & Vozzhennikova (1990, p. 82), and do not follow Pourtoy's emendation.

Batioladinium paeminosum sp. nov. (Figs 4A-P)

?1990 *Necrobroomea* sp.; Below, pl. 13, fig. 20.
1994 *Batioladinium* sp. A; Bint & Marshall, fig. 5.2.

Previous Australian usage
1986 ?*Batioladinium* sp. cf. *B. micropodum* (Eisenack & Cookson 1960) Brideaux 1975; Parker, p. 38, 39, pl. 2, fig. 9.
Batioladinium protojaegeri – Helby.

Description. An intermediate to large species of *Batioladinium* which is slightly dorsoventrally flattened with a thick, robust autophragm and low ornamentation. The autophragm is about 2µm thick and is covered with dense, nontabular rugulate to verrucate ornamentation. The rugulae comprise relatively short, undulose ridges, mostly 2 to 3µm wide, which may break up into irregular verrucae. The high density and irregular nature of the verrucae, particularly on the hypocyst, may give rise to a "scrollwork" pattern of ornamentation. The ornamentation varies in height from about 0.5 to 1µm and becomes markedly more prominent towards the antapical area. The paracingulum is slightly indented, has reduced ornamentation and may bear low, discontinuous, parasutural ridges and reduced ornamentation. The epicyst is longer than the hypocyst. The anterior part of the parasulcus lies in the area between the offset ends of the paracingulum and below the ventral notch (6"/1') of the principal archaeopyle suture. The single apical and paired antapical horns are variable in length, typically have solid distal portions and are rounded to pointed distally. The left antapical horn is larger than the right and both antapical horns may be markedly reduced.

Dimensions (µm, n=30): Min. (Mean) Max.
Length of entire cyst incl. horns: 82 (109) 146
Length of loisthocyst incl. horns: 55 (72) 93
Length of operculum: 44 (66) 81
Maximum width: 25 (33) 45
Length of apical horn: 10 (30) 55
Length of the left antapical horn: 4 (11) 22

The measured specimens are from conventional core samples in Lambert-2 well at 3101.00m, Lorikeet-1 well at 1761.20m and 1759.10m, Mutineer-1B well at 3132.25m, Wanaea-2 well at 2880.50m and 2875.30m and sidewall cores from Avocet-1A well at 1780.00m, 1778.00m, 1777.00m and 1771.50m, Scafell-1 well at 1418.00m and Zeewulf-1 well at 3085.00m.

Comments. Batioladinium paeminosum is characterised by the prominent rugulate-verrucate autophragm, especially on the hypocyst, the size of ornament elements diminishing towards the apex (Fig. 4). The ornamentation may be slightly irregular, variable in height and/or reduced in some specimens (Fig. 4). Many forms have relatively short antapical horns and the length of the apical horn is extremely variable (see above). In most specimens, the horns are distally rounded and in some individuals the outline of the antapical horns is disrupted by the ornamentation. Individuals with highly reduced antapical horns and in which the archaeopyle has not opened could be misidentified as *Pareodinia* Deflandre 1947 (Fig. 4M). Species of *Pareodinia* resembling *B. paeminosum* occur throughout the stratigraphical range of the latter. Rarely, morphotypes similar to *Batioladinium paeminosum*, but with a microreticulate autophragm have been observed.

Comparison. Necrobroomea sp. of Below (1990, pl. 13, fig. 20), from the Volgian of the Russian Platform, closely resembles *Batioladinium paeminosum*, and is indistinguishable from some end members of the species. The ornamentation of the specimens of *Necrobroomea micropoda* (Eisenack & Cookson 1960) Wiggins 1975 emend. Below 1990, as figured by Below (1990, pl. 13, figs 17-19) closely resembles that of *B. paeminosum*.

Batioladinium paeminosum differs from the other species of the genus by the rugulate/verrucate ornamentation which diminishes in size apically. The majority of species of this genus, including the genotype *Batioladinium jaegeri* (Alberti 1961) Brideaux 1975, are psilate or have extremely low relief ornamentation (Alberti, 1961). *Batioladinium daviesii* Lentin & Vozzhennikova 1990, *B. matyjae* Poulsen 1996 and *B. micropodum*, however, have a granulate autophragm. The early Cretaceous species *Batioladinium? gochtii* (Alberti 1961) Lentin & Williams 1977 has a tuberculate autophragm, is pareodinioid in outline,

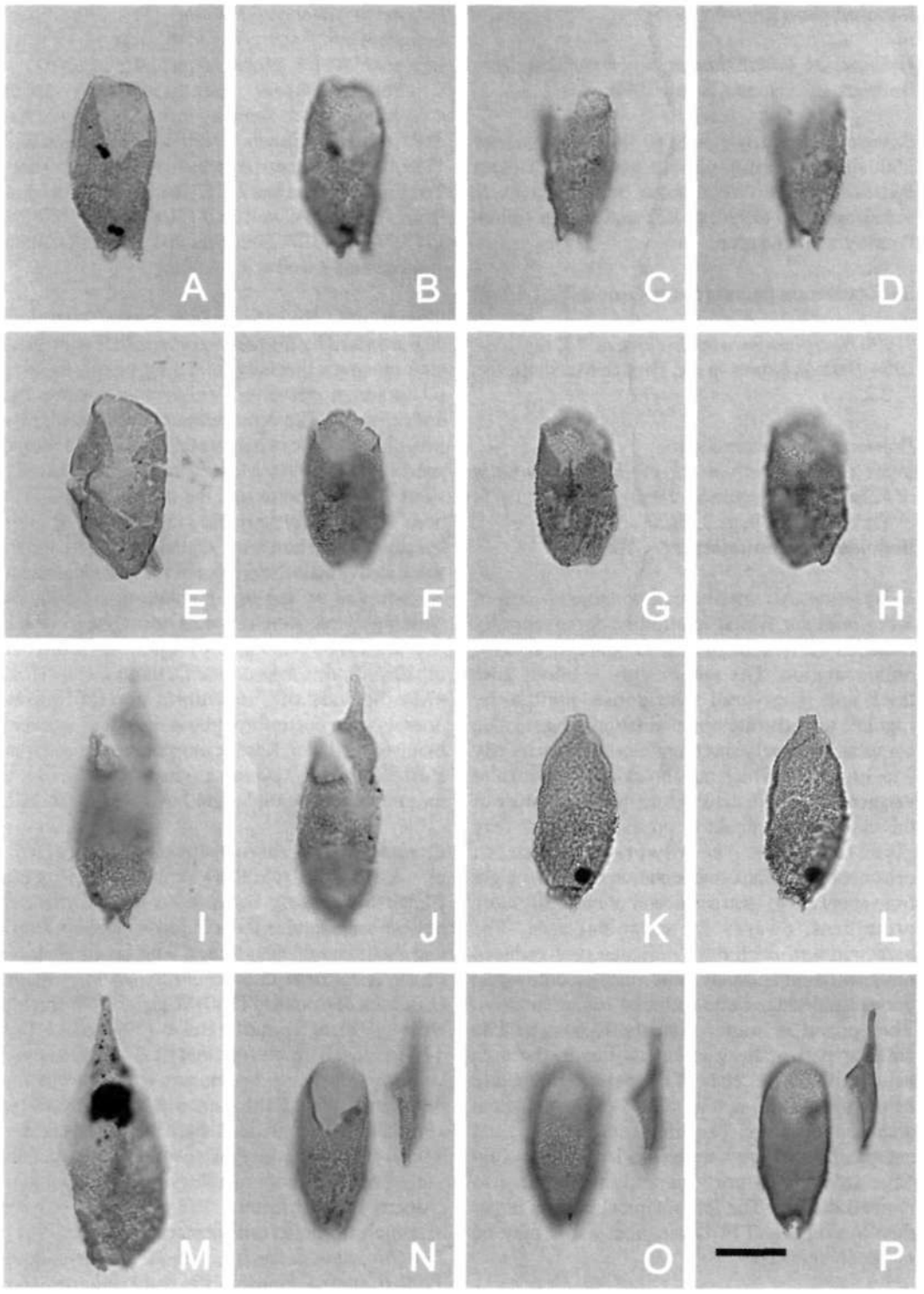

Fig. 4. Batioladinium paeminosum sp. nov. Specimens from conventional core samples in Lorikeet-1 well at 1759.10m (Figs 4N-P), Mutineer-1B well at 3132.25 (Fig. 4E) and Wanaea-2 well at 3375.34m (Figs 4K-L), 2880.50m (Figs 4F-H) and 2875.30m (Figs 4A-D, I, J, M). All photomicrographs taken using plain transmitted light. The scale bar in Fig. 4P refers to all photomicrographs and is 25µm. Figs 4N-P are the holotype; the remainder, paratypes. Note the thick autophragm covered with dense, nontabular (continued opposite)

has only a single antapical horn and is normally more squat than *B. paeminosum*. *Batioladinium? pelliferum* (Alberti 1961) Brideaux 1975 is also relatively squat and has an autophragm which is densely covered in short, slender spines and ornament that Alberti (1961) referred to as 'fur-like'. The lower Neocomian species, *B. reticulatum* Stover & Helby 1987, is holocavate and has a reticulate ectophragm (Stover & Helby, 1987).

Derivation of name. From the Latin, *paeminosus* meaning rough or uneven, referring to the coarse rugulate-verrucate ornamentation of this species.

Holotype and type locality. Figures 4N-P, CPC 35917, from a conventional core sample in Lorikeet-1 well at 1759.10m.

Stratigraphical distribution. *B. paeminosum* is confined to the Tithonian *Pseudoceratium iehiense* Zone (subzones 4ciiib to 4cib) (Foster, this volume; Helby & Partridge, in prep.).

Belowia gen. nov.

Type species. *Belowia balteus* sp. nov.

Diagnosis. Intermediate to large dinoflagellate cysts, which vary from proximate to chorate. The subspherical to ellipsoidal cyst body is markedly indented at the parasulcus. A hollow ectophragmal projection occurs at the paracingulum. The hypocyst commonly bears a further ectophragmal development which, in most cases, encompasses the major processes, where developed. This hypocystal ectophragm is highly variable: in the chorate forms, it may be virtually absent and the major hypocystal processes may be well developed. The paratabulation is standard gonyaulacalean, indicated by the intratabular postcingular processes, where developed, and the principal archaeopyle suture. Archaeopyle apical; operculum free.

Comments. *Belowia* is a morphologically complex and unusual genus; Figs 5 to 8 illustrate the principal features. It is ellipsoidal to subcircular in polar outline and has an apical archaeopyle. The cyst wall comprises autophragm and ectophragm. The ectophragm separates from the autophragm on the posterior part of the precingular paraplate series. Major processes in the postcingular paraplate series may support and/or may be incorporated into the hypocystal ectophragm. Numerous trabecular processes also emerge from the vicinity of the anterior and posterior paracingular parasutures to form a hollow paracingular ectophragmal tunnel, which is interrupted at the parasulcus.

Comparison. The Kimmeridgian-Tithonian genus *Hadriana* Riding & Helby (this volume) is very similar to *Belowia*. They both have a small, essentially smooth epicyst, devoid of processes, and wall separation occurring close to the posterior limits of the precingular paraplates. Although there are marked hypocystal differences, both genera display major ectophragmal development at and below the paracingulum. However, *Hadriana* lacks a paracingular tunnel, large processes and the ectophragm is widely open antapically (the opening is about twice the autocyst diameter).

Stephodinium Deflandre 1939 emend. Davey 1970 is characterised by an inflated paracingular periphragmal protrusion. It is distinguished from *Belowia* by having a cavate wall relationships, a precingular archaeopyle and by lacking trabeculate ectophragmal processes. *Belowia* differs from trabeculate chorate dinoflagellate cyst genera like *Adnatosphaeridium* Williams & Downie 1966, *Hapsidaulax* Sarjeant 1975, *Hystrichosphaerina* Alberti 1961, *Polystephanephorus* Sarjeant 1961 and *Rigaudella* Below 1982 in having a distinctive ectophragmal tunnel along the paracingulum and in lacking intratabular processes in the apical and precingular paraplate series. *Balteocysta* Stover & Evitt 1978 has a

---

rugulate-verrucate ornamentation which typically increases in height antapically, the paracingulum low on the cyst body, the relatively short polar horns and the apical archaeopyle. A, B - CPC 35910, paratype; ventral view, high and low focus respectively. Note principal archaeopyle suture and prominent parasulcal notch. C, D - CPC 35911, paratype; oblique dorsal view, median and low focus respectively. Note small antapical horns. E - CPC 35912, paratype; ventral view, high focus. Slightly damaged,, note parasulcal notch. F-H - CPC 35913, paratype; dorsal view, high to low focus sequence. Note low-relief ornamentation and parasulcal notch in 4G. I, J - CPC 35914, paratype; right lateral view, high and median focus respectively. Note slightly offset operculum with prominent apical horn. K, L - CPC 35915, paratype; dorsal view, high and median/low focus respectively. Note damaged apical horn. M - CPC 35916, paratype; oblique left lateral view, high focus. Note prominent apical horn and reduced antapical horns. N-P - CPC 35917, holotype; ventral view, high to low focus sequence. Note offset operculum and parasulcal notch in 4N. The operculum has been digitally relocated closer to the loisthocyst.

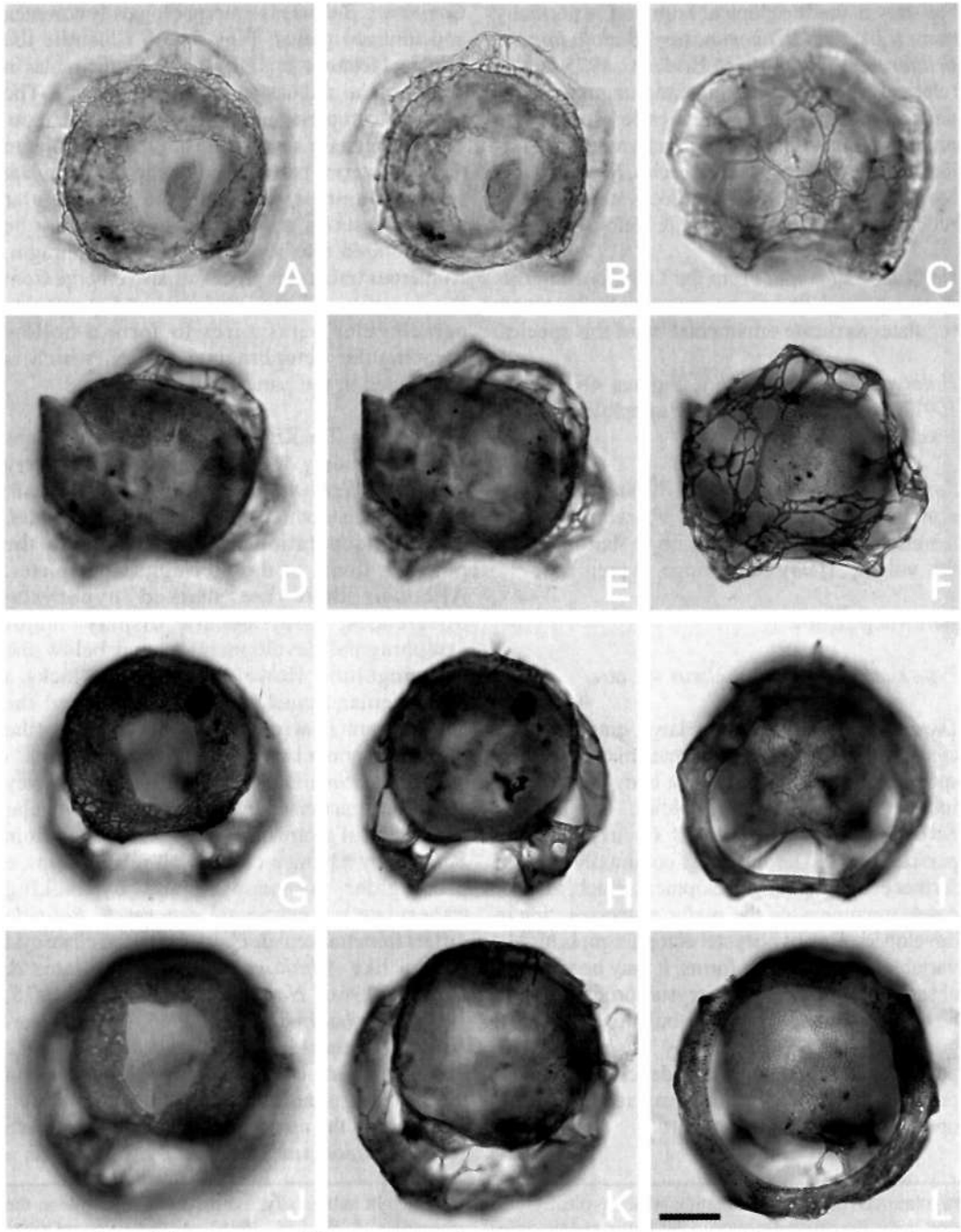

Fig. 5. Belowia halteus sp. nov. All are paratypes from outcrop sample 81FH11, Lelinta Formation, Misool, eastern Indonesia (Hasibuan, 1990) and are examples of the larger, more common morphotype 1. All photomicrographs taken using plain transmitted light. The scale bar in Fig. 5L refers to all photomicrographs and is 25µm. Note ellipsoidal cyst body, indented parasulcal region, short paracingular processes, trabeculate ectophragmal skirt-like structure which envelops hypocyst, and apical archaeopyle. A-C - CPC 35918, paratype; apical view, high to low focus sequence. Note short paracingular processes and apical archaeopyle. D-F - CPC 35919, paratype; antapical view, low to high focus sequence. Note skirt-like, distinctly trabeculate ectophragmal structure covering hypocyst. G-I - CPC 35920, paratype; apical view, high to low focus sequence. Note relatively wide postcingular processes which connect autophragm of the cyst body to ectophragm, and prominent antapical opening in the ectophragm (Fig. 5I). J-L - CPC 35921, paratype; antapical view, low to high focus sequence. Note wide postcingular processes and subcircular opening in ectophragm at antapex (Fig. 5L).

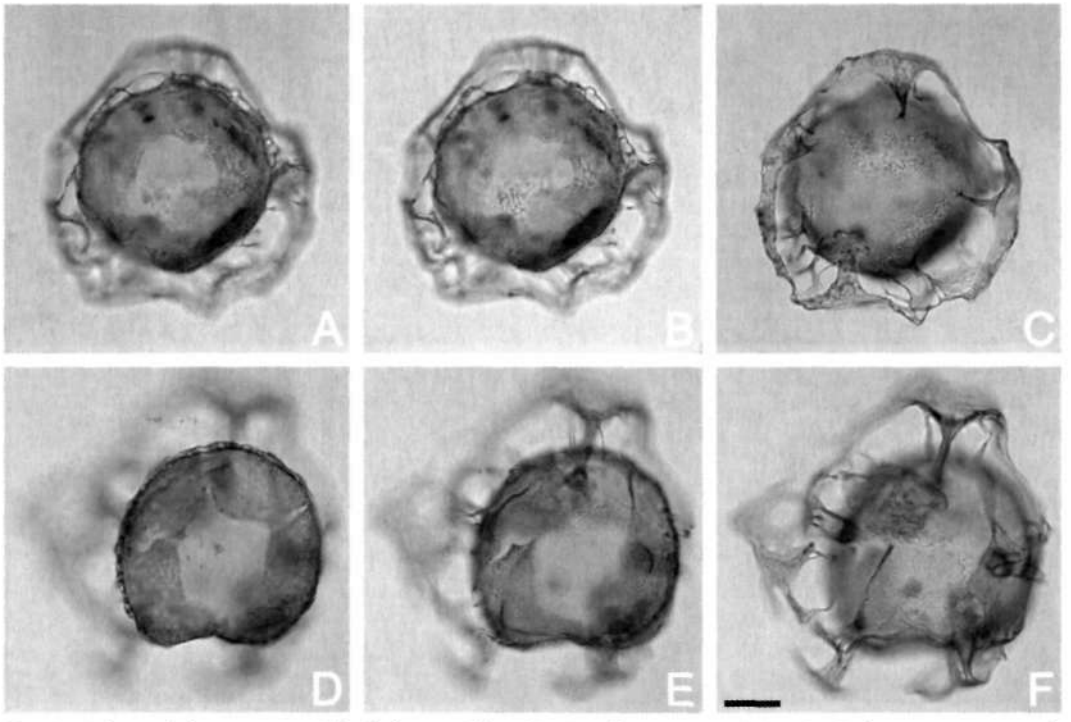

Fig. 6. Belowia balteus sp. nov. The holotype (Figs 6A-C) and a paratype (Figs 6D-F) from outcrop sample 81FH11 of the Lelinta Formation, Misool, eastern Indonesia (Hasibuan, 1990). Examples of the larger and more common morphotype 1. All photomicrographs taken using plain transmitted light. The scale bar in Fig. 6F refers to all the photomicrographs and is 25µm. Note subspherical/ellipsoidal cyst body with indented parasulcal region, short paracingular processes spanning paracingular region, trabeculate ectophragmal skirt-like structure which envelops hypocyst and is supported by intratabular postcingular processes, and apical archaeopyle. A-C - CPC 35922, holotype; antapical view, low to high focus sequence. Note relatively low paracingular ectocoel and prominent intratabular postcingular processes. D-F - CPC 35923, paratype; apical view, high to low focus sequence. Note wide hypocystal ectocoel supported by intratabular postcingular processes.

subspherical cyst body and an ectophragm which is confined to the paracingular region.

Derivation of name. For Dr Raimond Below.

Belowia balteus sp. nov. (Figs 5A-L, 6A-F, 7A-L)

Previous Australian usage
Belowia sp. – Helby.

Description. A species of *Belowia* with an ellipsoidal cyst body, that in polar view, is indented at the parasulcus. The autophragm is 1-1.5µm thick and usually densely striate to occasionally rugulate, especially close to the postcingular processes. It may also be verrucate and irregularly and sparsely reticulate. The ectophragm is extremely variable in form, ranging from a sparse trabeculum, through a wide, complex trabeculum, to a thin (0.5µm), perforate wall. Relatively short, solid, trabeculate processes consistently emerge from the vicinity of the anterior and posterior paracingular sutures. These form a projecting ectophragmal tunnel along the paracingulum, terminating at the relatively broad parasulcus. Close to the top of the postcingular paraplate series, a skirt-like ectophragmal structure is generally developed which extends antapically. This ectophragmal skirt may be supported by five intratabular postcingular processes representing paraplates 2''' to 6''', or by a variable number of nontabular processes. The processes are displaced toward the anterior margin of the paraplates. Where developed, the processes are extremely variable and may be slender, solid, wide or hollow and occasionally merge distally with the ectophragm. The ectophragmal skirt commonly terminates antapically in an open, solid girdle-like structure (Figs 5I, L), but this structure is sometimes absent (Fig. 7L). The strongly indented parasulcus is frequently indicated by a low, smooth parasutural ridge. The operculum is

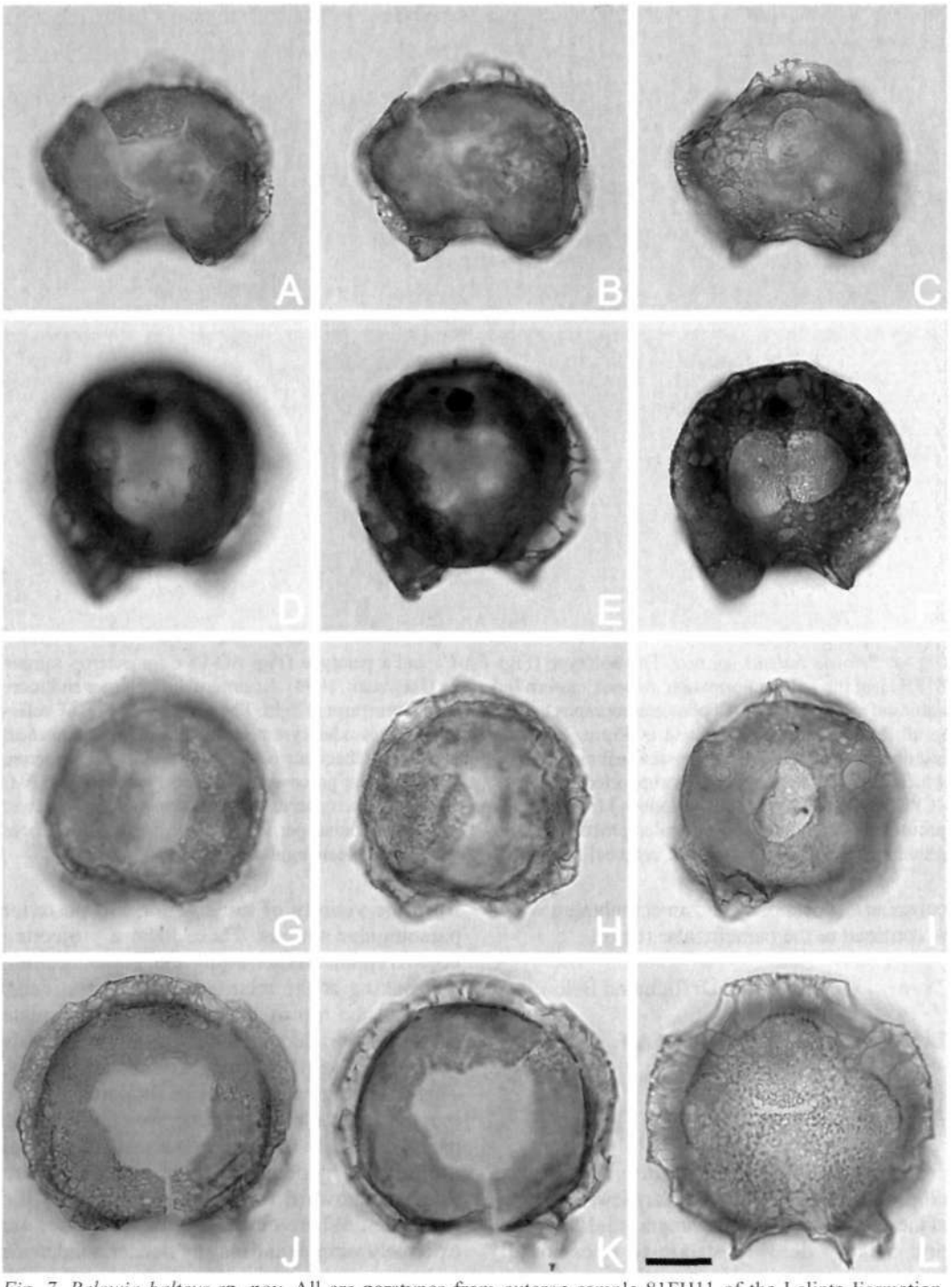

Fig. 7. Belowia balteus sp. nov. All are paratypes from outcrop sample 81FH11 of the Lelinta Formation, Misool, eastern Indonesia (Hasibuan, 1990) and are examples of the smaller, relatively rarer morphotype 2. All photomicrographs were all taken using plain transmitted light. The scale bar in Fig. 7L refers to all the photomicrographs and is 25µm. Note oblate ellipsoidal cyst body with markedly indented parasulcal region, narrow ectocoel below the reticulate ectophragm surrounding the hypocyst, the absence of intratabular postcingular processes and the apical archaeopyle. A-C - CPC 35924, paratype; antapical view, low to high focus sequence. Note apical archaeopyle in Fig. 7A and prominent antapical lacuna in Fig. 7C. D-F - CPC 35925, paratype; antapical view, low to high focus sequence. Note angular principal archaeopyle suture and (continued opposite)

normally free, but specimens were observed where the operculum has fallen back into the autocyst.

Dimensions (µm, n=57): Min. (Mean) Max.
Maximum overall lateral diameter: 83 (118) 159
Maximum lateral diameter of cyst body: 64 (91) 107
Maximum overall dorsoventral diameter: 80 (110) 151
Maximum dorsoventral diameter of cyst body: 63 (85) 105
Height of paracingular processes/trabeculum: 3 (8) 19
Height of postcingular processes/trabeculum: 8 (18) 35

The measured specimens are from ditch cuttings in Tenacious-1 ST1 well between 2975.00m and 2980.00m and outcrop material from the Tithonian Lelinta Formation (Fageo Group) of Misool, eastern Indonesia (Hasibuan, 1990; Helby & Hasibuan, 1988).

The 57 specimens in the above table comprise 37 of a larger morphotype 1 with distinct postcingular processes (Figs 5, 6), 14 examples of the smaller morphotype 2, with a more continuous perforate ectophragm (Fig. 7), and 6 intermediate forms. The dimensions of morphotypes 1 and 2 are set out below to document the size differences between these two end members of a continuously variable complex. The dimensions of the intermediate forms are not tabulated. The tables below principally illustrate the difference in the size of the ectophragm of the two morphotypes. Thus the maximum overall lateral and dorsoventral diameters are significantly different while other measurements are comparable.

Morphotype 1, Dimensions (µm, n=37): Min. (Mean) Max.
Maximum overall lateral diameter: 83 (124) 159
Maximum lateral diameter of cyst body: 64 (92) 107
Maximum overall dorsoventral diameter: 86 (116) 151
Maximum dorsoventral diameter of cyst body: 63 (85) 102
Height of paracingular processes/trabeculum: 3 (8) 19
Height of postcingular processes/trabeculum: 12 (19) 35

The above specimens are from Tenacious-1 ST1 well at 2975.00m-2980.00m and the Tithonian part of the Lelinta Formation of Misool, eastern Indonesia.

Morphotype 2, Dimensions (µm, n=14): Min. (Mean) Max.
Maximum overall lateral diameter: 91 (104) 130
Maximum lateral diameter of cyst body: 78 (89) 105
Maximum overall dorsoventral diameter: 80 (100) 118
Maximum dorsoventral diameter of cyst body: 66 (85) 105
Height of paracingular processes/trabeculum: 4 (8) 14
Height of postcingular processes/trabeculum: 8 (14) 29

The above specimens are all from sample 81FH11 in the Lelinta Formation of Misool, eastern Indonesia (Tithonian).

Comments. The morphology of the processes and the ectophragm are extremely variable. As indicated above, two morphotypes are recognised, both of which are mainly found as polar compressions. The relatively common morphotype 1 (Figs 5, 6) normally has intratabular postcingular processes which support a skirt-like ectophragmal trabeculum that is open antapically and terminates in a solid, girdle-like structure (Figs 5I, L). The postcingular processes are located unusually high on the postcingular paraplate series. Because the ectophragm is made up of thin elements, it is prone to folding. Thus the size and polar outline of the ectocyst are somewhat variable (Figs 5, 6). The relatively rare morphotype 2 (Fig. 7), lacks postcingular processes, the ectocoel is relatively narrow and the ectophragm is reticulate with lacunae of varying sizes (Fig. 7). Most lacunae are relatively small (1-3µm), but some may be considerably larger. These two variants are not assigned to separate taxa because intermediate forms occur and all variants have the same stratigraphical range.

Comparison. *Belowia* is currently a monotypic genus and thus the principal comparisons with other taxa are at the generic level (see above). Specimens of morphotype 1 of *Belowia balteus* and *Belowia* sp. A herein, however, resemble variants of *Rigaudella aemula* (Deflandre 1939) Below 1982. This similarity is confined to the postcingular paraplate series, where the

large, paired antapical lacunae. G-I - CPC 35926, paratype; antapical view, low to high focus sequence. A pale specimen, note large antapical lacuna in Fig. 7I. J-L - CPC 35927, paratype; apical view, high to low focus sequence. Note the prominent, relatively broad ectocoel.

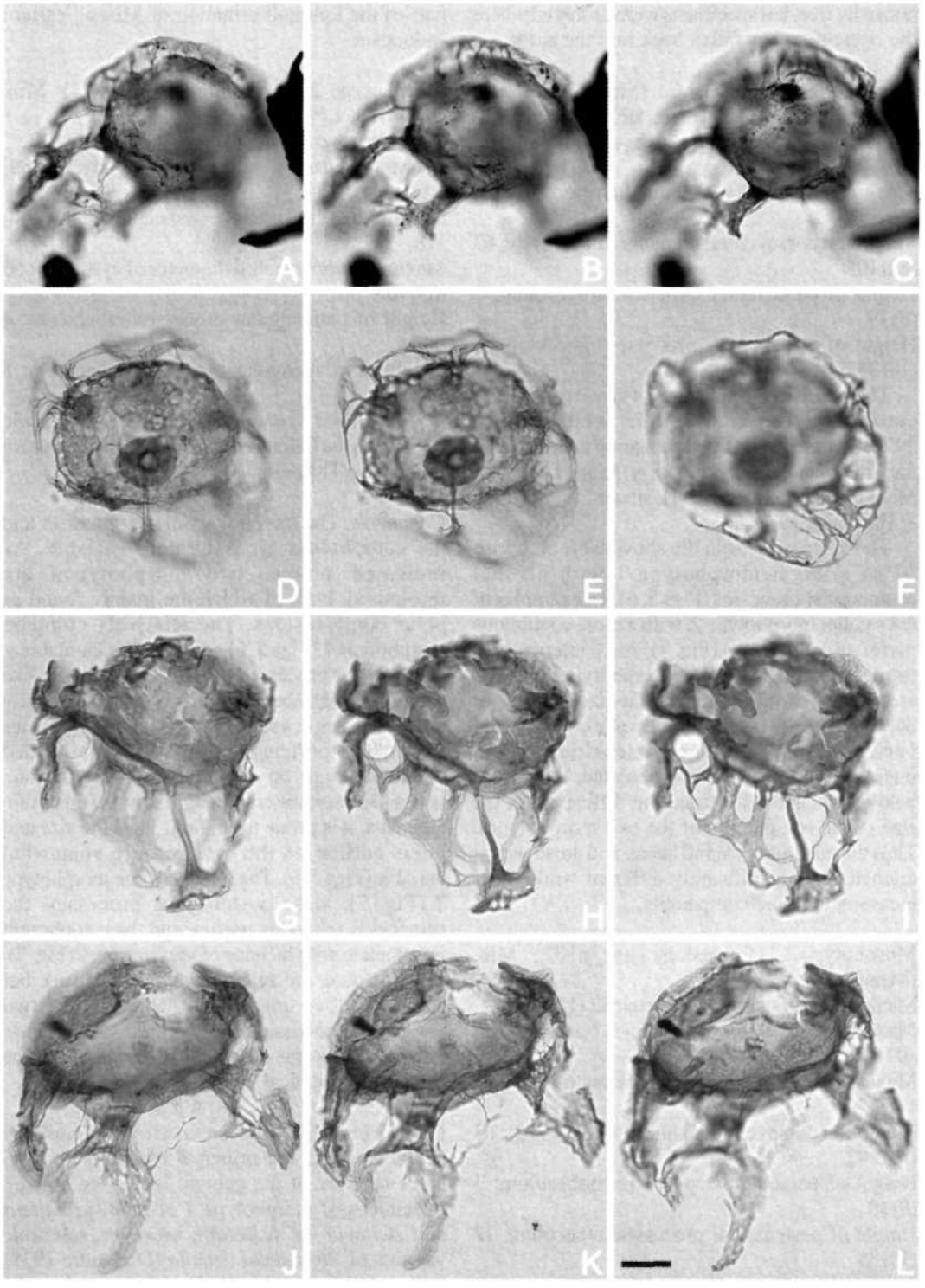

Fig. 8. Belowia sp. A. All are from ditch cuttings between 2945.00m and 2950.00m in Crux-1 well. All photomicrographs were taken using plain transmitted light. The scale bar in Fig. 8L refers to all photomicrographs and is 25µm. Note large overall size, ellipsoidal cyst body, short trabeculate processes in paracingular region, prominent intratabular, trabeculate postcingular processes which vary significantly in morphology, and apical archaeopyle. A-C - CPC 35928, slightly oblique apical view, high to low focus sequence. (continued opposite)

intratabular processes are connected distally by narrow trabeculae (compare Below, 1982, figs 22-34). The other paraplate series lack these, therefore the two forms can be readily distinguished.

Derivation of name. From the Latin *balteus*, meaning girdle or belt and referring to the characteristic variable ectophragm which surrounds the majority of the hypocyst.

Holotype and type locality. Figures 6A-C, CPC 35922, from outcrop material of the Lelinta Formation, Misool, eastern Indonesia. This is a specimen of morphotype 1.

Stratigraphical distribution. Belowia balteus has been recorded from the Tithonian *Cribroperidinium perforans* Zone (5d) to the *Omatia montgomeryi* Zone (5c) in the Timor Sea region (Foster, this volume; Helby & Partridge, in prep.). The species is also present in the Tithonian lower part of the Lelinta Formation (Fageo Group) of Misool, eastern Indonesia.

Belowia sp. A (Figs 8A-L)

Previous Australian usage
Belowia sp. – Helby.

Description. A relatively large form of *Belowia* with an ellipsoidal cyst body which is slightly indented at the parasulcus. The autophragm is smooth, occasionally microscabrate and may be irregularly microreticulate. Relatively short, solid, trabeculate processes emerge from the anterior and posterior paracingular sutural regions. These processes form a projecting ectophragmal tunnel of variable height along the paracingulum which terminates at the parasulcus (Figs 8A, B). Large, extremely variable intratabular postcingular processes, which flare distally and are connected distally by trabecular filaments, are present. The processes may be slender, solid, wide or hollow and occasionally appear to merge distally with the ectophragmal trabeculum. These prominent intratabular processes vary in width from 3-19µm. They are also highly variable in length (Fig. 8); the shortest and longest observed measured 17µm and 55µm in length respectively. The filaments of the trabeculum are solid and vary from 1-9µm. The operculum is normally free; however, specimens were observed where the operculum has fallen into the autocyst.

Dimensions (µm, n=17): Min. (Mean) Max.
Maximum overall lateral diameter: 101 (144) 193
Maximum lateral diameter of cyst body: 77 (94) 113
Maximum overall dorsoventral diameter: 97 (123) 143
Maximum dorsoventral diameter of cyst body: 61 (83) 96
Height of paracingular processes/trabeculum: 4 (10) 22
Height of postcingular processes/trabeculum: 21 (34) 55

All specimens are from a ditch cuttings sample in Crux-1 well between 2945.00m and 2950.00m.

Comments. This form is not given a specific name because sufficient material is currently unavailable. *Belowia* sp. A lacks the hypocystal ectophragmal skirt which is characteristic of *B. balteus*. The ectophragm is confined to trabecular filaments which connect the large postcingular processes and the paracingular ectophragmal tunnel (Fig. 8). The postcingular processes which prominently flare distally may occasionally split into several distal trabecular strands. Because of the large postcingular processes, oblique compressions of this morphotype are common (Fig. 8). The paracingular processes are relatively variable in height (see *Dimensions*, above).

Comparison. Belowia sp. A differs from *B. balteus* in being slightly larger, lacking a hypocystal ectophragmal skirt and having large intratabular postcingular processes connected by distal trabeculae.

Stratigraphical distribution. Belowia sp. A has been recorded from the Tithonian *Cribroperidinium perforans* Zone (5d) to the *Omatia montgomeryi* Zone (5c) in the Timor Sea, (Foster, this volume; Helby & Partridge, in prep.).

Biorbifera Habib 1972 emend.

1972 *Biorbifera* Habib, p. 377.
1987 *Biorbifera* Habib 1972 emend. Below, p. 63.

Type species. Biorbifera johnewingii Habib 1972

Note ectophragmal 'tunnel' formed by short, solid paracingular processes in 8A-B. D-F - CPC 35929, apical view, high to low focus sequence. Morphotype with relatively short postcingular processes. G-I - CPC 35930, oblique apical view, high to low focus sequence. Note highly variable length of postcingular processes. J-L - CPC 35931, lateral view, high to low focus sequence. Note extremely wide postcingular process to left.

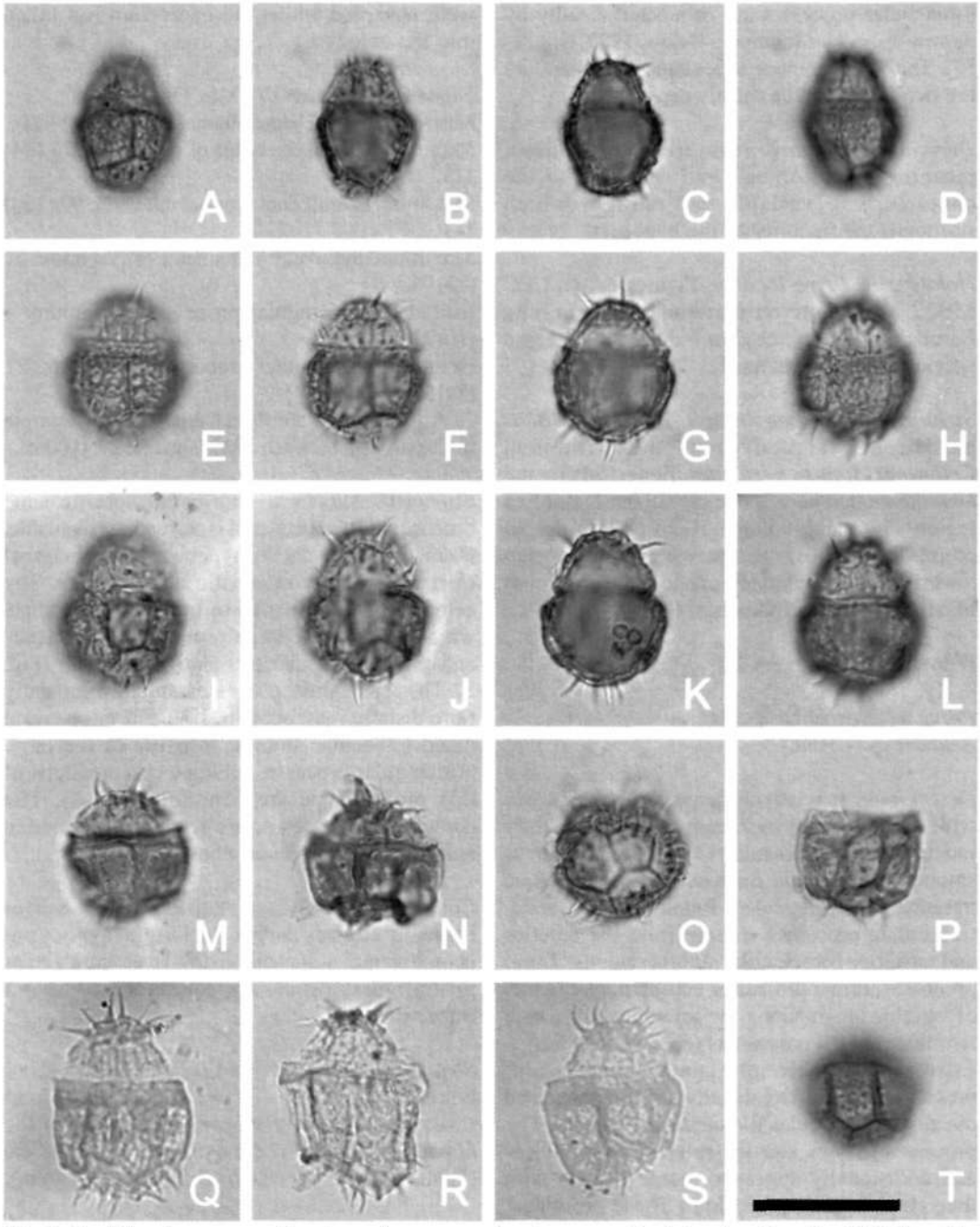

Fig. 9. Biorbifera ferox sp. nov. Specimens from conventional core samples in Lambert-2 well at 3101.00m (Fig. 9P), Lorikeet-1 well at 1761.20m (Figs 9M, O), Mutineer-1B well at 3132.24m (Fig. 9N) and Wanaea-3 well at 2929.67m (Fig. 9T), sidewall core samples in Avocet-1A well at 1771.50m (Figs 9E-L) and ditch cuttings from Avocet-1A well between 1770.00m and 1775.00m (Figs 9A-D) and Broome-1 Bore at 297.79m (Figs 9Q-S). All photomicrographs taken using plain transmitted light. The scale bar in Fig. 9T refers to all photomicrographs and is 25µm. Figs 9I-L are the holotype, the remainder are paratypes. Fig. 9R is a composite photomicrograph. Note small size, thick, microreticulate autophragm, prominent paracingulum, partiform paratabulation pattern, polar concentration of processes and epicystal archaeopyle. A-D - CPC 35932, paratype; lateral view, high to low focus sequence. Note elongate ellipsoidal outline. E-H - CPC 35933, paratype; lateral view, high to low focus sequence. Note polar processes and epicystal archaeopyle. I-L - CPC 35934, holotype; lateral view, high to low focus sequence. Note gonal nature of many of the processes. M - CPC 35935, paratype; (continued opposite)

emend. Below 1987

Emended diagnosis. The diagnosis given by Below (1987, p. 63) is further emended to include the fact that *Biorbifera* has a partiform gonyaulacalean paratabulation pattern which may be indicated by parasutural ridges, crests or processes. The paratabulation formula of ?pr, 4', ?2a, 6'', ?6c, 6''', 2'''', Xs was determined during the study of *Biorbifera ferox* sp. nov.

Comments. The original generic diagnosis of Habib (1972) was emended by Below (1987, p. 63) to include proximochorate and chorate forms, the processes of which may be nontabular and/or parasutural and gave a paratabulation formula. The material of *Biorbifera johnewingii* which was studied by Below (1987, pl. 27, figs 1-7, 13, 14, 19, 20), however, exhibits few unequivocal parasutural features. Australian material of *B. johnewingii* exhibits slender, low parasutural ridges (unpublished information). The material of *B. ferox* in this study has a full partiform gonyaulacalean paratabulation (Evitt, 1985), indicated by prominent, low, smooth parasutural ridges. A paratabulation formula of ?pr, 4', ?2a, 6'', ?6c, 6''', 2'''', Xs has been determined.

Biorbifera ferox sp. nov. (Figs 9A-T)

1994 *Biorbifera* sp.; Bint & Marshall, fig. 5.6-5.11.

Previous Australian usage
Biorbifera aggressiva – Helby.

Description. A species of *Biorbifera* with a small, elongate ellipsoidal outline, which is slightly dorsoventrally compressed. The autophragm is microreticulate and robust, between 1-1.5µm thick. The prominent paracingulum, which may be slightly incised, bears reduced ornamentation. The paracingulum is slightly displaced anteriorly, thereby making the hypocyst consistently larger that the epicyst. The hypocyst is normally wider than long and has a flattened to angular antapex. The epicyst is flattened or rounded apically. A partiform gonyaulacalean paratabulation pattern is indicated by thick, low, smooth parasutural ridges. The parasutural ridges vary from 1 to 1.5µm in width and height and indicate a paratabulation formula of ?pr, 4', ?2a, 6'', ?6c, 6''', 2'''', Xs. Slender, solid, distally pointed processes are concentrated at the polar areas. They are mainly parasutural (gonal and intergonal), but nontabular processes are also present. The parasulcus is narrow and not obviously subdivided.

Dimensions (µm, n=35) excl. processes where appropriate: Min. (Mean) Max.
Length of entire cyst: 19 (24) 33
Length of epicyst*: 6 (8) 11
Length of paracingulum: 2 (2.5) 4
Length of hypocyst*: 11 (14) 20
Equatorial width of cyst: 16 (21) 26
Length of spines: 3 (4) 6
* - measured dorsally

The measured specimens are from conventional core samples in Lorikeet-1 well at 1761.20m and Mutineer-1B well at 3132.25m, sidewall core samples from Avocet-1A well at 1771.50m and 1778.00m and ditch cuttings samples from Avocet-1A well at between 1770.00m and 1775.00m and Broome-1 Bore at 297.79m.

Comments. Biorbifera ferox is a distinctive small cyst readily identifiable by the epicystal archaeopyle, thick autophragm, well marked paratabulation, particularly on the hypocyst and the apparent concentration of spines at the poles. In poorly preserved material, these processes may be lost. The processes on the precingular paraplates appear to be especially susceptible to damage. Processes have not been observed on the postcingular paraplates apart from the antapical margins. The parasutural ridges suggest a partiform gonyaulacalean paratabulation pattern with a formula of ?pr, 4', ?2a, 6'', ?6c, 6''', 2'''', Xs (Fig. 9). The paired antapical paraplates are the most characteristic feature of this pattern (Figs 9O, T). No well preserved isolated epicysts were encountered, therefore the number and configuration of preapical and anterior intercalary paraplates could not be precisely determined. At least two anterior intercalary paraplates appear to

M - CPC 35935, paratype; lateral view, low focus. Relatively squat specimen. N - CPC 35936, paratype; dorsal view, median focus. Unusually broad specimen; note thick autophragm. O - CPC 35937, paratype; antapical view, high focus. Note characteristic partiform antapical paratabulation pattern with paired antapical paraplates; ventral side uppermost. P - CPC 35938, paratype; dorsal view, high focus. An isolated hypocyst. Q - CPC 35939, paratype; dorsal view, median focus. Relatively large form; note prominent solid, distally-pointed polar processes. R - CPC 35940, paratype; lateral view, composite photomicrograph. Large, elongate morphotype. S - CPC 35941, paratype; oblique dorsal view, median focus. Pale specimen; note prominent wide parasutural ridges. T - F.49311, paratype; dorsal view, high focus. Isolated hypocyst; note middorsal postcingular paraplate.

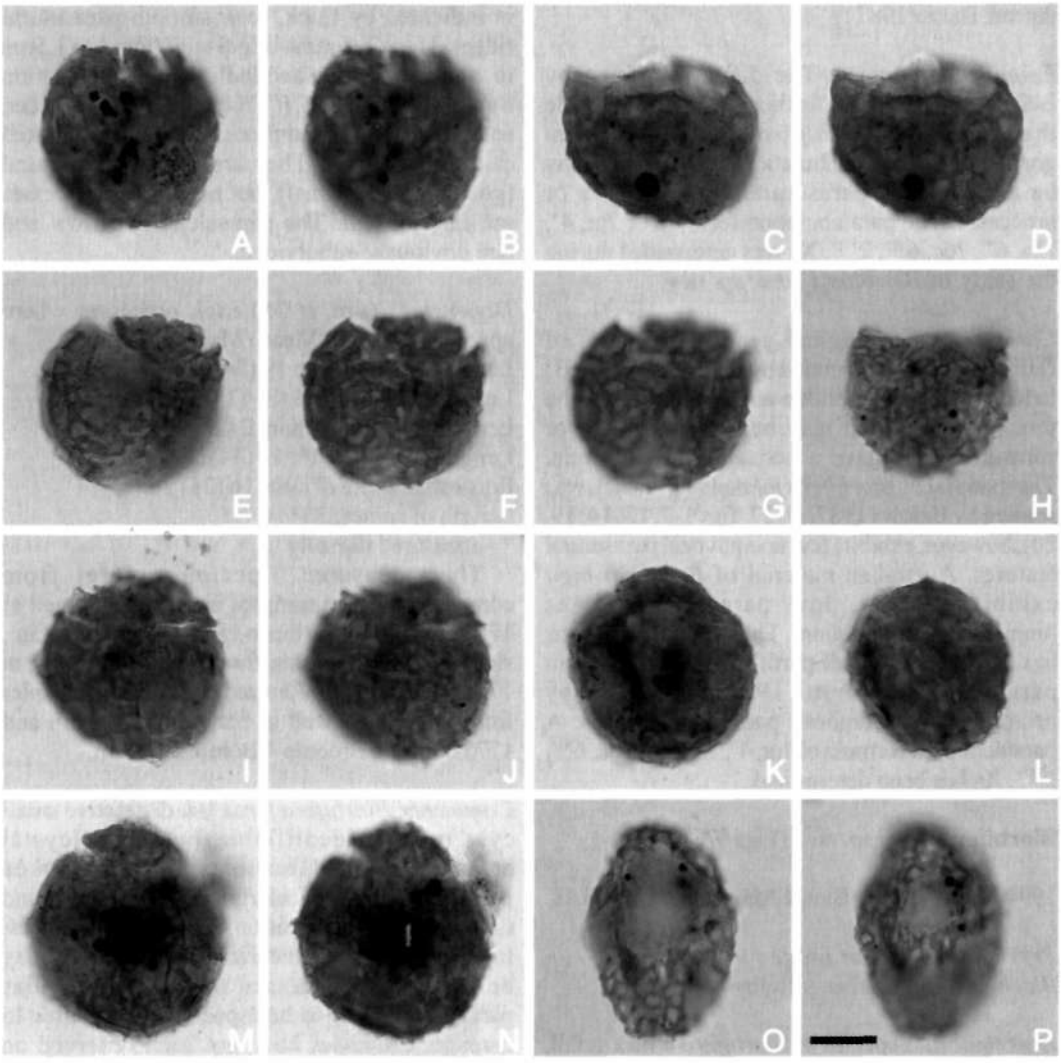

Fig. 10. Cassiculosphaeridia solida sp. nov. Specimens from ditch cuttings from Crux-1 well between 3045.00m and 3050.00m (Figs 10A-D, H-K, M-P) and 2945.00m to 2950.00m (Figs 10E-G, L). All photomicrographs taken using plain transmitted light. The scale bar in Fig. 10P refers to all photomicrographs and is 25µm. Figs 10E-G are the holotype; the remainder, paratypes. Note subcircular outline, extremely thick autophragm with strong, corrugate ornamentation, ridges which may form an irregular reticulum, and apical archaeopyle. A, B - CPC 35942, paratype; loisthocyst in ventral view, median and low focus respectively. Note accessory archaeopyle sutures and crude reticulate pattern formed by autophragmal ridges. C, D - CPC 35943, paratype; loisthocyst in dorsal view, high and median focus respectively. Note relatively smooth paracingulum. E-G - CPC 35944, holotype; loisthocyst and operculum in dorsal view, high to low focus sequence. Note relatively well developed reticulum. H - CPC 35945, paratype; loisthocyst in dorsal view, median focus. Note apical archaeopyle. I, J - CPC 35946, paratype; full cyst in dorsal view, high and median focus respectively. Note principal archaeopyle suture. K - CPC 35947, paratype; full cyst in ventral view, median focus. Note relatively inflated operculum. L - CPC 35948, paratype; full cyst in dorsal view, median focus. Note extremely small apical protuberance. M, N - CPC 35949, paratype; loisthocyst and operculum in dorsal view, high and median focus respectively. Note variable nature of reticulum. O, P - CPC 35950, paratype; full cyst in ?ventral view, high and median focus respectively. Elongate specimen.

be present (Fig. 9L). Furthermore, the paratabulation of the paracingulum and parasulcus was not determined with certainty. In poorly preserved material, the epicyst commonly collapses into the hypocyst.

Comparison. Biorbifera ferox differs from the genus type, *B. johnewingii.* in being slightly smaller, having prominent parasutural ridges and much fewer, but longer, robust spines which are largely confined to the polar areas. An unpublished Tithonian species of *Biorbifera,* recorded in both Australia and New Zealand, is characterised by small processes and a prominent inflation on each of the major paraplates.

Derivation of name. From the Latin, *ferox*, spirited, daring, proud, referring to its very distinct, paratabulation, in contrast to that on the genotype.

Holotype and type locality. Figures 9I-L, CPC 35934, from a sidewall core sample in Avocet-1A well at 1771.50m.

Stratigraphical distribution. Biorbifera ferox is confined to the Tithonian, ranging from the upper *Dingodinium jurassicum* Zone (5aia) to the mid *Pseudoceratium iehiense* Zone (4ciia) (Foster, this volume; Helby & Partridge, in prep.).

Cassiculosphaeridia Davey 1969

Type species. Cassiculosphaeridia reticulata Davey 1969

Cassiculosphaeridia solida sp. nov. (Figs 10A-P)

Previous Australian usage
1986 ?*Cassiculosphaeridia* sp. A; Parker, p. 50, pl. 5, fig. 6.
Valensiella sp. A – Helby.
M.P. 98 (proto) – Helby.

Description. A species of *Cassiculosphaeridia,* intermediate in size and with an ellipsoidal to subcircular outline. The autophragm is extremely thick (1.5-4µm) and covered with strong, corrugate ornamentation. The ornamentation comprises an irregular network of discontinuous, arcuate, anastomosing ridges 1-4µm in height and 2-6µm wide. These ridges frequently form an irregular reticulate pattern, the muri enclosing subcircular to subpolygonal lacunae 1-6µm in diameter. The ridges may be short and occasionally form isolated irregular verrucae. Indications of paratabulation are lacking except for the principal archaeopyle suture, which is angular and indicative of four apical and six precingular paraplates. Accessory archaeopyle sutures may be present. Rarely, a small (2-4µm high) apical protuberance may be developed.

Dimensions (µm, n=27): Min. (Mean) Max.
Length of entire cyst: 72 (79) 89
Length of loisthocyst: 53 (67) 80
Length of operculum: 15 (20) 27
Equatorial width: 58 (74) 91
Width of archaeopyle: 37 (53) 72

The measured specimens are from a sidewall core sample from Yering-1 well at 2563.50m and ditch cuttings samples from Crux-1 well between 3045.00m-3050.00m and 2945.00m-2950.00m.

Comments. This species of *Cassiculosphaeridia* is characterised by the extremely thick autophragm, covered by prominent ridges, which form a corrugate-rugulate ornamentational pattern. The ridges are highly variable and form a discontinuous and anastomosing configuration (Fig. 10). This variability ranges from short, irregular ridges giving a pseudo-verrucate pattern (Figs 10A, B) to longer elements which form a coarse reticulum (Figs 10E-G). The angular nature of the principal archaeopyle suture is indicative of a gonyaulacalean paratabulation pattern. The lack of indications of paratabulation means that orientation is difficult in specimens where the archaeopyle has not opened (Figs 10O, P). The species is frequently flattened during preservation and this tends to artificially expand the diameter of the archaeopyle. Due to the characteristic ornamentation, isolated opercula are commonly identified.

The lack of both paratabulation and ectophragm precludes the assignment of this species to *Ellipsoidictyum* Klement 1960 or *Valensiella* Eisenack 1963 respectively (see Stover & Evitt, 1978). Courtinat (1989, p. 182) considered *Cassiculosphaeridia* to be a junior synonym of *Valensiella* and transferred all the species of *Cassiculosphaeridia* to *Valensiella*. Lentin & Williams (1993, p. 82, 83) accepted these transfers. Subsequently, Slimani (1994) retained *Cassiculosphaeridia*. Williams et al. (1998) followed the Slimani interpretation.

Comparison. Cassiculosphaeridia solida differs from the other species of the genus in its distinctive, extremely thick autophragm and robust, highly irregular arcuate/reticulate ridges.

The majority of the other species of *Cassiculosphaeridia* have a regular reticulum and are smaller than *C. solida*. *Cassiculosphaeridia magna* Davey 1974 and *C? tocheri* Schiøler 1993 are similar in size to *C. solida*. Furthermore the ridges/crests in *C. magna* are also anastomosing (Davey, 1974). However, *C. magna* has smaller ridges that form a denser reticulate pattern than those in *C. solida*; and *C? tocheri* has a regular reticulum. Both *C. magna* and *C? tocheri* have a significantly thinner autophragm than *C. solida*. In terms of ornamentation, the most similar species to *C. solida* is *C. tunicata* Harding (in Williams et al., 1998). This species has relatively few prominent, arcuate/anastomosing ridges (Harding, 1990, pl. 27, figs 9-14.). However, *C. tunicata* is considerably smaller than *C. solida* and the former species is holocavate, has a relatively thin autophragm and the lumina formed by the ridges have a wide range of diameters. A similar, but less robust, unnamed form is recorded in the Tithonian lower *Pseudoceratium iehiense* Zone (4ciii) on the North-West Shelf. *Cassiculosphaeridia pygmaeus* Stevens 1987 is much smaller, with smaller, more delicate and regular fenestration and is commonly more ellipsoidal than *C. solida*.

Derivation of name. From the Latin, *solidus* meaning thick or dense, referring to the distinctive broad ridges of this species.

Holotype and type locality. Figures 10E-G, CPC 35944, from a ditch cuttings sample in Crux-1 well between 2945.00m and 2950.00m.

Stratigraphical distribution. *Cassiculosphaeridia solida* ranges from the Oxfordian *Wanaea spectabilis* Zone (6c) to the Tithonian upper *Dingodinium jurassicum* Zone (5a). It forms a marker acme in the upper part of the lower *D. jurassicum* Zone (5bi) (Foster, this volume; Helby & Partridge, in prep.).

Dissimulidinium May *et al.* 1987 emend.

Type species. *Dissimulidinium lobispinosum* May *et al.* 1987

Emended diagnosis. *Dissimulidinium* is emended here to accommodate forms with processes evenly distributed over the entire cyst except the paracingulum and parasulcus. Occasional isolated processes may occur on the paracingulum. Furthermore, the processes may be entirely nontabular or a mixture of elements of a nontabular and parasutural or penitabular disposition.

Comments. The generic concept of May *et al.* (1987) is extended to include forms with evenly distributed processes, some of which may be parasutural and/or penitabular. The original generic diagnosis confined the processes to nontabular elements located on the paired antapical lobes and the apical region (May *et al.*, 1987). The generic emendation was necessitated by the our observations of the morphology of *Dissimulidinium purattense* sp. nov. (see below).

A distinct *Dissimulidinium* lineage is recognised during the mid Tithonian to Berriasian interval. The genus first appeared during the mid Tithonian (upper *Dingodinium jurassicum* Zone – 5aii). This root-stock is characterised by a distinct lateral flattening and a minor equatorial constriction, foreshadowing the lobation developed in younger forms. In the early forms, the processes are both parasutural and nontabular. Elements of this root-stock have been described as *Egmontodinium egreticum* by Parker (1986, p. 59, 60, fig. 5.18, pl. 8, figs 2-4). There is a small stratigraphical gap prior to the appearance of the late Tithonian *Dissimulidinium purattense*, which represents the mid point of the lineage. In this species the lobation is slightly more pronounced, the dorsal to ventral inclination of the principal archaeopyle suture is substantially stronger than in the root-stock and the processes are significantly sparser in the equatorial region (Fig. 11). This trend culminates in the Berriasian species *Dissimulidinium lobispinosum* (*D. lobispinosum* Zone to the lower *Batioladinium reticulatum* Zone; subzones 4bi-4aiv), where the lobation can be extreme, the inclination of the principal archaeopyle suture is consistently developed and the processes are almost entirely restricted to the polar lobes (May *et al.*, 1987, figs 4H-I).

Dissimulidinium purattense sp. nov. (Figs 11A-P)

1986 *Ampulladinium robustum;* Parker, p. 29, pl. 1, figs. 1-3.
1994 *Dissimulidinium* sp. A; Bint & Marshall, fig. 5.4.
1994 *Dissimulidinium* sp. B; Bint & Marshall, fig. 5.5.

Previous Australian usage
Dissimulidinium purattiense – Helby.
MP 178C – Helby.

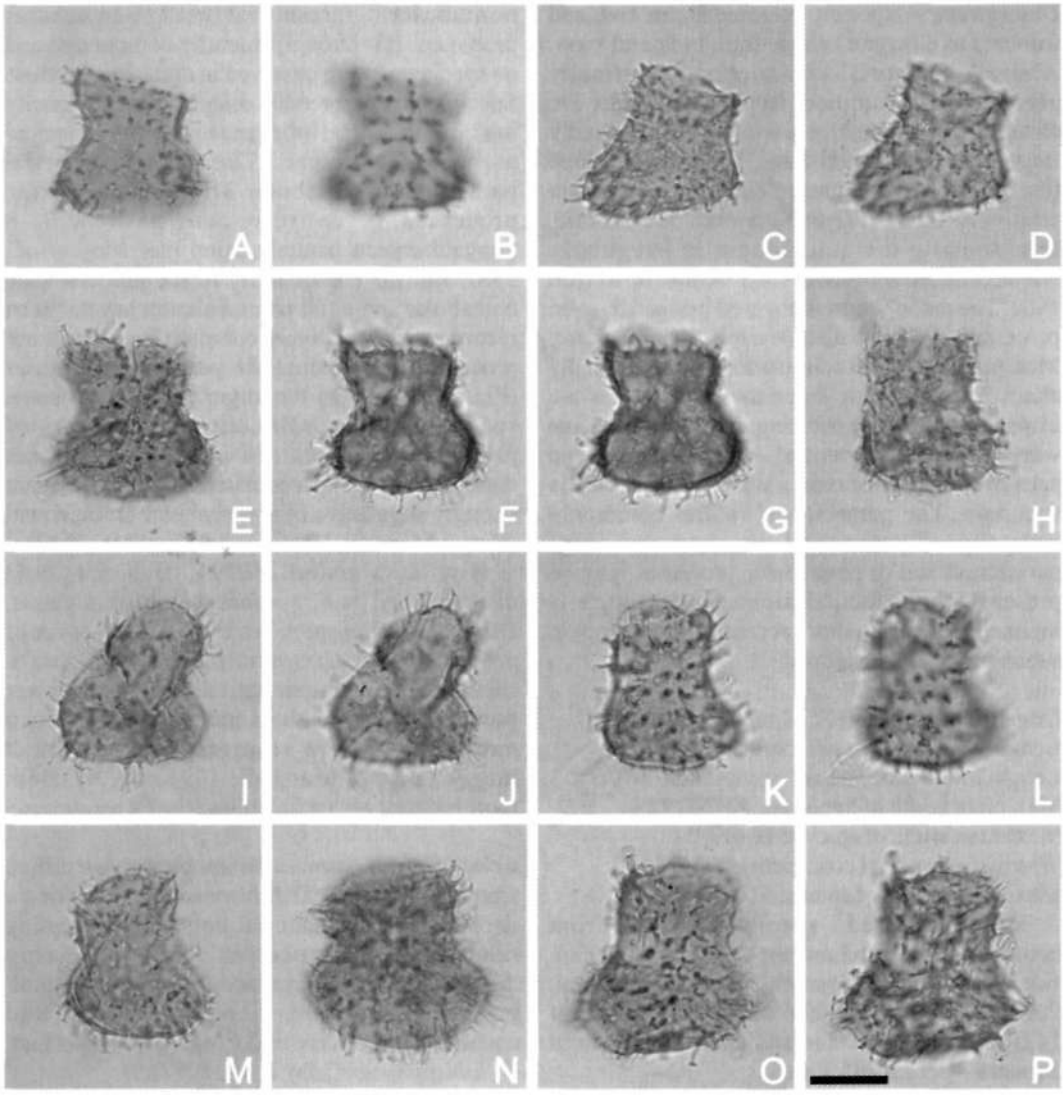

Fig. 11. Dissimulidinium purattense sp. nov. Specimens from sidewall core samples in Scafell-1 well at 1421.00m (Figs 11A-G, K-N) and 1418.00m (Figs 11H-J, O, P). All photomicrographs taken using plain transmitted light. The scale bar in Fig. 11P refers to all photomicrographs and is 25µm. Figures 11C-D are the holotype; the remainder, paratypes. Note trilobate/subquadrate outline, variable equatorial constriction, hypocystal lobes (of which dorsal lobe is largest), mixture of nontabular and parasutural/penitabular processes, and inclined principal archaeopyle suture of apical archaeopyle. A, B - CPC 35951, paratype; loisthocyst in right lateral view, high and low focus respectively. Note apparently parasutural processes which indicate paracingulum, and distinctly inclined principal archaeopyle suture. C, D - CPC 35952, holotype; loisthocyst in right lateral view, high and low focus respectively. Note solid processes, some of which may be penitabular. E-G - CPC 35953, paratype; loisthocyst in right lateral view, high to low focus sequence. Note penitabular processes on the hypocyst in Fig. 11E. H - CPC 35954, paratype; loisthocyst in left lateral view, median focus respectively. Note small equatorial constriction and apical archaeopyle. I, J - CPC 35955, paratype; loisthocyst in right lateral view, high and median focus respectively. Note relatively slender epicyst. K, L - CPC 35956, paratype; loisthocyst and operculum in left lateral view, high and low focus respectively. Note relatively flat operculum and evenly inserted processes, some of which may be parasutural. M - CPC 35957, paratype; loisthocyst and operculum in left lateral view, high focus. Note strong equatorial constriction. N - CPC 35958, paratype; full cyst in left lateral view, high focus. Note relatively large size. O, P - CPC 35959, paratype; full cyst in right lateral view, high and median focus respectively. Note possible penitabular nature of some processes.

Description. A species intermediate in size and trilobate to elongate subquadrate in lateral view. A slight equatorial constriction is normally present. The prominent hypocystal lobes are distally rounded and the dorsal lobe is markedly larger than the ventral lobe. The epicystal lobe (the apical area) is flattened distally. Autophragm relatively thick (1-2µm), smooth to scabrate. Occasionally the autophragm is irregularly microreticulate with subcircular lacunae up to 1µm wide. The autophragm is covered in slender, solid processes which are distally capitate or bifurcate. Most processes are 1-1.5µm wide, but occasionally attain 3µm in width. Intratabular processes are extremely rare on the paracingulum. No specimens were observed in ventral view, therefore the presence of processes on the parasulcus is uncertain. The paracingular sutures commonly have aligned parasutural processes and some parasutural and/or penitabular processes may be present. The principal archaeopyle suture is inclined ventrally; short accessory archaeopyle sutures may be developed.

Dimensions (µm, n=30): Min. (Mean) Max.
Length of entire cyst excl. spines: 52 (62) 71
Length of loisthocyst excl. spines: 43 (60) 76
Maximum width of hypocyst: 40 (52) 72
Maximum width of epicyst: 28 (39) 51
Width of equatorial constriction: 22 (35) 47
Maximum length of spines: 6 (9) 14

The measured specimens are from conventional core in Lambert-2 well at 3101.00m, sidewall core from Cossack-1 well at 3025.00m, Puratte-1 well at 172.00m and Scafell-1 well at 1421.00m and 1418.00m and ditch cuttings from Broome-1 Bore at 297.79m.

Comments. This species of *Dissimulidinium* is characterised by a robust autophragm, the slight equatorial constriction and the cover of nontabular, parasutural and penitabular processes. It is strongly laterally compressed and no specimens were observed in dorsoventral view. Specimens can be readily oriented by the disparity in size of the dorsal lobes and the sloping principal archaeopyle suture. The possible partial parasutural/penitabular arrangement of the processes is entirely consistent with a gonyaulacalean paratabulation (see May *et al.*, 1987, fig. 2). The majority of the processes are nontabular and a full paratabulation has not been recorded. It is relatively common for parasutural processes to surmount the paracingular sutures (Figs 11B, K). On the larger hypocyst in some specimens, discontinuous aligned rows of processes are present. In many of these cases these are closely spaced parallel rows, which are strongly suggestive of a penitabular arrangement (Bint & Marshall, 1994, fig. 5.4; Figs 11E, K, O).

Bint & Marshall (1994, figs 5.4, 5.5) distinguished two morphotypes of this genus. *Dissimulidinium* sp. A has a substantial cover of processes and *Dissimulidinium* sp. B has a slightly thicker autophragm and marginally fewer processes. These authors indicated that the two morphotypes have stratigraphically distinct ranges (Bint & Marshall, 1994, fig. 4). Both morphotypes are included here in *D. purattense*.

Comparison. *Dissimulidinium purattense* differs from the genotype, *D. lobispinosum*, in lacking a deeply incised equatorial constriction, having relatively wide processes which are evenly distributed over the cyst and may be parasutural/penitabular. Furthermore the epicyst and equatorial regions are wider in *D. purattense* than *D. lobispinosum* (May *et al.*, 1987).

Derivation of name. From the Puratte-1 well, where we first recorded this species.

Fig. 12. Gardodinium angustum Riding, Helby & Stevens sp. nov. Entire specimens from conventional core samples in Lorikeet-1 well at 1759.10m (Figs 12C-D, I-L, O-P), a sidewall core sample in Avocet-1A well at 1771.50m (Figs 12E-H, M-N) and ditch cuttings in Avocet-1A well between 1775.00m and 1780.00m (Figs 12A-B). Figs 12E-H are the holotype; the remainder, paratypes. All photomicrographs taken using plain transmitted light. The scale bar in Fig. 12P refers to all photomicrographs and is 25µm. Note elongate ellipsoidal outline, holocavate cyst organisation with numerous processes between two cyst walls, prominent apical horn formed of ectophragm, gonyaulacalean paratabulation and apical archaeopyle. A, B - CPC 35960, paratype; dorsal view, high and low focus respectively. Note distorted apical horn, penitabular nature of ectophragmal processes and low parasutural ridges on ectophragm. C - CPC 35961, paratype; dorsal view, median focus. Note holocavate cyst organisation and prominent apical horn. D - CPC 35962, paratype; dorsal view, low focus. Note long, straight, parallel-sided apical horn and straight (L-style), median parasulcus. E-H - CPC 35963, holotype; oblique ventral/left lateral view, high to low focus sequence. Exceptionally well-preserved; note partially penitabular nature of processes, apical archaeopyle and indented paracingulum. I, L - CPC 35964, paratype; slightly oblique ventral view, high to low focus sequence. Note relatively small, distorted apical horn (continued opposite)

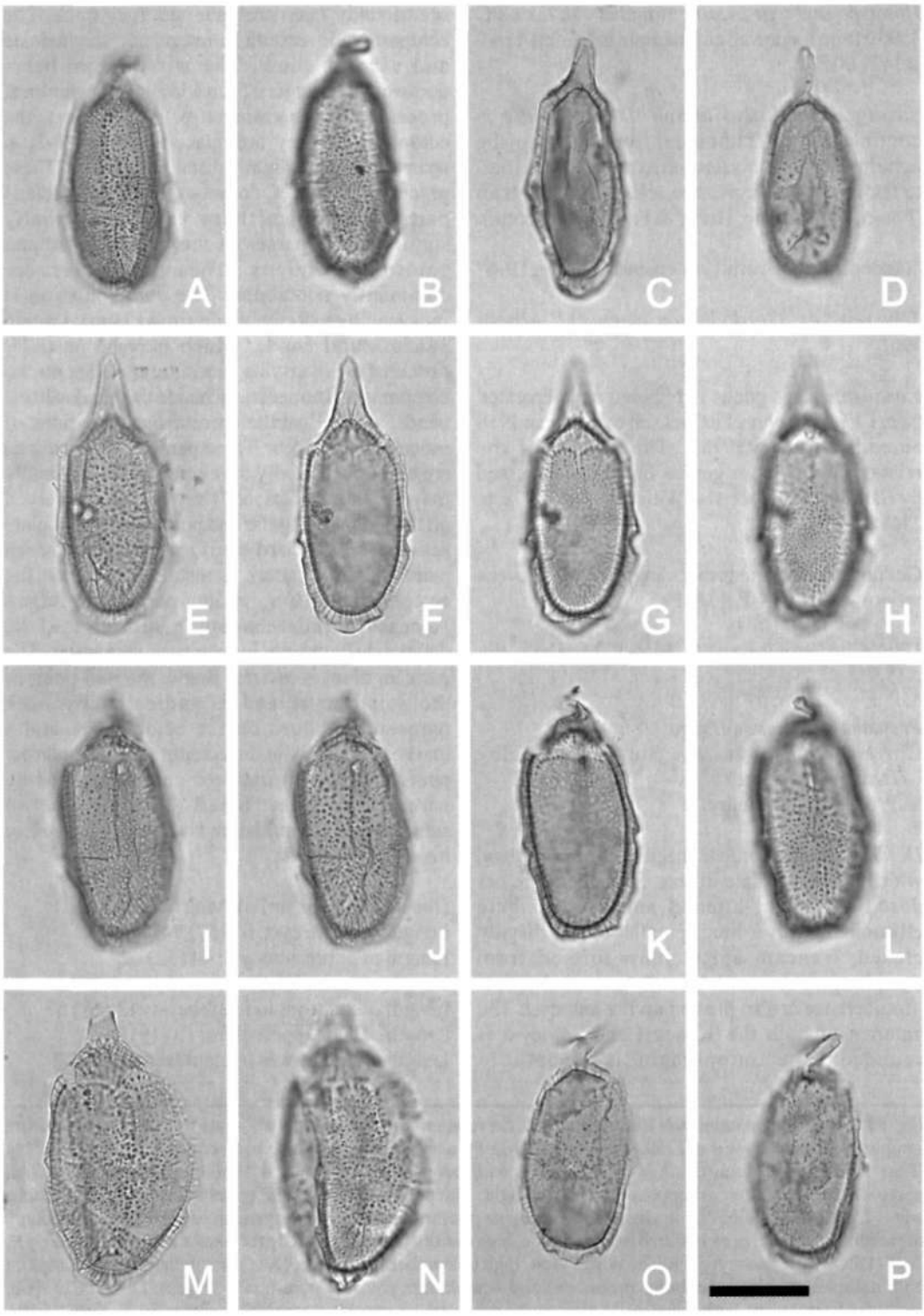

and long precingular paraplate series. M, N - CPC 35965, paratype; left lateral view, high and low focus respectively. Relatively large, wide specimen; note processes do not extend into apical horn. O, P - CPC 35966, paratype; dorsal view, high and median focus respectively. Note relatively narrow ectocoel and slightly distorted apical horn.

Holotype and type locality. Figures 11C-D, CPC 35952 from a sidewall core sample in Scafell-1 well at 1421.00m.

Stratigraphical distribution. *D. purattense* is confined to the Tithonian, ranging from the uppermost *Dingodinium jurassicum* Zone (5ai) to the mid *Pseudoceratium iehiense* Zone (4cic) (Foster, this volume; Helby & Partridge, in prep.).

Gardodinium Alberti 1961 emend. Harding 1996

Type species. *Gardodinium eisenackii* Alberti 1961.

Comments. This genus is retained and separated from *Chlamydophorella* Cookson & Eisenack 1958 emend. Duxbury 1983. The history of the relationship of these genera has been discussed by Harding (1996; see also Williams *et al.*, 1998, p. 234).

Gardodinium angustum Riding, Helby & Stevens sp. nov. (Figs 12A-P, 13A-P)

1994 *Gardodinium* sp. A; Bint & Marshall, fig. 5.3.

Previous Australian Usage
Gardodinium angustum Stevens & Helby (manuscript name).
M.P. 677 (pars) – Helby.

Description. An elongate species of *Gardodinium*, which is intermediate in size. Specimens are not dorsoventrally flattened and are elongate ellipsoidal, with a long, parallel-sided, distally closed, truncate apical horn formed from ectophragm. A small, distally rounded apical protuberance is also present on the autocyst. The antapex of both the autocyst and ectocyst is rounded. The autophragm is smooth to occasionally microscabrate and 1µm thick. The ectophragm is smooth to irregularly shagreenate and <0.5µm thick. The autophragm bears numerous slender (c. 0.5µm wide) solid, cylindrical processes which connect to, and support, the ectophragm. They are spaced between 1-3µm apart and may be slightly distally expanded. These processes, however, do not extend into the distal part of the apical horn and are normally significantly sparser in the paracingular and parasulcal regions. These processes are dominantly nontabular. The paratabulation is indicated by extremely thin (up to 1µm), smooth pandasutural bands, which may be partially obscured by overlying parasutural ridges on the ectophragm. Immediately inside the pandasutural bands, several parallel penitabular lineations of processes may occur. These penitabular lineations are normally partially developed and occasionally may be entirely absent. They are best observed on the long precingular and postcingular paraplate series. The standard sexiform gonyaulacacean paratabulation pattern is also expressed on the ectophragm by low, smooth parasutural ridges. Accessory endarchaeopyle sutures may be developed in the precingular paraplate series. The paracingulum is inserted below the mid-point of the loisthocyst and is indicated by both parasutural ridges on the ectophragm and a marked concavity in the ectophragm. The narrow parasulcus is also indented and surrounded by parasutural ridges. Small (3-5µm diameter) subspherical accumulation bodies may be present inside the autocyst.

Dimensions (µm, n=26): Min. (Mean) Max.
Length of entire cyst: 61 (67) 74
Length of entire autocyst: 44 (52) 62
Length of entire loisthocyst: 46 (53) 69
Length of autocyst in loisthocyst: 42 (48) 57
Length of entire operculum: 13 (19) 26
Length of autocyst in operculum: 10 (11) 13

Fig. 13. Gardodinium angustum Riding, Helby & Stevens sp. nov. Paratype loisthocysts from conventional core sample in Lorikeet-1 well at 1759.10m (Figs 13D-L, P), a sidewall core sample in Avocet-1A well at 1771.50m (Figs 13M-O) and ditch cuttings in Avocet-1A well between 1775.00m and 1780.00m (Figs 13A-C). All photomicrographs taken using plain transmitted light. The scale bar in Fig. 13P refers to all photomicrographs and is 25µm. Note variability in size, slender elongate outline, penitabular arrangement of processes at periphery of paraplates, angular principal archaeopyle suture, high density of ectophragmal processes and apical archaeopyle. A-C - CPC 35967, paratype; oblique dorsal view, high to low focus sequence. Note paratabulation is indicated on both autophragm (by penitabular processes) and ectophragm (by low parasutural ridges). D - CPC 35968, paratype; lateral view, high focus. Note penitabular processes on precingular paraplate series. E, F - CPC 35969, paratype; dorsal view, high and low focus respectively. Note penitabular processes on both precingular and postcingular paraplate series. Processes significantly less dense on the paracingulum and parasulcus. G, H - CPC 35970, paratype; lateral view, high and median focus respectively. Note indented paracingulum and penitabular processes. I-K - CPC 35971, paratype; lateral view, high to low focus sequence. (continued opposite)

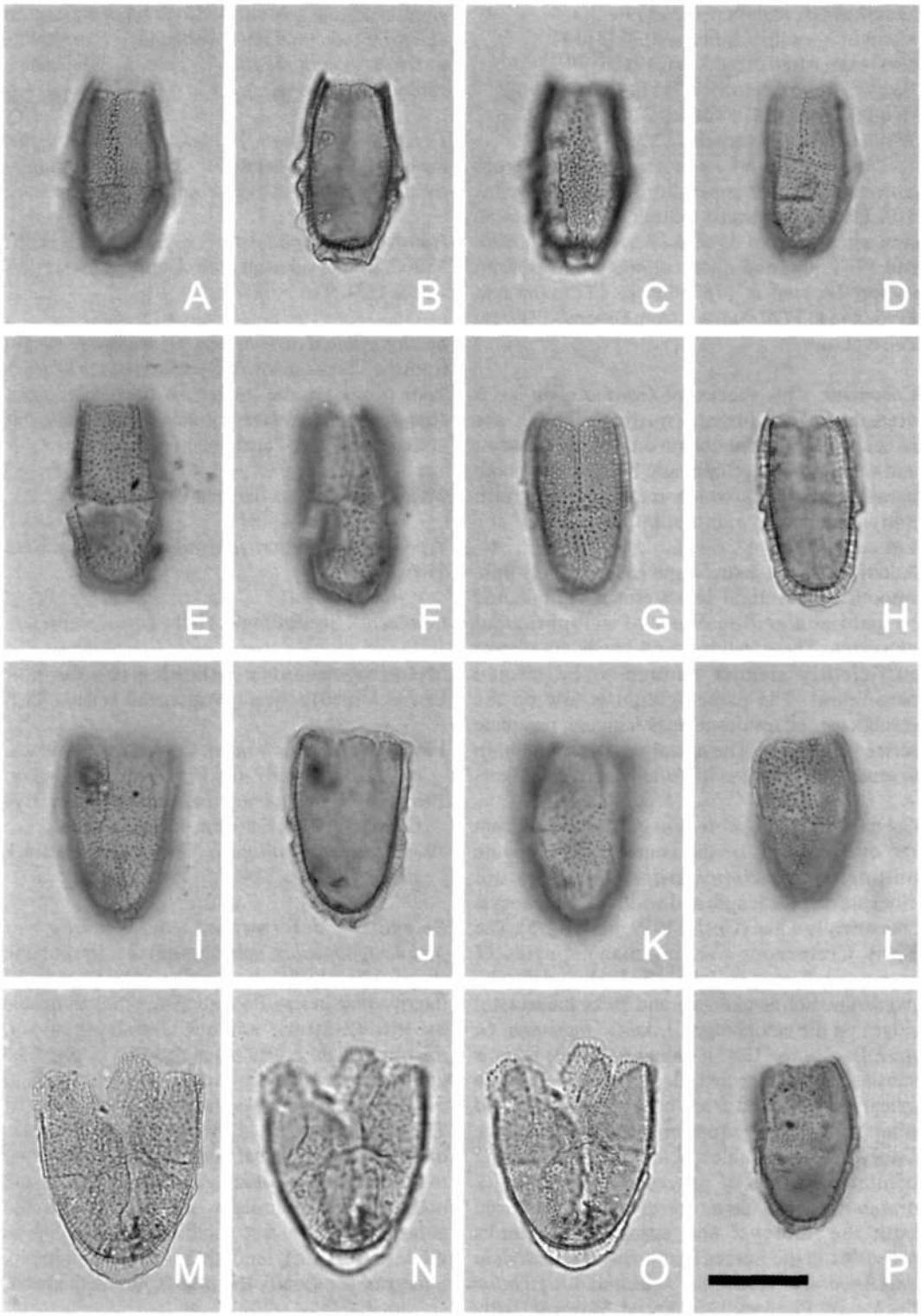

Note accessory archaeopyle sutures in Fig. 13J. L, P - CPC 35972, paratype; oblique dorsal view, high and low focus respectively. Relatively small specimen; note strong penitabular processes on middorsal precingular paraplates in Fig. 13L. M-O - CPC 35973, paratype; ventral view, high to low focus sequence. Relatively large specimen; note prominent accessory archaeopyle sutures.

Length of apical horn: 8 (12) 17
Maximum width of entire cyst: 25 (31) 44
Maximum width of autocyst: 19 (26) 39
Height of apical ectocoel: 7 (11) 16
Height of antapical ectocoel: 2 (4) 6
Width of lateral ectocoel: 1 (2.5) 4

The measured specimens are from conventional core samples from Lambert-2 well at 3101.00m and Lorikeet-1 well at 1759.10m, sidewall core samples from Avocet-1A well at 1778.00m and 1771.50m and ditch cuttings samples from Avocet-1A well at 1780.00m to 1775.00m and 1775.00m to 1770.00m and from Broome-1 Bore at 297.79m.

Comments. This species of *Gardodinium* has a distinctively elongate outline. There are indications of paratabulation on both the autocyst and ectocyst. The ectophragm bears low, smooth parasutural ridges which indicate a sexiform gonyaulacacean paratabulation pattern; the formula is: ?pr, 4', 6", 6c, 6"', 1p, 1"", Xs. Additionally, the autophragm has extremely thin, smooth pandasutural bands and is surmounted by penitabular lineations of ectophragmal processes. These pandasutural bands are almost sufficiently slender enough to be termed parasutural. The paracingulum is low on the loisthocyst and results in the precingular paraplate series being long. The apical ectophragmal horn is somewhat flimsy as it is often distorted or bent.

Comparison. *Gardodinium angustum* differs from the other species of the genus in its elongate outline. *Gardodinium trabeculosum* is not elongate and the length and width of the autocyst are normally equal (Gocht, 1959, pl. 4, fig. 5). The Early Cretaceous (Valanginian) species *G. attenuatum* Stover & Helby 1987 is larger than *G. angustum*, not as elongate and lacks parasutural ridges on the ectophragm. Like *G. angustum*, *G. lowii* Backhouse 1987 is elongate, but the latter is substantially larger and has an extremely large apical horn formed from both autophragm and ectophragm. The European species *G. ordinale* Davey 1974 resembles *G. angustum* in having penitabular rows of processes. However, *G. ordinale* is squat, has an apical horn formed from both the autocyst and ectocyst and lacks processes in the intratabular areas. *Gardodinium angustum* also resembles *Belodinium dysculum* Cookson & Eisenack 1960 emend. Stover & Helby 1987 in being elongate and holocavate. However, *B. dysculum* has highly variable penitabular to nontabular autophragmal processes and a significantly longer antapical ectocoel and has an antapical claustrum representing the 1"" paraplate in the ectophragm, like *B. nereidis* Stevens & Helby (1987, fig. 5).

Derivation of name. From the Latin *angustus*, meaning narrow, slender or thin, and referring to the characteristic elongate outline of this species.

Holotype and type locality. Figures 12E-H, CPC 35963, from a sidewall core sample in Avocet-1A well at 1771.50m.

Stratigraphical distribution. *G. angustum* ranges from the Tithonian lower *Pseudoceratium iehiense* Zone (4ciiic) to the lowermost Berriasian upper *Pseudoceratium iehiense* Zone (4cib) (Foster, this volume; Helby & Partridge, in prep.).

Meiourogonyaulax Sarjeant 1966

Type species. *Meiourogonyaulax valensii* Sarjeant 1966

Comments. See Riding & Helby (this volume).

Meiourogonyaulax bulloidea (Cookson & Eisenack 1960) Sarjeant 1969 emend. (Figs. 14A-I)

1960 *Gonyaulax bulloidea*; Cookson & Eisenack, p. 247, fig. 4, pl. 37, fig. 11.
1969 *Meiourogonyaulax bulloidea* (Cookson & Eisenack 1958); Sarjeant, p. 14.
1976 *Lithodinia bulloidea* (Cookson & Eisenack 1958); Gocht, p. 334.

Emended description. A species of *Meiourogonyaulax*, subspherical to ellipsoidal in shape; slightly dorsoventrally compressed and intermediate in size. Paratabulation fully indicated by low (2-3µm), narrow, distally smooth, microreticulate crests up to 5µm in height. The crests are occasionally irregularly fenestrate and are highest at gonal points and at the antapex. The crests coalesce at the apex to form a low, distally rounded apical horn or protuberance, up to 5µm high. The paracingulum is equatorial and not subdivided. Similarly, the slightly indented parasulcus is also not subdivided. Autophragm thick (1.5 -3µm), smooth and microreticulate. Fenestrae are usually less than 0.5µm in diameter.

Dimensions (µm, n=12) incl. crests, horns etc. where appropriate: Min. (Mean) Max.
Length of entire cyst: 75 (83) 90

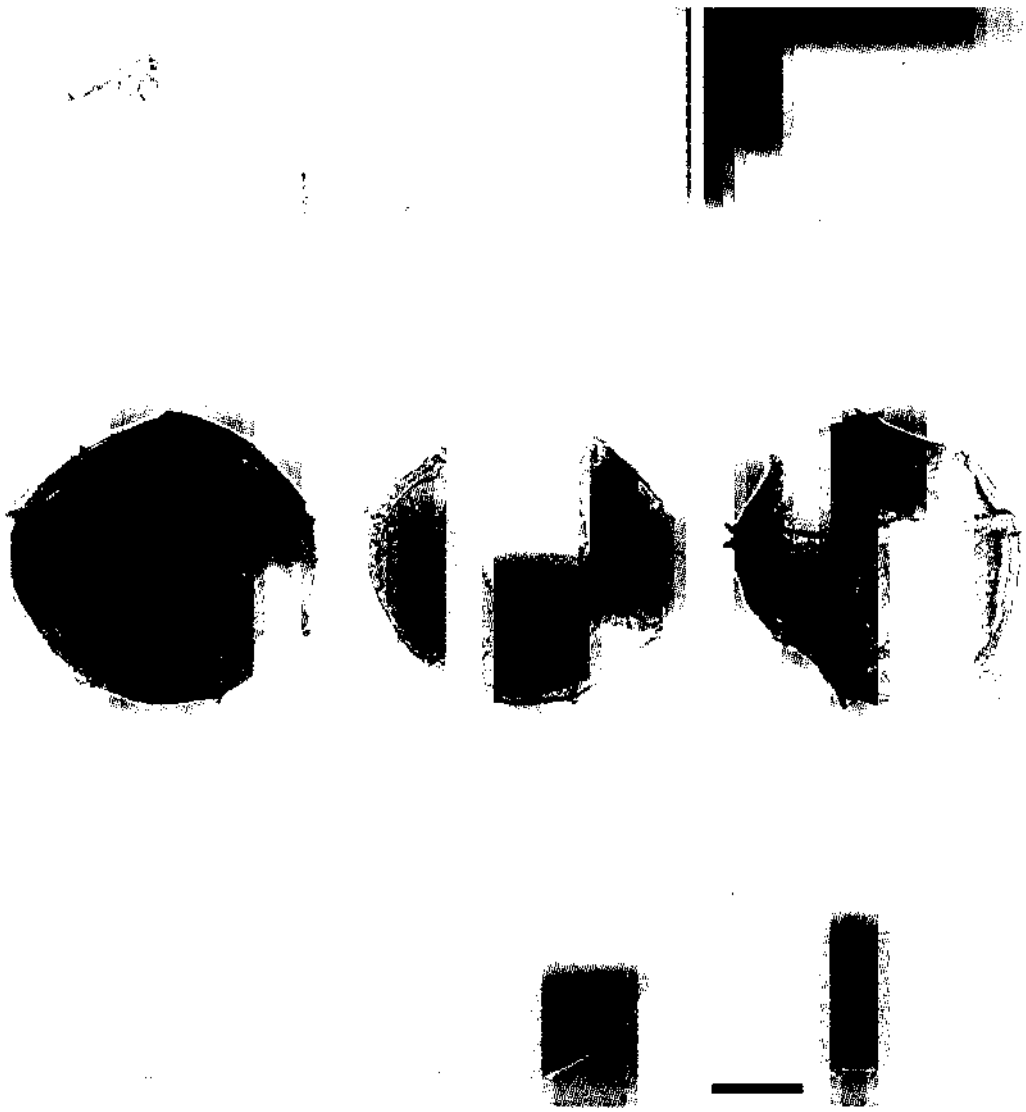

Fig. 14. Meiourogonyaulax bulloidea (Cookson & Eisenack 1960) Sarjeant 1969 emend. All are topotypes from ditch cuttings at 297.79m in Broome-1 Bore. All photomicrographs taken using plain transmitted light. The scale bar in Fig. 14I refers to all photomicrographs and is 25µm. Note robust, microreticulate autophragm, distinct apical horn or protuberance and narrow, distally-smooth parasutural crests which may be fenestrate and are highest at the gonal points. A - CPC 35974, topotype; apical view, low focus. Note relatively thick autophragm. B, C - CPC 35975, topotype; antapical view, high and median focus respectively. Note apical archaeopyle and relatively high, fenestrate parasutural crests at paracingulum. D, E - CPC 35976, topotype; oblique dorsal view, median and low focus respectively. Note extremely thick autophragm and much reduced apical horn/protuberance. F - CPC 35977, topotype; ventral view, median focus. Relatively angular specimen; note apical archaeopyle. G, H - CPC 35978, topotype; dorsal view, median and low focus respectively. Note ellipsoidal outline. I - CPC 35979, topotype; dorsal view, low focus. Note small apical horn/protuberance.

Length of loisthocyst: 65 (73) 83
Width of cyst: 76 (83) 91

All specimens measured are topotypes from ditch cuttings in the Jarlemai Siltstone (Tithonian) of Broome-1 Bore, Western Australia at 297.79m.

Comments. The thick, microreticulate autophragm is characteristic of this taxon. The subspherical shape and the broadly similar size and shape of the epicyst and hypocyst of *M. bulloidea* mean that typically these cysts are equatorially and laterally symmetrical. The parasutural crests are distinctively smooth and microreticulate, and typically about 3µm high (Fig. 14F). However,

crests are higher gonally and close to the antapex. In some specimens, the parasutural crests appear to be significantly reduced in height ventrally. This can make the paratabulation difficult to discern, and the orientation problematical.

This species is emended to record the characteristic microreticulate nature of the autophragm and parasutural crests. In the original description, the cyst wall and 'ledges' were described as '±granular' (Cookson & Eisenack, 1960, p. 247). The 12 topotype specimens studied are slightly larger than the type material of Cookson & Eisenack (1960). This emendation is based entirely on topotypes and does not take into account the wider morphological variation of this species noted in other material.

Comparison. Meiourogonyaulax bulloidea is distinctive in being significantly larger than most other species of the genus. However, the relatively large *M. pertusa* (Duxbury 1977) Below 1981 closely resembles *M. bulloidea* in that it also has thick, perforate autophragm and low, distally smooth parasutural crests. Duxbury (1977, p. 42, fig. 42) showed that the paracingulum and parasulcus of *M. pertusa* are subdivided.

Parasutures within the paracingular and parasulcal areas of *M. bulloidea* have not been observed. Furthermore, *M. pertusa* is slightly smaller than *M. bulloidea* and is more elongate. *Meiourogonyaulax strongyla* Sarjeant 1972, another large cyst, has denticulate parasutural crests and a granulate autophragm. The Bathonian *M. superornata* (W. Wetzel 1967) Sarjeant 1969 is also large, but differs from *M. bulloidea* in having very high parasutural crests. *Meiourogonyaulax bulloidea* also closely resembles *M. viriosa* Riding & Helby (this volume) in shape and in having a microreticulate autophragm. However, the latter is normally smaller than *M. bulloidea* and may have distally denticulate parasutural crests (see below). Moreover, the apical protuberance in *M. viriosa* is a solid boss-like feature; by contrast, the apical structure in *M. bulloidea* is formed by the coalescence of parasutural crests. Backhouse (1988, p. 95) noted that the Early Cretaceous form *Meiourogonyaulax stoveri* Millioud 1969 may be a variant of *M. bulloidea*. *Meiourogonyaulax stoveri* has distally smooth parasutural crests and a perforate/reticulate autophragm. The fenestrae in the autophragm of *M. stoveri* are, however, much larger than those in *M. bulloidea*. Also, the outline of *Meiourogonyaulax stoveri* is also much more elongate than that of *M. bulloidea* and the former lacks an apical structure of any kind.

Holotype and type locality. The holotype is from ditch cuttings in the upper portion of Jarlemai Siltstone (Tithonian) in Broome-1 Bore, Western Australia at 297.79m. It is in the Museum of Victoria, Melbourne as specimen number P.17788 (Cookson & Eisenack, 1960).

Stratigraphical distribution. Meiourogonyaulax bulloidea ranges from the Tithonian *Cribroperidinium perforans* Zone (5d) to the lowermost Valanginian *Egmontodinium torynum* Zone (4ai/4aii). It occurs consistently from the Tithonian upper *Dingodinium jurassicum* Zone (5ai) to the Berriasian *Cassiculosphaeridia delicata* Zone (4bii) (Foster, this volume; Helby & Partridge, in prep.).

Pseudoceratium Gocht 1957 emend. Helby 1987

Type species. Pseudoceratium pelliferum Gocht 1957

Pseudoceratium robustum sp. nov. (Figs 15A-L)

Previous Australian usage
Pseudoceratium iehiense (pars)– Helby.

Fig. 15. Pseudoceratium robustum sp. nov. Specimens from sidewall core in Scafell-1 well at 1418.00m (F-H) and from ditch cuttings between 3150.00m and 3155.00m in Mindil-1 well (A-E, I-L). Figures 15J-K are the holotype; the remainder are paratypes. All photomicrographs taken using plain transmitted light. The scale bar in Fig. 15L refers to all photomicrographs and is 25µm. Note apical, paracingular/postcingular and antapical horns, short, solid processes which emerge from autophragm and are connected distally by a thin, trabeculate, vacuolate ectophragm, and apical archaeopyle. A, B - CPC 35995, paratype; dorsal view, high and low focus respectively. Note equatorial position of the lateral horn. C - CPC 35996, paratype; dorsal view, median focus. Note vacuolate nature of the ectophragm. D, E - CPC 35997, paratype; ventral view, median and low focus respectively. Note angular nature of principal archaeopyle suture and vague indications of paracingulum. F - CPC 35998 paratype, dorsal view, median/low focus. Note relatively small, narrow horns. G - CPC 35999 paratype, ventral view, median focus. Note offset parasulcal notch. H - CPC 36000 paratype, dorsal view, median focus. Note highly angular principal archaeopyle suture. I - CPC 36001, paratype; dorsal view, median focus. Angular specimen; note narrow antapical horn. J, K - CPC 36002, holotype; ventral view, high and median focus respectively. Note prominent apical horn and irregularly vacuolate nature of the ectophragm. L - CPC 36003, paratype; dorsal view, median focus. Elongate specimen; note reduced lateral horn.

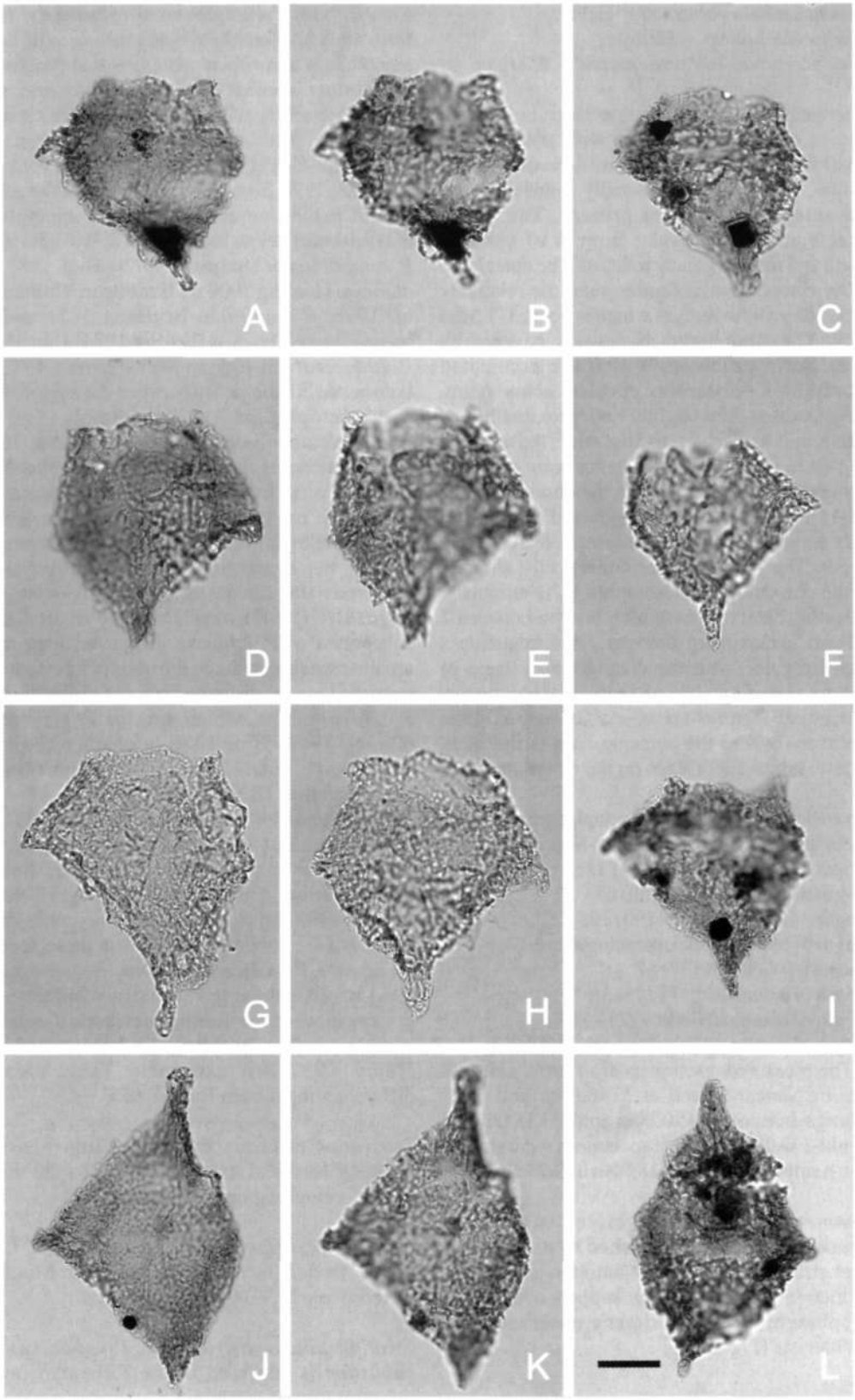
A
B
C
D
E
F
G
H
I
J
K
L

Pseudoceratium robustum – Helby.
Pseudoceratium sp. – Helby.
Pseudoceratium iehiense 'macro' – Morgan

Description. An intermediate to large, holocavate species of *Pseudoceratium* with a somewhat angular compressed ceratioid dorsoventral outline. Relatively large distally rounded apical and antapical horns are present. The single paracingular/postcingular horn is of variable length and may be greatly reduced. The outer layer of the ectophragm is thinner than the relatively thick, robust autophragm which is about 1-1.5µm thick. The autophragm is densely covered by short, solid processes which are connected distally by a trabeculate/reticulate ectophragm. The processes flare slightly both proximally and distally and vary from 1 to 5µm wide; the majority are 1-2µm in width. These elements are normally between 1 and 4µm in height; the observed range is 1-11µm. Close to the antapex and at the distal parts of the horns, the processes are frequently longer. The processes are consistently shortest on the operculum. The ectophragm is reticulate, with ellipsoidal to subcircular fenestra between 2 and 6µm in maximum diameter. The reticulation is often irregular, with the diameter and shape of fenestra varying widely on individual specimens. Parasutural features are absent, except in some specimens where the paracingulum is indicated by low, subparallel ridges on the ectophragm.

Dimensions (µm, n=32) incl. ectophragm and horns where appropriate: Min. (Mean) Max.
Length of entire cyst: 97 (124) 136
Length of operculum: 45 (50) 65
Length of loisthocyst: 74 (90) 105
Length of hypocyst incl. paracingulum: 47 (57) 69
Equatorial width: 61 (77) 87
Length of apical horn: 15 (25) 36
Length of antapical horn: 9 (21) 33
Length of right postcingular horn: 5 (11) 17

The measured specimens are from a sidewall core in Nancar-1 well at 3240.00m and ditch cuttings between 3150.00m and 3155.00m in Mindil-1 well. Additional specimens were studied from a sidewall core at 1418.00m in Scafell-1 well.

Comments. This distinctive species of *Pseudoceratium* is distinguished by its relatively large size, the thick, robust autophragm and the distinctive processes which support a vacuolate ectophragm. Most specimens observed were loisthocysts (Fig. 15).

Comparison. *Pseudoceratium robustum* differs from other species of *Pseudoceratium* in its thick autophragm and robust ectophragmal processes. Most other species have more numerous and slender autophragmal projections and are variably holocavate. The latter include the genotype, *P. pelliferum* Gocht 1970, as well as *P. retusum* Brideaux 1977. Some representatives of the genus do not exhibit an ectophragm, for example *P. almohadense* (Below 1984) Lentin & Williams 1989, *P. anaphrissum* (Sarjeant 1966) Bint 1986, *P. aulaeum* Harding 1990 ex Harding in Williams *et al*. 1998, *P. expolitum* Brideaux 1971 and *P. securigerum* (Davey & Verdier 1974) Bint 1986. *Pseudoceratium toveae* Nøhr-Hansen 1993 is holocavate but the cavity between the autophragm and ectophragm is extremely small. *Pseudoceratium gochtii* Neale & Sarjeant 1962 has longer horns than *P. robustum* and the short spines arising from the autophragm indicate a ceratioid paratabulation. *Pseudoceratium iehiense* Helby & May (in Helby, 1987) is extremely similar, but is marginally larger and has more numerous and slender ectophragmal processes. Arguably, *P. robustum* could be treated as a subspecies of *P. iehiense*. However, we prefer separate specific status on the basis of its extremely restricted range, disjunct from the range base of *P. iehiense*. The Albian species *P. eisenackii* (Davey 1969) Bint 1986 is characterised by extremely small horns and marginate ornamentation (Bint, 1986, pl. 2, figs 14, 15). *Pseudoceratium interiorense* Bint 1986 is holocavate, but is unusually elongate and is cornucavate at the extremities of the horns. Holocavation is developed in *P. iveri* Nøhr-Hansen 1993 and *P. plerum* (Duxbury 1983) Bint 1986, but the pandasutural areas in these species are acavate. *Pseudoceratium spitiense* Jain & Garg 1984 is very similar to *P. robustum*, but the poor preservation of the former precludes a detailed comparison. The three horns in *P. weymouthense* Helby 1987 are extremely long, clearly differentiating it from *P. robustum*.

Derivation of name. From the Latin *robustus*, meaning hard and strong, referring to the thick, robust, ectophragmal processes.

Holotype and type locality. Figures 15J-K, CPC 36002, from a ditch cuttings sample in Mindil-1 well between 3150.00m and 3155.00m.

Stratigraphical distribution. *Pseudoceratium robustum* is confined to the Tithonian lower

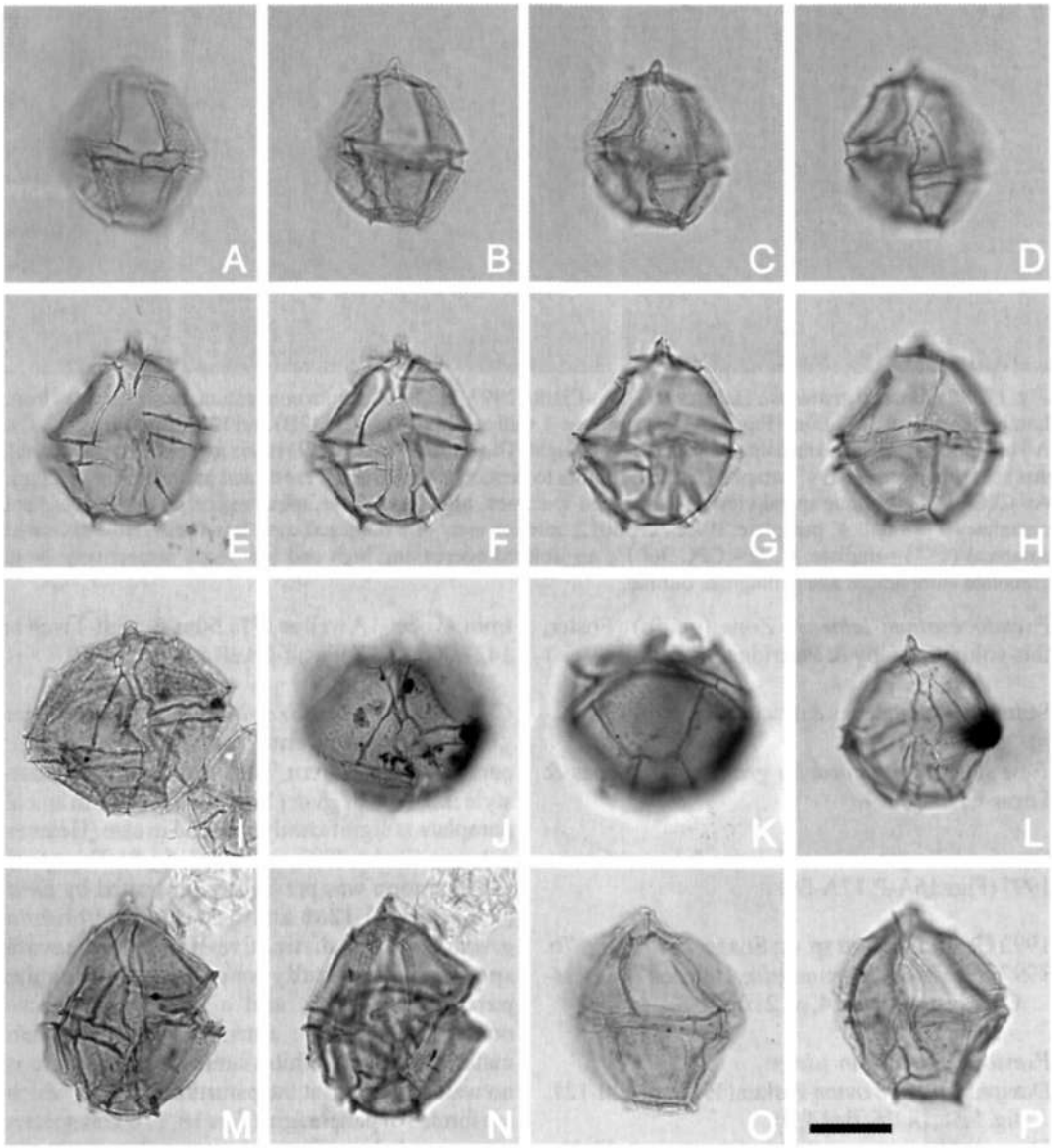

Fig. 16. Stanfordella granulosa Helenes & Lucas-Clarke 1997. Specimens from conventional core samples from Mutineer-1B well at 3132.25m (Figs 16M-N) and Wanaea-2 well at 3375.34m (Figs 16A-D, L), 2880.50m (Figs 16J-K) and 2875.30m (Figs 16O-P) and sidewall core samples from Avocet-1A well at 1771.50m (Figs 16E-H) and Zeewulf-1 well at 3085.00m (Fig. 16I). All photomicrographs taken using plain transmitted light. The scale bar in Fig. 16P refers to all photomicrographs and is 25µm. Note slight cavation developed at the apical horn, gonyaulacacean paratabulation comprising an extremely small 4' paraplate and sigmoidal (S-style) parasulcus, smooth to denticulate parasutural crests, granulate autophragm and precingular (type P) archaeopyle. A-D - CPC 36004; dorsal view, high to low focus sequence. Note highly offset paracingulum in Fig. 16D. E-H - CPC 36005; ventral view, high to low focus sequence. Note relatively wide, sigmoidal parasulcus and monocornucavate cyst organisation. I - CPC 36006; ventral view, high focus. Note characteristic subtriangular shape of the 6'' paraplate. J, K - CPC 36007; oblique ventral view, high and low focus respectively. Note subtriangular 6'' paraplate in Fig 16J and centrally-positioned middorsal postcingular paraplate (4''') in Fig. 16K. The latter indicates this species has not undergone torsion. L - CPC 36008; dorsal view, low focus. Relatively small specimen. M, N - CPC 36009; ventral view, high and low focus respectively. Slightly damaged specimen; note cavation at apical horn. O, P - CPC 36010; dorsal view, high and median focus respectively. Note single paraplate precingular archaeopyle.

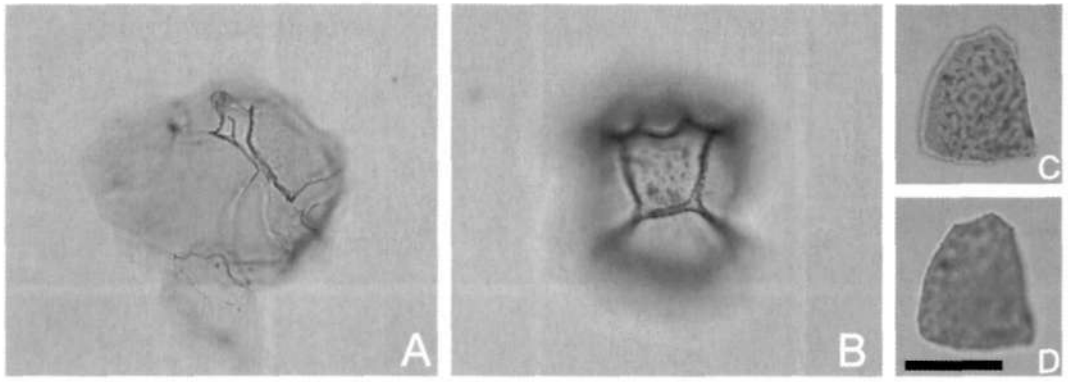

Fig. 17. Stanfordella granulosa Helenes & Lucas-Clarke 1997. Specimens from conventional core samples from Lambert-2 well at 3101.00m (Fig. 17A) and Lorikeet-1 well at 1759.10m (Fig. 17B) and 1756.70m (Fig. 17C-D). All photomicrographs taken using plain transmitted light. The scale bar in Fig. 17D refers to all photomicrographs and is 25µm. Note small 4' paraplate, robust, smooth to denticulate parasutural crests and granulate autophragm. A - CPC 36011; oblique apical view of a damaged specimen, high focus. Note apical region including preapical paraplates and small 4' paraplate. B - CPC 36012; interior view of a damaged cyst, low focus. Note six-sided antapical (1'''') paraplate. C, D - CPC 36013; an isolated operculum, high and low focus respectively. Note granulate autophragm and pentagonal outline.

Pseudoceratium iehiense Zone (4ciiib) (Foster, this volume; Helby & Partridge, in prep.).

Stanfordella Helenes & Lucas-Clarke 1997

Type species. Stanfordella granulosa Helenes & Lucas-Clarke 1997.

Stanfordella granulosa Helenes & Lucas-Clarke 1997 (Figs 16A-P, 17A-D)

1992 *Gonyaulacysta* sp. A; Snape, p. 273, fig. 7b.
1997 *Stanfordella granulosa*; Helenes & Lucas-Clarke, p. 182, fig. 4, pl. 2, figs 1-8.

Previous Australian usage
Dampierodinium ovum Parker (1986, p. 120-121, fig. 5.56, pl. 26, figs 4, 5).
Farragodinium curiosum Stevens & Helby (manuscript name).
M.P. 175 – Helby.
M.P. 654 – Helby.

Dimensions (µm, n=27) incl. parasutural crests where appropriate: Min. (Mean) Max.
Length of cyst incl. apical horn: 46 (59) 77
Length of apical horn: 3 (5) 9
Equatorial width of cyst: 44 (55) 70
Maximum height of parasutural crests: 1 (2) 5

The measured specimens are from conventional core samples in Lambert-2 well at 3101.00m, Lorikeet-1 well at 1759.10m, Mutineer-1B well at 3132.25m, Wanaea-2 well at 3375.34m, 2880.50m and 2875.30m and sidewall core samples from Avocet-1A well at 1771.50m, Scafell-1 well at 1421.00m and Zeewulf-1 well at 3085.00m.

Comments. Stanfordella is a distinctive gonyaulacacean genus with a characteristic paratabulation pattern. The ventral paratabulation style is S-type of Evitt (1985) and the fourth apical paraplate is significantly reduced in size (Helenes & Lucas-Clarke, 1997, fig. 4, pl. 2, fig. 8). This apical configuration was previously illustrated by Evitt (1985, figs 5.12M and 5.16G). *Stanfordella granulosa* is a distinctive monocornucavate species with distally smooth to denticulate parasutural crests and a relatively sparse nontabular granulate ornament. The Australian material does not exhibit suturocavation; there is no wall separation at the parasutural crests, which are formed of periphragm (Figs 16, 17). This species was recorded as *Gonyaulax granulosa* from the late Tithonian to the Valanginian (Early Cretaceous) of the Great Valley Sequence of McCarty Creek, California by Warren (1967).

Stanfordella granulosa is illustrated here (Figs 16, 17) as this is the first record of this species in the Australian region and also because of its stratigraphical importance.

Stratigraphical distribution. In Australia, *Stanfordella granulosa* ranges from the Tithonian upper *Dingodinium jurassicum* Zone (5aii) to the Berriasian upper *Cassiculosphaeridia delicata* Zone (4biia) (Foster, this volume; Helby & Partridge, in prep.).

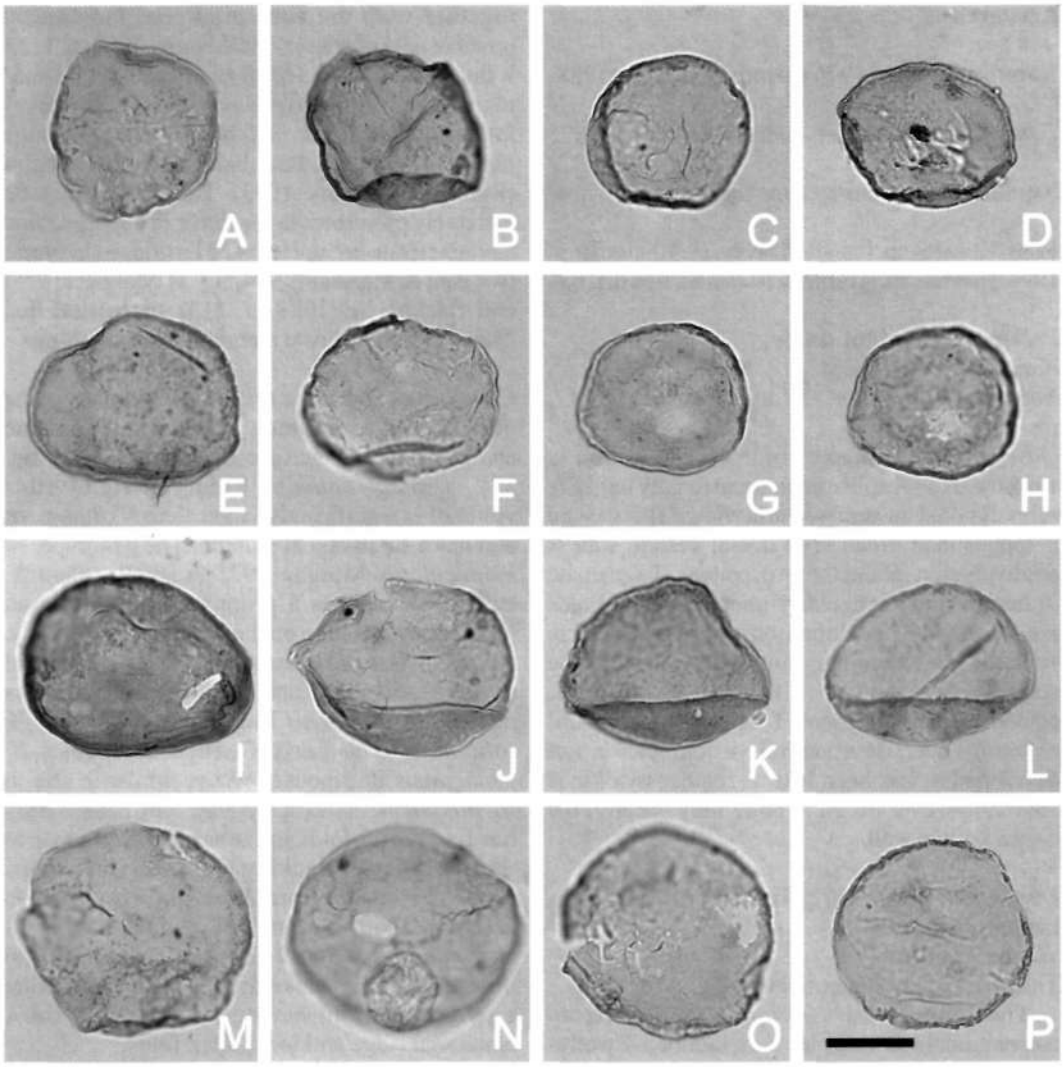

Fig. 18. Nummus tithonicus sp. nov. Specimens from conventional cores from Lambert-2 well at 318.69m (Figs 18C, J-K, N-O), Lorikeet-1 well at 1761.20m (Fig. 18P) and Mutineer-1B well at 3147.60m (Figs 18B, D-E, I) and 3132.25m (Figs 18A, G-H) and a sidewall core from Nancar-1 well at 3420.00m (Figs 18F, M). Fig. 18E is the holotype; remainder are paratypes. All photomicrographs taken using plain transmitted light. Scale bar in Fig. 18P refers to all photomicrographs and is 25µm. Note ellipsoidal to subcircular outline which is normally elongate; thin, largely smooth dorsal vesicle wall susceptible to irregular folding; lack of a ventral vesicle wall; thickened equatorial rim and absence of a consistently developed pylome. A - CPC 35980, paratype; dorsal view, high focus. Subcircular specimen. B - CPC 35981, paratype; ventral view, high focus. Note ventral thickened equatorial rim and slightly folded dorsal vesicle wall. C - CPC 35982, paratype; ventral view, median focus. Subcircular specimen with few folds. D - CPC 35983, paratype; ventral view, high focus. Relatively small, elongate specimen. E - CPC 35984, holotype; dorsal view, high focus. Note folds on dorsal surface, close to periphery. F - CPC 35985, paratype; ventral view, median focus. Note prominent, arcuate fold. G, H - CPC 35986, paratype; ventral view, high and median focus respectively. Small, subcircular thinning in dorsal vesicle wall probably a preservational artefact. I - CPC 35987, paratype; ventral view, median focus. Note thick vesicle wall. J - CPC 35988, paratype; dorsal view, high focus. Elongate specimen which has not been folded. K - CPC 35989, paratype; dorsal view, high focus. Note lack of folding of dorsal vesicle wall and absence of a pylome. L - CPC 35990, paratype; ventral view, high focus. Note large, straight fold on dorsal vesicle wall. M - CPC 35991, paratype; ventral view, high focus. Relatively large, subcircular specimen. N - CPC 35992, paratype; ventral view, median focus. Note small ellipsoidal hole in the dorsal vesicle wall; this is not considered to be a pylome. O - CPC 35993, paratype; dorsal view, median focus. Note slightly degraded dorsal vesicle wall. P - CPC 35994, paratype; ventral view, median focus. Note prominent thickened ventral equatorial rim.

Acritarch

Nummus Morgan 1975 emend. Backhouse 1988

Type species. Nummus monoculatus Morgan 1975

Nummus tithonicus sp. nov. (Figs 18A-P)

1988 *Nummus* sp. (small); Davey, pl. 10, fig. 10.
1994 *Nummus* sp. A; Bint & Marshall, figs 6.7, 6.8.

Previous Australian usage
Nummus spp. – Helby
Nummus 'minisimilis' - Morgan.

Description. A species of *Nummus* which is ellipsoidal to subspheroidal, occasionally partially subpolygonal in dorsoventral view. The vesicle is longer than broad. The dorsal vesicle wall is relatively thin (about 0.5µm), psilate, shagreenate to occasionally irregularly microscabrate. Folds are frequently developed on the dorsal vesicle wall; these are irregular, short or long and may be straight or arcuate. A thickened, ovoidal, equatorial rim is present. This forms the ventral extremity because a ventral vesicle wall is not developed or has been lost. A regular pylome is absent, however irregular holes may occur in the dorsal vesicle wall.

Dimensions (µm, n=30): Min. (Mean) Max.
Length: 44 (58) 74
Width: 33 (50) 64
Thickness of the equatorial rim: 2 (2.5) 5

The measured specimens are from conventional core samples from Lambert-2 well at 3118.69m, Lorikeet-1 well at 1761.20m and Mutineer-1B well at 3147.60m and 3132.25m and sidewall core samples from Avocet-1A well at 1780.00m, Nancar-1 well at 3240.00m and Scafell-1 well at 1418.00m.

Comments. This species of *Nummus* is relatively large and lacks a definite pylome (Fig. 18). However, in some specimens, subcircular, ellipsoidal or irregularly shaped holes are present in the dorsal vesicle wall (Figs 18G-H, N). These are considered to be the result of physico-chemical damage and not primary features because of their inconsistent and irregular nature and the lack of a thickened rim. The central folds on the dorsal wall are normally straight and the rarer folds close to the periphery are generally arcuate. These features are due to compaction of the vesicle. *Nummus tithonicus* does not have a ventral wall and this, together with the equatorial rim, indicates a possible adherent habit (Backhouse, 1988, p. 112). It thus resembles the hemispherical Jurassic non-marine acritarch *Truncatisphaeridium clevelandense* Riding & Duxbury 1993. *Nummus tithonicus* may also have had an encrusting habit (Riding & Duxbury, 1993). This species may be extremely prominent in the lower *Pseudoceratium iehiense* Zone sensu Helby & Partridge (in prep.) (see Bint & Marshall, 1994, fig. 4). Morgan (1975) and Backhouse (1988, p. 113) speculated that *Nummus* may indicate marginal marine settings.

Comparison. Nummus tithonicus differs from the other species of the genus in the lack of a pylome and in its size range (see Backhouse, 1988, fig. 33). *Nummus apiculus* Riding & Helby (this volume) is significantly larger than *N. tithonicus* and has a small apical pylome. The genotype, *N. monoculatus* Morgan 1975 is smaller than *N. tithonicus* and has a prominent pylome in an 'intercalary' position on the dorsal side. Similarly, the small size, consistent presence of an apical pylome and equatorial/lateral constrictions distinguish *N. parvus* Backhouse 1988 from *N. tithonicus*. The Early Cretaceous species *N. pentagonus* Backhouse 1988 is similar in size to *N. tithonicus*, lacks a pylome, but consistently has five dorsal folds in the vesicle wall close to the periphery (Backhouse, 1988). *Nummus tithonicus* differs from *N. similis* (Cookson & Eisenack 1960) Burger 1980 and the similar *N. mallajoharensis* Jain & Garg (in Jain *et al.*, 1984) in normally being markedly ellipsoidal and lacking a pylome, and in having an extremely thick equatorial ridge and long, thick folds.

Derivation of name. From the Tithonian Stage.

Holotype and type locality. Figure 18E, CPC 35984, from a conventional core sample in Mutineer-1B well at 3147.60m.

Stratigraphical distribution. Nummus tithonicus ranges from the Oxfordian *Wanaea spectabilis* Zone (6c) to the Berriasian *Batioladinium reticulatum* Zone (4aiii). The species has a characteristic acme in the upper part of the lower *Pseudoceratium iehiense* Zone (4ciii) (Foster, this volume; Helby & Partridge, in prep.).

ACKNOWLEDGEMENTS

The authors are grateful to Dr Clinton B. Foster (AGSO) for promoting and facilitating this work and for editorial guidance and advice. Christian

Thun and Andrew Kelman (AGSO) provided invaluable help with preparations and the manipulation of digital images. Eddie Resiak of the core and cuttings repository at AGSO, courteously provided access to sample material. BHP Petroleum Pty. Ltd., Esso Australia Ltd., Nippon Oil Exploration, Santos Ltd. and the Geological Survey of Western Australia kindly provided sample material on request. Dr Neil G. Marshall (Woodside) facilitated our restudy of the figured specimens of Bint & Marshall (1994). Dr Fauzie Hasibuan of the Geological Research and Development Center, Bandung, Indonesia supplied the sample material from Misool, eastern Indonesia. Laola Pty. Ltd. (Perth) gave support via the careful preparation of key samples. Drs R. A. Fensome and J. Goodall are thanked for reviewing the manuscript. J. B. Riding publishes with the permission of the Chief Executive Officer, AGSO.

REFERENCES

ALBERTI, G., 1961. Zur Kenntnis mesozoischer und alttertiärer Dinoflagellaten und Hystrichosphaerideen von Nord- und Mitteldeutschland sowie einigen anderen europäischen gebieten. *Palaeontographica Abteilung A 116*, 1-58.

BACKHOUSE, J., 1988. Late Jurassic and Early Cretaceous palynology of the Perth Basin, Western Australia. *Geological Survey of Western Australia Bulletin 135*, 233 p.

BELOW, R., 1982. *Rigaudella*, ein neues Genus von Dinoflagellaten-Zysten. *Neues Jahrbuch für Geologie und Paläontologie Monatshefte 1982/3*, 137-150.

BELOW, R., 1987. Evolution und Systematik von Dinoflagellaten-Zysten aus der Ordnung Peridiniales. II. Cladopyxiaceae und Valvaeodiniaceae. *Palaeontographica Abteilung B 206*, 1-115.

BELOW, R., 1990. Evolution und Systematik von Dinoflagellaten-Zysten aus der Ordnung Peridiniales. III. Familie Pareodiniaceae. *Palaeontographica Abteilung B 220*, 1-96.

BINT, A.N., 1986. Fossil Ceratiaceae: a restudy and new taxa from the mid-Cretaceous of the Western Interior, U.S.A. *Palynology 10*, 135-180.

BINT, A.N. & MARSHALL, N.G., 1994. High resolution palynostratigraphy of the Tithonian Angel Formation in the Wanaea and Cossack oil fields, Dampier sub-basin. 543-554 in Purcell, P.G. & Purcell, R.R. (eds). The Sedimentary Basins of Western Australia. *Proceedings of the Petroleum Exploration Society of Australia Symposium, Perth, 1994*.

BUJAK, J.P. & DAVIES, E.H., 1983. Modern and fossil Peridiniineae. *American Association of Stratigraphic Palynologists Contributions Series No. 13*, 203 p.

COOKSON, I.C. & EISENACK, A., 1958. Microplankton from Australian and New Guinea Upper Mesozoic sediments. *Proceedings of the Royal Society of Victoria (New Series) 70*, 19-79.

COOKSON, I.C. & EISENACK, A., 1960. Upper Mesozoic microplankton from Australia and New Guinea. *Palaeontology 2*, 243-261.

COOKSON, I.C. & EISENACK, A., 1974. Mikroplankton aus australischen mesozoischen und tertiären Sedimenten. *Palaeontographica Abteilung B 148*, 44-93.

COURTINAT, B., 1989. Les organoclastes des formations lithologiques du Malm dans le Jura Méridional. Systématique, biostratigraphie et éléments d'interprétation paléoécologique. *Documents des Laboratoires de Géologie Lyon 105*, 361 p.

DAVEY, R.J., 1974. Dinoflagellate cysts from the Barremian of the Speeton Clay, England. In: Symposium on Stratigraphic Palynology. *Birbal Sahni Institute of Palaeobotany, Special publication No. 3*, 41-75.

DUXBURY, S., 1977. A palynostratigraphy of the Berriasian to Barremian of the Speeton Clay of Speeton, England. *Palaeontographica Abteilung B 160*, 17-67.

EVITT, W.R., 1985. *Sporopollenin dinoflagellate cysts. Their morphology and interpretation*. American Association of Stratigraphic Palynologists Foundation, Dallas, 333 p.

FENSOME, R.A., TAYLOR, F.J.R., NORRIS, G., SARJEANT, W.A.S., WHARTON, D.I. & WILLIAMS, G.L., 1993. A classification of living and fossil dinoflagellates. *Micropaleontology Special Publication No. 7*, 351 p.

FOSTER, C.B., this volume. Introduction.

GOCHT, H., 1959. Mikroplankton aus dem nordwestdeutschen Neokom (Teil II). *Paläontologische Zeitschrift 33*, 50-89.

GOCHT, H., 1976. *Hystrichosphaeropsis quasicribrata* (O. Wetzel), ein Dinoflagellat aus dem Maastricht Nordeuropas. Mit einem nomenklatorischen Nachtrag zur Gattung *Lithodinia* Eis. *Neues Jahrbuch für Geologie und Paläontologie, Monatshefte 1976(6)*, 331-336.

HABIB, D., 1972. Dinoflagellate stratigraphy Leg 11, Deep Sea Drilling Project. *Initial Reports of the Deep Sea Drilling Project 11*, 367-425.

HARDING, I.C., 1990. A dinocyst calibration of the European Boreal Barremian. *Palaeontographica Abteilung B 218*, 1-76.

HARDING, I.C., 1996. Taxonomic stabilisation of dinoflagellate cyst taxa, as exemplified by two

morphologically complex Early Cretaceous species. *Review of Palaeobotany and Palynology 92*, 351-366.

HASIBUAN, F., 1990. *Mesozoic stratigraphy and paleontology of Misool Archipelago, Indonesia.* Unpublished Ph.D. thesis, University of Auckland, 384p., 22pl.

HELBY, R. & HASIBUAN, F., 1988. A Jurassic dinoflagellate sequence from Misool, Indonesia. *7 International Palynological Congress Brisbane, Abstracts Volume*, p. 69.

HELBY, R. MORGAN, R. & PARTRIDGE, A.D., 1987. A palynological zonation of the Australian Mesozoic. *Memoir of the Association of Australasian Palaeontologists 4*, 1-94.

HELBY, R. & PARTRIDGE, A.D., in prep. A palynological zonation of the Australian Mesozoic: an update.

HELENES, J. & LUCAS-CLARK, J., 1997. Morphological variations among species of the fossil dinoflagellate genus *Gonyaulacysta*. *Palynology 21*, 173-196.

LENTIN, J.K & VOZZHENNIKOVA, T.F., 1990. Fossil dinoflagellates from the Jurassic, Cretaceous and Paleogene deposits of the USSR – a re-study. *American Association of Stratigraphic Palynologists Contributions Series No. 23*, 221 p.

LENTIN, J.K. & WILLIAMS, G.L., 1993. Fossil dinoflagellates: index to genera and species. 1993 edition. *American Association of Stratigraphic Palynologists Contributions Series No. 28*, 856 p.

MAY, F.E., STEVENS, J. & PARTRIDGE, A.D. 1987. The Early Cretaceous dinoflagellate, *Dissimulidinium lobispinosum* gen. et sp. nov. from Western Australia. *Memoir of the Association of Australasian Palaeontologists 4*, 199-204.

MORGAN, R., 1975. Some Early Cretaceous organic-walled microplankton from the Great Australian Basin, Australia. *Journal and Proceedings of the Royal Society of New South Wales 108*, 157-167.

MORGAN, R., 1980. Palynostratigraphy of the Australian Early and Middle Cretaceous. *Memoirs of the Geological Survey of New South Wales. Palaeontology 18*, 153 p.

PARKER, F.M., 1986. *Late Jurassic palynology of the Dampier Sub-Basin, Carnarvon Basin, Western Australia*. Unpublished PhD thesis, University of Western Australia, vol. 1: 306 + A28p; vol. 2: pl. 1-63.

POURTOY, D., 1988. Le genre *Aprobolocysta* Duxbury, 1977, emend.: révision et comparison avec le genre *Batioladinium* Brideaux, 1975, emend. *Bulletin de Centres de Recherches Exploration-Production Elf-Aquitaine 12*, 383-403.

RIDING, J.B., 1984. A palynological investigation of Toarcian to early Aalenian strata from the Blea Wyke area, Ravenscar, North Yorkshire. *Proceedings of the Yorkshire Geological Society 45*, 109-122.

RIDING, J.B., 1994. A taxonomic study of the Mesozoic dinoflagellate cysts *Phallocysta elongata* (Beju 1971) comb. nov., emend. nov. and *Wallodinium cylindricum* (Habib 1970) Duxbury 1983 emend. nov. *Palynology* 18, 11-22.

RIDING, J.B. & DUXBURY, S., 1993. A new non-marine acritarch from the Middle Jurassic of Britain. *Special Papers in Palaeontology No. 48*, 57-66.

RIDING, J.B. & HELBY, R., this volume. Microplankton from the Mid Jurassic (late Callovian) *Rigaudella aemula* Zone in the Timor Sea, north-western Australia.

RIDING, J.B. & THOMAS, J.E., 1988. Dinoflagellate cyst stratigraphy of the Kimmeridge Clay (Upper Jurassic) from the Dorset coast, southern England. *Palynology 12*, 65-88.

SARJEANT, W.A.S., 1969. Taxonomic changes. *Bulletin of the British Museum (Natural History) Geology Series, Appendix to Supplement 3*, 7-15.

SARJEANT, W.A.S., LACALLI, T. & GAINES, G., 1987. The cysts and skeletal elements of dinoflagellates: speculations on the ecological causes for their morphology and development. *Micropaleontology 33*, 1-36.

SLIMANI, H., 1994. Les dinokystes des Craies du Campanien au Danien a Halembaye, Turnhout (Belgique) et a Beutenaken (Pays-Bas). *Mémoires pour servir à l'Explication des Cartes Géologiques et Minières de la Belgique - Toelichtende Verhandelingen voor de Geologische en Mijnkaarten van België No. 37*, 173 p.

SNAPE, M.G., 1992. Dinoflagellate cysts from an allochthonous block of Nordenskjöld Formation (Upper Jurassic), north-west James Ross Island. *Antarctic Science 4 (3)*, 267-278.

STEVENS, J. & HELBY, R., 1987. Some Early Cretaceous dinoflagellates encountered in the Australian *Kalyptea wisemaniae* Zone. *Memoir of the Association of Australasian Palaeontologists 4*, 165-184.

STEVENS, J. & HELBY, R., unpublished manuscript. Some Late Jurassic dinoflagellates from the Exmouth Plateau, Western Australia: *Endoceratium iehiense* Zone. 75 p.

STOVER, L.E., 1975. Observations on some Australian Eocene dinoflagellates. *Geoscience and Man 11*, 35-45.

STOVER, L.E. & EVITT, W.R., 1978. Analyses of Pre-Pleistocene organic-walled dinoflagellates. *Stanford University Publications, Geological Sciences 15*, 300 p.

STOVER, L.E. & HELBY, R., 1987. Some Australian

Mesozoic microplankton index species. *Memoir of the Association of Australasian Palaeontologists 4*, 101-134.

WARREN, J.S., 1967. *Dinoflagellates and acritarchs from the Upper Jurassic and Lower Cretaceous rocks on the west side of the Sacremento Valley, California.* Unpublished PhD thesis, Stanford University, 409 p.

WHITTAM, D.B., NORVICK, M.S. & McINTYRE, C.L., 1996. Mesozoic and Cainozoic tectono-stratigraphy of western ZOCA and adjacent areas. *The APPEA Journal 36*, 209-232.

WILLIAMS, G.L., LENTIN, J.K. & FENSOME, R.A., 1998. The Lentin and Williams Index of fossil dinoflagellates 1998 edition. *American Association of Stratigraphic Palynologists Contributions Series No. 34*, 817 p.

APPENDIX 1: LOCATIONS AND OPERATORS OF WELLS AND BORES FROM WHICH MATERIAL HAS BEEN STUDIED

Well Name and Number	Latitude	Longitude	Operator
Avocet-1A	11° 22' 18.05"S	125° 45' 22.29"E	Bond
Broome-1 Bore	17° 57' 40"S	122° 14' 20"E	PWD*
Broome-3 Town Bore	17° 57' 31"S	122° 14' 20"E	WAMD**
Cossack-1	19° 33' 16.94"S	116° 29' 50.01"E	Woodside
Crux-1	12° 94' 40.25"S	124° 45' 25.89"E	Nippon
Jurabi-1	21° 37' 07.30"S	114° 11' 59.81"E	Esso
Lambert-2	19° 26' 25.10"S	116° 29' 03.90"E	Woodside
Lorikeet-1	11° 10' 20.77"S	125° 37' 08.89"E	BHP
Mindil-1	10° 57' 47.69"S	125° 41' 21.45"E	Woodside
Mutineer-1B	19° 15' 01.53"S	116° 38' 11.44"E	Santos
Nancar-1	10° 59' 15.64"S	125° 45' 08.55"E	BHP
Peak-1	21° 36' 16.99"S	114° 30' 21.99"E	WAPET
Puratte-1	17° 05' 16.12"S	123° 14' 17.39"E	ESSO
Scafell-1	21° 32' 43.79"S	114° 01' 08.02"E	BHP
Wanaea-2	19° 36' 44.60"S	116° 24' 45.20"E	Woodside
Wanaea-3	19° 34' 41.81"S	116° 27' 00.09"E	Woodside
Yering-1	12° 36' 41.85"S	124° 31' 05.38"E	BHP
Zeewulf-1	21° 06' 27.51"S	113° 37' 17.02"E	Esso

*PWD – Public Works Department

**WAMD – Department of Mines, Western Australia

Well completion reports on all the listed offshore wells are publicly available five years after completion.

Outcrop Material: Misool, Eastern Indonesia

Sample Number	Lithostratigraphy	Age	Reference
81FH11	Lelinta Formation (Fageo Group)	Tithonian	Hasibuan (1990)

APPENDIX 2: REGISTER OF FIGURED SPECIMENS

All palynomorph specimens figured in this paper are listed here, together with essential details. The vast majority of the specimens are curated in the Commonwealth Palaeontological Collection (CPC) of the Australian Geological Survey Organisation, Canberra. However, two of the specimens illustrated here are housed in the collections of the Geological Survey of Western Australia, Perth.

The dinoflagellate cyst and acritarch genera and species are listed alphabetically here and the location of the specimens on the microscope slides are all 'England-Finder' co-ordinates (EF). These were taken with the slide label to the left of the observer; the microscope stage opening toward the microscope user. The coding for types is as follows: H = holotype; P = paratype; T = topotype. All specimens of new taxa examined during this study contributed to the specific concepts described. Therefore, all figured specimens of new taxa, which are not holotypes are paratypes. SGM = single grain mount. SSM = single species mount. The single mounts do not have unique numbers; they are numbered sequentially for each species within a particular sample. The specimens are from conventional core, sidewall core and ditch cutting samples.

Species	Type	Fig(s)	SGM/Slide No.	EF	Well (depth, m.)	CPC No.
A. clavata	P	1A-C	SSM 14 (i)	H27/4	Lorikeet-1 (759.10)	35883
A. clavata	P	1D	SGM 1 (i)	P35	Wanaea-2 (3375.34)	35884
A. clavata	P	1E	SGM 2 (i)	M34/3	Wanaea-2 (2875.30)	35885
A. clavata	P	1F,G	SSM 14 (ii)	H27/2	Lorikeet-1 (1759.10)	35886
A. clavata	P	1H	SGM 3 (ii)	O29	Wanaea-2 (2875.30)	35887
A. clavata	H	1I-L	SGM 2 (i)	L29	Wanaea-2 (2880.50)	35888
A. clavata	P	1M,N	SGM 83 (i)	L35/3	Avocet-1A (1771.50)	35889
A. clavata	P	1O,P	SGM 106 (i)	L27/4	Avocet-1A (1771.50)	35890
A. variabile	P	2A,B	SSM 9 (ii)	N33/4	Lorikeet-1 (1759.10)	35891
A. variabile	P	2C	SSM 9 (i)	N34/3	Lorikeet-1 (1759.10)	35892
A. variabile	P	2D	SGM 1 (i)	M35/3	Mutineer-1B (3132.25)	35893
A. variabile	P	2E-F	SGM 1 (i)	S34/1	Lorikeet-1 (1756.70)	35894
A. variabile	P	2H	SGM 2 (ii)	L21/1	Mutineer-1B (3132.25)	35895
A. variabile	H	2I-L	SGM 1 (i)	S32	Avocet-1A (1775.00*)	35896
A. variabile	P	2M-O	SGM 1 (i)	O28	Peak-1 (1493.54**)	35897
A. variabile	P	2P	SGM 1 (ii)	K32	Jurabi-1 (1140.00)	35898
B. cheleusis	P	3A-B	SGM 3 (ii)	M32/3	Scafell-1 (1421.00)	35899
B. cheleusis	P	3C	SGM 2 (i)	N27/4	Scafell-1 (1421.00)	35900
B. cheleusis	P	3D	SGM 2 (iii)	P27/4	Mindil-1 (3150.00*)	35901
B. cheleusis	H	3E-F	Ass. sl. 2	O28/4	Wanaea-3 (2964.00)	F.49309**
B. cheleusis	P	3G, 3H	SGM 7 (i)	N36	Scafell-1 (1418.00)	35902
B. cheleusis	P	3I	SGM 3 (i)	K28/3	Mindil-1 (3150.00*)	35903
B. cheleusis	P	3J, 3K	SGM 2 (ii)	R27	Mindil-1 (3150.00*)	35904
B. cheleusis	P	3L	SGM 3 (i)	N33/2	Scafell-1 (1421.00)	35905
B. cheleusis	P	3M	SGM 1 (iv)	N23/4	Mindil-1 (3150.00*)	35906
B. cheleusis	P	3N	SGM 1 (i)	O34/2	Scafell-1 (1418.00)	35907
B. cheleusis	P	3O	SGM 2 (ii)	M33/2	Nancar-1 (3240.00)	35908
B. cheleusis	P	3P	SGM 1 (iii)	O23/2	Mindil-1 (3150.00*)	35909
B. paeminosum	P	4A-B	SGM 2 (iii)	O25	Wanaea-2 (2875.30)	35910
B. paeminosum	P	4C-D	SGM 3 (iii)	J27/4	Wanaea-2 (2875.30)	35911
B. paeminosum	P	4E	SGM 1 (ii)	M17	Mutineer-1B (3132.25)	35912
B. paeminosum	P	4F-H	SGM 1 (i)	N35/3	Wanaea-2 (2880.50)	35913
B. paeminosum	P	4I-J	SGM 3 (i)	K27/4	Wanaea-2 (2875.30)	35914
B. paeminosum	P	4K-L	SGM 1 (iii)	S32/1	Wanaea-2 (3375.34)	35915
B. paeminosum	P	4M	SGM 3 (ii)	K26/2	Wanaea-2 (2875.30)	35916
B. paeminosum	H	4N-P	SSM 10 (i)	M32	Lorikeet-1 (1759.10)	35917
B. balteus morph. 1	P	5A-C	SGM 105 (ii)	L32/4	Misool, 81FH11	35918
B. balteus morph. 1	P	5D-F	SGM 103 (v)	N18	Misool, 81FH11	35919
B. balteus morph. 1	P	5G-I	SGM 101 (iii)	N30	Misool, 81FH11	35920
B. balteus morph. 1	P	5J-L	SGM 100 (ii)	J38/3	Misool, 81FH11	35921
B. balteus morph. 1	H	6A-C	SGM 103 (vii)	N17/2	Misool, 81FH11	35922
B. balteus morph. 1	P	6D-F	SGM 102 (iii)	J29	Misool, 81FH11	35923
B. balteus morph. 2	P	7A-C	SGM 106 (v)	K32	Misool, 81FH11	35924
B. balteus morph. 2	P	7D-7F	SGM 101 (v)	M30/3	Misool, 81FH11	35925
B. balteus morph. 2	P	7G-7I	SGM 102 (i)	K28	Misool, 81FH11	35926
B. balteus morph. 2	P	7J-7L	SSM 30	Q32/4	Misool, 81FH11	35927

* - range depth: 1775.00m-1780.00m

** - range depth: 1493.54m-1496.59m

* - range depth: 3150.00m-3155.00m

** - Geological Survey of Western Australia type/figured slide collection number

Species	Type	Fig(s)	SGM/Slide No.	EF	Well (depth, m.)	CPC No.
Belowia sp. A		8A-C	Ass. sl. 2	V21/1	Crux-1 (2945.00*)	35928
Belowia sp. A		8D-F	SGM 3 (v)	N33/3	Crux-1 (2945.00*)	35929
Belowia sp. A		8G-I	SGM 1 (ii)	S30/3	Crux-1 (2945.00*)	35930
Belowia sp. A		8J-L	SGM 1 (iii)	R30	Crux-1 (2945.00*)	35931
* - range depth: 2945.00m-2950.00m						
B. ferox	P	9A-D	SGM 1 (iii)	L29	Avocet-1A (1770.00*)	35932
B. ferox	P	9E-H	SGM 48 (i)	N36	Avocet 1A (1771.50)	35933
B. ferox	H	9I-L	SGM 38 (i)	N34	Avocet 1A (1771.50)	35934
B. ferox	P	9M	SGM 3 (i)	P31/3&4	Lorikeet-1 (1761.20)	35935
B. ferox	P	9N	SGM 1 (i)	J29/2	Mutineer-1B (3132.25)	35936
B. ferox	P	9O	SGM 1 (i)	F29/3	Lorikeet-1 (1761.20)	35937
B. ferox	P	9P	SGM 1 (i)	J31	Lambert-2 (3101.00)	35938
B. ferox	P	9Q	SGM 55 (i)	N34	Broome-1 (297.79)	35939
B. ferox	P	9R	SGM 90 (ii)	N34/2	Broome-1 (297.79)	35940
B. ferox	P	9S	SGM 52 (i)	R38	Broome-1 (297.79)	35941
B. ferox	P	9T	Ass. sl. 2	S43/2&4	Wanaea-3 (2929.67)	F.49311**
* - range depth: 1770.00m-1775.00m						
** - Geological Survey of Western Australia type/figured slide collection number						
C. solida	P	10A-B	SGM 3 (iii)	L23/1	Crux-1 (3045.00*)	35942
C. solida	P	10C-D	SGM 2 (iii)	N35/1	Crux-1 (3045.00*)	35943
C. solida	H	10E-G	SGM 1 (ii)	Q31/4	Crux-1 (2945.00**)	35944
C. solida	P	10H	SGM 3 (vi)	K24/1	Crux-1 (3045.00*)	35945
C. solida	P	10I-J	SGM 4 (vii)	O34/4	Crux-1 (3045.00*)	35946
C. solida	P	10K	SGM 1 (iv)	K35	Crux-1 (3045.00*)	35947
C. solida	P	10L	SGM 1 (i)	R31/1	Crux-1 (2945.00**)	35948
C. solida	P	10M-N	SGM 2 (ii)	N35	Crux-1 (3045.00*)	35949
C. solida	P	10O-P	SGM 3 (v)	K25	Crux-1 (3045.00*)	35950
* - range depth: 3045.00m-3050.00m						
** - range depth: 2945.00m-2950.00m						
D. purattense	P	11A-B	SGM 1 (iv)	K31/3	Scafell-1 (1421.00)	35951
D. purattense	H	11C-D	SGM 4 (i)	L32/4	Scafell-1 (1421.00)	35952
D. purattense	P	11E-G	SGM 1 (i)	L29	Scafell-1 (1421.00)	35953
D. purattense	P	11H	SGM 3 (iv)	H38/4	Scafell-1 (1418.00)	35954
D. purattense	P	11I-J	SGM 1 (i)	M37	Scafell-1 (1418.00)	35955
D. purattense	P	11K-L	SGM 1 (ii)	L30	Scafell-1 (1421.00)	35956
D. purattense	P	11M	SGM 2 (i)	P34/3	Scafell-1 (1421.00)	35957
D. purattense	P	11N	SGM 3 (i)	N35	Scafell-1 (1421.00)	35958
D. purattense	P	11O-P	SGM 2 (ii)	L32	Scafell-1 (1418.00)	35959
G. angustum	P	12A-B	SGM 1 (iv)	M37/2	Avocet-1A (1775.00*)	35960
G. angustum	P	12C	SSM 3 (i)	N28	Lorikeet-1 (1759.10)	35961
G. angustum	P	12D	SSM 3 (ii)	M28/3	Lorikeet-1 (1759.10)	35962
G. angustum	H	12E-H	SGM 31 (i)	P20	Avocet-1A (1771.50)	35963
G. angustum	P	12I-L	SSM 2 (iii)	J40/3	Lorikeet-1 (1759.10)	35964
G. angustum	P	12M-N	SGM 128 (i)	Q32	Avocet 1A (1771.50)	35965
G. angustum	P	12O-P	SSM 2 (vi)	G38/3	Lorikeet-1 (1759.10)	35966
G. angustum	P	13A-C	SGM 1 (v)	L35/4	Avocet-1A (1775.00*)	35967
G. angustum	P	13D	SSM 2 (v)	H39/4	Lorikeet-1 (1759.10)	35968
G. angustum	P	13E-F	SSM 3 (iii)	M28	Lorikeet-1 (1759.10)	35969
G. angustum	P	13G-H	SSM 1 (iii)	R29/2	Lorikeet-1 (1759.10)	35970
G. angustum	P	13I-K	SSM 3 (iv)	K28/3	Lorikeet-1 (1759.10)	35971

Species	Type	Fig(s)	SGM/Slide No.	EF	Well (depth, m.)	CPC No.
G. angustum	P	13L,P	SSM 4 (iii)	J40/1	Lorikeet-1 (1759.10)	35972
G. angustum	P	13M-O	SGM 9 (i)	N34	Avocet-1A (1771.50)	35973
* - range depth: 1775.00m-1780.00m						
M. bulloidea	T	14A	SGM 131 (i)	N38/4	Broome-1 (297.79)	35974
M. bulloidea	T	14B-C	SGM 29	L38	Broome-1 (297.79)	35975
M. bulloidea	T	14D-E	SGM 131 (ii)	N38/3	Broome-1 (297.79)	35976
M. bulloidea	T	14F	SGM 129	M34/4	Broome-1 (297.79)	35977
M. bulloidea	T	14G-H	SGM 28 (ii)	N33/1	Broome-1 (297.79)	35978
M. bulloidea	T	14I	SGM 28 (i)	M33	Broome-1 (297.79)	35979
N. tithonicus	P	18A	SGM 1(iv)	O32/4	Mutineer-1B (3132.25)	35980
N. tithonicus	P	18B	SGM 2 (iii)	R34	Mutineer-1B (3147.60)	35981
N. tithonicus	P	18C	SGM 1 (ii)	O28/1&3	Lambert-2 (3118.69)	35982
N. tithonicus	P	18D	SGM 2 (ii)	S35	Mutineer-1B (3147.60)	35983
N. tithonicus	H	18E	SGM 1 (ii)	K36/4	Mutineer-1B (3147.60)	35984
N. tithonicus	P	18F	SGM 1 (iv)	P32/3	Nancar-1 (3420.00)	35985
N. tithonicus	P	18G,H	SGM 1 (vi)	O31/2	Mutineer-1B (3132.25)	35986
N. tithonicus	P	18I	SGM 1 (v)	H37/3	Mutineer-1B (3147.60)	35987
N. tithonicus	P	18J	SGM 2 (i)	O34	Lambert-2 (3118.69)	35988
N. tithonicus	P	18K	SGM 1 (vi)	N27/2	Lambert-2 (3118.69)	35989
N. tithonicus	P	18L	SGM 2 (vii)	L37	Lambert-2 (3118.69)	35990
N. tithonicus	P	18M	SGM 1 (iii)	Q31/4	Nancar-1 (3420.00)	35991
N. tithonicus	P	18N	SGM 2 (vi)	L38/3	Lambert-2 (3118.69)	35992
N. tithonicus	P	18O	SGM 1 (iv)	O26	Lambert-2 (3118.69)	35993
N. tithonicus	P	18P	SGM 1 (i)	T37/3	Lorikeet-1 (1761.20)	35994
P. robustum	P	15A-B	SGM 3 (i)	J23/3	Mindil-1 (3150.00*)	35995
P. robustum	P	15C	SGM 2 (ii)	L25/4	Mindil-1 (3150.00*)	35996
P. robustum	P	15D-E	SGM 4 (iv)	L29/3	Mindil-1 (3150.00*)	35997
P. robustum	P	15F	SGM 1 (i)	N34/2	Scafell-1 (1418.00)	35998
P. robustum	P	15G	SGM 1 (ii)	J37/3	Scafell-1 (1418.00)	35999
P. robustum	P	15H	SGM 1 (iii)	L36/3	Scafell-1 (1418.00)	36000
P. robustum	P	15I	SGM 3 (ii)	H23	Mindil-1 (3150.00*)	36001
P. robustum	H	15J-K	SGM 5 (ii)	P28	Mindil-1 (3150.00*)	36002
P. robustum	P	15L	SGM I (i)	S23	Mindil-1 (3150.00*)	36003
* - range depth: 3150.00m-3155.00m						
S. granulosa		16A-D	SGM 2 (ii)	M39/3	Wanaea-2 (3375.34)	36004
S. granulosa		16E-H	SGM 14 (i)	L37/2	Avocet-1A (1771.50)	36005
S. granulosa		16I	SSM 1 (iii)	M27/3	Zeewulf-1 (3085.00)	36006
S. granulosa		16J-K	SGM 2 (iii)	Q26	Wanaea-2 (2880.50)	36007
S. granulosa		16L	SGM 4 (ii)	K37	Wanaea-2 (3375.34)	36008
S. granulosa		16M-N	SGM 1 (iii)	J29	Mutineer-1B (3132.25)	36009
S. granulosa		16O-P	SGM 5 (ii)	J38/1	Wanaea-2 (2875.30)	36010
S. granulosa		17A	SGM 1 (i)	J30/4	Lambert-2 (3101.00)	36011
S. granulosa		17B	SSM 5 (i)	J26/2	Lorikeet-1 (1759.10)	36012
S. granulosa		17C-D	SGM 1 (i)	N32/3	Lorikeet-1 (1756.70)	36013